

**Transition Metal- and Electro-Catalyzed C–H and B–H
Activation for the Efficient Synthesis of Carborane
Derivatives**

Dissertation

for the award of the degree

“Doctor rerum naturalium” (Dr.rer.nat.)

of the Georg-August-Universität Göttingen



in the doctoral program of chemistry

of the Georg-August-Universität School of Science (GAUSS)

Submitted by

Jei Becky Bongsuiru

From Kumbo (Cameroon)

Göttingen, 2022

Thesis Committee

Prof. Dr. Lutz Ackermann, Institute of Organic and Biomolecular Chemistry, Georg-August-Universität Göttingen Germany.

Professor Dr. Alexander Breder, Institute of Organic Chemistry, Universität Regensburg, Germany.

Prof. Dr. Shoubhik Das, ORSY Division, Department of Chemistry, Universiteit Antwerpen, Belgium.

Members of the Examination Board

Reviewer: Prof. Dr. Lutz Ackermann, Institute of Organic and Biomolecular Chemistry, Göttingen.

Second Reviewer: Professor Dr. Alexander Breder, Institute of Organic Chemistry, Universität Regensburg, Germany.

Further members of the Examination Board

Prof. Dr. Dr. h.c. Lutz-F. Tietze, Institute of Organic and Biomolecular Chemistry, Georg-August-Universität Göttingen Germany.

Prof. Dr. Dietmar Stalke, Institute of Inorganic Chemistry, Georg-August-Universität Göttingen Germany.

Dr. Michael John, Institute of Organic and Biomolecular Chemistry, Georg-August-Universität Göttingen Germany.

Dr. Daniel Janßen-Müller, Institute of Organic and Biomolecular Chemistry, Göttingen

Date of the Oral Examination: 15.12.2022

Acknowledgements

I wish to express my indebted gratitude to my supervisor Professor Dr. Lutz Ackermann, for acting as a portal to study at this prestigious university. His consistent professional mentorship and guidance fuelled the successes I achieved throughout my Ph.D. In addition, I sincerely appreciate the Georg-August University Göttingen for the lifetime privilege to study in this accredited institution. My second appreciation goes to the other members of my thesis committee: Prof. Dr. Alexander Breder and Prof. Dr. Shuobik Das, for their unsolicited support throughout my studies. Furthermore, my sincere appreciation also goes to all the members of my examination board for committing to be part of the final and key step of my Doctoral studies.

My heart felt gratitude goes to the German Academic Exchange Service (DAAD) for funding my studies through their doctoral grant scheme. Without their financial coverage I would not have been opportune to have a taste the prestigious German research environment.

The entire analytical department of the institute of Organic and Biomolecular Chemistry especially the NMR and mass department are herein appreciated for always providing quality analytical data. Dr Christopher Golz is also appreciated for providing X-ray crystallographic data.

In addition, I wish to appreciate the alumni and current members of the Ackermann group for their enormous contributions to the success of my studies. Special appreciation is ascribed to Dr. Long Yang, Dr. Cuiju Zhu, Alexej Scheremetjew, Dr. Fabio Pescioili, Dr. Uttam, Dr. Rositha Kuniyil, and Dr. Liang Yu-Feng for the fruitful collaboration in the past projects. Dr. Zi-Jing Zhang, Dr. Leonardo Massignan, Dr. Xuefeng Tan, Dr. Nikolaos Kaplaneris, Dr. Tjark Meyer, Dr. Maximilian Stangier, Ms. Julia Struwe, Adelina Kopp and for their respective assistance rendered to me.

Moreover, I am very grateful to Dr. Svenja Warratz, Dr. Joao Carlos Agostinho de Oliveira, Dr. Nikolaos Kaplaneris, Alexej Scheremetjew, Julia Struwe, Xiaoyan Hou, Hendrik Simon, and Tsuyoshi Ohyama for proofreading my dissertation. I am also grateful to Simon Homölle and Hendrik Simon for translating my executive summary to German. Next, I will not forget to thank Dr. Svenja Warratz, Ms. Gabriel Kiel-

Knepel, Ms. Bianca Spitalieri, Mr. Stefan Beußhausen, and Mr. Karsten Rauch for their undiluted technical and administrative assistance.

Many thanks go to my family, loved ones in Germany, Cameroon, and the world for their love, care, and moral support.

Finally, I want to thank God almighty for the grace to push through this critical phase of my life.

Deutsche Zusammenfassung

Kreuzkupplungsreaktionen stellen attraktive Wege zur Bildung von C–C und C–Het Bindungen dar. Dennoch sind auch sie, mit gewissen Nachteilen verbunden, die im Rahmen der C–H Funktionalisierung berücksichtigt werden. Die Entwicklung von übergangsmetallkatalysierten Methoden hat zu Durchbrüchen beim Aufbau komplexer molekularer Strukturen beigetragen. Zudem unterstützt die Elektrokatalyse zum umweltfreundlicheren Aufbau von Zielmolekülen, indem chemische Oxidationsmittel und harsche Reaktionsbedingungen vermieden werden und somit die Bildung unerwünschter Nebenprodukte unterdrückt wird. Carborane sind wichtige Verbindungen mit diversem einsatz in der Medizin, den Materialwissenschaften und der Koordinationschemie. Daraus resultiert die Notwendigkeit, Methoden für die selektive Käfigfunktionalisierung dieser Molekülklasse zu entwickeln. Deren Anwendbarkeit ist jedoch durch hohe Reaktionstemperaturen, den Einsatz von Edelmetallkatalysatoren und stöchiometrische chemischer oxidationsmittel eingeschränkt.

In unserem Forschungsprogramm zur nachhaltigen Katalyse, der Verwendung von 3d-Metallen als Katalysatoren und der Elektrokatalyse wurden effiziente Synthesewege zur Funktionalisierung von Carboranderivaten untersucht. Insbesondere das kostengünstige und in der Erdkruste vorkommende Mangan hat sich als nützlich erwiesen, carboranhaltige Peptide über selektive Hydroarylierung herzustellen. Zudem wurde die Käfigchalkogenierung von *o*-Carborane mittels Cupraelektro-katalyse bei Raumtemperatur erreicht und ermöglichte so den Zugang zu chalkogenhaltigen Carboranen. Außerdem wurden die weniger reaktiven *nido*-Carborane elektrokatalytisch über B–N Bindungsknüpfung an bioaktive Moleküle, wie BODIPY-Fluoreszenzmarker und Aminosäuren gebunden.

Alle Moleküle wurden mittels spektroskopischer, spektrometrischer, chromatographischer und kristallographischer Methoden detailliert analysiert. Basierend auf bereits bekannten Anwendungen der individuellen Molekülfragmente können die synthetisierten Verbindungen in der Medizin als Neutronenfänger in der Bestrahlungstherapie oder in den Materialwissenschaften als optoelektronische Materialien eingesetzt werden.

Table of Content

1.0 Introduction	1
1.1 Transition Metal-Catalyzed C–H Functionalization	1
1.2 General Mechanisms for Transition Metal-Catalyzed C–H Activation	2
1.3 General Approaches to Transition Metal-Catalyzed C–H Activation.....	3
1.4 Manganese-Catalyzed C–H Activations	5
1.4.1 Manganese-Catalyzed C–H Hydroarylation.....	7
1.4.2 Manganese-Catalyzed Domino-Initiated C–H Activation	11
1.4.3 Manganese-Catalyzed Substitutive C–H Activation.....	15
1.5 Manganese-Catalyzed Late-Stage Diversification of Peptides.....	18
1.6 Transition Metal-Catalyzed Electrochemical C–H Activation	18
1.6.1 Iron-Catalyzed Electrooxidative C–H Activation.....	26
1.6.2 Cobalt-electro-oxidative C–H Activation	26
1.6.3 Nickel-Catalyzed Electrooxidative C–H Activation	26
1.6.4 Copper-Catalyzed Electrooxidative C–H Activation	27
1.6.5 Palladium-Catalyzed Electro-Oxidative C–H Activation	28
1.6.6 Ruthenium-Catalyzed Electro-Oxidative C–H Activation.....	30
1.6.7 Rhodoelectro-Oxidative C–H Activation	32
1.6.8 Iridaelectro-Oxidative C–H Activation	34
1.6.9 Manganese-Catalyzed Electrooxidative C–H Activation	35
1.7 Transition Metal-Catalyzed Cage Functionalization of o-Carboranes.....	36
1.7.1 Transition Metal-Catalyzed Cage B(3, 6)–H Functionalization.....	37
1.7.2 Transition Metal-Catalyzed B(8,9,10,12)–H Functionalization	39
1.7.3 Transition Metal-Catalyzed Cage B(4,5,7,11)–H Functionalization	40
1.8 Electrochemical Cage Functionalization of Carboranes	49
2.0 Objectives	50
3. Results and Discussion	52
3.1 Electrochemical B–H Nitrogenation of <i>nido</i> -Carboranes.....	52
3.1.1 Optimization and Scope	52
3.1.2 Competition Experiments	58
3.1.3 Cyclic Voltammetry and Stability of 240a	59
3.1.4 Spectroscopic Data of BODIPY-Labelled <i>nido</i> -Carborane.....	60

Table of Content

3.1.5 Proposed Mechanism	61
3.2 Cupra- electro-catalyzed Cage Chalcogenation of <i>o</i> -Carboranes.....	62
3.2.1 Optimization and Scope	60
3.2.2 Late-Stage Functionalization	67
3.2.3 Mechanistic Studies	67
3.2.4 Proposed Mechanism	69
3.3 Manganese-Catalyzed Selective Labeling of Peptides with <i>o</i> -Carboranes <i>via</i> C–H Activation.	70
3.3.1 Optimization and Scope	71
3.3.2 Scale up Reaction and Late-Stage Amidation	72
3.3.3 Mechanistic Studies	77
3.3.4 Proposed Mechanism	78
4. Summary and Outlook	80
5.0 Experimental Section	82
5.1 General Remarks	82
5.2 General Procedures	82
5.3 Experimental Procedures and Analytical Data.....	87
5.3.1 Electrochemical B–H Nitrogenation of <i>nido</i> -Carboranes.....	87
5.3.2 Cupraelectro-Catalyzed Chalcogenations of <i>o</i> -Carboranes.....	117
5.3.3 Manganese-Catalyzed Selective Labeling of Peptides with <i>o</i> -Carboranes <i>via</i> C–H Activation.	139
6.0 References.....	164
7.0 NMR spectra	164

List of Abbreviations

Ac	acetyl
acac	acetyl acetate
Ad	Adamantane
Alk	alkyl
AMLA	ambiphilic metal-ligand activation
aq.	aqueous
Ar	aryl
atm	atmospheric pressure
BDMAE	bis(2-dimethylaminoethyl)ether
BHT	butylated hydroxytoluene
BIES	base-assisted internal electrophilic substitution
Bn	benzyl
BNCT	boron neutron capture therapy
Boc	<i>tert</i> -butoxycarbonyl
bpy	2,2'-bipyridyl
BQ	1,4-benzoquinone
Bu	butyl
Bz	benzoyl
calc.	calculated
<i>cat.</i>	catalytic
CCE	constant current electrolysis
CMD	concerted-metalation-deprotonation
cod	1,5-cyclooctadiene
conv.	conversion
Cp	cyclopentadienyl
Cp*	1,2,3,4,5-pentamethylcyclopenta-1,3-dienyl
Cy	cyclohexyl
δ	chemical shift
d	doublet
DBU	1,8-diazabicyclo[5.4.0]undec-7-ene
DCE	1,2-dichloroethane
DCIB	dichloro- <i>iso</i> -butane

List of Abbreviations

dcype	1,2-bis-(dicyclohexylphosphino)ethane
dd	doublet of doublet
DFT	density functional theory
DG	directing group
DME	dimethoxyethane
DMA	<i>N,N</i> -dimethylacetamide
DMAP	4-dimethylaminopyridine
DMF	<i>N,N</i> -dimethylformamide
DMPU	1,3-dimethyltetrahydropyrimidin-2(1 <i>H</i>)-one
dppbz	1,2-bis(diphenylphosphino)benzene
dt	doublet of triplet
EI	electron ionization
EPR	Electron paramagnetic resonance
equiv	equivalent
ES	electrophilic substitution
ESI	electrospray ionization
Et	ethyl
Fc	Ferrocene
FG	functional group
g	gram
GC	gas chromatography
GVL	γ -valerolactone
h	hour
Hal	halogen
Het	heteroatom
Hept	heptyl
Hex	hexyl
HFIP	1,1,1,3,3,3-hexafluoro-2-propanol
HPLC	high performance liquid chromatography
HR-MS	high resolution mass spectrometry
Hz	Hertz
i	iso
IPr•HCl	1,3-bis-(2,6-diisopropylphenyl) imidazolinium chloride

List of Abbreviations

IR	infrared spectroscopy
IES	internal electrophilic substitution
J	coupling constant
KIE	kinetic isotope effect
L	ligand
<i>m</i>	meta
m	multiplet
M	molar
[M] ⁺	molecular ion peak
Me	methyl
Mes	mesityl
mg	milligram
MHz	megahertz
min	minute
mL	milliliter
mmol	millimole
M.p.	melting point
MQ	6-methylquinoline
MS	mass spectrometry
<i>m/z</i>	mass-to-charge ratio
NBA	nitrobenzoic acid
NBE	Norbornene
NCTS	<i>N</i> -Cyano- <i>N</i> -phenyl- <i>p</i> -toluenesulfonamide
NMO	<i>N</i> -methylmorpholine oxide
NMP	<i>N</i> -methylpyrrolidinone
NMR	nuclear magnetic resonance
n.r.	no reaction
<i>o</i>	<i>ortho</i>
OPV	oil pump vacuum
<i>p</i>	<i>para</i>
PAHs	<i>polycyclic aromatic hydrocarbons</i>
Ph	phenyl
Phen	1,10-phenanthroline

List of Abbreviations

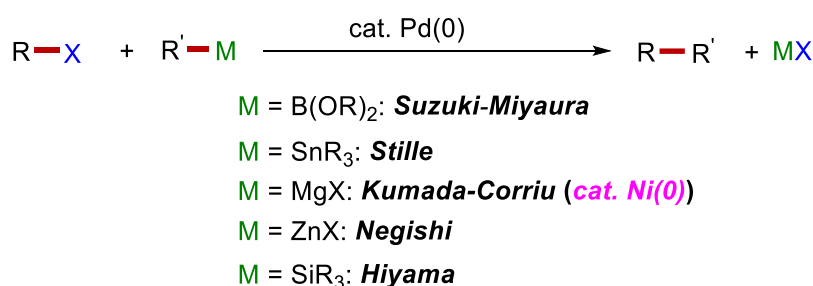
Piv	pivaloyl
ppm	parts per million
Pr	propyl
Phth	phthalic
Py	pyridyl
Pym	pyrimidyl
PyO	2-aminopyridine-1-oxide
q	quartet
Q	quinoline
RT	room temperature
s	singlet
sat.	saturated
SCE	saturated calomel electrode
SPS	solvent purification system
<i>t</i>	<i>tert</i>
t	triplet
T	temperature
TBAA	tetrabutylammonium acetate
TBAB	tetrabutylammonium bromide
TBAI	tetrabutylammonium iodide
TBHP	<i>tert</i> -butyl hydroperoxide
TEMPO	2,2,6,6-Tetramethylpiperidine-1-oxyl
Tf	triflate
TFE	2,2,2-trifluoroethanol
THF	tetrahydrofuran
TIPS	triisopropylsilyl
TM	transition metal
TMA	tetramethylammonium
TMEDA	<i>N,N,N',N'</i> -tetramethylethane-1,2-diamine
TMS	trimethylsilyl
Ts	<i>para</i> -toluenesulfonyl

1 Introduction

Organic compounds have a plethora of applications in pharmaceutical, agrochemical, materials, and cosmetic industries, among others.^[1] C–C and C–Het bonds are the main structural motif of most organic compounds. The selective formation of carbon-carbon(C–C),^[2] and carbon-heteroatom(C–Het)^[3] bonds has evolved as a reliable route to access diverse organic structures. In regard of the increasing environmental challenges, the use of expensive transition metal catalysts, harsh reaction conditions, environmentally unfriendly chemicals, and hazardous waste generated from chemical reactions should be avoided. Therefore, there has been a quest to develop cost-effective and environmentally benign methods for assembling complex molecular structures.^[4]

1.1 Transition Metal-Catalyzed C–H Activation

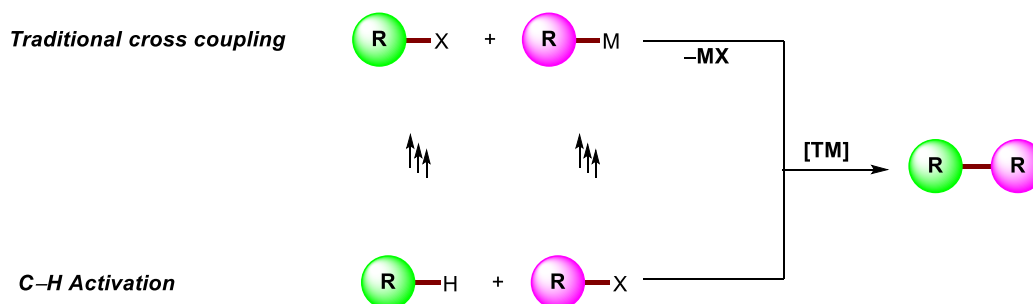
Transition metal-catalyzed cross-coupling reactions, such as the Suzuki-Miyaura,^[5] Kumada-Corriu,^[6] Hiyama,^[7] Negishi,^[8] and Stille couplings^[9] constitute key methods for C–C bond formations (Scheme 1). These reactions involve the coupling of an aryl or heteroaryl halide with an organometallic reagent. Furthermore, Goldberg-Ullmann couplings,^[10] Buchwald-Hartwig aminations,^[11] and Chan-Evans-Lam couplings^[12] are established methods for C–Het bond formation (Scheme 1).



Scheme 1. Transition metal-catalyzed cross-coupling reactions.

Despite the advancements of transition metal-catalyzed cross-coupling reactions, they suffer from significant drawbacks, making them less sustainable. These methods hence usually require pre-functionalized substrates, which are laborious to synthesize. Furthermore, the organometallic reagents (Grignard reagents, organostannanes, and

organozinc compounds) are difficult to handle and responsible for stoichiometric amounts of unwanted by-products.^[13] The development of the transition metal-catalyzed C–H activation as an alternative to cross-coupling reactions for C–C and C–Het bond formation unveiled a new era for synthetic chemists (Scheme 2).^[14]



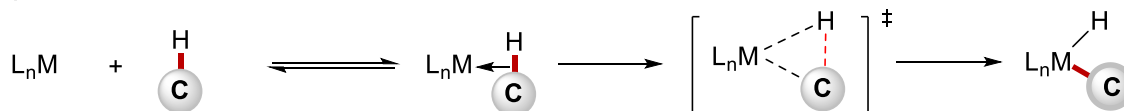
Scheme 2. Traditional cross-coupling reactions *versus* C–H activation.

1.2 General Mechanisms for Transition Metal-Catalyzed C–H Activation

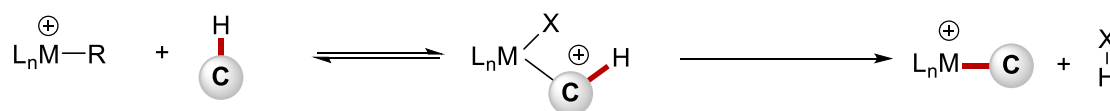
The cleavage of a C–H bond is the crucial step of all C–H activation pathways. Supporting evidence for this concept has been provided by the results of experimental investigations and computational calculations.^[15] Generally, transition metal-catalyzed C–H activation proceeds *via* five alternative pathways: oxidative addition, σ -bond metathesis, electrophilic substitution, 1,2 addition, and base-assisted metalation. The electronic properties and nature of the metal are the major factors dictating the exact mode of the C–H cleavage. While oxidative addition is the most favorable pathway for late transition metal complexes due to their electron-rich nature (Scheme 3a),^[16] σ -bond metathesis is the most probable for early transition metal complexes (Scheme 3c).^[17] Additionally, the electrophilic substitution pathway is mainly adopted by late transition metal complexes in their higher oxidation states as they exhibit high Lewis acidity (Scheme 3b).^[18] The 1,2 addition mode is often employed by metal complexes with M=X bonds (Scheme 3d).^[19] The base assisted metalation pathway can be linked to electrophilic substitution though it proceeds with assistance from the coordinated base (Scheme 3e).^[15b, 20] After detailed investigations, the base-assisted metalation pathway was further understood in terms of concerted metalation-deprotonation (CMD),^[21] or amphiphilic metal-ligand activation

(AMLA),^[22] and base-assisted internal electrophilic substitution (BIES).^[23] While the BIES mechanism is favorable for electron-rich arenes, CMD/AMLA are more favorable for electron-deficient substrates. Radical C–H functionalization *via* hydrogen atom transfer (HAT) constitutes a pathway that proceeds *via* the generation of carbon centered radicals and subsequent downstream manifolds.^[24]

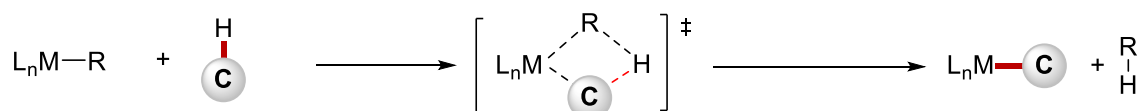
a) Oxidative addition



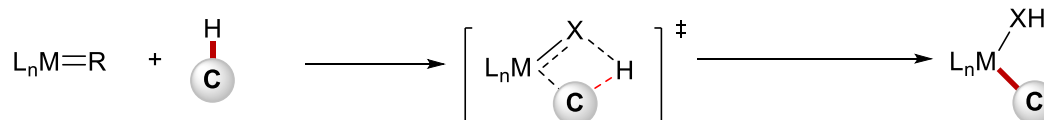
b) Electrophilic substitution



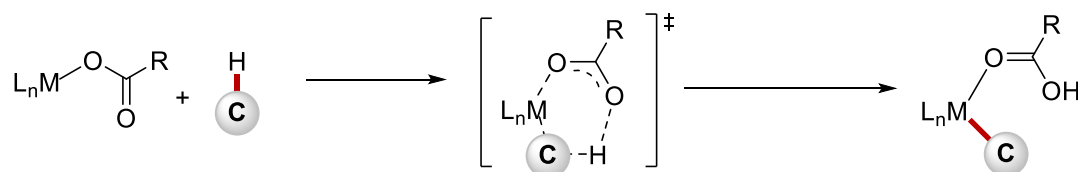
c) σ -Bond metathesis



d) 1,2-Addition



e) Base-assisted metalation

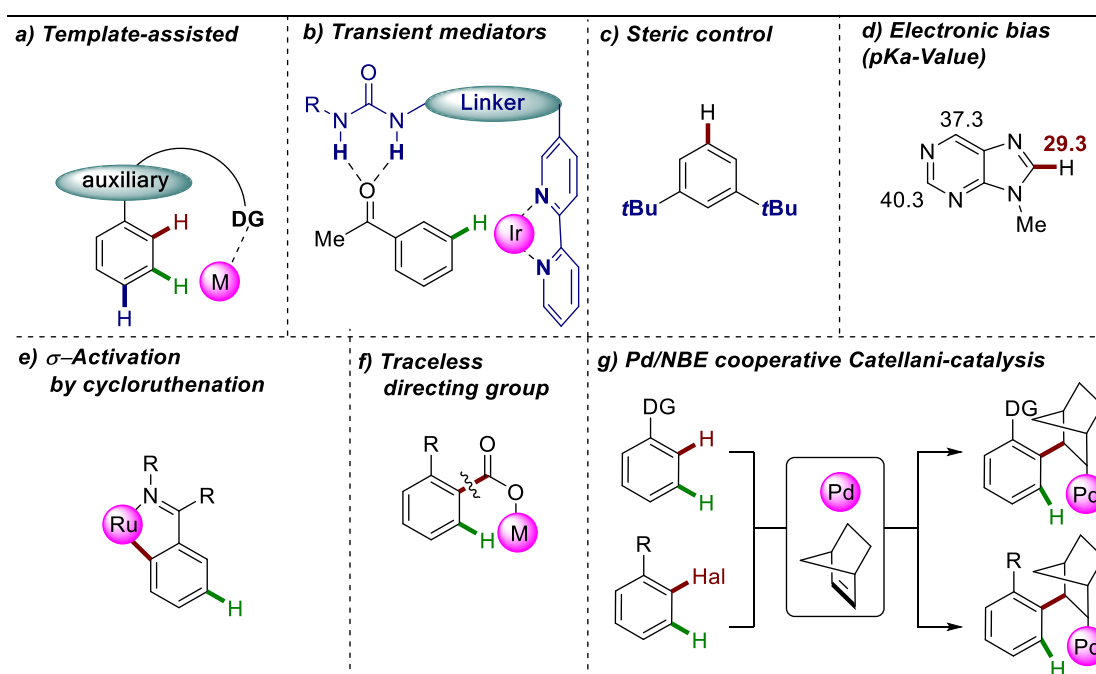


Scheme 3. Generalized mechanisms for transition metal-catalyzed C–H activation

1.3 General Approaches to Transition Metal-Catalyzed C–H Activation

The selective activation of C(sp²)–H bonds is challenging due to the similarity in the bond dissociation energy of the aromatic C–H bonds.^[25] In the past decade, diverse strategies have been developed to achieve the site-selective functionalization of organic molecules (Scheme 4). The introduction of a Lewis-basic directing group to assist the pre-coordination of the metal, thereby

activating the proximal C–H bond to facilitate the C–H activation step, has successfully been achieved (Scheme 4a).^[26] These directing groups could be transient directing groups generated during the reaction or a traceless removable directing group. Due to the *in-situ* installation and deconstruction/removal, transient directing groups are envisaged as more promising owing its step economical features (Scheme 4b).^[27] An alternative strategy is the introduction of bulky substituents on the substrates, which due to the steric hinderance prevents access to adjacent C–H bonds (Scheme 4c). In the case of heterocycles, the inherent reactivity in the kinetic acidities and bond dissociation energies of the constituent C–H bonds maps out their differences (Scheme 4d).^[28]



Scheme 4. Strategies for selective C–H functionalization

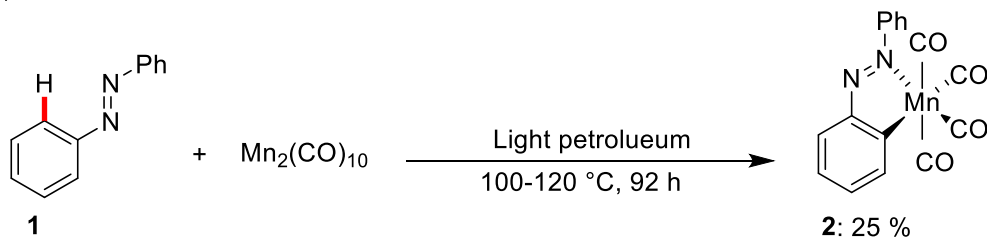
In addition, sigma-activation strongly influences the electronic properties of the arene leading to *meta*-functionalization (Scheme 4e).^[29] Also, exploiting carboxylic acids as traceless directing groups (Scheme 4f) *via* ruthenium catalysis has been established as an ideal strategy for remote *meta*-selective C–H activation.^[30] In addition, the palladium/norbornene(NBE) cooperative Catellani-type reaction has also emerged as a promising route for *meta*-selective C–H activation (Scheme 4g).^[31] The Pd/NBE facilitates *ortho*-C–H

activation to generate a palladium-norbornene species, which subsequently activates an adjacent C–H bond to achieve the remote functionalization of the *meta*-C–H bond.

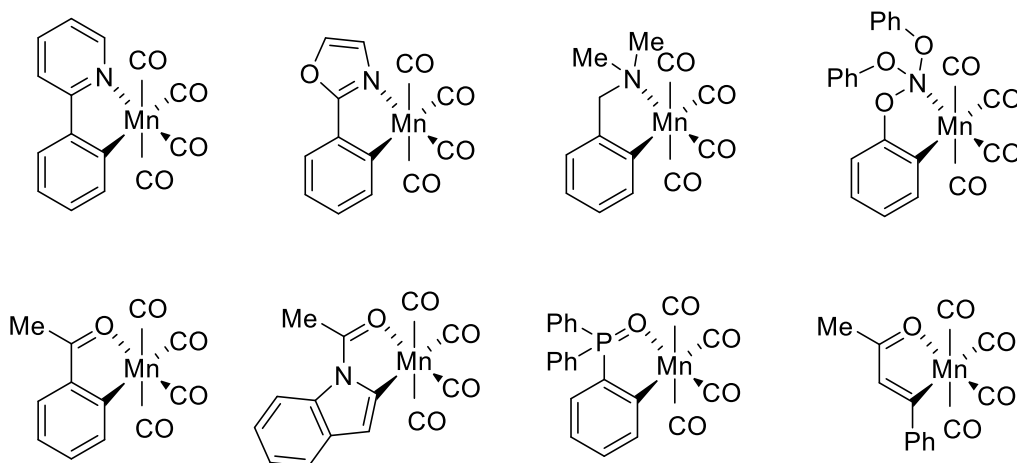
1.4 Manganese-Catalyzed C–H Activation

Manganese is the 12th most abundant element on the earth's crust and the third most abundant transition metal. Opposed to the traditionally used precious 4d transition metals, manganese catalysis has unveiled environmentally benign protocols with unique applications over the years.^[32] Over the years, this has also been established as robust technique for efficiently synthesizing diverse molecular entities *via* C–H activation as the main pathway.^[33] The early report of Stone and Bruce in 1970 was arguably the first example of manganese-assisted C–H activation. In this report, they achieved the activation of azobenzene **1** *via* the formation of a five-membered manganacycle **2**.^[34] Subsequent reports by the Nicholson/Main,^[35] Woodgate,^[36] and Liebeskind^[37] groups, among others, constituted the foundational evidence for the potency of manganese intermediates in stoichiometric synthetic chemistry (Scheme 5).

a) Bruce & Stone

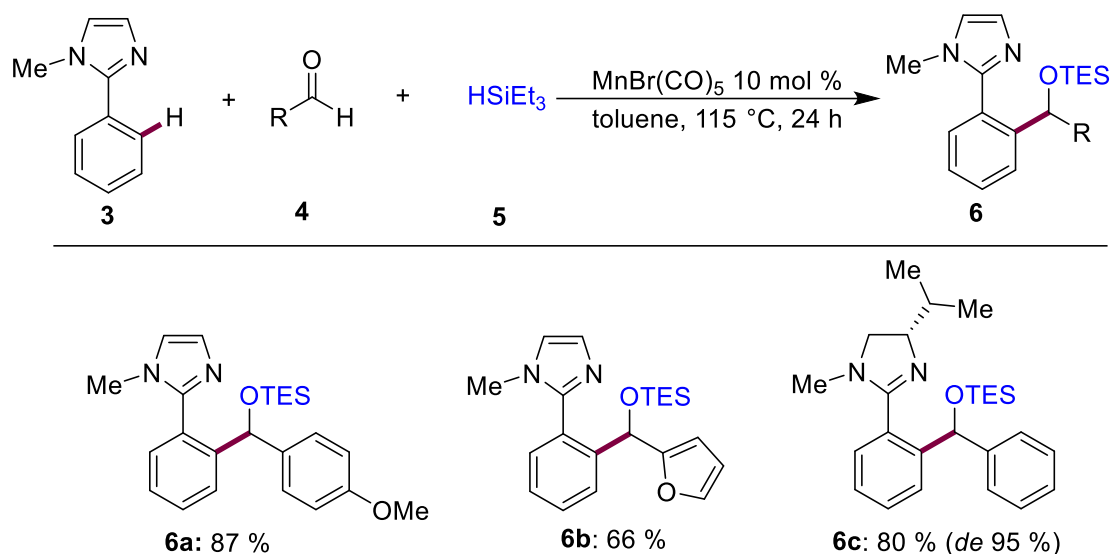


b) Nicholson/Main, Woodgate, Liebeskind

**Scheme 5:** Selected isolated manganacycles

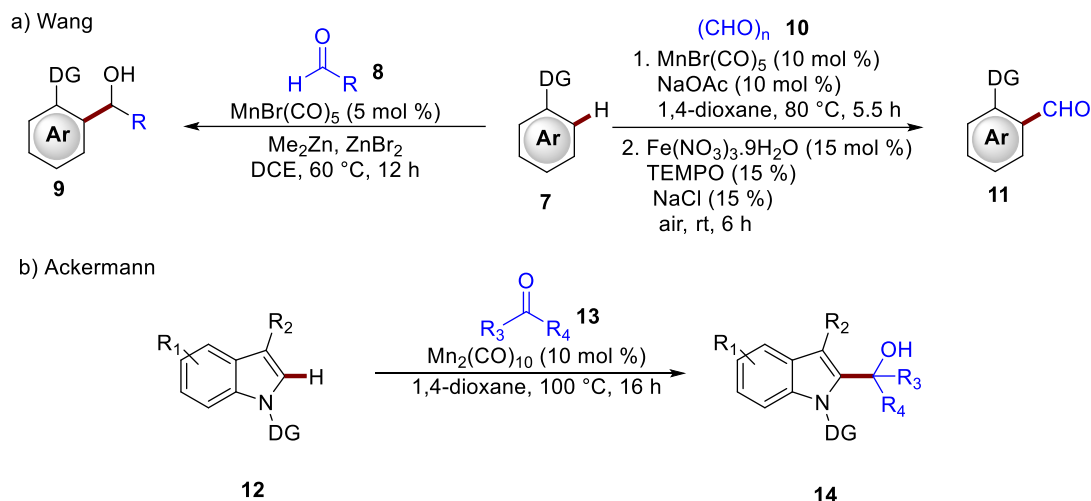
In an early report by Kuninobu and Takai, a versatile protocol to access silylated arylimidazoles and aryloxazolines *via* manganese(I) catalysis was established.^[38] The protocol featured a three-component system consisting of silanes and electrophilic aldehydes in the presence of catalytic amounts of $\text{MnBr}(\text{CO})_5$. Notably, the regime was tolerant to oxazolines bearing chiral substituents **3c** without altering the stereochemistry of the substrate. In addition, the manganese(I) regime tolerated electron-poor and rich aldehydes. Mechanistic studies led to the proposal that the reaction proceeded *via* cleavage of the C–H bond by oxidative addition followed by selective insertion of the C–Mn bond into the aldehyde and then silyl protection with the evolution of H_2 (Scheme 6).

Kuninobu & Takai, 2007

**Scheme 6:** Manganese-catalyzed access to silylated imidazoles.

1.4.1 Manganese-Catalyzed C–H Hydroarylation

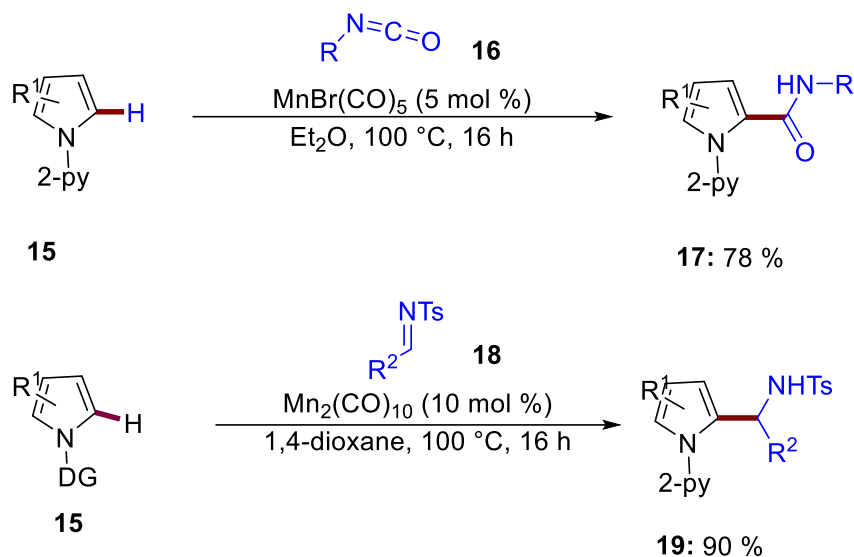
Manganese catalysis has gained ground in selective hydroarylation of alkenes with heterocyclic compounds. The report of Wang and co-workers unveiled a straightforward method for synthesizing aromatic alcohols and ketones *via* manganese catalysis (Scheme 7a).^[39] This report revealed that optimum transformations were achieved in the presence of Me_2Zn and ZnBr_2 which were responsible for activating the manganese pre-catalyst, thereby forming the more active $\text{MnMe}(\text{CO})_5$ complex. In contrast, Ackermann and co-workers reported the manganese catalyzed hydroarylation of ketones with nitrogen-containing heterocycles (Scheme 7b).^[40] Furthermore, Glorius recently achieved the formylation of arenes *via* a manganese(I)/iron(III) sequential catalysis broad substrate scope (Scheme 7a).^[41]



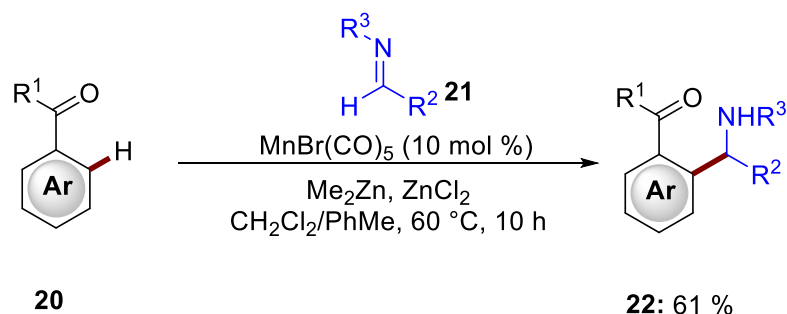
Scheme 7. Manganese-catalyzed addition of carbonyls to arenes and heterocycles

Manganese catalysis has proven resourceful for functionalizing nitrogen-containing heterocycles. The groups of Ackermann and Wang made enormous contributions to this achievement. Ackermann reported the efficient C-2 selective aminocarbonylation of indoles and pyrroles *via* manganese catalysis. The reaction proceeded successfully without an additive with industrially relevant imines and isocyanates as reaction partners. The same group also realized the C-2 selective C–H activation of indoles with imines *via* a manganese(I) regime (Scheme 8a).^[42] Wang, in an extension unraveled a chemo-selective coupling of ketones with imines to furnish benzylic amines (Scheme 8b).^[43]

a) Ackermann



b) Wang

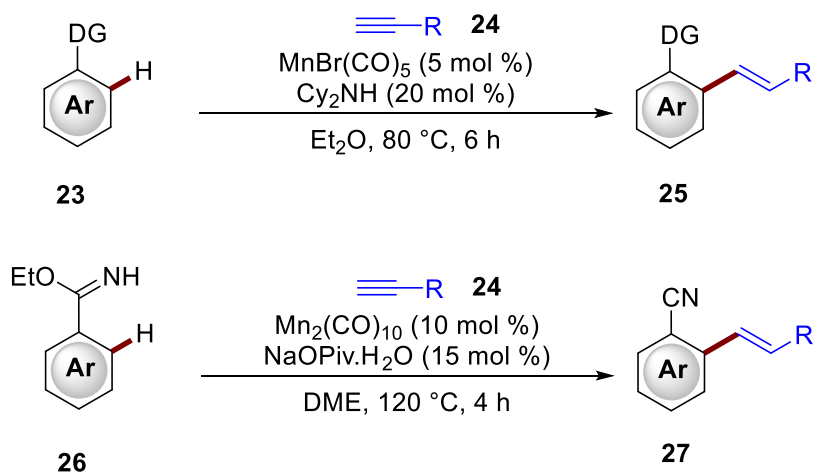


Scheme 8. Manganese-catalyzed addition of imines and isocyanates to arenes and heterocycles

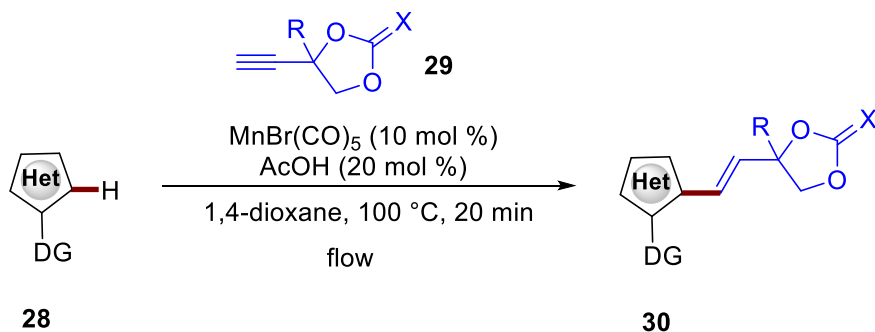
The manganese(I)-catalyzed C–H hydroarylation was not limited to carbonyl compounds but was expanded to include alkenes and alkynes. Wang and co-workers demonstrated this concept in two reports, with the manganese-catalyzed selective alkenylation of arenes with terminal alkynes.^[44] In one account, they established an environmentally-benign protocol to access highly functionalized molecules *via* a base-promoted mechanism. Further, they developed a reliable regime to construct synthetically relevant nitriles from imidates and terminal alkynes. Interestingly, high regio-selectivity was achieved in both cases (Scheme 9a). Also, Ackermann reported Brønsted acid-assisted C-2 selective alkenylation of indole derivatives with propargylic carbonates under manganese(I) catalysis. This regime enabled the successful synthesis of target molecules within a short reaction time facilitated by a flow

setup (Scheme 9b).^[45] In addition, Lei and Li extended the scope of manganese(I) catalyzed hydroarylation of indole derivatives to internal alkynes with high regioselectivity (Scheme 9c).^[46]

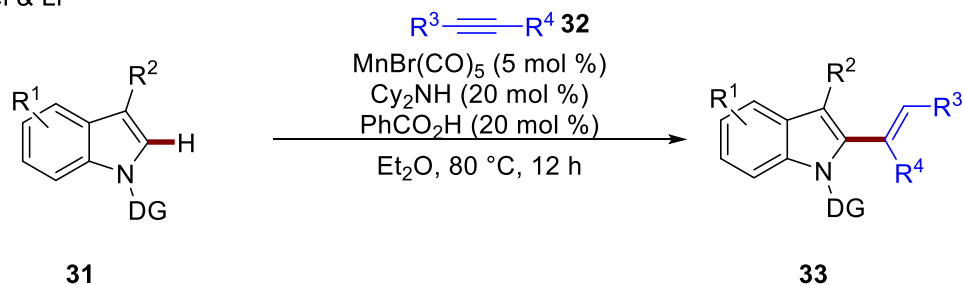
a) Wang



b) Ackermann



c) Lei & Li

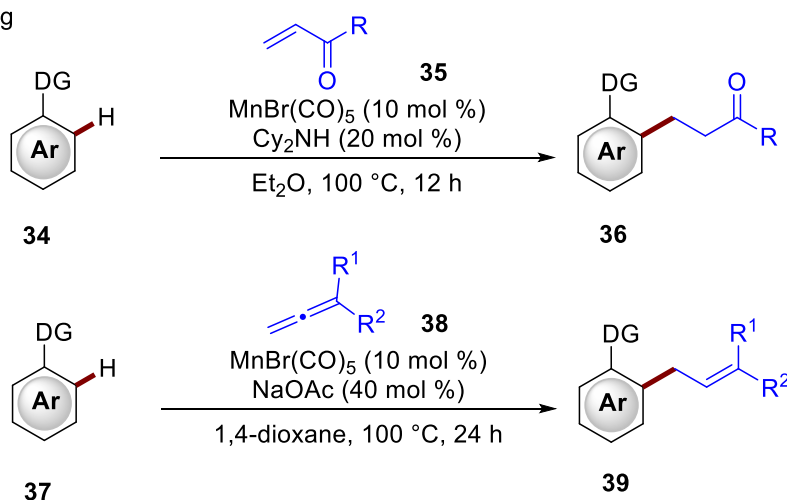


Scheme 9. Manganese-catalyzed C–H activation for hydroarylations.

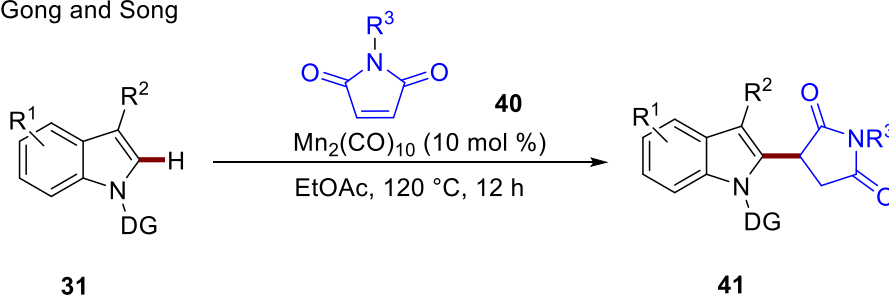
In addition to terminal alkynes, manganese(I) catalysis has proven beneficial for the selective alkylation of electron-deficient arenes. In this regard, the Wang group reported manganese(I)-catalyzed alkylation of arenes with α,β -unsaturated carbonyls.^[47] This approach was highly favorable to mono-

alkylation (Scheme 10a). Likewise, the same group efficiently achieved the alkylation of arenes, with allenes as coupling partners.^[48] Notably, fused five-membered heterocycles were well tolerated in the manganese catalysis (Scheme 10a). The subsequent report from Gong and Song extended the protocol to maleimides **40** for the selective alkylation of five-membered heterocycles (Scheme 10b).^[49] Furthermore, Glorius reported a robust protocol for the manganese(I)-catalyzed alkylation of arenes using α,β -diazo ketones **43**. This protocol proceeded *via* the *in situ* generation of α,β -unsaturated ketones assisted by a silver(I) salt (Scheme 10c).^[50]

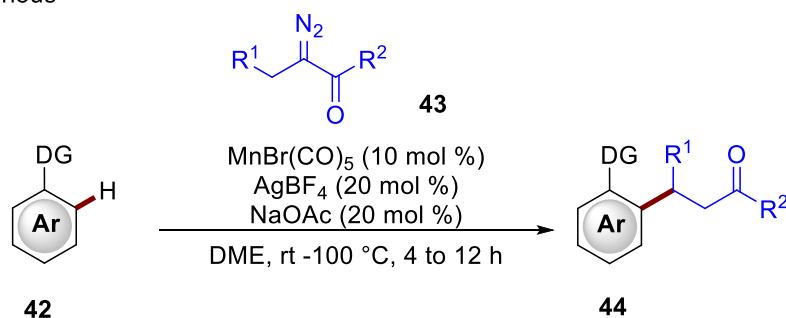
a) Wang



b) Gong and Song



c) Glorius

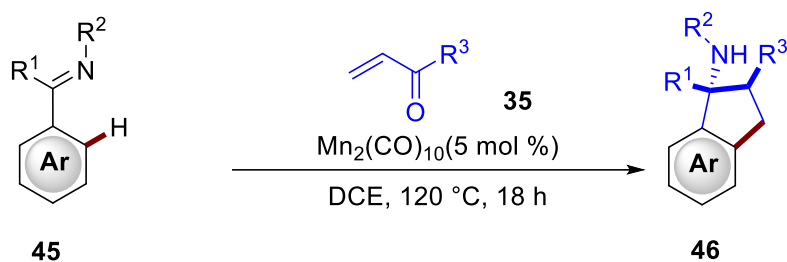


Scheme 10. Manganese(I)-catalyzed C–H hydroarylation

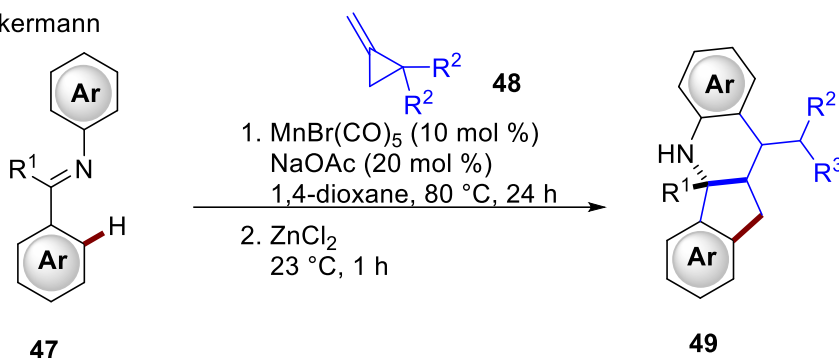
1.4.2 Manganese-Catalyzed Domino C–H Activation

Over the years, Domino-reactions have emerged as a promising strategy for the construction of structurally complex molecules.^[51] Irrespective of the advancements of these protocols, Domino reactions face challenges, such as the probable generation of side products that jeopardize their synthetic efficiency.^[51a, 52] The efficiency of manganese catalysis has also been fruitful for the simultaneous construction of multiple bonds in a single step. The Ackermann group reported the practical synthesis of cis- β -amino acid esters^[42] and tetrahydroquinolines^[53] *via* domino-manganese(I) catalysis. In the former, they reported an imine-directed manganese(I)-catalyzed domino C–H activation, which proceeded by the interception of the intermediate, which follows the insertion of the manganacycle to the acrylate. The latter proceeded *via* a zinc-mediated Michael addition of the electron-rich aniline to the newly formed α,β -unsaturated ester to form a fused tetrahydroquinoline **46** as the product (Scheme 11a). Later, Wang and co-workers devised another method to access tetrahydroquinolines **49** with aromatic ketimines **47** and 1,1-disubstituted allenes in a AgOTf catalyzed Povarov protocol (Scheme 11b).^[54] Recently, Chang, and Li developed the cascade regime for the hydroarylation of indoles to deliver seven-membered cyclic alkane side chains **51** (Scheme 11c).^[55] This reaction featured the alkyne insertion into the manganacycle followed by a retro-aldol reaction of the bicyclo[3.2.0]heptane system resulting from the addition of the Mn–C bond to the tethered ketone.

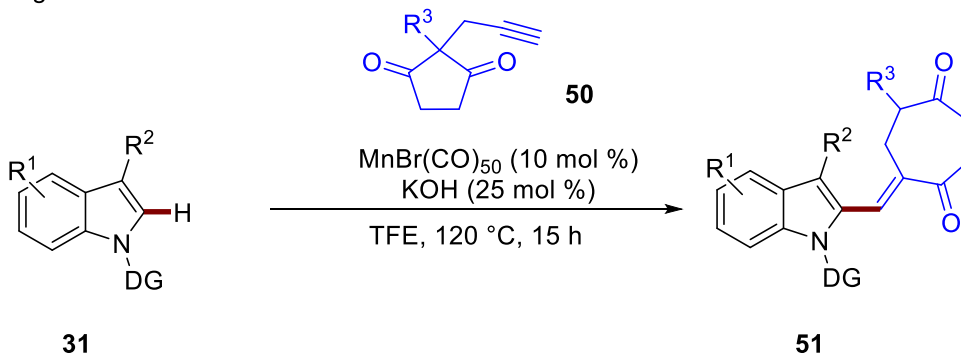
a) Ackermann



b) Ackermann



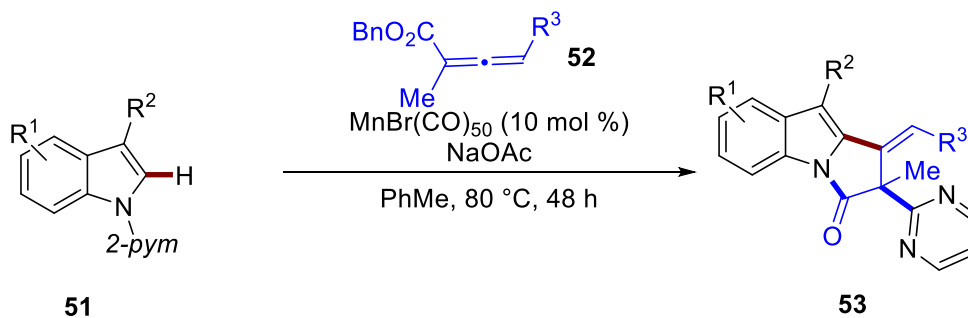
c) Chang & Li

**Scheme 11.** Manganese(I)-catalyzed domino C–H hydroarylation

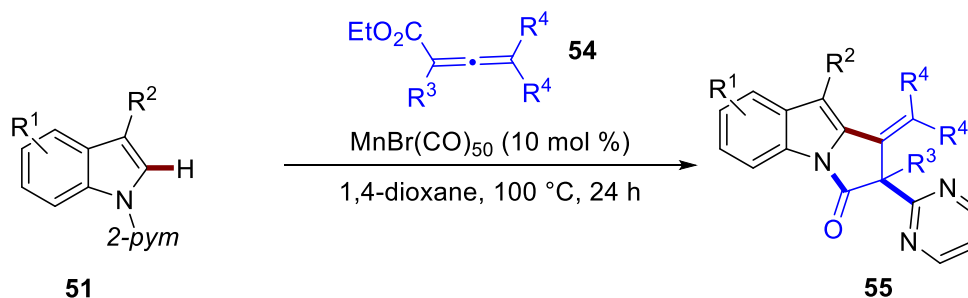
Manganese-catalyzed domino protocols have also been applied to hydroarylation of allenes (Scheme 12). The reports of the Rueping^[56] and Wang/Li^[57] groups in 2017 highlighted the hydroarylation of indoles with electron-deficient allenes (Scheme 12a/b). This reaction proceeded *via* migration of the directing group resulting from Smiles rearrangement of the hydroarylated intermediate. In the case of Rueping, temperatures played a crucial role in selectively furnishing the desired products (Scheme 12a). While lower temperatures favored the protodemetalation pathway for the formation of the desired product, the Smiles rearrangement of the intermediate resulting from the allene insertion was favored at higher temperatures. Next, Wang and Lu carried out a similar transformation with ketenimines featuring directing group migration, as was the case with the Rueping&Wang/Li report (Scheme

12c).^[58] Recently, Ruan, Ackermann, and co-workers have extended this concept to rhenium and manganese(I) catalysis for the hydroarylation of 6-indole-purines with ketenimines without migration of the directing group (Scheme 12d).^[59]

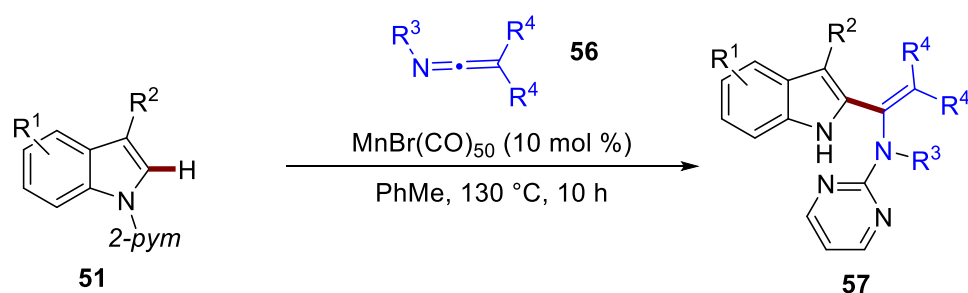
a) Rueping



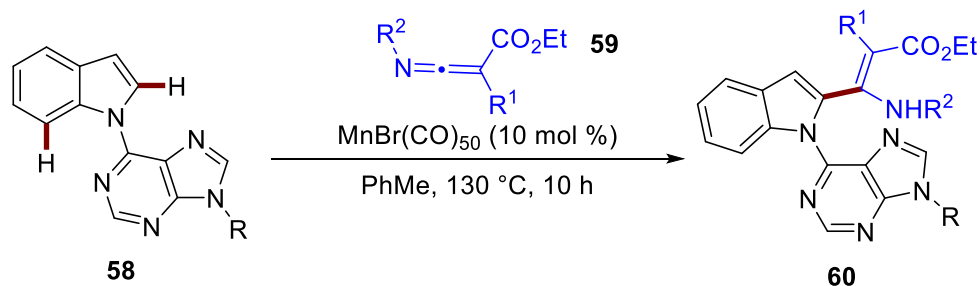
b) Wang & Li



c) Wang & Lu



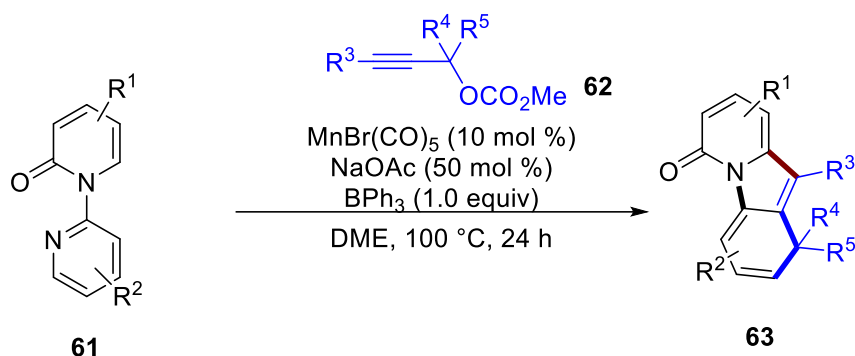
d) Ruan, Ackermann



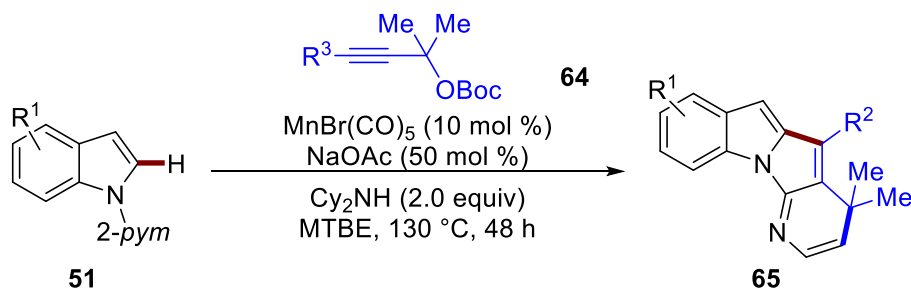
Scheme 12. Manganese(I)-catalyzed domino C–H hydroarylation with allenes

On a different note, Ackermann reported a manganese(I)-catalyzed sequential C–H allenylation/Diels-Alder reaction with directing group migration to furnish a highly polycyclic system **63**. In their findings, the Lewis acid (BPh_3) was crucial for the domino sequence, as revealed by computational calculations (Scheme 13a).^[60] In addition, Li and co-workers developed a similar transformation in the presence of Cy_2NH to access fused indoles **65** (Scheme 13b).^[61]

a) Ackermann



b) Li



Scheme 13. Manganese(I)-catalyzed domino C–H hydroarylation with propargylic esters/ethers

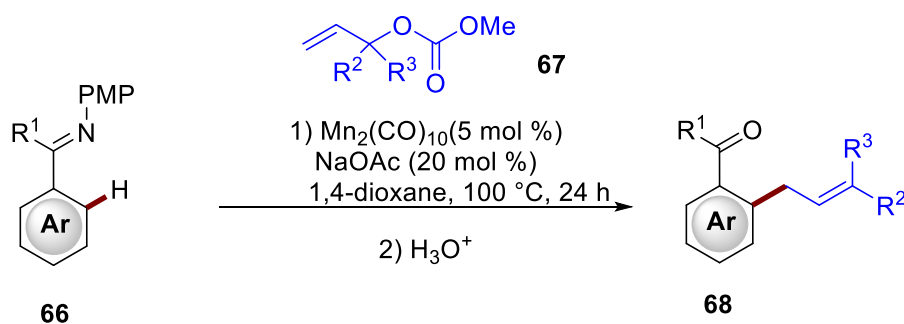
1.4.3 Manganese-Catalyzed Substitutive C–H Activation

1.4.3.1 Manganese-Catalyzed C–H Allylation

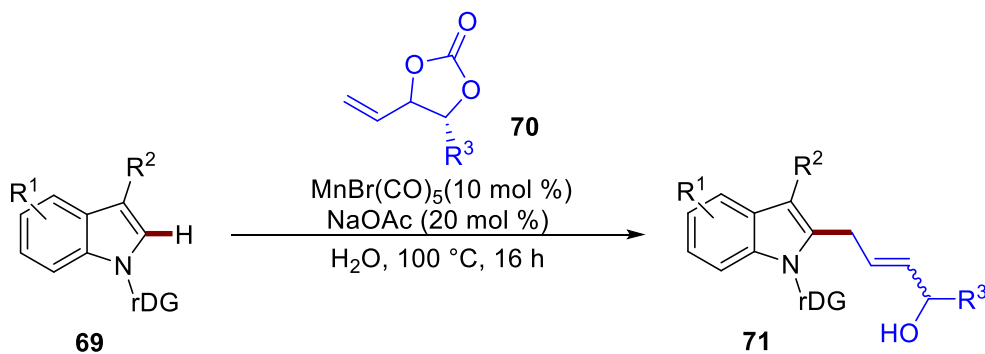
Allyl groups are of significant interest to organic chemists as reactive intermediate to access a variety of functional groups.^[62] C–H activation-enabled protocols have been established as an ideal tool to synthetically access allylic compounds. Ackermann was first to demonstrate this concept in their manganese(I)-catalyzed C–H allylation of ketimines with allyl methyl-carbonates **67** (Scheme 14a).^[63] Notably, electrophilic and nucleophilic groups

were excellently tolerated in the catalysis. In the continuous quest for eco-friendly protocols, the same group effectively achieved the manganese(I)-catalyzed allylation in water as green reaction media to access allylic alcohol-containing indoles **71** (Scheme 14b).^[64] Later, Zhang showed the selective 3,3-difluoroallylation of arenes with 3-bromo-3,3-difluoropropene by manganese(I) catalysis. Synthetically relevant heterocycles, like pyridine derivatives **73**, were well tolerated (Scheme 14c).^[65] In addition, Wang reported manganese(I)-catalyzed *ortho*-allylation of ketones assisted by Me_3Zn and $\text{Cu}(\text{OTf})_2$.^[66] Furthermore, Glorius disclosed the robustness of manganese(I)-catalyzed propargylation of arenes with good regioselectivity.^[67]

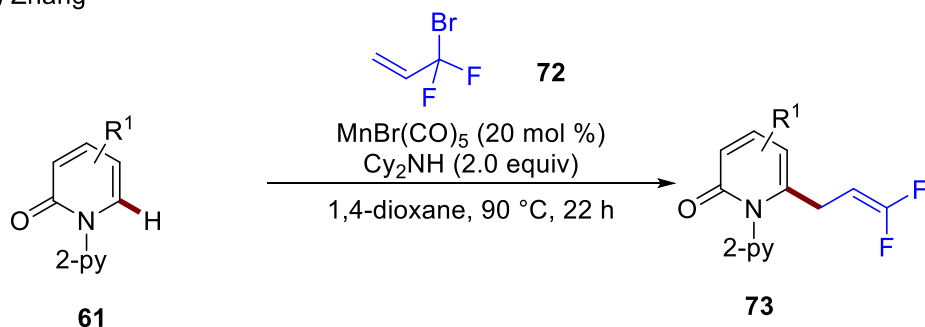
a) Ackermann



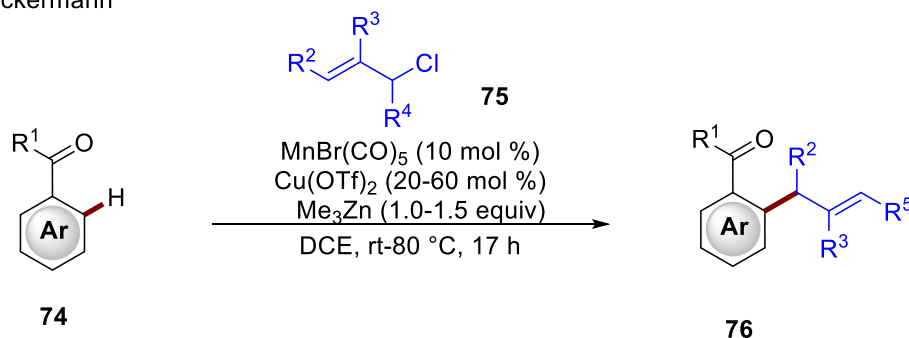
b) Ackermann



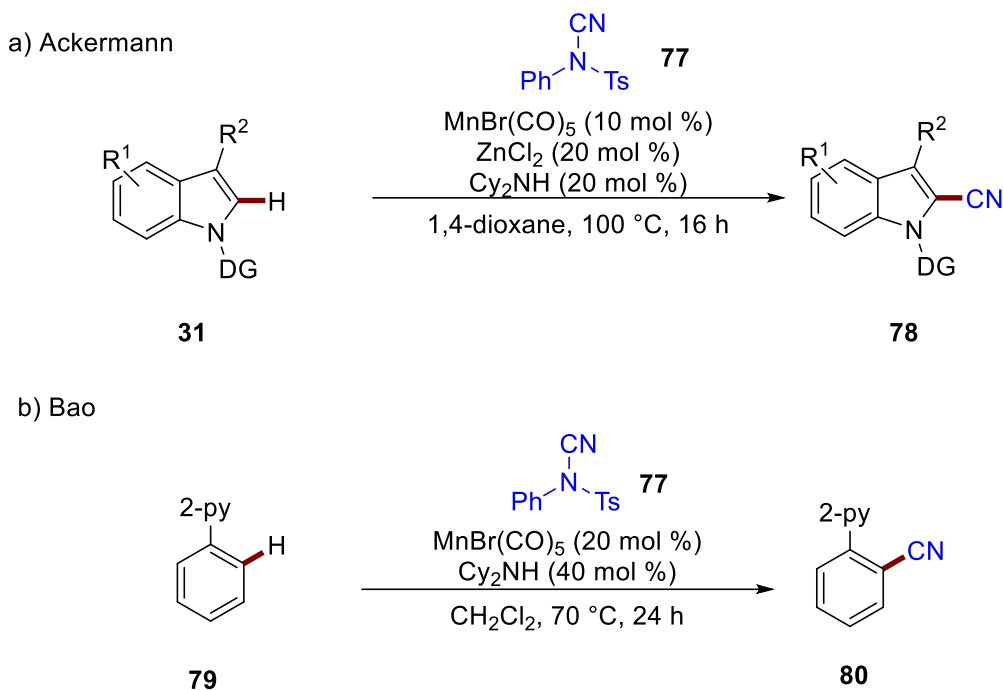
c) Zhang



d) Ackermann

**Scheme 14.** Manganese(I)-catalyzed C-H allylation**1.4.3.2 Manganese-Catalyzed C-H Cyanation.**

The transition metal-catalyzed cyanation of arenes and heterocycles has been extensively achieved with NCTS as the cyanation agent. In 2016, Ackermann demonstrated the robustness of manganese(I) catalysis in the synthesis of nitriles.^[68] In this regime, NCTS was used as cyanation agent for the user-friendly cyanation of indole scaffolds enabled by a $\text{MnBr}(\text{CO})_5$ and $\text{Cy}_2\text{NH}/\text{ZnCl}_2$ co-catalysis. Computational and mechanistic insights revealed that the reaction proceeds *via* coordination of ZnCl_2 to the cyano-toluenesulfonamide, thereby facilitating the transfer of the cyano group *via* an addition/elimination reaction (Scheme 15a). Subsequently, Bao and co-workers extended the scope of this reaction to the cyanation of pyridyl arenes. Then, cyanation was successful with a double loading of the catalyst and Cy_2NH , as reported by Ackermann.^[69] It was highlighted that ZnCl_2 then played no unique role in this reaction (Scheme 15b).



Scheme 15. Manganese(I)-catalyzed C–H cyanation

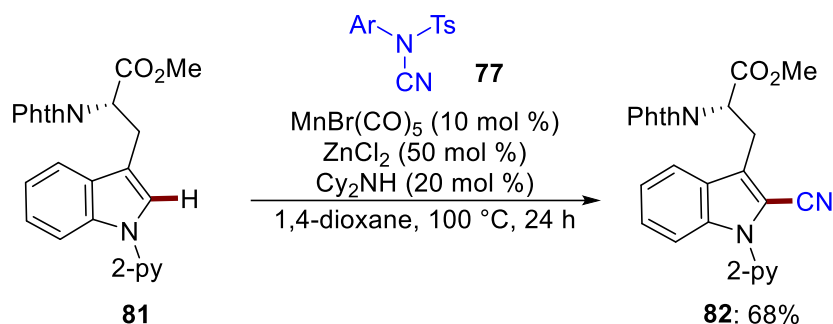
1.5 Manganese-Catalyzed Late-Stage Diversification of Peptides

Amino acids are the building blocks of proteins and peptides which are important for cell metabolism.^[70] Their increasing application in medicine has made their functionalization of great interest to organic chemists. Recently, transition metal catalysis has found applications in the late-stage modification of peptides using C–H activation.^[71] This method has evolved as an atom economical strategy for the late-stage modification of peptides and preserves the stereochemistry of the amino acid residues. Transition metal complexes of palladium,^[72] ruthenium,^[73] rhodium,^[74] and gold^[75] have fuelled significant progress in the selective functionalization of peptides.^[76] Most interestingly, earth-abundant 3d manganese has proven to be promising for the functionalization of peptides. It has notably been proven resourceful in the C-2 selective functionalization of tryptophan-containing peptides in a sustainable, atom/step economical, and cost-efficient fashion. The introduction of a coordinating nitrogen-containing directing group on the indole substituent of tryptophan enabled the site- and regio-selective functionalization of tryptophan.

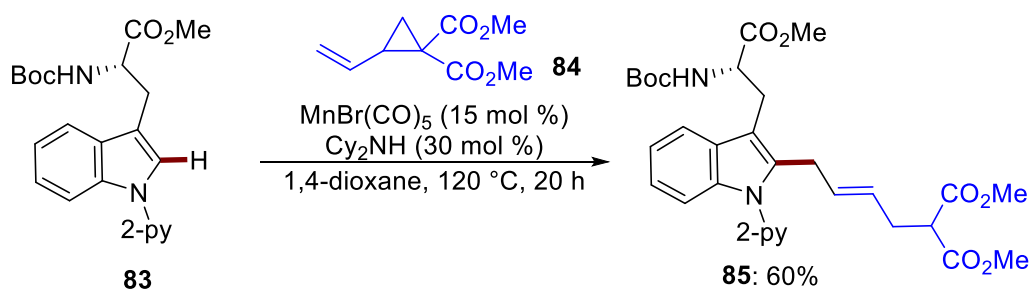
Ackermann achieved the C-2 selective cyanation and allylation of tryptophan-derivatives using manganese(I) catalysis. While cyanation was achieved *via*

substitutive C–H activation (Scheme 16a),^[68] allylation was achieved through C–H/C–C bond activation (Scheme 16b/16c),^[77] and C–H/C–O bond activation.^[64] Irrespective of the successes of these protocols, the applicability of these protocols were only reported with amino acid derivatives without any extension to peptides (Scheme 16).

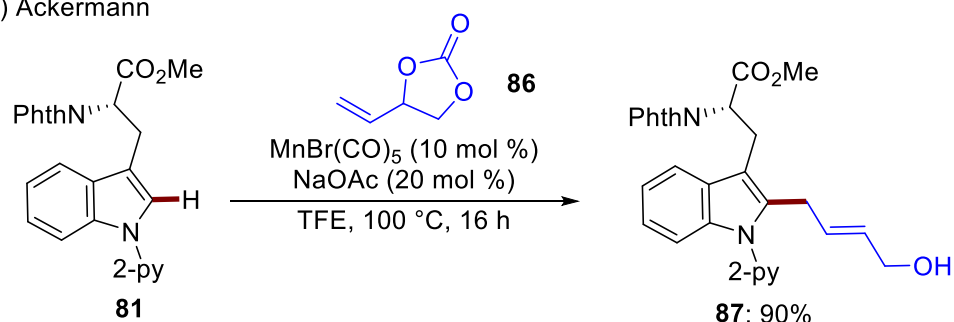
(a) Ackermann



(b) Ackermann



(c) Ackermann

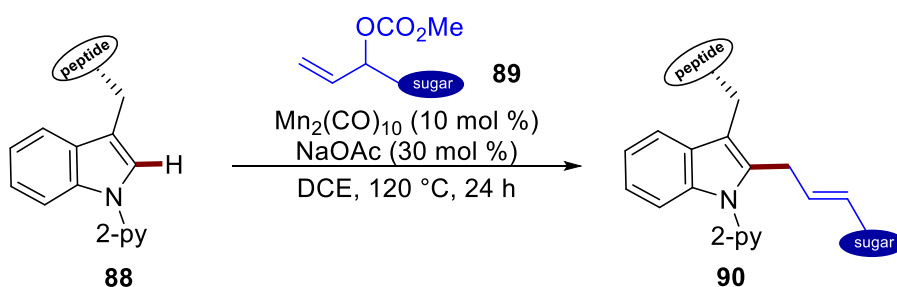


Scheme 16. Manganese(I)-catalyzed C-2 selective functionalization of tryptophan.

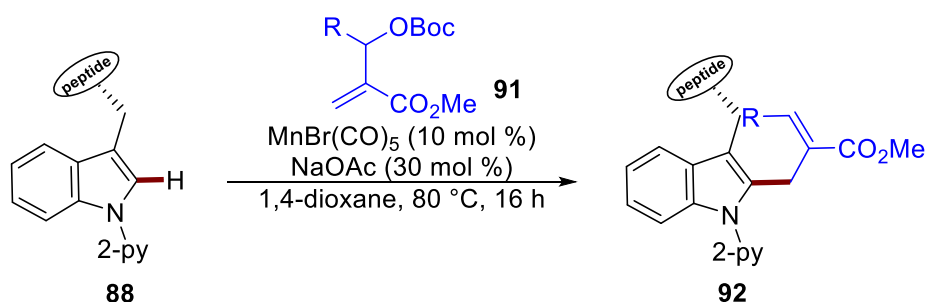
Glycopeptides are known to participate in important cell activities, thereby accounting for their use as therapeutic agents. The utility of manganese(I) complexes for constructing structurally complex peptides was extended to the selective allylation of tryptophan-containing peptides by Ackermann in 2018. This report employed Morita-Baylis–Hillman adducts as the allylating agents to successfully functionalize peptides, while tolerating complex structures and oxidation-sensitive alkyl side chains (Scheme 17b).^[78] Subsequently,

Ackermann achieved the efficient synthesis of glycopeptides *via* manganese(I) catalysis.^[79] This regime unraveled a C-2 selective allylation of tryptophan-containing peptides by a Linch-pin approach. It is worth noting that the strategy was racemization free and provided a step-economical access to glycopeptides (Scheme 17a).

a) Ackermann



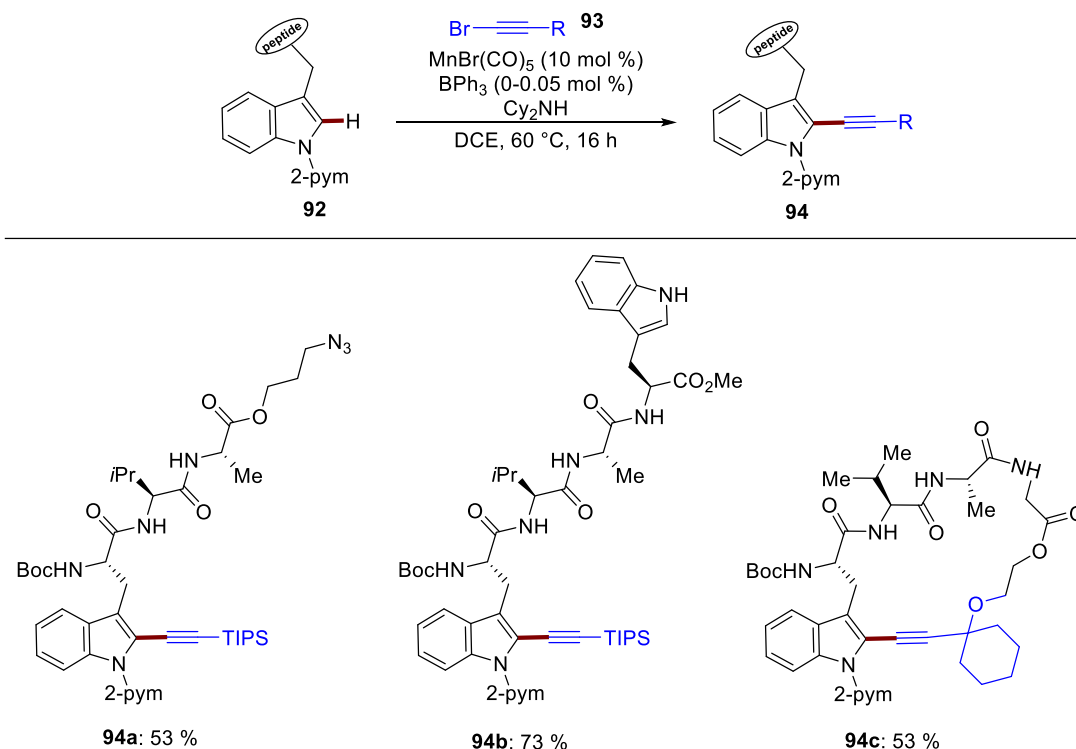
b) Ackermann



Scheme 17. Manganese(I)-catalyzed C-2 selective allylation of tryptophan-containing peptides.

Based on previous reports on manganese(I) catalysis in the selective C-sp² functionalization of indoles, Ackermann developed a manganese(I) catalysis enabling peptide modification. Ackermann reported the first C-2 selective alkynylation of tryptophan-containing peptides with 1-bromo-alkynes.^[80] This reaction proceeded successfully in the presence of catalytic amounts of BPh_3 , which was employed to facilitate the β -Br elimination step. This regime was functional group friendly to the free amine terminal of the amino acid residue **94b** and the azide functional group **94a**. In addition, this manganese catalysis system permitted the construction of structurally complex peptides with alkyl and arylbromoalkynes. Notably, the intramolecular alkynylation was achieved to furnish cyclic peptides **94c** (Scheme 18).

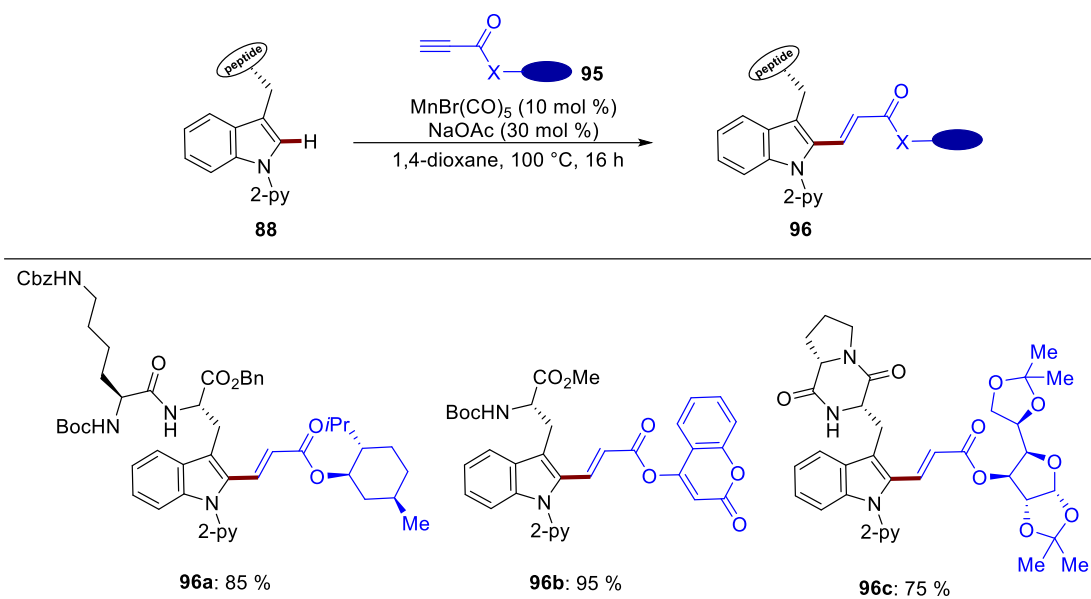
Ackermann



Scheme 18. Manganese(I)-catalyzed C-2 selective alkynylation of tryptophan-containing peptides.

Encouraged by the previous findings, Ackermann and co-workers recently reported the manganese(I)-catalyzed hydroarylation of tryptophan with acrylates **95**. The notable feature of this report included excellent E/Z ratios, high functional group tolerance, and broad substrate scope. Moreover, this manifold was applicable to acrylates with pharmacologically useful fragments such as menthol **96a**, coumarin **96b**, and sugar moiety **96c**. The undisputable relevance of this regime was expressed in the successful construction of cyclic polypeptides *via* intramolecular C-2 alkenylation under mild conditions (Scheme 19).^[81]

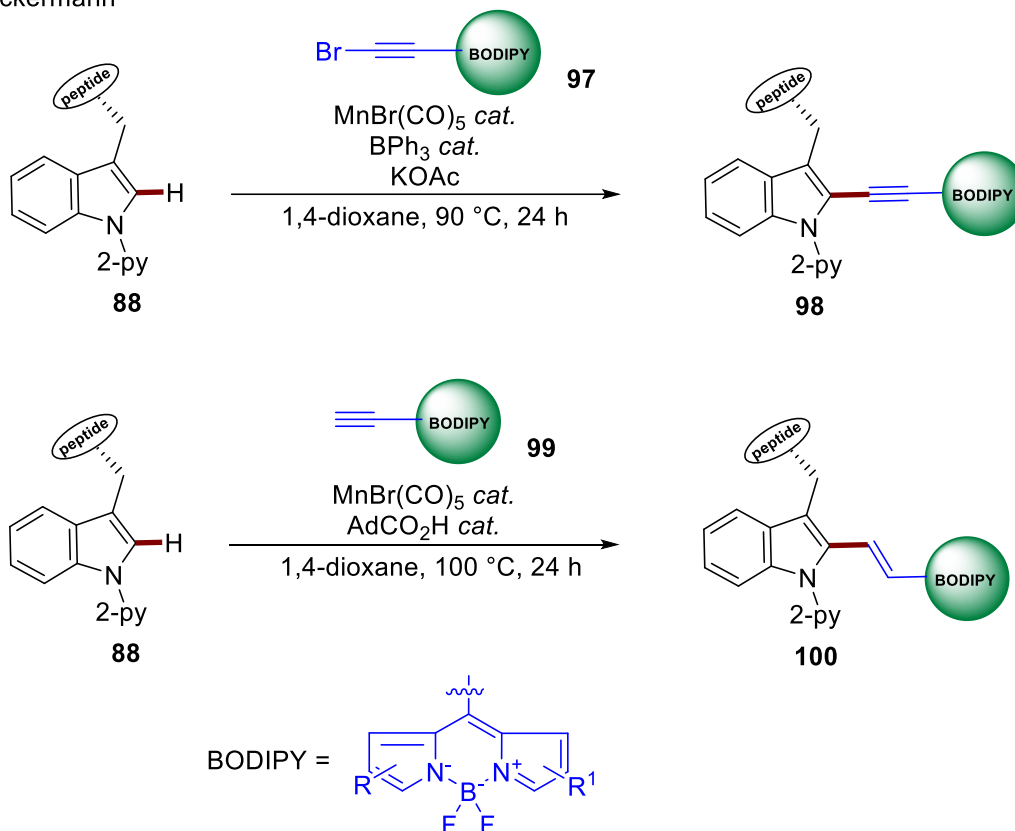
Ackermann



Scheme 19. Manganese(I)-catalyzed C-2 selective hydroarylation of tryptophan-containing peptides.

In a subsequent report, Ackermann and co-workers reported manganese(I) catalyzed C–H activation for the assembly of BODIPY labeled peptides.^[82] In this report, the previously established manganese(I) regime was applied to achieve alkynylation with BODIPY labeled bromoalkynes **97** (Scheme 20a). The same report also documented a Bronsted acid-assisted hydroarylation of tryptophan-containing peptides with BODIPY labeled terminal arylalkynes **99** featuring high E/Z selectivities (Scheme 20b). Furthermore, fluorescence studies illustrated the potential use of the products as fluorogenic probes (Scheme 20).

Ackermann



Scheme 20. Manganese(I)-catalyzed C-2 selective hydroarylation of tryptophan-containing peptides.

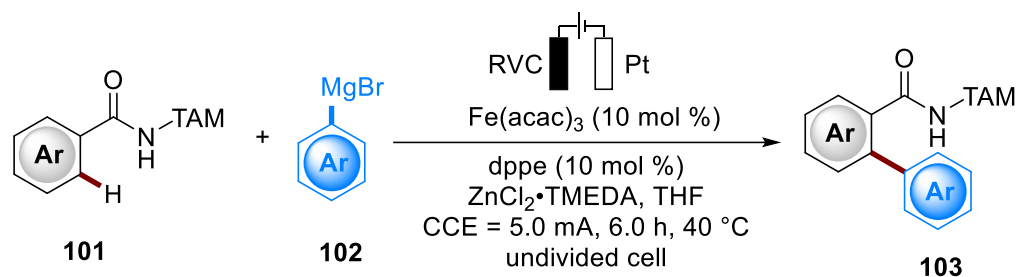
1.6 Transition Metal-Catalyzed Electrochemical C–H Activation

Electrosynthesis has evolved as a promising synthetic tool for the assembly of molecular entities, with pioneering works of Volta,^[83] Faraday,^[84] and Kolbe^[85] being the foundations of electro-mediated synthesis.^[86] In sharp contrast to chemical oxidants, electricity presents an environmentally friendly protocol with high-cost efficiency, minimum environmentally harmful waste, and a high resource economy.^[87] Over the last decade, metalla-electrocatalysis has presented a platform for C–C or C–Het bond formation *via* transition metal-catalyzed site-selective C–H activations.^[88]

1.6.1 Iron-Catalyzed Electro-Oxidative C–H Activation

The last decade has witnessed an increasing demand for more sustainable methods. In this regard, the use of iron as an earth-abundant, non-toxic, and cheap 3d transition metal is a promising tool. The merger of iron catalysis^[89] and electrosynthesis presents a much more sustainable platform for molecular

synthesis. Despite the advancements in the oxidative iron-catalyzed C–H functionalization, the unavoidable generation of unwanted waste resulting from the use of 1,2-dichloroisobutane (DCIB) as a sacrificial oxidant has been a key challenge. This restriction was overcome in the recent findings of the Ackermann group through the oxidative C–H arylation with Grignard reagents, including detailed mechanistic studies and insights (Scheme 21).^[90]

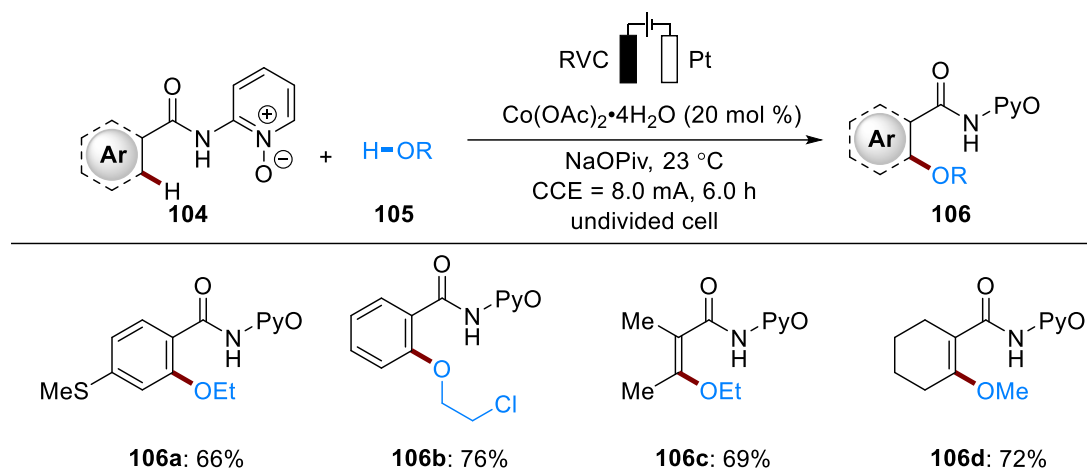


Scheme 21. Ferra-electrooxidative C–H activation.

1.6.2 Cobalta-Electrooxidative C–H Activation

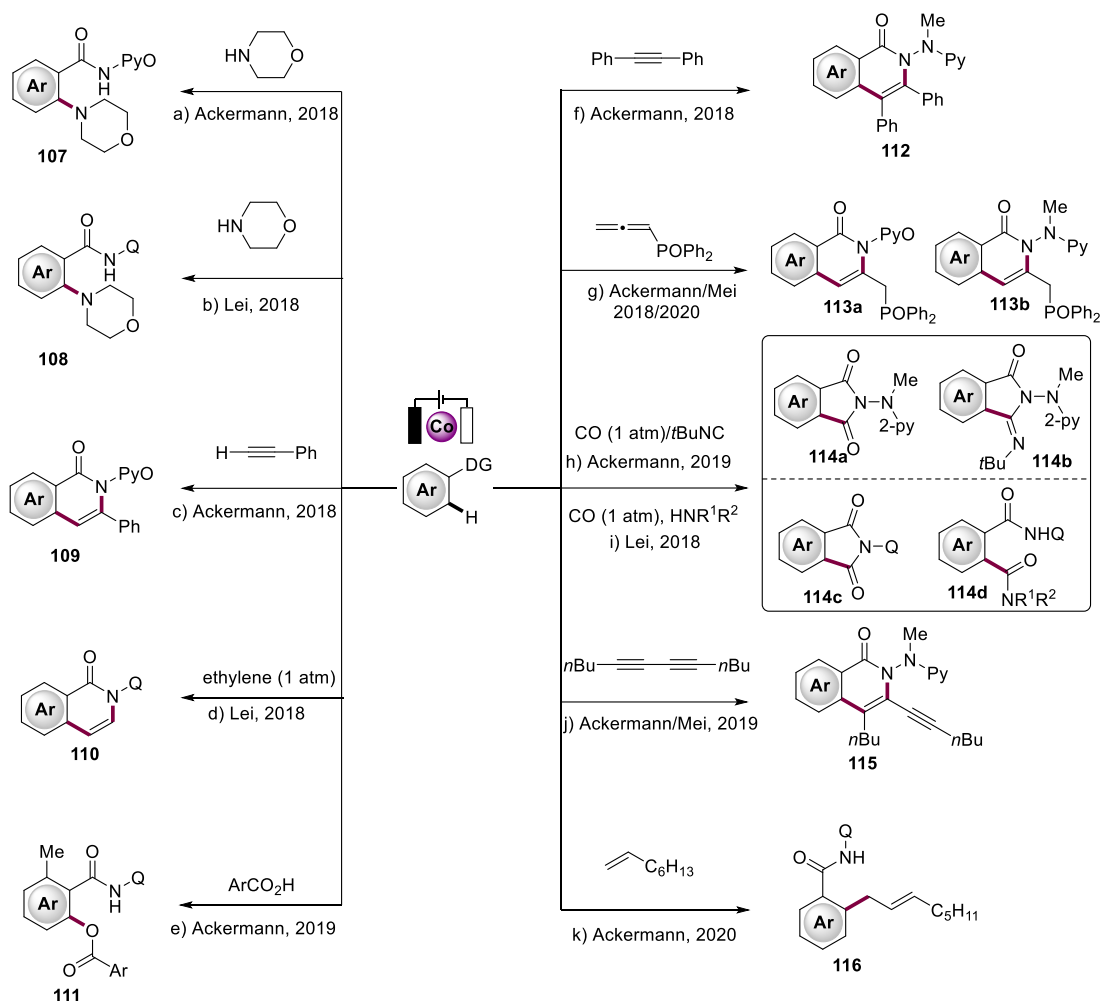
Irrespective of the achievements towards electrocatalytic C–H activation with 4d and 5d transition metals, the continuous need for the development of sustainable protocols is still in high demand. This leaves the earth-abundant, less toxic, and inexpensive 3d metals as the most promising alternatives.

The Ackermann group has made enormous contributions to 3d metallaelectro-catalyzed C–H activation with their pioneering work in 2017 unraveling a cobaltaelectro-catalyzed C–H oxygenation of aryl and alkenyl amides with earth-abundant, inexpensive cobalt(II) salt [Co(OAc)₂·4H₂O] as catalyst (Scheme 22).^[91] This reaction was proposed to proceed *via* a Co(III/IV/II) manifold based on detailed mechanistic investigations.^[92]



Scheme 22. Cobalta-electrooxidative aryl and vinylic C–H oxygenation

The Ackermann and later the Lei groups established intramolecular C–H amination under mild reaction conditions facilitated by directing groups containing N,O- and N, N-coordinating amides for the formation of C–Het bonds (Scheme 23).^[93] In addition, an electro-assisted cobalt-catalyzed C–H alkoxylation with carboxylic acids was reported by Ackermann and co-workers.^[94] Also, the robustness of cobalta-electrocatalysis for the synthesis of biologically relevant molecules has been demonstrated in the efficient C–H/N–H bond annulation of arenes with alkynes,^[94] allenes,^[95] alkenes,^[96] isocyanides, and carbon monoxide.^[95] Furthermore, cobalt catalysis has enabled the synthesis of allylated benzamides *via* electrochemical C–H activation with γ -valerolactone (GVL) as solvent.^[97]



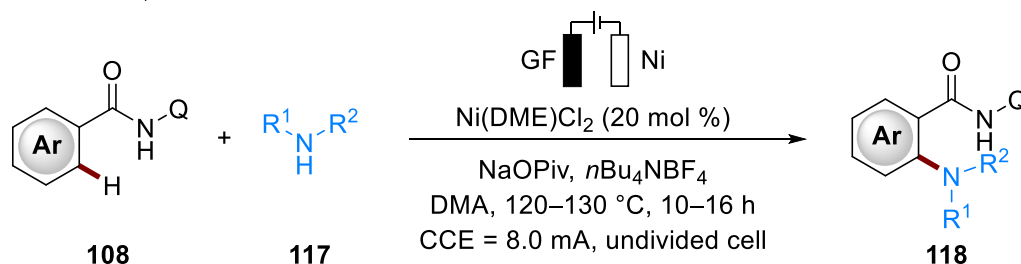
Scheme 23. Cobalta-electrooxidative C–H activation

1.6.3 Nickel-Catalyzed Electrooxidative C–H Activation

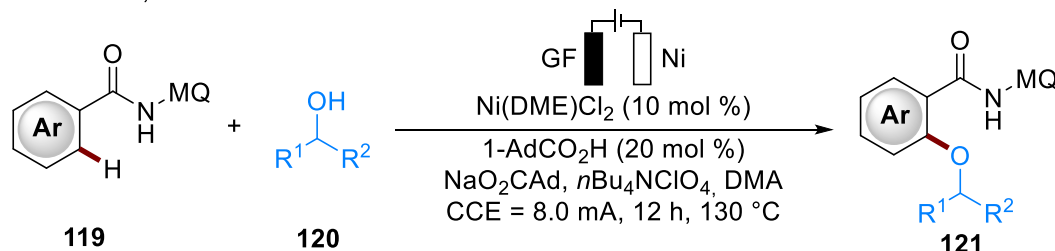
A vast number of transformations have been achieved using nickel catalysis as it is earth-abundant, less costly, and has unique reactivity compared to its 4d and 5d counterparts (palladium and platinum).^[98] Irrespective of the advancement in this area, the utility of electrochemistry in the nickel-catalyzed C–H functionalization has been unfruitful until the recent contributions of Ackermann (Scheme 24). The report of Ackermann in 2018 unraveled the first nickel catalyzed electrooxidative C–H activation featuring broad substrate scope, high levels of chemo- and regio-selectivity (Scheme 24a).^[99] The same group successively achieved the selective C–H alkylation of arenes at room temperature. Later, Ackermann also developed the nickella-electrocatalyzed alkoxylation (Scheme 24b)^[100] and phosphorylation of arenes (Scheme 24c).^[101] All reactions proceeded with H_2 gas as the sole byproduct. All these findings

were accompanied by detailed, mechanistic studies providing evidence for a nickel(III/IV/III) pathway.

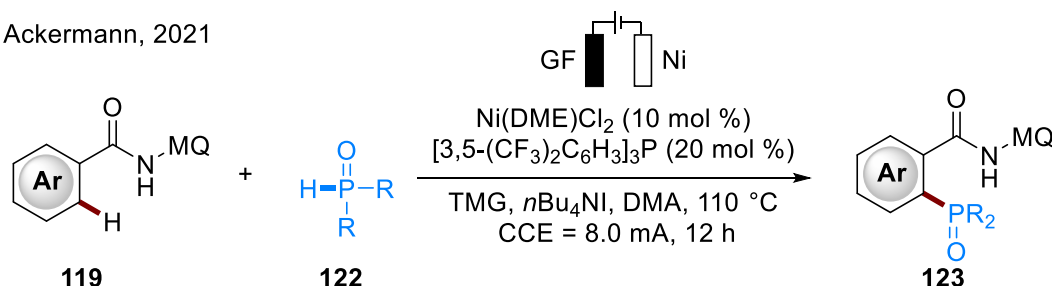
a) Ackermann, 2018



b) Ackermann, 2020



c) Ackermann, 2021



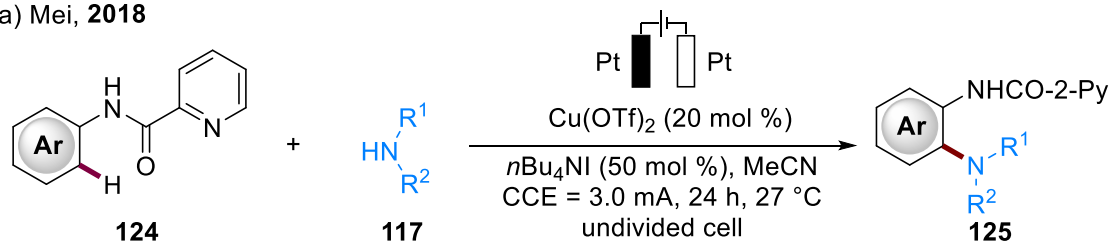
Scheme 24. Nickella-electrooxidative C–H activation

1.6.4 Copper-Catalyzed Electrooxidative C–H Activation

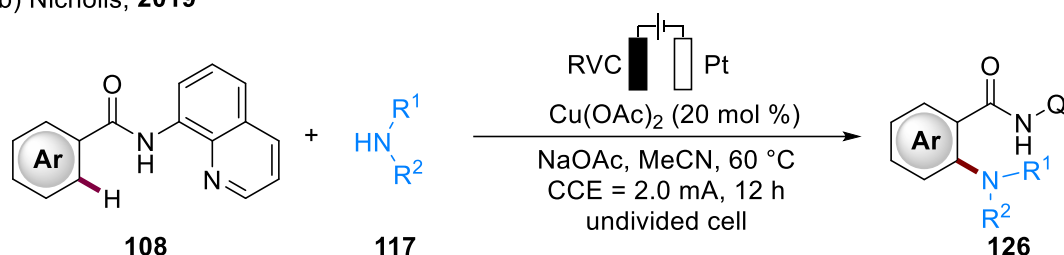
The use of copper catalysis in organic reactions is dated as far back as the Hay-Glaser coupling,^[102] and Ullmann-Goldberg coupling.^[103] Apart from acting as chemical oxidants in stoichiometric amounts, copper salts have recently found application as catalysts in C–H functionalization protocols (Scheme 24). In this regard, Mei in 2018 achieved the electrochemical *ortho*-selective C–H amination of arenes with arylamines using Cu(OTf)₂ as catalyst and *n*-Bu₄NI as redox mediator (Scheme 25a).^[104] They suggested a single electron transfer pathway to proceed *via* a high-valent copper(III) species. Nicholls reported a cupraelectro-oxidative C–H amination of benzamides without a redox mediator (Scheme 25b).^[105] This protocol was applicable to a variety of functional groups and pharmaceutically relevant molecules.

In contrast, in a subsequent report, Ackermann achieved the dehydrogenative and decarboxylative C–H/N–H alkyne annulation *via* cupraelectro-catalysis. This regime facilitated access to bioactive five-membered isoindolones **128** (Scheme 25c).^[106]

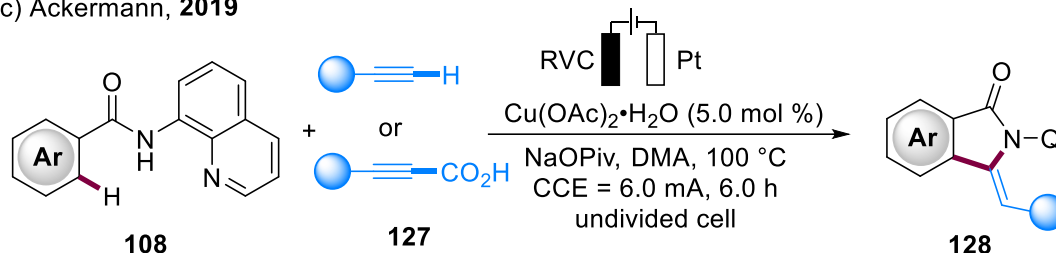
a) Mei, 2018



b) Nicholls, 2019



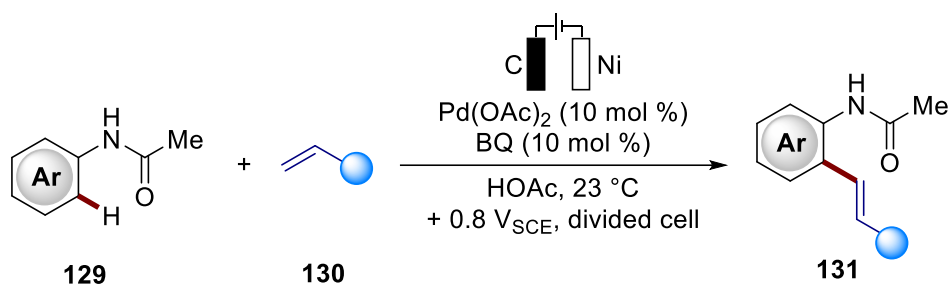
c) Ackermann, 2019



Scheme 25. Cupra-electrooxidative C–H activation

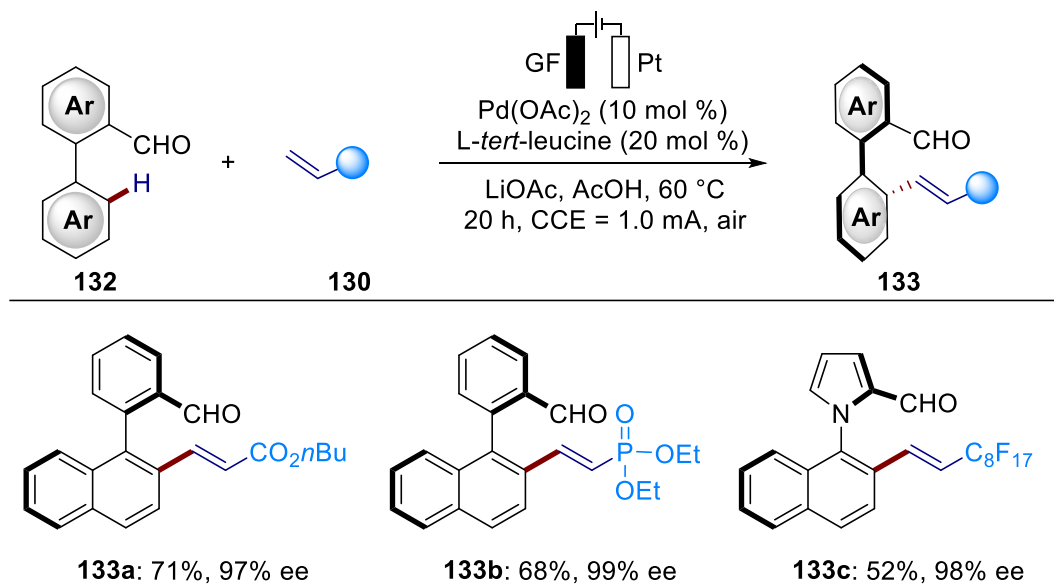
1.6.5 Palladium-Catalyzed Electro-Oxidative C–H Activation

Palladaelectro-catalytic C–H activation had its first report made by Amatore and Jutand in 2007.^[107] They reported an electro-oxidative C–H olefination of arenes as a modified version of the Fujiwara-Moritani-type reaction.^[108] In this report, they used catalytic amounts of benzoquinone as a redox mediator at room temperature (Scheme 26).



Scheme 26. Pallada-electrooxidative Fujiwara-Moritani-type C–H olefination

Oxidative olefination was recently achieved by Ackermann and co-workers in an asymmetric fashion. They accomplished the transient directing group-assisted atroposelective olefination to access axially chiral biaryls *via* palladaelectro-catalysis. Most recently, the same group reported the atroposelective C–H olefination of anilides with sunlight as the power source and thioether-enabled C–H olefination for N–C and C–C axial chirality (Scheme 25).^[109]

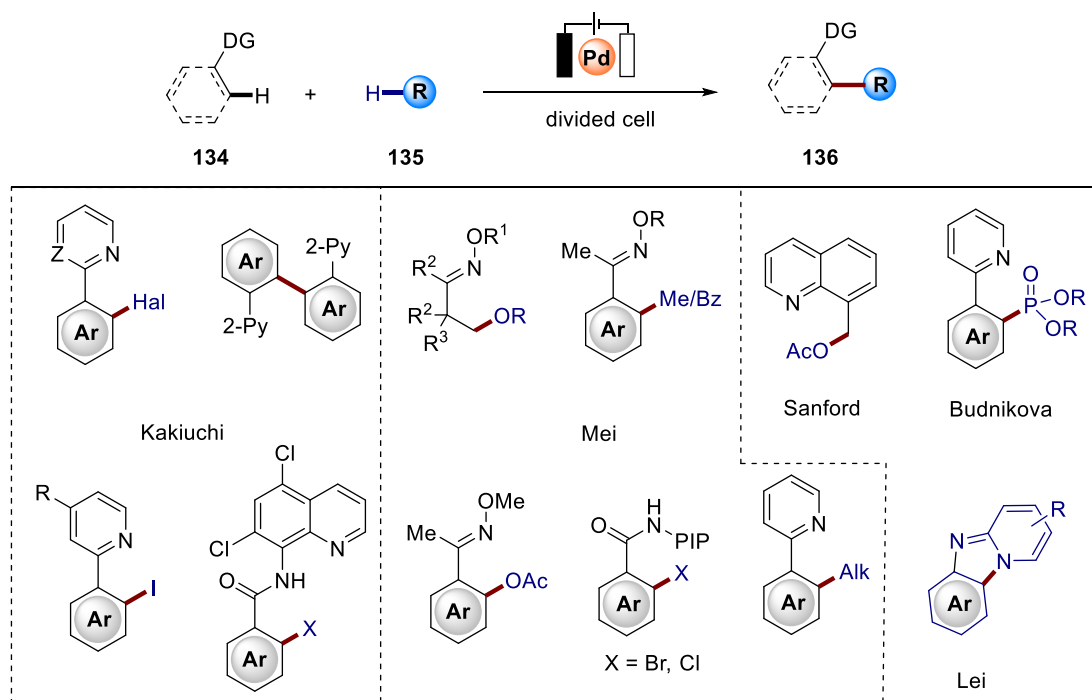


Scheme 26. First enantioselective pallada-electrooxidative asymmetric C–H olefination

Furthermore, Mei in 2017 reported a palladium-catalyzed electrochemical C(sp³)–H oxygenation under mild reaction conditions, thereby furnishing a variety of synthetically relevant oximes.^[110] In a later report, the same group developed the oxidative *ortho*-C(sp²)–H methylation and benzoylation of oximes using methyl trifluoroborates and benzoyl acetic acid as coupling partners.^[111] Interestingly, pallada-electrocatalysis allowed for the *ortho*-

C(sp²)-H halogenation,^[112] acetoxylation,^[113] and alkoxylation^[114] in the subsequent research findings of Mei and co-workers.

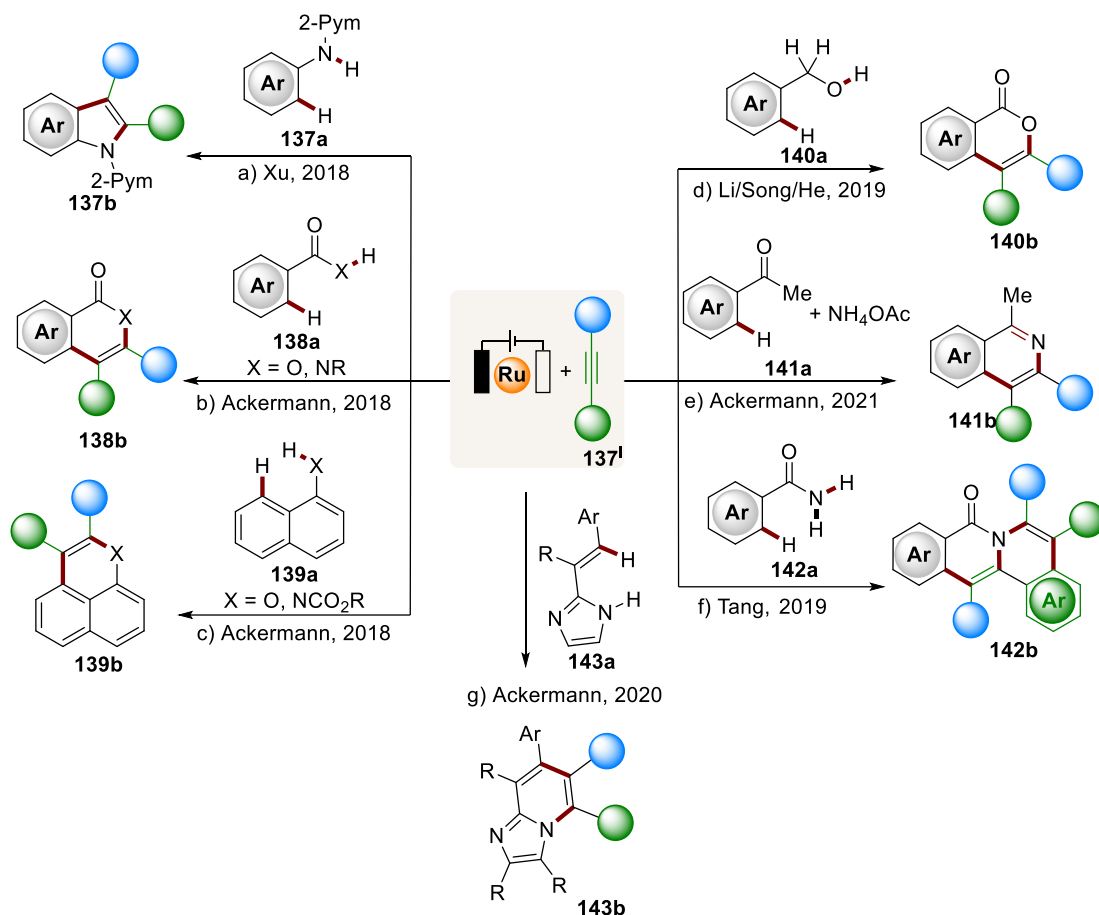
It is worth noting that more contributions to the palladaelectro-catalyzed C-H activation were made by the Stanford,^[115] Budnikova,^[116] and Lei groups.^[117]



Scheme 27. Pallada-electrooxidative C-H activation.

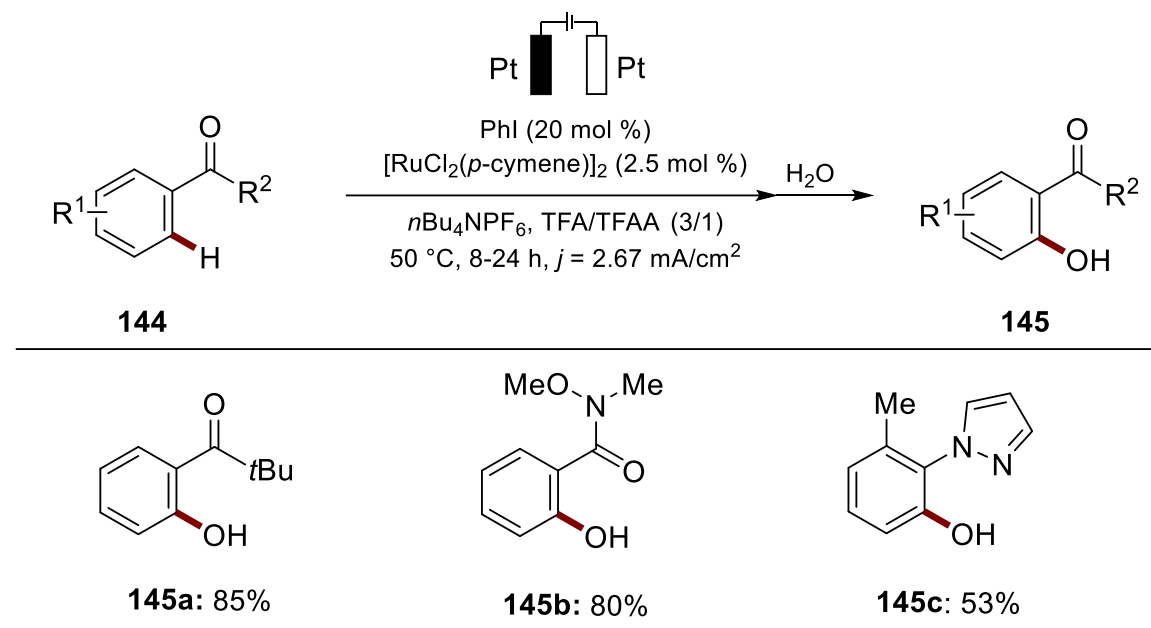
1.6.6 Ruthenium-Catalyzed Electro-Oxidative C-H Activation.

As of 2018, the versatility of ruthenium catalysis in oxidative C-H activation had been well established.^[118] However, these protocols relied on the use of stoichiometric amounts of copper(II) salts and molecular oxygen as oxidants which jeopardized the sustainability of the protocol. To tackle this challenge, Xu and Ackermann^[119] unraveled a promising protocol to access indoles and isocoumarins *via* the electro-oxidative C-H alkyne annulation of arenes bearing weakly coordinating benzoic acids with aniline derivatives as partners. Ackermann later reported the C-H/N-H annulation of imidazoles with internal alkynes to furnish a variety of azaindoles with high functional group tolerance.^[120] Next, the dehydrogenative C-H/Het-H alkyne annulation was proven applicable with naphthol, benzylic alcohols, acetophenones, benzylamides, and aromatic carbamates *via* electro-oxidative ruthenium catalysis (Scheme 28).^[121]



Scheme 28. Ruthena-electrooxidative C-H/X-H annulation. (X = N, O).

Furthermore, Ackermann and co-workers contributed further to the field of ruthenium-catalyzed electro-oxidative C-H activation in their report in 2020, revealing the hypervalent iodine(III) co-catalyzed ruthena-electrochemical C-H oxygenation of amides and ketones.^[122] In their report, a variety of synthetically beneficial amides **145b** and ketones **145a** were oxygenated with high functional group tolerance (Scheme 29).



Scheme 29. Ruthenaelectro-catalyzed C–H activation of ketones, amides and pyrazoles **144**.

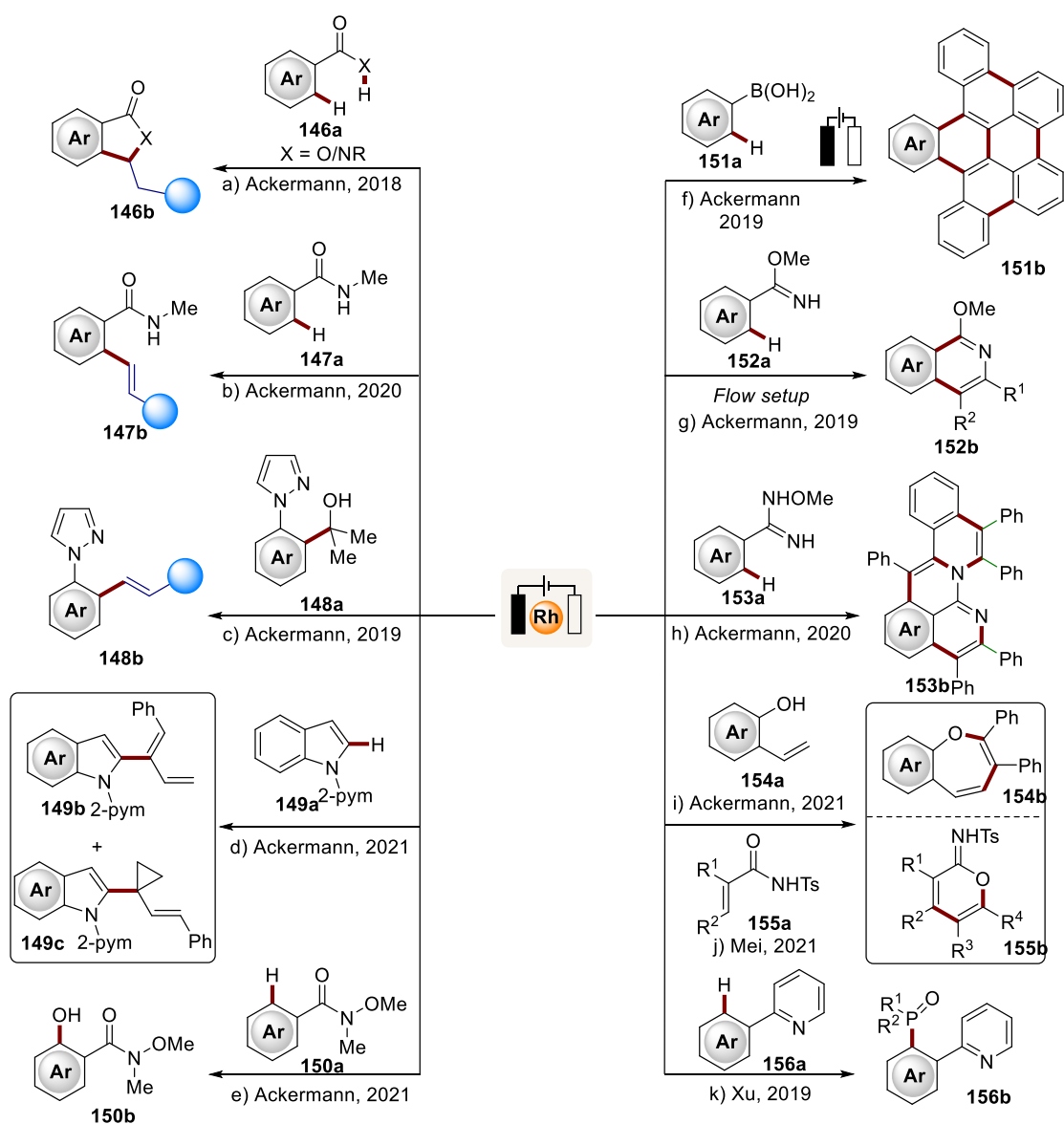
1.5.7 Rhodaelectro-Oxidative C–H Activation

Rhodaelectro-oxidative C–H activation has experienced significant advancement owing to the enormous contribution of Ackermann and co-workers.^[123] The first report was made in 2018 with the electrochemical rhodium-catalyzed alkene annulation of benzoic acids, amides, and indoles in a cross dehydrogenative fashion. In subsequent reports by the same group, rhodaelectro-catalysis facilitated the olefination of benzamides and the *ortho*-selective oxidative alkenylation of arenes *via* C–C bond activation.^[124] The developed C–C activation regime featured high chemo- and positional selectivity, thereby providing access to poly-substituted arenes, which had initially proven inaccessible with pre-existing protocols. Furthermore, the viability of rhodaelectro-catalysis was extendable to the synthesis of polyaromatic hydrocarbons by cascade annulation of alkynes with simple boronic acids^[125] and amidoximes^[126] respectively.

In 2019, Ackermann established the first flow-rhodaelectro-catalyzed annulation of arenes with imines as directing group. This reaction proceeded through an electro-oxidatively-induced reductive elimination pathway on a rhodium(III) species.^[127] Moreover, Xu reported an *ortho*-selective pyridine-directed electrochemical rhodium-catalyzed C–H phosphorylation,^[128] while

Mei recently reported an electro-oxidative alkyne annulation of amides *via* rhodium catalysis.^[129]

Most recently, Ackermann has documented the rhoda-electrooxidative C–H activation of indoles,^[130] alkyne annulation of phenols^[129] *via* C–H/O–H bond activation, C–H oxygenation of amides,^[131] and alkyne annulation of 2-hydroxybenzaldehydes to access synthetically relevant chromones (Scheme 30).^[132]

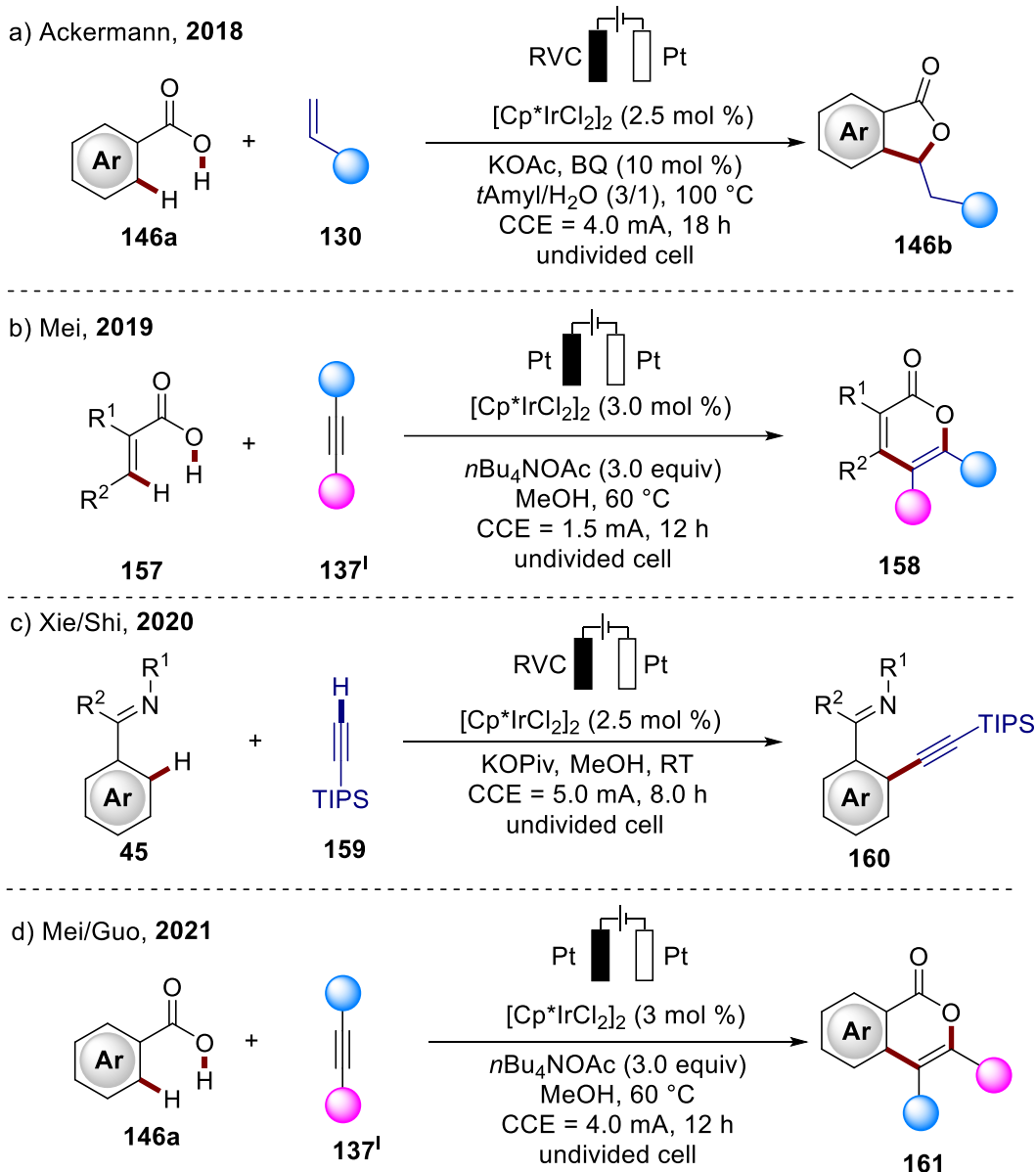


Scheme 30. Rhoda-electrooxidative C–H activations.

1.6.8 Iridaelectro-Oxidative C–H Activation

Iridium catalyzed electrooxidative C–H activation was pioneered by Ackermann and co-workers in 2018, where they achieved iridaelectro-oxidative C–H alkenylation *via* C–H/O–H bond activation.^[133] The high functional group tolerance of this regime was enabled by the metal-free redox mediator through indirect electro-catalysis (Scheme 31a). Mei and Guo subsequently reported the electrooxidative synthesis of α -pyrones under mild conditions *via* the alkyne annulation of benzoic acids and acrylic acids, respectively (Scheme 31b/d).^[134] These reactions proceeded *via* iridaelectro-catalysis with good to excellent yields and were proven to be dependent on anodic oxidation to release the product while regenerating the iridium(III) catalyst.

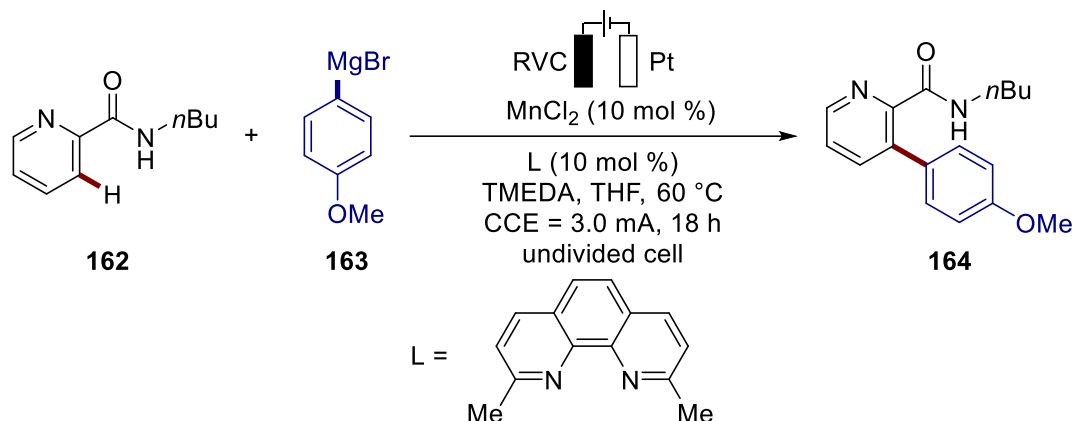
In 2020, Xie and Shi independently reported the alkynylation of arenes under electrooxidative iridium catalysis under mild reaction conditions. This protocol promoted positional and chemo-selective synthesis of unsymmetric alkynes with good functional group tolerance (Scheme 31c).^[135]



Scheme 31. Irida-electrooxidative C–H/O–H annulation.

1.6.9 Manganese-Catalyzed Electrooxidative C–H Activation

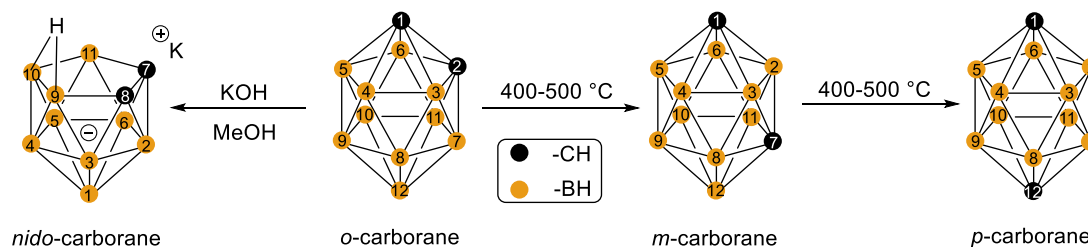
Manganese is one of the earth-abundant, cheap, and safe 3d transition metals that is not exempted within the framework of metallacyclocatalysis. Ackermann and co-workers reported the only example of manganese-electrocatalytic C–H activation. This protocol employed readily available MnCl_2 catalyst assisted by zinc salts for the C–H arylation of picolinic amides with aryl Grignard reagents as the arylating agent (Scheme 32).^[90]



Scheme 32. Manganaelectro-oxidative C–H arylation.

1.7 Transition Metal-Catalyzed Cage Functionalization of *o*-Carboranes

Carboranes are carbon-boron clusters with an icosahedral geometry bearing a three-dimensional electronic delocalization. Each *closo*-carborane cluster contains ten boron atoms and two neighboring carbon atoms.^[136] Due to the similarity in B–B, C–B, and C–C bond lengths, carboranes exhibit similar reactivity to arenes leading to their regard as three-dimensional analogs of benzene.^[137] *Closo*-carboranes exist as three main isomers, *ortho*, *meta*, and *para*-carborane, with *para*-carborane being the least reactive due to its high stability (Scheme 33). Another derivative of carboranes is the *nido*-carborane, an open cage derivative of *o*-carborane with one boron-vertex less. The extensive application of carboranes in material science,^[138] optoelectronics,^[139] coordination chemistry,^[140] and medicine as boron neutron capture therapy agents^[141] has attracted the interest of scientists of diverse backgrounds.

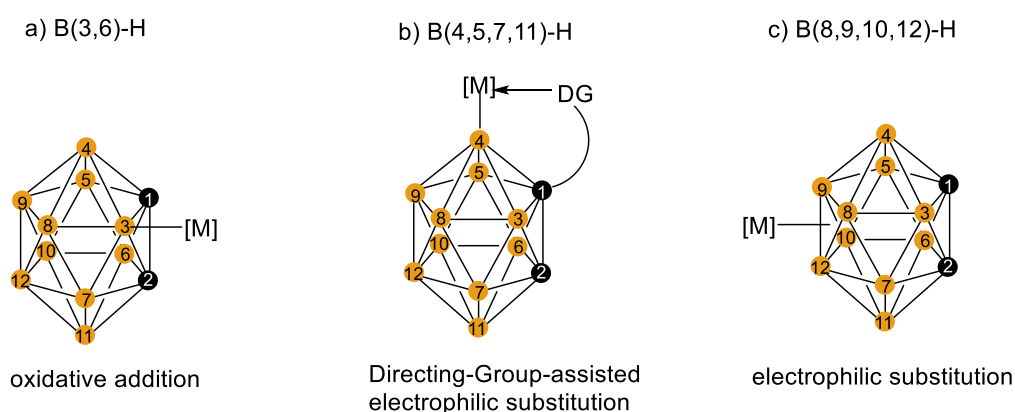


Scheme 33. Molecular *nido*-carborane and geometry of *o*-, *m*-, *p*-dicarb-closo-dodecarboranes, IUPAC numbering of the cage atoms and their chemical transformations.

o-Carboranes have a pK_a of 22.0 owing to the strong electron-withdrawing character of *o*-carborane cage towards the cage carbons.^[142] Hence, the early reactions of *o*-carborane were focused on the deprotonation of the cage C–H

bond with organometallic reagents, followed by an electrophilic attack. The symmetrical nature and similar charge distribution of the *o*-carboranes was a major challenge to achieve high selectivity, as all the boron atoms exhibit comparable reactivities. In addition, the different electron densities exhibited by the 10 B–H bonds triggers the formation of carborane derivatives with different reactivity rates to electrophilic substitution reactions in the order B(9,12)–H > B(8,10)–H > B(4,5,7,11)–H > B(3,6)–H.^[143]

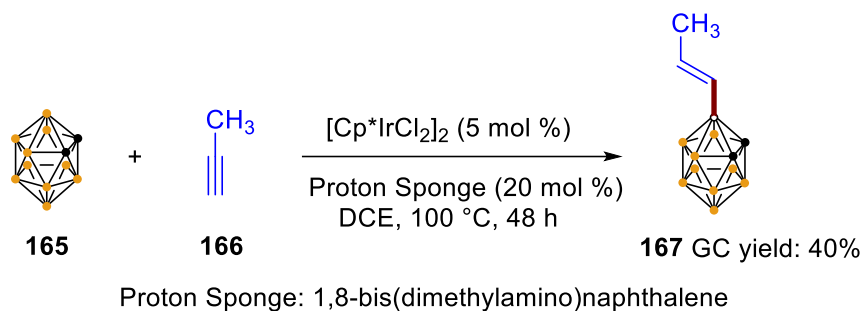
Transition metal catalysis came into play as a promising strategy to selectively functionalize B–H bonds. This strategy entails three main principles (Scheme 34): ^[144] (1) the use of electron-rich transition metal catalysts, which exhibits a preferential reactivity with the electron-deficient B(3,6)–H bonded to the two carbons; (2) installing a directing group in addition to an electrophilic transition metal catalyst is ideal for the functionalization of B(4, 5, 7, 11)–H; and (3) preferential functionalization of electron-rich B(8,9,10,12)–H bonds by electrophilic transition metal catalysts.



Scheme 34. The general strategy for catalytic selective cage B–H functionalization.

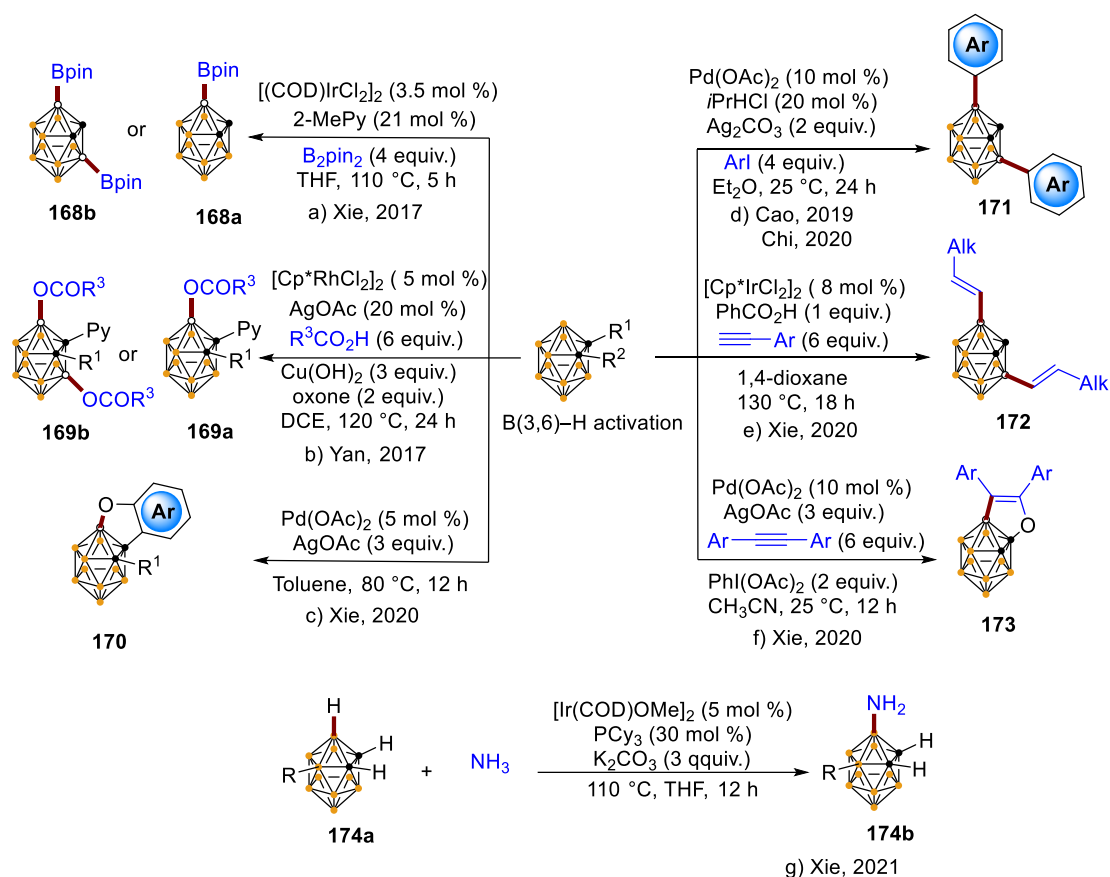
1.7.1 Transition Metal-Catalyzed Cage B(3, 6)–H Functionalization

The B(3,6) selective transition metal-catalyzed B–H functionalization was first reported by Hawthorne in 1977, in which he achieved the selective B–H deuteration with D₂.^[145] Then, the selective cage B(3)–H propenylation of *o*-carboranes with propyne *via* iridium/sponge catalysis was reported by Sneddon in 1988 (Scheme 35).^[146] Though this reaction faced the challenge of low reaction efficacy and investigations were limited to propyne, it provided a proof of concept for selective cage B–H functionalization.



Scheme 35. Iridium-catalyzed cage B(3)-propenylation of *o*-carborane.

In 2017, Xie reported an iridium-catalyzed B-3/B-6 selective diborylation of *o*-carboranes with B_2pin_2 as coupling partner in good to excellent yields.^[147] Yan later documented a pyridine-directed rhodium-catalyzed B-3/B-6 selective acyloxylation of *o*-carboranes.^[148] Subsequently, Xie reported a palladium-catalyzed intramolecular B-3 dehydrogenative coupling,^[149] acid-assisted iridium-catalyzed B-3/B-6 selective diakenylation of *o*-carboranes,^[150] and recently B-3 selective palladium-catalyzed oxidative annulation of *o*-carboranes with internal alkynes.^[151] Furthermore, Cao^[152] and Chi^[153] established an NHC ligand-assisted palladium-catalyzed B-3/B-6 selective diarylation of *o*-carboranes under mild reaction conditions. Recently, Xie reported the B-3 selective iridium-catalyzed B–H amination with ammonia *via* B–H/N–H dehydrocoupling with broad substrate scope (Scheme 36).^[154]

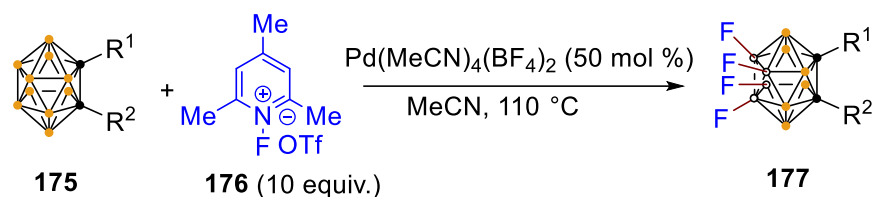


Scheme 36. Cage B(3,6)-halogenation, alkenylation, arylation, and tetraacetoxylation of *o*-carboranes

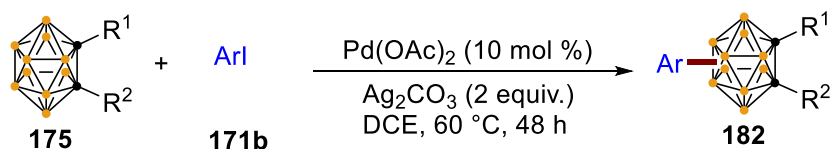
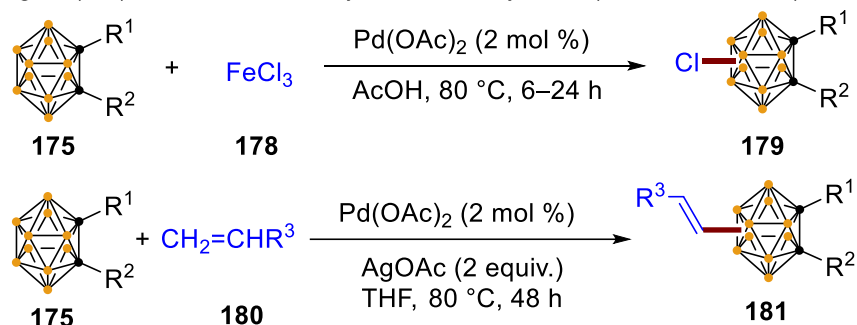
1.7.2 Transition Metal-Catalyzed B(8,9,10,12) Functionalization

The pioneering work of Xie in 2013 unraveled the first palladium-catalyzed B(8,9,10,12) fluorination of *o*-carboranes using F^+ species as fluorine sources and oxidants (Scheme 37a).^[155] As an extension of the concept, Cao later reported a directing group-free B(8,9) palladium-catalyzed chlorination,^[156] alkenylation,^[157] and arylation^[158] of *o*-carboranes respectively (Scheme 37b). In addition, the B(8)-arylation was achieved by palladium catalysis enabled by a B(4) amide directing group in the report made by Xie in 2018 (Scheme 37c).^[159] Furthermore, the palladium-catalyzed directing group-free B(8,9,10,12) functionalization could be applied to acetoxylation, as reported by Chao. They demonstrated the selective mono and tetra-acetoxylation of *o*-carboranes using $\text{PhI}(\text{OAc})_2$ as an acetoxylating agent and oxidant (Scheme 37d).^[160]

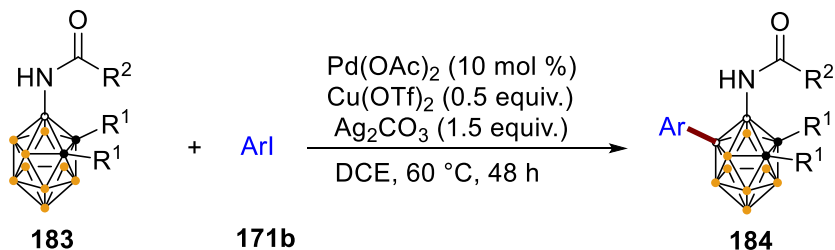
a) Cage B(8,9,10,12)-tetrafluorination (Xie, 2013)



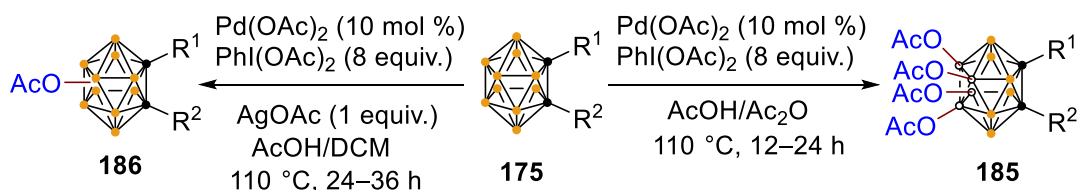
b) Cage B(8/9)-chlorination, alkenylation and arylation (Cao, 2015-2017)



c) Cage B(8)-arylation (Xie, 2019)



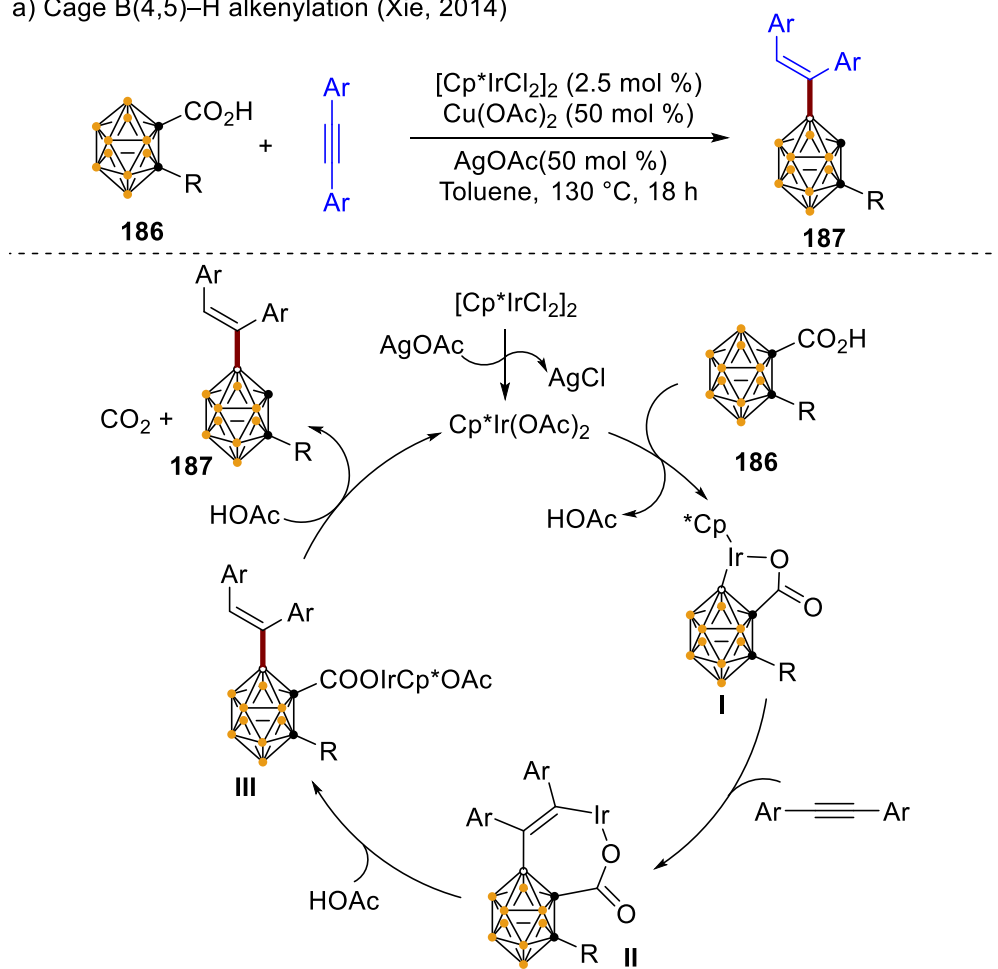
d) Cage B(8,9,10,12)-tetraacetoxylation (Cao, 2016/2018)

**Scheme 37.** Transition metal-catalyzed Cage B(8,9,10,12) functionalization of o-carboranes**1.7.3 Transition Metal-Catalyzed Cage B(4,5,7,11)–H Functionalization**

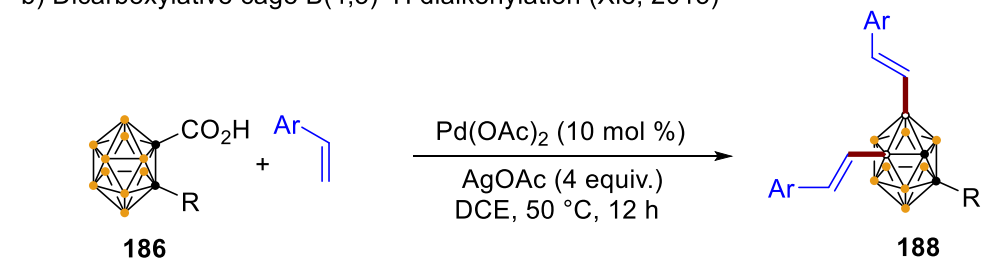
The B(4,5,7,11)–H selective functionalization has generally been achieved by installing a directing group on the cage carbon vertices, as was first reported by Xie in 2014. Their findings showed the iridium catalyzed B-4 selective alkenylation using a weakly coordinating traceless carboxylic acid directing group (Scheme 38a).^[161] Their reaction furnished a wide range of B-4-

alkenylated *o*-carboranes with excellent regioselectivities. This reaction was proposed to proceed by cage B(4)–H activation followed by alkyne insertion, then protonation and decarboxylation to generate the final product. In a subsequent report, the same group employed palladium catalysis to achieve the B(4,5)-dialkenylation of *o*-carboranes (Scheme 38b).^[162] Lu and co-workers later utilized the palladium catalyst [Pd(TFA)] to accomplish B(4,5)-dialkenylation of *o*-carboranes with acrylates in good to excellent yields (Scheme 38c).^[163]

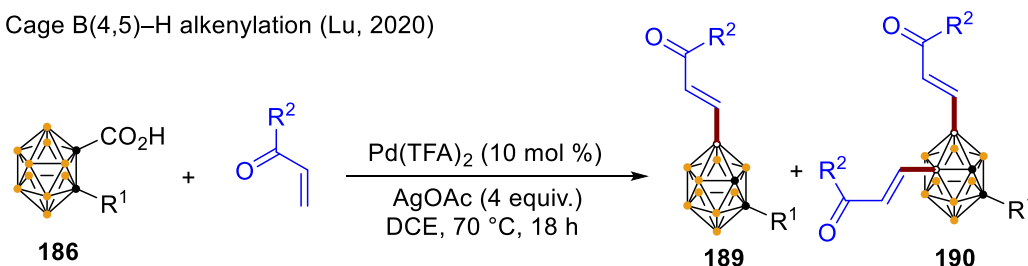
a) Cage B(4,5)–H alkenylation (Xie, 2014)



b) Dicarboxylative cage B(4,5)–H dialkenylation (Xie, 2015)



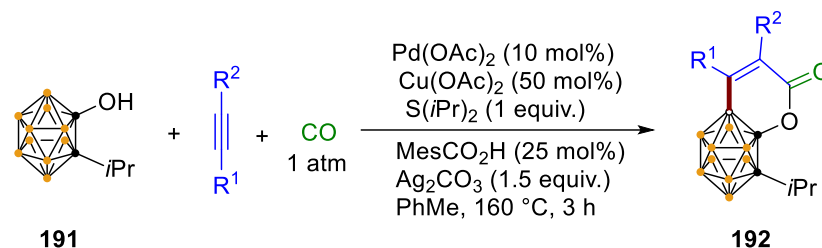
c) Cage B(4,5)-H alkenylation (Lu, 2020)



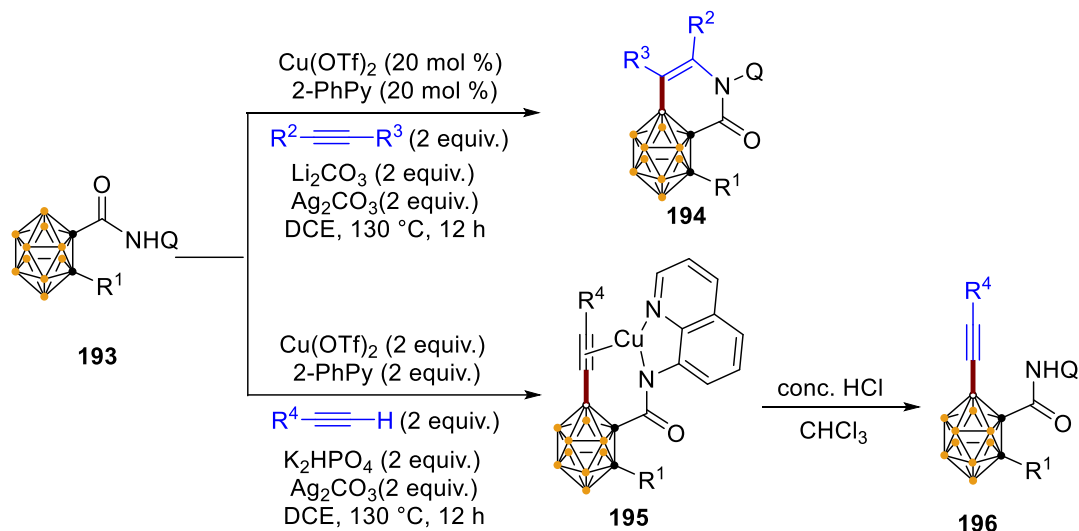
Scheme 38. Cage B(4,5)-H alkenylation of *o*-carboranes.

In a comprehensive study, Xie enormously contributed to the major advancements in the B(4,5) selective functionalization of *o*-carboranes. In 2019, they reported the bidentate 8-aminoquinoline-directed copper-catalyzed annulation of *o*-carboranes to afford carboranyl isoquinoline-1(2*H*)-one derivatives *via* B(4)-H/N-H annulation with internal alkynes. In the same year, they extended the scope of the same system to the dehydrogenative B(4) selective alkynylation of *o*-carboranes with terminal alkynes (Scheme 39b).^[164] In 2020, Xie established a palladium-catalyzed three-component annulation of 1-hydroxy-*o*-carboranes with internal alkynes and 1 atm of carbon monoxide to afford carborane-coumarin derivatives in good to excellent yields (Scheme 39a).^[165]

a) Cage B(4)–H carbonylative annulation (Xie, 2020)



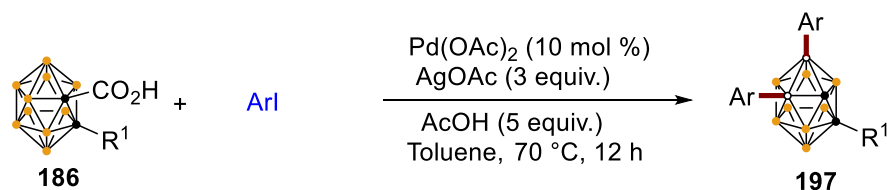
b) Cage B(4)–H alkyne annulation (Xie, 2019)



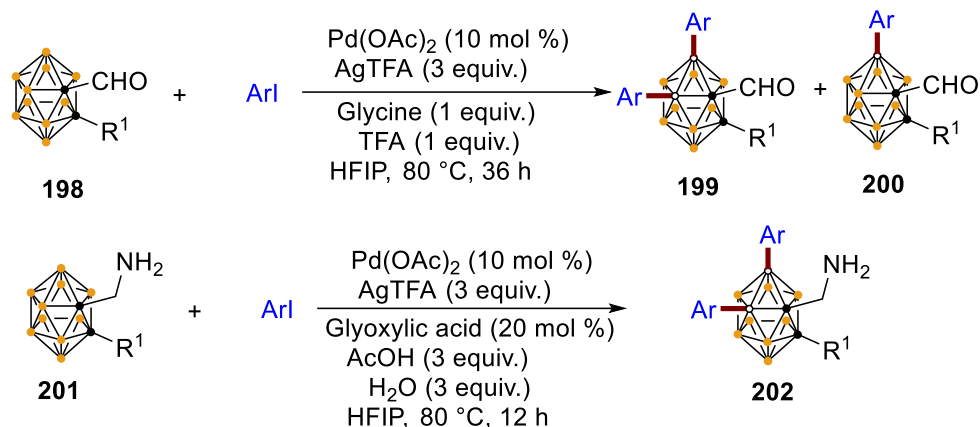
Scheme 39. Cage B(4)–H annulation of *o*-carboranes

The B(4,5)-selective arylation of *o*-carboranes has significantly advanced with the reports of the Xie, Yan, and Cao groups. In 2016, Xie reported a B(4,5)-palladium-catalyzed diarylation of *o*-carboranes in a decarboxylative manner (Scheme 40a).^[166] In addition, Yan, in 2017 and 2018, established a palladium-catalyzed B(4,5) selective diarylation using a transient directing group with aryl iodides as arylating agents (Scheme 40b).^[167] Cao later achieved a Suzuki-type coupling reaction to afford B(4)-monoarylated carboranes.^[168] These methods recorded high regioselectivity and functional group tolerance (Scheme 40c). Interestingly, Xie, in 2018, developed the first enantioselective B(4) intramolecular arylation of *o*-carboranes in the presence of a chiral phosphine ligand.^[169] This protocol facilitated the synthesis of carborane-fluoren-9-one derivatives (Scheme 40d).

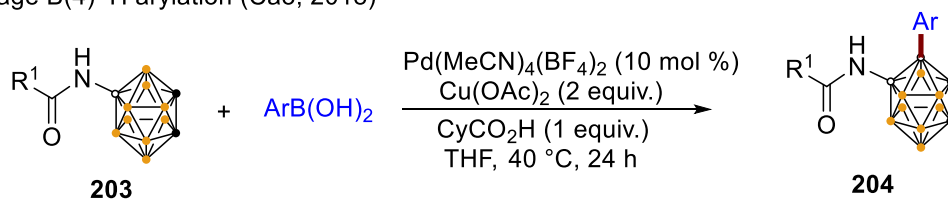
a) Cage B(4,5)-H diarylation (Xie, 2016)



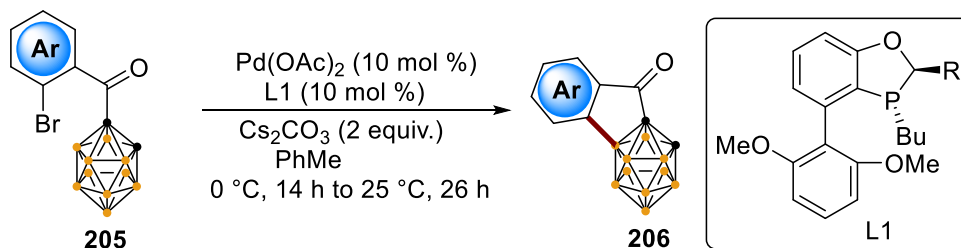
b) Cage B(4,5)-H arylation by transient DG (Yan, 2017/2018)



c) Cage B(4)-H arylation (Cao, 2018)

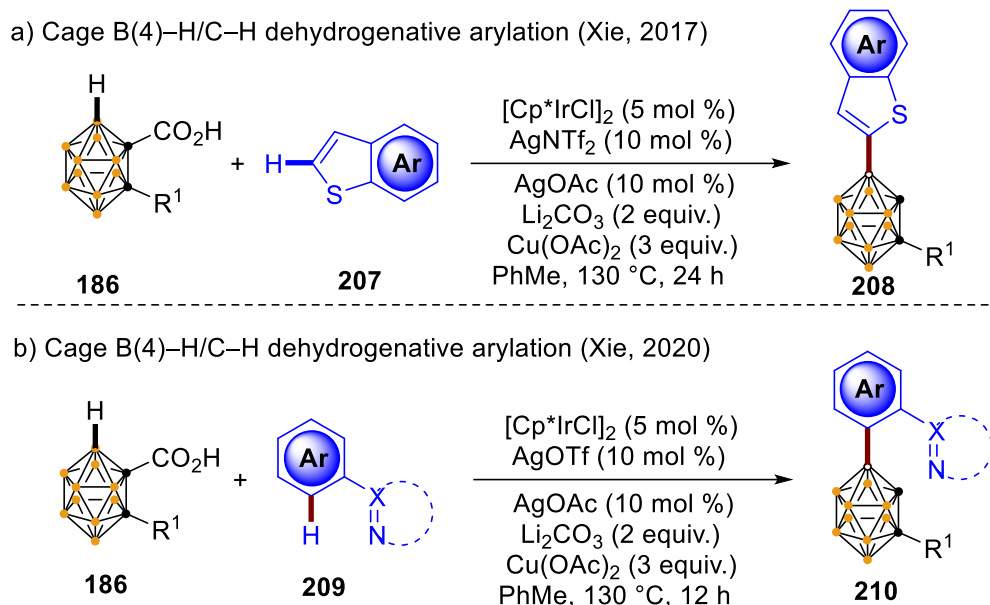


d) Intramolecular B(4)-H enantioselective arylation (Xie, 2018)

**Scheme 40.** Transition metal-catalyzed Cage B(4,5)-H arylation of *o*-carboranes

In addition to the protocols mentioned earlier for the selective arylation of *o*-carboranes, Xie also reported a carboxylic acid-directed iridium-catalyzed cross-dehydrogenative coupling to afford hetero-arylated **208** and arylated carboranes **210**.^[170] While the former protocol enabled the synthesis of B(4)-thienylated carboranes with thiophenes, the latter was achieved using a

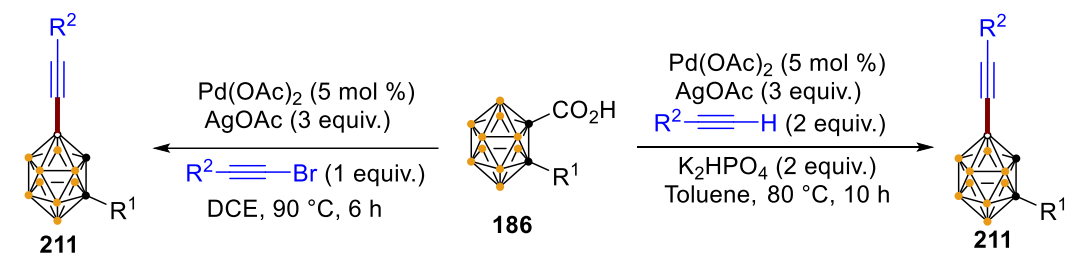
double directing group strategy leading to moderate to excellent yields (Scheme 41).^[171]



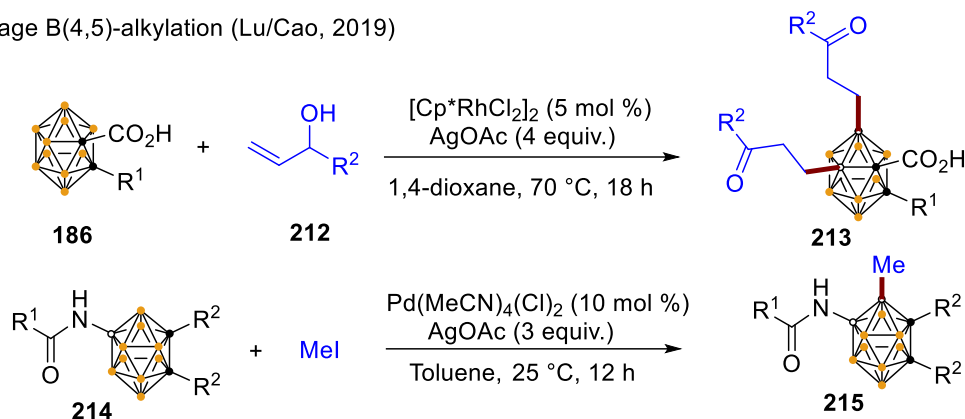
Scheme 41. Iridium-catalyzed Cage B(4)–H/C–H dehydrogenative arylation of *o*-carboranes

A broad scope of the B(4) selective functionalization was proven in the palladium-catalyzed B–H alkynylation of carboranyl carboxylic acids with bromoalkynes and terminal alkynes.^[172] This protocol granted access to B(4)-internal alkynyl carboranes in moderate to excellent yields (Scheme 42a). Additionally, B(4,5) dialkylation of carboranyl carboxylic acid was achieved *via* rhodium catalysis by Lu and co-workers.^[173] Here, they reported an efficient synthesis of carboranyl β -aryl and β -alkyl ketones (Scheme 42b). In sharp contrast, the versatility of palladium catalysis was demonstrated in the B(9)-acyl amino group directed B(4) selective methylation of *o*-carboranes employing methyl iodide as the coupling partner.^[174] Furthermore, the decarboxylative B(4) hydroxylation of *o*-carboranes by rhodium catalysis with oxygen gas in good to excellent yields was unraveled by Xie in 2016 (Scheme 42c).^[175]

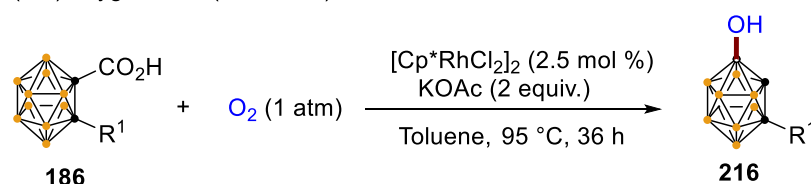
a) Cage B(4)-alkynylation (Xie, 2016)



b) Cage B(4,5)-alkylation (Lu/Cao, 2019)

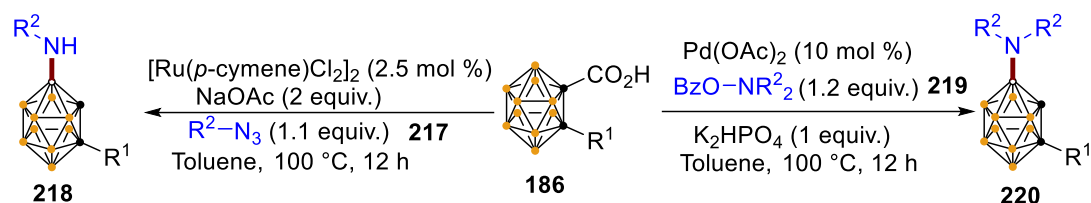


c) Cage B(4,5)-oxygenation (Xie, 2016)

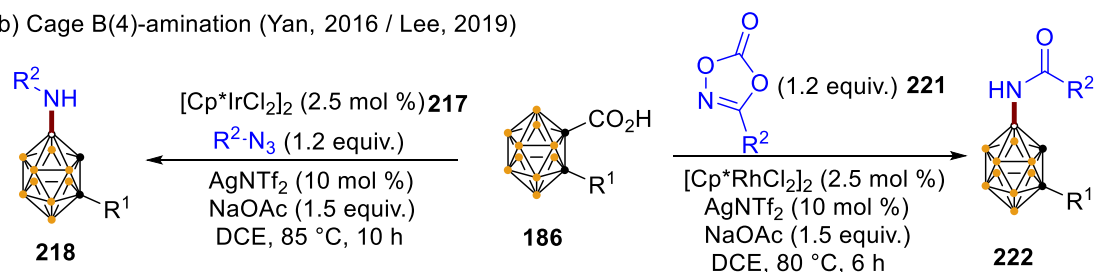
**Scheme 42.** Cage B(4,5)-alkylation, alkylation, oxygenation of *o*-carboranes

The transition metal-catalyzed selective B(4)-functionalization has also been proven viable for B(4)-amination. This was demonstrated in the research work of Xie in 2016, where he achieved the B(4) selective amination of *o*-carboranes.^[176] This report revealed two pathways involving ruthenium-catalyzed amination with organic azides as amination agents to afford secondary amines and palladium-catalyzed amination with *o*-benzoyl hydroxyl amines to furnish tertiary amines (Scheme 43a). Also, Yan unveiled the iridium-catalyzed B(4) selective access to secondary amines using organic azides as amination agents. More progress was made in B–N bond formation with the B(4)-amidation of carboranes *via* rhodium catalysis using dioxazolones in a decarboxylative fashion (Scheme 43b).^[177]

a) Cage B(4)-amination (Xie, 2016)

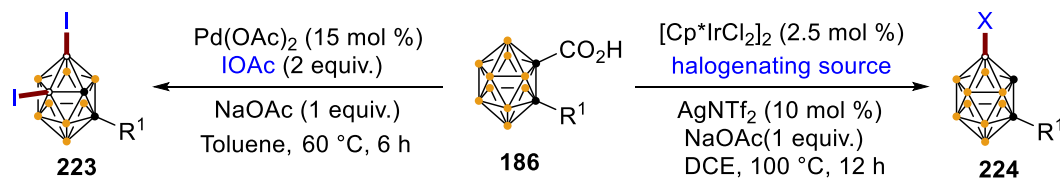


b) Cage B(4)-amination (Yan, 2016 / Lee, 2019)

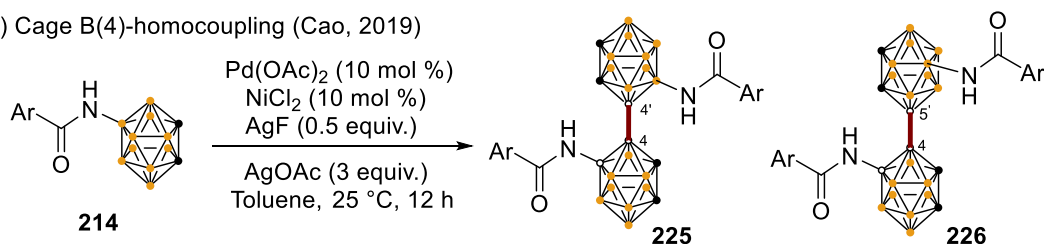
**Scheme 43.** Cage B(4,5)-amination of *o*-carboranes

Recent reports have further exploited the potential of transition metal catalysis in the selective B(4)-halogenation, B(4)-homocoupling,^[178] B(4,5)-diiodination,^[179] and B(4,5)-disulfenylation^[180] of *o*-carboranes reported by the Xie and Cao groups (Scheme 44).

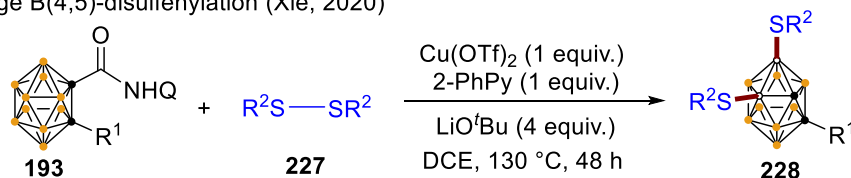
a) Cage B(4,5)-halogenation (Xie, 2017)



b) Cage B(4)-homocoupling (Cao, 2019)



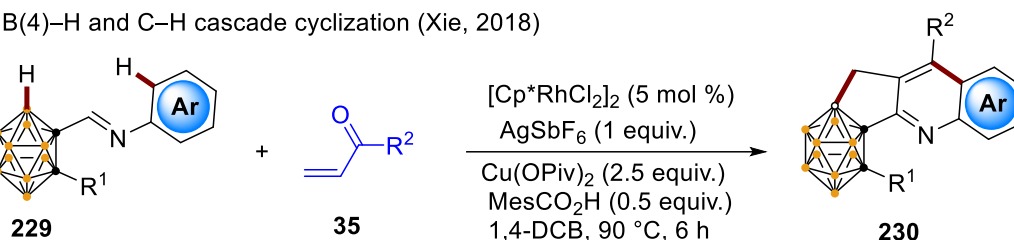
c) Cage B(4,5)-disulfenylation (Xie, 2020)

**Scheme 44.** Cage B(4,5)-halogenation, homocoupling, and disulfenylation of *o*-carboranes

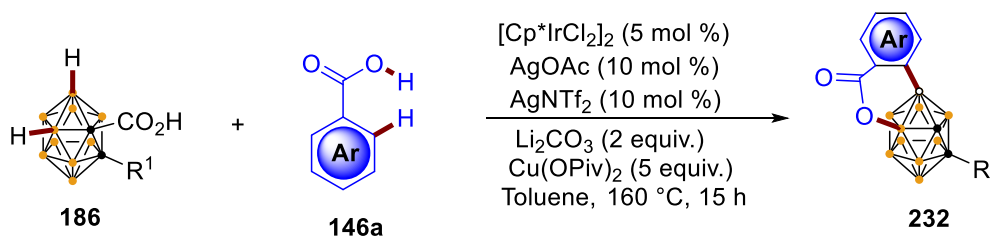
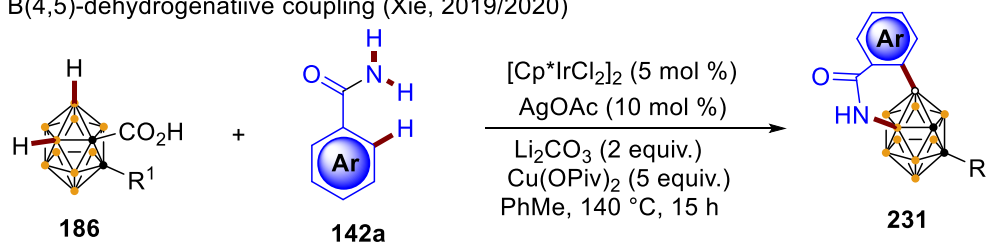
Considering the recent prospects presented by the one-pot protocols, the noble late transition metal catalysts have demonstrated their versatility in the

step-economical synthesis of bio-relevant scaffolds. With respect to this, Xie established an efficient synthesis of carboranyl quinolines **230** via a rhodium-catalyzed C–H/B–H cascade cyclization of carboranyl *N*-arylimines (Scheme 45a).^[181] Xie also reported the cascade B(4,5)-cross-dehydrogenative coupling involving sequential B–H, C–H, and N–H bonds activation via iridium catalysis to furnish carboranyl isoquinolin-1(2*H*)-ones **231** and carboranyl isochromen-1-ones **232** (Scheme 45b).^[182] A further report by Lee in 2020 illustrated the iridium-catalyzed B(4)-indenylolation of *o*-carboranyl carboxylic acid with propargylic alcohols (Scheme 45c).^[183]

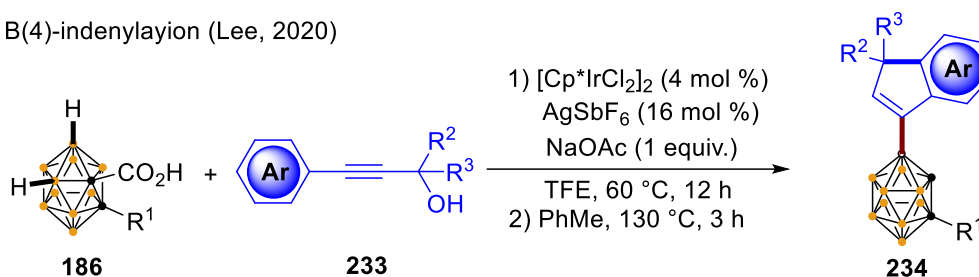
a) B(4)–H and C–H cascade cyclization (Xie, 2018)



b) B(4,5)-dehydrogenative coupling (Xie, 2019/2020)



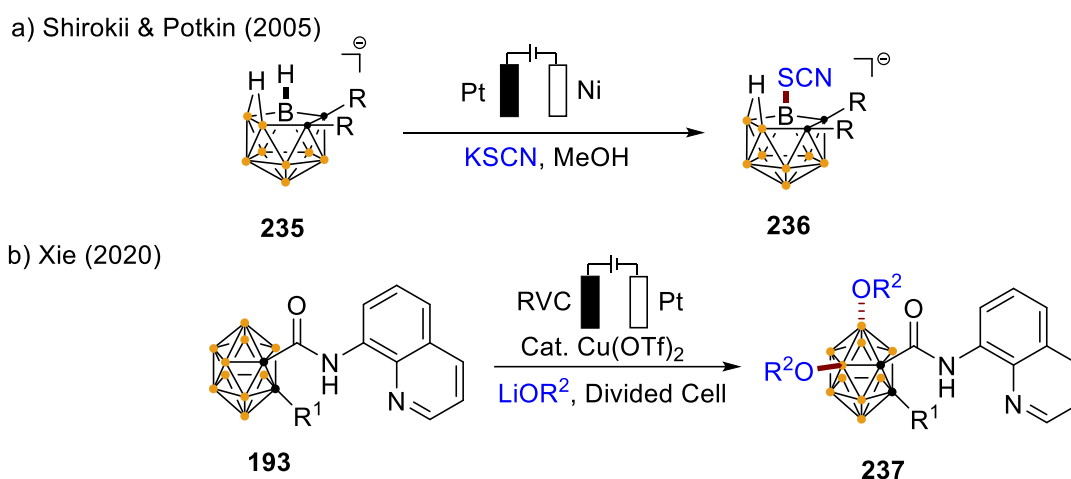
c) B(4)-indenylolation (Lee, 2020)



Scheme 45. Cage B(4,5) cascade cyclization reactions

1.8 Electrochemical Cage Functionalization of Carboranes

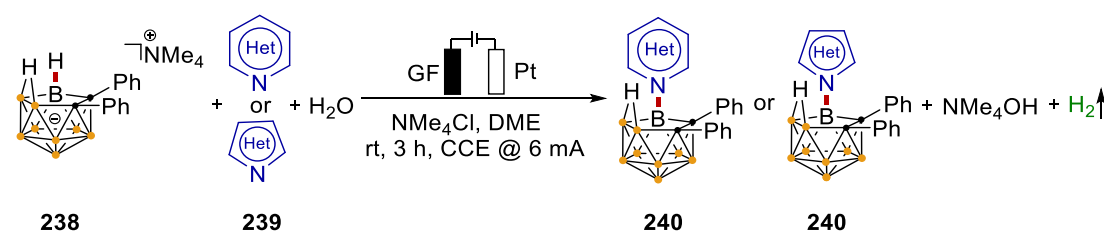
With the emergence of electrical energy as a more sustainable alternative to chemical oxidants in transition metal-catalyzed C–H activation, electrocatalysis is unfolding as a promising protocol for the selective functionalization of carboranes. In 2005, Shirokii and Potkin reported the metal-free electrochemical thiocyanation of *nido*-carboranes (Scheme 46a).^[184] During the preparation of this thesis, Xie and co-workers reported a copper-catalyzed electrochemical B–H oxygenation of *o*-carboranes using a detachable aminoquinoline directing group in a divided cell at room temperature. This protocol is environmentally friendly as it has hydrogen gas and lithium salts as the only side-products (Scheme 46b).^[185]



Scheme 46. Electrochemical cage functionalization of *o*-carborane

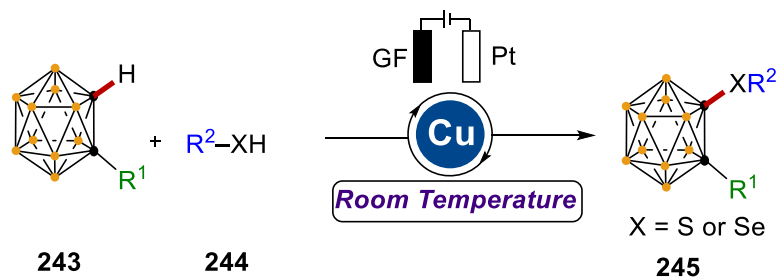
2 Objectives

Nitrogen-containing heterocycles are essential to drug discovery as they are widely distributed in bioactive molecules. The carboranyl analogues of these compounds are gaining the attention of medicinal chemists owing to their potentials in drug discovery and medicinal chemistry. Amidst the advancements in the selective functionalization of *closo*-carboranes, the selective functionalization of *nido*-carboranes is still in its infancy. The negative charge of the *nido*-carborane cage resulting from the detachment of one boron vertices restrains the susceptibility of B–H bonds of the *nido*-carborane clusters to nucleophilic attack. Notwithstanding the advancements in electro-catalysis in the functionalization of C–H bonds, electrochemical B–H activation is still scarcely explored. Therefore, exploring electrocatalysis in the selective functionalization of *nido*-carboranes is envisaged.



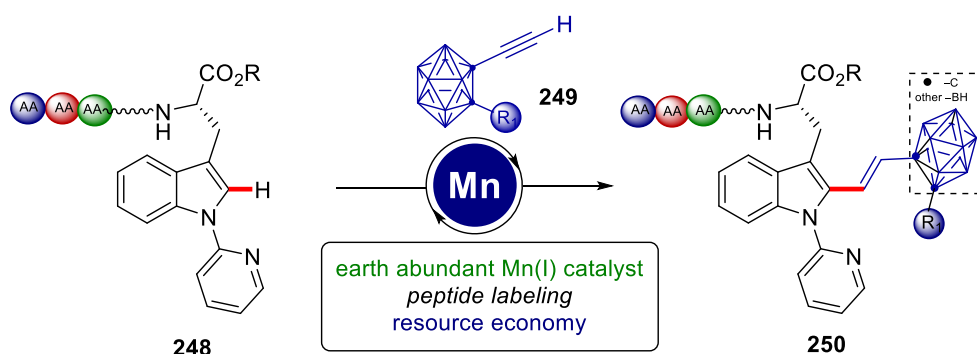
C–chalcogen-substituted compounds have been of interest to scientists due to their wide distribution in bioactive molecules. However, despite the already established protocols for efficiently synthesizing chalcogen-containing compounds, a negligible account has been made for synthesizing chalcogen-containing carboranes. The pre-existing protocols have encountered drawbacks such as the use of stoichiometric amounts of organolithium reagents which require special care. This makes them impractical thereby leading to a high demand for sustainable alternatives. First, the strong coordination of thiols to transition metals results in the deactivation of the catalyst, thus interrupting the entire synthetic process. Second, the selective functionalization of carboranes has only been achieved with noble transition metals. In addition, stoichiometric amounts of silver salts as oxidants have been proven unavoidable for the established protocols. Hence, the merger of 3d transition metal catalysis, electrochemistry, and cage C–H activation is

envisioned as a sustainable protocol for assembling chalcogen-containing carboranes.



The efficient modification of peptides has attracted the interest of synthetic chemists owing to their application in medicine as anticancer agents. Manganese catalysis has evolved as a sustainable tool for assembling a wide range of bio-relevant molecular entities. They have been proven viable for clean, step economical, and cost-efficient synthesis of various synthetically valuable molecules with unique reactivities compared to their late 3d counterparts. In addition, carboranes have found applications in cancer therapy, most notably boron neutron capture therapy. This has rapidly advanced selective cage functionalization of carboranes during the last decade.

Nonetheless, the application of 3d transition metals in the assembly of carborane-containing molecules is in its infancy. The application of manganese(I) catalysis in the C-2 selective hydroarylation of tryptophan derivatives is considered a promising pathway to access carborane labelled peptides following reported literature.



3. Results and Discussion

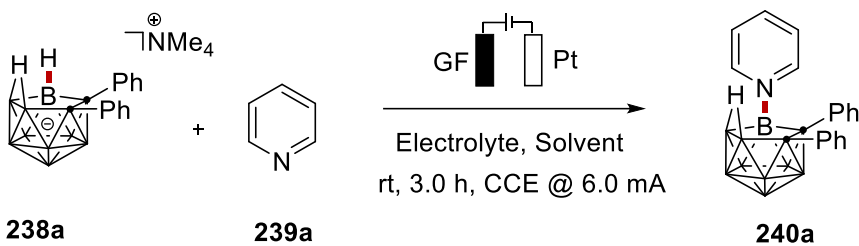
3.1 Electrochemical B–H Nitrogenation of *nido*-Carboranes

Nitrogen-containing heterocycles are privileged scaffolds in a variety of natural products, pharmacologically relevant molecules, and in catalysis.^[186] Due to the negative charge on the *nido*-carborane cluster, they exhibit less susceptibility to nucleophilic substitution. Therefore, the direct functionalization of *nido*-carboranes is still in its infancy, despite the recent advancements in the cage functionalization of their *closo*-carborane counterparts. The use of electricity as a redox reagent has unfolded over the years as a viable and environmentally-friendly protocol for the assembly of synthetically useful molecules. In addition, the employment of green strategies for the selective functionalization of *nido*-carboranes is gradually advancing. The merger of electrosynthesis with cage B–H functionalization of carboranes is still unexplored and therefore is envisaged as promising tool to access a variety of synthetically useful *nido*-carborane derivatives.

3.1.1 Optimization and Scope

The optimization of the reaction conditions was carried out by Dr. Long Yang (PhD thesis by Dr. Long Yang, 2021). Our intended electrochemically catalyzed B–N coupling was initiated with *nido*-carborane **238a** and pyridine **239a** at room temperature in an undivided cell setup equipped with a GF (Graphite Felt) anode and a Pt-plate cathode (Table 1). Detailed screening of various reaction conditions resulted in the isolation of the desired B-pyridine coupled *nido*-carborane product **240a** in a 60% yield in DME/H₂O as solvent (entries 1-4). In addition, NMe₄Cl emerged as the best electrolyte for our electrocatalytic system among other ammonium salts (entries 5-7). We observed that, an increase in the amount of H₂O diminished the efficiency of our electrocatalysis system (entries 8-9) while a decrease in the amount of H₂O improved the yields of our desired product **240a** to 83% (entry 10). Furthermore, the role of the H₂O, electricity, NMe₄Cl additive, and the GF as the anode material were confirmed by control experiments that resulted in significant decrease in yields when these parameters were altered (entries 11-16).

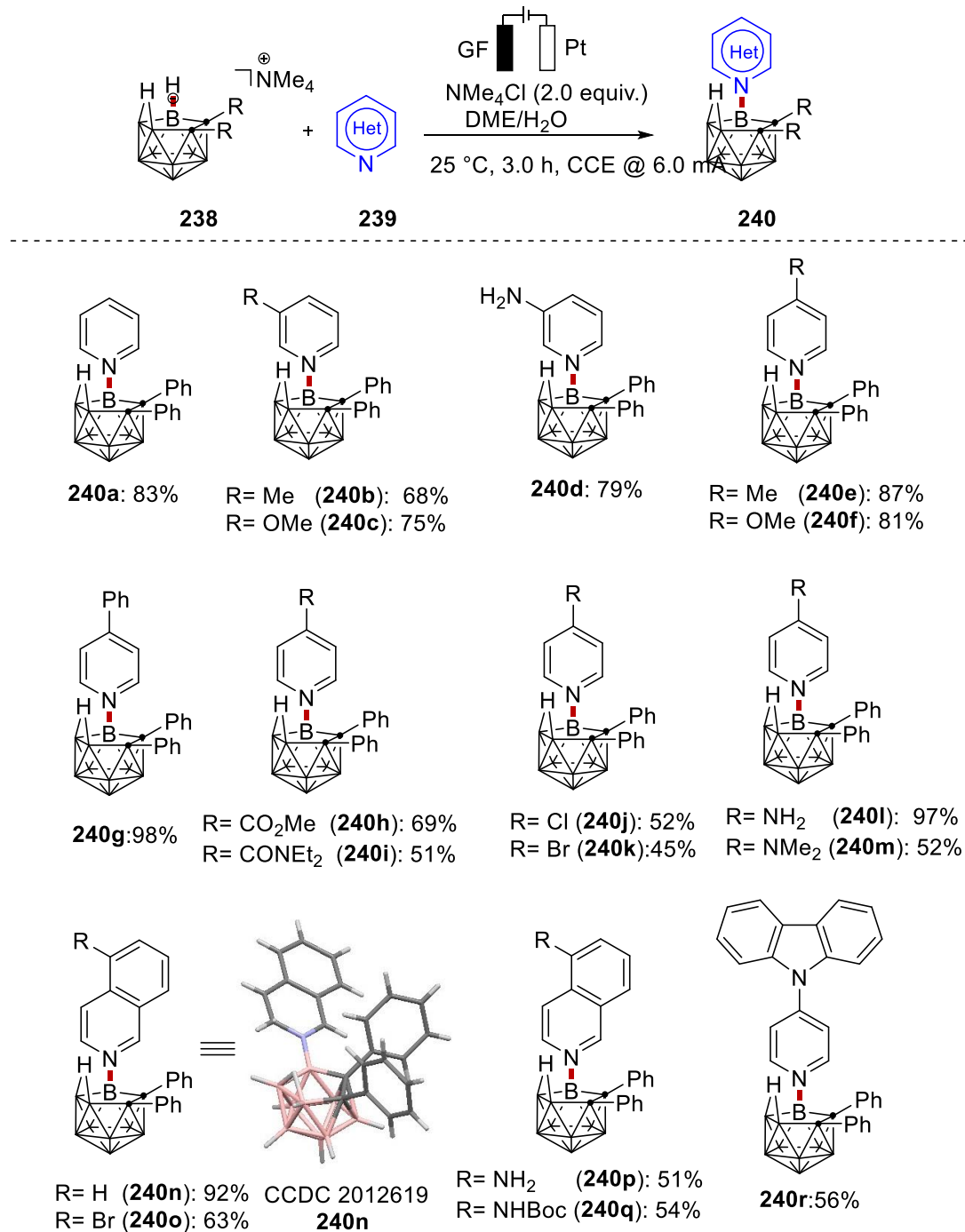
Table 1: Optimization of the reaction conditions.^[a]

			
238a	239a		240a
Entry	Electrolyte	Solvent	Yield [%] ^[b]
1	---	MeOH/H ₂ O	8% ^[c]
2	---	THF/H ₂ O	36% ^[c]
3	---	CH ₃ CN/H ₂ O	40% ^[c]
4	---	DME/H ₂ O	60% ^[c]
5	<i>n</i> BuNPF ₆	DME/H ₂ O	20% ^[c]
6	<i>n</i> BuNBF ₄	DME/H ₂ O	63% ^[c]
7	NMe ₄ Cl	DME/H ₂ O	65% ^[c]
8	NMe ₄ Cl	DME/H ₂ O	32% ^[d]
9	NMe ₄ Cl	DME/H ₂ O	50% ^[e]
10	NMe₄Cl	DME/H₂O	87% (83%)^[f]
11	NMe ₄ Cl	DME	10%
12	NMe ₄ Cl	DME/H ₂ O	--- ^[g]
13	---	DME/H ₂ O	67%
14	KCl	DME/H ₂ O	75%
15	NaCl	DME/H ₂ O	70%
16	NMe ₄ Cl	DME/H ₂ O	73% ^[h]

[a] Reaction conditions: **238a** (0.10 mmol), **239a** (0.30 mmol), electrolyte (2 equiv.), DME (4.0 mL), H₂O (0.2 mL), 25 °C, 3 h. [b] Yield was determined by ¹H NMR with CH₂Br₂ as the standard. [c] H₂O (0.5 mL). [d] H₂O (1.0 mL). [e] DME (5.0 mL), H₂O (1.0 mL). [f] Isolated yields in parenthesis. [g] No electricity. [h] Pt-plate as the anode. DME = 1,2-Dimethoxyethane, THF = Tetrahydrofuran. All optimization experiments were performed by Dr. Long Yang.

The versatility of the electrochemical B–N coupling of *nido*-carboranes **238** with different *N*-heterocyclic substrates **239** was explored with the optimized reaction conditions. Thus, a variety of nitrogen-containing heterocycles,

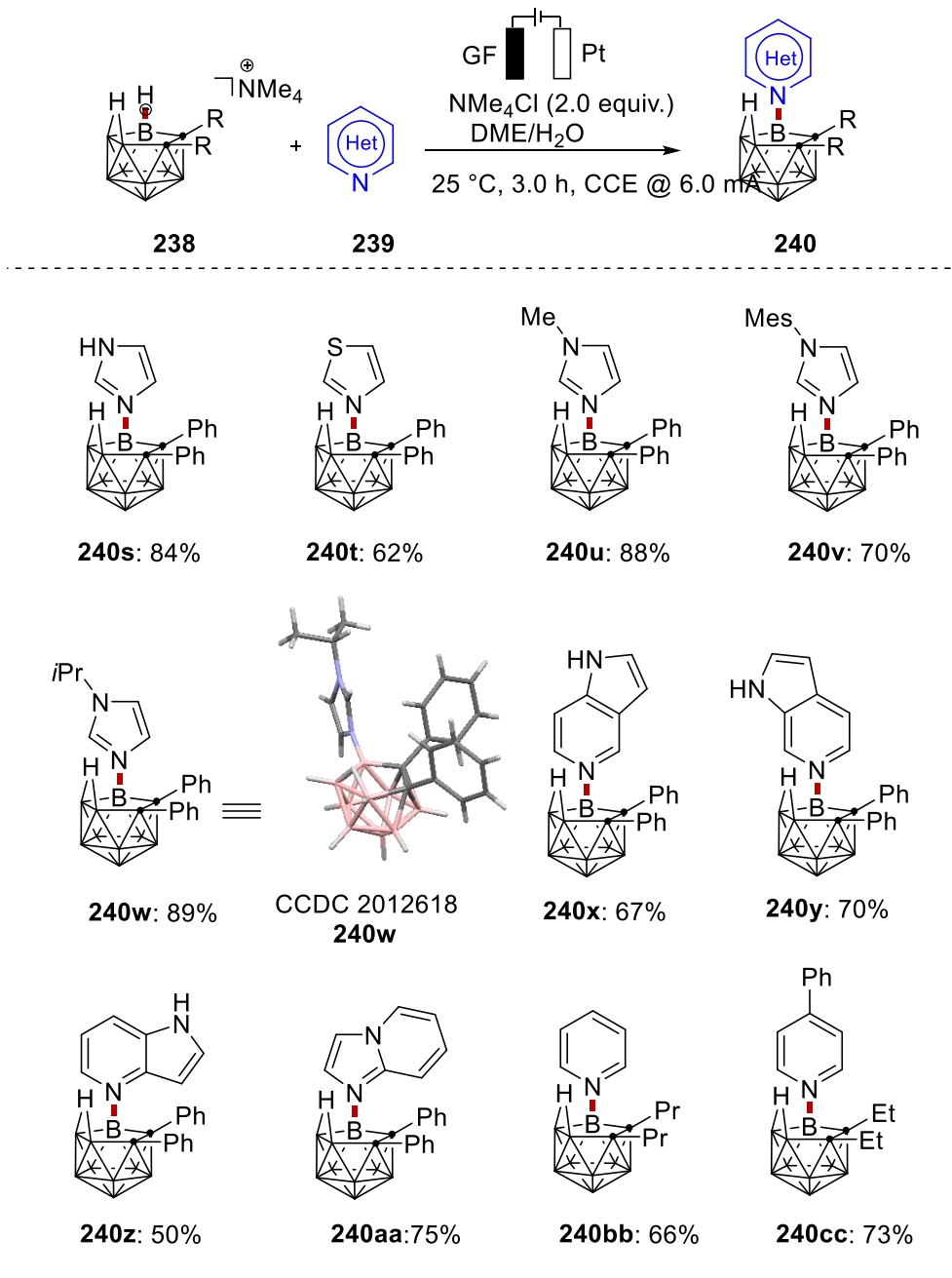
including fused rings, five-membered as well as six-membered rings were employed in our electrocatalytic system. First, decorated pyridines with electron-rich as well as electron-deficient groups **239** were tolerated in the electrocatalytic regime in good to excellent yields (**240a-240m**). Also, interesting pyridine derivatives such as the Steglich catalyst 4-dimethylaminopyridine (DMAP) and carbazole-substituted pyridine also furnished their respective desired products (**240m**, **240r**) with good efficacy. Synthetically useful functional groups, notably ester (**240h**), amide (**240i**), chloro (**240j**), and bromo (**240k**) groups, were fully tolerated. These could be resourceful for further late-stage transformation, especially with the already established cross-coupling reactions with aryl halides. In addition, isoquinolines (**240n-240q**) were successfully coupled to *nido*-carborane, even though the amine-substituted and *Boc*-protected amino isoquinoline products (**240p-240q**) were isolated in somewhat lower yields. This unique selectivity of our B–N coupling system was demonstrated in the tolerance of the free amino group (**240d**, **240l**) under the mild electro-oxidative conditions (Scheme 47a).



Scheme 47a. Electrooxidative B–H nitrogenation of *nido*-carborane with *N*-heterocycles. (**240a**, **240h**, **240l–240p**, and **240r** by Dr. Long Yang)

At this point we were keen to explore the robustness of the electrooxidative B–N coupling to five-membered *N*-heterocyclic rings. To our delight, imidazoles and thiazole were applicable to our system delivering the desired products (**240s–240w**). In addition, fused *N*-heterocycles like the pharmacologically relevant azaindole scaffold, yielded the corresponding B–N

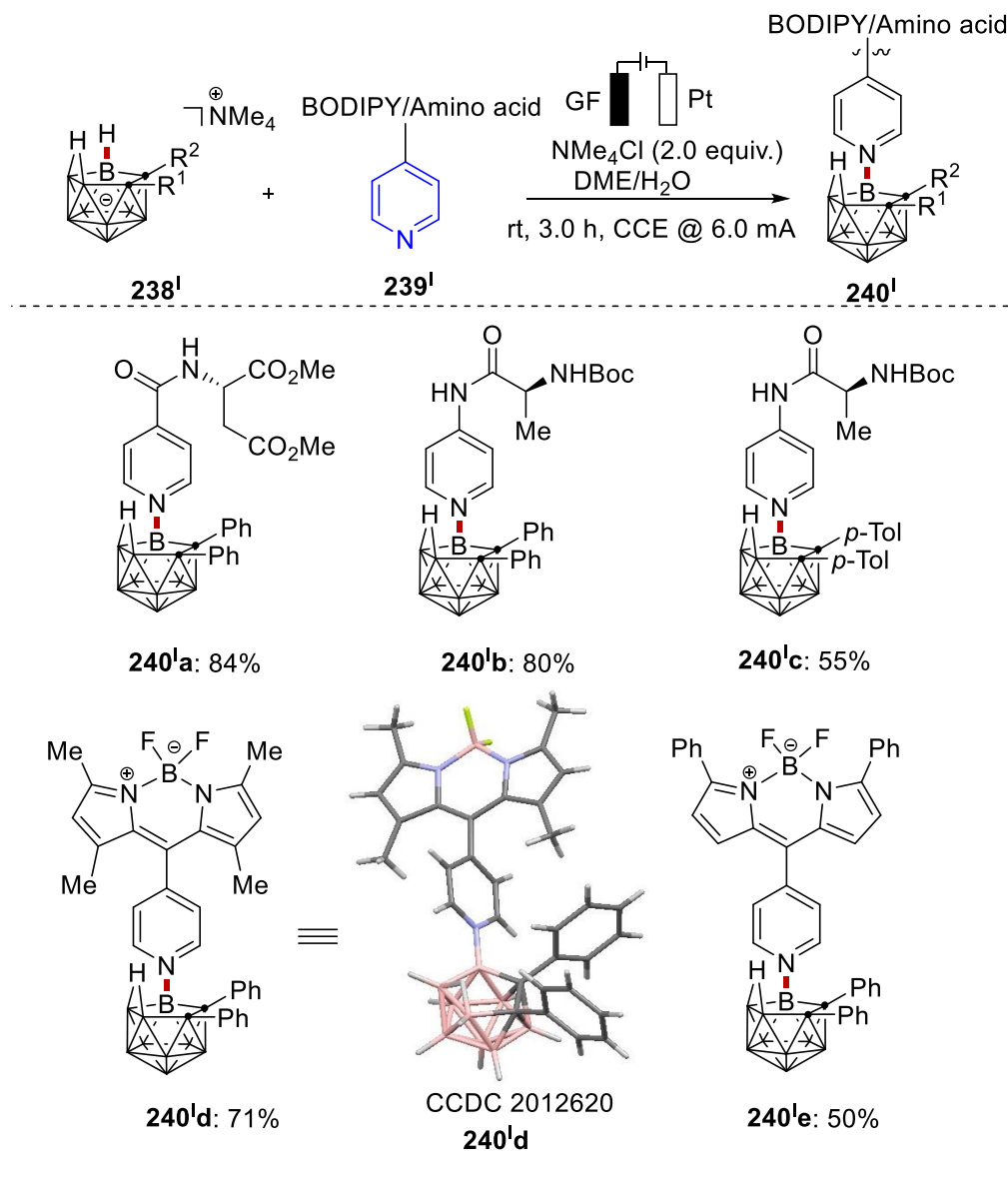
products in good to excellent yields (**240x-240aa**). Unfortunately, purines and quinine derivatives failed to undergo the desired transformation. In contrast, our regime was not limited to 1,2-diphenyl-*nido*-carboranes, as 1,2-dialkyl-*nido*-carboranes underwent our transformation, furnishing the corresponding B–N coupled products in good yields (**240bb-240cc**). Our established electrochemical oxidative B–N coupling provides a convenient and versatile route for the synthesis of *N*-heterocycle-containing *nido*-carboranes (Scheme 47b). Also, this established protocol is an intermediary step to access more complex *nido*-carborane-containing derivatives owing to the tolerance of functional groups, such as free amine and halides, which are suitable precursors to a variety of important functional groups.



Scheme 47b. Electrooxidative B-H nitrogenation of *nido*-carborane with *N*-heterocycles. (240u-240w, 240bb and 240cc by Dr Long Yang)

The wide functional group tolerance exhibited by our regime intrigued us to explore the robustness of our protocol to more decorated *N*-heterocyclic substrates. To our delight, pyridines with amino acid residues and BODIPY scaffolds were conveniently transformed to their corresponding products **240'a-240'e** (Scheme 48). This outcome highlighted prospective application of our protocol to the sustainable synthesis of complex *nido*-carborane

derivatives, such as highly conjugated fluorescent probes and *nido*-carborane-containing peptides.

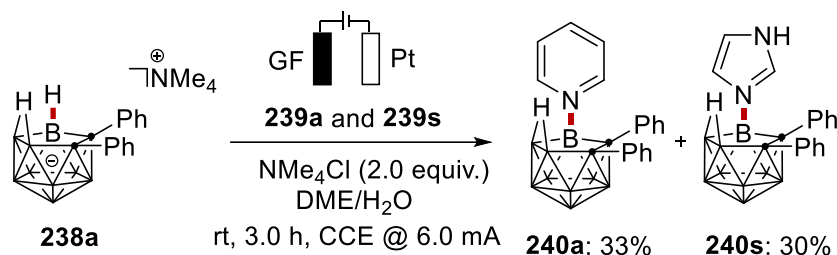


Scheme 48. Electrooxidative B–H nitrogenation of *nido*-carborane with amino acids and BODIPY pyridines. (**240^I a**, **240^Ib**, **240^Id** and **240^Ie** by Dr Long Yang)

3.1.2 Competition Experiments by Dr Long Yang

Motivated by the high efficiency of the electrocatalyzed B–N coupling of *nido*-carboranes with *N*-heterocycles, we were keen to understand the mode of action of our regime. Thus, our regime revealed a slight preference for pyridine over imidazole in an intermolecular competition experiment leading to the isolation of the corresponding products (**240a**, **240s**) in 33% and 30% yields, respectively. This could be attributed to the higher nucleophilicity of

pyridine ($N = 11.05$ in H_2O) as compared to that of imidazole ($N = 9.63$ in H_2O)^[187] (Scheme 50).



Scheme 49. Competition experiments (by Dr. Long Yang)

3.1.3 Cyclic Voltammetry and Stability of **240a**

To further delineate the mode of action of our electrocatalytic B–N coupling regime, cyclic voltammetric analysis of the *nido*-carborane was performed by MSc. Alexej Scheremetjew in the Ackermann group (Scheme 51). Thus, an irreversible oxidation of the *nido*-carborane at $E_{p/2} = 0.56$ V vs. Ag/Ag^+ at ambient temperature was observed. This was indicative of a direct oxidation of the *nido*-carborane under electrochemical conditions. Furthermore, computational studies using DFT calculations by Dr. Rositha Kuniyil revealed the calculated half-wave oxidation potential of **238a** at the B97D3/def2-QZVP+ CPCM(DME)//B97D3/def2-TZVP level of theory is in good agreement with the one observed in our CV studies (exp: $E_{p/2} = 0.87$ V vs. SCE, calc: $E_{1/2} = 0.86$ V vs. SCE). Also, compound **240a** was confirmed to be relatively stable as minor decomposition was observed after heating **240a** in 0.4 mL DMSO-d_6 to 120 °C for 10 h and treating the solution of **240a** (0.4 mL CD_3CN) with 0.1 mL H_2O , HCl , or NaOH , respectively. ^{11}B NMR experiments confirmed the excellent stability of **240a** in a neutral environment though not stable in strongly acidic or alkaline environments.

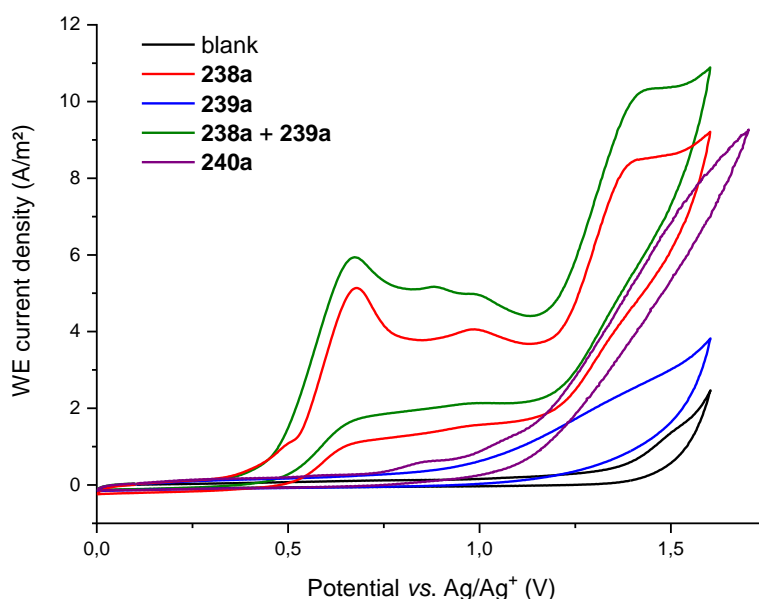


Figure 1. Cyclic voltammograms at 100 mV/s, $n\text{Bu}_4\text{NPF}_6$ (0.1M in DME), concentration of substrates 1.0 mM. CV was performed by MSc. Alexej Scheremetjew.

3.1.4 Spectroscopic Data of BODIPY-Labeled *nido*-Carborane

To further investigate the potential application of our BODIPY-labeled *nido*-carboranes **240'd** and **240'e** in fluorescent materials, UV-Vis absorption and fluorescence spectroscopic measurements was conducted in five different solvents (Table 2). It was observed that *nido*-carboranes **240'd** and **240'e** displayed intense absorption in the ultraviolet and visible region, with an absorption maximum between 507–582 nm and high Stokes shift. This could be rationalized by the possible donor-acceptor-donor structure of the compounds **240'd** and **240'e**, as the *nido*-carborane core is an electron acceptor. This data therefore was supportive of the potential applications of the thus-obtained BODIPY-labeled *nido*-carborane compounds in medicine, luminescent materials, and bioimaging.

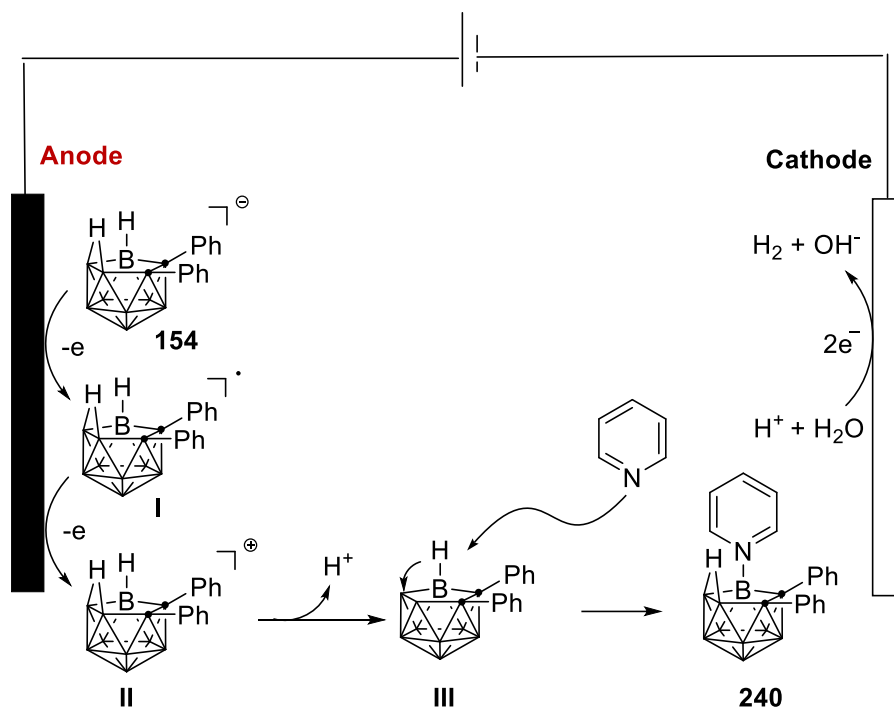
3 Results and Discussion

Table 2. Spectroscopic data of BODIPY-labelled *nido*-carboranes **240'd** and **240'e**.

Compound	Solvent	$\lambda_{\text{abs}}^{\text{Max}}$ [nm]	$\lambda_{\text{em}}^{\text{Max}}$ [nm]	Stokes shift [cm^{-1}]	ϵ_{max} [$\text{M}^{-1}\text{cm}^{-1}$]
240'd	DCM	512	569	1956	68812
	CHCl_3	513	567	1856	69790
	Acetone	507	559	1834	73746
	DMF	509	561	1821	69557
	THF	509	562	1852	72549
240'e	DCM	577	634	1558	63459
	CHCl_3	582	640	1557	60882
	Acetone	570	623	1492	65681
	DMF	574	602	810	58557
	THF	575	630	1518	67718

3.1.5 Proposed Mechanism

Based on the CV analysis, computational data and literature reports, a plausible reaction mechanism is proposed in Scheme 52. This commences with a single electron-transfer (SET) process from *nido*-carborane anion to form intermediate **I** at the anode. Next is the oxidation of intermediate **I** to generate intermediate **II**. Deprotonation of the bridge proton generates an open-cage carborane intermediate **III**. Lastly, nucleophilic attack on the electron-deficient B(9/11)–H site of intermediate **III** by pyridine with the consecutive hydrogen transfer to the B(10/11) furnishes a new bridge proton. This results in the generation of molecular H_2 , as the sole by-product through cathodic proton reduction as was confirmed by head-space GC analysis conducted by MSc. Alexej Scheremetjew.



Scheme 50. Proposed reaction mechanism.

3.2 Cupra-electro-catalyzed Cage Chalcogenation of *o*-Carboranes

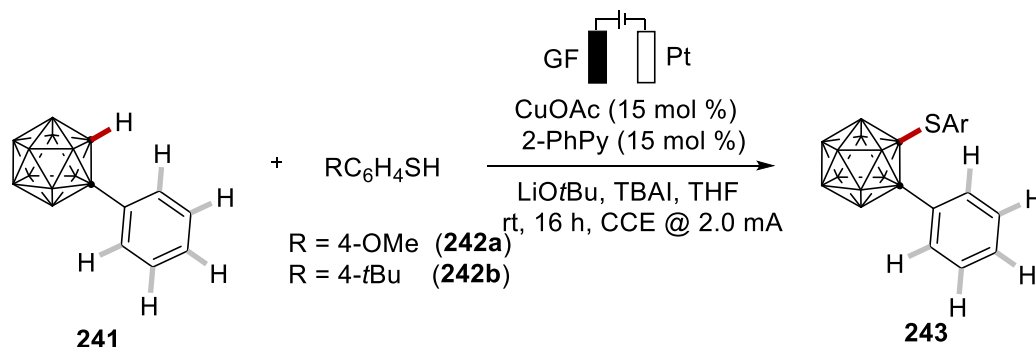
Sulfenylated/Selenylated carboranes have found wide-spread applications in optoelectronics where the chalcogen atom modulates the molecular band gap and induces charge transfer.^[188] The synthesis of chalcogen-coupled carboranes traditionally made use of stoichiometric amounts of organolithium reagents which renders these protocols largely impractical.^[189] In recent years, electrooxidative coupling^[190] and copper-assisted oxidative catalysis^[191] have proven promising for the construction of C–chalcogen bonds. Motivated by the growing need for advancement in sustainable synthesis, cupraelectrocatalysis stands the chances of being an ideal strategy for the synthesis of chalcogen-containing carboranes. An electro-assisted one-pot protocol for constructing cage C–S/C–Se bonds under mild conditions is unraveled through our findings, thereby highlighting the potential of cupraelectrocatalysis in the activation of inert cage C–H bonds of *o*-carboranes.

3.2.1 Optimization and Scope

At the onset of our studies, we probed various reaction conditions for our intended copper-catalyzed cage C–H thiolation of *o*-carborane in an operationally simple undivided cell setup equipped with a GF anode and a Pt cathode (Table 3). First, subjecting *o*-carborane **241** and aryl thiol **242** to a

system containing CuOAc as catalyst, 2-phenylpyridine as ligand, LiOtBu as the base, and *n*-Bu₄NI as the electrolyte at room temperature under a constant current of 2 mA furnished the thiolated carborane in 85 % isolated yields (entry 1). A decrease in yields was observed when alternative copper sources were used (entries 2-5). Notably, the dual role of *n*-Bu₄NI as an electrolyte and redox mediator was demonstrated in the failure of *n*-Bu₄NPF₆ to furnish the thiolated carborane (entry 6). In addition, it was observed that an increase in the amount of the electrolyte or use of KI had no positive impact on the catalytic efficiency of our cupra-electrocatalytic regime (entries 7,8). While no product was formed upon using DCE as the solvent, a drop in the catalytic performance was observed with CH₃CN as solvent (entries 9,10). Control experiments confirmed the indispensibility of electricity and the catalyst (entries 11,12). Interestingly, sequential procedure proved more favorable for the performance of our system (entries 13-15).

Table 3: Optimization of the reaction conditions.^[a]



Entry	Deviation from standard conditions	Yield [%] ^[b]
1	none	90% (85%) ^[c,g]
2	Cu(OAc) ₂ instead of CuOAc	51% ^[g]
3	CuI instead of CuOAc	43%
4	2,6-Lutidine instead of 2-PhPy	71% ^[g]
5	1,10-Phen instead of 2-PhPy	16% ^[g]
6	TBAPF ₆ instead of TBAI	--- ^[g]
7	TBAI (3 equiv.)	49%
8	KI (1 equiv) as additive	67%
9	DCE instead of THF	--- ^[g]

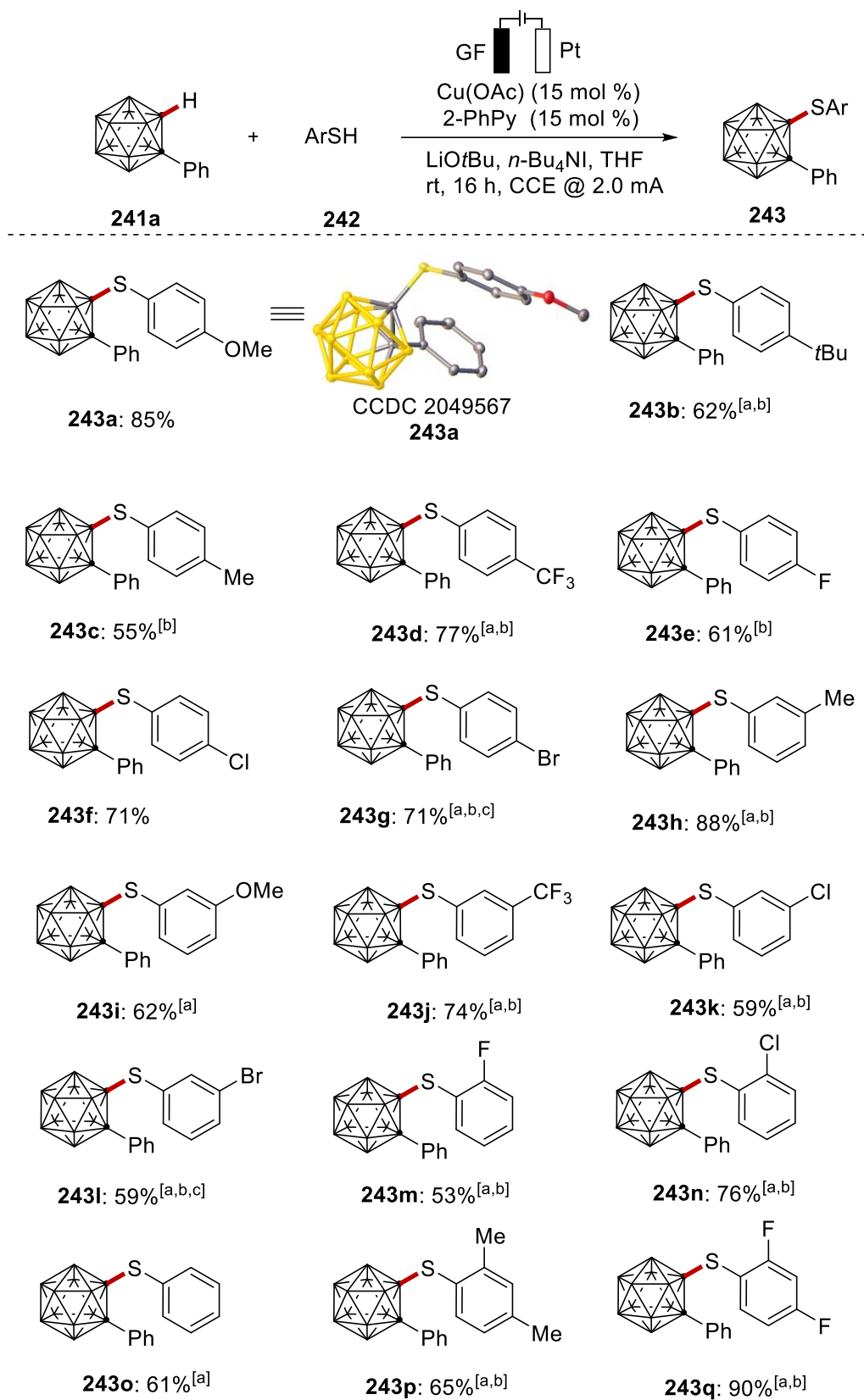
3 Results and Discussion

10	CH ₃ CN instead of THF	49% ^[g]
11	No electricity	14% ^[d,g]
12	No [Cu]	--- ^[g]
13	Procedure B (242b)	66% (62%) ^[e,d,g]
14	Procedure B: second step without electricity (242b)	--- ^[f,g]
15	Procedure B (242a)	92% ^[e,g]

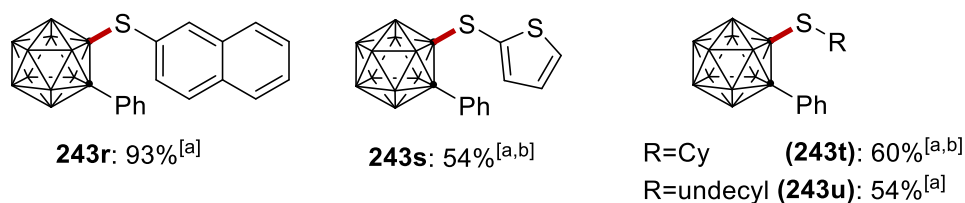
[a] Reaction conditions: Procedure A: **241a** (0.10 mmol), **242a** (0.3 mmol), CuOAc (15 mol %), 2-PhPy (15 mol %), LiOtBu (0.2 mmol), TBAI (2.0 equiv.), solvent (3.0 mL), platinum cathode (10 mm × 15 mm × 0.25 mm), graphite felt (GF) anode (10 mm × 15 mm × 6 mm), 2 mA, under air, rt, 16 h. [b] Yield was determined by ¹H NMR with CH₂Br₂ as the internal standard. [c] Isolated yields in parenthesis. [d] KI (1.0 equiv) as additive. [e] Procedure B: **241a** (0.3 mmol), LiOtBu (0.2 mmol), TBAI (2.0 equiv), solvent (3.0 mL), 2 mA, rt, 3 h, then adding **241a** (0.10 mmol), 2-PhPy (15 mol %), CuOAc (15 mol %), 2 mA, rt, 16 h. [f] **242b** (0.3 mmol), LiOtBu (0.2 mmol), KI (1.0 equiv.), TBAI (2.0 equiv.), solvent (3.0 mL), 2 mA, rt, 3 h, then adding **241a** (0.10 mmol), 2-PhPy (15 mol %), CuOAc (15 mol %), rt, 16 h. [g] performed by Dr. Long Yang

With the optimized reaction conditions in hand, we explored the versatility of the cage C–H thiolation of *o*-carborane **241a** with different thiols **242** (Scheme 53). The viability of our approach with differences in electronic properties as well as substitution patterns of the arylthiols **242** were thus investigated. First, electron-rich and electron-deficient substituents on the arenes were found suitable for the electrocatalyzed C–H activation, providing the corresponding thiolated carboranes **243a-243o**. This led to the synthesis of a variety of thiolated *o*-carboranes anchoring easily transformable functional groups, such as fluoro (**243e** and **243m**), chloro (**243f**, **243k**, and **243n**), and bromo (**243g** and **243l**), thereby making them suitable for late-stage modifications. In addition, disubstituted aryl thiols and heterocyclic thiols afforded the corresponding cage-thiolated products (**243p-243s**) in quantitative yields. Notably, aliphatic thiols efficiently underwent the electrochemical transformation to provide the corresponding cage alkyl-thiolated products (**243t-243u**).

3 Results and Discussion

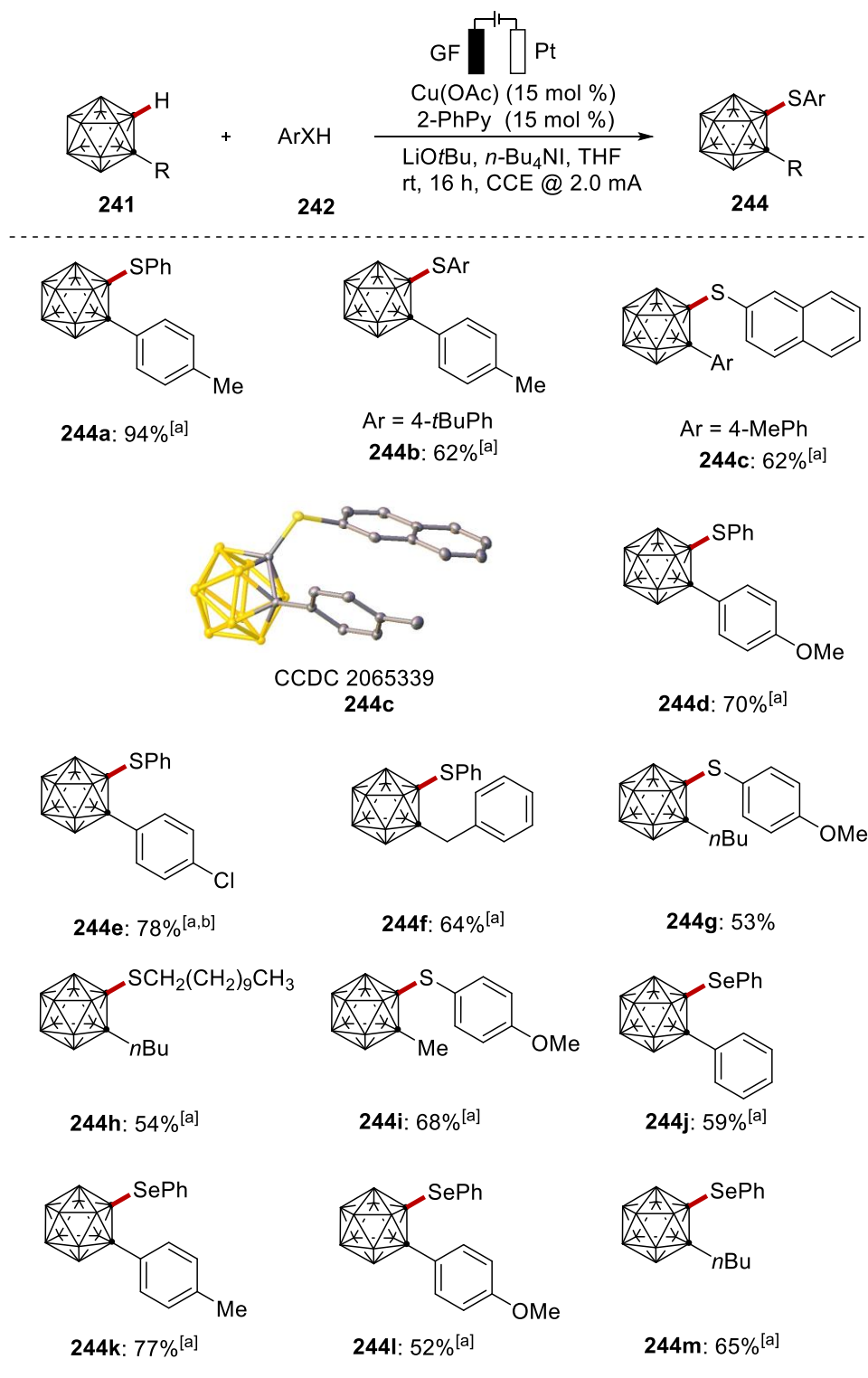


3 Results and Discussion



Scheme 51. Electrochemical C–H thiolation of *o*-carborane. ^[a] Procedure B. ^[b] KI (1 equiv.). ^[c] CuI as the catalyst. (**243a**, **243b**, **243e**, **243f**, **243i**, **243m**, **243o**, **243s**, and **243u** performed by Dr Long Yang)

Motivated by the efficiency of the cupraelectro-oxidative regime in the cage C–H thiolation of *o*-carboranes, we became keen to explore the sulfenylation and C–H selenylation of differently decorated *o*-carboranes **241** (Scheme 54). Electronically diverse *o*-carboranes **241** served as competent coupling partners, giving the corresponding thiolation products (**243a–243e**) with high efficacy and high positional selectivity. The strategy was not restricted to phenyl-substituted *o*-carboranes, as substrates bearing benzyl and even alkyl groups underwent transformation to deliver the desired products (**243f–243i**). It is noteworthy that the C–H activation approach also proved compatible with a selenol to give the *o*-carborane **243j**.

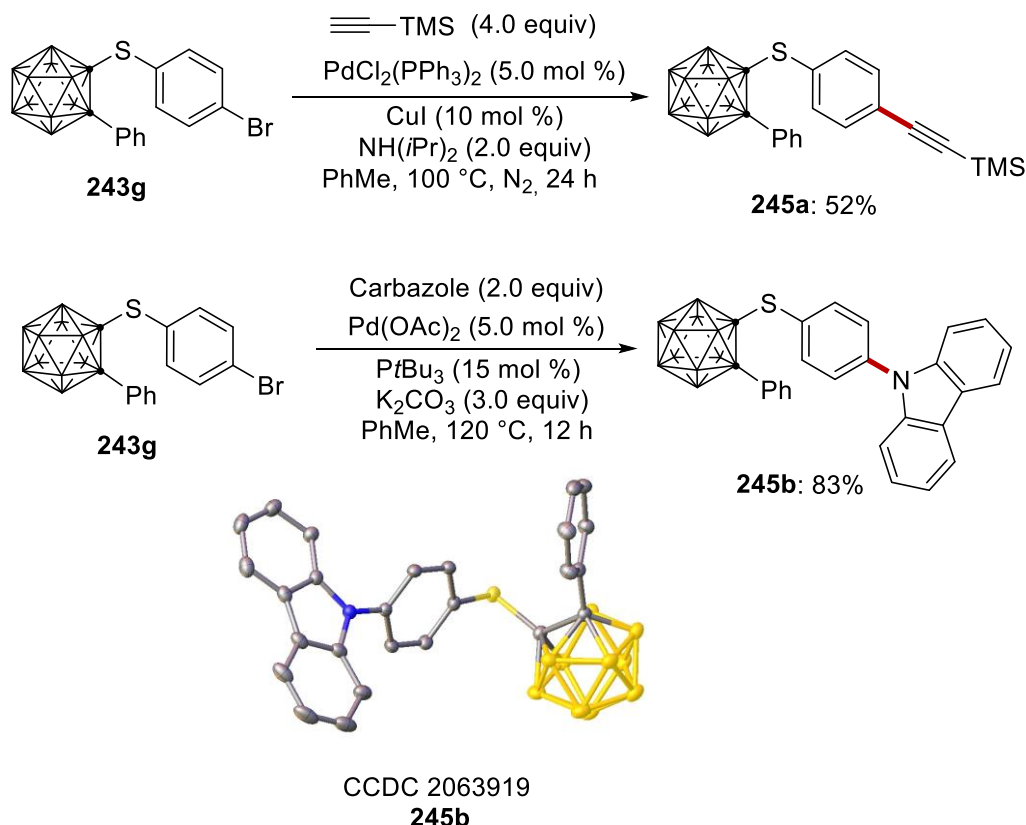


Scheme 52. Electrochemical C–H chalcogenation of *o*-carboranes. ^[a] Procedure B. ^[b] KI (1 equiv.). (**244b**, **244f–244m** performed by Dr. Long Yang).

3.2.2 Late-Stage Functionalization

Considering the role of aryl halides as suitable electrophilic coupling partners, the late-stage functionalization of the thus-obtained carborane **243g** was studied. Sonogashira-Hagihara coupling^[192] of carborane **243g** with

trimethylsilylacetylene gave the alkynylated derivative **245a** in good yield (Scheme 54). Also, Buchwald-Hartwig amination^[11] of carborane **243g** with carbazole furnished the amine **245b** in excellent yield, thereby unveiling a new route to access cage C-substituted carborane-based host materials for possible applications to phosphorescent organic light-emitting diodes.^[193]



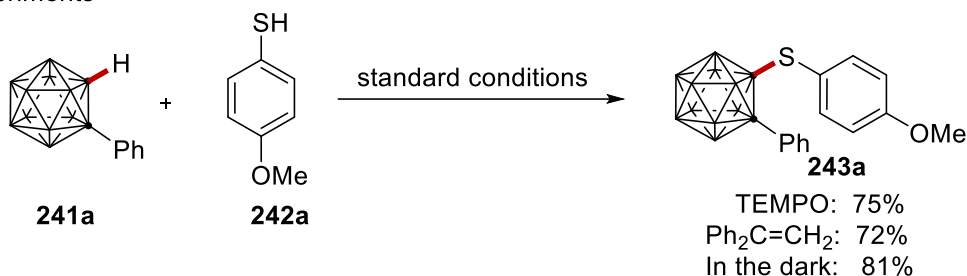
Scheme 53. Late-stage diversification (by Dr Long Yang).

3.2.3 Control Experiments and Cyclic Voltammograms

The high efficacy of the cupraelectro-catalyzed cage C–H chalcogenation motivated us to delineate the mode of action. To this end, control experiments were performed by Dr. Long Yang (Scheme 55). Electrocatalysis in the presence of TEMPO or $\text{Ph}_2\text{C}=\text{CH}_2$ gave the desired product **243a**. In addition, the cupraelectro-catalysis occurred efficiently in the dark. Furthermore, detailed cyclovoltammetric analysis of the thiol and iodide mediator by MSc. Alexej Scheremetjew (figure 3) showed an irreversible oxidation of the thiol anion at $E_p = -0.62\text{ V}$ vs. Ag/Ag^+ and two oxidation events for the iodide at $E_p = 0.12\text{ V}$ vs. Ag/Ag^+ and $E_p = 0.44\text{ V}$ vs. Ag/Ag^+ . This agrees with the literature

reported iodide oxidation potential^[104, 194] and is suggestive of the preferential oxidation of the iodide as redox mediator. Moreover, the use of *n*-Bu₄NI as a redox mediator to achieve copper-catalyzed electrochemical C–H amination of arenes was also documented.^[104]

Control experiments



Scheme 54. Control experiments (by Dr. Long Yang)

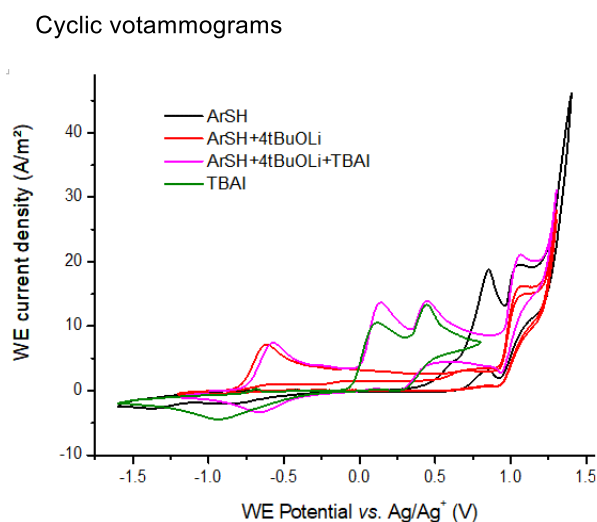
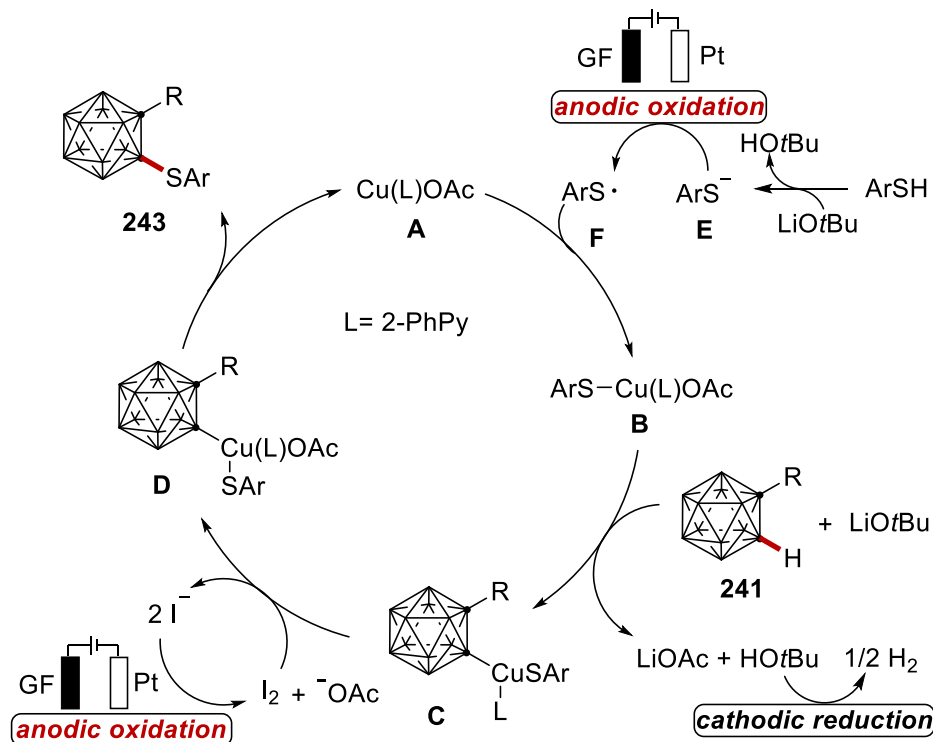


Figure 3. Cyclic voltammograms (CV studies were done by MSc. Alexej Scheremetjew)

3.2.4 Proposed Mechanism

Based on our findings, a plausible reaction mechanism is proposed in Scheme 56. Our reaction commences with an anodic single electron-transfer (SET) oxidation of the thiol anion **E** to form the sulfur-centered radical **F**. Subsequently, the copper(I) species **A** reacts with the sulfur radical **F** to deliver copper(II) complex **B**, which then reacts with *o*-carborane **241a** in the presence of LiO*t*Bu to generate a copper(II)-*o*-carborane complex **C**. The complex **C** is then oxidized by the anodically generated redox mediator I₂ to

furnish the copper(III) species **D**, which in turn undergoes reductive elimination, generating the final product **242** to regenerate the catalytically active complex **A**. Alternatively, the direct oxidation of copper(II) complex **C** by electricity to generate copper(III) species **D** can not be excluded at this stage.



Scheme 55. Proposed reaction mechanism.

3.3 Manganese-Catalyzed Selective Peptide Labeling with o-Carboranes via C–H Activation.

The extensive application of peptides in cancer therapy and carboranes in boron neutron capture therapy (BNCT) has attracted interest in the selective assembly of carborane-containing peptides. The synthesis of 1-alkenyl-o-carboranes have been achieved with different reactions, such as the condensation of decaborane with alkenes,^[195] Ullmann-type coupling,^[196] and Wittig-type reactions.^[197] In addition, nickel-mediated cross-coupling,^[198] and organophosphine catalysis^[199] have proven viable for the construction of 1-alkenyl-o-carboranes. However, these protocols suffered from limitations such as the use of stoichiometric amounts of nickel salts, organolithium reagents, long reaction time required, and a strong dependence of the reactivity on the electronic properties of the alkene substrate. Therefore, there is need to explore the versatility of more sustainable strategies to access 1-alkenyl-o-

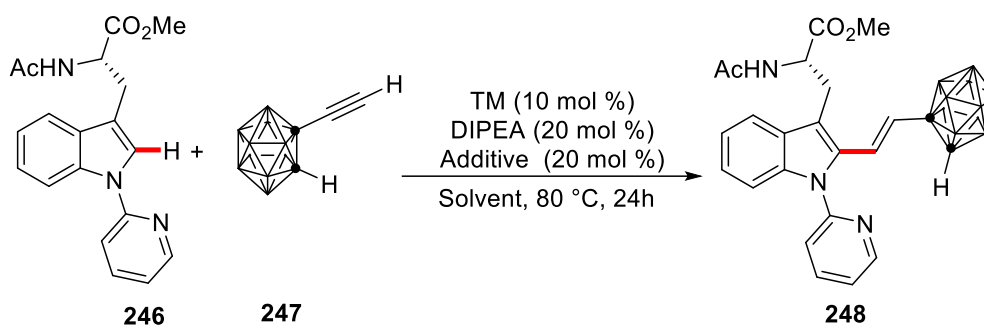
carboranes. With the above-mentioned successes of manganese catalysis in the selective hydroarylation of C–H bonds, a regime that enables the labeling of simple as well as complex peptides using earth-abundant, cost-efficient manganese(I) catalyst was developed. We also present a robust protocol that yields novel boron neutron capture agents.

3.3.1 Optimization and Scope

We commenced our studies with a system consisting of tryptophan **246a** with *o*-carboranyl alkyne **247a** in the presence of a $\text{MnBr}(\text{CO})_5$, PhCO_2H , and DIPEA in Et_2O at 80 °C for 24 h. The manganese(I) catalyst successfully furnished the carborane-labeled alkenylated tryptophan **250a** in 74% isolated yield (entry 1). An improvement in yield of the alkene **250a** to 81% was observed with AcOH as the additive (entry 2). In addition, altering the solvent from Et_2O to 1,4-dioxane resulted in an appreciable increase in the catalytic efficiency (entry 3). Comparatively, NaOAc was shown to be less effective as compared to AcOH (entry 4). Additionally, we investigated the efficacy of other transition metal catalysts, such as $(\text{ReBr}(\text{CO})_5)$, $[\text{Cp}^*\text{RhCl}_2]_2$, and $(\text{Mn}_2(\text{CO})_{10})$, in the C-2 selective alkenylation. Interestingly, the formation of product **250a** was only enabled by $\text{MnBr}(\text{CO})_5$ (entries 5-7). Furthermore, an increase in the reaction temperature to 100 °C diminished the efficacy of our manganese(I) catalyst (entry 8). Control experiments revealed the importance of each component of the system. First, the principal role of the manganese(I) catalyst was indisputably reflected by the inability to achieve the transformation in the absence of the metal catalyst (entry 9). Second, the unique role of the additive in the manganese(I) regime was expressed in a drastic drop in the yield in its absence (entry 10). Next, the robust and user-friendly nature of manganese(I) catalysis allowed the catalysis to proceed efficiently under air (entry 11). The catalysis was effective in the absence of DIPEA (96%, entry 12). Overall optimal yields were obtained with an equimolar amount of substrates **246a** and **247a** with $\text{MnBr}(\text{CO})_5$ (10 mol %) as catalyst, with AcOH (20 mol %) in 1,4 dioxane at 80 °C for 16 h (entry 12).

3 Results and Discussion

Table 4: Optimization of the reaction conditions.^[a]



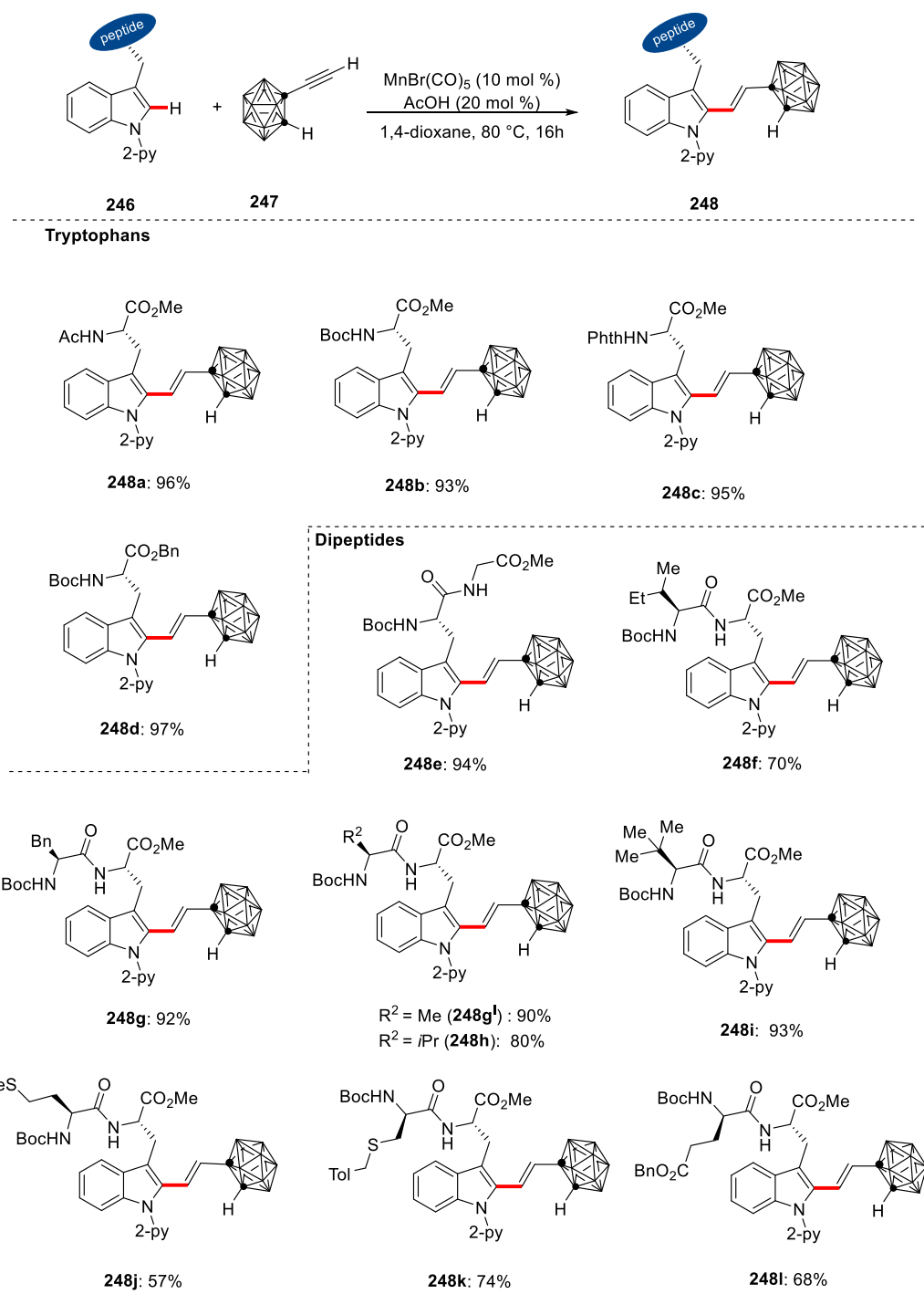
Entry	TM	Additive	Solvent	yield (%)
1	MnBr(CO) ₅	PhCO ₂ H	Et ₂ O	74
2	MnBr(CO) ₅	AcOH	Et ₂ O	81
3	MnBr(CO) ₅	AcOH	1,4-dioxane	94
4	MnBr(CO) ₅	NaOAc	1,4-dioxane	85
5	Mn ₂ (CO) ₁₀	AcOH	1,4-dioxane	---
6	ReBr(CO) ₅	AcOH	1,4-dioxane	---
7	[Cp*RhCl ₂] ₂	AcOH	1,4-dioxane	---
8	MnBr(CO) ₅	AcOH	1,4-dioxane	80 ^[b]
9	---	AcOH	1,4-dioxane	---
10	MnBr(CO) ₅	---	1,4-dioxane	28
11	MnBr(CO) ₅	AcOH	1,4-dioxane	94 ^[c]
12	MnBr(CO) ₅	AcOH	1,4-dioxane	96 ^[d]

[a] Reaction conditions: **246a** (0.10 mmol), **247a** (0.10 mmol), MnBr(CO)₅ (10 mol %), AcOH (20 mol %), DIPEA (20 mol %) solvent (1.0 mL), under N₂, 80 °C, 24 h. Isolated yields are reported. [b] At 100 °C. [c] Under air. [d] No DIPEA for 16 h.

With the optimized reaction conditions in hand, we were excited to explore the robustness of our manganese(I) catalyst (Scheme 55). Generally, excellent *E*-stereoselectivity of >20/1 was observed for most of the products. First, *N*-protected tryptophans with Boc, acetyl, and the phthalimide groups **248a**, **248b**, and **248c**, respectively, were transformed into the desired products in excellent yields. The removable benzyl ester was also transformed into the desired product **248d** in excellent yield. It is worthy of note that the manganese catalyst was tolerant to a variety of dipeptides furnishing the

3 Results and Discussion

desired products, without jeopardizing the tolerance of sensitive functional groups on the amino acid side chains. The robustness of the manganese(I) catalyst was hence highlighted with the successful transformation of dipeptides with alkyl side chains (**248f-248i**), and oxidation-sensitive groups found in methionine (**248j**), and modified cysteine (**248k**).

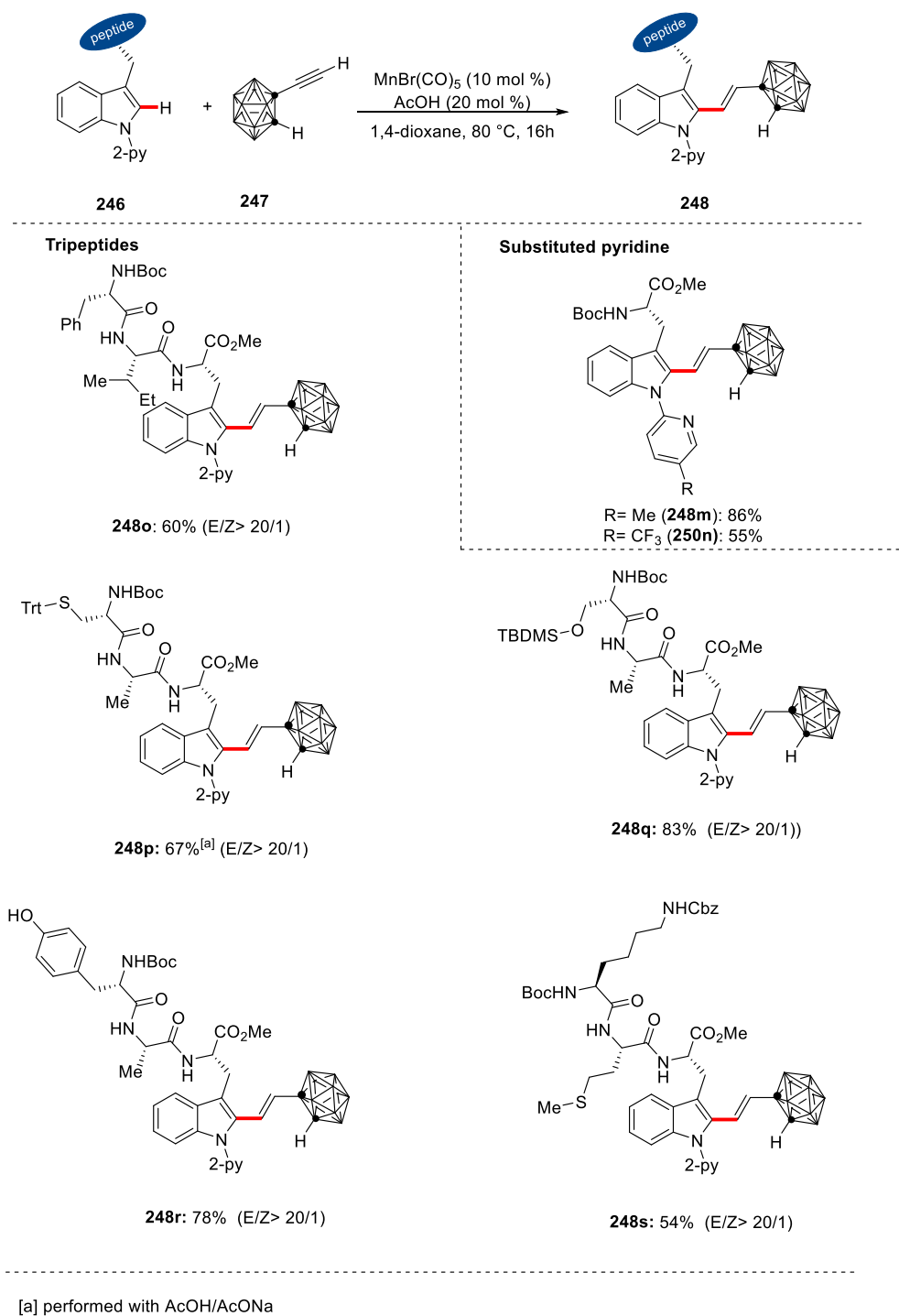


Scheme 56. Manganese-catalyzed alkenylation of tryptophan derivatives and peptides (**248h**, **248i**) by Dr. Long Yang).

Furthermore, we were keen to investigate the effect of electronic properties of the substrate on our manganese(I) regime. To our delight, electron-donating (Me: **248m**) and electron-withdrawing (CF₃: **248n**) substituents on the pyridine directing group successfully furnished the desired products in good yields.

To ascertain the validity of our manganese(I) catalysis to structurally complex substrates, we extended our scope to include tripeptides. Interestingly, tripeptides with hydroxyl groups, such as tyrosine (**248r**) and O-silylated serine (**248q**) furnished the alkenylated peptides with high chemo- and *E*-stereoselectivities. In addition, protected cysteine-containing tripeptide (**248p**) also afforded the desired product in the presence of AcOH/AcONa buffer system in good yields.

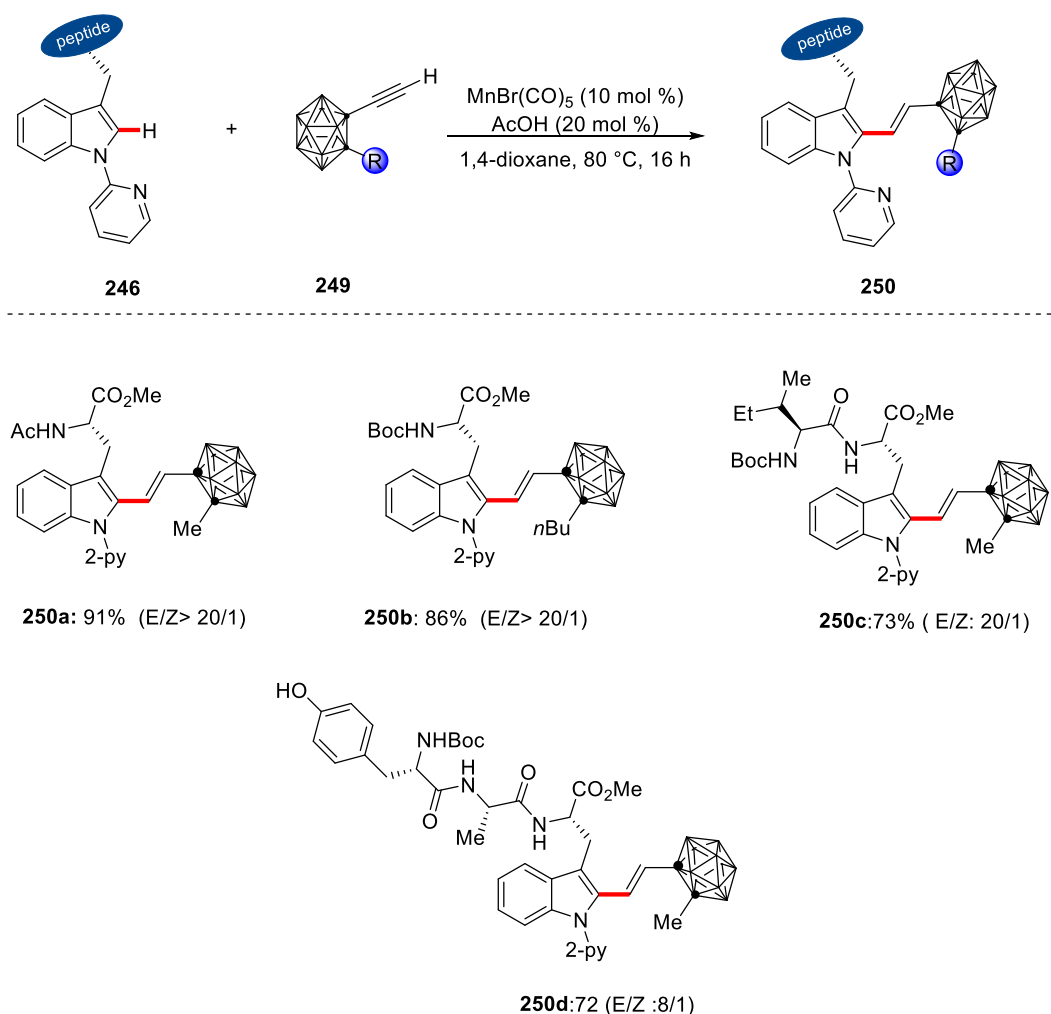
3 Results and Discussion



Scheme 57. Manganese(I)-catalyzed alkenylation of tryptophan derivatives and peptides

Next, we probed the effect of different alkyl substituents on the 2-*o*-carboranyl cage carbon (Scheme 57). Hence, methyl and *n*-butyl decorated *o*-carboranes selectively furnished the products with the amino acid **250a** and **250b**, dipeptide **250c**, and tripeptide **250d**, respectively.

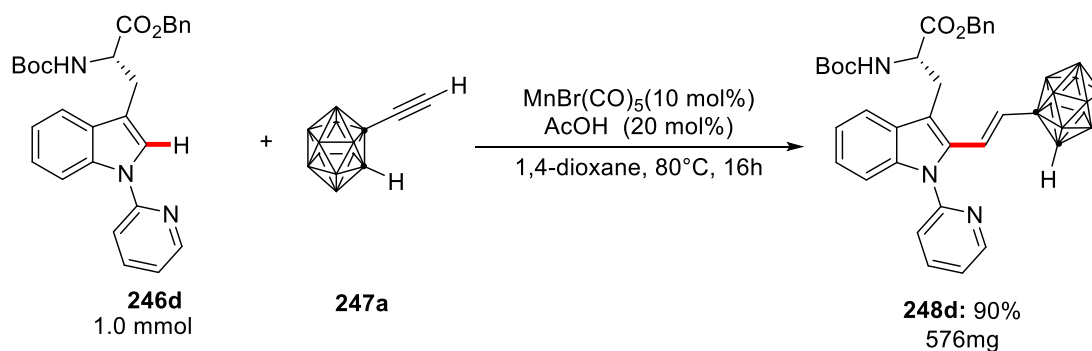
3 Results and Discussion



Scheme 58. Manganese(I)-catalyzed alkenylation of tryptophan derivatives and peptides

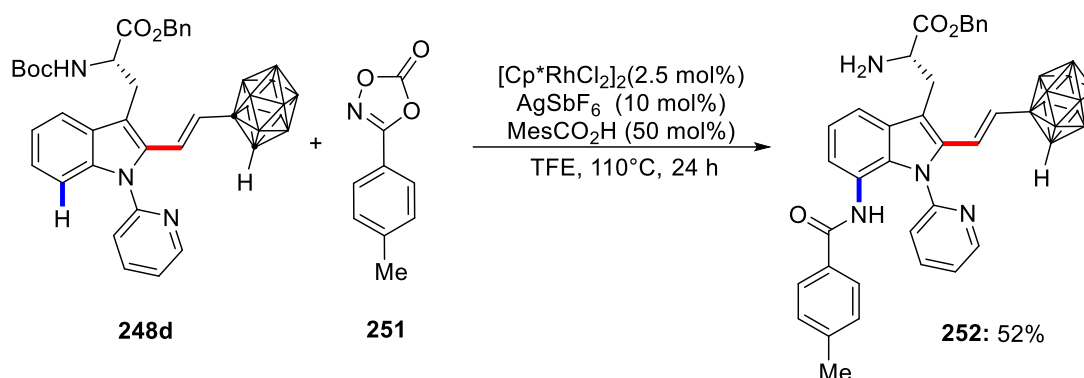
3.3.2 Scale up Reaction and Late-Stage Amidation

The applicability of our approach on a 1.0 mmol scale was demonstrated for the manganese(I) catalysis. Interestingly, the alkenylated product **248d** was isolated in high yield (Scheme 58).



Scheme 59. 1.0 mmol scale manganese(I)-catalyzed C–H alkenylation

At this stage, the possible derivatization of our obtained products was of key importance to us. We, therefore, subjected the thus-obtained amino acid **248d** to a slightly modified rhodium(III) catalysis as reported in literature.^[74] The C-7 amidation of **248d** was successfully achieved to afford NH₂-free amine **252** in good yield (Scheme 59). This presents a promising strategy to access more complex peptides through subsequent coupling of **252** with other amino acid residues.

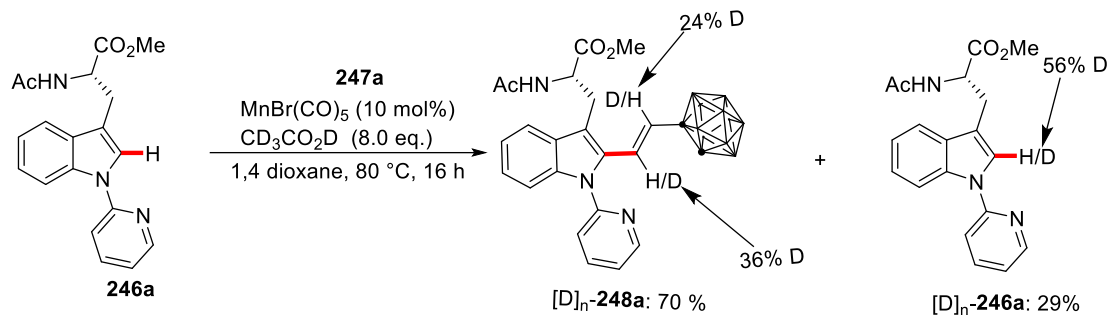


Scheme 60. C-7 Late-stage C–H amidation of conjugated **248d**

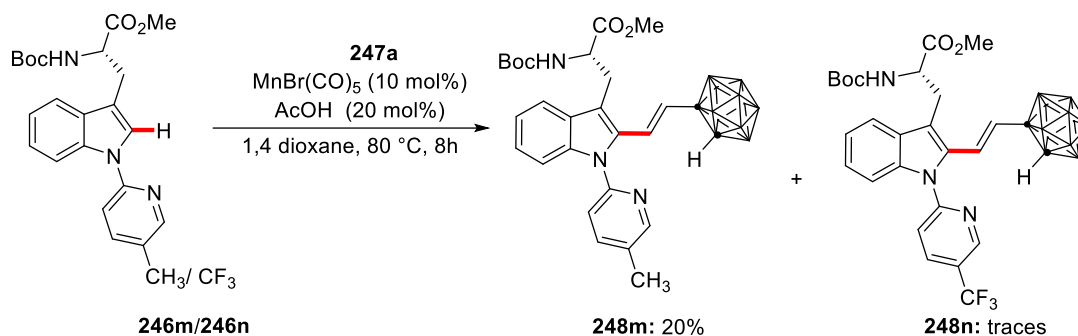
3.3.3 Mechanistic Studies

Given the unique selectivity of our manganese(I) catalysis regime, we became interested to ascertain the catalyst's mode of action. First, A notable H/D scrambling at the C-2 position of the indole moiety was observed in the re-isolated [D]_n-**246**, as was confirmed by ¹H NMR in the presence of excess deuterated acetic acid. This was supportive of a reversible C-2–H activation step. Second, deuterium incorporation was also observed for the olefinic protons of product [D]_n-**248a** (Scheme 60a), supporting the existence of H/D exchange in the reaction. Third, an intermolecular competition experiment revealed a preferential reactivity of electron-donating substituent **246m** over the electron-withdrawing group **246n** on the pyridine directing group (Scheme 60b).

a) Deuterium scrambling for C–H



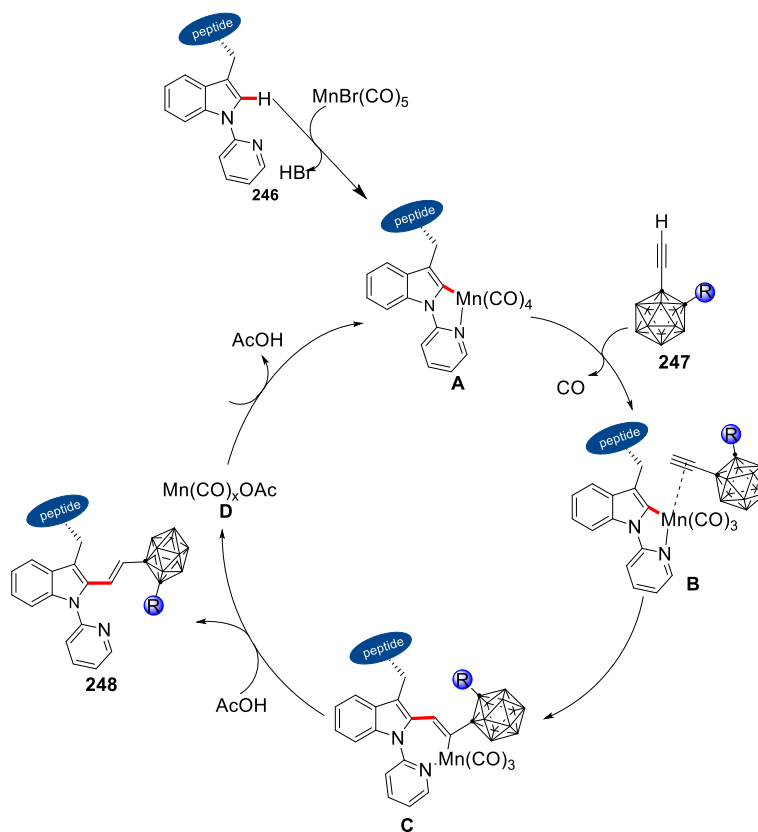
b) Intermolecular competition experiment



Scheme 61. a) H/D exchange experiments; b) intermolecular competition experiments.

3.3.4 Proposed Mechanism

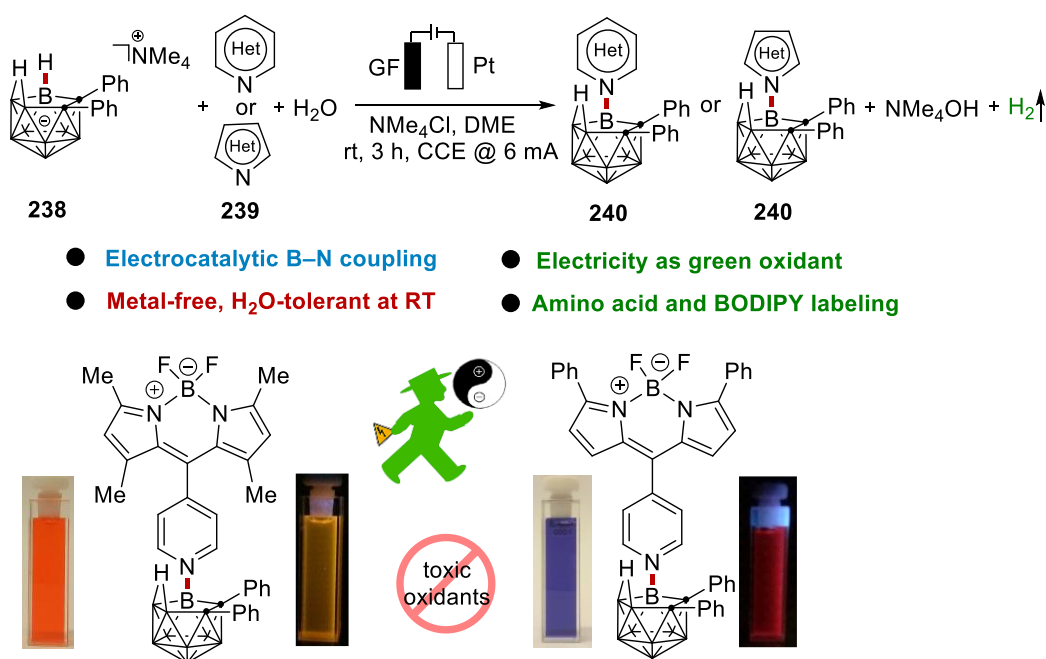
Based on our studies,^[46] I propose the C-2 selective manganese(I)-catalyzed alkenylation to proceed as follows. The reaction commences with the reversible C-2–H activation by the manganese(I) complex to give the cyclometalated complex **A**. Next, the addition of alkyne **247** to complex **A** results in the formation of complex **B**, which undergoes migratory insertion of the alkyne at C-2 to form the seven-membered cyclometalated complex **C**. Proto-demetalation from acetic acid furnishes the desired product **248**. Concurrently, complex **D** is generated and releases the acetate, which further reacts with tryptophan **246** and alkyne **247** to regenerate complex **B** (Scheme 61).



Scheme 62. Proposed catalytic cycle

4. Summary and Outlook

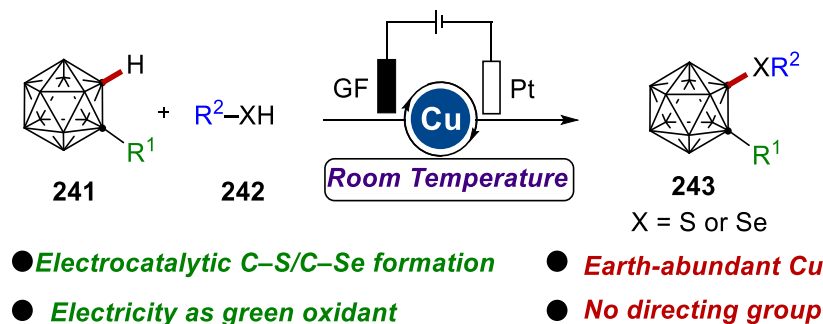
We established the metal-free electrocatalyzed direct B–H oxidative functionalization of *nido*-carborane with *N*-heterocyclic compounds at room temperature with molecular hydrogen as the sole by-product (Scheme 62). The key features of this protocol were mild reaction conditions, high functional group tolerance, and environmentally-friendly access to various amino acid- and BODIPY-labeled *nido*-carboranes. Cyclic voltammetry studies and computational calculations provided support for a plausible mechanism. In addition, the thus-obtained BODIPY-labeled *nido*-carborane displayed enhanced spectroscopic features thereby presenting their potential for application in optoelectronic materials, cancer therapy and bioimaging. Furthermore, the successful coupling of privileged scaffolds in drugs, such as pyridine, isoquinolines and indazoles, also highlighted their possible application in diverse pharmaceutical formulations.



Scheme 63. Electrocatalyzed B–H nitrogenation of *nido*-carboranes.

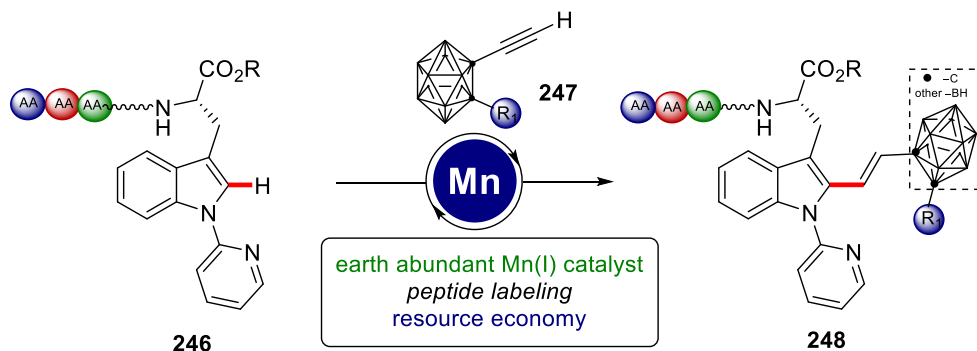
Second, an efficient and operationally-feasible electrocatalytic organometallic cage C–H chalcogenation of *o*-carboranes at room temperature with thiols and selenols has been achieved (Scheme 63). The notable features of this protocol include mild reaction conditions, high functional group tolerance, facile assembly of a series of *o*-carboranes, and a potential platform for the

design of cage C–S/Se substituted *o*-carboranes by environmentally-sound electricity. A plausible mechanism was proposed based on data from control experiments, cyclic voltammetry studies, and electron paramagnetic resonance (EPR) studies. The developed strategy is considered as the basis to further investigate the versatility of electrocatalysis and 3d metallalectrocatalysis cage C–H activation to access more decorated carborane derivatives.



Scheme 64. Cupraelectro-catalyzed C–H chalcogenation of *o*-carboranes **243**.

Finally, we have developed the first manganese(I)-catalyzed direct alkenylation to access *o*-carborane-decorated tryptophan-containing peptides to assemble structurally complex boron-rich peptides (Scheme 64). The strategy is atom-economical, cost-efficient, and demonstrates excellent chemo/stereo-selectivity therefore presents prospects of extension to other earth-abundant 3d transition metals. The novel synthesized boron-rich compounds are available for further modification with the prospects for future applications as potential candidates for anti-cancer therapy within a boron neutron capture therapy.



Scheme 65. Manganese(I)-catalyzed labeling of peptides (**246**) with *o*-carboranes **247**.

5 Experimental Section

5.1 General Remarks

Catalytic reactions under an atmosphere of air were conducted in sealed or Schlenk tubes. Unless stated otherwise, other reactions were performed under N₂ atmosphere using pre-dried glassware and standard Schlenk techniques.

If not stated otherwise, yields refer to isolated compounds estimated to be >95% pure as determined by ¹H NMR.

Vacuum

The following pressures were measured on the used vacuum pump uncorrected: membrane pump vacuum (MPV): 0.5 mbar, oil pump vacuum (OPV): 0.1 mbar.

Melting Points (M.p.)

Melting points were measured using a *Stuart*® Melting Point Apparatus *SMP3* from BARLOWORLD SCIENTIFIC. The reported values are uncorrected.

Chromatography

Analytical thin layer chromatography (TLC) was performed on 0.25 mm silica gel 60F-plates (MACHEREY-NAGEL) with a 254 nm fluorescent indicator from MERCK. Plates were visualized under UV light. Chromatographic purification of products was accomplished by flash column chromatography on MERCK silica gel, grade 60 (0.040–0.063 mm and 0.063–0.200 mm).

Gas Chromatography (GC)

The conversions of the reactions were monitored by applying coupled gas chromatography/mass spectrometry using G1760C GCDplus with mass detector *HP 5971, 5890 Series II* with mass detector *HP 5972* from HEWLETT-PACKARD and 7890A *GC-System* with mass detector *5975C (Triplex-Axis-Detector)* from AGILENT TECHNOLOGIES equipped with *HP-5MS* columns (30 m × 0.25 mm × 0.25 m).

Gel Permeation Chromatography (GPC)

GPC purifications were performed on a JAI system (JAI-LC-9260 II NEXT) equipped with two sequential columns (*JAIGEL-2HR*, gradient rate: 5.000; *JAIGEL-2.5HR*, gradient rate: 20.000; internal diameter = 20 mm; length = 600 mm; Flush rate = 10.0 mL/min and chloroform (HPLC-quality with 0.6% ethanol as stabilizer) was used as the eluent.

Chiral High-Performance Liquid Chromatography (HPLC)

Chiral HPLC chromatograms were recorded on an Agilent 1290 Infinity using CHIRALPAK® IA-3, IB-3, IC-3, ID-3, IE-3, and IF-3 columns (3.0 μm particle size; \varnothing : 4.6 mm and 250 mm length) at ambient temperature.

Infrared Spectroscopy

Infrared spectra were recorded with a BRUKER *Alpha-P ATR FT-IR* spectrometer. Liquid samples were measured as a film and solid samples neat. The analysis of the spectra was carried out using the software from BRUKER *OPUS 6*. The absorption was reported in wave numbers (cm^{-1}), and the spectra were recorded in the range 4000–400 cm^{-1} .

Mass Spectrometry

Electron-ionization (EI) mass spectra were recorded on a Jeol AccuTOF instrument at 70 eV. Electrospray-ionization (ESI) mass spectra were obtained on Bruker micrOTOF and maXis instruments. All systems were equipped with time-of-flight (TOF) analyzers. The ratios of mass to charge (m/z) were reported, and the intensity relative to the base peak ($I = 100$) is given in parenthesis.

Nuclear Magnetic Resonance Spectroscopy (NMR)

Nuclear magnetic resonance (NMR) spectra were recorded on Bruker Avance Neo 600, Bruker Avance III HD 500, Bruker Avance III HD 400, Bruker Avance III 400, Bruker Avance Neo 400, Bruker Avance III HD 300, Bruker Avance III 300 and *HD 500* spectrometers. All chemical shifts were given as δ -values in ppm relative to the residual proton peak of the deuterated solvent or its carbon atom. ^1H and ^{13}C NMR spectra were referenced using

the residual proton or solvent carbon peak (see table), respectively. ^{13}C and ^{19}F NMR were measured as proton-decoupled spectra.

	^1H NMR	^{13}C NMR
CDCl_3	7.26	77.16
$[\text{D}]_6\text{-DMSO}$	2.50	39.52

The observed resonance-multiplicities were described using the following abbreviations: s (singlet), d (doublet), t (triplet), q (quartet), hept (heptet), m (multiplet), or analogous representations. The coupling constants J were reported in Hertz (Hz). Analysis of the recorded spectra was carried out with *MestReNova 10* software.

EPR Spectroscopy

EPR spectra were measured on a Bruker ELEXSYS E500 spectrometer, equipped with the digital temperature control system ER 4131VT using nitrogen as the coolant. All spectra were measured at room temperature or temperatures around 150K and were recorded at about 9.4 GHz microwave frequency, 100 kHz field modulation frequency, and around 10 mW microwave power.

Electrochemistry

Platinum electrodes (10 mm × 15 mm × 0.25 mm, 99.9%; obtained from ChemPur® Karlsruhe, Germany) and graphite felt (GF) electrodes (10 mm × 15 mm × 6 mm, SIGRACELL®GFA 6 EA, obtained from SGL Carbon, Wiesbaden, Germany) were connected using stainless steel adapters. Electrolysis was conducted using an AXIOMET AX-3003P potentiostat in constant current mode. For reactions performed with the standardized electrochemistry kit, *ElectraSyn 2.0* from Ika, the commercialized electrodes and 10 mL undivided cells were used, if not stated otherwise. CV studies were performed using a Metrohm Autolab PGSTAT204 workstation and Nova 2.0 software. Divided cells separated by a P4-glassfrit were obtained from Glasgerätebau Ochs Laborfachhandel e. K. (Bovenden, Germany).

Solvents

All solvents for reactions involving moisture-sensitive reagents were dried, distilled and stored under inert atmosphere (N₂) according to the following standard procedures. Purified by solvent purification system (SPS-800, M. Braun): CH₂Cl₂, toluene, tetrahydrofuran, dimethylformamide, diethylether, 1,2-dichloroethane, *N*-methyl-2-pyrrolidone (NMP), *N,N*-dimethylacetamide (DMA), dimethylsulfoxide (DMSO), and γ -valerolactone (GVL) was dried over CaH₂ for 8 h, degassed and distilled under reduced pressure. 1,2-dimethoxyethane (DME) was dried over sodium and freshly distilled under N₂. 2,2,2-trifluoroethanol (TFE) was stirred over CaSO₄ and distilled under reduced pressure. Water was degassed by repeated *Freeze-Pump-Thaw* degassing procedure. 1,4-dioxane and di-*n*-butyl-ether (*n*Bu₂O) were distilled from sodium benzophenone ketyl.

Reagents

Chemicals obtained from commercial sources with purity above 95% were used without further purification. The following compounds were known and were synthesized according to previously described methods **238**, **239a**^l, **239b**^l, **239d**^l, **239e**^l, **243**, **248**, and **249**.

Cooperation clarification

In the project on metal-free electrocatalytic B–H nitrogenation of *nido*-carboranes, Dr. Long Yang carried out experiments for the optimization of reaction conditions, some scope (**240a**, **240h**, **240l**, **240m**, **240n**, **240o**, **240p**, **240r**, **240u**, **240v**, **240w**, **240bb**, **240cc**, **240'a**, **240'b**, **240'd**, **240'e**, **242a**, and **242b**), mechanistic studies and fluorescent studies of the BODIPY labeled *nido*-carboranes. Alexej Scheremetjew carried out GC-Headspace analysis and CV studies. Dr. Rositha Kuniyil performed DFT calculations.

In the project of cupraelectro-catalytic C–H chalcogenation of *o*-carboranes, Dr. Long Yang carried out some experiments for optimization, the scope (**243a**, **243b**, **243e**, **243f**, **243i**, **243m**, **243o**, **243s**, **243u**, **244b**, **244f**, **244g**, **244h**, **244i**, **244j**, **244k**, **244l**, and **244m**), mechanistic studies and late stage diversification. Alexej Scheremetjew carried out CV studies.

Binbin Yuan carried out DFT studies. Dr. A. Claudia Stückl carried out EPR measurements and analyzed all EPR data. Dr. Christopher Golz analyzed all the X-ray data in the thesis.

In the project of manganese-catalyzed selective labeling of peptides with *o*-carboranes *via* C–H activation, Dr. Long Yang carried out some experiments for the scope (**248h** and **248i**).

5.2 General Procedures

General Procedure A: Electrochemical-Catalyzed B–H Nitrogenation of *nido*-Carboranes

The electrocatalysis was carried out in an undivided cell under air, with a graphite felt (GF) anode (10 mm × 15 mm × 6 mm) and a platinum cathode (10 mm × 15 mm × 0.25 mm). *nido*-Carborane **238** (0.10 mmol, 1.0 equiv), pyridine **239** (0.30 mmol, 3.0 equiv), and NMe₄Cl (0.20 mmol, 2.0 equiv) were dissolved in DME (4.0 mL) and H₂O (0.20 mL). Electrocatalysis was performed at room temperature with a constant current of 6.0 mA maintained for 3 h. The GF anode was washed with CH₂Cl₂ (3×10 mL). Evaporation of the solvent and subsequent purification by column chromatography on silica gel with CH₂Cl₂/*n*-hexane (1/1) afforded the corresponding products **240**.

General Procedure B: Cupraelectro-Catalyzed C–H Chalcogenation of *o*-Carboranes

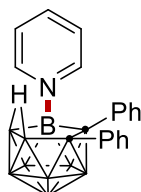
The electrocatalysis was carried out in an undivided cell under air, with a graphite felt (GF) anode (10 mm × 15 mm × 6 mm) and a platinum cathode (10 mm × 15 mm × 0.25 mm). *o*-Carborane **241** (0.10 mmol, 1.0 equiv), thiol **242** (0.30 mmol, 3.0 equiv), CuOAc (15 mol %), 2-PhPy (15 mol %), LiOtBu (0.20 mmol, 2.0 equiv) and TBAI (0.20 mmol, 2.0 equiv) were dissolved in THF (3.0 mL). Electrocatalysis was performed at room temperature with a constant current of 2.0 mA maintained for 16 h. The GF anode was washed with ethyl acetate (3×10 mL). Evaporation of the solvent and subsequent purification by column chromatography on silica gel with *n*-hexane or gel permeation chromatography (GPC) afforded the corresponding products **243**.

General Procedure C: Cupraelectro-Catalyzed C–H Chalcogenation of *o*-Carboranes

The electrocatalysis was carried out in an undivided cell under air, with a graphite felt (GF) anode (10 mm × 15 mm × 6 mm) and a platinum cathode (10 mm × 15 mm × 0.25 mm). Thiol **242** (0.30 mmol, 3.0 equiv), LiOtBu (0.20 mmol, 2.0 equiv) and TBAI (0.20 mmol, 2.0 equiv) were dissolved in THF (3.0 mL). Electrocatalysis was performed at room temperature with a constant current of 2.0 mA maintained for 3 h. Then, *o*-carborane **241** (0.10 mmol, 1.0 equiv), CuOAc (15 mol %), and 2-PhPy (15 mol %) were added to the reaction mixture, and electrocatalysis was performed at room temperature with a constant current of 2.0 mA maintained for another 16 h. The GF anode was washed with ethyl acetate (3×10 mL). Evaporation of the solvent and subsequent purification by column chromatography on silica gel with *n*-hexane or gel permeation chromatography (GPC) afforded the corresponding products **243**.

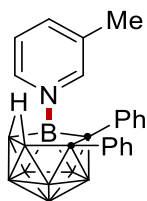
General Procedure D: Manganese(I)-Catalyzed C–2 Alkenylation of Tryptophan

Amino acid or peptide **246** (0.10 mmol, 1.0 equiv), ethynyl-*o*-carborane **247** (0.1 mmol, 1.0 equiv.), MnBr(CO)₅ (2.7 mg, 10 mol %), AcOH (1.2 μL, 20 mol %), and 1,4-dioxane (1.0 mL) were placed in a 25 mL oven-dried Schlenk tube and stirred at 80 °C for 16 h. After cooling to room temperature, the reaction mixture was transferred to a round bottom flask with 10 mL of ethyl acetate and concentrated in vacuum. Column chromatography in *n*-hexane/EtOAc followed by gel permeation chromatography(GPC) afforded the desired products **248** and **250**.

5.3 Experimental Procedures and Analytical Data**5.3.1 Electrochemical B–H Nitrogenation of *nido*-Carboranes****5.3.1.1 Characterization Data**

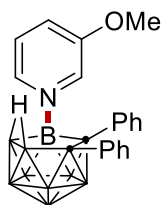
7,8-diphenyl-11-pyridyl-*nido*-carborane

240a. The representative procedure **A** was followed using *nido*-carborane **238a** (36.0 mg, 0.10 mmol) and pyridine **239a** (24.0 mg, 0.30 mmol). Isolation by column chromatography (*n*-hexane/CH₂Cl₂: 1/1) yielded **240a** (30.0 mg, 83%) as a colorless solid. **M.p.** = 280 – 282 °C. **¹H NMR** (300 MHz, CD₂Cl₂): δ = 8.75 (d, *J* = 5.2 Hz, 2H), 8.07 (tt, *J* = 7.7, 1.5 Hz, 1H), 7.56 – 7.48 (m, 2H), 7.35 – 7.28 (m, 2H), 7.08 – 6.96 (m, 3H), 6.94 – 6.82 (m, 5H), -1.97 (s, 1H). **¹³C NMR** (101 MHz, CD₂Cl₂): δ = 147.7 (CH), 142.4 (CH), 138.7 (C_q), 136.2 (C_q), 132.1 (CH), 131.1 (CH), 127.5 (CH), 127.1 (CH), 126.6 (CH), 126.3 (CH), 125.8 (CH). **¹¹B NMR** (96 MHz, CD₂Cl₂): δ = 4.92 (1B), -3.89 (1B), -11.50 (1B), -15.73 (2B), -20.65 (1B), -26.08 (1B), -30.97 (1B), -35.87 (1B). **IR** (ATR): 2558, 2536, 2510, 1486, 1456, 1445, 1171, 764, 698 cm⁻¹. **MS** (ESI) *m/z* (relative intensity): 387 (100) [M+Na]⁺, 365 (20) [M+H]⁺. **HR-MS** (ESI): *m/z* calcd. for C₁₉H₂₄¹⁰B₁¹¹B₈N [M+Na]⁺: 387.2688, found: 387.2680. The analytical data corresponds with those reported in the literature.^[200]

**7,8-diphenyl-11-(3-methylpyridyl)-*nido*-carborane**

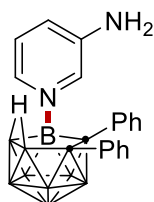
240b. The representative procedure **A** was followed using *nido*-carborane **238a** (36.0 mg, 0.10 mmol) and 3-methylpyridine **239b** (27.9 mg, 0.30 mmol). Isolation by column chromatography (*n*-hexane/CH₂Cl₂: 1/1) yielded **240b** (26.0 mg, 68%) as a white solid. **M.p.** = 280 – 283 °C. **¹H NMR** (500 MHz, CDCl₃): δ = 8.54 (d, *J* = 6.1 Hz, 1H), 8.45 (s, 1H), 7.76 (d, *J* = 7.7 Hz, 1H), 7.32 (dd, *J* = 7.9, 5.9 Hz, 1H), 7.28 – 7.24 (m, 2H), 7.00 – 6.87 (m, 3H), 6.86 – 6.77 (m, 5H), 2.27 (s, 3H), -2.08 (s, 1H). **¹³C NMR** (126 MHz, CDCl₃): δ = 147.5 (CH), 144.9 (CH), 142.4 (CH), 138.5 (C_q), 136.4 (C_q), 136.4 (C_q), 132.1 (CH), 131.1 (CH), 127.4 (CH), 127.1 (CH), 126.6 (CH), 126.2 (CH), 124.9 (CH), 18.5 (CH₃). **¹¹B NMR** (128 MHz, CDCl₃): δ = 4.46 (1B), -4.56 (1B), -11.28 (1B), -15.95 (2B), -21.01 (1B), -26.04 (1B), -30.94 (1B), -35.69 (1B). **IR** (ATR): 3059, 1487, 1443, 1201, 1155, 1056, 907, 734, 696 cm⁻¹. **MS** (ESI)

m/z (relative intensity): 401 (90) $[M+Na]^+$, 379 (20) $[M+H]^+$. **HR-MS** (ESI): m/z calcd. for $C_{20}H_{26}^{10}B_1^{11}B_8N$ $[M+Na]^+$: 401.2845, found: 401.2850. The analytical data corresponds with those reported in the literature.^[200]



7,8-diphenyl-11-(3-methoxypyridyl)-*nido*-carborane

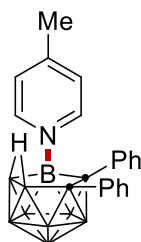
240c. The representative procedure **A** was followed using *nido*-carborane **238a** (36.0 mg, 0.10 mmol) and 3-methoxypyridine **239c** (32.0 mg, 0.30 mmol). Isolation by column chromatography (*n*-hexane/ CH_2Cl_2 : 1/1) yielded **240c** (30.0 mg, 75%) as a yellow solid. **M.p.** = 220 – 223 °C. **1H NMR** (500 MHz, CD_2Cl_2): δ = 8.47 (d, J = 5.8 Hz, 1H), 8.13 (d, J = 2.7 Hz, 1H), 7.51 (ddd, J = 8.7, 2.7, 1.1 Hz, 1H), 7.40 (dd, J = 8.7, 5.8 Hz, 1H), 7.28 – 7.25 (m, 2H), 6.99 – 6.93 (m, 3H), 6.91 – 6.83 (m, 5H), 3.65 (s, 3H), -2.01 (s, 1H). **^{13}C NMR** (126 MHz, CD_2Cl_2): δ = 157.1 (C_q), 140.8 (CH), 139.0 (C_q), 136.7 (C_q), 134.7 (CH), 132.4 (CH), 131.5 (CH), 128.2 (CH), 127.8 (CH), 127.4 (CH), 127.0 (CH), 126.6 (CH), 126.3 (CH), 56.8 (CH_3). **^{11}B NMR** (128 MHz, CD_2Cl_2): δ = 4.82 (1B), -4.05 (1B), -11.74 (1B), -15.83 (2B), -20.58 (1B), -26.13 (1B), -31.13 (1B), -35.90 (1B). **IR** (ATR): 2526, 1572, 1487, 1443, 1298, 1259, 1056, 881, 693 cm^{-1} . **MS** (ESI) m/z (relative intensity): 417 (100) $[M+Na]^+$, 395 (20) $[M+H]^+$. **HR-MS** (ESI): m/z calcd. for $C_{20}H_{26}^{10}B_1^{11}B_8NO$ $[M+Na]^+$: 417.2794, found: 417.2796. The analytical data corresponds with those reported in the literature.^[200]



7,8-diphenyl-11-(3-aminopyridyl)-*nido*-carborane

240d. The representative procedure **A** was followed using *nido*-carborane **238a** (36.0 mg, 0.10 mmol) and pyridin-3-amine **239d** (28.2 mg, 0.30 mmol).

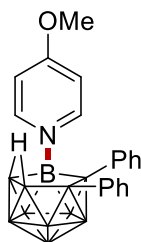
Isolation by column chromatography (*n*-hexane/CH₂Cl₂: 1/1) yielded **240d** (30.0 mg, 79%) as a yellow solid. **M.p.** = 250 – 253 °C. **¹H NMR** (500 MHz, CD₂Cl₂): δ = 8.07 (d, *J* = 2.4 Hz, 1H), 8.04 (d, *J* = 5.1 Hz, 1H), 7.29 – 7.24 (m, 2H), 7.20 – 7.14 (m, 2H), 6.99 – 6.92 (m, 3H), 6.88 – 6.82 (m, 5H), 4.13 (s, 2H), -2.00 (s, 1H). **¹³C NMR** (126 MHz, CD₂Cl₂): δ = 145.0 (C_q), 139.1 (C_q), 137.8 (CH), 136.8 (C_q), 134.2 (CH), 132.4 (CH), 131.3 (CH), 127.5 (CH), 127.3 (overlapped, CH), 126.8 (CH), 126.5 (CH), 126.0 (CH). **¹¹B NMR** (128 MHz, CD₂Cl₂): δ = 4.99 (1B), -4.38 (1B), -12.03 (1B), -15.78 (2B), -21.02 (1B), -26.20 (1B), -31.14 (1B), -36.05 (1B). **IR** (ATR): 3480, 3388, 2539, 1623, 1583, 1442, 1164, 697 cm⁻¹. **MS** (ESI) *m/z* (relative intensity): 402 (100) [M+Na]⁺, 380 (50) [M+H]⁺. **HR-MS** (ESI): *m/z* calcd. for C₁₉H₂₅¹⁰B₁¹¹B₈N₂ [M+Na]⁺: 402.2797, found: 402.2796. The analytical data corresponds with those reported in the literature.^[200]



7,8-diphenyl-11-(4-methylpyridyl)-*nido*-carborane

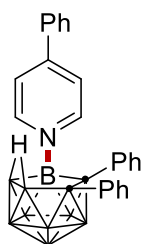
240e. The representative procedure **A** was followed using *nido*-carborane **238a** (36.0 mg, 0.10 mmol) and 4-methylpyridine **239e** (27.9 mg, 0.30 mmol). Isolation by column chromatography (*n*-hexane/CH₂Cl₂: 1/1) yielded **240e** (33.0 mg, 87%) as a white solid. **M.p.** = 247 – 250 °C. **¹H NMR** (500 MHz, CDCl₃): δ = 8.52 (d, *J* = 6.6 Hz, 2H), 7.26 – 7.24 (m, 1H), 7.24 – 7.23 (m, 1H), 7.21 (d, *J* = 7.5 Hz, 2H), 6.95 – 6.88 (m, 3H), 6.85 – 6.77 (m, 5H), 2.45 (s, 3H), -2.06 (s, 1H). **¹³C NMR** (126 MHz, CDCl₃): δ = 155.4 (C_q), 146.9 (CH), 138.5 (C_q), 136.5 (C_q), 132.1 (CH), 131.1 (CH), 127.1 (CH), 127.1 (CH), 126.6 (CH), 126.2 (overlapped, CH), 21.7 (CH₃). **¹¹B NMR** (128 MHz, CDCl₃): δ = 4.43 (1B), -3.98 (1B), -11.46 (1B), -15.82 (2B), -20.70 (1B), -26.00 (1B), -30.91 (1B), -35.77 (1B). **IR** (ATR): 3058, 2540, 2159, 1495, 1444, 761, 697 cm⁻¹. **MS** (ESI) *m/z* (relative intensity): 401 (100) [M+Na]⁺, 479 (20) [M+H]⁺. **HR-MS** (ESI): *m/z* calcd. for C₂₀H₂₆¹⁰B₁¹¹B₈N [M+Na]⁺: 401.2845, found:

401.2842. The analytical data corresponds with those reported in the literature.^[200]



7,8-diphenyl-11-(4-methoxypyridyl)-*nido*-carborane

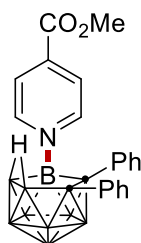
240f. The representative procedure **A** was followed using *nido*-carborane **238a** (36.0 mg, 0.10 mmol) and 4-methoxypyridine **239f** (32.7 mg, 0.30 mmol). Isolation by column chromatography (*n*-hexane/CH₂Cl₂: 1/1) yielded **240f** (32.0 mg, 81%) as a white solid. **M.p.** = 314 – 317 °C. **¹H NMR** (500 MHz, CD₂Cl₂): δ = 8.49 (d, *J* = 7.5 Hz, 2H), 7.27 (d, *J* = 6.6 Hz, 2H), 7.00 – 6.93 (m, 3H), 6.89 – 6.82 (m, 7H), 3.92 (s, 3H), -2.02 (s, 1H). **¹³C NMR** (126 MHz, CD₂Cl₂): δ = 169.8 (C_q), 149.5 (CH), 139.1 (C_q), 136.8 (C_q), 132.4 (CH), 131.4 (CH), 127.6 (CH), 127.3 (CH), 126.8 (CH), 126.5 (CH), 111.5 (CH), 57.3 (CH₃). **¹¹B NMR** (128 MHz, CD₂Cl₂): δ = 4.80 (1B), -3.95 (1B), -11.52 (1B), -15.65 (2B), -20.30 (1B), -25.96 (1B), -30.82 (1B), -35.66 (1B). **IR** (ATR): 2570, 2525, 1631, 1516, 1319, 1162, 1005, 847 cm⁻¹. **MS** (ESI) *m/z* (relative intensity): 417 (100) [M+Na]⁺, 395 (20) [M+H]⁺. **HR-MS** (ESI): *m/z* calcd. for C₂₀H₂₆¹⁰B₁¹¹B₈NO [M+Na]⁺: 417.2794, found: 417.2794. The analytical data corresponds with those reported in the literature.^[200]



7,8-diphenyl-11-(4-phenylpyridyl)-*nido*-carborane

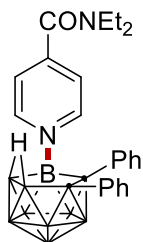
240g. The representative procedure **A** was followed using *nido*-carborane **238a** (36.0 mg, 0.10 mmol) and 4-phenylpyridine **239g** (46.5 mg, 0.30 mmol). Isolation by column chromatography (*n*-hexane/CH₂Cl₂: 1/1) yielded **240g** (43.2 mg, 98%) as a yellow solid. **M.p.** = 242 – 245 °C. **¹H NMR** (500 MHz,

CD₂Cl₂): δ = 8.67 (d, J = 7.0 Hz, 2H), 7.68 – 7.65 (m, 4H), 7.58 – 7.53 (m, 3H), 7.31 – 7.27 (m, 2H), 7.01 – 6.95 (m, 3H), 6.93 – 6.89 (m, 2H), 6.87 – 6.83 (m, 3H), -1.91 (s, 1H). **¹³C NMR** (126 MHz, CD₂Cl₂): δ = 154.4 (C_q), 147.8 (CH), 139.1 (C_q), 136.6 (C_q), 134.6 (C_q), 132.4 (CH), 131.9 (CH), 131.5 (CH), 129.9 (CH), 127.8 (CH), 127.7 (CH), 127.4 (CH), 126.9 (CH), 126.6 (CH), 123.1 (CH). **¹¹B NMR** (128 MHz, CDCl₃): δ = 6.28 (1B), -0.08 (1B), -7.92 (1B), -10.65 (2B), -16.32 (1B), -20.79 (1B), -26.45 (1B), -31.72 (1B). **IR** (ATR): 2532, 1626, 1486, 1431, 1219, 1172, 1013, 763, 698 cm⁻¹. **MS** (ESI) m/z (relative intensity): 463 (100) [M+Na]⁺, 441 (50) [M+H]⁺. **HR-MS** (ESI): m/z calcd. for C₂₅H₂₈¹⁰B₁¹¹B₈N [M+Na]⁺: 463.3005, found: 463.2997. The analytical data corresponds with those reported in the literature.^[200]



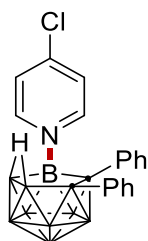
7,8-diphenyl-11-methylisonicotinyl-*nido*-carborane

240h. The representative procedure **A** was followed using *nido*-carborane **238a** (36.0 mg, 0.10 mmol) and methyl isonicotinate **239h** (41.0 mg, 0.30 mmol). Isolation by column chromatography (*n*-hexane/CH₂Cl₂: 1/1) yielded **240h** (29.0 mg, 69%) as a colorless solid. **M.p.** = 242 – 246 °C. **¹H NMR** (300 MHz, CD₂Cl₂): δ = 8.84 (d, J = 6.9 Hz, 2H), 8.00 (d, J = 7.0 Hz, 2H), 7.34 – 7.28 (m, 2H), 7.06 – 6.97 (m, 3H), 6.94 – 6.87 (m, 5H), 4.00 (s, 3H), -1.89 (s, 1H). **¹³C NMR** (101 MHz, CD₂Cl₂): δ = 162.5 (C_q), 148.4 (CH), 142.2 (C_q), 138.6 (C_q), 135.9 (C_q), 132.1 (CH), 131.2 (CH), 127.7 (CH), 127.1 (CH), 126.9 (CH), 126.4 (CH), 125.2 (CH), 53.7 (CH₃). **¹¹B NMR** (128 MHz, CD₂Cl₂): δ = 4.45 (1B), -3.67 (1B), -11.05 (1B), -15.83 (2B), -20.08 (1B), -26.03 (1B), -30.77 (1B), -35.42 (1B). **IR** (ATR): 2529, 1743, 1440, 1427, 1289, 1112, 767, 690 cm⁻¹. **MS** (ESI) m/z (relative intensity): 445 (100) [M+Na]⁺, 423 (20) [M+H]⁺. **HR-MS** (ESI): m/z calcd. for C₂₁H₂₆¹⁰B₁¹¹B₈NO₂ [M+H]⁺: 423.2925, found: 423.2897. The analytical data corresponds with those reported in the literature.^[200]



7,8-diphenyl-11-(*N*, *N*-diethylisonicotinamide)-*nido*-carborane

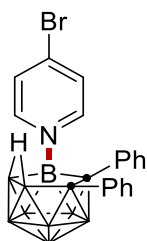
240i. The representative procedure **A** was followed using *nido*-carborane **238a** (36.0 mg, 0.10 mmol) and *N*, *N*-diethylisonicotinamide **239i** (53.4 mg, 0.30 mmol). Isolation by column chromatography (CH₂Cl₂) yielded **240i** (24.0 mg, 51%) as a yellow solid. **M.p.** = 251 – 254 °C. **¹H NMR** (400 MHz, CD₂Cl₂): δ = 8.72 (d, *J* = 6.8 Hz, 2H), 7.41 – 7.34 (m, 2H), 7.31 – 7.23 (m, 2H), 7.00 – 6.91 (m, 3H), 6.89 – 6.80 (m, 5H), 3.47 (q, *J* = 7.1 Hz, 2H), 2.99 (q, *J* = 7.1 Hz, 2H), 1.19 (t, *J* = 7.2 Hz, 3H), 1.02 (t, *J* = 7.1 Hz, 3H), -2.00 (s, 1H). **¹³C NMR** (101 MHz, CD₂Cl₂): δ = 165.4 (C_q), 150.9 (C_q), 148.4 (CH), 138.9 (C_q), 136.4 (C_q), 132.4 (CH), 131.5 (CH), 127.9 (CH), 127.4 (CH), 127.1 (CH), 126.7 (CH), 123.3 (CH), 43.4 (CH₂), 39.9 (CH₂), 14.2 (CH₃), 12.7 (CH₃). **¹¹B NMR** (128 MHz, CD₂Cl₂): δ = 4.59 (1B), -3.84 (1B), -11.22 (1B), -15.78 (2B), -20.43 (1B), -26.04 (1B), -30.87 (1B), -35.68 (1B). **IR** (ATR): 2530, 2223, 2177, 2035, 1991, 1628, 1053, 696 cm⁻¹. **MS** (ESI) *m/z* (relative intensity): 486 (50) [M+Na]⁺, 464 (100) [M+H]⁺. **HR-MS** (ESI): *m/z* calcd. for C₂₄H₃₃¹⁰B₁¹¹B₈N₂O [M+Na]⁺: 486.3375, found: 486.3392.



7,8-diphenyl-11-(4-chloropyridine)-*nido*-carborane

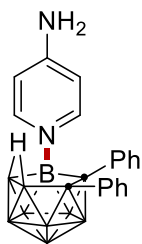
240j. The representative procedure **A** was followed using *nido*-carborane **238a** (36.0 mg, 0.10 mmol) and 4-chloropyridine hydrochloride **239j** (45.0 mg, 0.30 mmol). Isolation by column chromatography (*n*-hexane/CH₂Cl₂: 3/1) yielded **240j** (20.0 mg, 53%) as a yellow solid. **M.p.** = 232 – 234 °C. **¹H NMR** (300 MHz, CDCl₃): δ = 8.62 (d, *J* = 7.0 Hz, 2H), 7.44 (d, *J* = 7.1 Hz, 2H), 7.31

– 7.29 (m, 1H), 7.28 – 7.26 (m, 1H), 7.02 – 6.94 (m, 3H), 6.91 – 6.85 (m, 5H), -2.09 (s, 1H). **¹³C NMR** (101 MHz, CDCl₃): δ = 151.3 (C_q), 148.1 (CH), 138.4 (C_q), 136.1 (C_q), 132.04 (CH), 131.2 (CH), 127.7 (CH), 127.2 (CH), 126.9 (CH), 126.4 (CH), 126.1 (CH). **¹¹B NMR** (128 MHz, CDCl₃): δ = 4.15 (1B), -3.56 (1B), -10.88 (1B), -15.95 (2B), -20.21 (1B), -25.97 (1B), -30.85 (1B), -35.56 (1B). **IR** (ATR): 3112, 2538, 1615, 1487, 1433, 1115, 1055, 696 cm⁻¹. **MS** (ESI) *m/z* (relative intensity): 421 (100) [M+Na]⁺, 399 (20) [M+H]⁺. **HR-MS** (ESI): *m/z* calcd. for C₁₉H₂₃¹⁰B₁¹¹B₈³⁵ClN [M+Na]⁺: 421.2303, found: 421.2298. The analytical data corresponds with those reported in the literature.^[200]



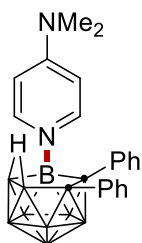
7,8-diphenyl-11-(4-bromopyridine)-*nido*-carborane

240k. The representative procedure **A** was followed using *nido*-carborane **238a** (36.0 mg, 0.10 mmol) and 4-bromopyridine hydrochloride **239k** (58.2 mg, 0.30 mmol). Isolation by column chromatography (*n*-hexane/CH₂Cl₂: 3/1) yielded **240k** (21.0 mg, 45%) as a yellow solid. **M.p.** = 233 – 236 °C. **¹H NMR** (500 MHz, CD₂Cl₂): δ = 8.46 (d, *J* = 7.0 Hz, 2H), 7.65 – 7.61 (m, 2H), 7.28 – 7.24 (m, 2H), 7.02 – 6.92 (m, 4H), 6.88 – 6.86 (m, 4H), -2.05 (s, 1H). **¹³C NMR** (126 MHz, CD₂Cl₂): δ = 147.9 (CH), 141.1 (C_q), 138.9 (C_q), 136.2 (C_q), 132.4 (CH), 131.5 (CH), 129.7 (CH), 128.0 (CH), 127.4 (CH), 127.2 (CH), 126.7 (CH). **¹¹B NMR** (128 MHz, CD₂Cl₂): δ = 4.35 (1B), -3.85 (1B), -11.36 (1B), -15.88 (2B), -20.30 (1B), -26.02 (1B), -30.90 (1B), -35.68 (1B). **IR** (ATR): 2923, 2852, 2149, 2030, 1974, 1723, 1459, 697 cm⁻¹. **MS** (ESI) *m/z* (relative intensity): 465 (100) [M+Na]⁺. **HR-MS** (ESI) *m/z* calcd for C₁₉H₂₃¹⁰B₁¹¹B₈⁷⁹BrN [M+Na]⁺ 465.1808, found 465.1807. The analytical data corresponds with those reported in the literature.^[200]



7,8-diphenyl-11-(4-aminopyridine)-*nido*-carborane

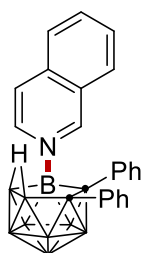
240l. The representative procedure **A** was followed using *nido*-carborane **238a** (36.0 mg, 0.10 mmol) and pyridin-4-amine **239l** (28.0 mg, 0.30 mmol). Isolation by column chromatography (*n*-hexane/CH₂Cl₂: 1/1) yielded **240l** (37.0 mg, 97%) as a colorless solid. **M.p.** = 293 – 296 °C. **¹H NMR** (400 MHz, Acetone-*d*₆): δ = 8.32 – 8.23 (m, 2H), 7.35 – 7.26 (m, 2H), 7.10 (s, 2H), 7.02 – 6.88 (m, 5H), 6.85 – 6.75 (m, 3H), 6.72 – 6.64 (m, 2H), -1.84 (s, 1H). **¹³C NMR** (101 MHz, Acetone-*d*₆): δ = 158.0 (C_q), 147.7 (CH), 139.4 (C_q), 137.4 (C_q), 132.2 (CH), 131.2 (CH), 126.8 (CH), 126.0 (CH), 125.9 (CH), 108.7 (CH), 108.6 (CH). **¹¹B NMR** (96 MHz, Acetone-*d*₆): δ = 5.24 (1B), -5.39 (1B), -13.34 (1B), -15.81 (2B), -22.06 (1B), -26.12 (1B), -31.54 (1B), -36.82 (1B). **IR** (ATR): 3475, 3375, 2538, 1644, 1527, 1182, 831, 694 cm⁻¹. **MS** (ESI) *m/z* (relative intensity): 402 (100) [M+Na]⁺, 380 (30) [M+H]⁺. **HR-MS** (ESI): *m/z* calcd. for C₁₉H₂₅¹⁰B₁¹¹B₈N [M+Na]⁺: 402.2797, found: 402.2792. The analytical data corresponds with those reported in the literature.^[200]



7,8-diphenyl-11-(*N,N*-dimethylpyridin-4-amino)-*nido*-carborane

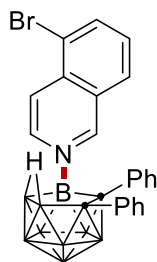
240m. The representative procedure **A** was followed using *nido*-carborane **238a** (36.0 mg, 0.10 mmol) and *N,N*-dimethylpyridin-4-amine **239m** (37.0 mg, 0.30 mmol). Isolation by column chromatography (*n*-hexane/CH₂Cl₂: 1/1) yielded **240m** (21.0 mg, 52%) as a colorless solid. **M.p.** = 336 – 338 °C. **¹H NMR** (300 MHz, DMSO-*d*₆): δ = 8.29 (d, *J* = 7.1 Hz, 2H), 7.30 (d, *J* = 6.4 Hz, 2H), 7.02 – 6.90 (m, 5H), 6.83 – 6.75 (m, 3H), 6.70 (d, *J* = 7.4 Hz, 2H), 3.05

(s, 6H), -1.56 (s, 1H). **¹³C NMR** (101 MHz, DMSO-*d*₆): δ = 155.7 (C_q), 147.0 (CH), 139.4 (C_q), 137.3 (C_q), 132.5 (CH), 131.4 (CH), 127.3 (CH), 127.2 (CH), 126.6 (CH), 126.5 (CH), 106.9 (CH), 39.8 (CH₃). **¹¹B NMR** (128 MHz, DMSO-*d*₆): δ = 5.14 (1B), -6.22 (1B), -15.59 (3B), -21.95 (1B), -26.05 (1B), -31.52 (1B), -37.12 (1B). **IR** (ATR): 2554, 2528, 2502, 1643, 1565, 1441, 1166, 820, 696 cm⁻¹. **MS** (ESI) *m/z* (relative intensity): 430 (100) [M+Na]⁺, 408 (30) [M+H]⁺. **HR-MS** (ESI): *m/z* calcd. for C₂₁H₂₉¹⁰B₁¹¹B₈N₂ [M+Na]⁺: 430.3111, found: 430.3110.



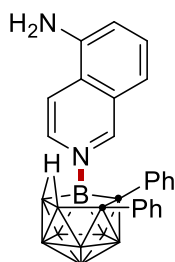
7,8-diphenyl-11-(isoquinolinyl)-*nido*-carborane

240n. The representative procedure **A** was followed using *nido*-carborane **238a** (36.0 mg, 0.10 mmol) and isoquinoline **239n** (39.0 mg, 0.30 mmol). Isolation by column chromatography (*n*-hexane/CH₂Cl₂: 1/1) yielded **240n** (38.0 mg, 92%) as a yellow solid. **M.p.** = 280 – 282 °C. **¹H NMR** (300 MHz, CD₂Cl₂): δ = 9.35 (s, 1H), 8.56 (dd, *J* = 6.8, 1.0 Hz, 1H), 8.03 – 7.96 (m, 3H), 7.87 – 7.81 (m, 2H), 7.37 – 7.32 (m, 2H), 7.06 – 6.99 (m, 3H), 6.97 – 6.93 (m, 2H), 6.85 – 6.78 (m, 3H), -1.85 (s, 1H). **¹³C NMR** (101 MHz, CD₂Cl₂): δ = 151.9 (CH), 139.1 (C_q), 139.0 (CH), 136.9 (C_q), 136.7 (C_q), 135.9 (CH), 132.5 (CH), 131.5 (CH), 130.7 (CH), 129.8 (CH), 127.7 (CH), 127.6 (C_q), 127.4 (CH), 126.9 (CH), 126.9 (CH), 126.6 (CH), 123.6 (CH). **¹¹B NMR** (128 MHz, CD₂Cl₂): δ = 4.98 (1B), -4.07 (1B), -11.80 (1B), -15.78 (2B), -20.56 (1B), -26.09 (1B), -31.06 (1B), -35.86 (1B). **IR** (ATR): 3376, 2544, 1644, 1598, 1494, 1443, 1179, 697 cm⁻¹. **MS** (ESI) *m/z* (relative intensity): 437 (100) [M+Na]⁺, 415 (30) [M+H]⁺. **HR-MS** (ESI): *m/z* calcd. for C₂₃H₂₆¹⁰B₁¹¹B₈N [M+Na]⁺: 437.2847, found: 437.2849.



7,8-diphenyl-11-(5-bromoisoquinolinyl)-*nido*-carborane

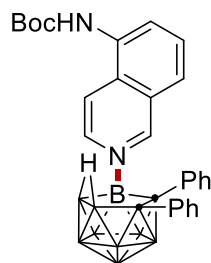
240o. The representative procedure **A** was followed using *nido*-carborane **238a** (36.0 mg, 0.10 mmol) and 5-bromoisoquinoline **239o** (62.0 mg, 0.30 mmol). Isolation by column chromatography (*n*-hexane/CH₂Cl₂: 1/1) yielded **240o** (31.0 mg, 63%) as a yellow solid. **M.p.** = 280 – 283 °C. **¹H NMR** (400 MHz, CD₂Cl₂): δ = 9.30 – 9.23 (m, 1H), 8.70 – 8.59 (m, 1H), 8.32 – 8.21 (m, 1H), 8.18 – 8.11 (m, 1H), 7.95 – 7.88 (m, 1H), 7.74 – 7.63 (m, 1H), 7.37 – 7.28 (m, 2H), 7.04 – 6.97 (m, 3H), 6.96 – 6.91 (m, 2H), 6.87 – 6.79 (m, 3H), -1.84 (s, 1H). **¹³C NMR** (101 MHz, CD₂Cl₂): δ = 151.5 (CH), 139.9 (CH), 139.0 (CH), 138.7 (C_q), 136.2 (C_q), 135.8 (C_q), 132.1 (CH), 131.3 (CH), 131.0 (CH), 129.3 (CH), 128.4 (C_q), 127.6 (CH), 127.1 (CH), 126.8 (CH), 126.3 (CH), 122.7 (CH), 121.5 (C_q). **¹¹B NMR** (96 MHz, CD₂Cl₂): δ = 4.90 (1B), -3.78 (1B), -11.27 (1B), -15.75 (2B), -20.22 (1B), -26.03 (1B), -31.02 (1B), -35.73 (1B). **IR** (ATR): 2923, 2543, 1637, 1595, 1490, 1443, 1215, 748, 698 cm⁻¹. **MS** (ESI) *m/z* (relative intensity): 516 (100) [M+Na]⁺, 494 (30) [M+H]⁺. **HR-MS** (ESI): *m/z* calcd. for C₂₃H₂₅¹¹B₉⁷⁹BrN [M+Na]⁺: 516.1952, found: 516.1946.



7,8-diphenyl-11-(isoquinolin-5-amino)-*nido*-carborane

240p. The representative procedure **A** was followed using *nido*-carborane **238a** (36.0 mg, 0.10 mmol) and isoquinolin-5-amine **239p** (43.0 mg, 0.30 mmol). Isolation by column chromatography (*n*-hexane/CH₂Cl₂: 1/1) yielded **240p** (22.0 mg, 51%) as a yellow solid. **M.p.** = 291 – 293 °C. **¹H NMR** (400

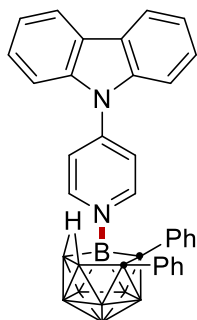
MHz, CD₂Cl₂): δ = 9.24 (s, 1H), 8.48 – 8.40 (m, 1H), 7.74 – 7.68 (m, 1H), 7.64 – 7.57 (m, 1H), 7.40 – 7.31 (m, 3H), 7.23 – 7.18 (m, 1H), 7.04 – 6.93 (m, 5H), 6.86 – 6.77 (m, 3H), 4.45 (s, 2H), -1.84 (s, 1H). **¹³C NMR** (101 MHz, CD₂Cl₂): δ = 151.9 (CH), 142.1 (C_q), 138.8 (C_q), 137.0 (CH), 136.4 (C_q), 132.2 (CH), 131.2 (CH), 131.2 (CH), 128.2 (C_q), 127.4 (CH), 127.1 (CH), 126.6 (CH), 126.3 (CH), 125.7 (C_q), 119.3 (CH), 117.7 (CH), 117.4 (CH). **¹¹B NMR** (96 MHz, CD₂Cl₂): δ = 5.02 (1B), -4.05 (1B), -11.73 (1B), -15.70 (2B), -20.59 (1B), -26.07 (1B), -31.04 (1B), -35.90 (1B). **IR** (ATR): 2529, 1627, 1596, 1494, 1399, 1385, 744, 693 cm⁻¹. **MS** (ESI) *m/z* (relative intensity): 452 (100) [M+Na]⁺, 430 (20) [M+H]⁺. **HR-MS** (ESI): *m/z* calcd. for C₂₃H₂₇¹⁰B₁¹¹B₈N₂ [M+Na]⁺: 452.2956, found: 452.2954.



7,8-diphenyl-11-(*tert*-butyl isoquinolin-5-ylcarbamyl)-*nido*-carborane

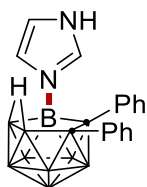
240q. The representative procedure **A** was followed using *nido*-carborane **238a** (36.0 mg, 0.10 mmol) and *tert*-butyl isoquinolin-5-ylcarbamate **239q** (53.4 mg, 0.30 mmol). Isolation by column chromatography (CH₂Cl₂) yielded **240q** (25.1 mg, 54%) as a yellow solid. **M.p.** = 198 – 201 °C. **¹H NMR** (400 MHz, CD₂Cl₂): δ = 9.27 (s, 1H), 8.49 (d, *J* = 8.0 Hz, 1H), 8.32 (d, *J* = 7.7 Hz, 1H), 7.81 – 7.73 (m, 2H), 7.71 – 7.66 (m, 1H), 7.32 – 7.27 (m, 2H), 7.01 – 6.94 (m, 3H), 6.93 – 6.86 (m, 3H), 6.82 – 6.76 (m, 3H), 1.52 (s, 9H), -1.88 (s, 1H). **¹³C NMR** (101 MHz, CD₂Cl₂): δ = 152.9 (C_q), 152.1 (CH), 139.1 (C_q), 138.5 (CH), 136.6 (C_q), 133.8 (C_q), 132.5 (CH), 131.6 (CH), 131.0 (CH), 130.0 (C_q), 128.2 (C_q), 127.8 (CH), 127.4 (overlapped, CH), 127.0 (CH), 126.6 (CH), 125.6 (CH), 117.7 (CH), 82.2 (C_q), 28.2 (CH₃). **¹¹B NMR** (128 MHz, CD₂Cl₂): δ = 4.81 (1B), -3.96 (1B), -11.51 (1B), -15.65 (2B), -20.31 (1B), -25.95 (1B), -30.82 (1B), -35.66 (1B). **IR** (ATR): 2540, 1682, 1521, 1491, 1444, 1252, 1151, 696 cm⁻¹. **MS** (ESI) *m/z* (relative intensity): 530 (50) [M+H]⁺, 552 (100)

$[M+Na]^+$. **HR-MS** (ESI): m/z calcd. for $C_{28}H_{35}^{10}B_1^{11}B_8N_2O_2$ $[M+Na]^+$: 552.3483, found: 552.3478.



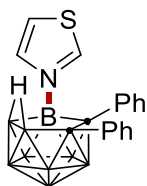
7,8-diphenyl-11-(9-(pyridin-4-yl)-9H-carbazyl)-*nido*-carborane

240r. The representative procedure **A** was followed using *nido*-carborane **238a** (36.0 mg, 0.10 mmol) and 9-(pyridin-4-yl)-9H-carbazole **239r** (73.0 mg, 0.30 mmol). Isolation by column chromatography (*n*-hexane/ CH_2Cl_2 : 1/1) yielded **240r** (30.0 mg, 56%) as a yellow solid. **M.p.** = 320 – 321 °C. **1H NMR** (300 MHz, $DMSO-d_6$): δ = 9.09 (d, J = 7.0 Hz, 2H), 8.28 (d, J = 7.4 Hz, 2H), 8.12 (d, J = 7.1 Hz, 2H), 7.66 – 7.59 (m, 2H), 7.52 (t, J = 7.1 Hz, 2H), 7.46 – 7.40 (m, 2H), 7.37 (d, J = 6.7 Hz, 2H), 7.09 – 6.94 (m, 5H), 6.90 – 6.81 (m, 3H), -1.42 (s, 1H). **^{13}C NMR** (101 MHz, $DMSO-d_6$): δ = 150.7 (CH), 150.0 (C_q), 139.1 (C_q), 138.3 (C_q), 136.6 (C_q), 132.5 (CH), 131.5 (CH), 127.7 (CH), 127.5 (CH), 127.4 (CH), 126.9 (CH), 126.7 (CH), 125.1 (C_q), 123.4 (CH), 121.5 (CH), 121.4 (CH), 111.1 (CH). **^{11}B NMR** (161 MHz, $DMSO-d_6$): δ = 19.79 (1B), 5.14 (1B), -5.31 (1B), -15.72 (2B), -21.29 (1B), -26.27 (1B), -31.13 (1B), -36.92 (1B). **IR** (ATR): 2216, 2176, 2149, 1961, 1510, 1443, 749 cm^{-1} . **MS** (ESI) m/z (relative intensity): 552 (100) $[M+Na]^+$, 530 (20) $[M+H]^+$. **HR-MS** (ESI): m/z calcd. for $C_{31}H_{31}^{10}B_1^{11}B_8N_2$ $[M+Na]^+$: 552.3274, found: 552.3265.



7,8-diphenyl-11-imidazo-*nido*-carborane

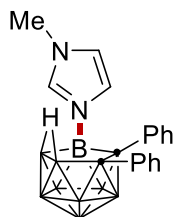
240s. The representative procedure **A** was followed using *nido*-carborane **238a** (36.0 mg, 0.10 mmol) and imidazole **239s** (20.4 mg, 0.30 mmol). Isolation by column chromatography (CH₂Cl₂) yielded **240s** (30.0 mg, 84%) as a white solid. **M.p.** = 283 – 285 °C. **¹H NMR** (500 MHz, Acetone-*d*₆): δ = 8.47 (t, *J* = 1.4 Hz, 1H), 7.33 (t, *J* = 1.6 Hz, 1H), 7.32 – 7.24 (m, 3H), 7.04 – 6.98 (m, 2H), 6.97 – 6.91 (m, 2H), 6.92 – 6.85 (m, 1H), 6.86 – 6.77 (m, 3H), 2.87 (s, 1H), -1.81 (s, 1H). **¹³C NMR** (126 MHz, Acetone-*d*₆): δ = 140.4 (C_q), 138.4 (C_q), 133.0 (CH), 132.1 (CH), 127.7 (CH), 127.6 (overlapped, CH), 127.3 (CH), 126.9 (CH), 126.7 (CH), 119.3 (CH). **¹¹B NMR** (128 MHz, Acetone *d*₆): δ = 6.28 (1B), -0.05 (1B), -7.84 (1B), -10.55 (2B), -16.20 (1B), -20.71 (1B), -26.25 (1B), -31.58 (1B). **IR** (ATR): 3350, 3151, 2535, 1693, 1494, 1444, 1245, 1058 cm⁻¹. **MS** (ESI) *m/z* (relative intensity): 376 (100) [M+Na]⁺, 354 (20) [M+H]⁺. **HR-MS** (ESI): *m/z* calcd. for C₁₇H₂₃¹⁰B₁¹¹B₈N₂ [M+Na]⁺: 376.2639, found: 376.2637. The analytical data corresponds with those reported in the literature.^[200]



7,8-diphenyl-11-thiazo-*nido*-carborane

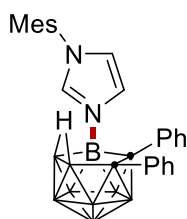
240t. The representative procedure **A** was followed using *nido*-carborane **238a** (36.0 mg, 0.10 mmol) and thiazole **239t** (25.5 mg, 0.30 mmol). Isolation by column chromatography (*n*-hexane/CH₂Cl₂: 1/1) yielded **240t** (23.0 mg, 62%) as a white solid. **M.p.** = 278 – 280 °C. **¹H NMR** (500 MHz, Acetone-*d*₆): δ = 9.62 (dd, *J* = 2.4, 1.2 Hz, 1H), 8.19 (dd, *J* = 3.6, 1.2 Hz, 1H), 8.01 (dd, *J* = 3.6, 2.3 Hz, 1H), 7.33 – 7.28 (m, 2H), 7.04 – 6.99 (m, 2H), 6.96 – 6.87 (m, 3H), 6.85 – 6.80 (m, 3H), -1.75 (s, 1H). **¹³C NMR** (126 MHz, Acetone-*d*₆): δ = 160.8 (CH), 142.5 (C_q), 139.9 (C_q), 137.7 (CH), 132.9 (CH), 131.9 (CH), 127.9 (CH), 127.7 (CH), 127.3 (CH), 126.9 (CH), 124.5 (CH). **¹¹B NMR** (128 MHz, Acetone-*d*₆): δ = 2.16 (1B), -4.51 (1B), -11.95 (1B), -15.68 (2B), -20.65 (1B), -25.91 (1B), -30.68 (1B), -36.28 (1B). **IR** (ATR): 3110, 2922, 2852, 1975, 1492, 1442, 1248, 688 cm⁻¹. **MS** (ESI) *m/z* (relative intensity): 393 (100) [M+Na]⁺, 371 (30) [M+H]⁺. **HR-MS** (ESI): *m/z* calcd. for C₁₇H₂₂¹⁰B₁¹¹B₈NS [M+Na]⁺:

393.2252, found: 393.2252. The analytical data corresponds with those reported in the literature.^[200]



7,8-diphenyl-11-(1-methyl-1*H*-imidazole)-*nido*-carborane

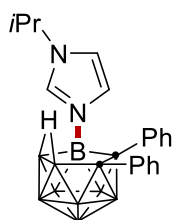
240u. The representative procedure **A** was followed using *nido*-carborane **238a** (36.0 mg, 0.10 mmol) and 1-methyl-1*H*-imidazole **239u** (25.0 mg, 0.30 mmol). Isolation by column chromatography (*n*-hexane/CH₂Cl₂: 1/1) yielded **240u** (32.0 mg, 88%) as a colorless solid. **M.p.** = 270 – 272 °C. **¹H NMR** (400 MHz, CD₂Cl₂): δ = 7.74 (s, 1H), 7.34 – 7.28 (m, 2H), 7.04 – 6.90 (m, 9H), 6.85 (t, *J* = 1.8 Hz, 1H), 3.67 (s, 3H), -1.98 (s, 1H). **¹³C NMR** (101 MHz, CD₂Cl₂): δ = 139.1 (C_q), 137.3 (C_q), 137.2 (CH), 132.2 (CH), 131.2 (CH), 127.2 (CH), 127.1 (CH), 127.0 (CH), 126.4 (CH), 126.1 (CH), 121.6 (CH), 35.5 (CH₃). **¹¹B NMR** (96 MHz, CD₂Cl₂): δ = 0.89 (1B), -4.66 (1B), -12.39 (1B), -15.64 (2B), -20.80 (1B), -25.99 (1B), -31.34 (1B), -36.47 (1B). **IR** (ATR): 3143, 2547, 2506, 1541, 1442, 1172, 829, 750, 689 cm⁻¹. **MS** (ESI) *m/z* (relative intensity): 390 (100) [M+Na]⁺, 368 (20) [M+H]⁺. **HR-MS** (ESI): *m/z* calcd. for C₁₈H₂₅¹⁰B₁¹¹B₈N₂ [M+Na]⁺: 390.2796, found: 390.2795. The analytical data corresponds with those reported in the literature.^[200]



7,8-diphenyl-11-(1-mesityl-1*H*-imidazole)-*nido*-carborane

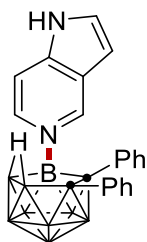
240v. The representative procedure **A** was followed using *nido*-carborane **238a** (36.0 mg, 0.10 mmol) and 1-mesityl-1*H*-imidazole **239v** (56.0 mg, 0.30 mmol). Isolation by column chromatography (*n*-hexane/CH₂Cl₂: 1/1) yielded **240v** (33.0 mg, 70%) as a colorless solid. **M.p.** = 237 – 239 °C. **¹H NMR** (300 MHz, CD₂Cl₂): δ = 7.72 (t, *J* = 1.5 Hz, 1H), 7.47 (t, *J* = 1.6 Hz, 1H), 7.36 – 7.30

(m, 2H), 7.04 – 6.95 (m, 7H), 6.93 – 6.87 (m, 4H), 2.35 (s, 3H), 1.94 (s, 3H), 1.60 (s, 3H), -2.01 (s, 1H). **¹³C NMR** (101 MHz, CD₂Cl₂): δ = 141.3 (C_q), 139.3 (C_q), 137.7 (C_q), 137.4 (CH), 134.8 (C_q), 134.7 (C_q), 132.5 (CH), 131.4 (CH), 131.0 (C_q), 129.7 (CH), 128.3 (CH), 127.6 (CH), 127.3 (CH), 126.7 (CH), 126.4 (CH), 122.5 (CH), 21.1 (CH₃), 17.2 (CH₃), 17.0 (CH₃). **¹¹B NMR** (128 MHz, CD₂Cl₂): δ = 0.52 (1B), -4.70 (1B), -12.44 (1B), -15.97 (2B), -21.20 (1B), -26.06 (1B), -31.28 (1B), -36.54 (1B). **IR** (ATR): 3475, 3375, 2534, 1644, 1527, 1181, 832, 695 cm⁻¹. **MS** (ESI) *m/z* (relative intensity): 494 (100) [M+Na]⁺, 472 (30) [M+H]⁺. **HR-MS** (ESI): *m/z* calcd. for C₂₆H₃₃¹⁰B₁¹¹B₈N₂ [M+Na]⁺: 494.3427, found: 494.3417.



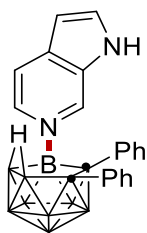
7,8-diphenyl-11-(1-isopropyl-1H-imidazole)-nido-carborane

240w. The representative procedure **A** was followed using *nido*-carborane **238a** (36.0 mg, 0.10 mmol) and 1-isopropyl-1H-imidazole **239w** (33.0 mg, 0.30 mmol). Isolation by column chromatography (*n*-hexane/CH₂Cl₂: 1/1) yielded **240w** (35.0 mg, 89%) as a colorless solid. **M.p.** = 213 – 216 °C. **¹H NMR** (300 MHz, CD₂Cl₂): δ = 7.50 (t, *J* = 1.6 Hz, 1H), 7.34 – 7.30 (m, 2H), 7.21 (t, *J* = 1.7 Hz, 1H), 7.05 – 6.97 (m, 3H), 6.96 – 6.91 (m, 6H), 4.24 (hept, *J* = 6.7 Hz, 1H), 1.35 (d, *J* = 2.5 Hz, 3H), 1.33 (d, *J* = 2.5 Hz, 3H), -2.07 (s, 1H). **¹³C NMR** (101 MHz, CD₂Cl₂): δ = 139.4 (C_q), 137.8 (C_q), 134.8 (CH), 132.4 (CH), 131.5 (CH), 127.6 (CH), 127.5 (CH), 127.3 (CH), 126.7 (CH), 126.4 (CH), 118.7 (CH), 52.4 (CH), 23.1 (CH₃), 22.9 (CH₃). **¹¹B NMR** (128 MHz, CD₂Cl₂): δ = 0.72 (1B), -5.08 (1B), -12.70 (1B), -15.94 (2B), -21.04 (1B), -26.22 (1B), -31.68 (1B), -36.64 (1B). **IR** (ATR): 3142, 2557, 2519, 1537, 1442, 1177, 838, 759, 657 cm⁻¹. **MS** (ESI) *m/z* (relative intensity): 418 (100) [M+Na]⁺, 396 (30) [M+H]⁺. **HR-MS** (ESI): *m/z* calcd. for C₂₀H₂₉¹⁰B₁¹¹B₈N₂ [M+Na]⁺: 418.3111, found: 418.3114.



7,8-diphenyl-11-(1*H*-pyrrolo[3,2-*c*]pyridyl)-*nido*-carborane

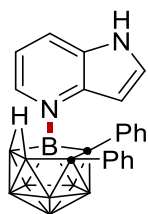
240x. The representative procedure **A** was followed using *nido*-carborane **239a** (36.0 mg, 0.10 mmol) and 1*H*-pyrrolo[3,2-*c*]pyridine **239x** (35.4 mg, 0.30 mmol). Isolation by column chromatography (CH₂Cl₂) yielded **240x** (27.0 mg, 67%) as a white solid. **M.p.** = 280 – 283 °C. **¹H NMR** (500 MHz, Acetone-*d*₆): δ = 11.51 (s, 1H), 9.40 (s, 1H), 8.57 (d, *J* = 7.8 Hz, 1H), 7.75 (dd, *J* = 3.4, 1.9 Hz, 1H), 7.66 (d, *J* = 6.8 Hz, 1H), 7.35 – 7.30 (m, 2H), 7.04 – 6.99 (m, 2H), 6.97 – 6.85 (m, 4H), 6.75 – 6.60 (m, 3H), -1.65 (s, 1H). **¹³C NMR** (126 MHz, Acetone-*d*₆): δ = 144.2 (CH), 141.7 (C_q), 140.2 (C_q), 139.9 (CH), 138.0 (C_q), 133.0 (CH), 132.0 (CH), 131.9 (CH), 127.7 (CH), 127.5 (CH), 126.8 (CH), 126.8 (CH), 125.6 (C_q), 108.8 (CH), 104.6 (CH). **¹¹B NMR** (128 MHz, Acetone-*d*₆): δ = 6.10 (1B), -4.91 (1B), -12.91 (1B), -15.57 (2B), -21.64 (1B), -26.01 (1B), -30.95 (1B), -36.54 (1B). **IR** (ATR): 3386, 2923, 2536, 1631, 1493, 1357, 1225, 697 cm⁻¹. **MS** (ESI) *m/z* (relative intensity): 426 (100) [M+Na]⁺, 404 (30) [M+H]⁺. **HR-MS** (ESI): *m/z* calcd. for C₂₁H₂₅¹⁰B₁¹¹B₈N₂ [M+Na]⁺: 426.2798, found: 426.2794.



7,8-diphenyl-11-(1*H*-pyrrolo[2,3-*c*]pyridyl)-*nido*-carborane

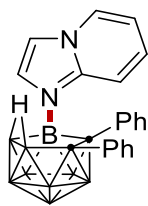
240y. The representative procedure **A** was followed using *nido*-carborane **238a** (36.0 mg, 0.10 mmol) and 1*H*-pyrrolo[2,3-*c*]pyridine **239y** (35.4 mg, 0.30 mmol). Isolation by column chromatography (CH₂Cl₂) yielded **240y** (28.2 mg, 70%) as a white solid. **M.p.** = 171 – 175 °C. **¹H NMR** (500 MHz, Acetone-*d*₆): δ = 11.55 (s, 1H), 9.23 (s, 1H), 8.53 (d, *J* = 6.6 Hz, 1H), 8.07 (d, *J* = 2.9 Hz,

1H), 7.80 (d, $J = 6.6$ Hz, 1H), 7.31 (d, $J = 7.2$ Hz, 2H), 6.99 (d, $J = 6.8$ Hz, 2H), 6.93 (t, $J = 7.4$ Hz, 2H), 6.92 – 6.85 (m, 1H), 6.79 (d, $J = 2.9$ Hz, 1H), 6.73 – 6.63 (m, 3H), -1.64 (s, 1H). **^{13}C NMR** (126 MHz, Acetone- d_6): $\delta = 140.1$ (C_q), 138.3 (CH), 137.9 (C_q), 137.9 (CH), 136.4 (C_q), 134.8 (CH), 133.0 (CH), 132.6 (C_q), 131.9 (CH), 127.7 (CH), 127.6 (CH), 126.9 (CH), 126.8 (CH), 116.7 (CH), 103.6 (CH). **^{11}B NMR** (128 MHz, Acetone- d_6): $\delta = 6.24$ (1B), -4.58 (1B), -12.66 (1B), -15.43 (2B), -21.41 (1B), -25.92 (1B), -30.88 (1B), -36.41 (1B). **IR** (ATR): 2539, 1710, 1639, 1494, 1321, 1140, 836, 693 cm^{-1} . **MS** (ESI) m/z (relative intensity): 426 (100) [M+Na]⁺, 404 (50) [M+H]⁺. **HR-MS** (ESI): m/z calcd. for C₂₁H₂₅¹⁰B₁¹¹B₈N₂ [M+Na]⁺: 426.2798, found: 426.2798. The analytical data corresponds with those reported in the literature.^[200]



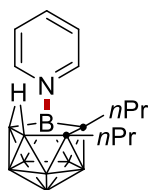
7,8-diphenyl-11-(1H-pyrrolo[3,2-b]pyridyl)-nido-carborane

240z. The representative procedure **A** was followed using *nido*-carborane **238a** (36.0 mg, 0.10 mmol) and 1H-pyrrolo[3,2-b]pyridine **239z** (35.4 mg, 0.30 mmol). Isolation by column chromatography (CH₂Cl₂) yielded **240z** (20.1 mg, 50%) as a white solid. **M.p.** = 283 – 285 °C. **^1H NMR** (500 MHz, Acetone- d_6): $\delta = 11.57$ (s, 1H), 8.69 (d, $J = 6.0$ Hz, 1H), 8.30 (d, $J = 8.1$ Hz, 1H), 8.22 (d, $J = 3.3$ Hz, 1H), 7.76 (d, $J = 3.3$ Hz, 1H), 7.38 – 7.29 (m, 3H), 7.02 – 6.85 (m, 5H), 6.62 – 6.50 (m, 3H), -1.67 (s, 1H). **^{13}C NMR** (126 MHz, Acetone- d_6): $\delta = 144.0$ (C_q), 142.6 (CH), 140.0 (C_q), 137.9 (C_q), 135.3 (CH), 133.1 (CH), 132.7 (CH), 131.6 (C_q), 127.8 (CH), 126.9 (CH), 126.9 (CH), 126.7 (CH), 126.6 (CH), 116.9 (CH), 101.9 (CH). **^{11}B NMR** (128 MHz, Acetone- d_6): $\delta = 4.40$ (1B), -4.77 (1B), -12.03 (1B), -15.09 (1B), -15.66 (1B), -22.01 (1B), -25.70 (1B), -29.83 (1B), -36.66 (1B). **IR** (ATR): 3386, 2540, 2199, 2021, 14958, 1425, 1367, 763, 698. cm^{-1} . **MS** (ESI) m/z (relative intensity): 426 (100) [M+Na]⁺, 404 (30) [M+H]⁺. **HR-MS** (ESI): m/z calcd. for C₂₁H₂₅¹⁰B₁¹¹B₈N₂ [M+Na]⁺: 426.2798, found: 426.2801.



7,8-diphenyl-11-(*H*-imidazo[1,2-*a*]pyridine)-*nido*-carborane

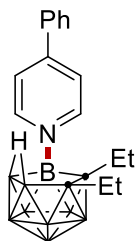
240aa. The representative procedure **A** was followed using *nido*-carborane **238a** (36.0 mg, 0.10 mmol) and *H*-imidazo[1,2-*a*]pyridine **239aa** (35.4 mg, 0.30 mmol). Isolation by column chromatography (CH₂Cl₂) yielded **240aa** (30.0 mg, 75%) as a white solid. **M.p.** = 265 – 268 °C. **¹H NMR** (500 MHz, CD₂Cl₂): δ = 8.76 (d, *J* = 9.3 Hz, 1H), 8.16 (dt, *J* = 6.7, 1.2 Hz, 1H), 7.82 (ddd, *J* = 9.3, 7.0, 1.3 Hz, 1H), 7.53 (d, *J* = 2.1 Hz, 1H), 7.39 (d, *J* = 1.3 Hz, 1H), 7.34 – 7.28 (m, 2H), 7.25 (td, *J* = 6.9, 1.1 Hz, 1H), 7.01 – 6.92 (m, 3H), 6.83 – 6.76 (m, 2H), 6.70 – 6.61 (m, 3H), -1.87 (s, 1H). **¹³C NMR** (126 MHz, CD₂Cl₂): δ = 143.8 (C_q), 139.4 (C_q), 137.8 (C_q), 132.4 (CH), 132.1 (CH), 130.9 (CH), 130.5 (CH), 127.9 (CH), 127.3 (CH), 127.0 (CH), 126.4 (CH), 126.2 (CH), 116.9 (CH), 115.0 (CH), 113.1 (CH). **¹¹B NMR** (128 MHz, CD₂Cl₂): δ = 0.00 (1B), -4.98 (1B), -11.82 (1B), -15.41 (1B), -16.03 (1B), -21.34 (1B), -25.59 (1B), -30.16 (1B), -36.53 (1B). **IR** (ATR): 3144, 2532, 1707, 1642, 1444, 1202, 752, 697 cm⁻¹. **MS** (ESI) *m/z* (relative intensity): 426 (100) [M+Na]⁺, 404 (50) [M+H]⁺. **HR-MS** (ESI): *m/z* calcd. for C₂₁H₂₅¹⁰B₁¹¹B₈N₂ [M+H]⁺: 426.2798, found: 426.2801.



7,8-dipropyl-11-pyridyl-*nido*-carborane

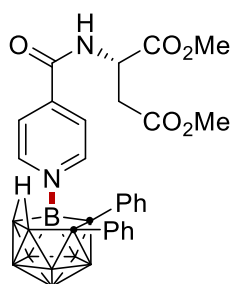
240bb. The representative procedure **A** was followed using *nido*-carborane **239b** (29.1 mg, 0.10 mmol) and pyridine **239a** (24.0 mg, 0.30 mmol). Isolation by column chromatography (*n*-hexane/CH₂Cl₂: 1/1) yielded **240bb** (19.5 mg, 66%) as a yellow solid. **M.p.** = 199 – 200 °C. **¹H NMR** (300 MHz, CD₂Cl₂): δ = 9.09 (d, *J* = 4.9 Hz, 2H), 8.33 (tt, *J* = 7.8, 1.5 Hz, 1H), 7.85 (dd, *J* = 7.7, 6.6 Hz, 2H), 2.04 – 1.85 (m, 6H), 1.01 – 0.86 (m, 5H), 0.61 (t, *J* = 7.3 Hz, 3H), -

2.76 (s, 1H). **¹³C NMR** (75 MHz, CD₂Cl₂): δ = 148.9 (CH), 143.1 (CH), 126.5 (CH), 36.7 (CH₂), 33.4 (CH₂), 24.1 (CH₂), 22.9 (CH₂), 14.3 (CH₃), 14.1 (CH₃). **¹¹B NMR** (96 MHz, CD₂Cl₂): δ = 4.42 (1B), -5.99 (1B), -12.19 (1B), -13.83 (1B), -17.06 (1B), -20.53 (1B), -27.25 (1B), -30.97 (1B), -37.54 (1B). **IR** (ATR): 2558, 2527, 2231, 2032, 1960, 1629, 572, 480 cm⁻¹. **MS** (ESI) m/z (relative intensity): 319 (100) [M+Na]⁺, 297 (50) [M+H]⁺. **HR-MS** (ESI): m/z calcd. for C₁₃H₂₈¹⁰B₁¹¹B₈N [M+Na]⁺: 319.2997, found: 319.2993.



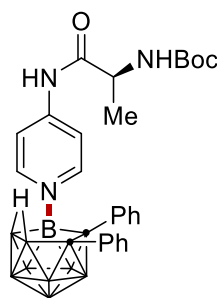
7,8-diethyl-11-(4-phenylpyridyl)-*nido*-carborane

240cc. The representative procedure **A** was followed using *nido*-carborane **238c** (26.3 mg, 0.10 mmol) and 4-phenylpyridine **239g** (46.5 mg, 0.30 mmol). Isolation by column chromatography (*n*-hexane/CH₂Cl₂: 1/1) yielded **240cc** (25.0 mg, 73%) as a yellow solid. **M.p.** = 84 – 85 °C. **¹H NMR** (300 MHz, CD₂Cl₂): δ = 9.06 (d, J = 5.6 Hz, 2H), 8.02 (d, J = 5.6 Hz, 2H), 7.90 – 7.80 (m, 2H), 7.71 – 7.62 (m, 3H), 2.19 – 1.98 (m, 2H), 1.92 – 1.80 (m, 2H), 1.15 (t, J = 7.5 Hz, 3H), 0.65 (t, J = 7.5 Hz, 3H), -2.72 (s, 1H). **¹³C NMR** (75 MHz, CD₂Cl₂): δ = 155.0 (C_q), 148.8 (CH), 134.4 (C_q), 131.8 (CH), 129.8 (CH), 127.6 (CH), 123.6 (CH), 27.1 (CH₂), 23.7 (CH₂), 14.9 (CH₃), 13.9 (CH₃). **¹¹B NMR** (96 MHz, CD₂Cl₂): δ = 4.3 (1B), -6.1 (1B), -12.5 (1B), -14.0 (1B), -17.2 (1B), -20.7 (1B), -27.3 (1B), -31.1 (1B), -37.6 (1B). **IR** (ATR): 2527, 2032, 1994, 1961, 1629, 766, 692, 446 cm⁻¹. **MS** (ESI) m/z (relative intensity): 367 (100) [M+Na]⁺, 345 (50) [M+H]⁺. **HR-MS** (ESI): m/z calcd. for C₁₇H₂₈¹⁰B₁¹¹B₈N [M+Na]⁺: 367.0000, found: 367.2993.



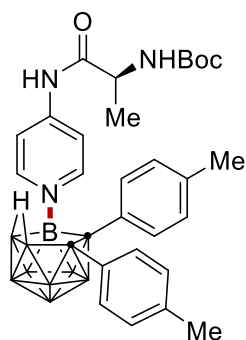
7,8-diethyl-11-(dimethyl isonicotinoyl-*L*-aspartate)-*nido*-carborane

240^{la}. The representative procedure **A** was followed using *nido*-carborane **238a** (36.0 mg, 0.10 mmol) and dimethyl isonicotinoyl-*L*-aspartate **239bb** (80.0 mg, 0.30 mmol). Isolation by column chromatography (MeOH/CH₂Cl₂: 1/100) yielded **240^{la}** (46.0 mg, 84%) as a yellow solid. **M.p.** = 183 – 187 °C. **¹H NMR** (400 MHz, CD₂Cl₂): δ = 8.83 (d, *J* = 6.7 Hz, 2H), 7.82 (d, *J* = 7.0 Hz, 2H), 7.49 – 7.42 (m, 1H), 7.32 (d, *J* = 6.5 Hz, 2H), 7.04 – 6.98 (m, 3H), 6.96 – 6.89 (m, 5H), 5.03 – 4.96 (m, 1H), 3.80 (s, 3H), 3.72 (s, 3H), 3.20 – 3.11 (m, 1H), 3.02 – 2.94 (m, 1H), -1.89 (s, 1H). **¹³C NMR** (101 MHz, CD₂Cl₂): δ = 171.4 (C_q), 170.2 (C_q), 161.8 (C_q), 148.3 (CH), 145.7 (C_q), 138.6 (C_q), 135.8 (C_q), 132.1 (CH), 131.2 (CH), 127.8 (CH), 127.1 (CH), 127.0 (CH), 126.4 (CH), 123.5 (CH), 53.1 (CH₃), 52.2 (CH₃), 49.3 (CH), 35.4 (CH₂). **¹¹B NMR** (96 MHz, CD₂Cl₂): δ = 4.58 (1B), -3.63 (1B), -11.19 (1B), -15.79 (2B), -20.13 (1B), -26.06 (1B), -30.87 (1B), -35.56 (1B). **IR** (ATR): 3335, 2954, 2541, 1738, 1708, 1676, 1434, 1220, 697 cm⁻¹. **MS** (ESI) *m/z* (relative intensity): 574 (100) [M+Na]⁺, 552 (20) [M+H]⁺. **HR-MS** (ESI): *m/z* calcd. for C₂₆H₃₃¹⁰B₁¹¹B₈N₂O₅ [M+Na]⁺: 574.3174, found: 574.3165.

**7,8-diphenyl-11-(*tert*-butyl(*S*)-(1-oxo-1-(pyridin-4-ylamino)propan-2-yl)carbamyl)-*nido*-carborane**

240^{lb}. The representative procedure **A** was followed using *nido*-carborane **238a** (36.0 mg, 0.10 mmol) and *tert*-butyl (*S*)-(1-oxo-1-(pyridin-4-ylamino)propan-2-yl)carbamate **239cc** (80.0 mg, 0.30 mmol). Isolation by column chromatography (MeOH/CH₂Cl₂: 1/100) yielded **240^{lb}** (44.0 mg, 80%)

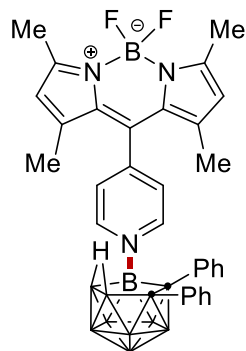
as a colorless solid. **M.p.** = 230 – 233 °C. **¹H NMR** (400 MHz, CDCl₃): δ = 10.00 (s, 1H), 8.47 (d, J = 3.3 Hz, 2H), 7.51 (t, J = 6.5 Hz, 2H), 7.33 – 7.28 (m, 2H), 7.00 – 6.93 (m, 3H), 6.89 – 6.80 (m, 5H), 4.98 – 4.84 (m, 1H), 4.33 – 4.20 (m, 1H), 1.48 (s, 9H), 1.42 (d, J = 7.2 Hz, 3H), -2.02 (s, 1H). **¹³C NMR** (101 MHz, CDCl₃): δ = 171.8 (C_q), 157.2 (C_q), 149.5 (C_q), 148.3 (CH), 138.6 (C_q), 136.5 (C_q), 132.1 (CH), 131.1 (CH), 127.4 (CH), 127.1 (CH), 126.6 (CH), 126.2 (CH), 113.9 (CH), 82.2 (C_q), 51.1 (CH), 28.2 (CH₃), 15.7 (CH₃). **¹¹B NMR** (96 MHz, CDCl₃): δ = 5.18 (1B), -3.87 (1B), -10.82 (1B), -15.36 (2B), -20.60 (1B), -26.03 (1B), -30.80 (1B), -35.93 (1B). **IR** (ATR): 3475, 3375, 2535, 1681, 1644, 1494, 1443, 1162, 695 cm⁻¹. **MS** (ESI) m/z (relative intensity): 573 (100) [M+Na]⁺, 551 (50) [M+H]⁺. **HR-MS** (ESI): m/z calcd. for C₂₇H₃₈¹⁰B₁¹¹B₈N₃O₃ [M+Na]⁺: 573.3698, found: 573.3708.



7,8-(*p*-ditoluoyl)-11-(*tert*-butyl(*S*)-(1-oxo-1-(pyridin-4-ylamino)propan-2-yl)carbamyl)-*nido*-carborane

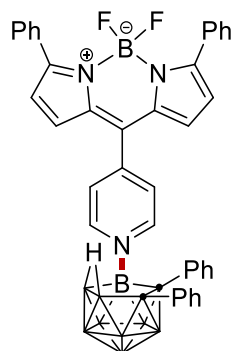
240lc. The representative procedure **A** was followed using the toluene derivative of the *nido*-carborane **238d** (38.8 mg, 0.10 mmol) and *tert*-butyl (*S*)-(1-oxo-1-(pyridin-4-ylamino)propan-2-yl)carbamate **239dd** (80.0 mg, 0.30 mmol). Isolation by column chromatography (CH₂Cl₂) yielded **240lc** (32.0 mg, 55%) as a white solid. **M.p.** = 220 – 222 °C. **¹H NMR** (300 MHz, CD₂Cl₂): δ = 9.91 (s, 1H), 8.48 (d, J = 7.3 Hz, 2H), 7.57 (d, J = 9.7 Hz, 2H), 7.19 (d, J = 8.1 Hz, 2H), 6.90 – 6.76 (m, 4H), 6.71 (d, J = 7.8 Hz, 2H), 5.01 (d, J = 6.5 Hz, 1H), 4.29 (q, J = 7.0 Hz, 1H), 2.18 (s, 3H), 2.10 (s, 3H), 1.48 (s, 9H), 1.42 (d, J = 7.1 Hz, 3H), -1.98 (s, 1H). **¹³C NMR** (101 MHz, CD₂Cl₂): δ = 171.9 (C_q), 149.7 (C_q), 148.3 (CH), 136.2 (C_q), 136.2 (C_q), 136.2 (C_q), 135.8 (C_q), 133.5 (C_q), 132.0 (CH), 131.0 (CH), 128.1 (CH), 127.8 (CH), 113.8 (CH), 81.8 (C_q), 29.7 (CH), 27.9 (CH₃), 20.6 (CH₃), 20.6 (CH₃), 20.5 (CH₃).

^{11}B NMR (128 MHz, CD_2Cl_2): δ = 6.10 (1B), -4.91 (1B), -12.91 (1B), -15.57 (2B), -21.64 (1B), -26.01 (1B), -30.95 (1B), -36.54 (1B). **IR** (ATR): 3210, 2539, 1633, 1517, 1312, 1171, 845, 697 cm^{-1} . **MS** (ESI) m/z (relative intensity): 596 (100) $[\text{M}+\text{NH}_4]^+$. **HR-MS** (ESI): m/z calcd. for $\text{C}_{29}\text{H}_{42}^{10}\text{B}_1^{11}\text{B}_8\text{N}_3\text{O}_3$ $[\text{M}+\text{NH}_4]^+$: 596.4458, found: 596.4449.



7,8-diphenyl-11-(5,5-difluoro-1,3,7,9-tetramethyl-10-(pyridin-4-yl)-5H-4 λ^4 ,5 λ^4 -dipyrrolo[1,2-c:2',1'-f][1,3,2]diazaborin-9-yl)-nido-carborane

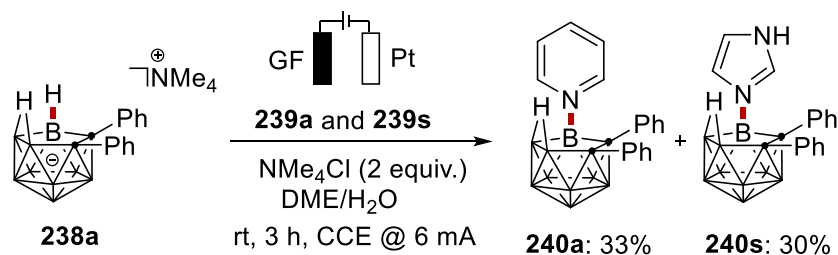
240'd. The representative procedure **A** was followed using *nido*-carborane **238a** (36.0 mg, 0.10 mmol) and 5,5-difluoro-1,3,7,9-tetramethyl-10-(pyridin-4-yl)-5H-4 λ^4 ,5 λ^4 -dipyrrolo[1,2-c:2',1'-f][1,3,2]diazaborinine **239ee** (98.0 mg, 0.30 mmol). Isolation by column chromatography ($\text{MeOH}/\text{CH}_2\text{Cl}_2$: 1/100) yielded **240'd** (43.0 mg, 71%) as a red solid. **M.p.** = 318 – 319 °C. **^1H NMR** (300 MHz, CD_2Cl_2): δ = 8.94 (d, J = 6.8 Hz, 2H), 7.59 (d, J = 6.8 Hz, 2H), 7.37 – 7.30 (m, 2H), 7.07 – 6.87 (m, 8H), 6.09 (s, 2H), 2.55 (s, 6H), 1.25 (s, 6H), -1.96 (s, 1H). **^{13}C NMR** (101 MHz, CD_2Cl_2): δ = 158.0 (C_q), 150.7 (C_q), 148.5 (CH), 142.1 (C_q), 138.5 (C_q), 136.0 (C_q), 133.5 (C_q), 132.1 (CH), 131.0 (CH), 129.4 (C_q), 127.7 (CH), 127.2 (CH), 126.9 (CH), 126.4 (overlapped, CH), 122.5 (CH), 15.1 (CH_3), 15.1 (CH_3), 14.5 (CH_3), 14.5 (CH_3). **^{11}B NMR** (128 MHz, CD_2Cl_2): δ = 4.61 (1B), 0.53 (t, J = 31.9 Hz, BF_2), -3.67 (1B), -10.68 (1B), -15.76 (2B), -20.49 (1B), -26.01 (1B), -30.72 (1B), -35.65 (1B). **^{19}F NMR** (377 MHz, CD_2Cl_2): δ = -146.29 (dd, J = 64.0, 32.5 Hz). **IR** (ATR): 3478, 3376, 2541, 1644, 1518, 1443, 1197, 1161, 695 cm^{-1} . **MS** (ESI) m/z (relative intensity): 633 (100) $[\text{M}+\text{Na}]^+$. **HR-MS** (ESI): m/z calcd. for $\text{C}_{32}\text{H}_{37}^{10}\text{B}_1^{11}\text{B}_9\text{F}_2\text{N}_3$ $[\text{M}+\text{Na}]^+$: 633.3821, found: 633.3823.



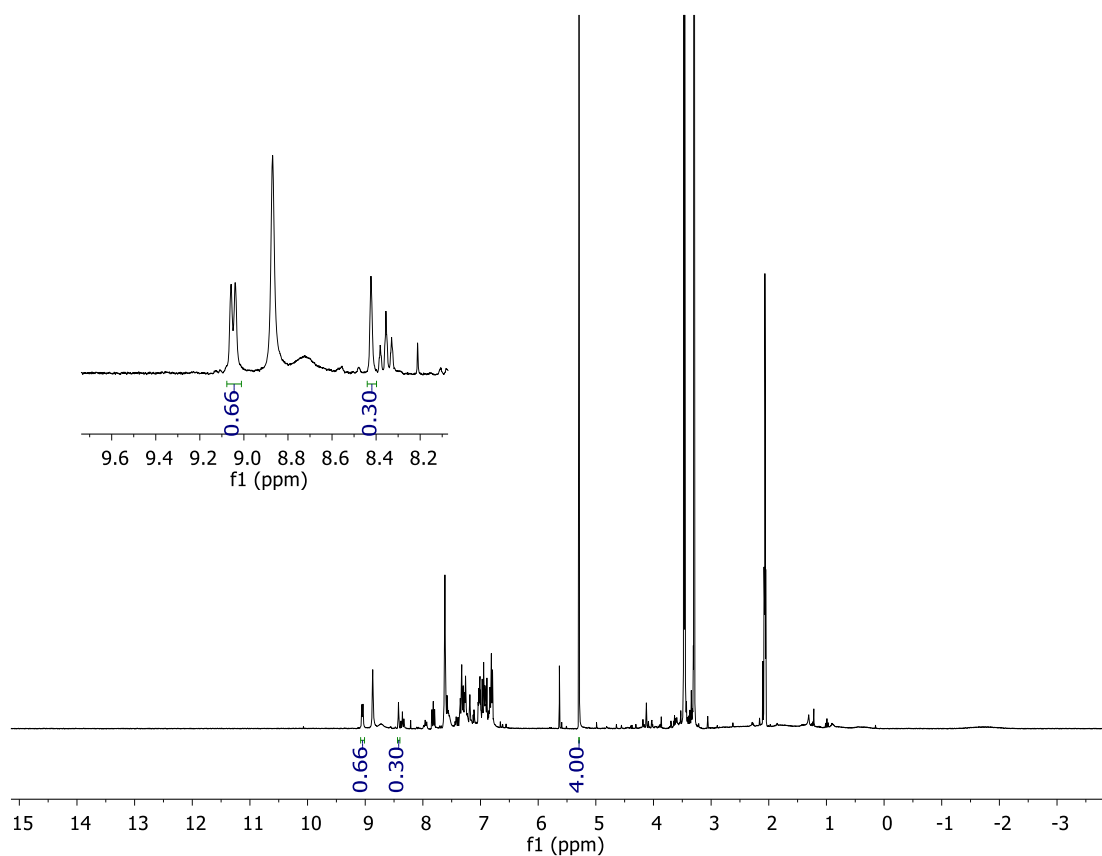
7,8-diphenyl-11-(5,5-difluoro-3,7-diphenyl-10-(pyridin-4-yl)-5H-4λ⁴,5λ⁴-dipyrrolo[1,2-c:2',1'-f][1,3, 2]diazaborininyl)-nido-carborane

240le. The representative procedure **A** was followed using *nido*-carborane **238a** (36.0 mg, 0.10 mmol) and 5,5-difluoro-3,7-diphenyl-10-(pyridin-4-yl)-5H-4λ⁴,5λ⁴-dipyrrolo[1,2-c:2',1'-f][1,3, 2]diazaborinine **239ff** (126.0 mg, 0.30 mmol). Isolation by column chromatography (MeOH/CH₂Cl₂: 1/100) yielded **240le** (35.0 mg, 50%) as a purple solid. **M.p.** = 310 – 312 °C. **¹H NMR** (300 MHz, CD₂Cl₂): δ = 8.91 (d, *J* = 6.8 Hz, 2H), 7.92 – 7.85 (m, 4H), 7.70 (d, *J* = 6.9 Hz, 2H), 7.55 – 7.47 (m, 6H), 7.40 – 7.33 (m, 2H), 7.09 – 6.95 (m, 8H), 6.78 (d, *J* = 4.3 Hz, 2H), 6.62 (d, *J* = 4.4 Hz, 2H), -1.90 (s, 1H). **¹³C NMR** (101 MHz, CD₂Cl₂): δ = 161.2 (C_q), 148.5 (C_q), 147.8 (CH), 138.6 (C_q), 136.2 (C_q), 135.4 (C_q), 134.9 (C_q), 132.1 (CH), 131.8 (C_q), 131.2 (CH), 130.3 (CH), 129.7 (CH), 129.5 (CH), 129.5 (CH), 129.4 (CH), 128.3 (CH), 127.7 (CH), 127.2 (CH), 127.0 (CH), 126.9 (CH), 126.4 (CH), 122.6 (CH). **¹¹B NMR** (128 MHz, CD₂Cl₂): δ = 4.61 (1B), 1.24 (t, *J* = 31.3 Hz, BF₂), -3.79 (1B), -10.90 (1B), -16.09 (2B), -20.64 (1B), -26.21 (1B), -31.07 (1B), -35.67 (1B). **¹⁹F NMR** (377 MHz, CD₂Cl₂): δ = -132.08 (dd, *J* = 63.1, 31.2 Hz). **IR** (ATR): 2220, 2160, 2148, 1990, 1569, 1289, 1136, 1073, 699 cm⁻¹. **MS** (ESI) *m/z* (relative intensity): 729 (100) [M+Na]⁺. **HR-MS** (ESI): *m/z* calcd. for C₄₀H₃₇¹⁰B₁¹¹B₉F₂N₃ [M+Na]⁺: 729.3822, found: 729.3833.

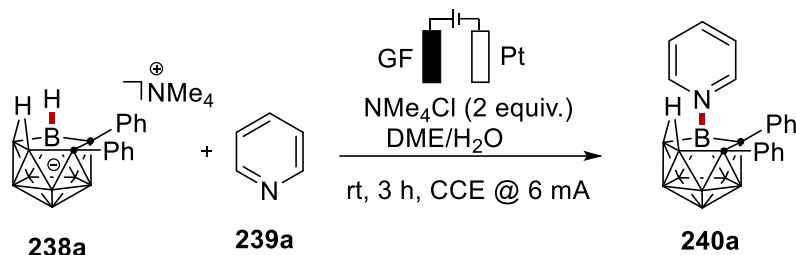
5.3.1.2 Competition Experiments



The general procedure **A** was followed using *nido*-carborane **238a** (36 mg, 0.10 mmol), pyridine **239a** (12 mg, 0.15 mmol) and imidazole **239s** (10 mg, 0.15 mmol). The conversions to **240a** and **240s** were determined by crude ^1H NMR spectroscopy with CH_2Br_2 as the internal standard.



5.3.1.3 GC-Headspace Detection



In an undivided cell equipped with a GF anode (10 mm × 15 mm × 6 mm) and a platinum cathode (10 mm × 15 mm × 0.25 mm), *nido*-Carborane **238a** (0.10 mmol, 1.0 equiv), pyridine **239a** (0.30 mmol, 3.0 equiv), and NMe₄Cl (0.20 mmol, 2.0 equiv) were dissolved in DME (4.0 mL) and H₂O (0.2 mL). Electrocatalysis was performed at room temperature under a constant current of 6.0 mA maintained for 3 h. After the reaction, 1.0 mL of the headspace volume was removed for GC analysis. The graphite felt anode was washed with CH₂Cl₂ (3 × 10 mL) in an ultrasonic bath. The yield of **240a** (86%) was determined by ¹H NMR spectroscopy.

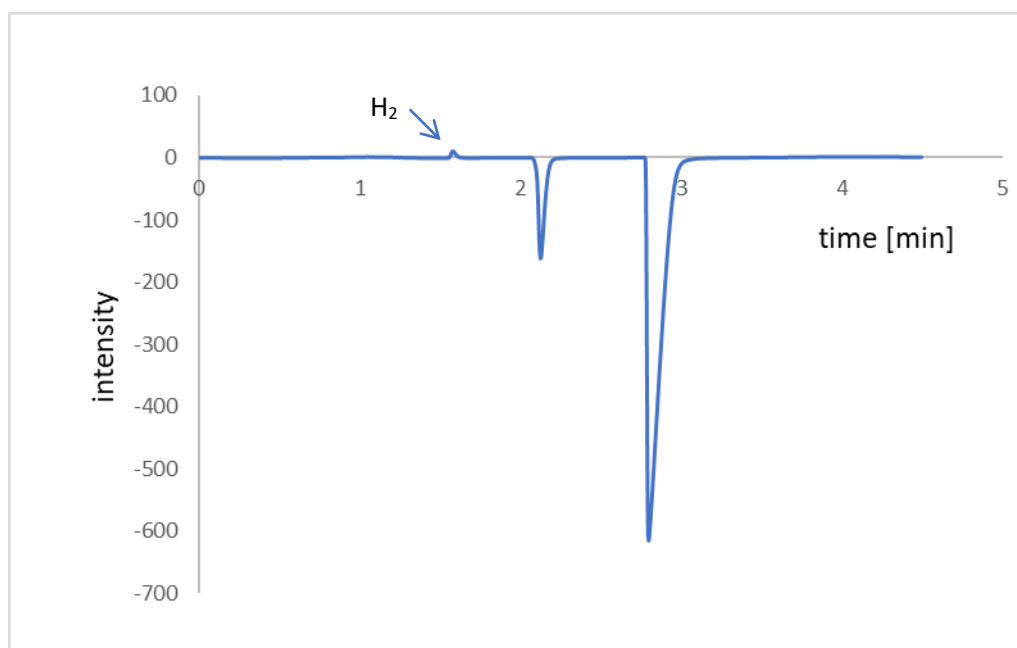


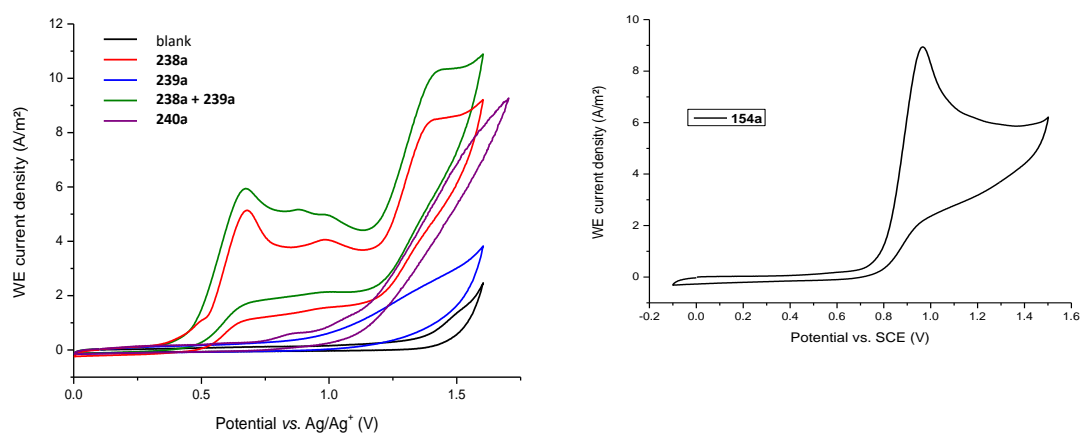
Figure 4: Headspace Gas Chromatography for **240a**

5.3.1.4 Cyclic Voltammetry

CV measurements were conducted with a Metrohm Autolab PGSTAT204 potentiostat and Nova 2.1 software. A glassy carbon working electrode (disk,

diameter: 3mm), a coiled platinum wire counter electrode, and a non-aqueous Ag/Ag⁺ reference electrode (ALS Japan) was employed. The voltammograms were recorded at room temperature in dry 1,2-dimethoxyethane (DME) at a substrate concentration of 1 mmol/L and with 100 mmol/L *n*-Bu₄NPF₆ as supporting electrolyte. All solutions were degassed with DME-saturated N₂ prior to measurement, and an overpressure of protective gas was maintained throughout the experiment. The scan rate is 100 mV/s. Deviations from the general experimental conditions are indicated in the respective figures and descriptions. The measured half-peak potential for the irreversible oxidation process of the *nido*-carborane standard substrate is: +0.87 V vs. SCE in DME/H₂O 19:1, +0.55 V vs. Ag/Ag⁺ in DME/H₂O 19:1, + 0.57 V vs. Ag/Ag⁺ in DME.

1) Reagents



2) Effect of H₂O

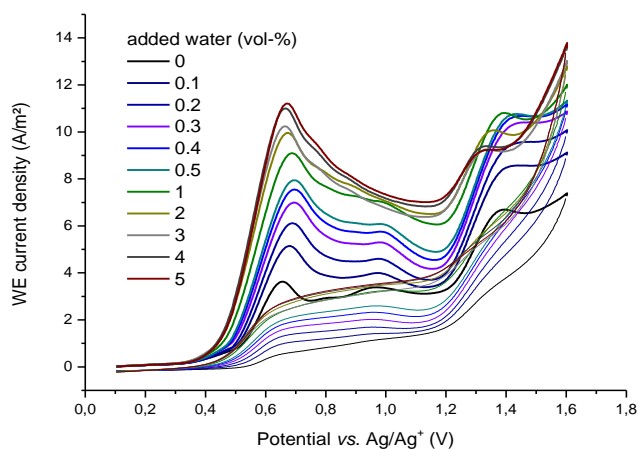


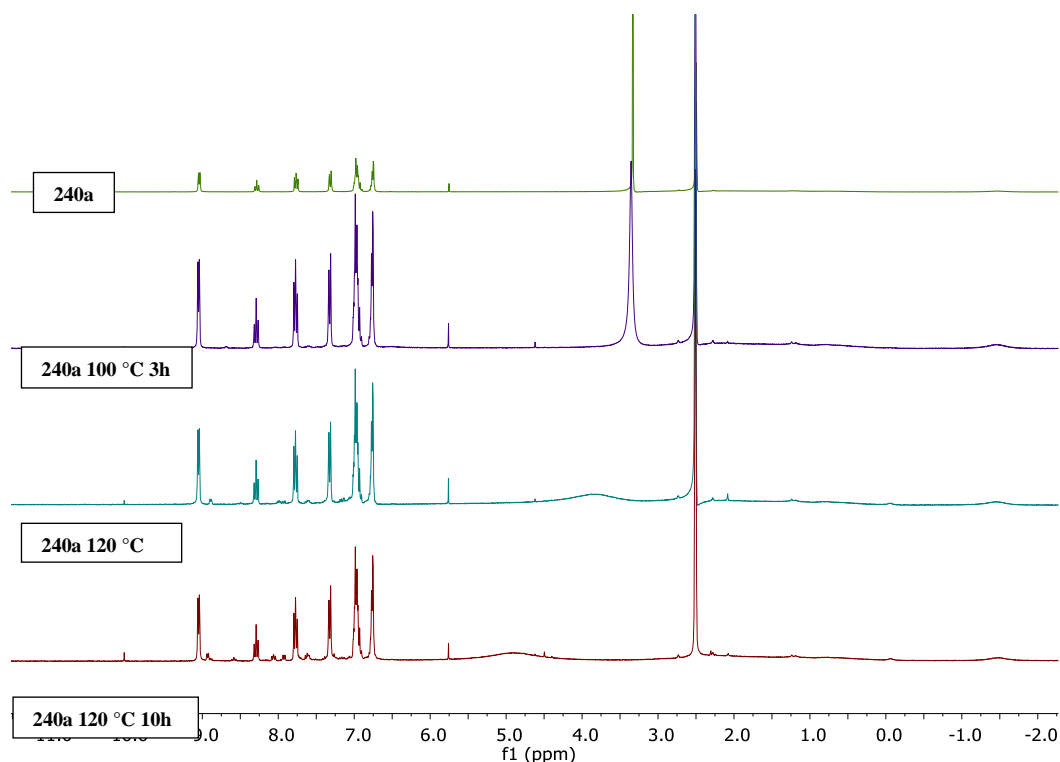
Figure 5. Cyclic Voltametric studies of **240a**

5.3.3.5 Stability Test

Thermal stability test: compound **240a** was dissolved in an NMR tube (0.4 mL DMSO- d_6), then heated to 100 °C for 3 h, 120 °C for 3 h, and 120 °C for 10 h, respectively. The ^1H NMR and ^{11}B NMR tracking experiments show that **240a** was relatively stable at 100 °C and 120 °C.

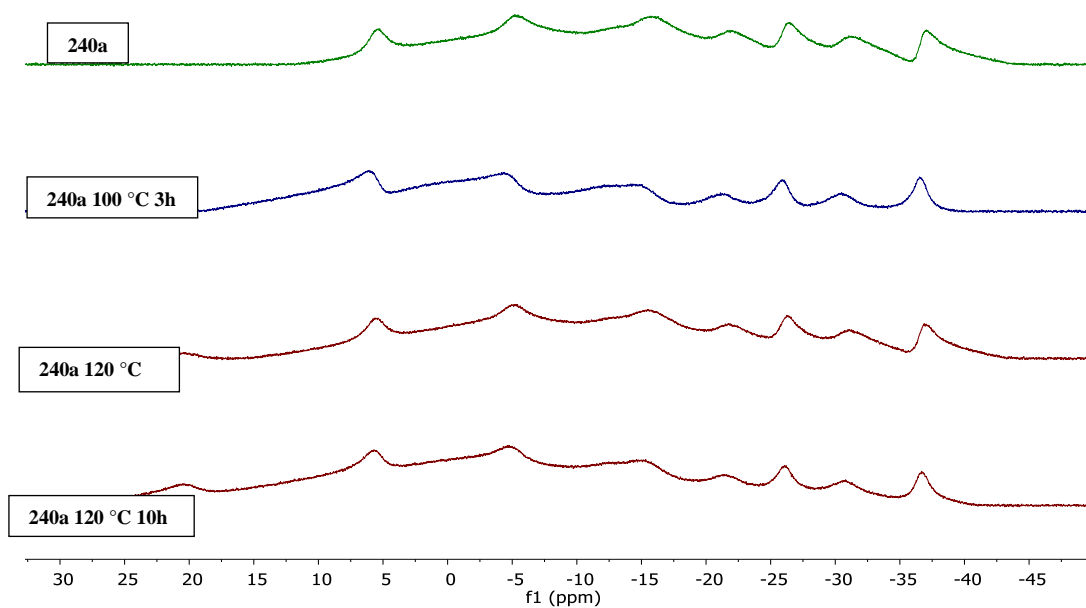
Chemical stability test: compound **240a** was dissolved in an NMR tube (0.4 mL CD_3CN), then 0.1 mL H_2O , HCl (1 M), or NaOH (1 M) was added into the NMR tube, respectively. The ^{11}B NMR tracking experiments show that **240a** was stable in a neutral environment. However, **240a** started to decompose in a strongly acidic or alkaline environment.

Note: although **240a** was not stable in strongly acidic or alkaline environments. Still, during our experiments, we found that these B-N coupled compounds are very stable in the solid state and even in liquid solution at room temperature for a long time.

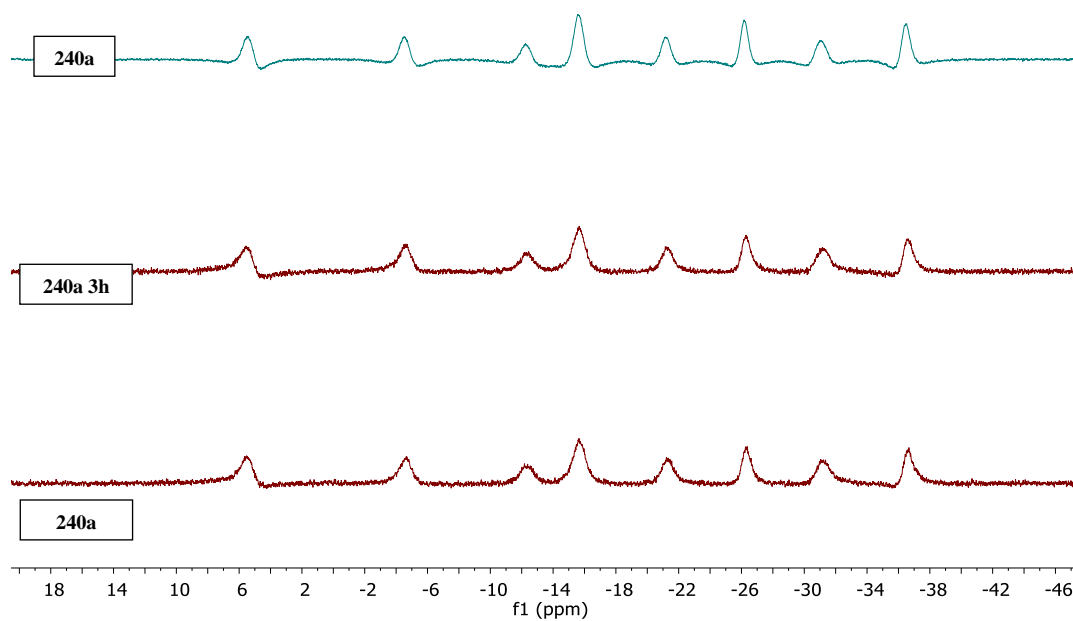


^1H NMR spectra of compound **240a** in DMSO- d_6 at different temperatures for stability test.

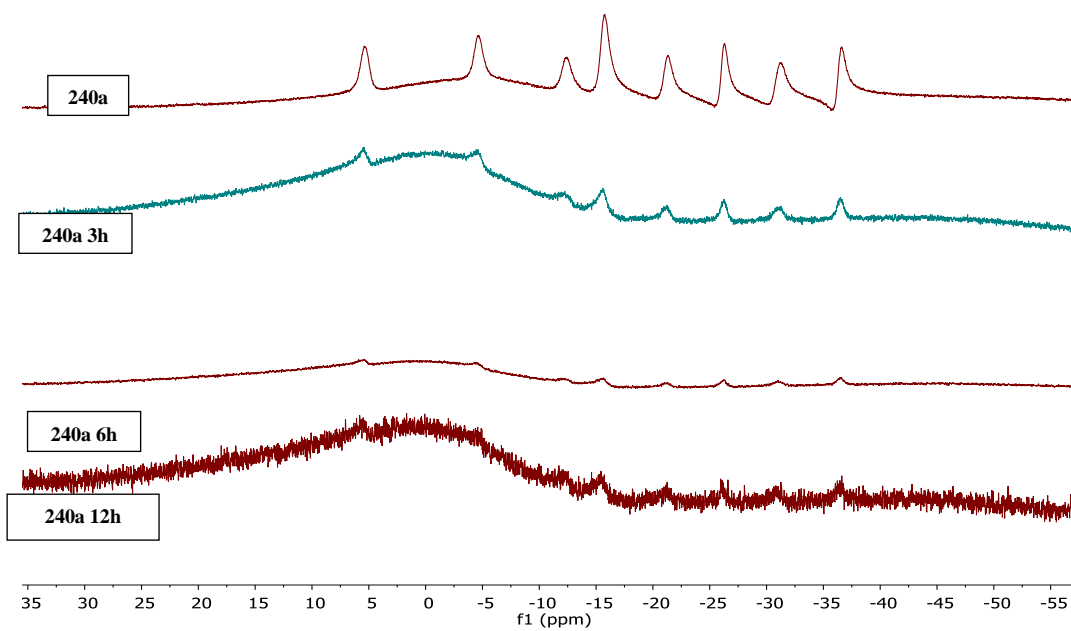
5 Experimental Section



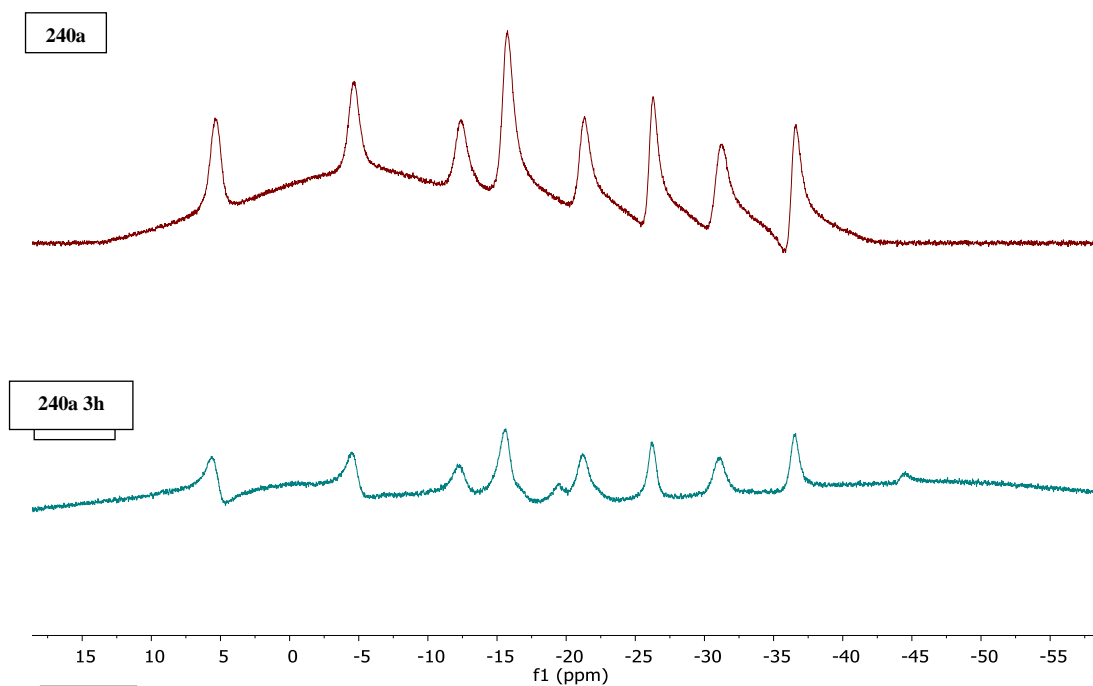
^{11}B NMR spectra of compound **240a** in $\text{DMSO}-d_6$ at different temperatures for thermal stability test.



^{11}B NMR spectra of compound **240a** in CD_3CN in 0.1 mL H_2O for chemical stability test.



^{11}B NMR spectra of compound **240a** in CD_3CN in 0.1 mL HCl (1M) for chemical stability test.

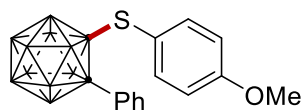


^{11}B NMR spectra of compound **240a** in CD_3CN in 0.1 mL NaOH (1M) for chemical stability test.

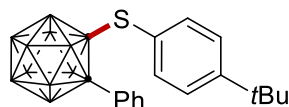
Figure 6: Stability studies of **240a**

5.3.2 Cupraelectro-Catalyzed Chalcogenations of *o*-Carboranes

5.3.2.1 Characterization Data

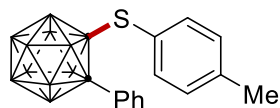
**1-phenyl-2-[(4-methoxyphenyl)-sulfanyl]-*o*-carborane**

243a. The representative procedure **B** was followed using *o*-carborane **241a** (22.0 mg, 0.10 mmol) and 4-methoxybenzenethiol **242a** (36.9 μ L, 0.30 mmol). Isolation by column chromatography (*n*-hexane) yielded **243a** (30.5 mg, 85%) as a colorless solid. **M.p.** = 141 – 143 °C. $^1\text{H NMR}$ (400 MHz, CDCl_3): δ = 7.66 (d, J = 8.0 Hz, 2H), 7.57 (t, J = 7.4 Hz, 1H), 7.48 (t, J = 7.6 Hz, 2H), 6.86 (d, J = 8.7 Hz, 2H), 6.77 (d, J = 8.8 Hz, 2H), 3.83 (s, 3H). $^{13}\text{C NMR}$ (101 MHz, CDCl_3): δ = 161.8 (C_q), 138.5 (CH), 132.2 (CH), 131.0 (C_q), 130.8 (CH), 128.5 (CH), 120.8 (C_q), 114.5 (CH), 87.9 (Cage C), 86.9 (Cage C), 55.4 (CH_3). $^{11}\text{B NMR}$ (96 MHz, CDCl_3): δ = -2.78 (2B), -9.14 (3B), -10.46 (3B), -11.59 (2B). **IR** (ATR): 2924, 2853, 2601, 2574, 2561, 1588, 1253, 1170, 1027 cm^{-1} . **MS** (EI) m/z : 358 [M] $^+$. **HR-MS** (EI): m/z calcd. for $\text{C}_{15}\text{H}_{22}^{10}\text{B}_2^{11}\text{B}_8\text{OS}$ [M] $^+$: 358.2397, found: 358.2386.

**1-phenyl-2-[(4-(tert-butyl)phenyl)-sulfanyl]-*o*-carborane**

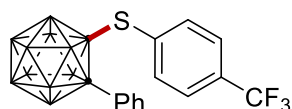
243b. The representative procedure **B** with KI (16.6 mg, 0.10 mmol) was followed using *o*-carborane **241a** (22.0 mg, 0.10 mmol) and 4-(*tert*-butyl)benzenethiol **242b** (49.9 μ L, 0.30 mmol). Isolation by column chromatography (*n*-hexane) yielded **243b** (24.0 mg, 62%) as a colorless solid. **M.p.** = 177 – 179 °C. $^1\text{H NMR}$ (400 MHz, CDCl_3): δ = 7.69 – 7.64 (m, 2H), 7.62 – 7.53 (m, 1H), 7.51 – 7.46 (m, 2H), 7.30 – 7.26 (m, 2H), 6.92 – 6.85 (m, 2H), 1.33 (s, 9H). $^{13}\text{C NMR}$ (101 MHz, CDCl_3): δ = 154.7 (C_q), 136.5 (CH), 132.2 (CH), 131.0 (C_q), 130.8 (CH), 128.5 (CH), 126.4 (C_q), 126.1 (CH), 88.1 (Cage C), 86.6 (Cage C), 34.9 (C_q), 31.1 (CH_3). $^{11}\text{B NMR}$ (96 MHz, CDCl_3): δ = -3.00 (2B), -9.24 (3B), -10.43 (2B), -11.65 (3B). **IR** (ATR): 2966, 2924, 2866,

2577, 2564, 1446, 1073, 687 cm^{-1} . **MS** (EI) m/z : 384 $[\text{M}]^+$. **HR-MS** (EI): m/z calcd. for $\text{C}_{18}\text{H}_{28}^{10}\text{B}_2^{11}\text{B}_8\text{S}$ $[\text{M}]^+$: 384.2919, found: 384.2904.



1-phenyl-2-[(4-methylphenyl)-sulfanyl]-o-carborane

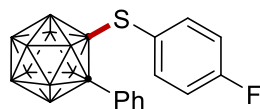
243c. The representative procedure **B** with KI (16.6 mg, 0.10 mmol) was followed using o-carborane **241a** (22.0 mg, 0.10 mmol) and 4-methylbenzenethiol **242c** (37.2 mg, 0.30 mmol). Isolation by column chromatography (*n*-hexane) yielded **243c** (18.9 mg, 55%) as a colorless solid. **M.p.** = 146 – 148 °C. **^1H NMR** (400 MHz, CDCl_3): δ = 7.65 – 7.58 (m, 1H), 7.55 – 7.49 (m, 2H), 7.47 – 7.39 (m, 2H), 7.03 (d, J = 7.8 Hz, 2H), 6.79 (d, J = 8.2 Hz, 2H), 2.32 (s, 3H). **^{13}C NMR** (101 MHz, CDCl_3): δ = 141.6 (C_q), 136.7 (CH), 132.2 (CH), 130.9 (C_q), 130.8 (CH), 129.8 (CH), 128.5 (C_q), 126.5 (CH), 88.0 (Cage C), 86.5 (Cage C), 21.37 (CH_3). **^{11}B NMR** (128 MHz, CDCl_3): δ = -2.59 (1B), -3.22 (1B), -8.51 (2B), -9.22 (2B), -10.42 (2B), -11.56 (2B). **IR** (ATR): 2954, 2598, 2568, 1973, 1492, 1446, 1179, 1073, 885 cm^{-1} . **MS** (EI) m/z : 342 $[\text{M}]^+$. **HR-MS** (EI): m/z calcd. for $\text{C}_{15}\text{H}_{22}^{10}\text{B}_2^{11}\text{B}_8\text{S}$ $[\text{M}]^+$: 342.2448, found: 342.2435.



1-phenyl-2-[(4-trifluoromethylphenyl)-sulfanyl]-o-carborane

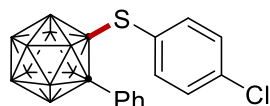
243d. The representative procedure **B** with KI (16.6 mg, 0.10 mmol) was followed using o-carborane **241a** (22.0 mg, 0.10 mmol) and 4-(trifluoromethyl)benzenethiol **242d** (41.1 μL , 0.30 mmol). Isolation by column chromatography (*n*-hexane) yielded **243d** (30.6 mg, 77%) as a colorless solid. **M.p.** = 84 – 86 °C. **^1H NMR** (400 MHz, CDCl_3): δ = 7.62 – 7.58 (m, 2H), 7.57 – 7.52 (m, 1H), 7.51 – 7.47 (m, 2H), 7.47 – 7.42 (m, 2H), 7.05 – 7.00 (m, 2H). **^{13}C NMR** (101 MHz, CDCl_3): δ = 137.0 (CH), 133.8 (C_q), 133.0 (q, $^2J_{\text{C-F}}$ = 33 Hz, C_q), 132.1 (CH), 131.0 (CH), 130.7 (C_q), 128.6 (CH), 125.9 (q, $^3J_{\text{C-F}}$ = 3.7 Hz, CH), 123.4 (q, $^1J_{\text{C-F}}$ = 273 Hz, C_q), 88.0 (Cage C), 84.7 (Cage C). **^{11}B NMR** (128 MHz, CDCl_3): δ = -2.47 (2B), -9.09 (4B), -10.22 (2B), -11.48 (2B).

^{19}F NMR (376 MHz, CDCl_3): δ = -63.07. **IR** (ATR): 2925, 2572, 1495, 1447, 1322, 1172, 1135, 1062, 842 cm^{-1} . **MS** (EI) m/z : 396 $[\text{M}]^+$. **HR-MS** (EI): m/z calcd. for $\text{C}_{15}\text{H}_{19}^{10}\text{B}_2^{11}\text{B}_8\text{F}_3\text{S}$ $[\text{M}]^+$: 396.2165, found: 396.2158.



1-phenyl-2-[(4-fluorophenyl)-sulfanyl]-o-carborane

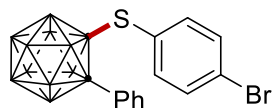
243e. The representative procedure **B** with KI (16.6 mg, 0.10 mmol) was followed using o-carborane **241a** (22.0 mg, 0.10 mmol) and 4-fluorobenzenethiol **242e** (32.0 μL , 0.30 mmol). Isolation by column chromatography (*n*-hexane) yielded **243e** (21.0 mg, 61%) as a colorless solid. **M.p.** = 103 – 105 $^{\circ}\text{C}$. **^1H NMR** (400 MHz, CDCl_3): δ = 7.69 – 7.61 (m, 2H), 7.61 – 7.54 (m, 1H), 7.51 – 7.44 (m, 2H), 7.01 – 6.87 (m, 4H). **^{13}C NMR** (101 MHz, CDCl_3): δ = 164.4 (d, $^1J_{\text{C-F}}$ = 254 Hz, C_q), 139.0 (d, $^3J_{\text{C-F}}$ = 8.9 Hz, CH), 132.1 (CH), 130.9 (CH), 130.8 (C_q), 128.6 (CH), 125.3 (d, $^4J_{\text{C-F}}$ = 3.6 Hz, C_q), 116.4 (d, $^2J_{\text{C-F}}$ = 22 Hz, CH), 87.8 (Cage C), 85.8 (Cage C). **^{11}B NMR** (96 MHz, CDCl_3): δ = -2.67 (2B), -8.91 (4B), -10.32 (2B), -11.54 (2B). **^{19}F NMR** (282 MHz, CDCl_3): δ = -107.68. **IR** (ATR): 2609, 2572, 2561, 1585, 1486, 1233, 1155, 835, 687 cm^{-1} . **MS** (EI) m/z : 346 $[\text{M}]^+$. **HR-MS** (EI): m/z calcd. for $\text{C}_{14}\text{H}_{19}^{10}\text{B}_2^{11}\text{B}_8\text{FS}$ $[\text{M}]^+$: 346.2197, found: 346.2185.



1-phenyl-2-[(4-chlorophenyl)-sulfanyl]-o-carborane

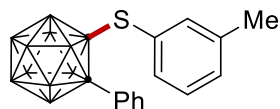
243f. The representative procedure **B** was followed using o-carborane **241a** (22.0 mg, 0.10 mmol) and 4-chlorobenzenethiol **242f** (43.0 mg, 0.30 mmol). Isolation by column chromatography (*n*-hexane) yielded **243f** (26.0 mg, 71%) as a colorless solid. **M.p.** = 108 – 110 $^{\circ}\text{C}$. **^1H NMR** (400 MHz, CDCl_3): δ = 7.68 – 7.62 (m, 2H), 7.61 – 7.54 (m, 1H), 7.52 – 7.44 (m, 2H), 7.28 – 7.22 (m, 2H), 6.90 – 6.81 (m, 2H). **^{13}C NMR** (101 MHz, CDCl_3): δ = 138.0 (CH), 137.9 (C_q), 132.1 (CH), 131.0 (CH), 130.8 (C_q), 129.4 (CH), 128.6 (CH), 128.1 (C_q), 87.9 (Cage C), 85.4 (Cage C). **^{11}B NMR** (96 MHz, CDCl_3): δ = -2.60 (2B), -8.90 (4B), -10.31 (2B), -11.54 (2B). **IR** (ATR): 2610, 2567, 1572, 1473, 1445,

1092, 1073, 746 cm^{-1} . **MS** (EI) m/z : 362 $[\text{M}]^+$. **HR-MS** (EI): m/z calcd. for $\text{C}_{14}\text{H}_{19}^{10}\text{B}_2^{11}\text{B}_8^{35}\text{ClS} [\text{M}]^+$: 362.1904, found: 362.1893.



1-phenyl-2-[(4-bromophenyl)-sulfanyl]-o-carborane

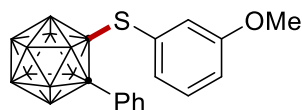
243g. The representative procedure **C** with KI (16.6 mg, 0.10 mmol) and CuI (2.9 mg, 15 mol %) was followed using o-carborane **241a** (22.0 mg, 0.10 mmol) and 4-bromobenzenethiol **242g** (56.1 mg, 0.30 mmol). Isolation by column chromatography (*n*-hexane) yielded **243g** (29.0 mg, 71 %) as a colorless solid. **M.p.** = 126 – 128 °C. **^1H NMR** (400 MHz, CDCl_3): δ = 7.62 – 7.58 (m, 2H), 7.56 – 7.50 (m, 1H), 7.46 – 7.41 (m, 2H), 7.39 – 7.34 (m, 2H), 6.78 – 6.70 (m, 2H). **^{13}C NMR** (101 MHz, CDCl_3): δ = 138.1 (CH), 132.4 (CH), 132.1 (CH), 130.9 (CH), 130.7 (C_q), 128.6 (C_q), 128.5 (CH), 126.3 (C_q), 87.9 (Cage C), 85.2 (Cage C). **^{11}B NMR** (128 MHz, CDCl_3): δ = -2.46 (2B), -9.13 (4B), -10.31 (2B), -11.52 (2B). **IR** (ATR): 2622, 2596, 1564, 1471, 1446, 1386, 1070, 1010, 810 cm^{-1} . **MS** (EI) m/z : 408 $[\text{M}]^+$. **HR-MS** (EI): m/z calcd. for $\text{C}_{14}\text{H}_{19}^{11}\text{B}_{10}\text{S}^{79}\text{Br} [\text{M}]^+$: 408.1363, found: 408.1358.



1-phenyl-2-[(3-methylphenyl)-sulfanyl]-o-carborane

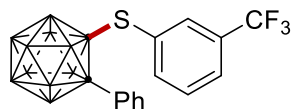
243h. The representative procedure **C** with KI (16.6 mg, 0.10 mmol) was followed using o-carborane **241a** (22.0 mg, 0.10 mmol) and 3-methylbenzenethiol **242h** (35.6 μL , 0.30 mmol). Isolation by column chromatography (*n*-hexane) yielded **243h** (30.3 mg, 88%) as a colorless solid. **M.p.** = 58 – 60 °C. **^1H NMR** (400 MHz, CDCl_3): δ = 7.63 – 7.59 (m, 2H), 7.56 – 7.51 (m, 1H), 7.46 – 7.41 (m, 2H), 7.20 – 7.16 (m, 1H), 7.13 (t, J = 7.6 Hz, 1H), 6.79 (d, J = 7.5 Hz, 1H), 6.55 (s, 1H), 2.22 (s, 3H). **^{13}C NMR** (101 MHz, CDCl_3): δ = 138.9 (C_q), 137.3 (CH), 133.6 (CH), 132.2 (CH), 131.8 (CH), 130.8 (C_q), 130.7 (CH), 129.4 (C_q), 128.8 (CH), 128.4 (CH), 87.8 (Cage C), 86.2 (Cage C), 21.1 (CH_3). **^{11}B NMR** (128 MHz, CDCl_3): δ = -2.43 (1B), -3.16 (1B), -8.42 (1B), -9.16 (2B), -10.45 (3B), -11.42 (2B). **IR** (ATR): 2922,

2564, 1591, 1494, 1474, 1446, 1377, 885, 780 cm^{-1} . **MS** (EI) m/z : 342 $[\text{M}]^+$. **HR-MS** (EI): m/z calcd. for $\text{C}_{15}\text{H}_{22}^{10}\text{B}_2^{11}\text{B}_8\text{S}$ $[\text{M}]^+$: 342.2448, found: 342.2434.



1-phenyl-2-[(3-methoxyphenyl)-sulfanyl]-o-carborane

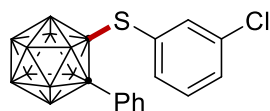
243i. The representative procedure **C** was followed using o-carborane **241a** (22.0 mg, 0.10 mmol) and 3-methoxybenzenethiol **242i** (37.2 μL , 0.30 mmol). Isolation by column chromatography (*n*-hexane) yielded **243i** (22.2 mg, 62%) as a colorless oil. **^1H NMR** (400 MHz, CDCl_3): δ = 7.66 (d, J = 8.0 Hz, 2H), 7.59 – 7.54 (m, 1H), 7.51 – 7.44 (m, 2H), 7.18 (t, J = 8.0 Hz, 1H), 6.97 (dd, J = 8.4, 2.5 Hz, 1H), 6.56 (d, J = 7.6 Hz, 1H), 6.50 (s, 1H), 3.75 (s, 3H). **^{13}C NMR** (101 MHz, CDCl_3): δ = 159.5 (C_q), 132.2 (CH), 131.0 (C_q), 130.8 (CH), 130.6 (C_q), 129.8 (CH), 129.0 (CH), 128.5 (CH), 121.5 (CH), 117.4 (CH), 88.1 (Cage C), 86.1 (Cage C), 55.4 (CH_3). **^{11}B NMR** (96 MHz, CDCl_3): δ = -2.69 (2B), -9.12 (4B), -10.34 (2B), -11.44 (2B). **IR** (ATR): 2961, 2934, 2597, 2564, 1589, 1479, 1249, 1231, 1040, 688 cm^{-1} . **MS** (EI) m/z : 358 $[\text{M}]^+$. **HR-MS** (EI): m/z calcd. for $\text{C}_{15}\text{H}_{22}^{10}\text{B}_2^{11}\text{B}_8\text{OS}$ $[\text{M}]^+$: 358.2397, found: 358.2385.



1-phenyl-2-[(3-trifluoromethylphenyl)-sulfanyl]-o-carborane

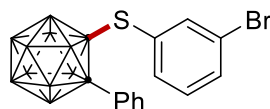
243j. The representative procedure **C** with KI (16.6 mg, 0.10 mmol) was followed using o-carborane **241a** (22.0 mg, 0.10 mmol) and 3-(trifluoromethyl)benzenethiol **242j** (40.8 μL , 0.30 mmol). Isolation by column chromatography (*n*-hexane) yielded **243j** (29.5 mg, 74%) as a colorless oil. **^1H NMR** (400 MHz, CDCl_3): δ = 7.65 (d, J = 7.8 Hz, 1H), 7.61 – 7.52 (m, 3H), 7.47 – 7.40 (m, 3H), 7.34 – 7.30 (m, 1H), 6.93 – 6.87 (m, 1H). **^{13}C NMR** (101 MHz, CDCl_3): δ = 139.9 (CH), 133.5 (q, $^3J_{\text{C-F}}$ = 3.8 Hz, CH), 132.0 (CH), 131.5 (q, $^2J_{\text{C-F}}$ = 33 Hz, C_q), 131.1 (CH), 130.8 (C_q), 130.5 (C_q), 129 (CH), 128.7 (CH), 127.9 (q, $^3J_{\text{C-F}}$ = 3.7 Hz, CH), 123.2 (q, $^1J_{\text{C-F}}$ = 273 Hz, C_q), 88.0 (Cage C), 84.9 (Cage C). **^{11}B NMR** (128 MHz, CDCl_3): δ = -2.31 (2B), -9.02 (4B), -10.25 (2B), -11.46 (2B). **^{19}F NMR** (376 MHz, CDCl_3): δ = -62.78. **IR** (ATR):

2755, 1580, 1420, 1320, 1272, 1165, 1122, 1071, 792 cm^{-1} . **MS** (EI) m/z : 396 $[\text{M}]^+$. **HR-MS** (EI): m/z calcd. for $\text{C}_{15}\text{H}_{19}^{10}\text{B}_2^{11}\text{B}_8\text{F}_3\text{S}$ $[\text{M}]^+$: 396.2165, found: 396.2154.



1-phenyl-2-[(3-chlorophenyl)-sulfanyl]-o-carborane

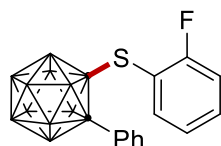
243k. The representative procedure **C** with KI (16.6 mg, 0.10 mmol) was followed using o-carborane **241a** (22.0 mg, 0.10 mmol) and 3-chlorobenzenethiol **242k** (34.5 μL , 0.30 mmol). Isolation by column chromatography (*n*-hexane) yielded **243k** (21.4 mg, 59%) as a colorless solid. **M.p.** = 60 – 62 $^{\circ}\text{C}$. **^1H NMR** (400 MHz, CDCl_3): δ = 7.63 – 7.52 (m, 3H), 7.49 – 7.42 (m, 2H), 7.37 (ddd, J = 8.1, 2.1, 1.0 Hz, 1H), 7.23 – 7.17 (m, 1H), 6.95 (ddd, J = 7.8, 1.7, 1.1 Hz, 1H), 6.62 (ddd, J = 2.1, 1.7, 0.4 Hz, 1H). **^{13}C NMR** (101 MHz, CDCl_3): δ = 136.4 (CH), 134.7 (CH), 134.4 (C_q), 132.1 (CH), 131.3 (CH), 131.1 (C_q), 131.0 (CH), 130.6 (C_q), 130.1 (CH), 128.6 (CH), 87.8 (Cage C), 85.1 (Cage C). **^{11}B NMR** (128 MHz, CDCl_3): δ = -2.37 (1B), -2.90 (1B), -9.11 (4B), -10.37 (2B), -11.46 (2B). **IR** (ATR): 2922, 2565, 1573, 1459, 1398, 1116, 1071, 864, 771 cm^{-1} . **MS** (EI) m/z : 362 $[\text{M}]^+$. **HR-MS** (EI): m/z calcd. for $\text{C}_{14}\text{H}_{19}^{10}\text{B}_2^{11}\text{B}_8\text{S}^{35}\text{Cl}$ $[\text{M}]^+$: 362.1904, found: 362.1893.



1-phenyl-2-[(3-bromophenyl)-sulfanyl]-o-carborane

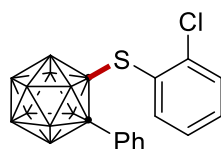
243l. The representative procedure **C** with KI (16.6 mg, 0.10 mmol) and CuI (2.9 mg, 15 mol %) was followed using o-carborane **241a** (22.0 mg, 0.10 mmol) and 3-bromobenzenethiol **242l** (31.0 μL , 0.30 mmol). Isolation by column chromatography (*n*-hexane) yielded **243l** (24.1 mg, 59%) as a colorless oil. **^1H NMR** (400 MHz, CDCl_3): δ = 7.62 – 7.57 (m, 2H), 7.57 – 7.50 (m, 2H), 7.49 – 7.42 (m, 2H), 7.15 (t, J = 7.9 Hz, 1H), 7.02 (ddd, J = 7.8, 1.7, 1.1 Hz, 1H), 6.75 (t, J = 1.8 Hz, 1H). **^{13}C NMR** (101 MHz, CDCl_3): δ = 139.2 (CH), 135.1 (CH), 134.2 (CH), 132.1 (CH), 131.4 (C_q), 131.0 (CH), 130.5 (C_q), 130.4 (CH), 128.7 (CH), 122.4 (C_q), 87.8 (Cage C), 85.1 (Cage C). **^{11}B NMR**

(128 MHz, CDCl₃): δ = -2.35 (2B), -9.11 (4B), -10.37 (2B), -11.44 (2B). **IR** (ATR): 2918, 2589, 1559, 1455, 1394, 1066, 866, 770, 672 cm⁻¹. **MS** (EI) m/z : 408 [M]⁺. **HR-MS** (EI): m/z calcd. for C₁₄H₁₉¹¹B₁₀S⁷⁹Br [M]⁺: 408.1363, found: 408.1360.



1-phenyl-2-[(2-fluorophenyl)-sulfanyl]-o-carborane

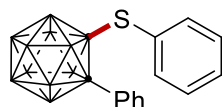
243m. The representative procedure **C** with KI (16.6 mg, 0.10 mmol) was followed using o-carborane **241a** (22.0 mg, 0.10 mmol) and 2-fluorobenzenethiol **242m** (32.0 μ L, 0.30 mmol). Isolation by column chromatography (*n*-hexane) yielded **243m** (18.5 mg, 53%) as a colorless solid. **M.p.** = 116 – 118 °C. **¹H NMR** (400 MHz, CDCl₃): δ = 7.73 – 7.66 (m, 2H), 7.61 – 7.54 (m, 1H), 7.53 – 7.44 (m, 3H), 7.17 – 7.03 (m, 2H), 6.94 – 6.84 (m, 1H). **¹³C NMR** (101 MHz, CDCl₃): δ = 163.3 (d, ¹J_{C-F} = 253 Hz, C_q), 139.4 (CH), 134.1 (d, ³J_{C-F} = 8.4 Hz, CH), 132.1 (CH), 130.9 (C_q), 130.9 (CH), 128.5 (CH), 124.5 (d, ³J_{C-F} = 4.0 Hz, CH), 117.0 (d, ²J_{C-F} = 18.2 Hz, C_q), 116.5 (d, ²J_{C-F} = 23.1 Hz, CH), 88.7 (Cage C), 85.2 (Cage C). **¹¹B NMR** (96 MHz, CDCl₃): δ = -2.87 (2B), -8.30 (2B), -9.21 (1B), -9.90 (3B), -11.53 (2B). **¹⁹F NMR** (282 MHz, CDCl₃): δ = -102.48. **IR** (ATR): 2598, 2557, 1470, 1261, 1223, 1067, 755, 689 cm⁻¹. **MS** (EI) m/z : 346 [M]⁺. **HR-MS** (EI): m/z calcd. for C₁₄H₁₉¹⁰B₂¹¹B₈FS [M]⁺: 346.2197, found: 346.2183.



1-phenyl-2-[(2-chlorophenyl)-sulfanyl]-o-carborane

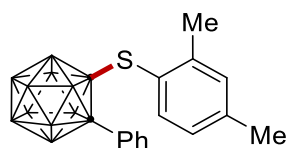
243n. The representative procedure **C** with KI (16.6 mg, 0.10 mmol) was followed using o-carborane **241a** (22.0 mg, 0.10 mmol) and 2-chlorobenzenethiol **242n** (33.6 μ L, 0.30 mmol). Isolation by column chromatography (*n*-hexane) yielded **243n** (27.5 mg, 76%) as a colorless solid. **M.p.** = 146 – 148 °C. **¹H NMR** (400 MHz, CDCl₃): δ = 7.72 – 7.64 (m, 2H),

7.56 – 7.47 (m, 1H), 7.49 – 7.40 (m, 3H), 7.40 – 7.31 (m, 1H), 7.21 – 7.12 (m, 1H), 7.02 (d, $J = 7.8$ Hz, 1H). ^{13}C NMR (101 MHz, CDCl_3): $\delta = 141.1$ (C_q), 140.0 (CH), 132.7 (CH), 132.1 (CH), 131.1 (C_q), 130.9 (CH), 130.6 (CH), 128.9 (C_q), 128.6 (CH), 127.1 (CH), 89.5 (Cage C), 85.7 (Cage C). ^{11}B NMR (128 MHz, CDCl_3): $\delta = -2.90$ (2B), -8.40 (2B), -9.57 (4B), -11.70 (2B). IR (ATR): 2500, 1945, 1447, 1321, 1259, 1166, 1134, 1070, 749 cm^{-1} . MS (EI) m/z : 362 $[\text{M}]^+$. HR-MS (EI): m/z calcd. for $\text{C}_{14}\text{H}_{19}^{10}\text{B}_2^{11}\text{B}_8\text{S}^{35}\text{Cl}$ $[\text{M}]^+$: 362.1904, found: 362.1893.



1-phenyl-2-phenylsulfanyl-o-carborane

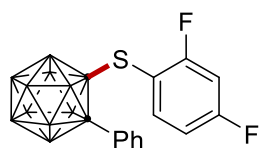
243o. The representative procedure **C** was followed using o-carborane **241a** (22.0 mg, 0.10 mmol) and benzenethiol **242o** (31.0 μL , 0.30 mmol). Isolation by column chromatography (*n*-hexane) yielded **243o** (20.0 mg, 61%) as a colorless solid. **M.p.** = 112 – 114 $^{\circ}\text{C}$. ^1H NMR (300 MHz, CDCl_3): $\delta = 7.66$ (d, $J = 7.6$ Hz, 2H), 7.61 – 7.54 (m, 1H), 7.51 – 7.40 (m, 3H), 7.32 – 7.25 (m, 2H), 6.96 (d, $J = 7.7$ Hz, 2H). ^{13}C NMR (75 MHz, CDCl_3): $\delta = 136.8$ (CH), 132.2 (CH), 131.1 (CH), 130.9 (C_q), 130.9 (CH), 129.8 (C_q), 129.1 (CH), 128.5 (CH), 88.1 (Cage C), 86.1 (Cage C). ^{11}B NMR (96 MHz, CDCl_3): $\delta = -2.78$ (2B), -9.14 (3B), -10.35 (3B), -11.50 (2B). IR (ATR): 2612, 2589, 2560, 1585, 1486, 1232, 1077, 686 cm^{-1} . MS (EI) m/z : 328 $[\text{M}]^+$. HR-MS (EI): m/z calcd. for $\text{C}_{14}\text{H}_{20}^{10}\text{B}_2^{11}\text{B}_8\text{S}$ $[\text{M}]^+$: 328.2291, found: 328.2279.



1-phenyl-2-[(2,4-dimethylphenyl)-sulfanyl]-o-carborane

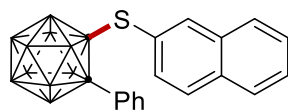
243p. The representative procedure **C** with KI (16.6 mg, 0.10 mmol) was followed using o-carborane **241a** (22.0 mg, 0.10 mmol) and 2,4-dimethylbenzenethiol **242p** (40.3 μL , 0.30 mmol). Isolation by column chromatography (*n*-hexane) yielded **243p** (23.1 mg, 65%) as a colorless solid. **M.p.** = 97 – 99 $^{\circ}\text{C}$. ^1H NMR (400 MHz, CDCl_3): $\delta = 7.71$ – 7.64 (m, 2H), 7.55 –

7.47 (m, 1H), 7.49 – 7.40 (m, 2H), 7.05 – 6.99 (m, 1H), 6.91 – 6.84 (m, 1H), 6.75 (d, $J = 7.9$ Hz, 1H), 2.29 (s, 3H), 2.21 (s, 3H). **^{13}C NMR** (101 MHz, CDCl_3): $\delta = 143.9$ (C_q), 141.9 (C_q), 138.6 (CH), 132.1 (CH), 131.7 (CH), 131.3 (C_q), 130.7 (CH), 128.6 (CH), 127.3 (CH), 126.1 (C_q), 89.5 (Cage C), 87.4 (Cage C), 21.3 (CH_3), 20.7 (CH_3). **^{11}B NMR** (128 MHz, CDCl_3): $\delta = -3.05$ (2B), -8.58 (2B), -9.80 (4B), -11.72 (2B). **IR** (ATR): 2919, 2851, 2586, 2569, 1600, 1446, 1232, 1074, 886 cm^{-1} . **MS** (EI) m/z : 356 $[\text{M}]^+$. **HR-MS** (EI): m/z calcd. for $\text{C}_{16}\text{H}_{24}^{10}\text{B}_2^{11}\text{B}_8\text{S}$ $[\text{M}]^+$: 356.2605, found: 356.2593.



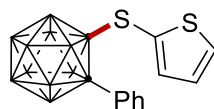
1-phenyl-2-[(2,4-difluorophenyl)-sulfanyl]-o-carborane

243q. The representative procedure **C** with KI (16.6 mg, 0.10 mmol) was followed using o-carborane **241a** (22.0 mg, 0.10 mmol) and 2,4-difluorobenzenethiol **242q** (33.1 μL , 0.30 mmol). Isolation by column chromatography (*n*-hexane) yielded **243q** (32.8 mg, 65%) as a colorless solid. **M.p.** = 109 – 111 $^{\circ}\text{C}$. **^1H NMR** (400 MHz, CDCl_3): $\delta = 7.69$ – 7.60 (m, 2H), 7.56 – 7.48 (m, 1H), 7.48 – 7.39 (m, 2H), 6.88 – 6.71 (m, 3H). **^{13}C NMR** (101 MHz, CDCl_3): $\delta = 165.4$ (dd, $^1J_{\text{C-F}} = 257$ Hz, $^3J_{\text{C-F}} = 10.8$ Hz, C_q), 163.9 (dd, $^1J_{\text{C-F}} = 256$ Hz, $^3J_{\text{C-F}} = 13.4$ Hz, C_q), 140.6 (dd, $^3J_{\text{C-F}} = 10.2$, 10.2 Hz, CH), 132.1 (CH), 131.0 (CH), 130.9 (C_q), 128.6 (CH), 112.9 (dd, $^2J_{\text{C-F}} = 18.5$ Hz, $^4J_{\text{C-F}} = 3.9$ Hz, C_q), 112.2 (dd, $^2J_{\text{C-F}} = 22.0$ Hz, $^4J_{\text{C-F}} = 3.9$ Hz, CH), 105.1 (dd, $^2J_{\text{C-F}} = 25.8$, 25.9 Hz, CH), 88.5 (Cage C), 84.9 (Cage C). **^{11}B NMR** (128 MHz, CDCl_3): $\delta = -2.20$ (1B), -3.38 (1B), -7.71 (2B), -9.26 (2B), -10.50 (2B), -12.38 (2B). **^{19}F NMR** (282 MHz, CDCl_3): $\delta = -97.08$ (d, $J = 11.5$ Hz), -101.85 (d, $J = 11.5$ Hz). **IR** (ATR): 3059, 1487, 1443, 1201, 1155, 1056, 907, 734 cm^{-1} . **MS** (EI) m/z : 364 $[\text{M}]^+$. **HR-MS** (EI): m/z calcd. for $\text{C}_{14}\text{H}_{18}^{10}\text{B}_2^{11}\text{B}_8\text{SF}_2$ $[\text{M}]^+$: 364.2102, found: 364.2098.



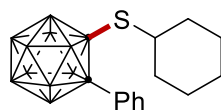
1-phenyl-2-[(2-naphthyl)-sulfanyl]-o-carborane

243r. The representative procedure **C** was followed using *o*-carborane **241a** (22.0 mg, 0.10 mmol) and naphthalene-2-thiol **242r** (43.2 mg, 0.30 mmol). Isolation by column chromatography (*n*-hexane) yielded **243r** (35.2 mg, 93%) as a colorless solid. **M.p.** = 129 – 131 °C. **¹H NMR** (400 MHz, CDCl₃): δ = 7.83 – 7.79 (m, 1H), 7.71 (d, *J* = 8.7 Hz, 1H), 7.64 – 7.44 (m, 8H), 7.18 – 7.15 (m, 1H), 7.08 (dd, *J* = 8.5, 1.8 Hz, 1H). **¹³C NMR** (101 MHz, CDCl₃): δ = 137.6 (CH), 133.9 (C_q), 132.8 (C_q), 132.3 (CH), 132.1 (CH), 130.9 (C_q), 130.8 (CH), 128.8 (CH), 128.5 (CH), 128.3 (CH), 128.0 (CH), 127.7 (CH), 126.8 (CH), 126.8 (C_q) 87.8 (Cage C), 85.9 (Cage C). **¹¹B NMR** (128 MHz, CDCl₃): δ = -2.37 (1B), -3.12 (1B), -8.44 (2B), -9.14 (2B), -10.49 (3B), -11.39 (1B). **IR** (ATR): 3057, 2594, 1581, 1494, 1446, 1072, 901, 859, 808, 743 cm⁻¹. **MS** (EI) *m/z*: 378 [M]⁺. **HR-MS** (EI): *m/z* calcd. for C₁₈H₂₂¹⁰B₂¹¹B₈S [M]⁺: 378.2449, found: 378.2436.



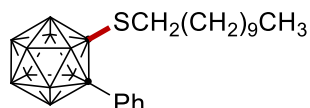
1-phenyl-2-[(2-thiophenyl)-sulfanyl]-*o*-carborane

243s. The representative procedure **C** with KI (16.6 mg, 0.10 mmol) was followed using *o*-carborane **241a** (22.0 mg, 0.10 mmol) and thiophen-2-thiol **242s** (27.8 μ L, 0.30 mmol). Isolation by column chromatography (*n*-hexane) yielded **243s** (18.0 mg, 54%) as a colorless solid. **M.p.** = 83 – 85 °C. **¹H NMR** (300 MHz, CDCl₃): δ = 7.68 (d, *J* = 7.6 Hz, 2H), 7.59 – 7.45 (m, 4H), 6.97 (dd, *J* = 5.3, 3.6 Hz, 1H), 6.64 (d, *J* = 3.9 Hz, 1H). **¹³C NMR** (75 MHz, CDCl₃): δ = 139.3 (CH), 134.1 (CH), 132.1 (CH), 130.9 (CH), 130.6 (C_q), 128.6 (CH), 127.7 (CH), 127.6 (C_q), 87.4 (Cage C), 85.6 (Cage C). **¹¹B NMR** (96 MHz, CDCl₃): δ = -2.70 (2B), -9.16 (3B), -10.37 (3B), -11.72 (2B). **IR** (ATR): 2922, 2852, 2605, 2589, 2559, 1399, 1218, 852, 710 cm⁻¹. **MS** (EI) *m/z*: 334 [M]⁺. **HR-MS** (EI): *m/z* calcd. for C₁₂H₁₈¹⁰B₂¹¹B₈S₂ [M]⁺: 334.1854, found: 334.1845.



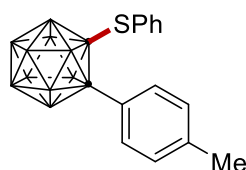
1-phenyl-2-cyclohexylsulfanyl-*o*-carborane

243t. The representative procedure **C** with KI (16.6 mg, 0.10 mmol) was followed using *o*-carborane **241a** (22.0 mg, 0.10 mmol) and cyclohexanethiol **242t** (35.5 μ L, 0.30 mmol). Isolation by column chromatography (*n*-hexane) yielded **243t** (20.0 mg, 60%) as a colorless oil. **¹H NMR** (400 MHz, CDCl₃): δ = 7.65 – 7.58 (m, 2H), 7.47 – 7.41 (m, 1H), 7.41 – 7.33 (m, 2H), 2.76 – 2.68 (m, 1H), 1.69 – 1.60 (m, 2H), 1.51 – 1.40 (m, 2H), 1.33 – 0.98 (m, 6H). **¹³C NMR** (101 MHz, CDCl₃): δ = 131.8 (CH), 131.0 (C_q), 130.6 (CH), 128.3 (CH), 88.6 (Cage C), 87.0 (Cage C), 50.5 (CH), 33.9 (CH₂), 25.7 (CH₂), 25.0 (CH₂). **¹¹B NMR** (128 MHz, CDCl₃): δ = -2.81 (2B), -8.18 (2B), -9.37 (2B), -10.21 (2B), -11.07 (2B). **IR** (ATR): 2932, 2852, 2557, 1494, 1447, 1321, 1261, 1075, 884 cm⁻¹. **MS** (EI) *m/z*: 334 [M]⁺. **HR-MS** (EI): *m/z* calcd. for C₁₄H₂₆¹⁰B₂¹¹B₈S [M]⁺: 334.2760, found: 334.2748.



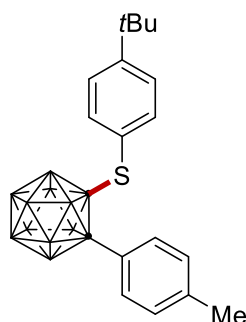
1-phenyl-2-undecylsulfanyl-*o*-carborane

243u. The representative procedure **C** was followed using *o*-carborane **241a** (22.0 mg, 0.10 mmol) and 1-undecanethiol **242u** (67.9 μ L, 0.30 mmol). Isolation by column chromatography (*n*-hexane) yielded **243u** (22.0 mg, 54%) as a colorless oil. **¹H NMR** (300 MHz, CDCl₃): δ = 7.65 (d, *J* = 7.6 Hz, 2H), 7.52 – 7.46 (m, 1H), 7.45 – 7.37 (m, 2H), 2.65 (t, *J* = 7.2 Hz, 2H), 1.37 – 1.12 (m, 18H), 0.95 – 0.88 (m, 3H). **¹³C NMR** (75 MHz, CDCl₃): δ = 131.6 (CH), 131.1 (C_q), 130.7 (CH), 128.5 (CH), 88.7 (Cage C), 86.7 (Cage C), 36.9 (CH₂), 31.9 (CH₂), 29.6 (CH₂), 29.5 (CH₂), 29.3 (2CH₂), 28.8 (CH₂), 28.3 (CH₂), 28.0 (CH₂), 22.7 (CH₂), 14.1 (CH₃). **¹¹B NMR** (96 MHz, CDCl₃): δ = -2.96 (2B), -8.35 (2B), -10.02 (5B), -11.34 (1B). **IR** (ATR): 2957, 2923, 2853, 2593, 1447, 1276, 766, 750 cm⁻¹. **MS** (EI) *m/z*: 406 [M]⁺. **HR-MS** (EI): *m/z* calcd. for C₁₉H₃₈¹⁰B₂¹¹B₈S [M]⁺: 406.3702, found: 406.3694.



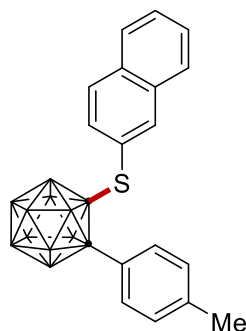
1-(*p*-tolyl)-2-phenylsulfanyl-*o*-carborane

244a. The representative procedure **C** was followed using *o*-carborane **241b** (23.4 mg, 0.10 mmol) and benzenethiol **242o** (30.8 μ L, 0.30 mmol). Isolation by column chromatography (*n*-hexane) yielded **244a** (32.2 mg, 94%) as a colorless solid. **M.p.** = 114 – 116 °C. **¹H NMR** (400 MHz, CDCl₃): δ = 7.51 – 7.46 (m, 2H), 7.42 – 7.37 (m, 1H), 7.28 – 7.21 (m, 4H), 7.01 – 6.96 (m, 2H), 2.43 (s, 3H). **¹³C NMR** (101 MHz, CDCl₃): δ = 141.3 (C_q), 137.0 (CH), 132.1 (CH), 131.1 (CH), 129.9 (C_q), 129.2 (CH), 129.1 (CH), 128.2 (C_q), 88.6 (Cage C), 86.3 (Cage C), 21.2 (CH₃). **¹¹B NMR** (128 MHz, CDCl₃): δ = -2.90 (2B), -9.10 (3B), -10.40 (3B), -11.55 (2B). **IR** (ATR): 2922, 2564, 1612, 1509, 1471, 1439, 1260, 1193, 888 cm⁻¹. **MS** (EI) *m/z*: 342 [M]⁺. **HR-MS** (EI): *m/z* calcd. for C₁₅H₂₂¹⁰B₂¹¹B₈S [M]⁺: 342.2448, found: 342.2436.



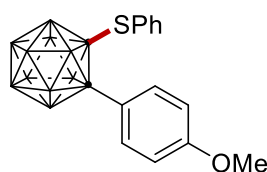
1-(4-methylphenyl)-2-[(4-(tert-butyl)phenyl)sulfanyl]-*o*-carborane

244b. The representative procedure **C** was followed using *o*-carborane **241b** (23.0 mg, 0.10 mmol) and 4-(*tert*-butyl)benzenethiol **242b** (49.9 μ L, 0.30 mmol). Isolation by column chromatography (*n*-hexane) yielded **244b** (24.7 mg, 62%) as a colorless solid. **M.p.** = 106 – 108 °C. **¹H NMR** (400 MHz, CDCl₃): δ = 7.51 (d, *J* = 8.4 Hz, 2H), 7.27 (d, *J* = 6.0 Hz, 2H), 7.25 (d, *J* = 6.0 Hz, 2H), 6.93 (d, *J* = 8.4 Hz, 2H), 2.45 (s, 3H), 1.30 (s, 9H). **¹³C NMR** (101 MHz, CDCl₃): δ = 154.6 (C_q), 141.2 (C_q), 136.6 (CH), 132.1 (CH), 129.2 (CH), 128.3 (C_q), 126.5 (C_q), 126.1 (CH), 88.6 (Cage C), 86.7 (Cage C), 34.9 (C_q), 31.1 (CH₃), 21.2 (CH₃). **¹¹B NMR** (96 MHz, CDCl₃): δ = -3.14 (2B), -9.15 (3B), -10.52 (3B), -11.76 (2B). **IR** (ATR): 2962, 2924, 2852, 2594, 2572, 1460, 1259, 765 cm⁻¹. **MS** (EI) *m/z*: 398 [M]⁺. **HR-MS** (EI): *m/z* calcd. for C₁₉H₃₀¹⁰B₂¹¹B₈S [M]⁺: 398.3076, found: 398.3064.



1-(4-methylphenyl)-2-[(2-naphthylsulfanyl)-o-carborane

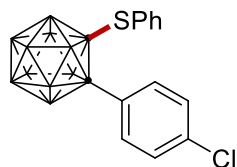
244c. The representative procedure **C** was followed using *o*-carborane **241b** (23.4 mg, 0.10 mmol) and naphthalene-2-thiol **242r** (43.2 mg, 0.30 mmol). Isolation by column chromatography (*n*-hexane) yielded **244c** (39.2 mg, 62%) as a colorless solid. **M.p.** = 165 – 166 °C. **¹H NMR** (400 MHz, CDCl₃): δ = 7.84 – 7.79 (m, 1H), 7.72 (dd, *J* = 8.5, 0.6 Hz, 1H), 7.62 – 7.58 (m, 1H), 7.57 – 7.53 (m, 1H), 7.53 – 7.47 (m, 3H), 7.27 – 7.24 (m, 2H), 7.22 (dd, *J* = 1.8, 0.9 Hz, 1H), 7.12 (dd, *J* = 8.5, 1.8 Hz, 1H), 2.49 (s, 3H). **¹³C NMR** (101 MHz, CDCl₃): δ = 141.3 (C_q), 137.6 (CH), 133.9 (C_q), 132.9 (C_q), 132.2 (CH), 132.2 (CH), 129.2 (CH), 128.8 (CH), 128.2 (CH), 128.2 (C_q), 128.0 (CH), 127.7 (CH), 126.9 (C_q), 126.8 (CH), 88.1 (Cage C), 86.0 (Cage C), 21.3 (CH₃). **¹¹B NMR** (128 MHz, CDCl₃): δ = -2.63 (2B), -9.08 (4B), -10.53 (2B), -11.48 (2B). **IR** (ATR): 2591, 1276, 1259, 816, 766, 748 cm⁻¹. **MS** (EI) *m/z*: 392 [M]⁺. **HR-MS** (EI): *m/z* calcd. for C₁₉H₂₄¹⁰B₂¹¹B₈S [M]⁺: 392.2606, found: 392.2600.



1-(4-methoxyphenyl)-2-phenylsulfanyl-o-carborane

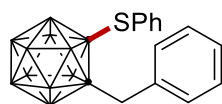
244d. The representative procedure **C** was followed using *o*-carborane **241c** (25.1 mg, 0.10 mmol) and benzenethiol **242o** (30.8 μL, 0.30 mmol). Isolation by column chromatography (*n*-hexane) yielded **244d** (25.1 mg, 70%) as a colorless oil. **¹H NMR** (400 MHz, CDCl₃): δ = 7.51 (d, *J* = 9.0 Hz, 2H), 7.42 – 7.37 (m, 1H), 7.28 – 7.22 (m, 2H), 6.99 (dd, *J* = 8.3, 1.3 Hz, 2H), 6.92 (d, *J* = 9.0 Hz, 2H), 3.88 (s, 3H). **¹³C NMR** (101 MHz, CDCl₃): δ = 161.6 (C_q), 136.9 (CH), 133.7 (CH), 131.1 (CH), 129.9 (C_q), 129.1 (CH), 123.3 (C_q), 113.7

(CH), 88.9 (Cage C), 86.7 (Cage C), 55.5 (CH₃). **¹¹B NMR** (128 MHz, CDCl₃): δ = -3.01 (2B), -9.06 (4B), -10.52 (2B), -11.55 (2B). **IR** (ATR): 2588, 1971, 1607, 1511, 1302, 1261, 1184, 835, 748 cm⁻¹. **MS** (EI) *m/z*: 358 [M]⁺. **HR-MS** (EI): *m/z* calcd. for C₁₅H₂₂¹⁰B₂¹¹B₈SO [M]⁺: 358.2395, found: 358.2391.



1-(4-chlorophenyl)-2-phenylsulfanyl-o-carborane

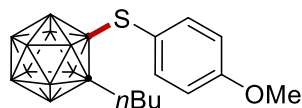
244e. The representative procedure **C** with KI (16.6 mg, 0.10 mmol) was followed using *o*-carborane **241d** (25.4 mg, 0.10 mmol) and benzenethiol **242o** (30.8 μ L, 0.30 mmol). Isolation by column chromatography (*n*-hexane) yielded **244e** (28.2 mg, 78%) as a colorless oil. **¹H NMR** (400 MHz, CDCl₃): δ = 7.55 (d, *J* = 8.6 Hz, 2H), 7.49 – 7.40 (m, 3H), 7.29 (t, *J* = 7.8 Hz, 2H), 7.00 (d, *J* = 7.6 Hz, 2H). **¹³C NMR** (101 MHz, CDCl₃): δ = 137.5 (C_q), 136.8 (CH), 133.4 (CH), 131.3 (CH), 129.7 (C_q), 129.6 (C_q), 129.2 (CH), 128.7 (CH), 87.1 (Cage C), 86.2 (Cage C). **¹¹B NMR** (128 MHz, CDCl₃): δ = -2.39 (1B), -3.00 (1B), -8.40 (2B), -9.20 (1B), -10.19 (3B), -11.56 (2B). **IR** (ATR): 2924, 2593, 1593, 1492, 1401, 1100, 1070, 1016, 887 cm⁻¹. **MS** (EI) *m/z*: 362 [M]⁺. **HR-MS** (EI): *m/z* calcd. for C₁₄H₁₉¹⁰B₂¹¹B₈S³⁵Cl [M]⁺: 362.1904, found: 362.1894.



1-benzyl-2-phenylsulfanyl-o-carborane

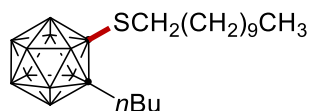
244f. The representative procedure **C** was followed using *o*-carborane **241e** (23.4 mg, 0.10 mmol) and benzenethiol **242o** (31.0 μ L, 0.30 mmol). Isolation by column chromatography (*n*-hexane) yielded **244f** (22.0 mg, 64%) as a colorless solid. **M.p.** = 119 – 121 °C. **¹H NMR** (300 MHz, CDCl₃): δ = 7.70 – 7.66 (m, 2H), 7.60 – 7.55 (m, 1H), 7.53 – 7.46 (m, 2H), 7.43 – 7.33 (m, 3H), 7.29 – 7.25 (m, 2H), 3.80 (s, 2H). **¹³C NMR** (75 MHz, CDCl₃): δ = 137.2 (CH), 135.6 (C_q), 131.5 (CH), 130.4 (CH), 130.0 (C_q), 129.6 (CH), 128.6 (CH), 128.0 (CH), 84.3 (Cage C), 84.2 (Cage C), 40.9 (CH₂). **¹¹B NMR** (96 MHz, CDCl₃): δ = -3.85 (2B), -9.37 (4B), -10.84 (4B). **IR** (ATR): 2923, 2852, 2577, 2560, 1493,

1470, 1439, 1419, 745 cm^{-1} . **MS** (EI) m/z : 342 $[\text{M}]^+$. **HR-MS** (EI): m/z calcd. for $\text{C}_{15}\text{H}_{22}^{10}\text{B}_2^{11}\text{B}_8\text{S}$ $[\text{M}]^+$: 342.2448, found: 342.2432.



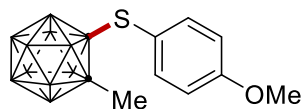
1-(*n*-butyl)-2-[(4-methoxyphenyl)sulfanyl]-*o*-carborane

244g. The representative procedure **B** was followed using *o*-carborane **241f** (20.0 mg, 0.10 mmol) and 4-methoxybenzenethiol **242a** (36.9 μL , 0.30 mmol). Isolation by column chromatography (*n*-hexane) yielded **244g** (18.0 mg, 53%) as a colorless oil. **^1H NMR** (400 MHz, CDCl_3): δ = 7.48 (d, J = 8.8 Hz, 2H), 6.94 (d, J = 8.7 Hz, 2H), 3.88 (s, 3H), 2.52 – 2.47 (m, 2H), 1.59 – 1.53 (m, 2H), 1.49 – 1.41 (m, 2H), 1.01 (t, J = 7.2 Hz, 3H). **^{13}C NMR** (101 MHz, CDCl_3): δ = 162.0 (C_q), 138.8 (CH), 120.9 (C_q), 114.9 (CH), 84.7 (Cage C), 84.6 (Cage C), 55.5 (CH_3), 35.0 (CH_2), 31.8 (CH_2), 22.5 (CH_2), 13.8 (CH_3). **^{11}B NMR** (96 MHz, CDCl_3): δ = -4.27 (2B), -9.91 (4B), -10.94 (4B). **IR** (ATR): 2959, 2930, 2564, 1591, 1493, 1254, 1172, 830 cm^{-1} . **MS** (EI) m/z : 338 $[\text{M}]^+$. **HR-MS** (EI): m/z calcd. for $\text{C}_{13}\text{H}_{26}^{10}\text{B}_2^{11}\text{B}_8\text{OS}$ $[\text{M}]^+$: 338.2709, found: 338.2703.



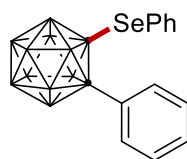
1-(*n*-butyl)-2-undecylsulfanyl-*o*-carborane

244h. The representative procedure **C** was followed using *o*-carborane **241f** (20.0 mg, 0.10 mmol) and 1-undecanethiol **242u** (67.9 μL , 0.30 mmol). Isolation by column chromatography (*n*-hexane) yielded **244h** (20.7 mg, 54%) as a colorless oil. **^1H NMR** (300 MHz, CDCl_3): δ = 2.86 (t, J = 7.2 Hz, 2H), 2.35 – 2.26 (m, 2H), 1.67 – 1.59 (m, 2H), 1.57 – 1.47 (m, 2H), 1.45 – 1.21 (m, 18H), 1.01 – 0.85 (m, 6H). **^{13}C NMR** (75 MHz, CDCl_3): δ = 85.0 (Cage C), 83.9 (Cage C), 37.2 (CH_2), 34.6 (CH_2), 31.9 (CH_2), 31.8 (CH_2), 29.6 (CH_2), 29.5 (CH_2), 29.4 (CH_2), 29.3 (CH_2), 29.0 (CH_2), 28.7 (CH_2), 28.2 (CH_2), 22.7 (CH_2), 22.4 (CH_2), 14.1 (CH_3), 13.7 (CH_3). **^{11}B NMR** (96 MHz, CDCl_3): δ = -4.29 (2B), -9.85 (4B), -10.95 (4B). **IR** (ATR): 2958, 2924, 2853, 2606, 2569, 1466, 1259, 748 cm^{-1} . **MS** (EI) m/z : 386 $[\text{M}]^+$. **HR-MS** (EI): m/z calcd. for $\text{C}_{17}\text{H}_{42}^{10}\text{B}_2^{11}\text{B}_8\text{S}$ $[\text{M}]^+$: 386.4014, found: 386.4008.



1-methyl-2-[(4-methoxyphenyl)sulfanyl]-o-carborane

244i. The representative procedure **C** was followed using o-carborane **241g** (15.8 mg, 0.10 mmol) and 4-methoxybenzenethiol **242a** (36.9 μ L, 0.30 mmol). Isolation by column chromatography (*n*-hexane) yielded **244i** (20.0 mg, 68%) as a colorless solid. **M.p.** = 81 – 83 °C. **¹H NMR** (300 MHz, CDCl₃): δ = 7.49 (d, *J* = 8.9 Hz, 2H), 6.94 (d, *J* = 9.0 Hz, 2H), 3.87 (s, 3H), 2.24 (s, 3H). **¹³C NMR** (75 MHz, CDCl₃): δ = 162.0 (C_q), 138.9 (CH), 121.0 (C_q), 114.9 (CH), 82.7 (Cage C), 79.3 (Cage C), 55.5 (CH₃), 23.6 (CH₃). **¹¹B NMR** (96 MHz, CDCl₃): δ = -3.86 (1B), -4.97 (1B), -8.82 (2B), -9.90 (6B). **IR** (ATR): 2838, 2600, 2571, 2557, 1590, 1493, 1254, 828 cm⁻¹. **MS** (EI) *m/z*: 296 [M]⁺. **HR-MS** (EI): *m/z* calcd. for C₁₀H₂₀¹⁰B₂¹¹B₈OS [M]⁺: 296.2238, found: 296.2230.

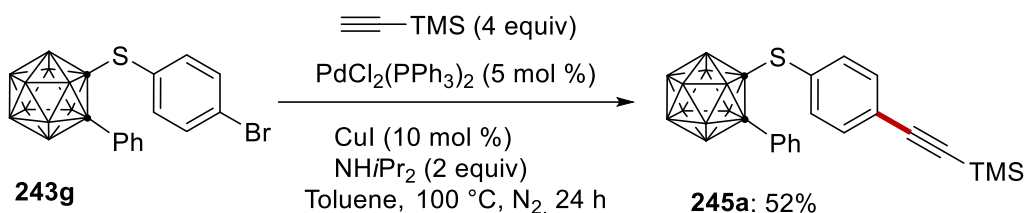


1-phenyl-2-phenylselanyl-o-carborane

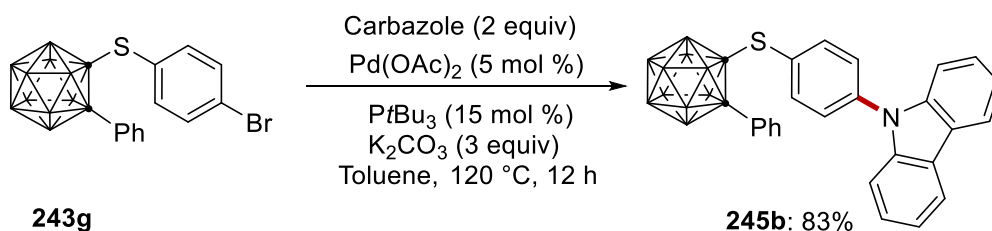
244j. The representative procedure **C** was followed using o-carborane **241a** (22.0 mg, 0.10 mmol) and benzeneselenol **242v** (31.9 μ L, 0.30 mmol). Isolation by column chromatography (*n*-hexane) yielded **244j** (22.0 mg, 59%) as a colorless solid. **M.p.** = 112 – 114 °C. **¹H NMR** (300 MHz, CDCl₃): δ = 7.63 – 7.52 (m, 3H), 7.45 (t, *J* = 7.5 Hz, 3H), 7.29 (t, *J* = 7.6 Hz, 2H), 7.16 (d, *J* = 7.3 Hz, 2H). **¹³C NMR** (75 MHz, CDCl₃): δ = 137.6 (CH), 132.0 (CH), 131.7 (C_q), 130.8 (CH), 130.7 (CH), 129.2 (CH), 128.5 (CH), 127.1 (C_q), 86.3 (Cage C), 72.7 (Cage C). **¹¹B NMR** (96 MHz, CDCl₃): δ = -2.44 (2B), -8.29 (1B), -9.00 (1B), -9.78 (3B), -11.45 (3B). **IR** (ATR): 2630, 2609, 2572, 2561, 1585, 1486, 1233, 754 cm⁻¹. **MS** (EI) *m/z*: 376 [M]⁺. **HR-MS** (EI): *m/z* calcd. for C₁₄H₂₀¹⁰B₂¹¹B₈Se [M]⁺: 376.1729, found: 376.1726.

5.3.2.2 Late-Stage Diversification

5 Experimental Section



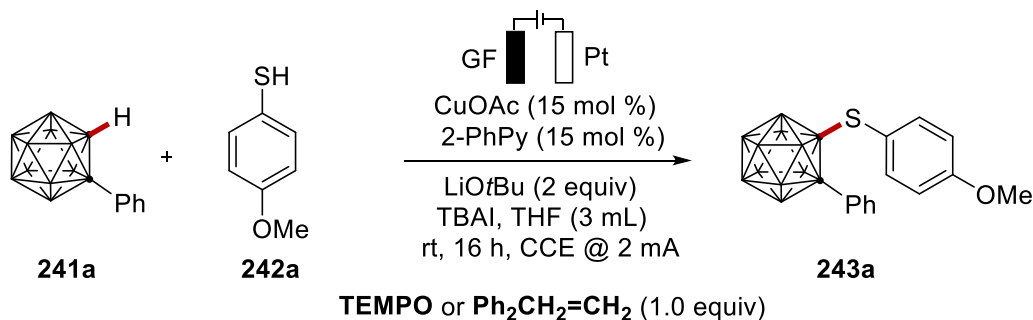
Compound **243g** (40.7 mg, 0.10 mmol), trimethylsilylacetylene (56.5 μL , 0.40 mmol), $\text{PdCl}_2(\text{PPh}_3)_2$ (3.5 mg, 0.005 mmol), CuI (1.9 mg, 0.01 mmol) and $\text{HN}i\text{Pr}_2$ (28.2 μL , 0.20 mmol) were combined in toluene (2.5 mL). The resulting mixture was heated at 100 °C for 24 h under N_2 . Then, the reaction was quenched with water (10 mL) and extracted with diethyl ether (10 mL x 3). The organic layers were combined and concentrated to dryness in vacuo. The residue was subjected to flash column chromatography on silica gel using *n*-hexane as eluent to give the product **245a** as a colorless oil (52%). **^1H NMR** (300 MHz, CDCl_3): δ = 7.66 – 7.60 (m, 2H), 7.60 – 7.53 (m, 1H), 7.47 (t, J = 7.6 Hz, 2H), 7.34 (d, J = 8.0 Hz, 2H), 6.86 (d, J = 8.0 Hz, 2H), 0.28 (s, 9H). **^{13}C NMR** (101 MHz, CDCl_3): δ = 136.6 (CH), 132.5 (CH), 132.3 (CH), 131.0 (CH), 130.9 (C_q), 129.9 (C_q), 128.7 (CH), 126.3 (C_q), 103.6 (C_q), 98.0 (C_q), 88.1 (Cage C), 85.8 (Cage C), 0.0 (CH_3). **^{11}B NMR** (96 MHz, CDCl_3): δ = -2.65 (2B), -8.99 (3B), -10.46 (5B). **IR** (ATR): 2958, 2923, 2594, 2575, 2158, 1480, 1250, 862, 841 cm^{-1} . **MS** (EI) m/z : 424 $[\text{M}]^+$. **HR-MS** (EI): m/z calcd. for $\text{C}_{19}\text{H}_{28}^{10}\text{B}_2^{11}\text{B}_8\text{SSi}$ $[\text{M}]^+$: 424.2690, found: 424.2678.



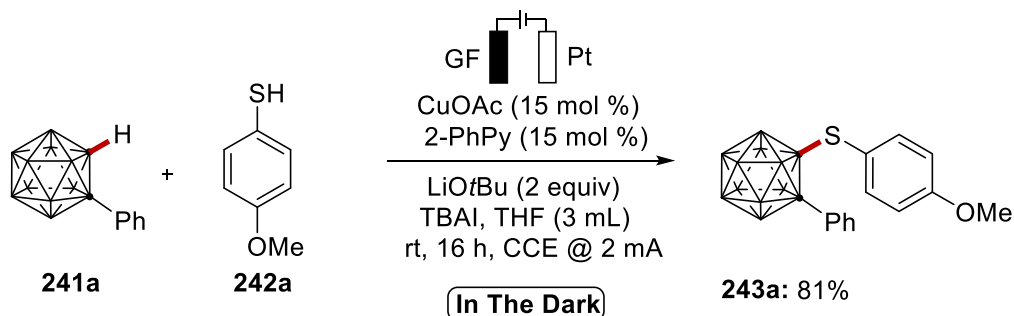
Compound **243g** (40.7 mg, 0.10 mmol), carbazole (33.4 mg, 0.20 mmol), $\text{Pd}(\text{OAc})_2$ (1.1 mg, 0.005 mmol), PtBu_3 (3.0 mg, 0.015 mmol), and K_2CO_3 (41.4 mg, 0.30 mmol) were combined together in toluene (2.5 mL). The resulting mixture was heated at 120 °C for 12 h. Then, the reaction was quenched with water (10 mL) and extracted with diethyl ether (10 mL x 3). The organic layers were combined and concentrated to dryness in vacuo. The residue was subjected to flash column chromatography on silica gel using *n*-hexane and ethyl acetate (20/1) as eluent to give the product **247b** as a

colorless solid (83%). M.p. = 214 – 216 °C. **¹H NMR** (300 MHz, CDCl₃): δ = 8.14 (d, *J* = 7.8 Hz, 2H), 7.70 (d, *J* = 7.7 Hz, 2H), 7.58 – 7.53 (m, 1H), 7.49 (d, *J* = 8.5 Hz, 4H), 7.45 – 7.39 (m, 4H), 7.32 (ddd, *J* = 8.0, 6.1, 2.1 Hz, 2H), 7.14 (d, *J* = 8.4 Hz, 2H). **¹³C NMR** (101 MHz, CDCl₃): δ = 140.5 (C_q), 140.1 (C_q), 138.4 (CH), 132.2 (CH), 131.0 (CH), 130.9 (C_q), 128.6 (CH), 128.0 (C_q), 127.0 (CH), 126.2 (CH), 123.8 (C_q), 120.7 (CH), 120.5 (CH), 109.6 (CH), 87.9 (Cage C), 85.7 (Cage C). **¹¹B NMR** (96 MHz, CDCl₃): δ = -2.51 (2B), -9.09 (4B), -10.13 (4B). **IR** (ATR): 2921, 2851, 2595, 2565, 2555, 1586, 1446, 1223, 720 cm⁻¹. **MS** (EI) *m/z*: 493 [M]⁺. **HR-MS** (EI): *m/z* calcd. for C₂₆H₂₇¹⁰B₂¹¹B₈NS [M]⁺: 493.2875, found: 493.2861.

5.3.2.3 Mechanistic Studies



The general procedure **B** was followed using *o*-carborane **241a** (0.10 mmol, 1.0 equiv), 4-methoxybenzenethiol **242a** (36.9 μL, 0.30 mmol) and TEMPO or Ph₂CH₂=CH₂ (0.1 mmol, 1.0 equiv). Electrocatalysis was performed at room temperature with a constant current of 2.0 mA maintained for 16 h. The GF anode was washed with ethyl acetate (3×10 mL). Evaporation of the solvent and subsequent purification by column chromatography on silica gel with *n*-hexane afforded the corresponding product **243a** (TEMPO: 75%, Ph₂CH₂=CH₂: 72%).



The general procedure **B** was followed using *o*-carborane **241a** (0.10 mmol, 1.0 equiv), 4-methoxybenzenethiol **242a** (36.9 μ L, 0.30 mmol). Electrocatalysis was performed in the dark at room temperature with a constant current of 2.0 mA maintained for 16 h. The GF anode was washed with ethyl acetate (3 \times 10 mL). Evaporation of the solvent and subsequent purification by column chromatography on silica gel with *n*-hexane afforded the corresponding product **243a** (81%).

5.3.2.4 Cyclic Voltammetry

CV measurements were conducted by MSc. Alexej Scheremetjew with a Metrohm Autolab PGSTAT204 potentiostat and Nova 2.1 software. A glassy carbon working electrode (disk, diameter: 3mm), a coiled platinum wire counter electrode, and a non-aqueous Ag/Ag⁺ reference electrode (ALS Japan, 10 mmol/L AgNO₃ and 100 mmol/L *n*-Bu₄NPF₆ in acetonitrile) were employed. The voltammograms were recorded at room temperature in dry acetonitrile at a substrate concentration of 5 mmol/L and 100 mmol/L *n*-Bu₄NPF₆ as supporting electrolyte. Prior to each measurement, the working electrode was thoroughly polished with 0.05 μ m alumina polishing powder and rinsed with water and methanol. All measured solutions were saturated with nitrogen gas, and an overpressure of protective gas was maintained throughout the experiment. The nitrogen gas was previously saturated with solvent vapor by passing it through a gas washing bottle with acetonitrile. The scan rate is 100 mV/s. Deviations from the general experimental conditions are indicated in the respective figures.

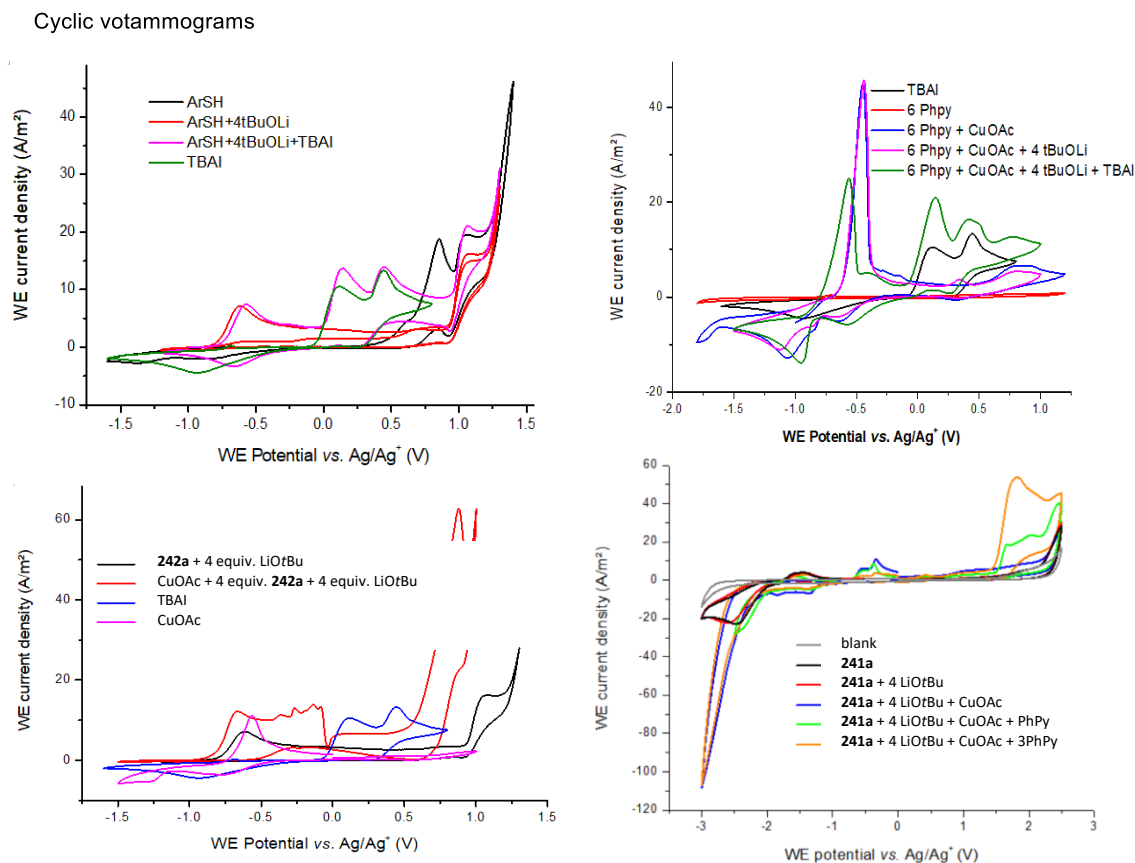


Figure 7. Cyclic voltametric studies of **241a**.

5.3.2.5 EPR Studies

The EPR spectroscopy analysis was carried out by Dr. A. Claudia Stückl. The electrocatalysis was carried out in an undivided cell under air, with a graphite felt (GF) anode (10 mm × 15 mm × 6 mm) and a platinum cathode (10 mm × 15 mm × 0.25 mm). *o*-Carborane **241a** (0.10 mmol, 1.0 equiv), 4-methoxybenzenethiol **242a** (0.30 mmol, 3.0 equiv), CuOAc (15 mol %), 2-PhPy (15 mol %), LiOtBu (0.2 mmol, 2.0 equiv) and TBAI (0.2 mmol, 2.0 equiv) were dissolved in THF (3.0 mL). Electrocatalysis was performed at room temperature with a constant current of 2.0 mA maintained for 2 h. Then PBN (*N*-tert-butyl- α -Phenylnitrone) (5 equiv) (if noted) was added to the reaction system. After stirring for 2 minutes, the mixture was immediately transferred into the EPR tube for EPR measurement.

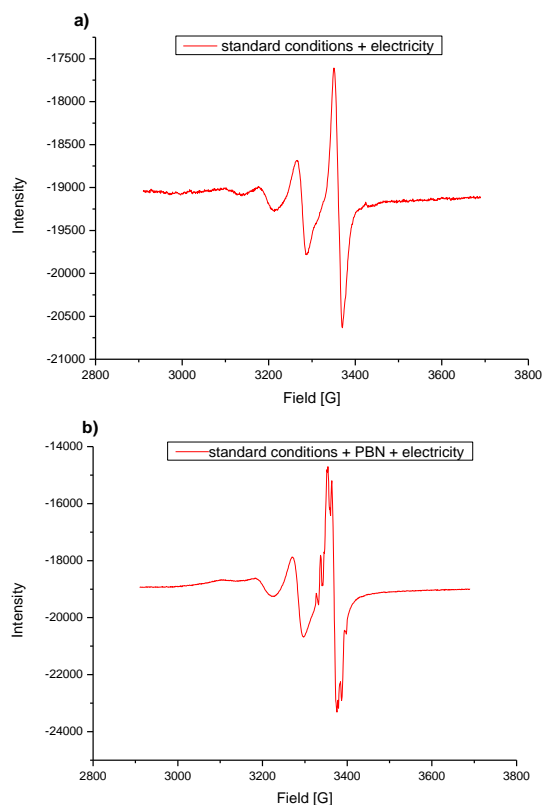


Figure 8. EPR analysis of **241a** and **242a**.

The electrocatalysis was carried out in an undivided cell under air, with a graphite felt (GF) anode (10 mm × 15 mm × 6 mm) and a platinum cathode (10 mm × 15 mm × 0.25 mm). 4-methoxybenzenethiol **241a** (0.30 mmol) and LiOtBu (0.2 mmol) were dissolved in THF (3.0 mL). Electrocatalysis was performed at room temperature with a constant current of 2.0 mA maintained for 2 h. Then PBN (*N*-tert-butyl- α -Phenylnitrone) (5 equiv.) was added to the reaction system. After stirring for 2 minutes, the mixture was immediately transferred into the EPR tube for EPR measurement. This EPR result showed a small radical signal, which is not stable for a long time even after trapping with PBN and might be attributed to one of the possible thiols containing radical species.

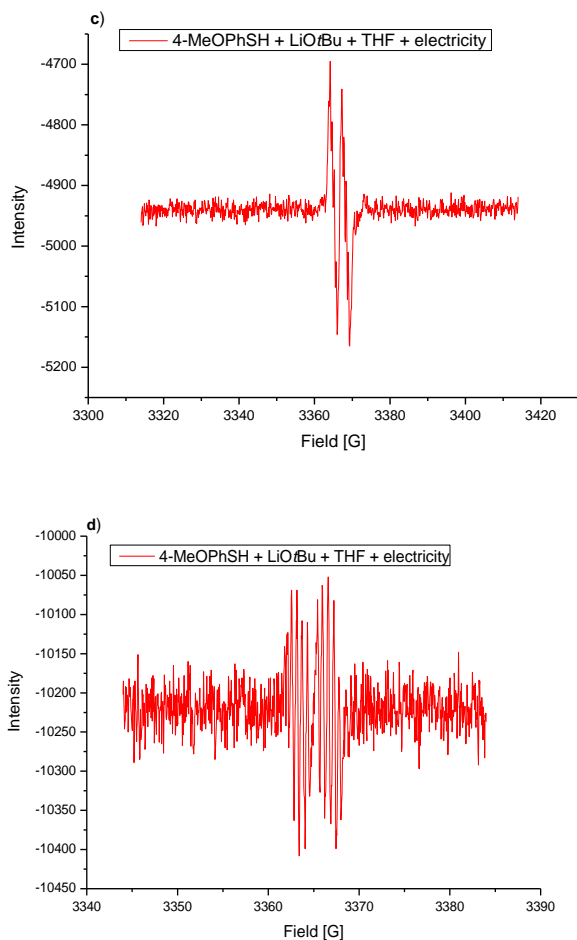


Figure 9. EPR analysis of **241a** and **242a**.

The electrocatalysis was carried out in an undivided cell under air, with a graphite felt (GF) anode (10 mm × 15 mm × 6 mm) and a platinum cathode (10 mm × 15 mm × 0.25 mm). *o*-carborane **241a** (0.10 mmol) and LiOtBu (0.2 mmol) were dissolved in THF (3.0 mL). Electrocatalysis was performed at room temperature with a constant current of 2.0 mA maintained for 2 h. Then PBN (*N*-tert-butyl- α -Phenylnitrone) (5 equiv) was added into the reaction system. After stirring for 2 minutes, the mixture was immediately transferred into the EPR tube for EPR measurement.^[201]

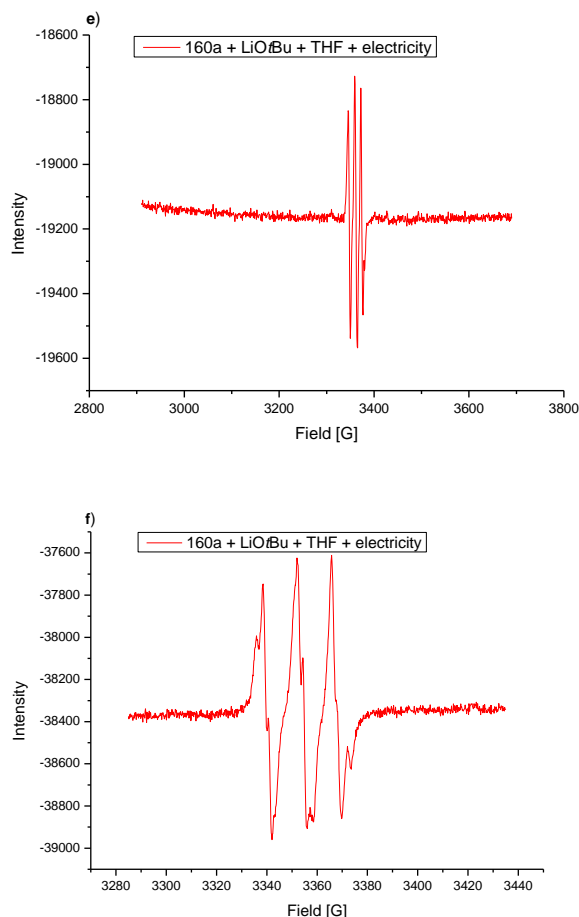
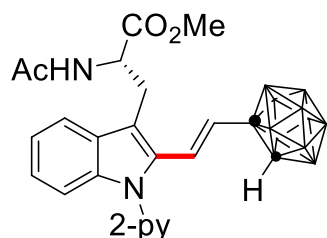


Figure 10. EPR analysis of **241a** and **242a**

5.3.3 Manganese(I)-Catalyzed Selective Labeling of Peptides with *o*-Carboranes *via* C–H Activation.

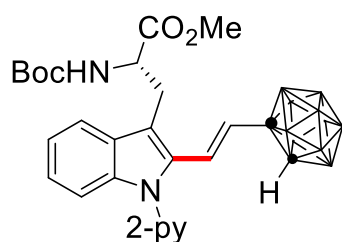
5.3.3.1 Characterization Data



Methyl (S, E)-2-acetamido-3-[2-(*o*-carboranyl-1-en-1-yl)]-1-(pyridin-2-yl)-1*H*-indol-3-ylpropanoate

248a. The general procedure was followed using methyl *N*_α-acetyl-1-(pyridin-2-yl)-*L*-tryptophanate **246a** (33.7 mg, 0.10 mmol) and 1-ethynyl-*o*-carborane **247a** (16.8 mg, 0.1 mmol). Column chromatography on silica (*n*-

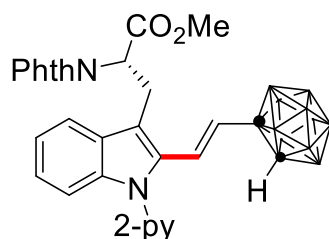
hexane/EtOAc = 4/1) afforded **248a** (48.7 mg, 96%) as yellow solid. **M.P.** = 101-103 °C. **¹H NMR** (300 MHz, CDCl₃): δ = 8.72 (dd, J = 4.9, 1.9 Hz, 1H), 7.94 (td, J = 7.7, 1.9 Hz, 1H), 7.53 – 7.45 (m, 2H), 7.41 (dd, J = 7.5, 4.9 Hz, 1H), 7.34 – 7.29 (m, 1H), 7.28 – 7.15 (m, 2H), 6.85 (d, J = 16.1 Hz, 1H), 6.30 (d, J = 7.8 Hz, 1H), 6.14 (d, J = 16.1 Hz, 1H), 4.75 (td, J = 8.5, 5.0 Hz, 1H), 4.34 (s, 1H), 3.48 (s, 3H), 3.43 – 3.20 (m, 2H), 2.05 (s, 3H). **¹³C NMR** (101 MHz, CDCl₃): δ = 172.5 (C_q), 169.7 (C_q), 150.9 (C_q), 149.4 (CH), 138.5 (CH), 137.4 (C_q), 131.7 (C_q), 128.6 (C_q), 125.8 (CH), 125.8 (CH), 125.7 (CH), 124.5 (CH), 122.6 (CH), 121.4 (CH), 118.9 (CH), 113.8 (C_q), 111.1 (CH), 74.2 (cage C_q), 60.7 (cage CH), 53.1 (CH), 52.6 (CH₃), 28.9 (CH₂), 23.2 (CH₃). **¹¹B NMR** (128 MHz, CDCl₃): δ = -2.61 (1B), -4.93 (1B), -9.06 (2B), -11.36 (3B), -12.76 (3B). **IR** (ATR): 3050, 2596, 1655, 1588, 1469, 1437, 1372, 1224, 744 cm⁻¹. **MS** (ESI) m/z (relative intensity): 507(90) [M]⁺. **HR-MS** (ESI): m/z calcd. for C₂₃H₃₁B₁₀N₃O₃ [M+H]⁺: 508.3369, found: 508.3373.



Methyl (S, E)-3-[2-(2-o-carboranyl-vinyl)-1-(pyridin-2-yl)-1H-indol-3-yl]-2-[(tert-butoxycarbonyl)amino]propanoate

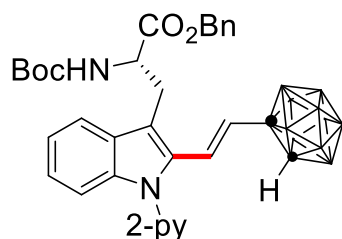
248b. The general procedure was followed using methyl *N* α -(*tert*-butoxycarbonyl)-1-(pyridin-2-yl)-*L*-tryptophanate **246b** (39.5 mg, 0.10 mmol) and 1-ethynyl-*o*-carborane **247a** (16.8 mg, 0.10 mmol). Column chromatography on silica in (*n*-hexane/EtOAc = 4/1) afforded **248b** (54.8 mg, 97%) as white foamy solid. **M.P.** = 102-103°C. **¹H NMR** (400 MHz, CDCl₃): δ = 8.71 – 8.65 (dd, J = 4.9, 2.0 Hz, 1H), 7.89 (td, J = 7.8, 2.0 Hz, 1H), 7.53 – 7.41 (m, 2H), 7.36 (ddd, J = 7.5, 4.9, 1.0 Hz, 1H), 7.27 (d, J = 8.0 Hz, 1H), 7.23 – 7.11 (m, 2H), 6.85 (d, J = 16.1 Hz, 1H), 6.09 (d, J = 16.1 Hz, 1H), 5.33 (d, J = 8.3 Hz, 1H), 4.56 – 4.36 (m, 1H), 4.33 (s, 1H), 3.41 (s, 3H), 3.25 (m, J = 14.1, 7.1 Hz, 2H), 1.43 (s, 9H). **¹³C NMR** (126 MHz): δ = 172.6 (C_q), 155.0 (C_q), 151.0 (C_q), 149.6 (CH), 138.4 (CH), 137.3 (C_q), 131.5 (C_q), 128.7 (C_q), 125.8 (CH), 125.7 (CH), 124.4 (CH), 122.4 (CH), 121.4 (CH), 121.4 (CH),

119.0 (CH), 114.15 (C_q), 111.1 (CH), 80.4 (C_q), 74.3 (cage C_q), 60.6 (cage CH), 54.5 (CH), 52.4 (CH₃), 29.7 (CH₂), 28.3 (3CH₃). **¹¹B NMR** (128 MHz, CDCl₃): δ = -2.52 (1B), -4.82 (1B), -8.97 (2B), -11.13 (6B). **IR** (ATR): 3051, 2976, 2596, 1743, 1698, 1588, 1469, 1437, 1365, 1172 cm⁻¹. **MS** (ESI) *m/z* (relative intensity): 565 (90) [M]⁺. **HR-MS** (ESI): *m/z* calcd. for C₂₆H₃₇B₁₀N₃O₄ [M+H]⁺: 566.3783, found: 566.3793.



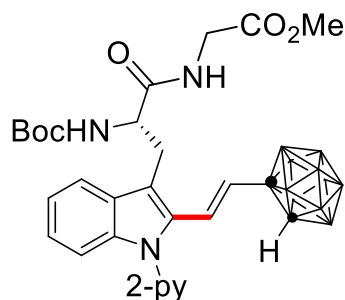
Methyl (S, E)-3-[2-(2-o-carboranyl-vinyl)]-1-(pyridin-2-yl)-1H-indol-3-yl)-2-(1,3-dioxoisindolin-2-yl)propanoate

248c. The general procedure was followed using methyl (S)-2-(1,3-dioxoisindolin-2-yl)-3-[1-(pyridin-2-yl)-1H-indol-3-yl]propanoate **246c** (43.9 mg, 0.10 mmol) and 1-ethynyl-o-carborane **247a** (16.8 mg, 0.10 mmol). Column chromatography on silica in (*n*-hexane/EtOAc = 3/2) afforded **248c** (56.6 mg, 95%) as yellow solid. **M.P.** = 154-155 °C. **¹H NMR** (400 MHz, CDCl₃): δ = 8.59 (dd, *J* = 4.9, 2.0 Hz, 1H), 7.80 (ddd, *J* = 8.0, 7.5, 2.0 Hz, 1H), 7.75 – 7.70 (m, 2H), 7.70 – 7.63 (m, 3H), 7.39 – 7.35 (m, 1H), 7.29 (ddd, *J* = 7.5, 4.9, 1.0 Hz, 1H), 7.20 – 7.11 (m, 2H), 7.07 (dt, *J* = 7.9, 1.0 Hz, 1H), 6.75 (d, *J* = 16.0 Hz, 1H), 5.54 (d, *J* = 16.0 Hz, 1H), 5.32 – 5.25 (m, 1H), 3.95 (s, 1H), 3.86 – 3.81 (m, 2H), 3.79 (s, 3H). **¹³C NMR** (126 MHz, CDCl₃): δ = 169.1 (C_q), 167.5 (C_q), 151.2 (C_q), 149.5 (CH), 138.4 (C_q), 138.1 (CH), 134.3 (C_q), 131.5 (C_q), 127.9 (CH), 126.1 (CH), 125.5 (CH), 124.8 (CH), 123.6 (CH), 122.4 (CH), 121.6 (CH), 121.5 (CH), 119.2 (CH), 115.3 (CH), 111.1 (C_q), 73.9 (cage C_q), 61.0 (cage CH), 53.1 (CH₃), 51.87 (CH), 24.6 (CH₂). **¹¹B NMR** (128 MHz, CDCl₃): δ = -2.04 (1B), -4.83 (1B), -9.20 (2B), -11.37 (6B). **IR** (ATR): 1746, 1712, 1586, 1467, 1434, 1385, 1185, 1069, 716 cm⁻¹. **MS** (ESI) *m/z* (relative intensity): 596 (30) [M+H]⁺. **HR-MS** (ESI): *m/z* calcd. for C₂₉H₃₁B₁₀N₃O₃ [M+H]⁺: 596.3318, found: 596.3324.



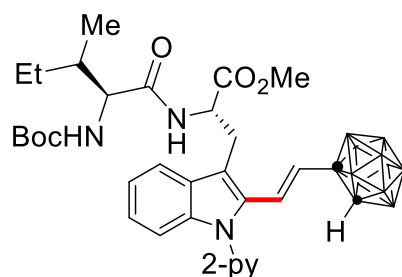
Benzyl (S, E)-3-[2-(2-o-carboranyl-vinyl)]-1-(pyridin-2-yl)-1*H*-indol-3-yl)-2-[(*tert* butoxycarbonyl) amino]propanoate

248d. The general procedure was followed using benzyl *N* α -(*tert*-butoxycarbonyl)-1-(pyridin-2-yl)-*L*-tryptophanate **246d** (47.1 mg, 0.10 mmol) and 1-ethynyl-*o*-carborane **247a** (16.8 mg, 0.10 mmol). Column chromatography on silica in (*n*-hexane/EtOAc = 4/1) afforded **248d** (59.6 mg, 93%) as yellow solid. **M.P.** = 84-86 °C. **¹H NMR** (400 MHz, CDCl₃): δ = 8.68 (dd, *J* = 5.0, 1.9 Hz, 1H), 7.88 (td, *J* = 7.7, 2.0 Hz, 1H), 7.49 (dd, *J* = 10.9, 8.1 Hz, 2H), 7.35 (ddd, *J* = 7.5, 4.9, 1.0 Hz, 1H), 7.30 – 7.10 (m, 6H), 6.85 – 6.74 (m, 3H), 6.14 (d, *J* = 16.2 Hz, 1H), 5.36 (d, *J* = 8.2 Hz, 1H), 4.97 (d, *J* = 12.1 Hz, 1H), 4.61 (d, *J* = 12.1 Hz, 1H), 4.45 (td, *J* = 8.9, 5.4 Hz, 1H), 4.29 (s, 1H), 3.27 (m, 2H), 1.42 (s, 9H). **¹³C NMR** (126 MHz, CDCl₃): δ = 172.2 (C_q), 155.0 (C_q), 150.9 (C_q), 149.6 (CH), 138.4 (CH), 137.3 (C_q), 134.4 (C_q), 131.6 (C_q), 128.7 (C_q), 128.4 (CH), 128.3 (CH), 128.3 (CH), 125.8 (CH), 125.7 (CH), 124.4 (CH), 122.4 (CH), 121.5 (CH), 121.3 (CH), 118.9 (CH), 113.9 (C_q), 111.1 (CH), 80.4 (C_q), 74.3 (cage C_q), 67.7 (CH₂), 60.6 (cage CH), 54.6 (CH), 29.8 (CH₂), 28.3 (CH₃), 27.4 (CH). **¹¹B NMR** (128 MHz, CDCl₃): δ = -2.77 (1B), -5.09 (1B), -9.16 (2B), -11.76 (3B), -13.24 (3B). **IR** (ATR): 3053, 2924, 2596, 1697, 1588, 1469, 1454, 1352, 1172, 742 cm⁻¹. [α]_D²⁰ : 36.0 (*c* = 1.00, CH₂Cl₂). **MS** (ESI) *m/z* (relative intensity): 642 (100) [M+H]⁺. **HR-MS** (ESI): *m/z* calcd. for C₃₂H₄₁B₁₀N₃O₄ [M+H]⁺: 642.4100, found: 642.4107.



Methyl (S, E)-{3-[2-(2-o-carboranyl-vinyl)]-1-(pyridin-2-yl)-1*H*-indol-3-yl)-2-[(*tert*-butoxycarbonyl)amino]propanoyl}glycinate

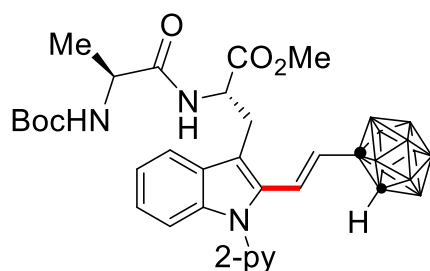
248e. The general procedure was followed using methyl *N* α -(*tert*-butoxycarbonyl)-1-(pyridin-2-yl)-*L*-tryptophylglycinate **246e** (40.9 mg, 0.1 mmol) and 1-ethynyl-*o*-carborane **247a** (16.8 mg, 0.1 mmol). Column chromatography on silica in (*n*-hexane/ EtOAc = 3/2) afforded **248e** (58.4 mg, 94%) as a white solid. **M.P.** = 115-117 °C. **¹H NMR** (400 MHz, CDCl₃): δ = 8.70 – 8.62 (dd, *J* = 6.9, 0.9 Hz, 1H), 7.92 (td, *J* = 7.8, 1.9 Hz, 1H), 7.47 (d, *J* = 7.8 Hz, 1H), 7.45 – 7.32 (m, 3H), 7.22 – 7.08 (m, 2H), 6.82 (d, *J* = 16.2 Hz, 1H), 6.33 (d, *J* = 16.2 Hz, 1H), 5.80 – 5.54 (m, 2H), 4.56 (s, 1H), 4.20 (s, 1H), 3.94 – 3.85 (m, 1H), 3.54 (s, 3H), 3.41 – 3.14 (m, 2H), 1.43 (s, 9H). **¹³C NMR** (126 MHz, CDCl₃): δ = 170.7 (C_q), 169.0 (C_q), 155.2 (C_q), 150.8 (C_q), 149.7 (CH), 138.6 (CH), 137.0 (C_q), 131.8 (C_q), 128.8 (C_q), 126.1 (CH), 125.3 (CH), 124.4 (CH), 122.6 (CH), 121.5 (CH), 121.4 (CH), 119.1 (CH), 113.6 (C_q), 110.9 (CH), 80.3 (C_q), 74.4 (cage C_q), 60.5 (cage CH), 55.6 (CH), 52.3 (CH₃), 41.2 (CH₂), 29.8 (CH₂), 28.3 (CH₃). **¹¹B NMR** (128 MHz, CDCl₃): δ = -2.83 (1B), -4.85 (1B), -8.97 (2B), -11.26 (6B). **IR** (ATR): 2360, 2167, 2056, 1596, 1560, 1428, 534 cm⁻¹. **MS** (ESI) *m/z* (relative intensity): 622 (100) [M]⁺. **HR-MS** (ESI): *m/z* calcd. for C₂₈H₄₀B₁₀N₄O₅ [M+H]⁺: 622.3929, found: 622.4055.



Methyl (S)-3-{2-[(*E*)-2-*o*-carboranyl-vinyl]-1-(pyridin-2-yl)-1*H*-indol-3-yl}-2-[(2*S*, 3*S*)-2-[(*tert*-butoxycarbonyl)amino]-3-methylpentanamido]propanoate

248f. The general procedure was followed using methyl *N* α -[(*tert*-butoxycarbonyl)-*L*-isoleucyl]-1-(pyridin-2-yl)-*L*-tryptophanate **246f** (50.8 mg, 0.1 mmol) and 1-ethynyl-*o*-carborane **247a** (16.8 mg, 0.1 mmol). Column chromatography on silica in (*n*-hexane/EtOAc = 3/2) afforded **248f** (47.3 mg, 70%) as yellow solid. **M.P.** = 108-110 °C. **¹H NMR** (400 MHz, CDCl₃): δ = 8.67 (dd, *J* = 5.7, 2.0 Hz, 1H), 7.90 (td, *J* = 7.7, 2.0 Hz, 1H), 7.52 – 7.42 (m, 2H), 7.35 (ddd, *J* = 7.5, 4.9, 1.0 Hz, 1H), 7.29 (dt, *J* = 8.0, 1.0 Hz, 1H), 7.23 – 7.14 (m, 2H), 6.81 (d, *J* = 16.1 Hz, 1H), 6.77 (s, 1H), 6.25 (d, *J* = 16.1 Hz,

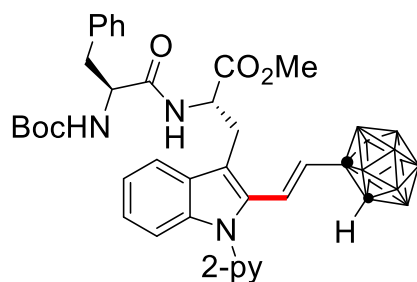
1H), 4.89 (s, 1H), 4.67 (q, $J = 7.6$ Hz, 1H), 4.49 (s, 1H), 3.97 (s, 1H), 3.41 (s, 3H), 3.41 – 3.22 (m, 2H), 1.94 – 1.83 (m, 2H), 1.45 (s, 9H), 1.33 – 1.19 (m, 1H), 0.97 – 0.85 (m, 6H). **^{13}C NMR** (126 MHz, CDCl_3): $\delta = 172.3$ (C_q), 171.4 (C_q), 150.8 (C_q), 149.6 (CH), 138.5 (CH), 137.1 (C_q), 131.7 (C_q), 128.6 (C_q), 126.1 (CH), 125.7 (CH), 124.4 (CH), 122.4 (CH), 121.5 (CH), 121.3 (CH), 118.8 (CH), 113.5 (C_q), 111.2 (CH), 80.3 (C_q), 74.3 (cage C_q), 60.7 (cage CH), 59.3 (CH), 53.2 (CH), 52.5 (CH_3), 37.0 (CH), 29.4 (CH_2), 28.2 (CH_3), 24.7 (CH_2), 15.6 (CH_3), 11.5 (CH_3). **^{11}B NMR** (128 MHz, CDCl_3): $\delta = -2.74$ (1B), -4.85 (1B), -8.94 (2B), -11.25 (6B). **IR** (ATR): 2963, 2565, 1713, 1652, 1588, 1519, 1469, 1436, 1366, 1173 cm^{-1} . **MS** (ESI) m/z (relative intensity): 678 (100) $[\text{M}]^+$. **HR-MS** (ESI): m/z calcd. for $\text{C}_{32}\text{H}_{48}\text{B}_{10}\text{N}_4\text{O}_5$ $[\text{M}+\text{H}]^+$: 679.4628, found: 679.4634.



Methyl (S)-3-{2-((E)-2-o-carboranyl-vinyl)-1-(pyridin-2-yl)-1H-indol-3-yl)-2-((S)-2-[(tert-butoxycarbonyl) amino] propanamido} propanoate

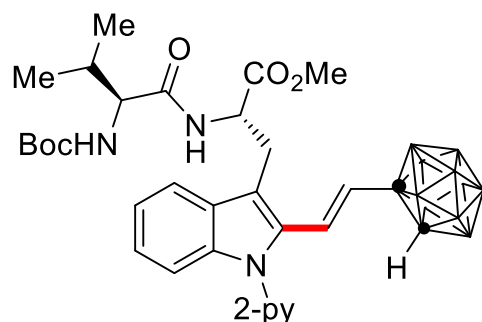
248g. The general procedure was followed using methyl N_α -[(tert-butoxycarbonyl)-L-alanyl]-1-(pyridin-2-yl)-L-tryptophanate **246g** (46.6 mg, 0.1 mmol) and 1-ethynyl-o-carborane **247a** (16.8 mg, 0.1 mmol). Column chromatography on silica in (*n*-hexane/EtOAc = 4/1) afforded **248g** (57.0 mg, 90%) as white solid. **M.P.** = 105-107 °C. **^1H NMR** (400 MHz, CDCl_3): $\delta = 8.67$ (dd, $J = 4.9, 2.0$ Hz, 1H), 7.90 (td, $J = 7.8, 2.0$ Hz, 1H), 7.50 – 7.41 (m, 2H), 7.36 (ddd, $J = 7.5, 4.9, 1.0$ Hz, 1H), 7.32 – 7.26 (m, 1H), 7.25 – 7.10 (m, 2H), 6.88 (d, $J = 8.0$ Hz, 1H), 6.80 (d, $J = 16.1$ Hz, 1H), 6.14 (d, $J = 16.1$ Hz, 1H), 4.89 (s, 1H), 4.68 (q, $J = 7.4$ Hz, 1H), 4.38 (s, 1H), 4.25 – 4.01 (m, 1H), 3.44 (s, 3H), 3.24 (d, $J = 7.3$ Hz, 2H), 1.43 (s, 9H), 1.29 (dd, $J = 7.0, 3.2$ Hz, 3H). **^{13}C NMR** (126 MHz, CDCl_3): $\delta = 172.4$ (C_q), 172.3 (C_q), 150.9 (C_q), 149.6 (CH), 138.5 (CH), 137.2 (C_q), 131.8 (C_q), 128.6 (C_q), 126.0 (CH), 125.9 (CH), 125.8 (CH), 124.5 (CH), 122.5 (CH), 121.4 (CH), 121.3 (CH), 118.9 (CH),

113.7 (C_q), 111.1 (CH), 80.4 (C_q), 74.2 (cage C_q), 60.8 (cage CH), 53.2 (CH), 52.6 (CH₃), 29.2 (CH₂), 28.2 (CH₃), 18.0 (CH₃). **¹¹B NMR** (128 MHz, CDCl₃): δ = -2.73 (1B), -5.01 (1B), -9.06 (2B), -11.45 (6B). **IR** (ATR): 2977, 2594, 1713, 1665, 1588, 1496, 1437, 1366, 1223, 1167 cm⁻¹. **MS** (ESI) *m/z* (relative intensity): 636 (100) [M]⁺. **HR-MS** (ESI): *m/z* calcd. for C₂₉H₄₃B₁₀N₄O₅ [M+H]⁺: 637.4159, found: 637.4164.



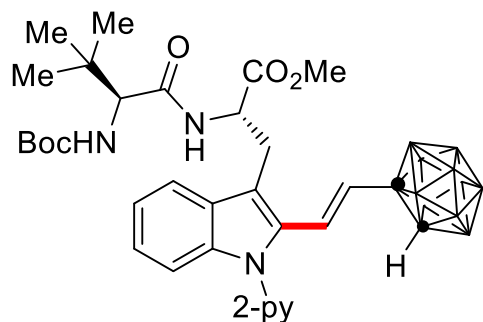
Methyl (S)-3-[2-(E)-(2-*o*-carboranyl)-vinyl]-1-(pyridin-2-yl)-1*H*-indol-3-yl)-2-[(S)-2-[(*tert*-butoxycarbonyl) amino]-3-phenylpropanamido)propanoate **248g**¹. The general procedure was followed using methyl *N*_α-[(*tert*-butoxycarbonyl)-*L*-phenylalanyl]-1-(pyridin-2-yl)-*L*-tryptophanate **246g**¹ (54.1 mg, 0.1 mmol) and 1-ethynyl-*o*-carborane **247a** (16.8 mg, 0.1 mmol). Column chromatography on silica in (*n*-hexane/EtOAc = 4/1) afforded **248g**¹ (65.2 mg, 92%) as yellow solid. **M.P.** = 104-106 °C. **¹H NMR** (300 MHz, CDCl₃): δ = 8.72 (dd, *J* = 5.2, 2.0 Hz, 1H), 7.95 (td, *J* = 7.7, 2.0 Hz, 1H), 7.50 (d, *J* = 8.2 Hz, 1H), 7.40 (dd, *J* = 7.5, 4.5 Hz, 2H), 7.32 (dd, *J* = 7.7, 5.9 Hz, 3H), 7.27 – 7.14 (m, 5H), 6.86 (d, *J* = 16.1 Hz, 1H), 6.64 (d, *J* = 7.8 Hz, 1H), 6.21 (d, *J* = 16.1 Hz, 1H), 4.93 (s, 1H), 4.72 – 4.58 (m, 1H), 4.43 (s, 1H), 4.36 (d, *J* = 9.9 Hz, 1H), 3.43 (s, 3H), 3.23 (qd, *J* = 14.2, 7.5 Hz, 2H), 3.04 (d, *J* = 6.8 Hz, 2H), 1.44 (s, 9H). **¹³C NMR** (101 MHz, CDCl₃): δ = 171.9 (C_q), 171.0 (C_q), 150.9 (C_q), 149.7 (CH), 138.5 (CH), 137.2 (C_q), 136.3 (C_q), 131.7 (C_q), 129.2 (CH), 128.7 (CH), 128.6 (C_q), 127.1 (CH), 125.8 (CH), 125.8 (CH), 124.5 (CH), 122.5 (CH), 121.5 (CH), 121.3 (CH), 118.81 (CH), 113.6 (C_q), 111.1 (CH), 80.5 (C_q), 74.3 (cage C_q), 60.7 (cage CH), 55.8 (CH), 53.2 (CH), 52.5 (CH₃), 38.2 (CH₂), 29.1 (CH₂), 28.2 (CH₃). **¹¹B NMR** (128 MHz, CDCl₃): δ = -2.67 (1B), -4.90 (1B), -8.98 (2B), -11.21 (3B), -13.04 (3B). **IR** (ATR): 2924, 2596, 2166, 1966, 1703, 1519, 1469, 1438, 1367, 744 cm⁻¹. **MS** (ESI) *m/z* (relative intensity): 712 (100) [M]⁺. **HR-MS** (ESI): *m/z* calcd. for C₃₅H₄₇B₁₀N₄O₅ [M+H]⁺:

713.4472, found: 713.4478.



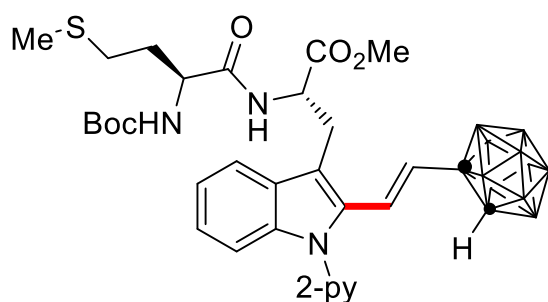
Methyl (S)-3-(2-((E)-2-*o*-carboranyl-vinyl)-1-(pyridin-2-yl)-1*H*-indol-3-yl)-2-((S)-2-((*tert*-butoxycarbonyl) amino)-3-methylbutanamido)propanoate

248h. The general procedure was followed using methyl *N* α -[(*tert*-butoxycarbonyl)-*L*-valyl]-1-(pyridin-2-yl)-*L*-tryptophanate **246h** (49.3 mg, 0.1 mmol) and 1-ethynyl-*o*-carborane **247a** (16.8 mg, 0.1 mmol). Column chromatography on silica in (*n*-hexane/EtOAc = 4/1) afforded **248h** (52.9 mg, 80%) as white solid. **M.P.** = 115-117 °C. **¹H NMR** (400 MHz, CDCl₃): δ = 8.67 (dd, *J* = 6.8, 0.8 Hz, 1H), 7.90 (ddd, *J* = 8.0, 7.5, 2.0 Hz, 1H), 7.49 – 7.43 (m, 2H), 7.35 (ddd, *J* = 7.5, 4.9, 1.0 Hz, 1H), 7.29 (dt, *J* = 8.0, 1.0 Hz, 1H), 7.25 – 7.11 (m, 2H), 6.81 (d, *J* = 16.1 Hz, 1H), 6.20 (d, *J* = 16.1 Hz, 1H), 4.93 (d, *J* = 8.6 Hz, 1H), 4.68 (q, *J* = 7.6 Hz, 1H), 4.45 (s, 1H), 3.97 – 3.87 (m, 1H), 3.42 (s, 3H), 3.23 (d, *J* = 7.5 Hz, 2H), 2.14 (dt, *J* = 7.0, 5.9 Hz, 2H), 1.44 (s, 9H), 0.93 (d, *J* = 6.8 Hz, 3H), 0.89 – 0.80 (d, *J* = 7.1 Hz, 3H). **¹³C NMR** (126 MHz, CDCl₃): δ = 172.3 (C_q), 171.4 (C_q), 155.8 (C_q), 150.9 (C_q), 149.6 (CH), 138.4 (CH), 137.1 (C_q), 131.7 (C_q), 128.6 (C_q), 126.0 (CH), 125.8 (CH), 124.4 (CH), 122.4 (CH), 121.5 (CH), 121.3 (CH), 118.8 (CH), 113.5 (C_q), 111.2 (CH), 80.3 (C_q), 74.3 (cage C_q), 60.7 (cage CH), 59.9 (CH), 53.2 (CH), 52.6 (CH₃), 30.5 (CH), 29.3 (CH₂), 28.2 (CH₃), 19.2 (CH₃), 17.5 (CH₃). **¹¹B NMR** (128 MHz, CDCl₃): δ = -2.67 (1B), -4.71 (1B), -8.92 (2B), -11.18 (6B). **IR** (ATR): 2961, 2594, 1656, 1499, 1469, 1437, 1366, 1214, 1174, 1018 cm⁻¹. **MS** (ESI) *m/z* (relative intensity): 664 (100) [M]⁺. **HR-MS** (ESI): *m/z* calcd. for C₃₁H₄₇B₁₀N₄O₅ [M+H]⁺: 665.4472, found: 665.4478.



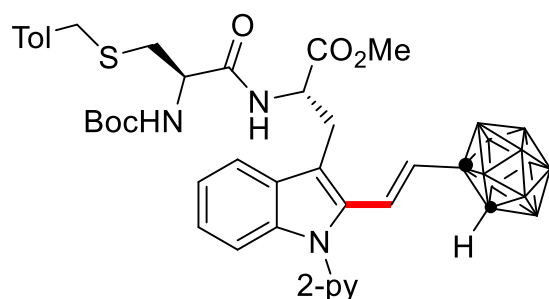
Methyl (S)-3-(2-((E)-2-o-carboranyl-vinyl)-1-(pyridin-2-yl)-1H-indol-3-yl)-2-((S)-2-((tert-butoxycarbonyl) amino)-3,3-dimethylbutanamido)propanoate

248i. The general procedure was followed using methyl N_{α} -((S)-2-[(tert-butoxycarbonyl)amino]-3,3-dimethylbutanoyl)-1-(pyridin-2-yl)-L-tryptophanate **246i** (50.8 mg, 0.1 mmol) and 1-ethynyl-o-carborane **247a** (16.8 mg, 0.1 mmol). Column chromatography on silica in (*n*-hexane/ EtOAc = 4/1) afforded **248i** (62.9 mg, 93%) as white solid. **M.P.** = 121-123 °C. **¹H NMR** (400 MHz, CDCl₃): δ = 8.67 (dd, J = 5.0, 1.9 Hz, 1H), 7.89 (td, J = 7.8, 1.9 Hz, 1H), 7.46 (td, J = 8.3, 1.0 Hz, 2H), 7.35 (ddd, J = 7.5, 5.0, 1.0 Hz, 1H), 7.28 (d, J = 8.0 Hz, 1H), 7.22 – 7.13 (m, 2H), 6.83 (d, J = 16.1 Hz, 1H), 6.55 (d, J = 7.8 Hz, 1H), 6.16 (d, J = 16.1 Hz, 1H), 5.11 (d, J = 8.7 Hz, 1H), 4.70 – 4.62 (m, 1H), 4.49 (s, 1H), 3.82 (d, J = 8.9 Hz, 1H), 3.40 (s, 3H), 3.24 (dd, J = 7.5, 4.9 Hz, 2H), 1.43 (s, 9H), 0.98 (s, 9H). **¹³C NMR** (126 MHz, CDCl₃): δ = 172.3 (C_q), 170.8 (C_q), 155.7 (C_q), 150.9 (C_q), 149.6 (CH), 138.4 (CH), 137.2 (C_q), 131.6 (C_q), 128.6 (C_q), 126.0 (CH), 125.6 (CH), 124.5 (CH), 122.4 (CH), 121.5 (CH), 121.3 (CH), 118.8 (CH), 113.6 (C_q), 111.1 (CH), 80.1 (C_q), 74.3 (cage C_q), 62.6 (CH), 60.7 (cage CH), 53.2 (CH), 52.5 (CH₃), 34.4 (CH₂), 29.2 (C_q), 28.3 (CH₃), 26.6 (CH₃). **¹¹B NMR** (128 MHz, CDCl₃): δ = -2.65 (1B), -4.79 (1B), -8.97 (2B), -10.99 (6B). **IR** (ATR): 3051, 2976, 2588, 1656, 1588, 1505, 1469, 1367, 1223, 1174 cm⁻¹. **MS** (ESI) m/z (relative intensity): 678 (100) [M]⁺. **HR-MS** (ESI): m/z calcd. for C₃₂H₄₉B₁₀N₄O₅ [M+H]⁺: 679.4628, found: 679.4634.



Methyl (S)-3-(2-((E)-2-*o*-carboranyl-vinyl)-1-(pyridin-2-yl)-1*H*-indol-3-yl)-2-((S)-2-((*tert*-butoxycarbonyl) amino)-4-(methylthio) butanamido)propanoate

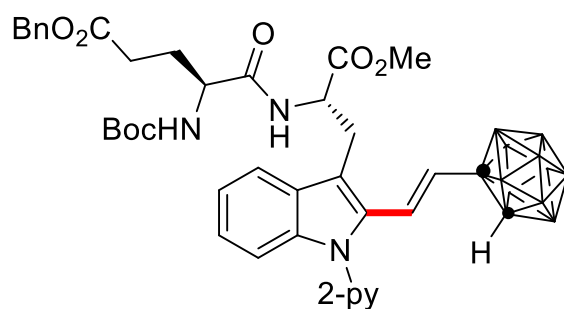
248j. The general procedure was followed using methyl *N*_α-[(*tert*-butoxycarbonyl)-*L*-methionyl]-1-(pyridin-2-yl)-*L*-tryptophanate **246j** (52.6 mg, 0.1 mmol) and 1-ethynyl-*o*-carborane **247a** (16.8 mg, 0.1 mmol). Column chromatography on silica in (*n*-hexane/EtOAc = 4/1) afforded **248j** (39.6 mg, 57% yield) as pale-yellow solid. **M.P.** = 89-91 °C. **¹H NMR** (300 MHz, CDCl₃): δ = 8.71 (dd, *J* = 5.0, 2.0 Hz, 1H), 7.95 (td, *J* = 7.8, 2.0 Hz, 1H), 7.50 (d, *J* = 7.8 Hz, 2H), 7.41 (dd, *J* = 7.5, 5.0 Hz, 1H), 7.34 (d, *J* = 8.0 Hz, 1H), 7.23 (t, *J* = 8.4 Hz, 2H), 6.96 (d, *J* = 8.2 Hz, 1H), 6.86 (d, *J* = 16.1 Hz, 1H), 6.13 (d, *J* = 16.1 Hz, 1H), 5.14 (s, 1H), 4.75 (m, 1H), 4.38 (s, 1H), 4.27 (d, *J* = 7.0 Hz, 1H), 3.52 (s, 3H), 3.31 (d, *J* = 7.2 Hz, 2H), 3.00 – 2.88 (m, 1H), 2.56 (t, *J* = 7.1 Hz, 3H), 2.09 (s, 3H), 1.48 (s, 9H). **¹³C NMR** (101 MHz, CDCl₃): δ = 172.1 (C_q), 171.3 (C_q), 155.4 (C_q), 150.9 (C_q), 149.7 (CH), 138.5 (CH), 137.3 (C_q), 131.8 (C_q), 128.5 (C_q), 125.9 (CH), 125.9 (CH), 124.5 (CH), 122.5 (CH), 121.5 (CH), 121.4 (CH), 118.9 (CH), 113.7 (C_q), 111.2 (CH), 80.5 (C_q), 74.2 (cage C_q), 60.8 (cage CH), 53.4 (CH), 53.1 (CH), 52.61 (CH₃), 31.3 (CH₂), 30.1 (CH₂), 28.9 (CH₂), 28.3 (CH₃), 15.2 (CH₃). **¹¹B NMR** (128 MHz, CDCl₃): δ = -2.61 (1B), -4.91 (1B), -9.00 (2B), -11.13 (6B). **IR** (ATR): 3049, 2976, 2565, 1663, 1558, 1507, 1469, 1366, 1226, 1167 cm⁻¹. **MS** (ESI) *m/z* (relative intensity): 696 (90) [M]⁺. **HR-MS** (ESI): *m/z* calcd. for C₃₁H₄₇B₁₀N₄O₅S [M+H]⁺: 697.4192, found: 697.4199.



Methyl (S)-3-(2-((E)-2-*o*-carboranyl-vinyl)-1-(pyridin-2-yl)-1*H*-indol-3-yl)-2-((R)-2-((*tert*-butoxycarbonyl) amino)-3-((4-methylbenzyl)thio)propanamido)propanoate

248k. The general procedure was followed using methyl *N*_α-[*N*-(*tert*-

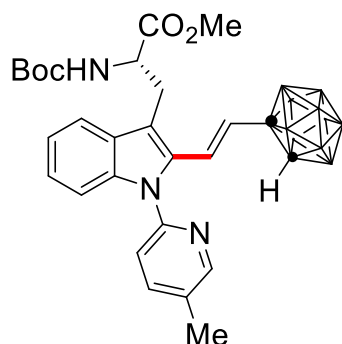
butoxycarbonyl)-S-(4-methylbenzyl)-L-cysteinyl]-1-(pyridin-2-yl)-L-tryptophanate **246k** (51.1 mg, 0.1 mmol) and 1-ethynyl-*o*-carborane **247a** (16.8 mg, 0.1 mmol). Column chromatography on silica in (*n*-hexane/ EtOAc = 4/1) afforded **248k** (57.0 mg, 74%) as white solid. **M.P.** = 115-117 °C. **¹H NMR** (300 MHz, CDCl₃): δ = 8.72 (dd, *J* = 4.9, 2.0 Hz, 1H), 7.94 (td, *J* = 7.7, 2.0 Hz, 1H), 7.54 – 7.47 (m, 2H), 7.40 (ddd, *J* = 7.5, 4.9, 1.0 Hz, 1H), 7.33 (d, *J* = 8.0 Hz, 1H), 7.27 – 7.09 (m, 7H), 6.86 (d, *J* = 16.1 Hz, 1H), 6.18 (d, *J* = 16.1 Hz, 1H), 5.31 – 5.14 (m, 1H), 4.76 – 4.65 (m, 1H), 4.38 (s, 1H), 4.30 – 4.18 (m, 1H), 3.71 (s, 2H), 3.47 (s, 3H), 3.33 – 3.27 (m, 2H), 2.87 – 2.66 (m, 2H), 2.35 (s, 3H), 1.49 (s, 9H). **¹³C NMR** (101 MHz, CDCl₃): δ = 172.4 (C_q), 170.4 (C_q), 155.3 (C_q), 150.9 (C_q), 149.7 (CH), 138.4 (CH), 137.2 (C_q), 137.0 (C_q), 134.5 (C_q), 131.7 (C_q), 129.4 (CH), 128.8 (CH), 128.6 (C_q), 125.9 (CH), 125.8 (CH), 124.5 (CH), 122.4 (CH), 121.5 (CH), 121.3 (CH), 118.9 (CH), 113.6 (C_q), 111.2 (CH), 80.7 (C_q), 74.3 (cage C_q), 60.7 (cage CH), 53.6 (CH), 52.6 (CH), 52.6 (CH₃), 36.2 (CH₂), 33.4 (CH₂), 29.1 (CH₂), 28.2 (CH₃), 21.1 (CH₃). **¹¹B NMR** (128 MHz, CDCl₃): δ = -2.61 (1B), -4.82 (1B), -8.98 (2B), -11.13 (6B). **IR** (ATR): 3049, 2924, 2596, 1664, 1588, 1513, 1469, 1366, 1210, 1167 cm⁻¹. **MS** (ESI) *m/z* (relative intensity): 772 (100) [M]⁺. **HR-MS** (ESI): *m/z* calcd. for C₃₇H₅₁B₁₀N₄O₅S [M+H]⁺: 773.4505, found: 773.4548.



Benzyl (S)-5-{[(S)-3-(2-((E)-2-*o*-carboranyl-vinyl)-1-(pyridin-2-yl)-1*H*-indol-3-yl)-1-methoxy-1-oxopropan-2-yl] amino}-4-[(*tert*-butoxycarbonyl) amino]-5-oxopentanoate

248I. The general procedure was followed using benzyl (S)-4-[(*tert*-butoxycarbonyl)amino]-5-{[(S)-1-methoxy-1-oxo-3-(1-(pyridin-2-yl))-1*H*-indol-3-yl]propan-2-yl}amino)-5-oxopentanoate **246I** (61.4 mg, 0.1 mmol) and 1-ethynyl-*o*-carborane **247a** (16.8 mg, 0.1 mmol). Column chromatography on silica in (*n*-hexane/EtOAc = 4/1) afforded **248I** (53.2 mg, 68%) as pale-yellow

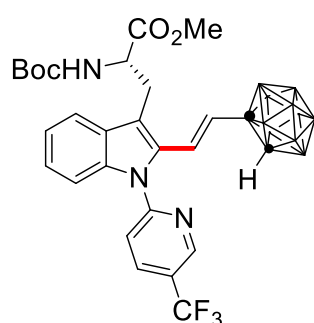
solid. **M.P.** = 84-86 °C. **¹H NMR** (400 MHz, CDCl₃): δ = 8.66 (dd, J = 5.8, 2.0 Hz, 1H), 7.89 (td, J = 7.7, 2.0 Hz, 1H), 7.49 – 7.42 (m, 2H), 7.37 – 7.28 (m, 7H), 7.22 – 7.12 (m, 2H), 6.99 (d, J = 6.1 Hz, 1H), 6.82 (d, J = 16.1 Hz, 1H), 6.09 (d, J = 16.1 Hz, 1H), 5.20 (d, J = 7.9 Hz, 1H), 4.75 – 4.64 (m, 1H), 4.34 (s, 1H), 4.23 – 4.08 (m, 1H), 3.46 (s, 3H), 3.25 (d, J = 7.3 Hz, 2H), 2.45 (m, 4H), 2.12 – 2.03 (m, 2H), 1.93 – 1.84 (m, 2H), 1.42 (s, 9H). **¹³C NMR** (126 MHz, CDCl₃): δ = 173.1 (C_q), 172.1 (C_q), 171.3 (C_q), 155.6 (C_q), 150.9 (C_q), 149.6 (CH), 138.5 (CH), 137.2 (C_q), 135.6 (C_q), 131.7 (C_q), 128.6 (CH), 128.5 (C_q), 128.3 (CH), 128.2 (CH), 125.9 (CH), 125.9 (CH), 124.5 (CH), 122.5 (CH), 121.5 (CH), 121.4 (CH), 118.9 (CH), 113.7 (C_q), 111.1 (CH), 80.4 (C_q), 74.2 (cage C_q), 66.6 (CH₂), 60.8 (cage CH), 53.7 (CH), 53.1 (CH), 52.6 (CH₃), 30.4 (CH₂), 29.0 (CH₂), 28.2 (CH₃), 27.6 (CH₂). **¹¹B NMR** (128 MHz, CDCl₃): δ = -2.72 (1B), -5.02 (1B), -9.18 (2B), -12.62 (6B). **IR** (ATR): 2924, 2850, 2361, 1735, 1260, 1095, 794, 601 cm⁻¹. **MS** (ESI) m/z (relative intensity): 784 (90) [M]⁺. **HR-MS** (ESI): m/z calcd. for C₃₈H₅₀B₁₀N₄O₇ [M+H]⁺: 785.4683, found: 785.4750.



Methyl (S, E)-3-(2-(2-o-carboranyl-vinyl)-1-(5-methylpyridin-2-yl)-1H-indol-3-yl)-2-((tert-butoxycarbonyl) amino)propanoate

248m. The general procedure was followed using methyl *N*_α-(tert-butoxycarbonyl)-1-(5-methylpyridin-2-yl)-L-tryptophanate **246m** (40.9 mg, 0.1 mmol) and 1-ethynyl-o-carborane **247a** (16.8 mg, 0.1 mmol). Column chromatography on silica in (*n*-hexane/EtOAc = 4/1) afforded **248m** (49.7 mg, 86 %) as a white solid. **M.P.** = 76-78 °C. **¹H NMR** (400 MHz, CDCl₃): δ = 8.49 (s, 1H), 7.69 (d, J = 8.2 Hz, 1H), 7.41 (m, 2H), 7.23 – 7.08 (m, 3H), 6.83 (d, J = 16.1 Hz, 1H), 6.12 (d, J = 16.1 Hz, 1H), 5.33 (d, J = 8.3 Hz, 1H), 4.48 – 4.37 (m, 1H), 4.34 (s, 1H), 3.40 (s, 3H), 3.33 – 3.15 (m, 2H), 2.45 (s, 3H), 1.43 (s,

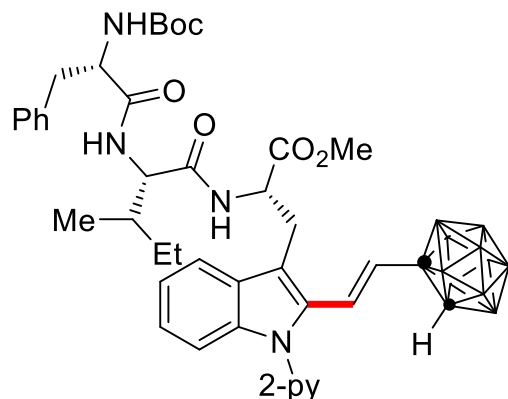
9H). **¹³C NMR** (126 MHz, CDCl₃): δ = 172.7 (C_q), 155.1 (C_q), 149.8 (CH), 148.6 (C_q), 139.0 (CH), 137.4 (C_q), 132.4 (C_q), 131.6 (C_q), 128.6 (C_q), 125.8 (CH), 125.5 (CH), 124.3 (CH), 121.2 (CH), 120.9 (CH), 118.9 (CH), 113.6 (C_q), 111.0 (CH), 80.4 (C_q), 74.5 (cage C_q), 60.7 (cage CH), 54.5 (CH), 52.4 (CH₃), 29.7 (CH₂), 28.3 (CH₃), 18.1 (CH₃). **¹¹B NMR** (128 MHz, CDCl₃): δ = -2.65 (1B), -5.00 (1B), -9.04 (2B), -11.08 (3B), -13.01 (3B). **IR** (ATR): 2586, 2147, 2027, 1984, 1691, 1482, 1453, 1364, 1151, 739 cm⁻¹. **MS** (ESI) *m/z* (relative intensity): 579 (80) [M]⁺. **HR-MS** (ESI): *m/z* calcd. for C₂₇H₄₀B₁₀N₃O₄ [M+H]⁺: 580.3944, found: 580.3949.



Methyl (S, E)-3-[2-(2-o-carboranyl-vinyl)]-1-[5-(trifluoromethyl)pyridin-2-yl]-1H-indol-3-yl]-2-((tert-butoxycarbonyl)amino) propanoate

248n. The general procedure was followed using methyl *N*_α-(*tert*-butoxycarbonyl)-1-(5-(trifluoromethyl)pyridin-2-yl)-*L*-tryptophanate **246n** (46.3 mg, 0.1 mmol) and 1-ethynyl-*o*-carborane **247a** (16.8 mg, 0.1 mmol). Column chromatography on silica in (*n*-hexane/EtOAc = 4/1) afforded **248n** (34.7 mg, 55 %) as a white solid. **M.P.** = 107-109 °C. **¹H NMR** (300 MHz, CDCl₃): δ = 8.97 (s, 1H), 8.15 (d, *J* = 10.9 Hz, 1H), 7.69 (d, *J* = 8.2 Hz, 1H), 7.46 (t, *J* = 8.2 Hz, 2H), 7.35 – 7.19 (m, 2H), 6.89 (d, *J* = 16.0 Hz, 1H), 6.35 (d, *J* = 16.1 Hz, 1H), 5.42 (d, *J* = 8.2 Hz, 1H), 4.55 – 4.36 (m, 2H), 3.43 (s, 3H), 3.34 – 3.17 (m, 2H), 1.47 (s, 9H). **¹³C NMR** (126 MHz, CDCl₃): δ = 172.5 (C_q), 155.0 (C_q), 153.7 (C_q), 146.7 (q, ³*J*_{C-F} = 4.1 MHz, CH), 136.6 (C_q), 135.6 (q, ³*J*_{C-F} = 3.3 MHz, CH), 131.4 (C_q), 129.2 (C_q), 126.6 (CH), 125.9 (CH), 125.0 (CH), 124.5 (q, ²*J*_{C-F} = 32.0 Hz, C_q), 123.2 (q, ¹*J*_{C-F} = 271.3 Hz, C_q), 122.2 (CH), 120.1 (CH), 119.1 (CH), 115.4 (C_q), 111.5 (CH), 80.5 (C_q), 74.0 (cage C_q), 60.6 (cage CH), 54.6 (CH), 52.5 (CH₃), 30.9 (CH), 29.9 (CH₂), 28.3 (CH₃). **¹¹B NMR** (128 MHz, CDCl₃): δ = -2.61 (1B), -4.75 (1B), -8.93 (2B), -11.45 (3B), -12.57

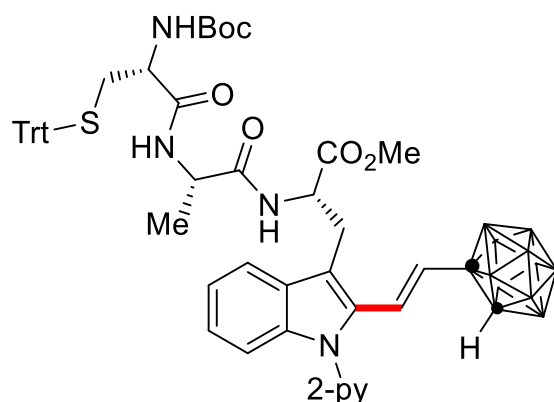
(3B). **^{19}F NMR** (376 MHz, CDCl_3): δ = -61.93. **IR** (ATR): 2586, 2147, 2027, 1984, 1691, 1482, 1453, 1364, 1151, 739 cm^{-1} . **MS** (ESI) m/z (relative intensity): 633 (80) $[\text{M}]^+$. **HR-MS** (ESI): m/z calcd. for $\text{C}_{27}\text{H}_{37}\text{B}_{10}\text{F}_3\text{N}_3\text{O}_4$ $[\text{M}+\text{H}]^+$: 634.3661, found: 634.3667.



Methyl (6S, 9S, 12S)-6-benzyl-12-((2-((E)-2-o-carboranyl-vinyl)-1-(pyridin-2-yl)-1H-indol-3-yl) methyl)-9-((R)-sec-butyl)-2,2-dimethyl-4,7,10-trioxo-3-oxa-5,8,11-triazatridecan-13-oate

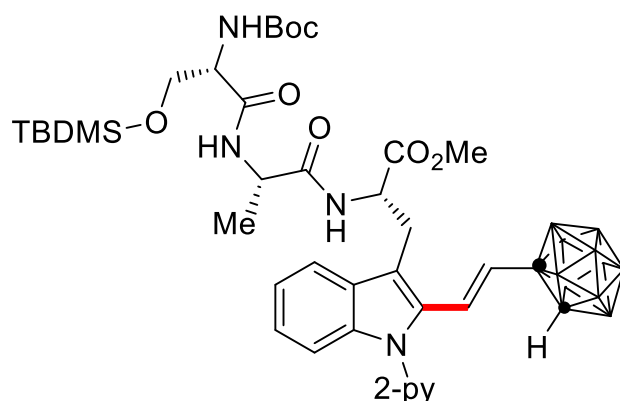
248o. The general procedure was followed using methyl N_α -(*tert*-butoxycarbonyl)-*L*-phenylalanyl-*L*-alloisoleucyl-1-(pyridin-2-yl)-*L*-tryptophanate **246o** (65.4 mg, 0.1 mmol) and 1-ethynyl-*o*-carborane **247a** (16.8 mg, 0.1 mmol). Column chromatography on silica in (*n*-hexane/EtOAc = 4/1) afforded **248o** (49.3 mg, 60%) as white solid. **M.P.** = 127-129 °C. **^1H NMR** (400 MHz, CDCl_3): δ = 8.65 (dd, J = 5.3, 2.4 Hz, 1H), 7.89 (td, J = 7.7, 1.9 Hz, 1H), 7.52 – 7.41 (m, 2H), 7.37 – 7.33 (m, 1H), 7.29 – 7.22 (m, 3H), 7.21 – 7.14 (m, 5H), 6.88 (s, 1H), 6.88 (d, J = 16.1 Hz, 1H), 6.43 (s, 1H), 6.07 (d, J = 16.1 Hz, 1H), 5.17 (d, J = 7.4 Hz, 1H), 4.68 – 4.58 (m, 1H), 4.37 (s, 1H), 4.33 – 4.21 (m, 2H), 3.46 (s, 3H), 3.23 (d, J = 7.5 Hz, 2H), 3.02 (d, J = 7.1 Hz, 2H), 1.90 – 1.80 (m, 1H), 1.40 (s, 9H), 1.37 – 1.28 (m, 1H), 1.03 – 0.91 (m, 1H), 0.86 – 0.80 (m, 6H). **^{13}C NMR** (126 MHz, CDCl_3): δ = 172.0 (C_q), 171.5 (C_q), 170.6 (C_q), 155.7 (C_q), 150.9 (C_q), 149.6 (CH), 138.5 (CH), 137.3 (C_q), 136.6 (C_q), 131.7 (C_q), 129.2 (CH), 128.8 (CH), 128.4 (C_q), 127.0 (CH), 126.0 (CH), 125.8 (CH), 124.5 (CH), 122.5 (CH), 121.5 (CH), 121.4 (CH), 119.0 (CH), 113.8 (C_q), 111.1 (CH), 80.5 (C_q), 74.2 (cage C_q), 60.8 (cage CH), 57.8 (CH), 53.2 (CH), 52.5 (CH_3), 37.5 (CH_2), 36.6 (CH), 28.6 (CH_2), 28.2 (CH_3), 24.5 (CH_2), 15.4 (CH_3), 11.4 (CH_3). **^{11}B NMR** (126 MHz, CDCl_3): δ = -2.61 (1B), -4.80 (1B), -9.10 (2B), -11.64 (6B). **IR** (ATR): 2361, 1760, 1643, 1559, 1429, 1377,

1342, 1097, 668 cm^{-1} . **MS** (ESI) m/z (relative intensity): 825 (100) $[\text{M}]^+$. **HR-MS** (ESI): m/z calcd. for $\text{C}_{41}\text{H}_{58}\text{B}_{10}\text{N}_5\text{O}_6$ $[\text{M}+\text{H}]^+$: 826,5312, found: 826,5379.



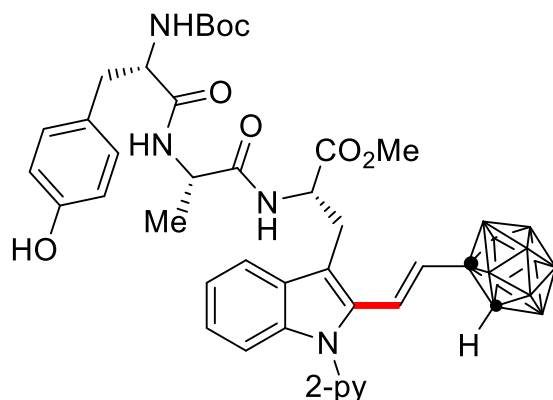
Methyl (6*R*, 9*S*, 12*S*)-12-((2-((*E*)-2-oxa-carboranyl-vinyl)-1-(pyridin-2-yl)-1*H*-indol-3-yl) methyl)-2,2,9-trimethyl-4,7,10-trioxo-6-((tritylthio)methyl)-3-oxa-5,8,11-triazatridecan-13-oate

248p. The general procedure was followed using methyl *N* α -*N*-(*tert*-butoxycarbonyl)-*S*-trityl-*L*-cysteinyl-*L*-alanyl-1-(pyridin-2-yl)-*L*-tryptophanate **246p** (66.6 mg, 0.1 mmol) and 1-ethynyl- α -carborane **247a** (16.8 mg, 0.1 mmol). Column chromatography on silica in (*n*-hexane/EtOAc = 1/1) afforded **248p** (65.7 mg, 67%) as white solid. **M.P.** = 185-187 °C. **^1H NMR** (400 MHz, CDCl_3): δ = 8.69 (dd, J = 5.2, 1.9 Hz, 1H), 7.90 (td, J = 7.8, 1.9 Hz, 1H), 7.51 – 7.44 (m, 2H), 7.43 – 7.34 (m, 7H), 7.31 – 7.14 (m, 12H), 7.02 (d, J = 7.8 Hz, 1H), 6.81 (d, J = 16.1 Hz, 1H), 6.28 (s, 1H), 6.03 (d, J = 16.1 Hz, 1H), 4.89 (s, 1H), 4.65 – 4.54 (m, 2H), 3.66 (s, 1H), 3.45 (s, 3H), 3.25 – 3.09 (m, 2H), 2.66 – 2.42 (m, 3H), 1.41 (s, 9H), 1.26 (d, J = 7.1 Hz, 3H). **^{13}C NMR** (126 MHz, CDCl_3): δ = 171.9 (C_q), 171.4 (C_q), 170.7 (C_q), 155.5 (C_q), 150.9 (C_q), 149.6 (CH), 144.3 (C_q), 138.5 (CH), 137.3 (C_q), 131.7 (C_q), 129.5 (CH), 128.5 (C_q), 128.1 (CH), 126.9 (CH), 125.9 (CH), 125.8 (CH), 124.5 (CH), 122.5 (CH), 122.4 (CH), 121.4 (CH), 119.1 (CH), 113.9 (C_q), 111.1 (CH), 80.5 (C_q), 74.2 (cage C_q), 67.3 (C_q), 60.8 (cage CH), 53.6 (CH), 53.2 (CH), 52.5 (CH_3), 48.8 (CH), 33.2 (CH_2), 28.6 (CH_2), 28.2 (CH_3), 17.2 (CH_3). **^{11}B NMR** (128 MHz, CDCl_3): δ = -2.45 (1B), -4.68 (1B), -8.98 (2B), -11.05 (6B). **IR** (ATR): 2361, 2184, 2043, 1649, 1488, 1446, 1156, 740, 699 cm^{-1} . **MS** (ESI) m/z (relative intensity): 981 (100) $[\text{M}]^+$. **HR-MS** (ESI): m/z calcd. for $\text{C}_{51}\text{H}_{62}\text{B}_{10}\text{N}_5\text{O}_6\text{S}$ $[\text{M}+\text{H}]^+$: 982.5346, found: 982.5414.



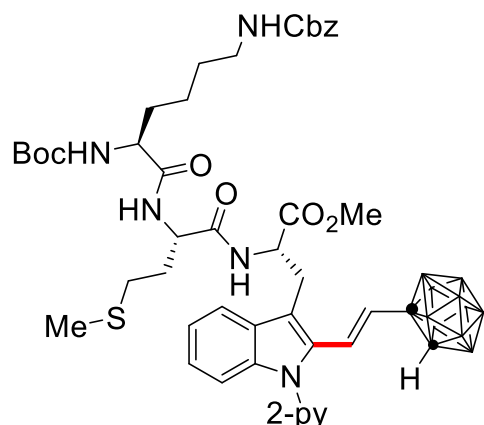
Methyl (6*S*, 9*S*, 12*S*)-12-((2-((*E*)-2-*o*-carboranyl-vinyl)-1-(pyridin-2-yl)-1*H*-indol-3-yl) methyl)-6-((*tert*-butoxycarbonyl) amino)-2,2,3,3,9-pentamethyl-7,10-dioxo-4-oxa-8,11-diaza-3-silatridecane-13-oate

248q. The general procedure was followed using methyl *N*_α-*N*-(*tert*-butoxycarbonyl)-*o*-(*tert*-butyldimethylsilyl)-*L*-seryl-*L*-alanyl-1-(pyridin-2-yl)-*L*-tryptophanate **246q** (66.5 mg, 0.1 mmol) and 1-ethynyl-*o*-carborane **249a** (16.8 mg, 0.1 mmol). Column chromatography on silica in (*n*-hexane/EtOAc = 1/1) afforded **248q** (69.1 mg, 83%) as white solid. **M.P.** = 111-113°C. **¹H NMR** (400 MHz, CDCl₃): δ = 8.69 (dd, *J* = 5.7, 1.3 Hz, 1H), 7.89 (td, *J* = 7.7, 1.9 Hz, 1H), 7.53 – 7.43 (m, 2H), 7.31 – 7.25 (m, 1H), 7.22 – 7.12 (m, 1H), 7.23 – 7.12 (m, 2H), 7.01 (s, 1H), 6.83 (d, *J* = 16.1 Hz, 2H), 6.04 (d, *J* = 16.1 Hz, 1H), 5.55 (d, *J* = 6.8 Hz, 1H), 4.60 (dd, *J* = 7.5, 1.2 Hz, 1H), 4.42 (t, *J* = 7.2 Hz, 1H), 4.35 (s, 1H), 4.10 (s, 1H), 3.90 (dd, *J* = 9.9, 4.0 Hz, 1H), 3.48 (s, 3H), 3.42 (m, 1H), 3.33 – 3.18 (m, 2H), 1.45 (s, 9H), 1.32 (d, *J* = 7.1 Hz, 3H), 0.86 (s, 9H), 0.04 (d, *J* = 7.6 Hz, 6H). **¹³C NMR** (126 MHz, CDCl₃): δ = 171.9 (C_q), 171.7 (C_q), 170.6 (C_q), 155.7 (C_q), 151.0 (C_q), 149.6 (CH), 138.5 (CH), 138.5 (CH), 137.3 (C_q), 131.8 (C_q), 128.4 (C_q), 126.0 (CH), 125.9 (CH), 124.5 (CH), 122.5 (CH), 121.5 (CH), 119.0 (CH), 113.7 (C_q), 111.2 (CH), 80.3 (C_q), 74.2 (cage C_q), 63.0 (C_q), 60.9 (cage CH), 53.2 (CH), 52.5 (CH), 52.5 (CH), 48.9 (CH₃), 28.4 (CH₂), 28.3 (CH₃), 25.8 (CH₃), 18.1 (CH₂), 17.6 (CH₃), -5.6 (CH₃). **¹¹B NMR** (128 MHz, CDCl₃): δ = -2.57 (1B), -4.87 (1B), -9.15 (2B), -11.74 (6B). **IR** (ATR): 2534, 2361, 2002, 1761, 1596, 1560, 1428, 1036, 823 cm⁻¹. **MS** (ESI) *m/z* (relative intensity): 837 (100) [M]⁺. **HR-MS** (ESI): *m/z* calcd. for C₃₈H₆₂B₁₀N₅O₇Si [M+H]⁺: 838.5344, found: 838.5410.



Methyl (6S, 9S, 12S)-12-((2-((E)-2-o-carboranyl-vinyl)-1-(pyridin-2-yl)-1H-indol-3-yl) methyl)-6-(4-hydroxybenzyl)-2,2,9-trimethyl-4,7,10-trioxo-3-oxa-5,8,11-triazatridecan-13-oate

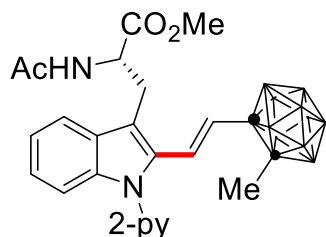
248r. The general procedure was followed using methyl *N*_α-(*tert*-butoxycarbonyl)-*L*-tyrosyl-*L*-alanyl-1-(pyridin-2-yl)-*L*-tryptophanate **246r** (62.8 mg, 0.1 mmol) and 1-ethynyl-*o*-carborane **247a** (16.8 mg, 0.1 mmol). Column chromatography on silica in (*n*-hexane/EtOAc = 1/1) afforded **248r** (62.1 mg, 78%) as white solid. **M.P.** = 173-175 °C. **¹H NMR** (300 MHz, CDCl₃): δ = 8.70 (dd, *J* = 4.9, 1.8 Hz, 1H), 7.99 (td, *J* = 7.7, 2.0 Hz, 1H), 7.58 – 7.49 (m, 1H), 7.48 – 7.36 (m, 3H), 7.24 – 6.72 (m, 2H), 7.03 (s, 1H), 6.92 – 6.72 (m, 4H), 6.55 – 6.46 (m, 2H), 6.23 (s, 1H), 5.94 (d, *J* = 16.1 Hz, 1H), 5.29 (d, *J* = 7.7 Hz, 1H), 4.63 (d, *J* = 7.3 Hz, 1H), 4.40 – 4.29 (m, 1H), 4.22 (s, 2H), 3.62 (s, 3H), 3.37 – 3.19 (m, 2H), 2.97 – 2.85 (m, 1H), 2.82 – 2.71 (m, 1H), 1.45 (s, 9H), 1.27 (d, *J* = 7.0 Hz, 3H). **¹³C NMR** (126 MHz, CDCl₃): δ = 171.9 (C_q), 171.7 (C_q), 171.4 (C_q), 155.6 (C_q), 155.3 (C_q), 150.8 (C_q), 149.5 (CH), 139.0 (CH), 137.5 (C_q), 131.7 (C_q), 130.1 (CH), 128.5 (C_q), 127.5 (C_q), 126.1 (CH), 125.8 (CH), 124.7 (CH), 122.9 (CH), 121.8 (CH), 121.7 (CH), 119.1 (CH), 115.6 (CH), 114.5 (C_q), 110.9 (CH), 80.4 (C_q), 74.1 (cage C_q), 60.9 (cage CH), 56.0 (CH), 53.6 (CH), 52.7 (CH), 48.8 (CH₃), 37.5 (CH₂), 30.9 (CH₃), 28.3 (CH₃), 28.0 (CH₂). **¹¹B NMR** (128 MHz, CDCl₃): δ = -2.31 (1B), -4.46 (1B), -9.09 (2B), -11.25 (6B). **IR** (ATR): 3400, 3050, 2595, 1648, 1516, 1469, 1437, 1366, 1221, 1171 cm⁻¹. **MS** (ESI) *m/z* (relative intensity): 799 (100) [M]⁺. **HR-MS** (ESI): *m/z* calcd. for C₃₈H₅₂B₁₀N₅O₇ [M+H]⁺: 800.4792, found: 800.4859.



Methyl (9S, 12S, 15S)-15-([2-((E)-2-*o*-carboranyl-vinyl)-1-(pyridin-2-yl)-1*H*-indol-3-yl) methyl]-9-((*tert*-butoxycarbonyl) amino]-12-(2-(methylthio)ethyl)-3,10,13-trioxo-1-phenyl-2-oxa-4,11,14-triazaheptadecan-16-oate

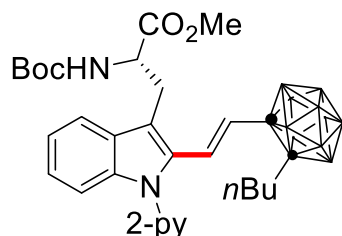
248s. The general procedure was followed using methyl *N*_α-*N*₆-[(benzyloxy)carbonyl]-*N*₂-(*tert*-butoxycarbonyl)-*L*-lysyl-*L*-methionyl-1-(pyridin-2-yl)-*L*-tryptophanate **246s** (78.7 mg, 0.1 mmol) and 1-ethynyl-*o*-carborane **247a** (16.8 mg, 0.1 mmol). Column chromatography on silica in (*n*-hexane/EtOAc = 3/2) afforded **248s** (51.6 mg, 54%) as white solid. **M.P.** = 91–93 °C. **¹H NMR** (400 MHz, CDCl₃): δ = 8.67 (dd, *J* = 4.7, 1.3 Hz, 1H), 7.89 (td, *J* = 7.7, 1.9 Hz, 1H), 7.47 (dd, *J* = 7.5, 1.3 Hz, 1H), 7.42 (d, *J* = 8.1 Hz, 1H), 7.39 – 7.22 (m, 7H), 7.23 – 7.07 (m, 3H), 6.98 (s, 1H), 6.83 (d, *J* = 16.0 Hz, 1H), 5.95 (d, *J* = 16.0 Hz, 1H), 5.34 (d, *J* = 7.1 Hz, 1H), 5.06 (s, 1H), 4.73 – 4.65 (m, 1H), 4.59 – 4.49 (m, 1H), 4.31 (s, 1H), 3.97 (s, 1H), 3.49 (s, 3H), 3.31 – 3.22 (m, 2H), 3.09 – 3.14 (m, 2H), 2.52 (t, *J* = 7.0 Hz, 3H), 2.08 – 1.98 (m, 6H), 1.96 – 1.88 (m, 2H), 1.70 (s, 2H), 1.42 (s, 9H), 1.27 (d, *J* = 12.3 Hz, 2H). **¹³C NMR** (126 MHz, CDCl₃): δ = 172.4 (C_q), 171.9 (C_q), 170.8 (C_q), 156.7 (C_q), 156.0 (C_q), 150.9 (C_q), 149.7 (CH), 138.5 (C_q), 137.5 (C_q), 136.5 (C_q), 131.8 (CH), 128.5 (C_q), 128.3 (CH), 128.1 (CH), 128.0 (CH), 126.0 (CH), 125.8 (CH), 124.5 (CH), 122.6 (CH), 121.5 (CH), 121.5 (CH), 119.0 (CH), 113.8 (C_q), 111.1 (CH), 80.3 (C_q), 74.1 (cage C_q), 66.6 (CH₂), 60.9 (cage CH), 54.4 (CH), 53.1 (CH), 52.6 (CH₃), 52.1 (CH), 40.0 (CH₂), 31.1 (CH₂), 30.5 (CH₂), 30.0 (CH₂), 29.3 (CH₂), 28.3 (CH₃), 28.3 (CH₂), 22.3 (CH₂), 15.0 (CH₃). **¹¹B NMR** (128 MHz, CDCl₃): δ = -2.25 (1B), -4.55 (1B), -8.93 (2B), -10.94 (6B). **IR** (ATR): 2956, 2594, 2362, 1982, 1700, 1650, 1520, 1231, 754 cm⁻¹. **MS** (ESI) *m/z* (relative intensity): 958 (90) [M]⁺. **HR-MS** (ESI): *m/z* calcd. for

$C_{45}H_{65}B_{10}N_5O_8S$ $[M+H]^+$: 959.5510, found: 959.5577.



Methyl (S, E)-2-acetamido-3-{2-[2-(2-methyl-o-carboranyl)-vinyl]-1-[pyridin-2-yl]-1H-indol-3-yl} propanoate

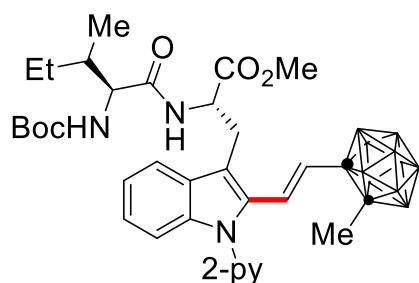
250a. The general procedure was followed using methyl N_α -acetyl-1-(pyridin-2-yl)-*L*-tryptophanate **246a** (33.7 mg, 0.1 mmol) and 1-ethynyl-2-methyl-o-carborane **249a** (18.3 mg, 0.1 mmol). Column chromatography on silica in (*n*-hexane/EtOAc = 4/1) afforded **250a** (47.3 mg, 91%) as pale-yellow solid. **M.P.** = 129-131 °C. **1H NMR** (400 MHz, $CDCl_3$): δ = 8.65 (dd, J = 6.8, 0.8 Hz, 1H), 7.90 (ddd, J = 8.0, 7.5, 2.0 Hz, 1H), 7.59 (dd, J = 1.5, 0.8 Hz, 1H), 7.41 – 7.33 (m, 2H), 7.28 (dt, J = 8.0, 1.0 Hz, 1H), 7.25 – 7.15 (m, 2H), 6.98 (d, J = 16.0 Hz, 1H), 6.06 (d, J = 7.9 Hz, 1H), 5.59 (d, J = 16.0 Hz, 1H), 4.89 (ddd, J = 8.0, 7.2, 5.9 Hz, 1H), 3.60 (s, 3H), 3.45 – 3.26 (m, 2H), 1.96 (s, 3H), 1.85 (s, 3H). **^{13}C NMR** (101 MHz, $CDCl_3$): δ = 172.2 (C_q), 169.6 (C_q), 151.4 (C_q), 149.8 (CH), 138.7 (CH), 138.4 (C_q), 131.8 (C_q), 129.1 (CH), 128.4 (C_q), 125.0 (CH), 123.2 (CH), 122.8 (CH), 121.9 (CH), 121.7 (CH), 119.4 (CH), 115.6 (C_q), 110.9 (CH), 78.1 (cage C_q), 75.7 (cage C_q), 52.9 (CH), 52.6 (CH_3), 28.1 (CH_2), 23.2 (CH_3), 23.2 (CH_3). **^{11}B NMR** (128 MHz, $CDCl_3$): δ = -3.78 (1B), -5.34 (1B), -10.11 (8B). **IR** (ATR): 2955, 2587, 1746, 1656, 1587, 1436, 1371, 1220, 743 cm^{-1} . **MS** (ESI) m/z (relative intensity): 521 (90) $[M]^+$. **HR-MS** (ESI): m/z calcd. for $C_{24}H_{34}B_{10}N_3O_3$ $[M+H]^+$: 522.3525, found: 522.3530.



Methyl (S,E)-3-{2-[2-(2-*n*-butyl-o-carboranyl)-vinyl]-1-[(pyridin-2-yl)-1H-indol-3-yl]-2-[(*tert*-butoxycarbonyl)] amino}propanoate

250b. The general procedure was followed using methyl N_α -(*tert*-

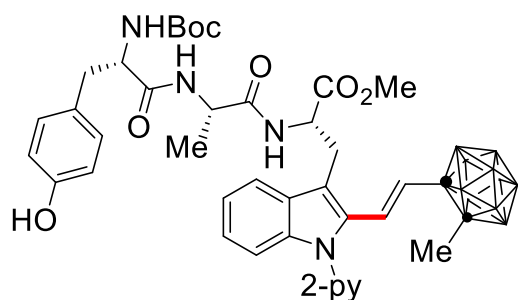
butoxycarbonyl)-1-(pyridin-2-yl)-*L*-tryptophanate **246b** (39.5 mg, 0.1 mmol) and 1-ethynyl-2-butyl-*o*-carborane **249c** (22.5 mg, 0.1 mmol). Column chromatography on silica in (*n*-hexane/EtOAc = 4/1) afforded **250c** (52.5 mg, 86%) as yellow solid. **M.P.** = 103-105 °C. **¹H NMR** (400 MHz, CDCl₃): δ = 8.64 (dd, *J* = 4.9, 1.2 Hz, 1H), 7.89 (td, *J* = 7.8, 2.0 Hz, 1H), 7.60 (d, *J* = 7.8 Hz, 1H), 7.41 – 7.32 (m, 2H), 7.28 (dt, *J* = 8.0, 1.0 Hz, 1H), 7.23 – 7.14 (m, 2H), 7.00 (d, *J* = 16.0 Hz, 1H), 5.61 (d, *J* = 16.0 Hz, 1H), 5.14 (d, *J* = 8.6 Hz, 1H), 4.66 – 4.53 (m, 1H), 3.61 (s, 3H), 3.40 – 3.24 (m, 2H), 2.06 – 1.96 (m, 2H), 1.46 – 1.30 (m, 10H), 1.30 – 1.09 (m, 3H), 0.87 (t, *J* = 7.3 Hz, 3H). **¹³C NMR** (126 MHz, CDCl₃): δ = 172.5 (C_q), 155.0 (C_q), 151.4 (C_q), 149.7 (CH), 138.6 (CH), 138.3 (C_q), 131.7 (C_q), 129.6 (CH), 128.4 (C_q), 124.9 (CH), 122.9 (CH), 122.7 (CH), 121.8 (CH), 121.6 (CH), 119.6 (CH), 115.8 (C_q), 110.8 (CH), 81.0 (C_q), 80.1 (cage C_q), 79.8 (cage C_q), 54.2 (CH), 52.4 (CH₃), 35.0 (CH₂), 31.7 (CH₂), 28.6 (CH₂), 28.2 (CH₃), 22.3 (CH₂), 13.7 (CH₃). **¹¹B NMR** (128 MHz, CDCl₃): δ = -4.37 (2B), -10.48 (8B). **IR** (ATR): 2958, 2566, 1713, 1587, 1468, 1366, 1170, 1031, 742 cm⁻¹. **MS** (ESI) *m/z* (relative intensity): 621 (90) [M]⁺. **HR-MS** (ESI): *m/z* calcd. for C₃₀H₄₆B₁₀N₃O₄ [M+H]⁺: 622.4413, found: 622.4448.



Methyl (S)-3-{2-[(E)-2(2-methyl-*o*-carboranyl-vinyl)-1-(pyridin-2-yl)-1*H*-indol-3-yl]-2-((2*S*, 3*S*)-2-[(*tert*-butoxycarbonyl) amino]-3-methylpentanamido)} propanoate

250c. The general procedure was followed using methyl *N*_α-[(*tert*-butoxycarbonyl)-*L*-isoleucyl]-1-(pyridin-2-yl)-*L*-tryptophanate **246f** (50.7 mg, 0.1 mmol) and 1-ethynyl-2-methyl-*o*-carborane **249b** (18.3 mg, 0.1 mmol). Column chromatography on silica in (*n*-hexane/EtOAc = 4/1) afforded **250c** (50.4 mg, 73%) as white solid. **M.P.** = 114-116 °C. **¹H NMR** (400 MHz, CDCl₃): δ = 8.63 (dd, *J* = 6.8, 0.9 Hz, 1H), 7.89 (ddd, *J* = 8.0, 7.5, 1.9 Hz, 1H), 7.67 – 7.60 (m, 1H), 7.41 – 7.32 (m, 2H), 7.29 (dt, *J* = 8.0, 0.9 Hz, 1H), 7.23 –

7.17 (m, 2H), 6.99 (d, $J = 16.0$ Hz, 1H), 6.59 (d, $J = 7.9$ Hz, 1H), 5.72 (d, $J = 16.0$ Hz, 1H), 4.99 – 4.78 (m, 2H), 3.95 (s, 1H), 3.57 (s, 3H), 3.40 – 3.23 (m, 2H), 1.89 (s, 3H), 1.85 (s, 2H), 1.42 (s, 9H), 1.33 – 1.16 (m, 1H), 0.87 – 0.78 (m, 6H). **^{13}C NMR** (126 MHz, CDCl_3): $\delta = 172.0$ (C_q), 171.2 (C_q), 155.6 (C_q), 151.2 (C_q), 149.7 (CH), 138.6 (CH), 138.1 (C_q), 131.6 (C_q), 129.4 (CH), 128.4 (C_q), 124.9 (CH), 123.3 (CH), 122.6 (CH), 121.7 (CH), 121.6 (CH), 119.4 (CH), 115.2 (C_q), 111.0 (CH), 80.0 (C_q), 78.2 (cage C_q), 75.8 (cage C_q), 59.2 (CH), 52.9 (CH), 52.5 (CH_3), 37.1 (CH), 28.4 (CH_2), 28.3 (CH_3), 24.4 (CH_2), 23.2 (CH_3), 15.4 (CH_3), 11.5 (CH_3). **^{11}B NMR** (128 MHz, CDCl_3): $\delta = -4.06$ (1B), -5.41 (1B), -10.31 (8B). **IR** (ATR): 2962, 2584, 1764, 1684, 1650, 1469, 1366, 1175, 742 cm^{-1} . **MS** (ESI) m/z (relative intensity): 692 (90) $[\text{M}]^+$. **HR-MS** (ESI): m/z calcd. for $\text{C}_{33}\text{H}_{51}\text{B}_{10}\text{N}_4\text{O}_5$ $[\text{M}+\text{H}]^+$: 693.4785, found: 693.4791.

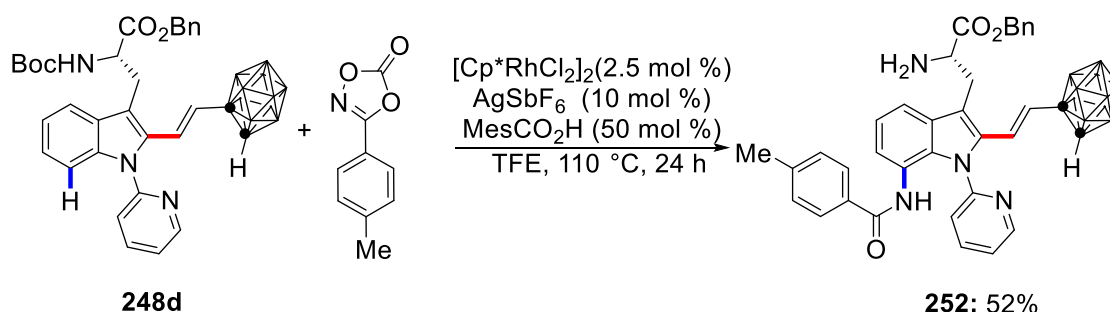


Methyl (6S, 9S, 12S)-12-(((E)-2(2-methyl-o-carboranyl-vinyl)-1-(pyridin-2-yl)-1H-indol-3-yl) methyl)-6-(4-hydroxybenzyl)-2,2,9-trimethyl-4,7,10-trioxo-3-oxa-5,8,11-triazatridecan-13-oate

250d. The general procedure was followed using methyl N_α -(*tert*-butoxycarbonyl)-*L*-tyrosyl-*L*-alanyl-1-(pyridin-2-yl)-*L*-tryptophanate **246r** (62.8 mg, 0.1 mmol) and 1-ethynyl-2-methyl-*o*-carborane **249b** (18.3 mg, 0.1 mmol). Column chromatography on silica in (*n*-hexane/EtOAc = 3/2) afforded **250d** (58.4 mg, 72%) as white solid. **M.P.** = 161-163 °C. **^1H NMR** (400 MHz, CDCl_3): $\delta = 8.64$ (dd, $J = 6.9, 0.8$ Hz, 1H), 7.94 (td, $J = 7.7, 2.0$ Hz, 1H), 7.63 – 7.56 (m, 1H), 7.50 (s, 1H), 7.43 – 7.29 (m, 3H), 7.23 – 7.16 (m, 2H), 6.99 (d, $J = 16.0$ Hz, 1H), 6.71 (d, $J = 8.2$ Hz, 2H), 6.44 – 6.35 (m, 2H), 6.20 (s, 2H), 5.68 (d, $J = 16.0$ Hz, 1H), 5.37 (s, 1H), 4.65 (q, $J = 7.2$ Hz, 1H), 4.36 – 4.25 (m, 1H), 4.15 (s, 2H), 3.66 (s, 3H), 3.40 – 3.25 (m, 2H), 2.80 (dd, $J = 13.7, 6.3$ Hz, 1H), 2.60 (dd, $J = 13.7, 7.9$ Hz, 2H), 2.15 (s, 3H), 1.40 (s, 9H), 1.18 (d, $J = 7.0$ Hz, 3H). **^{13}C NMR** (126 MHz, CDCl_3): $\delta = 171.7$ (C_q), 171.3 (C_q), 155.5

(C_q), 155.5 (C_q), 155.4 (C_q), 151.0 (C_q), 149.6 (CH), 139.2 (CH), 138.0 (C_q), 131.8 (C_q), 130.0 (CH), 129.3 (CH), 128.4 (C_q), 127.4 (C_q), 125.1 (CH), 123.7 (CH), 123.0 (CH), 122.1 (CH), 121.9 (CH), 119.5 (CH), 115.7 (C_q), 115.5 (CH), 110.7 (CH), 80.3 (C_q), 78.1 (cage C_q), 76.0 (cage C_q), 56.1 (CH), 53.7 (CH), 52.7 (CH₃), 48.6 (CH), 37.7 (CH₂), 28.3 (CH₃), 27.4 (CH₂), 23.2 (CH₃), 17.8 (CH₃). **¹¹B NMR** (128 MHz, CDCl₃): δ = -5.29 (2B), -10.10 (8B). **IR** (ATR): 2547, 2361, 2167, 1643, 1515, 1232, 1146, 726, 546 cm⁻¹. **MS** (ESI) *m/z* (relative intensity): 813 (100) [M]⁺. **HR-MS** (ESI): *m/z* calcd. for C₃₉H₅₄B₁₀N₅O₇ [M+H]⁺: 814.4948, found: 814.4952.

5.3.3.2 Late-Stage C–7 Amidation of **248d**

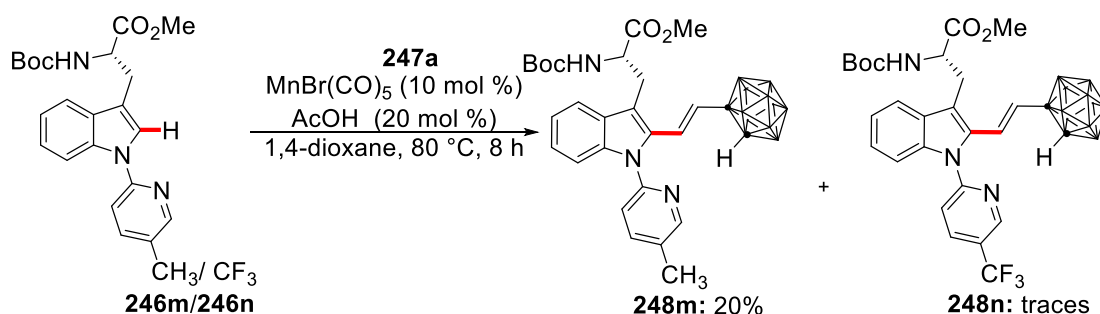


Benzyl (S,E)-2-amino-3-[2-(2-*o*-carboranyl-vinyl)-7-(4-methylbenzamido)]-1-(pyridin-2-yl)-1*H*-indol-3-yl]propanoate (252**)**

Alkenylated tryptophan **248d** (63.9 mg, 0.1 mmol), 3-(*p*-tolyl)-1,4,2-dioxazol-5-one (32.6 mg, 0.2 mmol), [Cp^{*}RhCl₂]₂ (1.5 mg, 2.5 mol %), AgSbF₆ (3.4 mg, 10 mol %), and MesCO₂H (8.3 mg, 50 mol %) in TFE (1.0 mL) was stirred at 100 °C for 24 h. After cooling to room temperature, the solvent was removed in vacuo. Column chromatography on silica gel (*n*-hexane/ EtOAc = 2/1) followed by gel permeation chromatography led to the isolation of product **252** (35.0 mg, 52%) as a yellow solid. **M.P.** 169–171 °C. **¹H NMR** (400 MHz, CDCl₃): δ = 8.66 (dd, *J* = 4.9, 2.8 Hz, 1H), 7.88 (ddd, *J* = 8.0, 7.5, 2.0 Hz, 1H), 7.48 – 7.42 (m, 2H), 7.37 (ddd, *J* = 7.5, 4.9, 1.0 Hz, 1H), 7.23 – 7.14 (m, 5H), 7.13 – 7.03 (m, 5H), 6.87 – 6.83 (m, 2H), 6.77 (d, *J* = 16.1 Hz, 1H), 6.66 (s, 1H), 6.10 (d, *J* = 16.1 Hz, 1H), 5.69 (d, *J* = 7.8 Hz, 1H), 4.98 (d, *J* = 12.1 Hz, 1H), 4.78 – 4.68 (m, 2H), 4.19 (s, 1H), 3.42 – 3.22 (m, 2H), 2.29 (s, 3H). **¹³C NMR** (126 MHz, CDCl₃): δ = 172.6 (C_q), 154.9 (C_q), 150.9 (C_q), 149.6 (CH), 138.5 (CH), 137.4 (C_q), 135.2 (C_q), 134.4 (C_q), 134.1 (C_q), 131.9 (C_q), 129.9

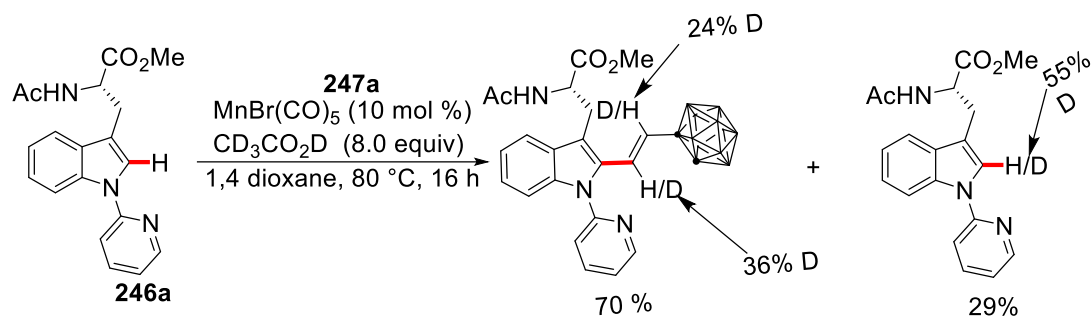
(CH), 128.6 (C_q), 128.5 (CH), 128.4 (CH), 128.3 (CH), 126.0 (CH), 125.7 (CH), 124.5 (CH), 122.5 (CH), 121.5 (CH), 121.4 (CH), 121.3 (CH), 119.0 (CH), 113.9 (C_q), 111.1 (CH), 74.2 (cage C_q), 67.8 (CH₂), 60.8 (cage CH), 54.0 (CH), 29.3 (CH₂), 20.8 (CH₃). **¹¹B NMR** (128 MHz, CDCl₃): δ = -2.65 (1B), -4.88 (1B), -9.16 (2B), -11.60 (2B), -12.80 (4B). **IR** (ATR): 2922, 2595, 1734, 1650, 1598, 1543, 1469, 1438, 1196 cm⁻¹. **MS** (ESI) *m/z* (relative intensity): 674 (90) [M]⁺. **HR-MS** (ESI): *m/z* calcd. for C₃₅H₄₁B₁₀N₄O₃ [M+H]⁺: 675.4104, found: 675.4111.

5.3.3.3 Intermolecular Competition Experiment

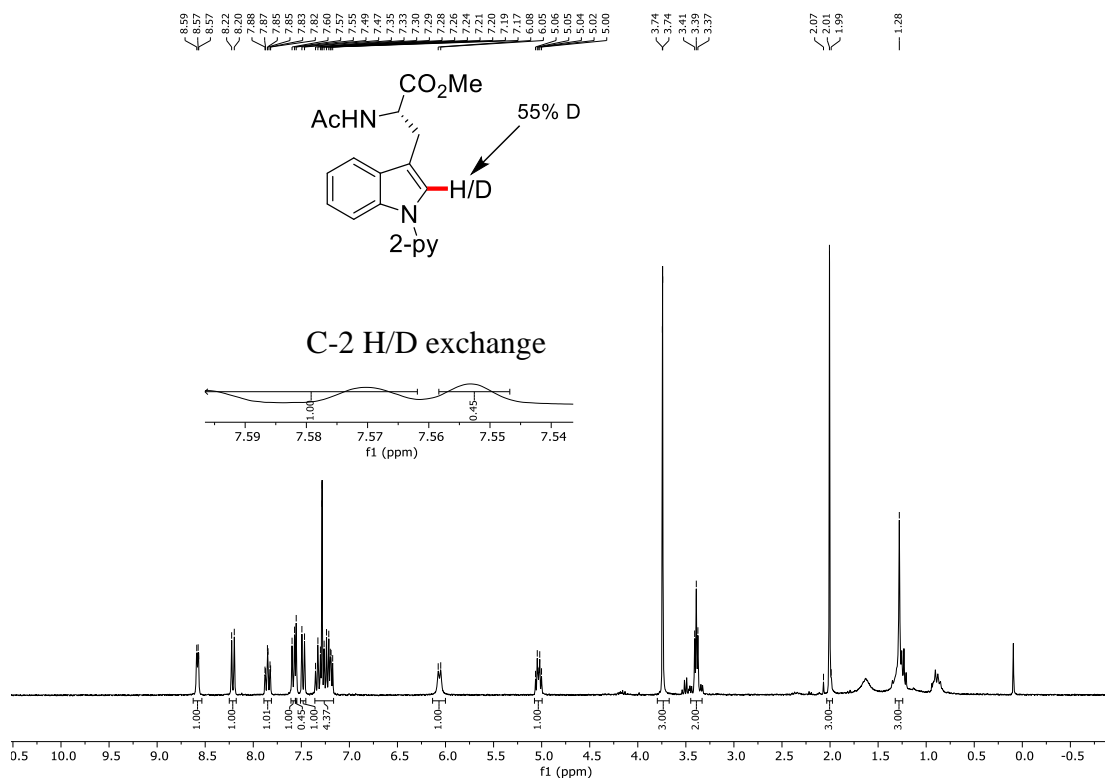


An oven dried Schlenk tube was charged with methyl N_α -(*tert*-butoxycarbonyl)-1-(5-methylpyridin-2-yl)-*L*-tryptophanate (**246m**) (0.2 mmol), methyl N_α -(*tert*-butoxycarbonyl)-1-(5-(trifluoromethyl)pyridin-2-yl)-*L*-tryptophanate (**247n**) (0.2 mmol), 1-ethynyl-*o*-carborane **247a** (0.1 mmol) and $\text{MnBr}(\text{CO})_5$ (10 mol %), AcOH (1.2 μL , 20 mol %) and 1,4-dioxane (1 mL). After stirring at 80 °C for 8 h and cooling to ambient temperature, the solvent was removed in vacuo. Purification by column chromatography on silica gel (*n*-hexane/EtOAc = 4/1) afforded **248m** (11.6 mg, 20%) as a white solid and traces of **248n**.

5.3.3.4 H/D Exchange Experiment



A solution of N^α-acetyl-1-(pyridin-2-yl)-L-tryptophanate (**246a**) (0.1 mmol), alkyne **247a** (0.1 mmol), MnBr(CO)₅ (10 mol %) and CD₃CO₂D (8.0 equiv.) in 1,4-dioxane was stirred at 80 °C for 16 h. After cooling to room temperature, the solvent was removed in vacuo. Column chromatography of the crude mixture (*n*-hexane/EtOAc = 3/2) afforded a mixture of the deuterium-labeled amino acid **246a** (9.8 mg, 29%) and **248a** (35.4 mg, 70 %).



5.3.3.5 Studies on Potential Racemization

DL-tryptophan **246d** was subjected to manganese(I)-catalyzed C–H alkenylation. HPLC **248d** revealed no racemization occurred during the reaction.

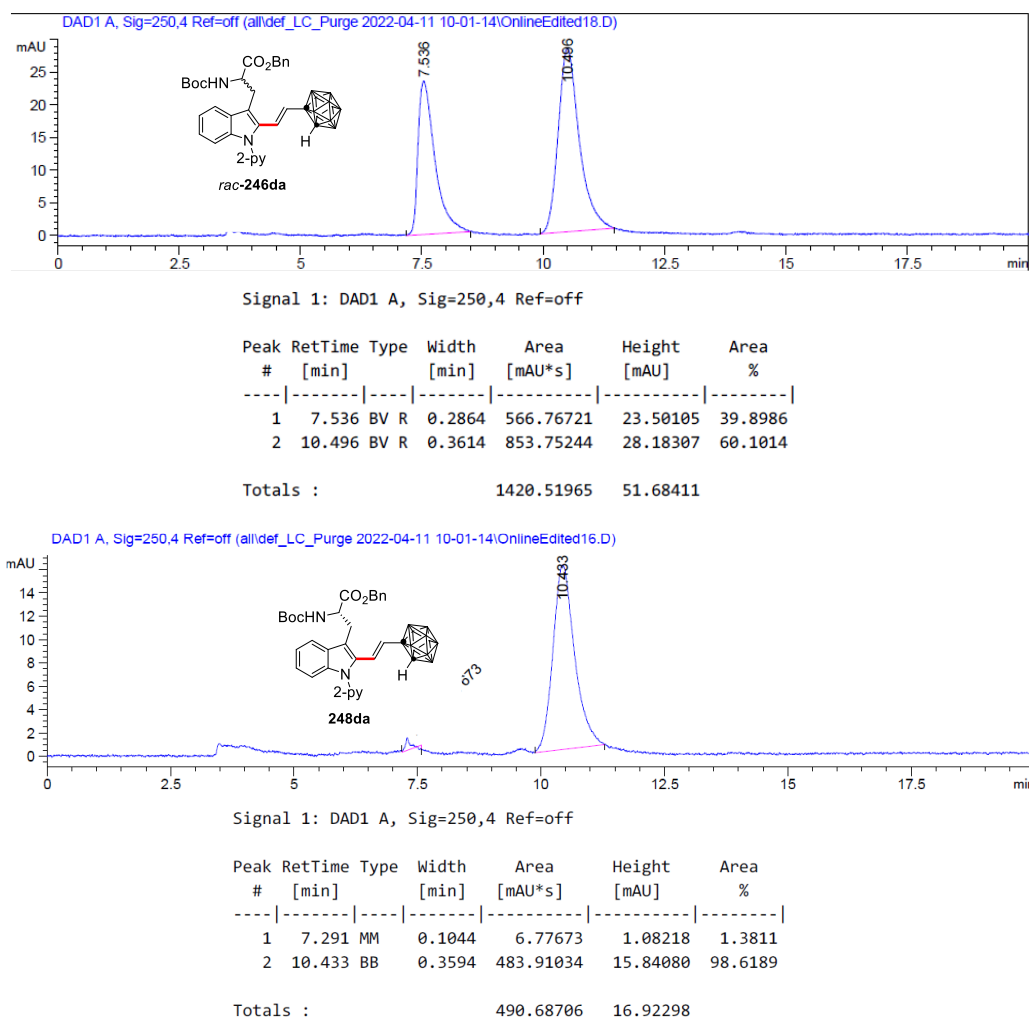


Figure 11. HPLC-Chromatogram of **248d**. These were recorded on an Agilent 1290 Infinity using the column CHIRALPAK® ID and *n*-hexane/*i*PrOH (90:10, 1 mL/min, detection at 250 nm).

6 References

- [1] a) J. Börgel, T. Ritter, *Chem* **2020**, *6*, 1877–1887; b) W. Wang, M. M. Lorion, J. Shah, A. R. Kapdi, L. Ackermann, *Angew. Chem. Int. Ed.* **2018**, *57*, 14700–14717; c) D. J. Schipper, K. Fagnou, *Chem. Mater.* **2011**, *23*, 1594–1600.
- [2] a) J. Xie, H. Jin, A. S. K. Hashmi, *Chem. Soc. Rev.* **2017**, *46*, 5193–5203; b) C. C. Johansson Seechurn, M. O. Kitching, T. J. Colacot, V. Snieckus, *Angew. Chem. Int. Ed.* **2012**, *51*, 5062–5085.
- [3] a) Q. Wang, Y. Su, L. Li, H. Huang, *Chem. Soc. Rev.* **2016**, *45*, 1257–1272; b) C. Shen, P. Zhang, Q. Sun, S. Bai, T. S. Hor, X. Liu, *Chem. Soc. Rev.* **2015**, *44*, 291–314.
- [4] S. A. Matlin, G. Mehta, H. Hopf, A. Krief, *Nat. Chem.* **2016**, *8*, 393–398.
- [5] a) N. Miyaoura, A. Suzuki, *Chem. Rev.* **1995**, *95*, 2457–2483; b) N. Miyaoura, K. Yamada, A. Suzuki, *Tetrahedron Lett.* **1979**, *20*, 3437–3440.
- [6] K. Tamao, Y. Kiso, K. Sumitani, M. Kumada, *J. Am. Chem. Soc.* **1972**, *94*, 9268–9269.
- [7] a) T. Hiyama, in *Metal-Catalyzed Cross-Coupling Reactions* (Eds.: A. de Meijere, F. Diederich), Wiley-VCH, Weinheim, **1998**; b) M. Fujita, T. Hiyama, *J. Org. Chem.* **1988**, *53*, 5415–5421; c) T. Hiyama, M. Obayashi, I. Mori, H. Nozaki, *J. Org. Chem.* **1983**, *48*, 912–914.
- [8] a) E.-I. Negishi, *Acc. Chem. Res.* **1982**, *15*, 340–348; b) E.-I. Negishi, A. O. King, N. Okukado, *J. Org. Chem.* **1977**, *42*, 1821–1823; c) S. Baba, E.-I. Negishi, *J. Am. Chem. Soc.* **1976**, *98*, 6729–6731.
- [9] a) J. K. Stille, *Angew. Chem. Int. Ed.* **1986**, *25*, 508–524; b) D. Milstein, J. K. Stille, *J. Am. Chem. Soc.* **1978**, *100*, 3636–3638; c) M. Kosugi, Y. Shimizu, T. Migita, *Chem. Lett.* **1977**, *6*, 1423–1424.
- [10] a) H. Lin, D. Sun, *Org. Prep. Proced. Int.* **2013**, *45*, 341–394; b) F. Monnier, M. Taillefer, *Angew. Chem. Int. Ed.* **2009**, *48*, 6954–6971.
- [11] a) J. F. Hartwig, *Nature* **2008**, *455*, 314–322; b) A. R. Muci, S. L. Buchwald, *Top. Curr. Chem.* **2002**, *219*, 131–209; c) J. F. Hartwig, *Angew. Chem. Int. Ed.* **1998**, *37*, 2046–2067.
- [12] J. X. Qiao, P. Y. S. Lam, *Synthesis* **2011**, 829–856.
- [13] L. Ackermann, *Modern Arylation Methods*, Wiley-VCH: Weinheim, **2009**.
- [14] a) R. C. Samanta, T. H. Meyer, I. Siewert, L. Ackermann, *Chem. Sci.* **2020**, *11*, 8657–8670; b) P. Gandeepan, L. H. Finger, T. H. Meyer, L. Ackermann, *Chem. Soc. Rev.* **2020**, *49*, 4254–4272; c) L. Ackermann, S.-L. You, M. Oestreich, S. Meng, D. MacFarlane, Y. Yin, *Trends Chem.* **2020**, *2*, 275–277; d) T. H. Meyer, L. H. Finger, P. Gandeepan, L. Ackermann, *Trends Chem.* **2019**, *1*, 63–76.
- [15] a) D. L. Davies, S. A. Macgregor, C. L. McMullin, *Chem. Rev.* **2017**, *117*, 8649–8709; b) L. Ackermann, *Chem. Rev.* **2011**, *111*, 1315–1345; c) D. Balcells, E. Clot, O. Eisenstein, *Chem. Rev.* **2010**, *110*, 749–823.
- [16] a) J. R. Webb, S. A. Burgess, T. R. Cundari, T. B. Gunnoe, *Dalton Trans.* **2013**, *42*, 16646–16665; b) T. G. P. Harper, P. J. Desrosiers, T. C. Flood, *Organometallics* **1990**, *9*, 2523–2528.
- [17] Z. Lin, *Coord. Chem. Rev.* **2007**, *251*, 2280–2291.
- [18] J. Kua, X. Xu, R. A. Periana, W. A. Goddard, *Organometallics* **2002**, *21*, 511–525.
- [19] a) T. R. Cundari, T. R. Klinckman, P. T. Wolczanski, *J. Am. Chem. Soc.* **2002**, *124*, 1481–1487; b) J. L. Bennett, P. T. Wolczanski, *J. Am. Chem. Soc.* **1997**, *119*, 10696–10719; c) C. C. Cummins, S. M. Baxter, P. T. Wolczanski, *J. Am. Chem. Soc.* **1988**, *110*, 8731–8733; d) P. J. Walsh, F. J. Hollander, R. G. Bergman, *J. Am. Chem. Soc.* **1988**, *110*, 8729–8731.
- [20] J. M. Duff, B. L. Shaw, *J. Chem. Soc., Dalton Trans.* **1972**, 2219–2225.
- [21] S. I. Gorelsky, D. Lapointe, K. Fagnou, *J. Am. Chem. Soc.* **2008**, *130*, 10848–10849.

6 References

- [22] a) Y. Boutadla, D. L. Davies, S. A. Macgregor, A. I. Poblador-Bahamonde, *Dalton Trans.* **2009**, 5887–5893; b) D. L. Davies, S. M. A. Donald, S. A. Macgregor, *J. Am. Chem. Soc.* **2005**, *127*, 13754–13755.
- [23] a) D. Zell, M. Bursch, V. Müller, S. Grimme, L. Ackermann, *Angew. Chem. Int. Ed.* **2017**, *56*, 10378–10382; b) W. Ma, R. Mei, G. Tenti, L. Ackermann, *Chem. Eur. J.* **2014**, *20*, 15248–15251.
- [24] H. Yi, G. Zhang, H. Wang, Z. Huang, J. Wang, A. K. Singh, A. Lei, *Chem. Rev.* **2017**, *117*, 9016–9085.
- [25] J. M. Brown, S. Murai, H. Alper, A. Furstner, P. Dixneuf, R. Gossage, S. Murai, V. Grushin, L. Hegedus, M. Hidai, *Activation of Unreactive Bonds and Organic Synthesis*, Springer-Verlag Berlin, Heidelberg, **1999**.
- [26] a) G. Cera, L. Ackermann, *Top. Curr. Chem.* **2016**, *374*, 57; b) L. Ackermann, J. Li, *Nat. Chem.* **2015**, *7*, 686–687; c) L. Ackermann, R. Vicente, *Top. Curr. Chem.* **2010**, *292*, 211–229; d) L. Ackermann, R. Vicente, A. R. Kapdi, *Angew. Chem. Int. Ed.* **2009**, *48*, 9792–9826; e) L. Ackermann, *Top. Organomet. Chem.* **2007**, 35–60.
- [27] a) L. Ackermann, K. Korvorapun, R. C. Samanta, T. Rogge, *Synthesis* **2021**, *53*, 2911–2946; b) P. Gandeepan, L. Ackermann, *Chem* **2018**, *4*, 199–222; c) C. Sambiagio, D. Schönbauer, R. Blicke, T. Dao-Huy, G. Pototschnig, P. Schaaf, T. Wiesinger, M. F. Zia, J. Wencel-Delord, T. Besset, B. U. W. Maes, M. Schnürch, *Chem. Soc. Rev.* **2018**, *47*, 6603–6743; d) J. Li, S. De Sarkar, L. Ackermann, *Top. Organomet. Chem.* **2016**, *55*, 217–257.
- [28] a) K. Shen, Y. Fu, J.-N. Li, L. Liu, Q.-X. Guo, *Tetrahedron* **2007**, *63*, 1568–1576; b) L. Ackermann, in *Directed Metallation* (Ed.: N. Chatani), Springer Berlin Heidelberg, Berlin, Heidelberg, **2007**, pp. 35–60.
- [29] a) K. Korvorapun, R. C. Samanta, T. Rogge, L. Ackermann, *Synthesis* **2021**, *53*, 2911–2946; b) J. A. Leitch, C. G. Frost, *Chem. Soc. Rev.* **2017**, *46*, 7145–7153.
- [30] a) M. Font, J. M. Quibell, G. J. P. Perry, I. Larrosa, *Chem. Commun.* **2017**, *53*, 5584–5597; b) N. Y. P. Kumar, A. Bechtoldt, K. Raghuvanshi, L. Ackermann, *Angew. Chem. Int. Ed.* **2016**, *55*, 6929–6932.
- [31] a) J. Wang, G. Dong, *Chem. Rev.* **2019**, *119*, 7478–7528; b) M. Catellani, F. Frignani, A. Ragoni, *Angew. Chem. Int. Ed.* **1997**, *36*, 119–122.
- [32] a) Y. Kuninobu, S. Sueki, N. Kaplaneris, L. Ackermann, in *Catalysis with Earth-abundant Elements*, The Royal Society of Chemistry, **2021**, pp. 139–230; b) J. R. Carney, B. R. Dillon, S. P. Thomas, *Eur. J. Org. Chem.* **2016**, 3912–3929.
- [33] a) T. Aneja, M. Neetha, C. M. A. Afsina, G. Anilkumar, *Catal. Sci. Technol.* **2021**, *11*, 444–458; b) R. Cano, K. Mackey, G. P. McGlacken, *Catal. Sci. Technol.* **2018**, *8*, 1251–1266; c) W. Liu, L. Ackermann, *ACS Catal.* **2016**, *6*, 3743–3752.
- [34] M. I. Bruce, M. Z. Iqbal, F. G. A. Stone, *J. Chem. Soc. A* **1970**, 3204–3209.
- [35] a) W. Tully, L. Main, B. K. Nicholson, *J. Organomet. Chem.* **1995**, *503*, 75–92; b) G. J. Depree, L. Main, B. K. Nicholson, *J. Organomet. Chem.* **1998**, *551*, 281–291.
- [36] a) R. C. Cambie, M. R. Metzler, P. S. Rutledge, P. D. Woodgate, *J. Organomet. Chem.* **1990**, *381*, C26–C30; b) R. C. Cambie, M. R. Metzler, P. S. Rutledge, P. D. Woodgate, *J. Organomet. Chem.* **1990**, *398*, C22–C24; c) R. C. Cambie, M. R. Metzler, P. S. Rutledge, P. D. Woodgate, *J. Organomet. Chem.* **1992**, *429*, 41–57.
- [37] L. S. Liebeskind, J. R. Gasdaska, J. S. McCallum, S. J. Tremont, *J. Org. Chem.* **1989**, *54*, 669–677.
- [38] Y. Kuninobu, Y. Nishina, T. Takeuchi, K. Takai, *Angew. Chem. Int. Ed.* **2007**, *46*, 6518–6520.
- [39] B. Zhou, Y. Hu, C. Wang, *Angew. Chem. Int. Ed.* **2015**, *54*, 13659–13663.
- [40] Y. F. Liang, L. Massignan, L. Ackermann, *ChemCatChem* **2018**, *10*, 2768–2772.
- [41] C. Zhu, T. Pinkert, S. Greßies, F. Glorius, *ACS Catal.* **2018**, *8*, 10036–10042.

6 References

- [42] W. Liu, J. Bang, Y. Zhang, L. Ackermann, *Angew. Chem. Int. Ed.* **2015**, *127*, 14343-14346.
- [43] B. Zhou, Y. Hu, T. Liu, C. Wang, *Nat. Commun.* **2017**, *8*, 1-9.
- [44] B. Zhou, H. Chen, C. Wang, *J. Am. Chem. Soc.* **2013**, *135*, 1264-1267.
- [45] H. Wang, F. Pesciaoli, J. C. Oliveira, S. Warratz, L. Ackermann, *Angew. Chem. Int. Ed.* **2017**, *129*, 15259-15263.
- [46] L. Shi, X. Zhong, H. She, Z. Lei, F. Li, *Chem. Commun.* **2015**, *51*, 7136-7139.
- [47] B. Zhou, P. Ma, H. Chen, C. Wang, *Chem. Commun.* **2014**, *50*, 14558-14561.
- [48] S.-Y. Chen, Q. Li, H. Wang, *J. Org. Chem.* **2017**, *82*, 11173-11181.
- [49] S.-L. Liu, Y. Li, J.-R. Guo, G.-C. Yang, X.-H. Li, J.-F. Gong, M.-P. Song, *Org. Lett.* **2017**, *19*, 4042-4045.
- [50] Q. Lu, S. Mondal, S. Cembellín, F. Glorius, *Angew. Chem. Int. Ed.* **2018**, *57*, 10732-10736.
- [51] a) L. F. Tietze, *Chem. Rev.* **1996**, *96*, 115-136; b) L. F. Tietze, N. Rackelmann, *Pure Appl. Chem.* **2004**, *76*, 1967-1983; c) L. F. Tietze, T. Kinzel, C. C. Brazel, *Acc. Chem. Res.* **2009**, *42*, 367-378; d) C. G. Shen Jinhai, Cui Xiuling, *Prog. Chem.* **2012**, *24*, 1324-1336; e) H. Pellissier, *Org. Prep. Proced. Int.* **2019**, *51*, 311-344; f) H. A. Döndaş, M. d. G. Retamosa, J. M. Sansano, *Organometallics* **2019**, *38*, 1828-1867.
- [52] a) H.-M. Huang, M. H. Garduño-Castro, C. Morrill, D. J. Procter, *Chem. Soc. Rev.* **2019**, *48*, 4626-4638; b) H. Pellissier, *Chem. Rev.* **2013**, *113*, 442-524; c) K. Nicolaou, J. S. Chen, *Chem. Soc. Rev.* **2009**, *38*, 2993-3009; d) K. Nicolaou, D. J. Edmonds, P. G. Bulger, *Angew. Chem. Int. Ed.* **2006**, *45*, 7134-7186.
- [53] Y. F. Liang, V. Müller, W. Liu, A. Münch, D. Stalke, L. Ackermann, *Angew. Chem. Int. Ed.* **2017**, *129*, 9543-9547.
- [54] S. Y. Chen, Q. Li, X. G. Liu, J. Q. Wu, S. S. Zhang, H. Wang, *ChemSusChem* **2017**, *10*, 2360-2364.
- [55] B. Liu, Y. Yuan, P. Hu, G. Zheng, D. Bai, J. Chang, X. Li, *Chem. Commun.* **2019**, *55*, 10764-10767.
- [56] C. Wang, A. Wang, M. Rueping, *Angew. Chem. Int. Ed.* **2017**, *129*, 10067-10070.
- [57] S. Y. Chen, X. L. Han, J. Q. Wu, Q. Li, Y. Chen, H. Wang, *Angew. Chem. Int. Ed.* **2017**, *56*, 9939-9943.
- [58] X. Zhou, Z. Li, Z. Zhang, P. Lu, Y. Wang, *Org. Lett.* **2018**, *20*, 1426-1429.
- [59] Z. Xu, Y. Wang, Y. Zheng, Z. Huang, L. Ackermann, Z. Ruan, *Org. Chem. Front.* **2020**, *7*, 3709-3714.
- [60] C. Zhu, R. Kuniyil, L. Ackermann, *Angew. Chem. Int. Ed.* **2019**, *58*, 5338-5342.
- [61] G. Zheng, J. Sun, Y. Xu, S. Zhai, X. Li, *Angew. Chem. Int. Ed.* **2019**, *58*, 5090-5094.
- [62] a) L. Ackermann, S. Fenner, *Chem. Commun.* **2011**, *47*, 430-432; b) S. Dutta, T. Bhattacharya, D. B. Werz, D. Maiti, *Chem* **2021**, *7*, 555-605.
- [63] W. Liu, S. C. Richter, Y. Zhang, L. Ackermann, *Angew. Chem. Int. Ed.* **2016**, *55*, 7747-7750.
- [64] H. Wang, M. M. Lorion, L. Ackermann, *Angew. Chem. Int. Ed.* **2017**, *56*, 6339-6342.
- [65] J. Ni, H. Zhao, A. Zhang, *Org. Lett.* **2017**, *19*, 3159-3162.
- [66] S. Ali, J. Huo, C. Wang, *Org. Lett.* **2019**, *21*, 6961-6965.
- [67] C. Zhu, J. L. Schwarz, S. Cembellin, S. Greßies, F. Glorius, *Angew. Chem. Int. Ed.* **2018**, *57*, 437-441.
- [68] W. Liu, S. C. Richter, R. Mei, M. Feldt, L. Ackermann, *Chem. Eur. J.* **2016**, *22*, 17958-17961.
- [69] X. Yu, J. Tang, X. Jin, Y. Yamamoto, M. Bao, *Asian J. Org. Chem.* **2018**, *7*, 550-553.
- [70] a) Q. Xu, H. Deng, X. Li, Z.-S. Quan, *Front. Chem.* **2021**, *9*, 650569; b) M. Miyajima, *Int. Immunol.* **2020**, *32*, 435-446.
- [71] a) D. G. Rivera, G. M. Ojeda-Carralero, L. Reguera, E. V. Van Der Eycken, *Chem. Soc.*

6 References

- Rev.* **2020**, *49*, 2039-2059; b) W. Wang, M. M. Lorion, J. Shah, A. R. Kapdi, L. Ackermann, *Angew. Chem. Int. Ed.* **2018**, *57*, 14700-14717; c) S. Sengupta, G. Mehta, *Tetrahedron Lett.* **2017**, *58*, 1357-1372.
- [72] a) S. H. Reisberg, Y. Gao, A. S. Walker, E. J. N. Helfrich, J. Clardy, P. S. Baran, *Science* **2020**, *367*, 458-463; b) W. Wang, M. M. Lorion, O. Martinazzoli, L. Ackermann, *Angew. Chem. Int. Ed.* **2018**, *57*, 10554-10558; c) Z. Bai, C. Cai, W. Sheng, Y. Ren, H. Wang, *Angew. Chem. Int. Ed.* **2020**, *59*, 14686-14692; d) H. Dong, C. Limberakis, S. Liras, D. Price, K. James, *Chem. Commun.* **2012**, *48*, 11644.
- [73] a) A. Schischko, H. Ren, N. Kaplaneris, L. Ackermann, *Angew. Chem. Int. Ed.* **2017**, *56*, 1576-1580; b) S. Preciado, L. Mendive-Tapia, F. Albericio, R. Lavilla, *J. Org. Chem.* **2013**, *78*, 8129-8135; c) L. Ackermann, A. V. Lygin, *Org. Lett.* **2011**, *13*, 3332-3335.
- [74] W. Wang, J. Wu, R. Kuniyil, A. Kopp, R. N. Lima, L. Ackermann, *Chem* **2020**, *6*, 3428-3439.
- [75] L. Song, C. Liu, G. Tian, L. Van Meervelt, J. Van der Eycken, E. V. Van der Eycken, *Mol. Catal.* **2022**, *522*, 112240.
- [76] X. Lu, S.-J. He, W.-M. Cheng, J. Shi, *Chin. Chem. Lett.* **2018**, *29*, 1001-1008.
- [77] T. H. Meyer, W. Liu, M. Feldt, A. Wuttke, R. A. Mata, L. Ackermann, *Chem. Eur. J.* **2017**, *23*, 5443-5447.
- [78] N. Kaplaneris, T. Rogge, R. Yin, H. Wang, G. Sirvinskaite, L. Ackermann, *Angew. Chem. Int. Ed.* **2019**, *58*, 3476-3480.
- [79] W. Wang, P. Subramanian, O. Martinazzoli, J. Wu, L. Ackermann, *Chem. Eur. J.* **2019**, *25*, 10585-10589.
- [80] Z. Ruan, N. Sauermann, E. Manoni, L. Ackermann, *Angew. Chem. Int. Ed.* **2017**, *129*, 3220-3224.
- [81] N. Kaplaneris, F. Kaltenhäuser, G. Sirvinskaite, S. Fan, T. D. Oliveira, L.-C. Conradi, L. Ackermann, *Sci. Adv.* **2021**, *7*, eabe6202.
- [82] N. Kaplaneris, J. Son, L. Mendive-Tapia, A. Kopp, N. D. Barth, I. Maksso, M. Vendrell, L. Ackermann, *Nat. Commun.* **2021**, *12*, 3389.
- [83] A. Volta, *Philos. Trans. R. Soc. London* **1800**, *90*, 403-431.
- [84] M. Faraday, *Philos. Trans. R. Soc. London* **1825**, 440-466.
- [85] a) H. Kolbe, *Liebigs Ann. Chem.* **1849**, *69*, 257-294; b) H. Kolbe, *Liebigs Ann. Chem.* **1848**, *64*, 339-341.
- [86] T. H. Meyer, L. H. Finger, P. Gandeepan, L. Ackermann, *Trends Chem.* **2019**, *1*, 63-76.
- [87] a) N. Sbei, A. V. Listratova, A. A. Titov, L. G. Voskressensky, *Synthesis* **2019**, *51*, 2455-2473; b) S. D. Minter, P. Baran, *Acc. Chem. Res.* **2020**, *53*, 545-546.
- [88] a) L. Ackermann, *Acc. Chem. Res.* **2020**, *53*, 84-104; b) Y. Qiu, J. Struwe, L. Ackermann, *Synlett* **2019**, *30*, 1164-1173; c) Q.-L. Yang, P. Fang, T.-S. Mei, *Chin. J. Chem.* **2018**, *36*, 338-352; d) S. Tang, Y. Liu, A. Lei, *Chem* **2018**, *4*, 27-45; e) C. Ma, P. Fang, T.-S. Mei, *ACS Catal.* **2018**, *8*, 7179-7189; f) N. Sauermann, T. H. Meyer, Y. Qiu, L. Ackermann, *ACS Catal.* **2018**, *8*, 7086-7103; g) N. Sauermann, T. H. Meyer, L. Ackermann, *Chem. Eur. J.* **2018**, *24*, 16209-16217.
- [89] a) R. Shang, L. Ilies, E. Nakamura, *Chem. Rev.* **2017**, *117*, 9086-9139; b) G. Cera, L. Ackermann, *Top. Curr. Chem.* **2016**, *374*, 191-224.
- [90] C. Zhu, M. Stangier, J. C. A. Oliveira, L. Massignan, L. Ackermann, *Chem. Eur. J.* **2019**, *25*, 16382-16389.
- [91] N. Sauermann, T. H. Meyer, C. Tian, L. Ackermann, *J. Am. Chem. Soc.* **2017**, *139*, 18452-18455.
- [92] T. H. Meyer, J. C. A. Oliveira, D. Ghorai, L. Ackermann, *Angew. Chem. Int. Ed.* **2020**, *59*, 10955-10960.
- [93] a) N. Sauermann, R. Mei, L. Ackermann, *Angew. Chem. Int. Ed.* **2018**, *57*, 5090-5094; b) X. Gao, P. Wang, L. Zeng, S. Tang, A. Lei, *J. Am. Chem. Soc.* **2018**, *140*, 4195-4199.

6 References

- [94] C. Tian, U. Dhawa, J. Struwe, L. Ackermann, *Chin. J. Chem.* **2019**, *37*, 552–556.
- [95] a) R. Mei, X. Fang, L. He, J. Sun, L. Zou, W. Ma, L. Ackermann, *Chem. Commun.* **2020**, *56*, 1393–1396; b) T. H. Meyer, J. C. A. Oliveira, S. C. Sau, N. W. J. Ang, L. Ackermann, *ACS Catal.* **2018**, *8*, 9140–9147.
- [96] S. Tang, D. Wang, Y. Liu, L. Zeng, A. Lei, *Nat. Commun.* **2018**, *9*, 798.
- [97] U. Dhawa, C. Tian, W. Li, L. Ackermann, *ACS Catal.* **2020**, *10*, 6457–6462.
- [98] P. Gandeepan, T. Müller, D. Zell, G. Cera, S. Warratz, L. Ackermann, *Chem. Rev.* **2019**, *119*, 2192–2452.
- [99] S.-K. Zhang, R. C. Samanta, N. Sauermann, L. Ackermann, *Chem. Eur. J.* **2018**, *24*, 19166–19170.
- [100] S.-K. Zhang, J. Struwe, L. Hu, L. Ackermann, *Angew. Chem. Int. Ed.* **2020**, *59*, 3178–3183.
- [101] S.-K. Zhang, A. Del Vecchio, R. Kuniyil, A. M. Messinis, Z. Lin, L. Ackermann, *Chem* **2021**, *7*, 1379–1392.
- [102] a) C. Glaser, *Justus Liebigs Ann. Chem.* **1870**, *154*, 137–171; bC. Glaser, *Ber. Dtsch. Chem. Ges.* **1869**, *2*, 422–424.
- [103] a) I. Goldberg, *Ber. Dtsch. Chem. Ges.* **1906**, *39*, 1691–1692; bF. Ullmann, *B. Dtsch. Chem. Ges.* **1903**, *36*, 2382–2384.
- [104] Q.-L. Yang, X.-Y. Wang, J.-Y. Lu, L.-P. Zhang, P. Fang, T.-S. Mei, *J. Am. Chem. Soc.* **2018**, *140*, 11487–11494.
- [105] S. Kathiravan, S. Suriyanarayanan, I. A. Nicholls, *Org. Lett.* **2019**, *21*, 1968–1972.
- [106] C. Tian, U. Dhawa, A. Scheremetjew, L. Ackermann, *ACS Catal.* **2019**, *9*, 7690–7696.
- [107] C. Amatore, C. Cammoun, A. Jutand, *Adv. Synth. Catal.* **2007**, *349*, 292–296.
- [108] a) Y. Fujiwara, I. Moritani, S. Danno, R. Asano, S. Teranishi, *J. Am. Chem. Soc.* **1969**, *91*, 7166–7169; b) Y. Fujiwara, I. Moritani, M. Matsuda, S. Teranishi, *Tetrahedron Lett.* **1968**, *9*, 633–636; c) I. Moritanl, Y. Fujiwara, *Tetrahedron Lett.* **1967**, *8*, 1119–1122.
- [109] U. Dhawa, C. Tian, T. Wdowik, J. C. A. Oliveira, J. Hao, L. Ackermann, *Angew. Chem. Int. Ed.* **2020**, *59*, 13451–13457.
- [110] K.-J. Jiao, Y.-K. Xing, Q.-L. Yang, H. Qiu, T.-S. Mei, *Acc. Chem. Res.* **2020**, *53*, 300–310.
- [111] C. Ma, C.-Q. Zhao, Y.-Q. Li, L.-P. Zhang, X.-T. Xu, K. Zhang, T.-S. Mei, *Chem. Commun.* **2017**, *53*, 12189–12192.
- [112] a) X.-Y. W. Q.-L. Yang, X.-J. Weng, X. Yang, X.-T. Xu, X., P. F. Tong, X.-Y. Wu, T.-S. Mei, , *Acta Chim. Sinica* **2019**, *77*, 866–873; b) Q.-L. Yang, X.-Y. Wang, T.-L. Wang, X. Yang, D. Liu, X. Tong, X.-Y. Wu, T.-S. Mei, *Org. Lett.* **2019**, *21*, 2645–2649.
- [113] Y.-Q. Li, Q.-L. Yang, P. Fang, T.-S. Mei, D. Zhang, *Org. Lett.* **2017**, *19*, 2905–2908.
- [114] Q.-L. Yang, C.-Z. Li, L.-W. Zhang, Y.-Y. Li, X. Tong, X.-Y. Wu, T.-S. Mei, *Organometallics* **2019**, *38*, 1208–1212.
- [115] A. Shrestha, M. Lee, A. L. Dunn, M. S. Sanford, *Org. Lett.* **2018**, *20*, 204–207.
- [116] T. V. Grayaznova, Y. B. Dudkina, D. R. Islamov, O. N. Kataeva, O. G. Sinyashin, D. A. Vicic, Y. H. Budnikova, *J. Organomet. Chem.* **2015**, *785*, 68–71.
- [117] Z. Duan, L. Zhang, W. Zhang, L. Lu, L. Zeng, R. Shi, A. Lei, *ACS Catal.* **2020**, *10*, 3828–3831.
- [118] L. Ackermann, *Acc. Chem. Res.* **2014**, *47*, 281–295.
- [119] a) F. Xu, Y.-J. Li, C. Huang, H.-C. Xu, *ACS Catal.* **2018**, *8*, 3820–3824; b) Y. Qiu, C. Tian, L. Massignan, T. Rogge, L. Ackermann, *Angew. Chem. Int. Ed.* **2018**, *57*, 5818–5822.
- [120] L. Yang, R. Steinbock, A. Scheremetjew, R. Kuniyil, L. H. Finger, A. M. Messinis, L. Ackermann, *Angew. Chem. Int. Ed* **2020**, *59*, 11130–11135.
- [121] a) X. Tan, X. Hou, T. Rogge, L. Ackermann, *Angew. Chem. Int. Ed.* **2021**, *60*, 4619–4624; b) L. Yang, R. Steinbock, A. Scheremetjew, R. Kuniyil, L. H. Finger, A. M. Messinis, L. Ackermann, *Angew. Chem. Int. Ed.* **2020**, *59*, 11130–11135; c) M.-J. Luo, M. Hu, R.-J. Song, D.-L. He, J.-H. Li, *Chem. Commun.* **2019**, *55*, 1124–1127; d) M.-J.

6 References

- Luo, T.-T. Zhang, F.-J. Cai, J.-H. Li, D.-L. He, *Chem. Commun.* **2019**, 55, 7251–7254; e) Z.-Q. Wang, C. Hou, Y.-F. Zhong, Y.-X. Lu, Z.-Y. Mo, Y.-M. Pan, H.-T. Tang, *Org. Lett.* **2019**, 21, 9841–9845; f) R. Mei, J. Koeller, L. Ackermann, *Chem. Commun.* **2018**, 54, 12879–12882.
- [122] L. Massignan, X. Tan, T. H. Meyer, R. Kuniyil, A. M. Messinis, L. Ackermann, *Angew. Chem. Int. Ed.* **2020**, 59, 3184–3189.
- [123] Y. Qiu, W.-J. Kong, J. Struwe, N. Sauermann, T. Rogge, A. Scheremetjew, L. Ackermann, *Angew. Chem. Int. Ed.* **2018**, 57, 5828–5832.
- [124] Y. Zhang, J. Struwe, L. Ackermann, *Angew. Chem. Int. Ed.* **2020**, 59, 15076–15080.
- [125] W.-J. Kong, L. H. Finger, J. C. A. Oliveira, L. Ackermann, *Angew. Chem. Int. Ed.* **2019**, 58, 6342–6346.
- [126] W.-J. Kong, Z. Shen, L. H. Finger, L. Ackermann, *Angew. Chem. Int. Ed.* **2020**, 59, 5551–5556.
- [127] W.-J. Kong, L. H. Finger, A. M. Messinis, R. Kuniyil, J. C. A. Oliveira, L. Ackermann, *J. Am. Chem. Soc.* **2019**, 141, 17198–17206.
- [128] Z.-J. Wu, F. Su, W. Lin, J. Song, T.-B. Wen, H.-J. Zhang, H.-C. Xu, *Angew. Chem. Int. Ed.* **2019**, 58, 16770–16774.
- [129] a) Y. Wang, J. C. A. Oliveira, Z. Lin, L. Ackermann, *Angew. Chem. Int. Ed.* **2021**, 60, 6419–6424; b) Y.-K. Xing, X.-R. Chen, Q.-L. Yang, S.-Q. Zhang, H.-M. Guo, X. Hong, T.-S. Mei, *Nat. Commun.* **2021**, 12, 930.
- [130] Z. Shen, I. Maksso, R. Kuniyil, T. Rogge, L. Ackermann, *Chem. Commun.* **2021**, 57, 3668–3671.
- [131] X. Tan, L. Massignan, X. Hou, J. Frey, J. C. A. Oliveira, M. N. Hussain, L. Ackermann, *Angew. Chem. Int. Ed.* **2021**, 60, 13264–13270.
- [132] M. Stangier, A. M. Messinis, J. C. A. Oliveira, H. Yu, L. Ackermann, *Nat. Commun.* **2021**, 12.
- [133] Y. Qiu, M. Stangier, T. H. Meyer, J. C. A. Oliveira, L. Ackermann, *Angew. Chem. Int. Ed.* **2018**, 57, 14179–14183.
- [134] Q.-L. Yang, H.-W. Jia, Y. Liu, Y.-K. Xing, R.-C. Ma, M.-M. Wang, G.-R. Qu, T.-S. Mei, H.-M. Guo, *Org. Lett.* **2021**, 23, 1209–1215.
- [135] X. Ye, C. Wang, S. Zhang, J. Wei, C. Shan, L. Wojtas, Y. Xie, X. Shi, *ACS Catal.* **2020**, 10, 11693–11699.
- [136] a) R. N. Grimes, *Dalton Trans.* **2015**, 44, 5939–5956; b) C. Douvris, J. Michl, *Chem. Rev.* **2013**, 113, 179–233.
- [137] J. Poater, M. Solà, C. Viñas, F. Teixidor, *Angew. Chem. Int. Ed.* **2014**, 53, 12191–12195.
- [138] a) A. Saha, E. Oleshkevich, C. Vinas, F. Teixidor, *Adv. Mater.* **2017**, 29, 1704238; b) E. A. Qian, A. I. Wixtrom, J. C. Axtell, A. Saebi, D. Jung, P. Rehak, Y. Han, E. H. Mouilly, D. Mosallaei, S. Chow, M. S. Messina, J. Y. Wang, A. T. Royappa, A. L. Rheingold, H. D. Maynard, P. Kral, A. M. Spokoiny, *Nat. Chem.* **2017**, 9, 333–340; c) C. J. Villagómez, T. Sasaki, J. M. Tour, L. Grill, *J. Am. Chem. Soc.* **2010**, 132, 16848–16854; d) M. Koshino, T. Tanaka, N. Solin, K. Suenaga, H. Isobe, E. Nakamura, *Science* **2007**, 316, 853–853.
- [139] a) C. Zhao, Y. Guo, Y. Zhang, N. Yan, S. You, W. Li, *J. Mater. Chem. A* **2019**, 7, 10174–10199; b) Y. Patil, R. Misra, *Chem. Asian J.* **2018**, 13, 220–229; c) W. Li, K. H. Hendriks, M. M. Wienk, R. A. J. Janssen, *Acc. Chem. Res.* **2016**, 49, 78–85; d) M. J. Robb, S.-Y. Ku, F. G. Brunetti, C. J. Hawker, *J. Polym. Sci., Part A: Polym. Chem.* **2013**, 51, 1263–1271; e) Y. Wu, W. Zhu, *Chem. Soc. Rev.* **2013**, 42, 2039–2058; f) Y. Li, P. Sonar, L. Murphy, W. Hong, *Energy Environ. Sci.* **2013**, 6, 1684–1710; g) B. Tieke, A. R. Rabindranath, K. Zhang, Y. Zhu, *Beilstein J. Org. Chem.* **2010**, 6, 830–845.
- [140] a) X. Zhang, H. Yan, *Coord. Chem. Rev.* **2019**, 378, 466–482; b) W.-B. Yu, P.-F. Cui, W.-X. Gao, G.-X. Jin, *Coord. Chem. Rev.* **2017**, 350, 300–319; c) Z.-J. Yao, G.-X. Jin, *Coord. Chem. Rev.* **2013**, 257, 2522–2535.

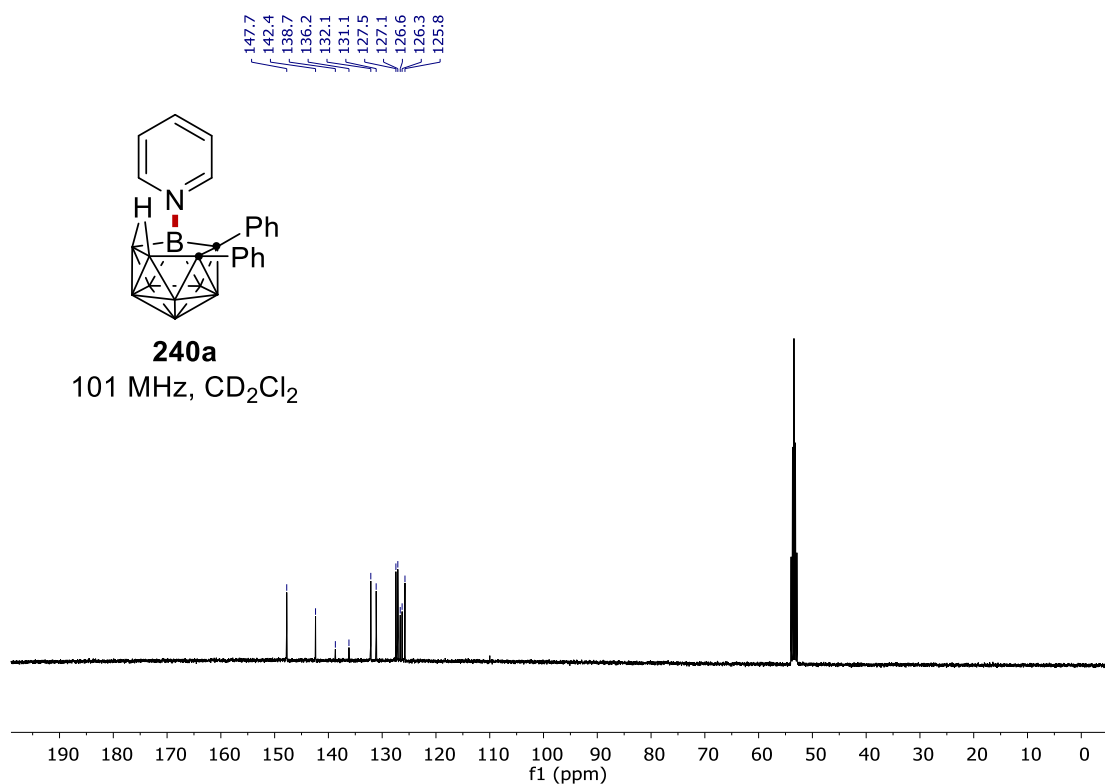
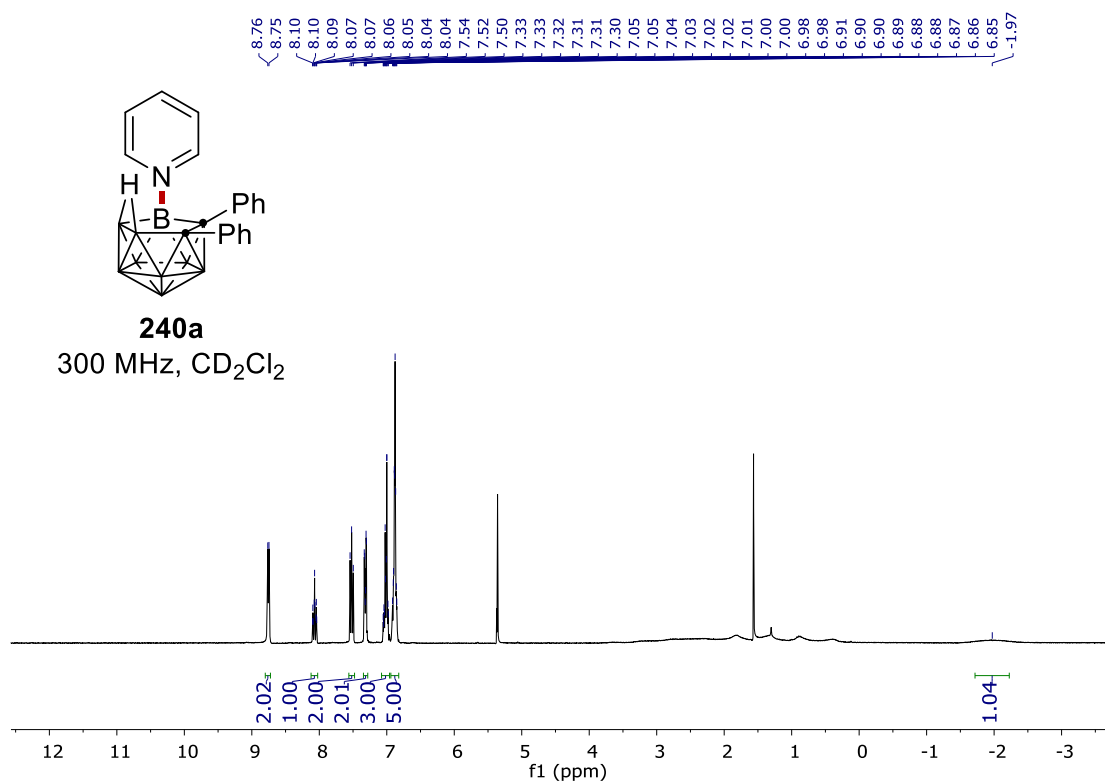
6 References

- [141] a) F. Issa, M. Kassiou, L. M. Rendina, *Chem. Rev.* **2011**, *111*, 5701–5722; b) M. Scholz, E. Hey-Hawkins, *Chem. Rev.* **2011**, *111*, 7035–7062.
- [142] a) V. Bregadze, Z. Xie, *Eur. J. Inorg. Chem.* **2017**, *2017*, 4344; b) R. N. Grimes, *Carboranes*, Academic Press, **2016**; c) Z. Xie, G.-X. Jin, *Dalton Trans.* **2014**, *43*, 4924–4924.
- [143] F. Teixidor, G. Barberà, A. Vaca, R. Kivekäs, R. Sillanpää, J. Oliva, C. Viñas, *J. Am. Chem. Soc.* **2005**, *127*, 10158–10159.
- [144] Y. Quan, Z. Qiu, Z. Xie, *Chem. Eur. J.* **2018**, *24*, 2795–2805.
- [145] E. L. Hoel, M. Talebinasab-Savari, M. Hawthorne, *J. Am. Chem. Soc.* **1977**, *99*, 4356–4367.
- [146] M. G. Mirabelli, L. G. Sneddon, *J. Am. Chem. Soc.* **1988**, *110*, 449–453.
- [147] R. Cheng, Z. Qiu, Z. Xie, *Nat. Commun.* **2017**, *8*, 14827.
- [148] C. X. Li, H. Y. Zhang, T. Y. Wong, H. J. Cao, H. Yan, C. S. Lu, *Org. Lett.* **2017**, *19*, 5178–5181.
- [149] C.-X. Cui, J. Zhang, Z. Qiu, Z. Xie, *Dalton Trans.* **2020**, *49*, 1380–1383.
- [150] R. Cheng, Z. Qiu, Z. Xie, *Chem. Eur. J.* **2020**, *26*, 7212–7218.
- [151] R. Cheng, Z. Qiu, Z. Xie, *Chin. J. Chem.* **2020**, *38*, 1575–1578.
- [152] T.-T. Xu, K. Cao, C.-Y. Zhang, J. Wu, L.-F. Ding, J. Yang, *Org. Lett.* **2019**, *21*, 9276–9279.
- [153] Z. Y. Zhang, X. Zhang, J. Yuan, C. D. Yue, S. Meng, J. Chen, G. A. Yu, C. M. Che, *Chem. Eur. J.* **2020**, *26*, 5037–5050.
- [154] Y. K. Au, J. Zhang, Y. Quan, Z. Xie, *J. Am. Chem. Soc.* **2021**, *143*, 4148–4153.
- [155] Z. Qiu, Y. Quan, Z. Xie, *J. Am. Chem. Soc.* **2013**, *135*, 12192–12195.
- [156] T. T. Xu, C. Y. Zhang, K. Cao, J. Wu, L. Jiang, J. Li, B. Li, J. Yang, *ChemistrySelect* **2017**, *2*, 3396–3399.
- [157] J. Wu, K. Cao, T.-T. Xu, X.-J. Zhang, L. Jiang, J. Yang, Y. Huang, *RSC Adv.* **2015**, *5*, 91683–91685.
- [158] K. Cao, Y. Huang, J. Yang, J. Wu, *Chem. Commun.* **2015**, *51*, 7257–7260.
- [159] H. Lyu, J. Zhang, J. Yang, Y. Quan, Z. Xie, *J. Am. Chem. Soc.* **2019**, *141*, 4219–4224.
- [160] a) T.-T. Xu, K. Cao, J. Wu, C.-Y. Zhang, J. Yang, *Inorg. Chem.* **2018**, *57*, 2925–2932; b) K. Cao, T.-T. Xu, J. Wu, L. Jiang, J. Yang, *Chem. Commun.* **2016**, *52*, 11446–11449.
- [161] Y. Quan, Z. Xie, *J. Am. Chem. Soc.* **2014**, *136*, 15513–15516.
- [162] H. Lyu, Y. Quan, Z. Xie, *Angew. Chem. Int. Ed.* **2015**, *54*, 10623–10626.
- [163] C. Zhang, Q. Wang, S. Tian, J. Zhang, J. Li, L. Zhou, J. Lu, *Org. Bio. Chem.* **2020**, *18*, 4723–4727.
- [164] Y. Chen, Y. K. Au, Y. Quan, Z. Xie, *Sci. China Chem.* **2018**, *62*, 74–79.
- [165] Y. K. Au, Y. Quan, Z. Xie, *Chem. Asian J.* **2020**, *15*, 2170–2173.
- [166] Y. Quan, Z. Xie, *Angew. Chem. Int. Ed.* **2016**, *55*, 1295–1298.
- [167] a) X. Zhang, H. Yan, *Chem. Sci.* **2018**, *9*, 3964–3969; b) X. Zhang, H. Zheng, J. Li, F. Xu, J. Zhao, H. Yan, *J. Am. Chem. Soc.* **2017**, *139*, 14511–14517.
- [168] T. T. Xu, K. Cao, C. Y. Zhang, J. Wu, L. Jiang, J. Yang, *Chem. Commun.* **2018**, *54*, 13603–13606.
- [169] R. Cheng, B. Li, J. Wu, J. Zhang, Z. Qiu, W. Tang, S.-L. You, Y. Tang, Z. Xie, *J. Am. Chem. Soc.* **2018**, *140*, 4508–4511.
- [170] Y. Quan, H. Lyu, Z. Xie, *Chem. Commun.* **2017**, *53*, 4818–4821.
- [171] Y. Chen, Y. Quan, Z. Xie, *Chem. Commun.* **2020**, *56*, 7001–7004.
- [172] Y. Quan, C. Tang, Z. Xie, *Chem. Sci.* **2016**, *7*, 5838–5845.
- [173] Q. Wang, S. Tian, C. Zhang, J. Li, Z. Wang, Y. Du, L. Zhou, J. Lu, *Org. Lett.* **2019**, *21*, 8018–8021.
- [174] K. Cao, C.-Y. Zhang, T.-T. Xu, J. Wu, L.-F. Ding, L. Jiang, J. Yang, *J. Organomet. Chem.* **2019**, *902*, 120956.
- [175] H. Lyu, Y. Quan, Z. Xie, *Angew. Chem. Int. Ed.* **2016**, *55*, 11840–11844.

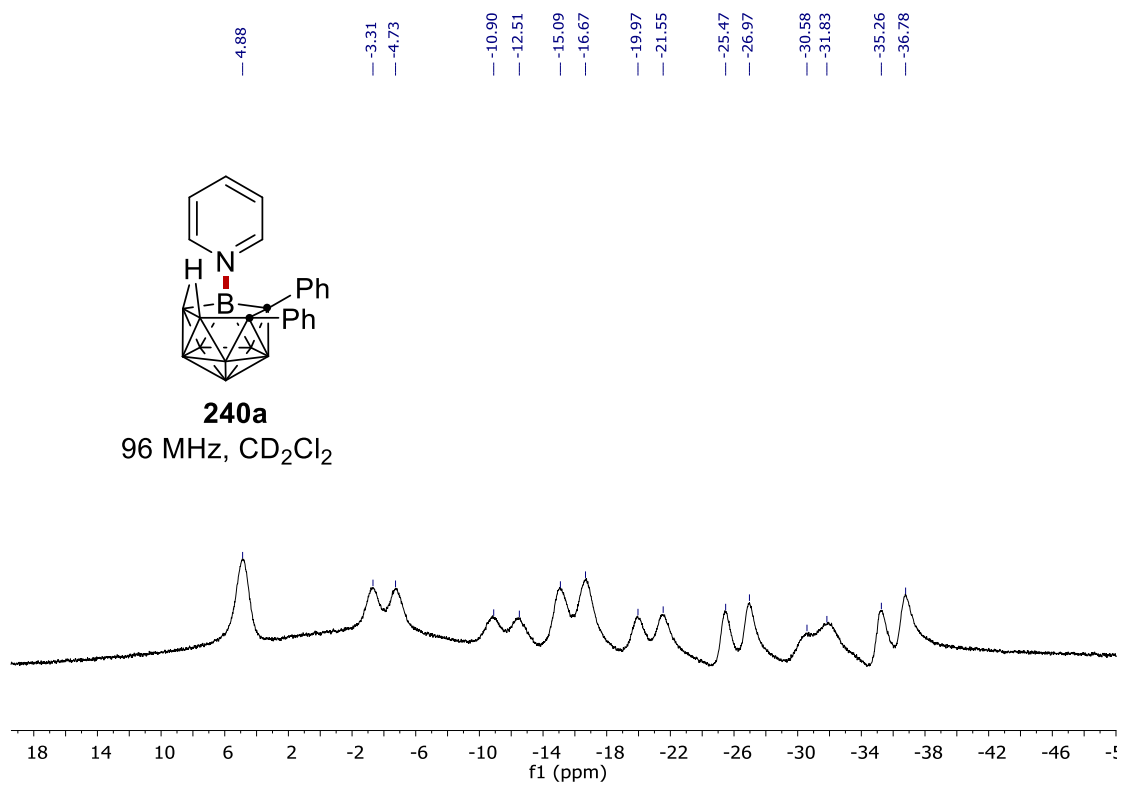
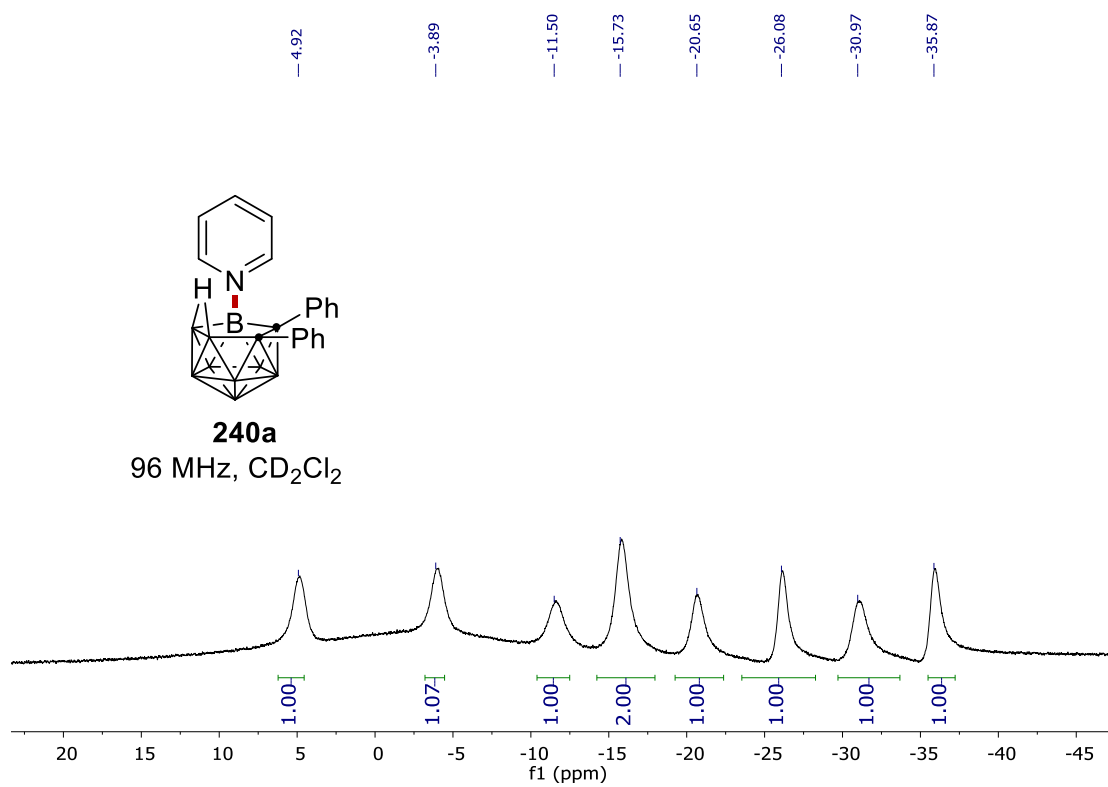
6 References

- [176] H. Lyu, Y. Quan, Z. Xie, *J. Am. Chem. Soc.* **2016**, *138*, 12727–12730.
- [177] a) Y. Baek, S. Kim, J.-Y. Son, K. Lee, D. Kim, P. H. Lee, *ACS Catal.* **2019**, 10418–10425; b) H. Li, F. Bai, H. Yan, C. Lu, V. I. Bregadze, *Eur. J. Org. Chem.* **2017**, *2017*, 1343–1352.
- [178] a) J. Wu, K. Cao, C. Y. Zhang, T. T. Xu, X. Y. Wen, B. Li, J. Yang, *Inorg. Chem.* **2020**, *59*, 17340–17346; b) J. Wu, K. Cao, C.-Y. Zhang, T.-T. Xu, L.-F. Ding, B. Li, J. Yang, *Org. Lett.* **2019**, *21*, 5986–5989.
- [179] H. Lyu, Y. Quan, Z. Xie, *Chem. Eur. J.* **2017**, *23*, 14866–14871.
- [180] Y. Chen, Y. Quan, Z. Xie, *Chem. Commun.* **2020**, *56*, 12997–13000.
- [181] H. Lyu, Y. Quan, Z. Xie, *Chem. Sci.* **2018**, *9*, 6390–6394.
- [182] a) Y. K. Au, H. Lyu, Y. Quan, Z. Xie, *Chin. J. Chem.* **2020**, *38*, 383–388; b) Y. K. Au, H. Lyu, Y. Quan, Z. Xie, *J. Am. Chem. Soc.* **2019**, *141*, 12855–12862.
- [183] Y. Baek, K. Cheong, G. H. Ko, G. U. Han, S. H. Han, D. Kim, K. Lee, P. H. Lee, *J. Am. Chem. Soc.* **2020**, *142*, 9890–9895.
- [184] a) D. A. Rudakov, V. I. Potkin, I. V. Lantsova, *Russ. J. Electrochem.* **2009**, *45*, 813–817; b) D. Rudakov, V. Shirokii, V. Potkin, N. Maier, V. Bragin, P. Petrovskii, I. Sivaev, V. Bregadze, A. Kisin, *Russ. Chem. Bull.* **2005**, *54*, 1599–1602.
- [185] Y. K. Au, H. Lyu, Y. Quan, Z. Xie, *J. Am. Chem. Soc.* **2020**, *142*, 6940–6945.
- [186] M. M. Heravi, V. Zadsirjan, *RSC Adv.* **2020**, *10*, 44247–44311.
- [187] a) H. Mayr, A. R. Ofial, *Acc. Chem. Res.* **2016**, *49*, 952–965; b) M. Baidya, F. Brotzel, H. Mayr, *Org. Bio. Chem.* **2010**, *8*, 1929–1935; c) F. Brotzel, B. Kempf, T. Singer, H. Zipse, H. Mayr, *Chem. Eur. J.* **2007**, *13*, 336–345.
- [188] X. Yang, B. Zhang, S. Zhang, G. Li, L. Xu, Z. Wang, P. Li, Y. Zhang, Z. Liu, G. He, *Org. Lett.* **2019**, *21*, 8285–8289.
- [189] a) O. Guzyr, C. Viñas, H. Wada, S. Hayashi, W. Nakanishi, F. Teixidor, A. V. Puga, V. David, *Dalton Trans.* **2011**, *40*, 3402–3411; b) F. Teixidor, M. A. Flores, C. Viñas, *Organometallics* **1999**, *18*, 5409–5411.
- [190] G. M. Martins, A. G. Meirinho, N. Ahmed, A. L. Braga, S. R. Mendes, *ChemElectroChem* **2019**, *6*, 5928–5940.
- [191] a) P. Gandeepan, J. Mo, L. Ackermann, *Chem. Commun.* **2017**, *53*, 5906–5909; b) F. Shibahara, T. Kanai, E. Yamaguchi, A. Kamei, T. Yamauchi, T. Murai, *Asian J. Chem.* **2014**, *9*, 237–244.
- [192] K. Sonogashira, *J. Organomet. Chem.* **2002**, *653*, 46–49.
- [193] a) K.-R. Wee, W.-S. Han, D. W. Cho, S. Kwon, C. Pac, S. O. Kang, *Angew. Chem. Int. Ed.* **2012**, *51*, 2677–2680; b) K.-R. Wee, Y.-J. Cho, S. Jeong, S. Kwon, J.-D. Lee, I.-H. Suh, S. O. Kang, *J. Am. Chem. Soc.* **2012**, *134*, 17982–17990.
- [194] F. Wang, S. S. Stahl, *Angew. Chem. Int. Ed.* **2019**, *58*, 6385–6390.
- [195] M. M. Fein, D. Grafstein, J. E. Paustian, J. Bobinski, B. M. Lichstein, N. Mayes, N. N. Schwartz, M. S. Cohen, *Inorganic Chemistry* **1963**, *2*, 1115–1119.
- [196] L. I. Zakharkin, A. I. Kovderov, V. A. Ol'Shevskaya, *Russ. Chem. Bull.* **1986**, *35*, 1260–1266.
- [197] A. Sousa-Pedrares, C. Viñas, F. Teixidor, *Chem. Commun.* **2010**, *46*, 2998–3000.
- [198] a) Y. Quan, Z. Qiu, Z. Xie, *J. Am. Chem. Soc.* **2014**, *136*, 7599–7602; b) Z. Qiu, Z. Xie, *Angew. Chem. Int. Ed.* **2008**, *47*, 6572–6575.
- [199] F. Zheng, T.-F. Leung, K.-W. Chan, H. H. Y. Sung, I. D. Williams, Z. Xie, G. Jia, *Chem. Commun.* **2016**, *52*, 10767–10770.
- [200] Z. Yang, W. Zhao, W. Liu, X. Wei, M. Chen, X. Zhang, X. Zhang, Y. Liang, C. Lu, H. Yan, *Angew. Chem. Int. Ed.* **2019**, *58*, 11886–11892.
- [201] O. Ito, M. Matsuda, *Bull. Chem. Soc. Jpn* **1984**, *57*, 1745–1749.

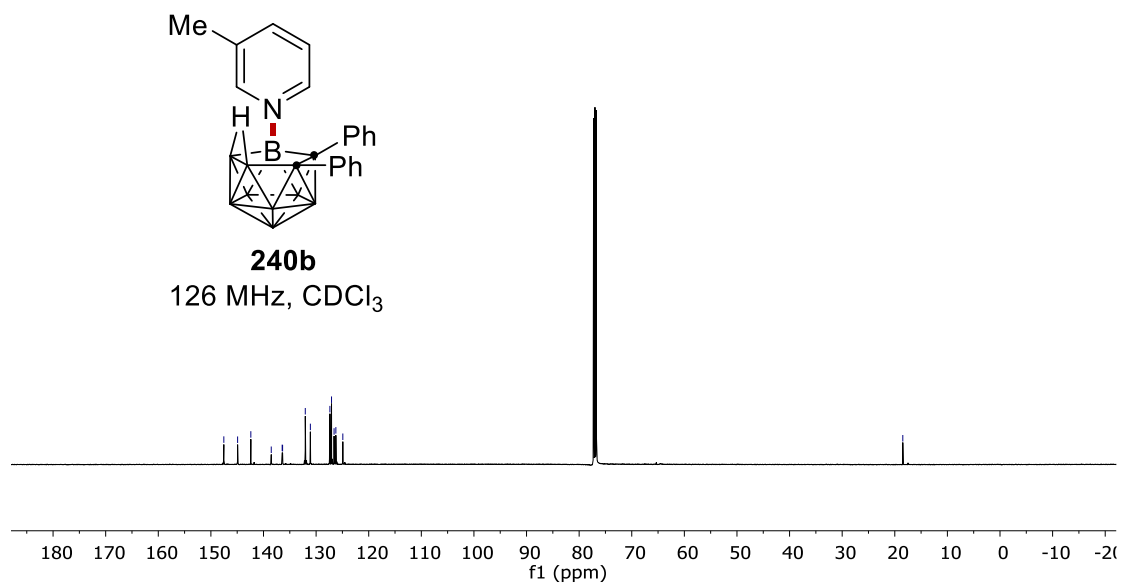
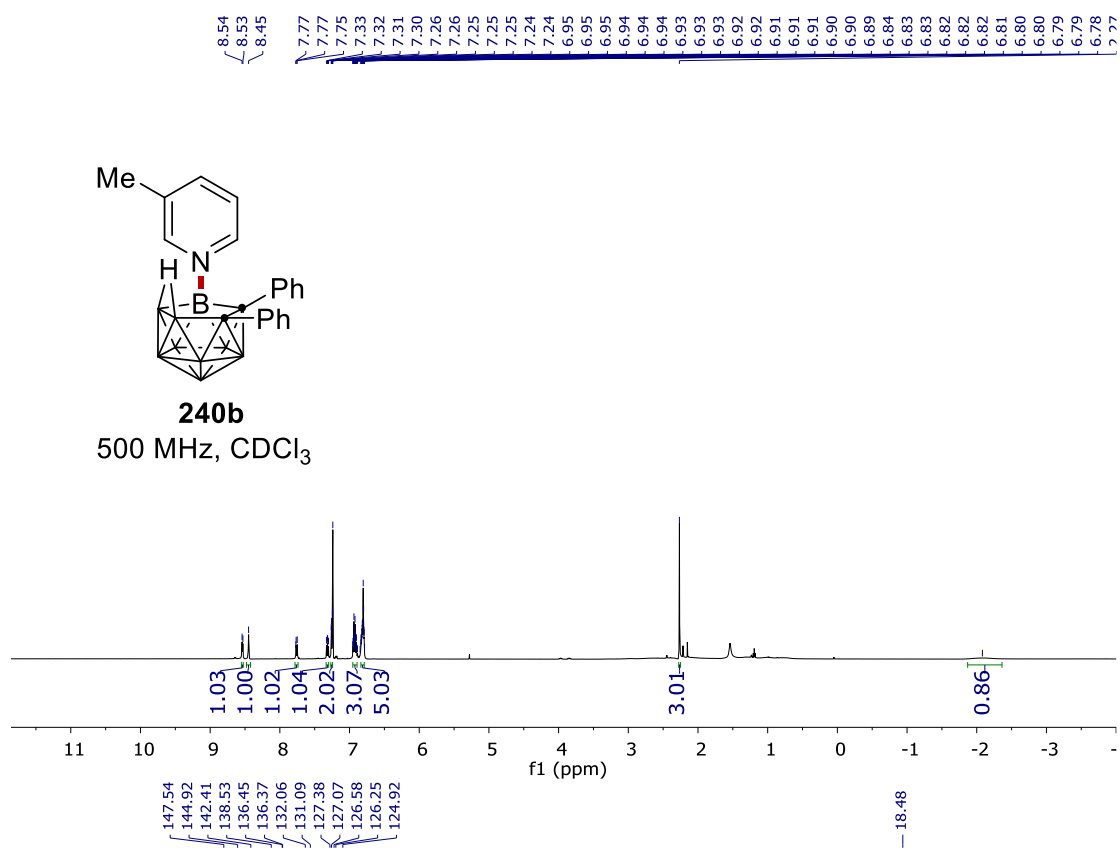
7. NMR spectra

7.1 Electrochemical B–H nitrogenation of *nido*-carboranes

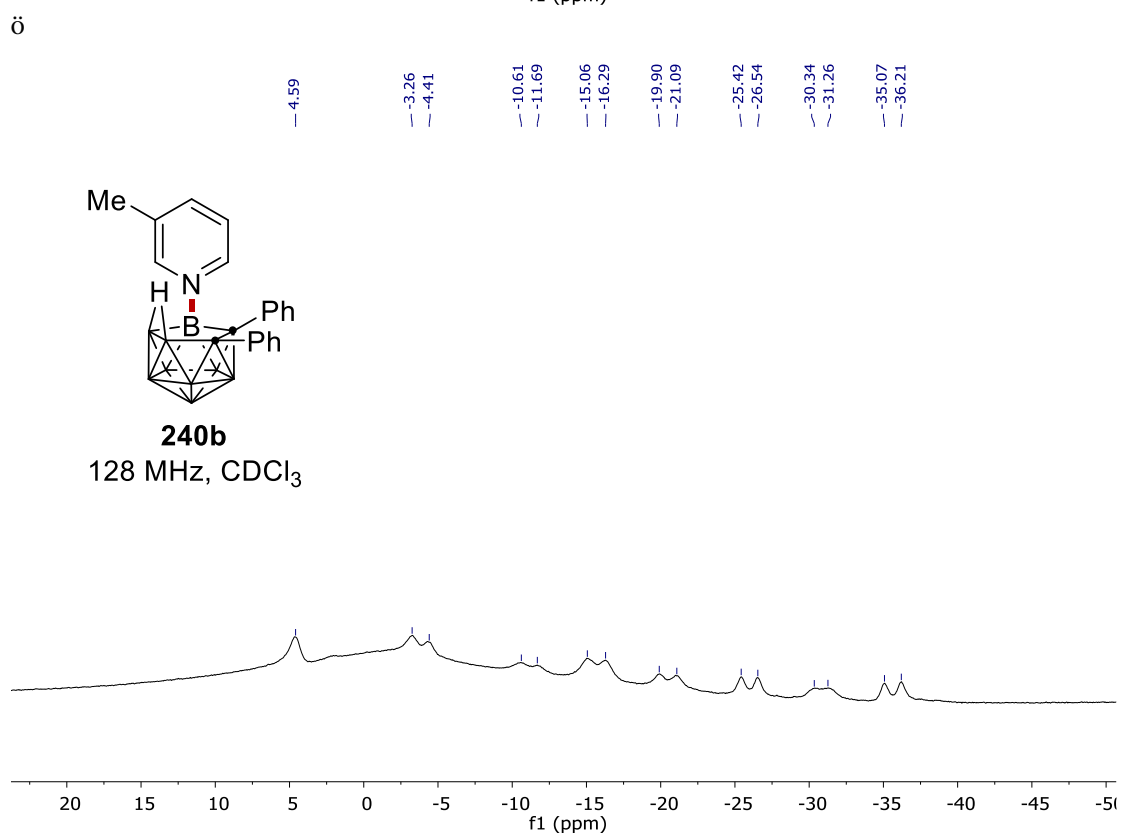
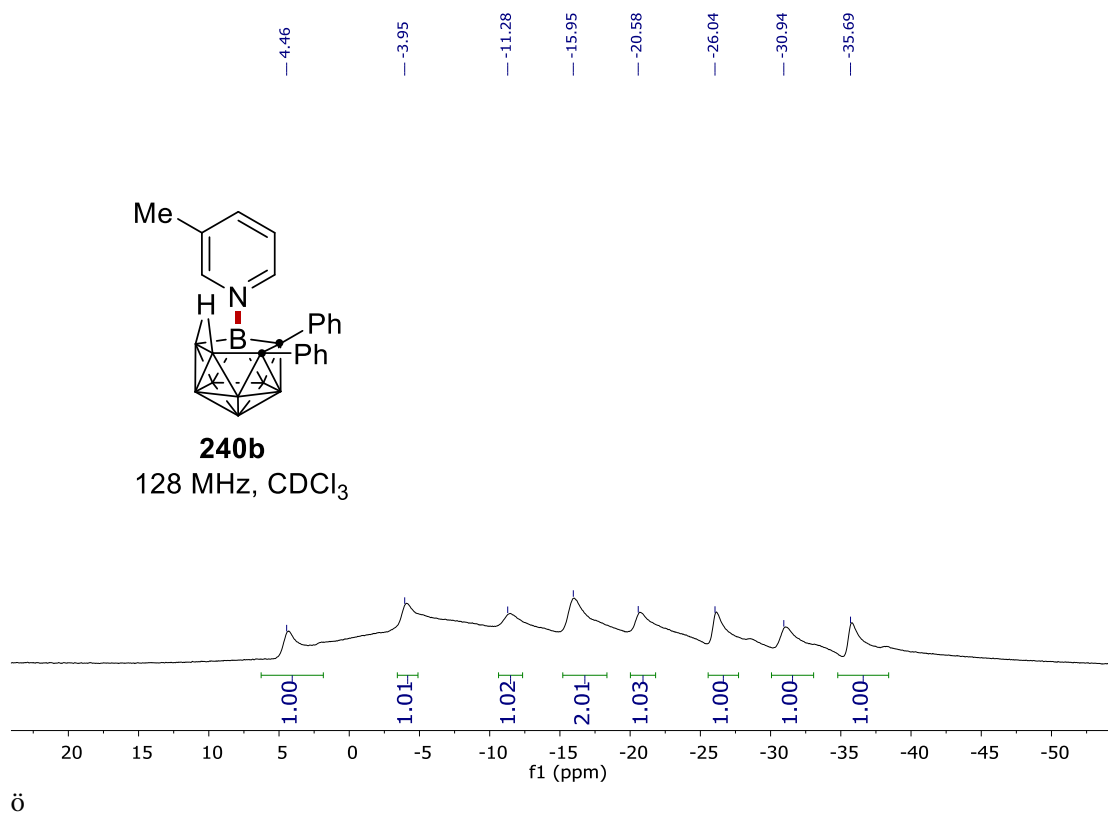
7. NMR Spectra



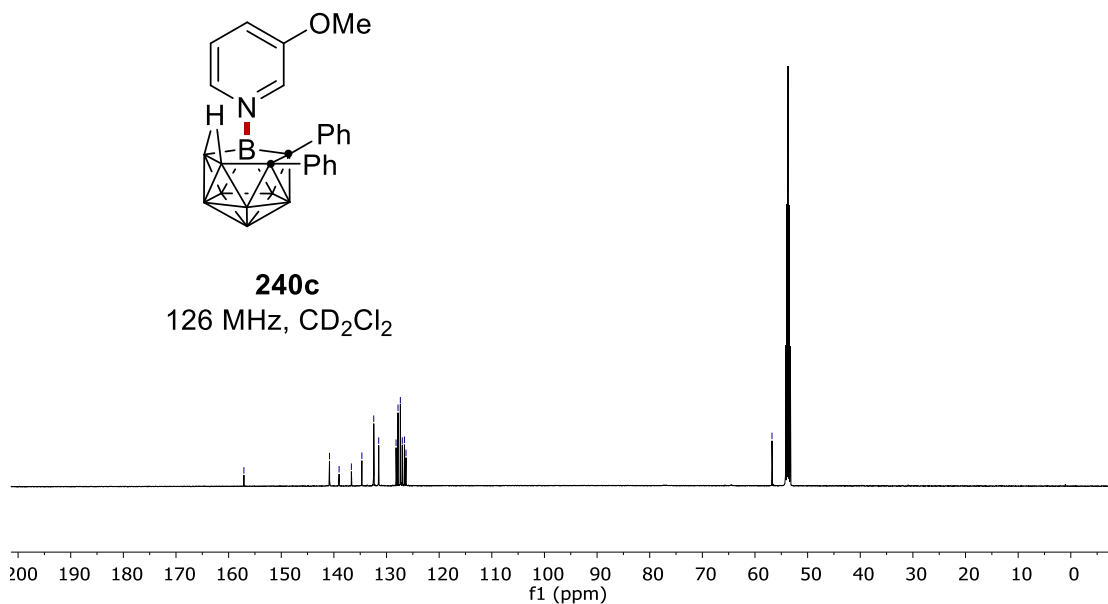
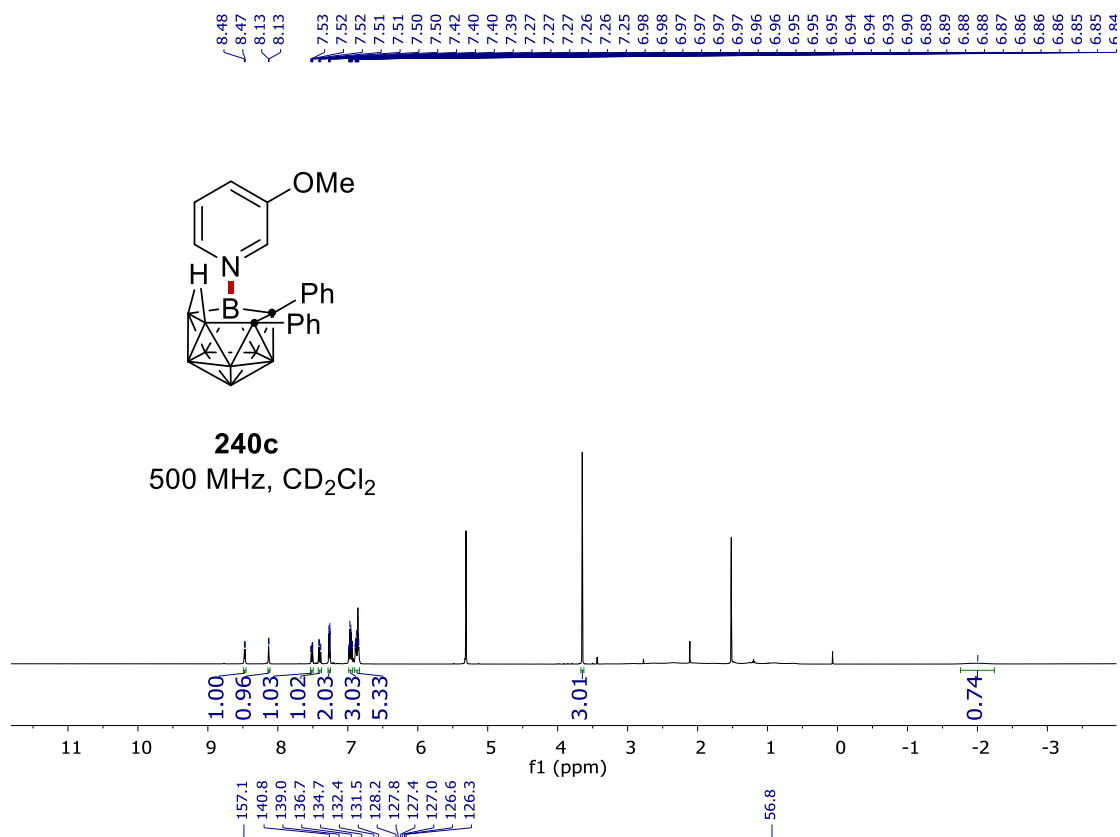
7. NMR Spectra



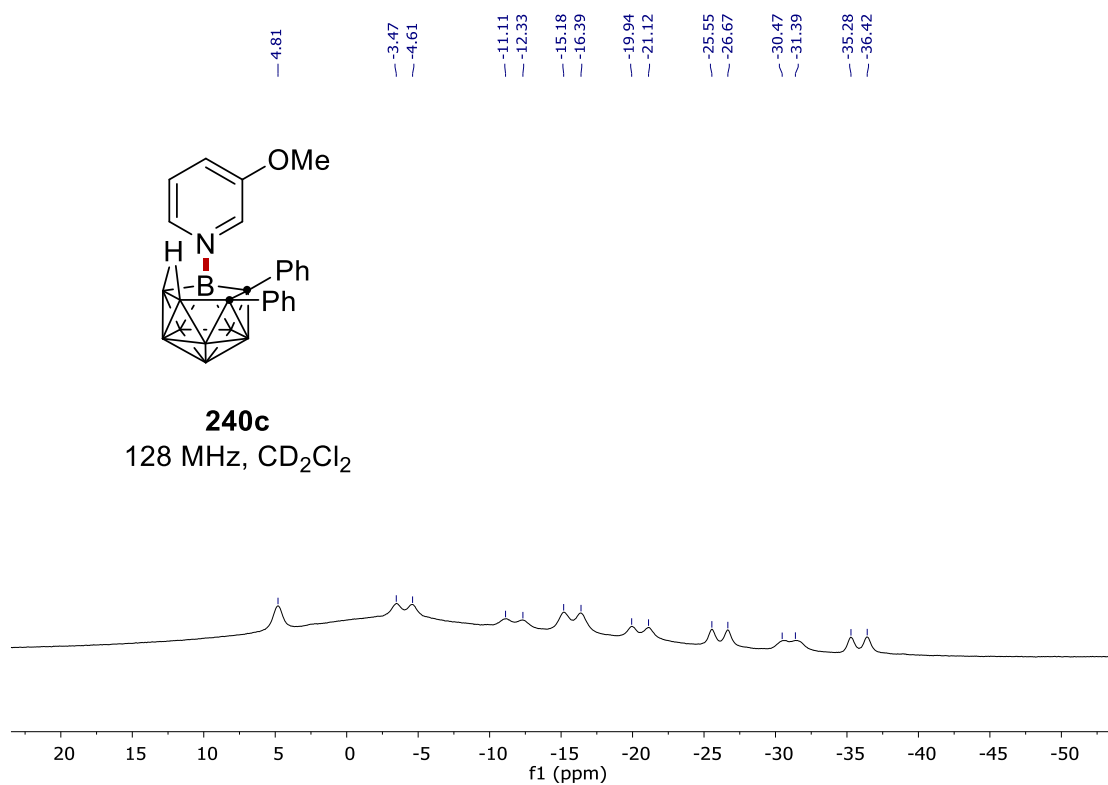
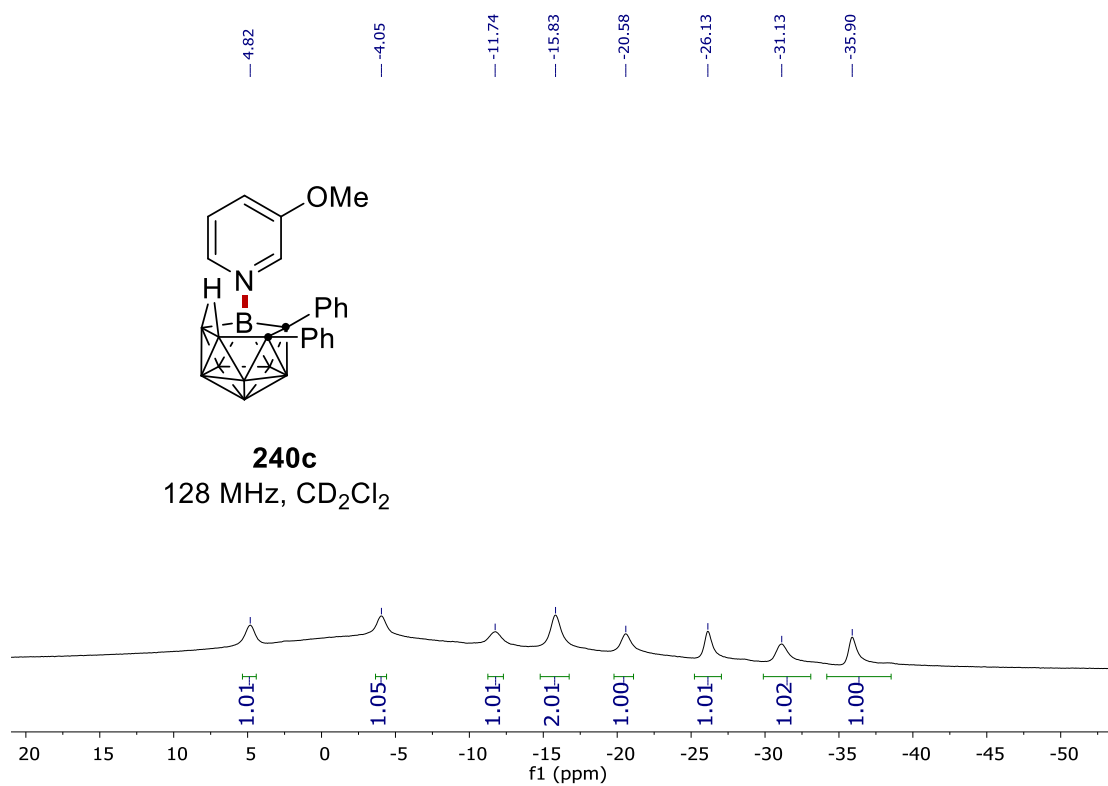
7. NMR Spectra



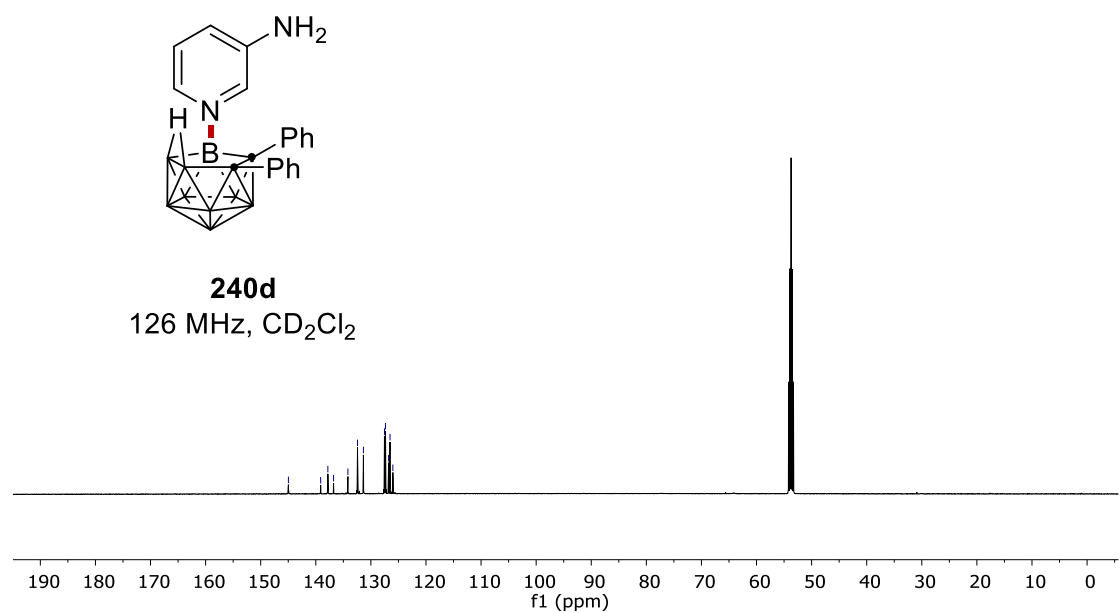
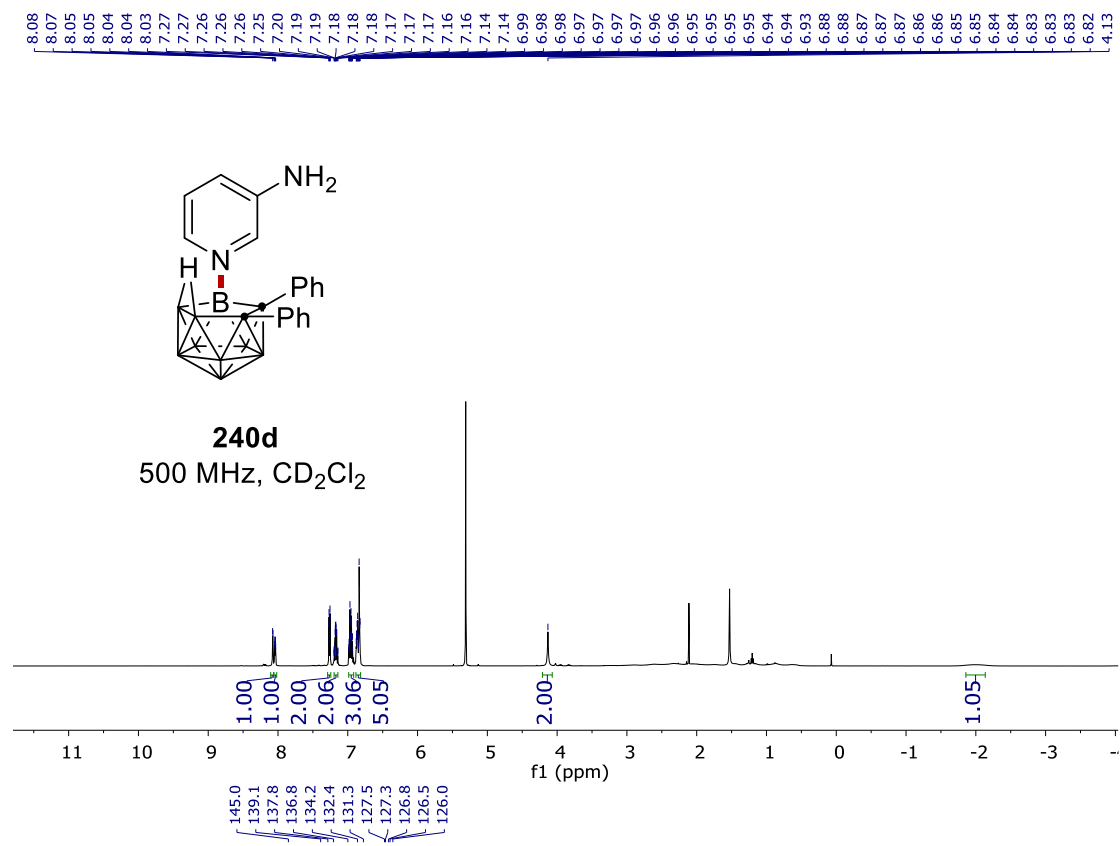
7. NMR Spectra



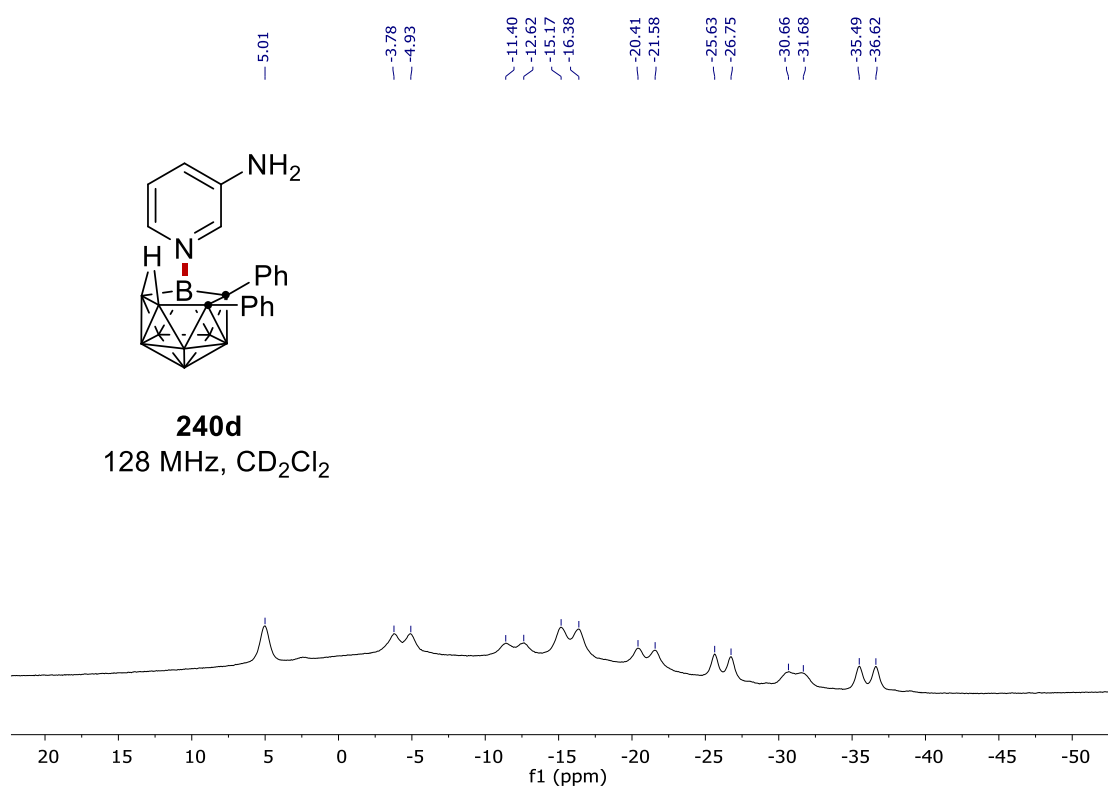
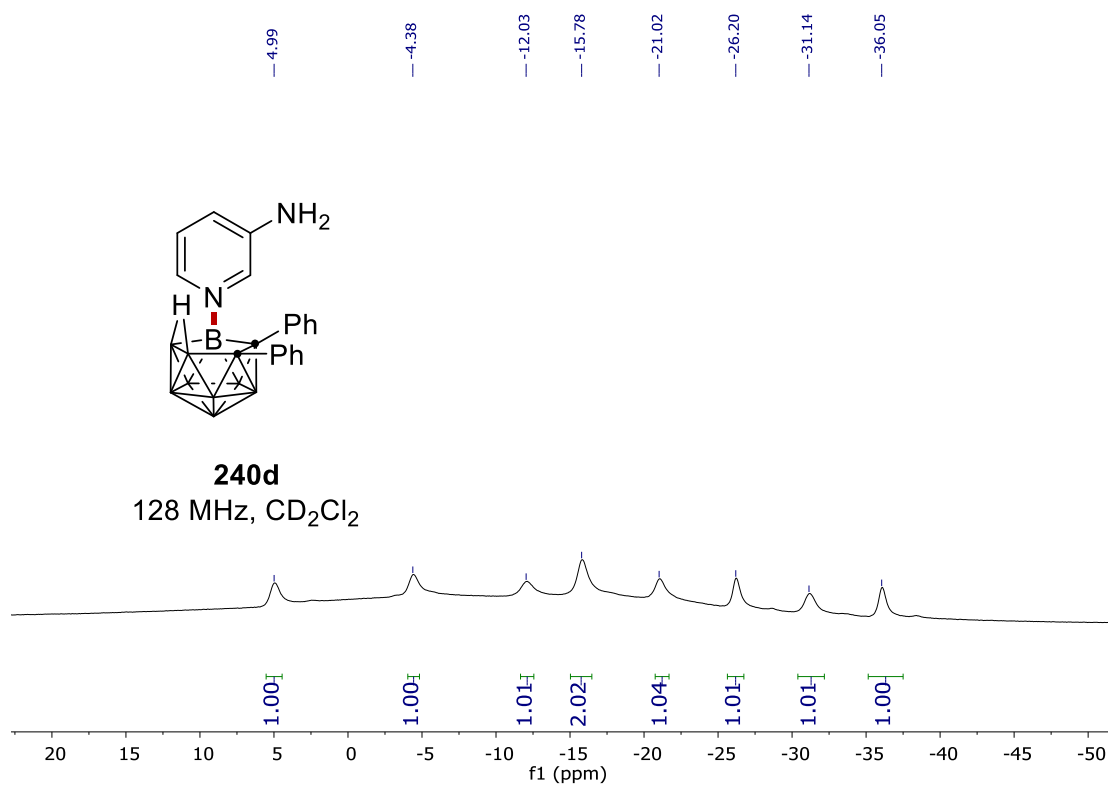
7. NMR Spectra



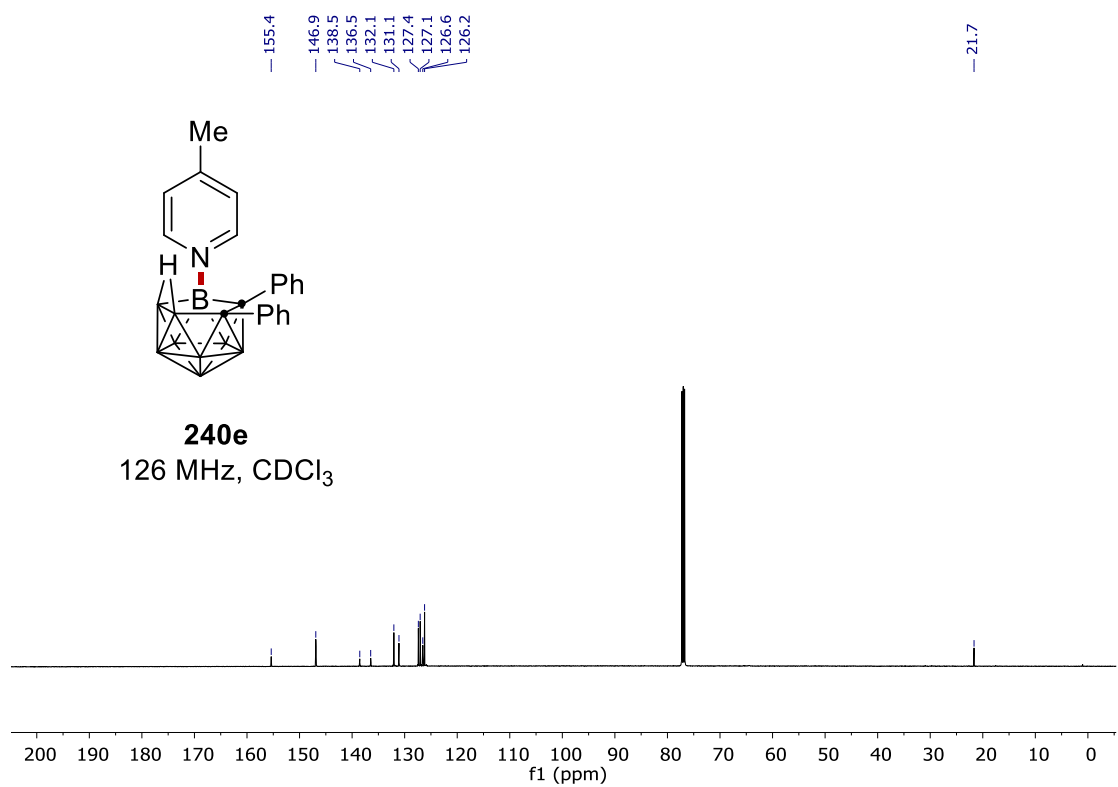
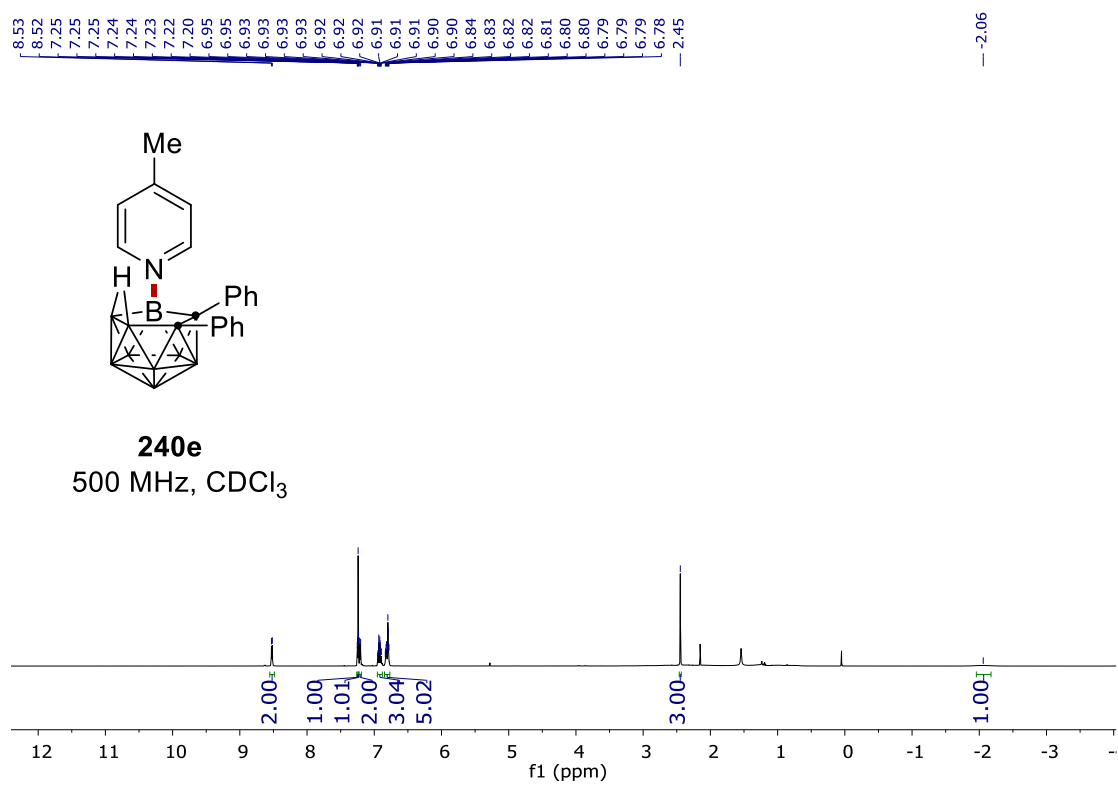
7. NMR Spectra



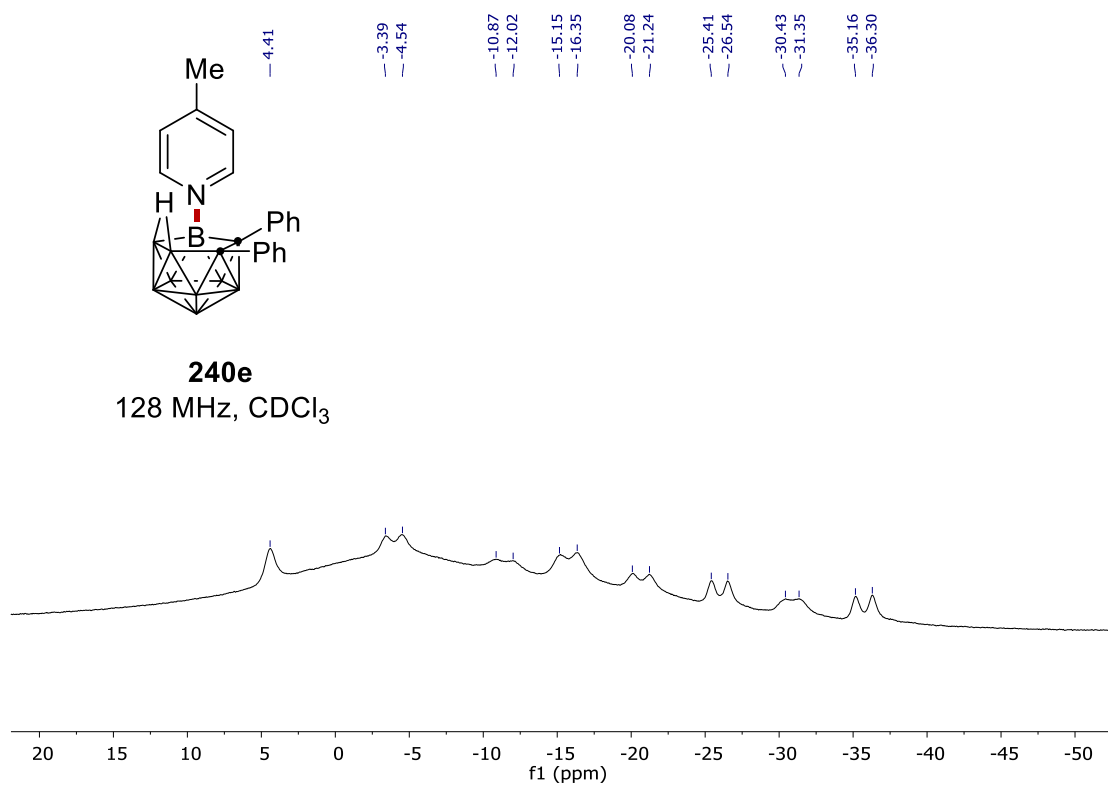
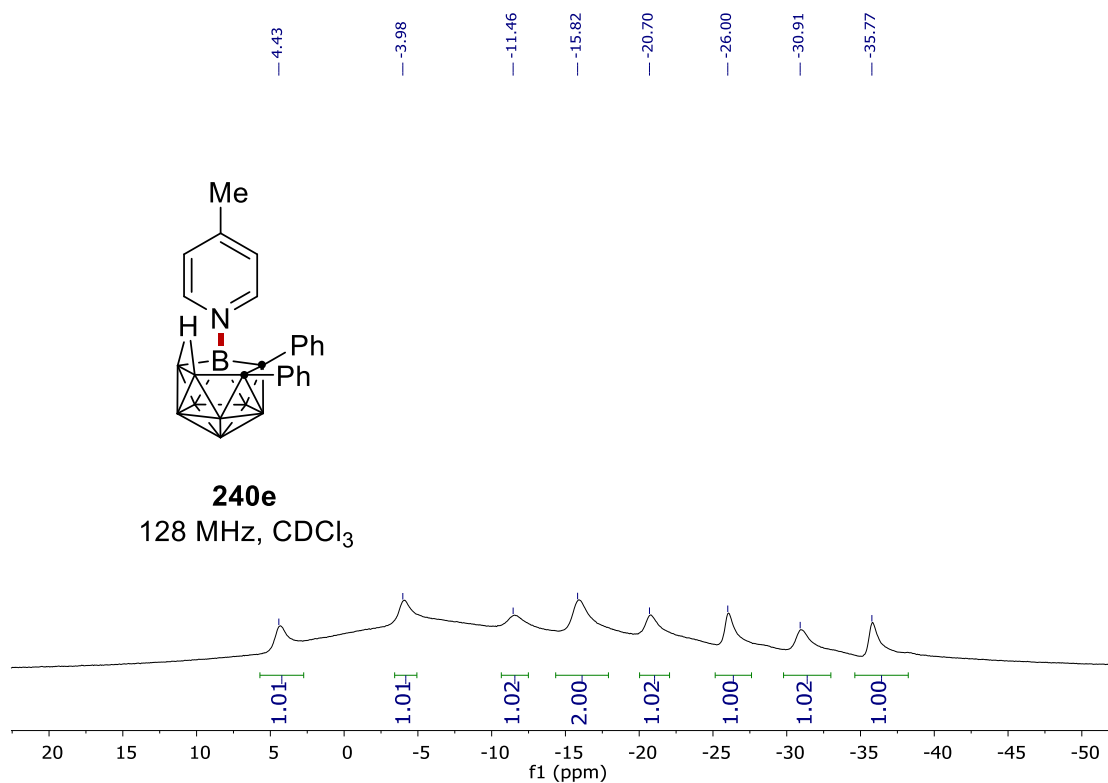
7. NMR Spectra

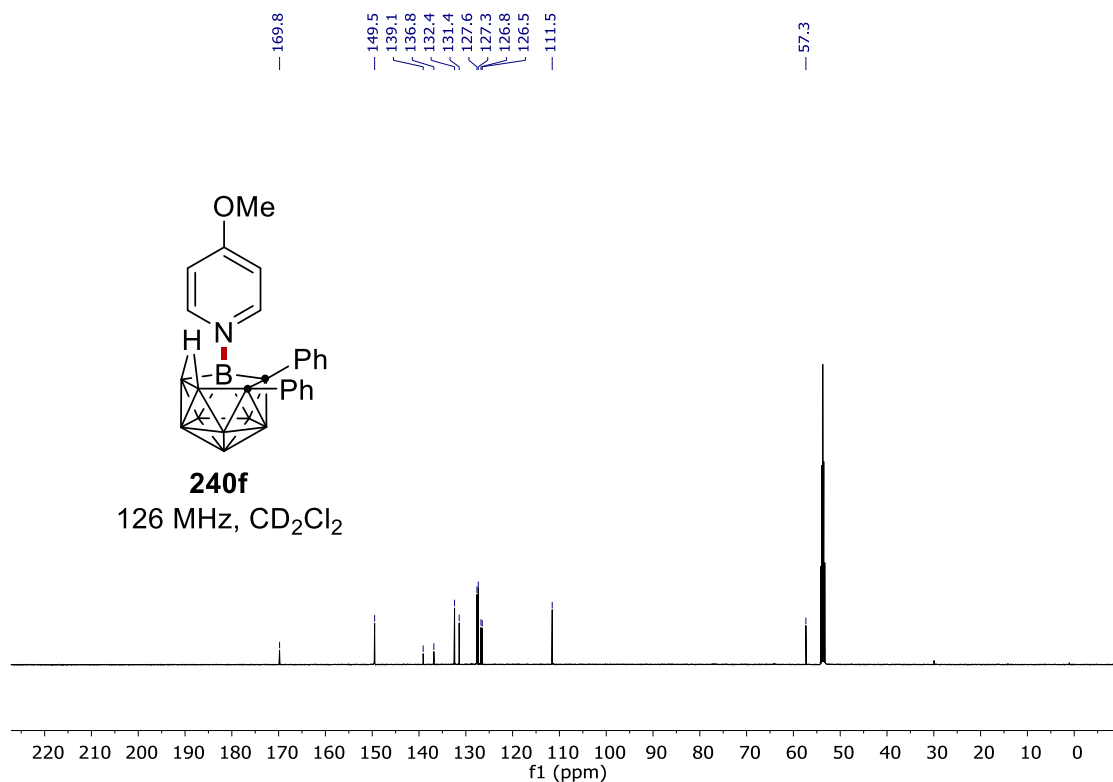


7. NMR Spectra

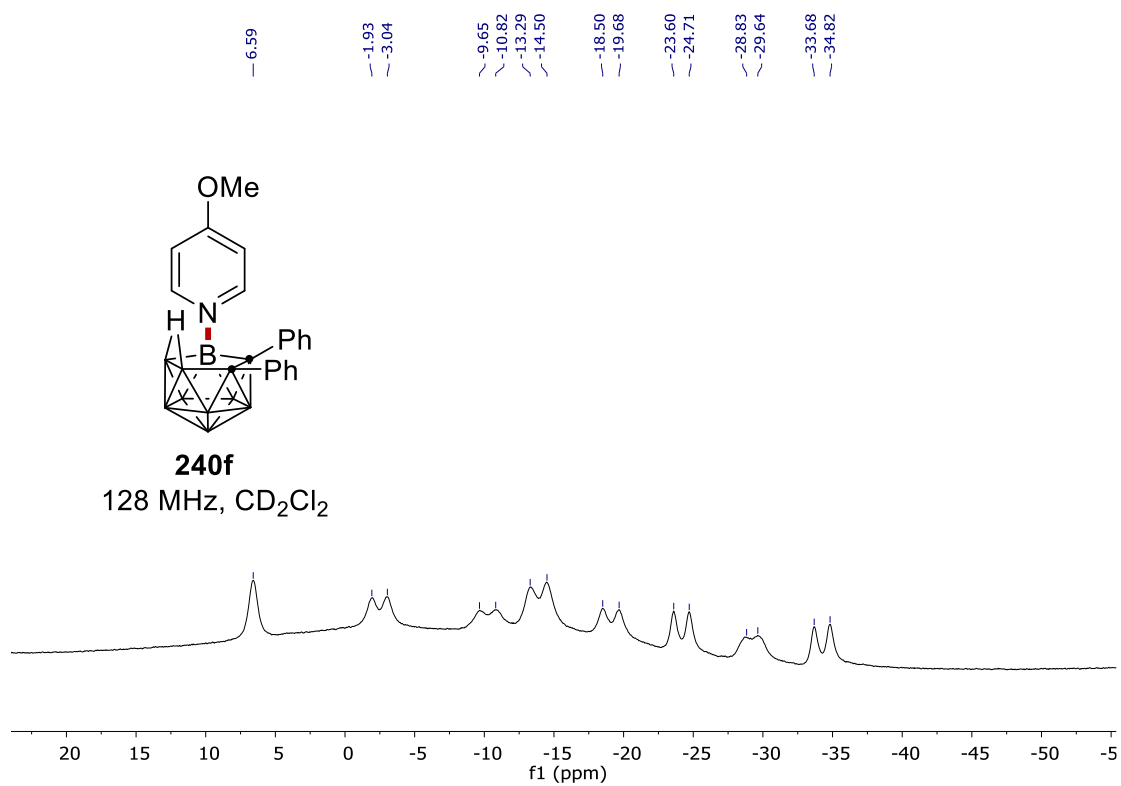
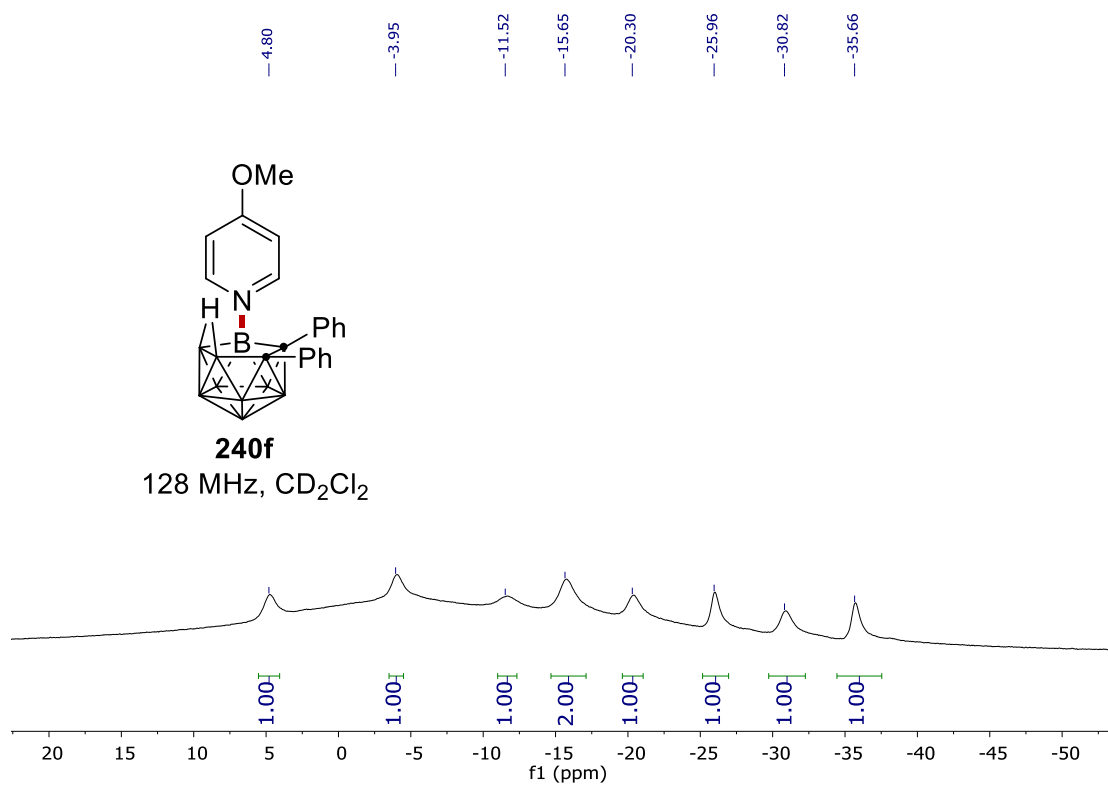


7. NMR Spectra

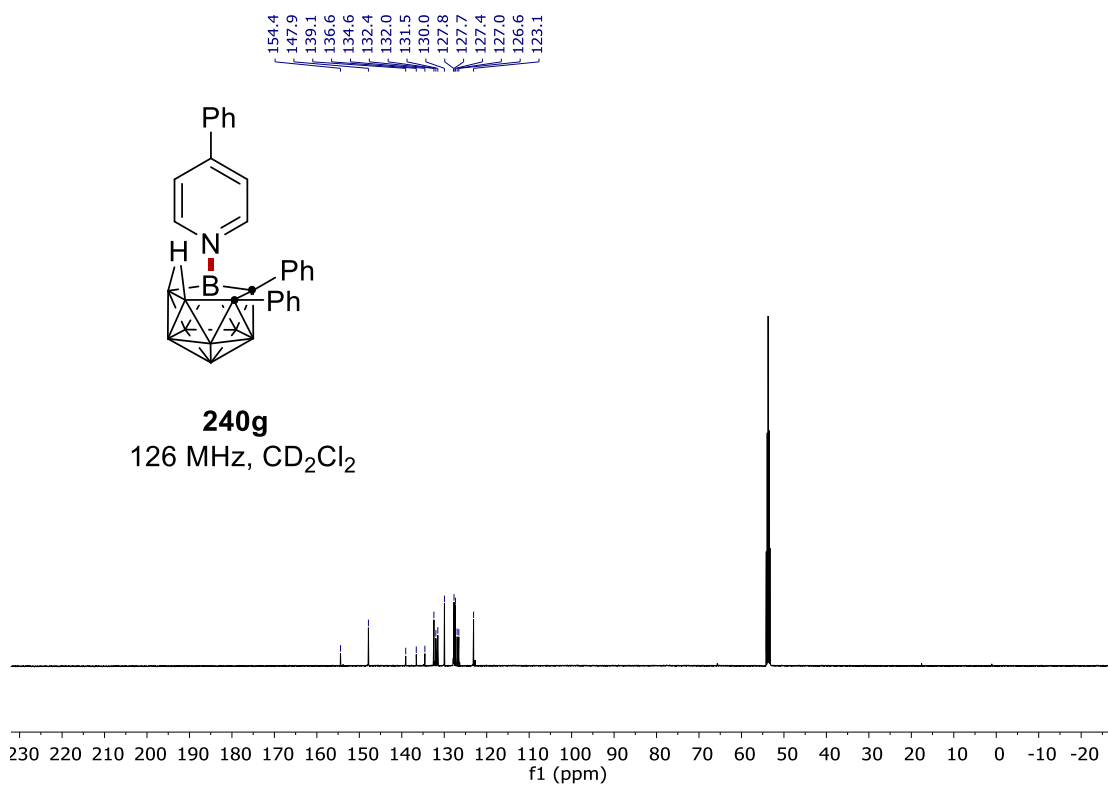
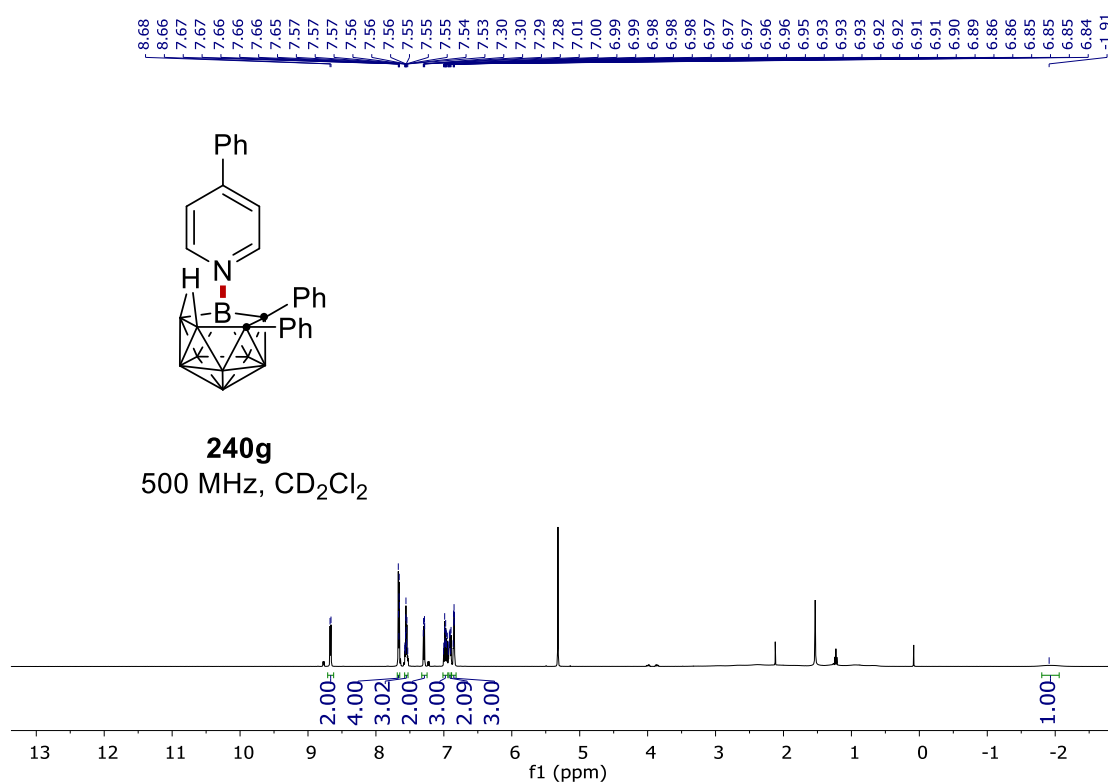




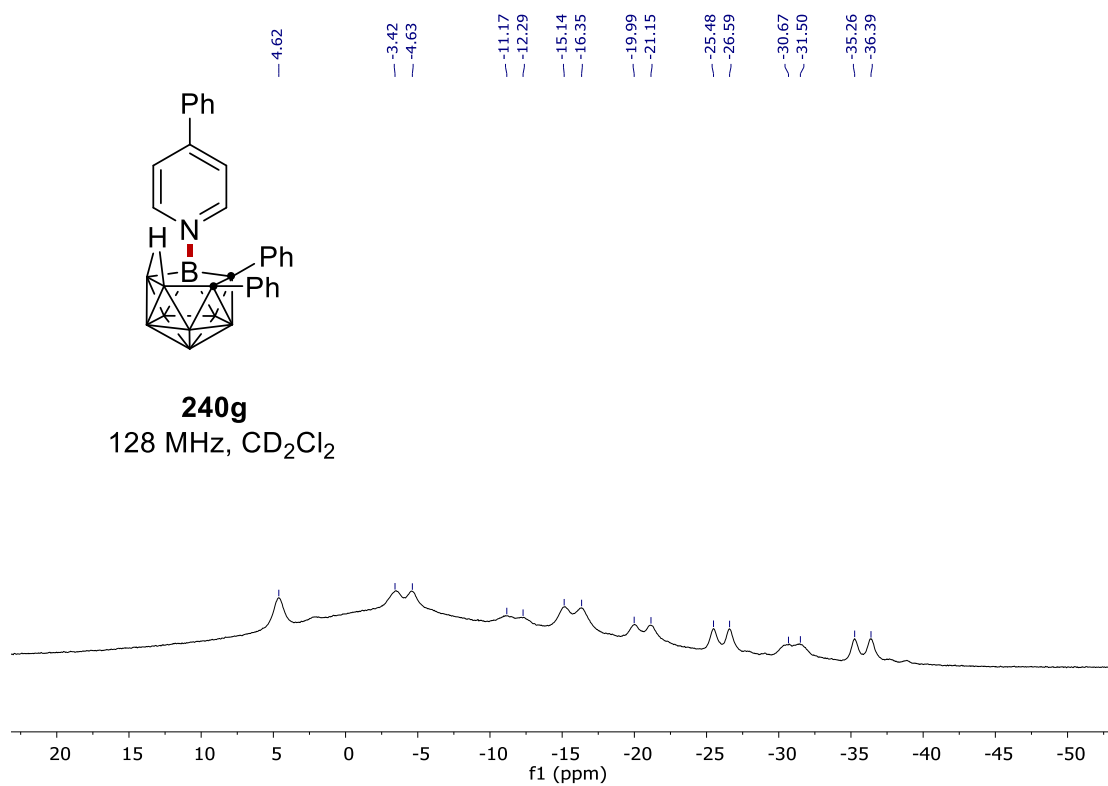
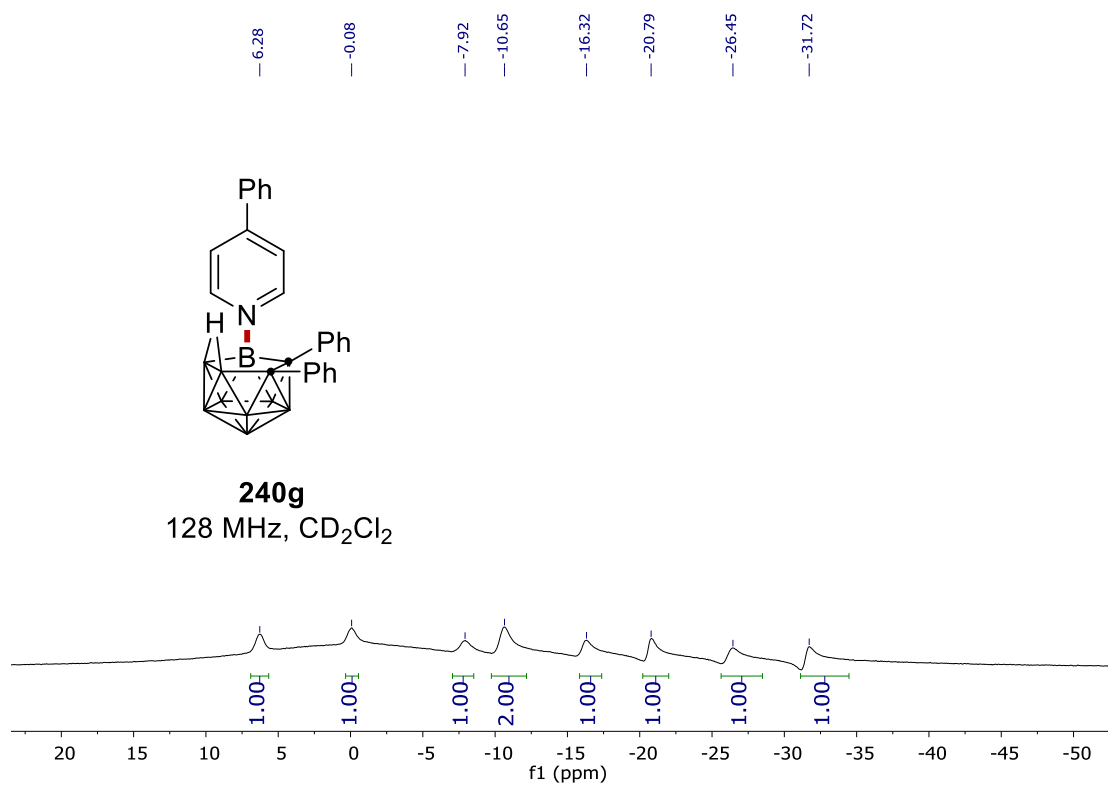
7. NMR Spectra



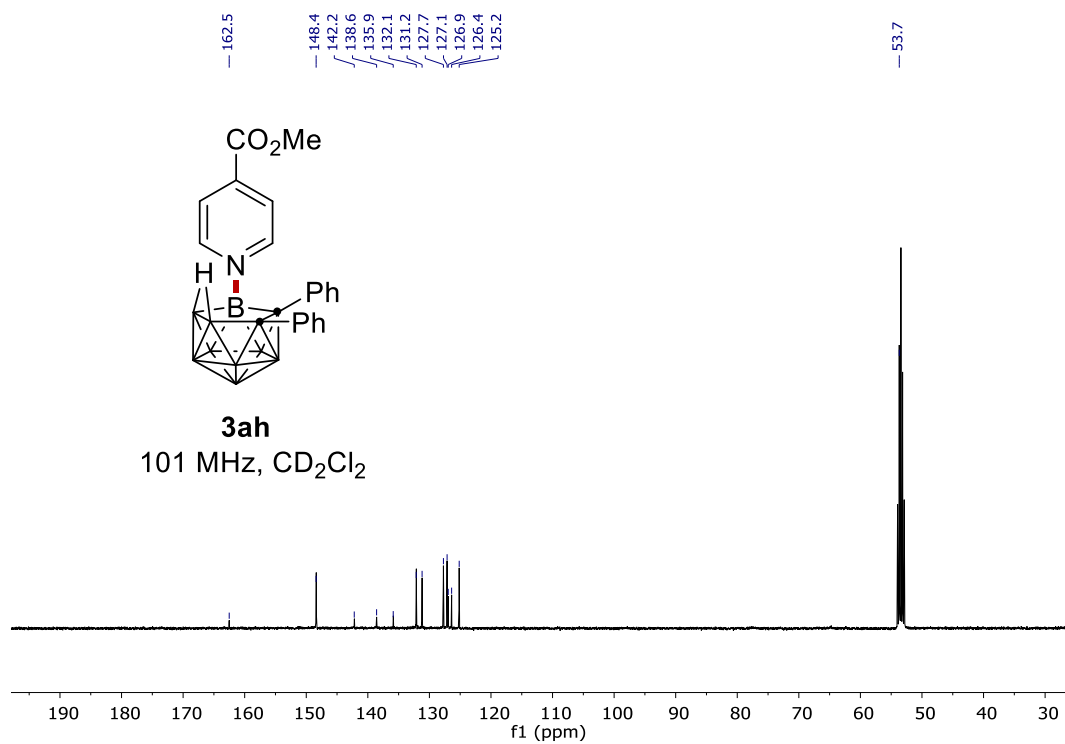
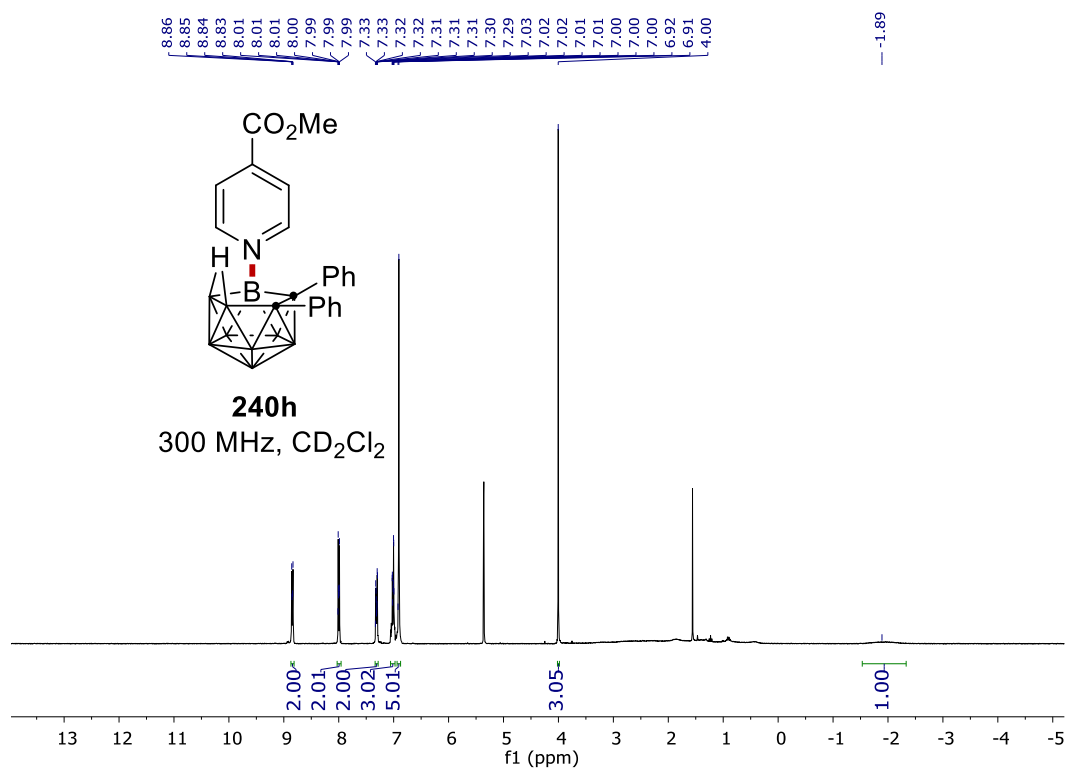
7. NMR Spectra



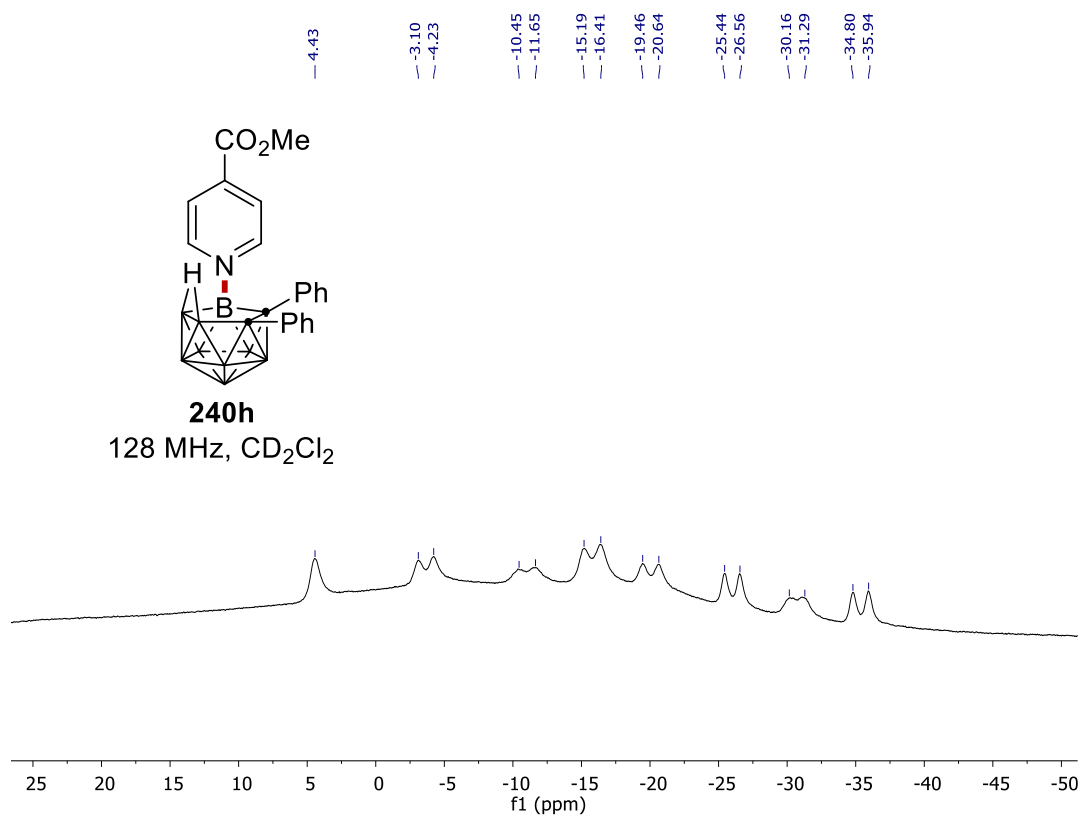
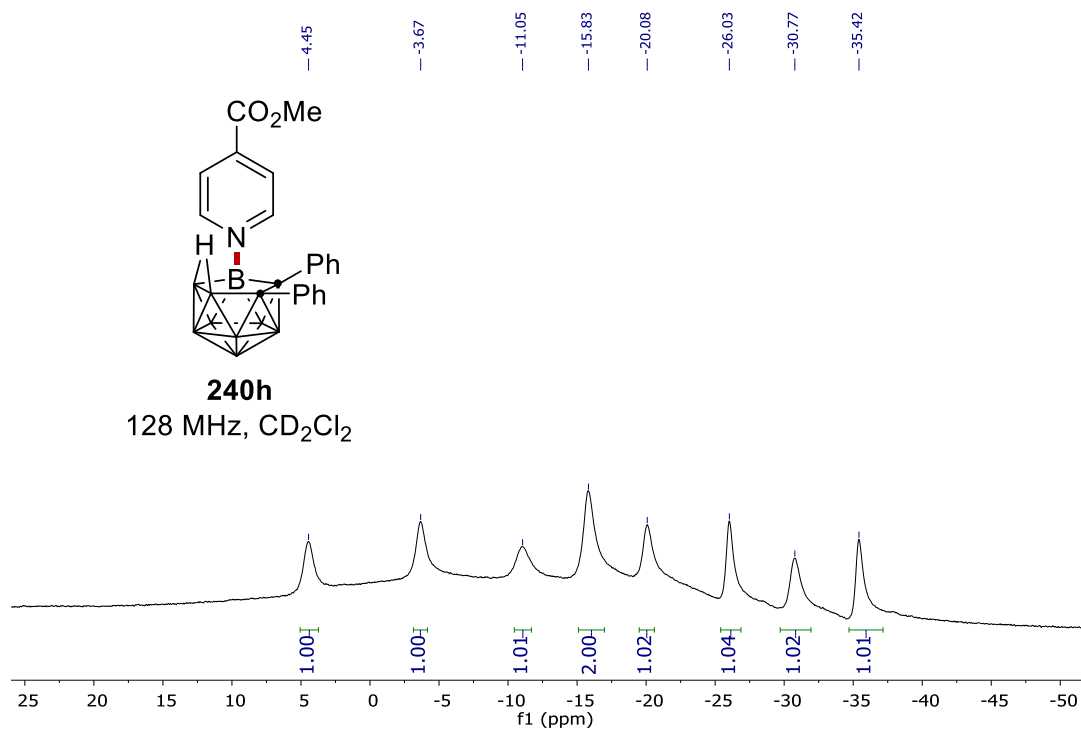
7. NMR Spectra



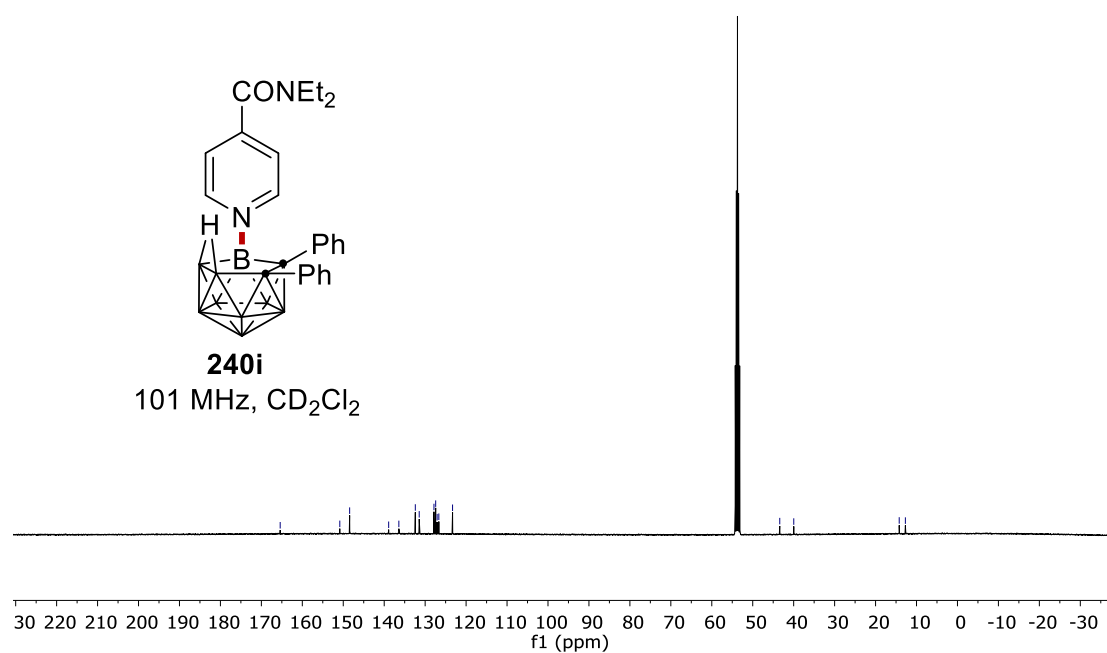
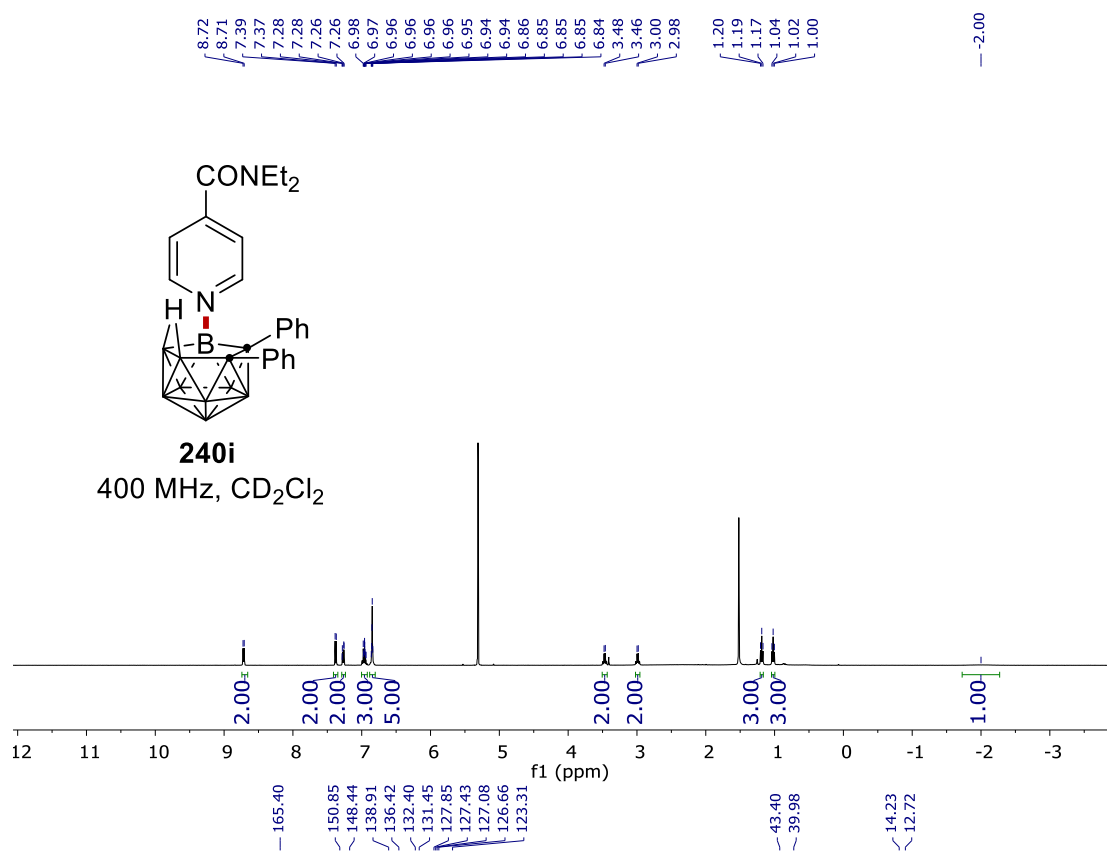
7. NMR Spectra



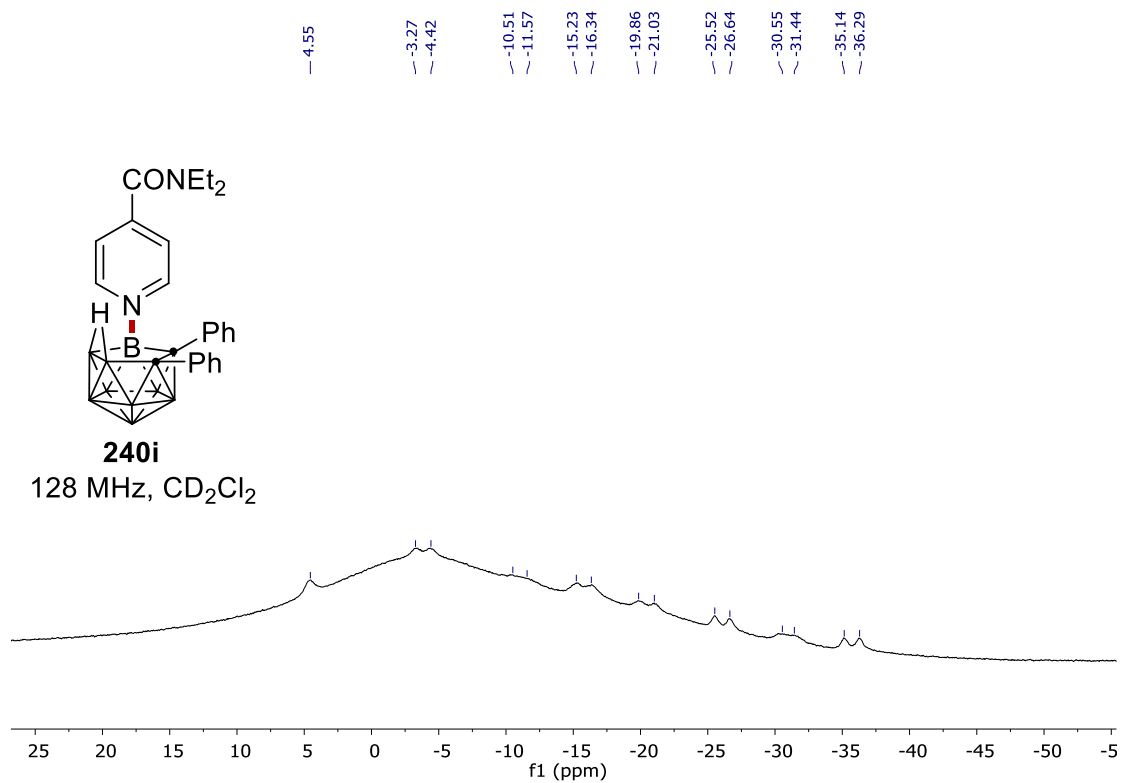
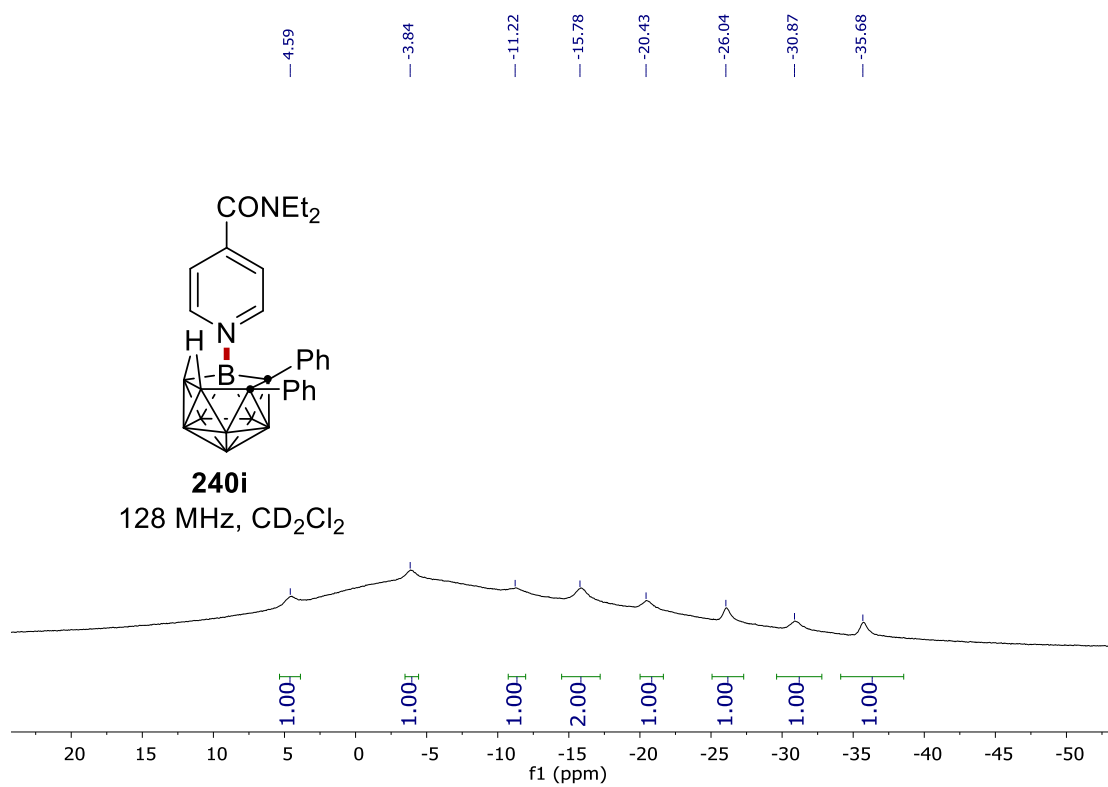
7. NMR Spectra



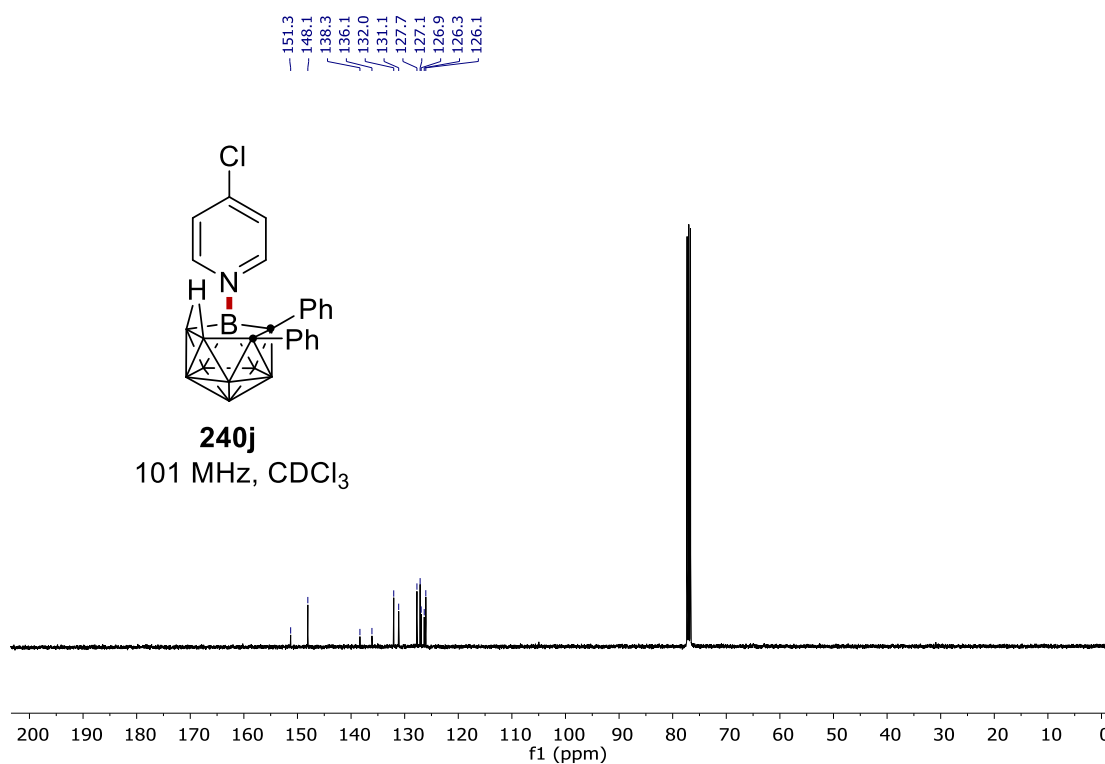
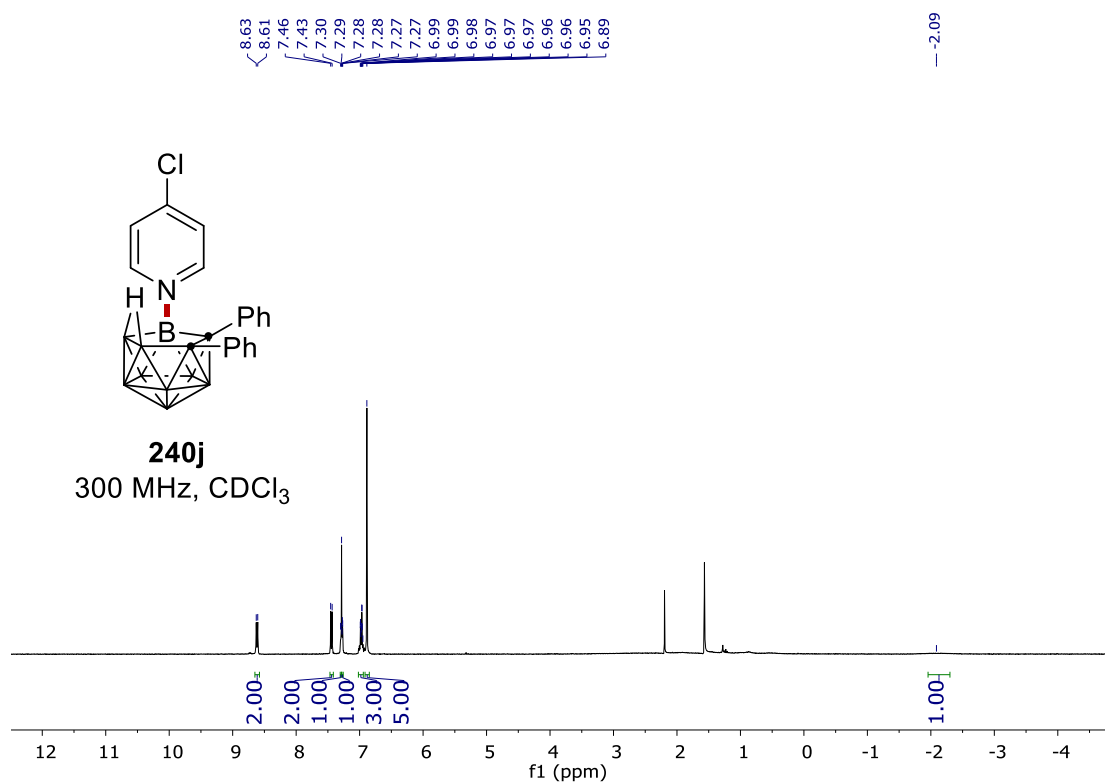
7. NMR Spectra



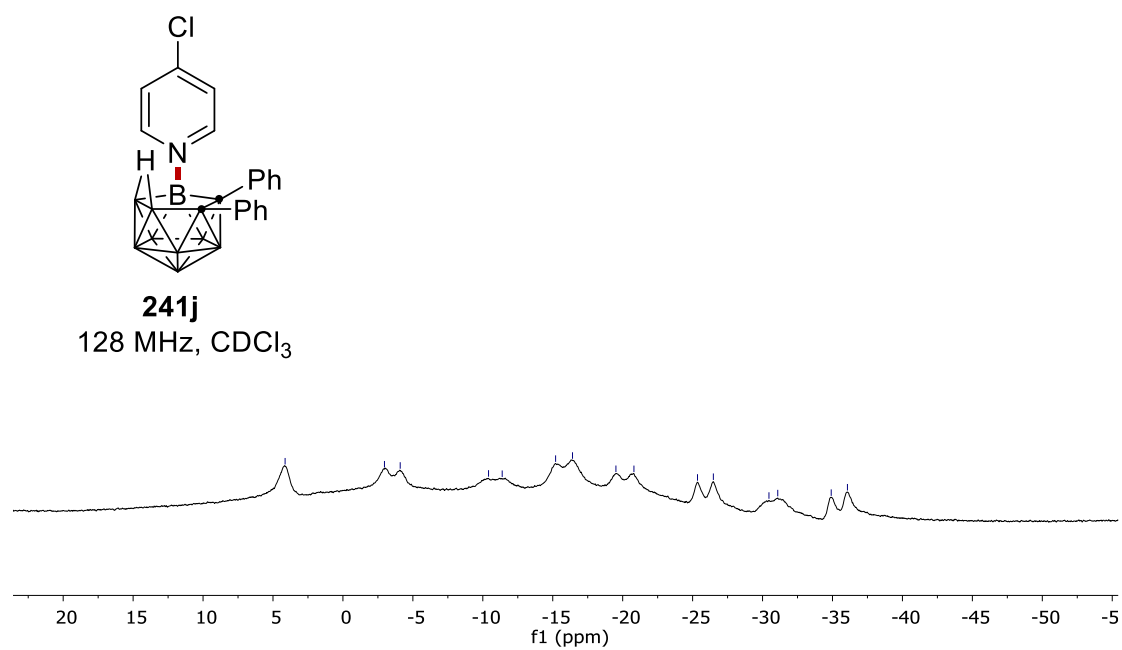
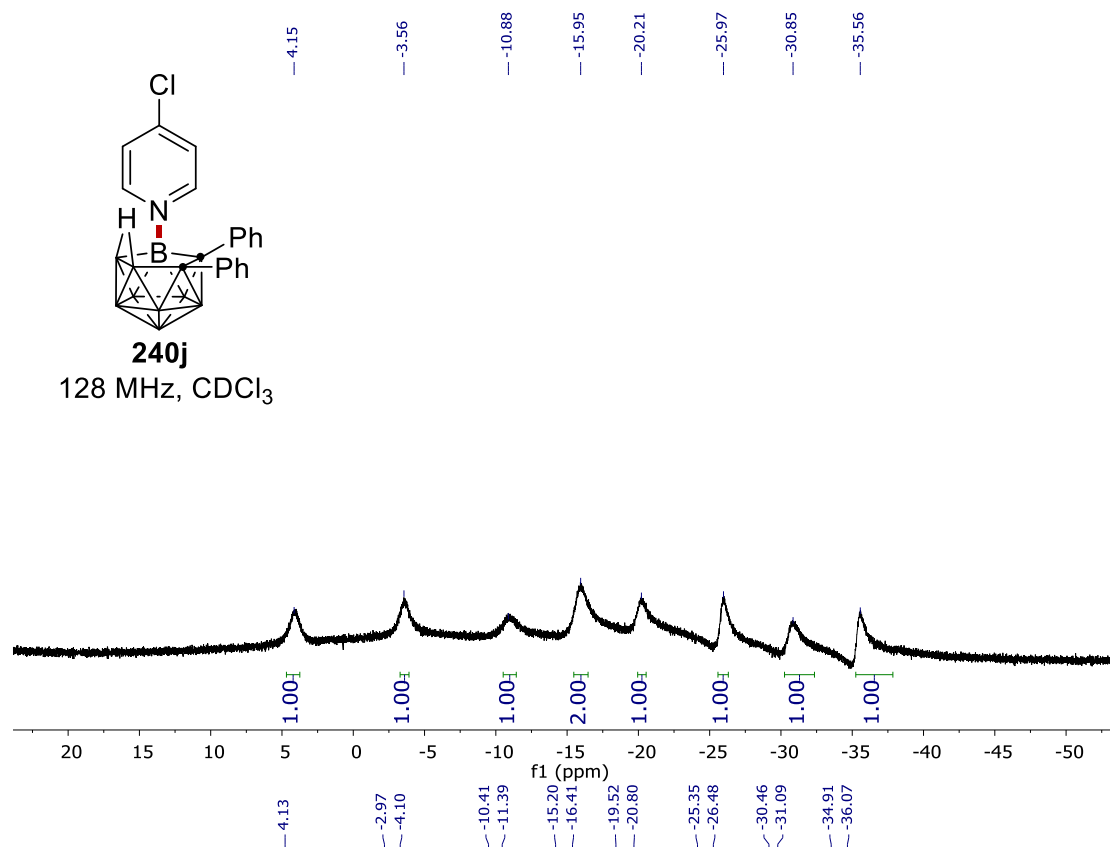
7. NMR Spectra



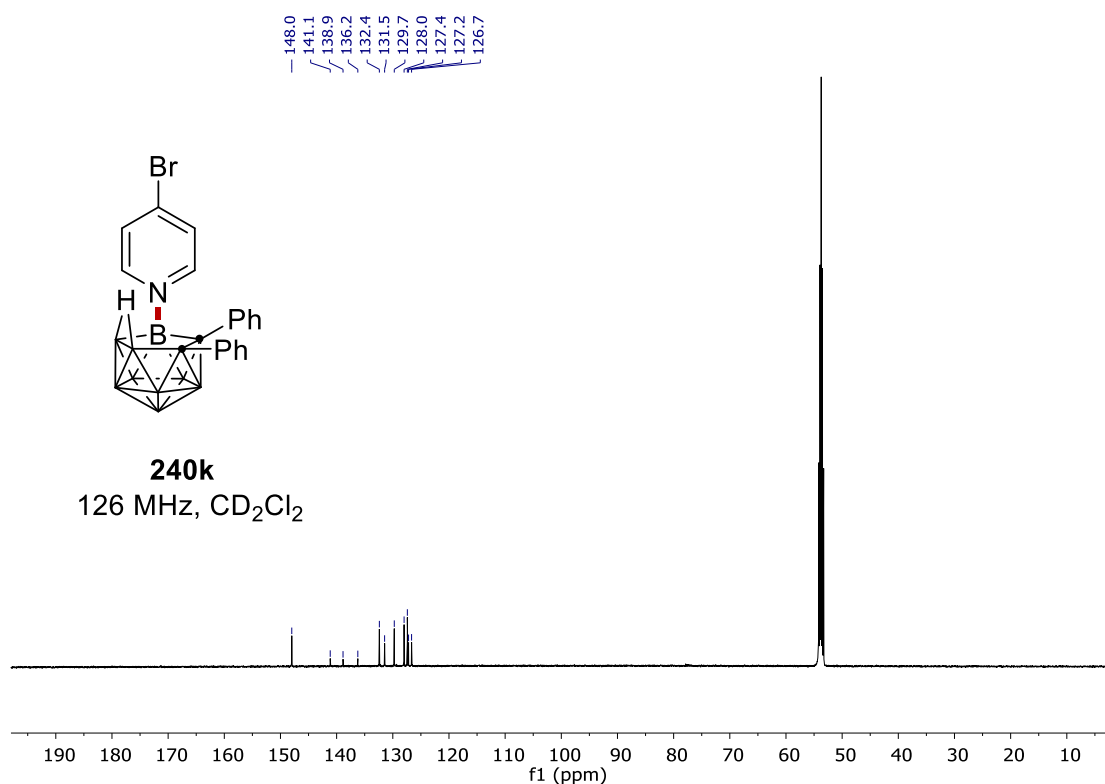
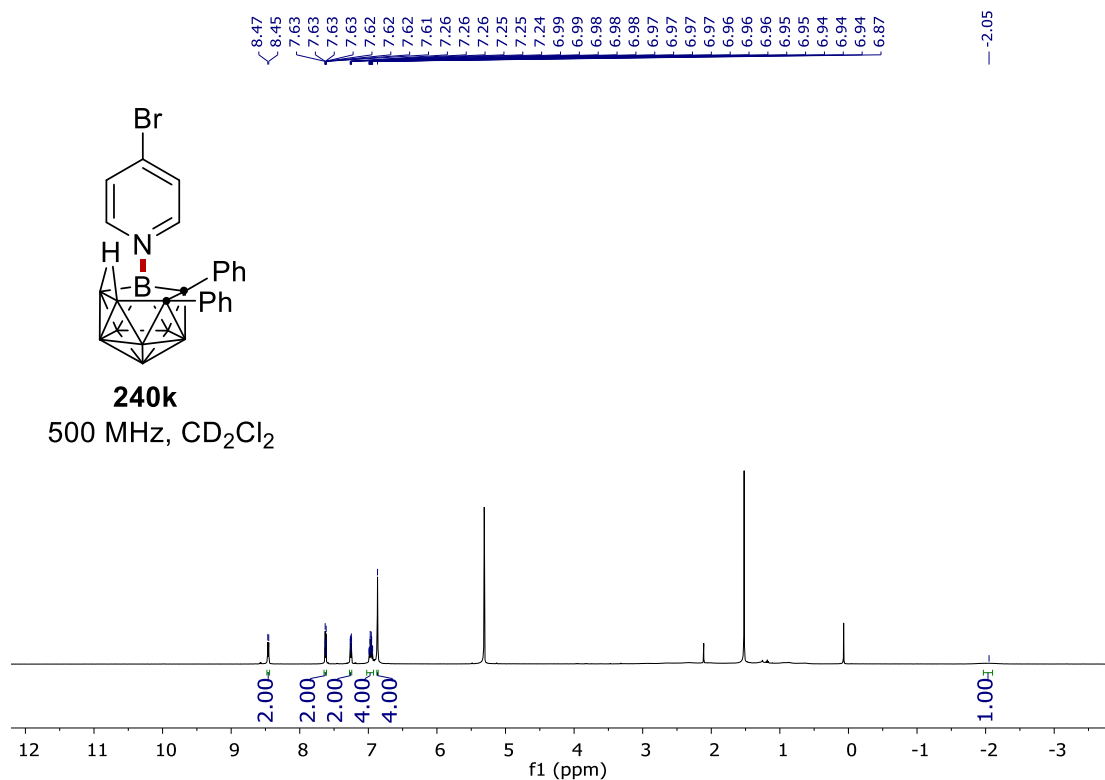
7. NMR Spectra



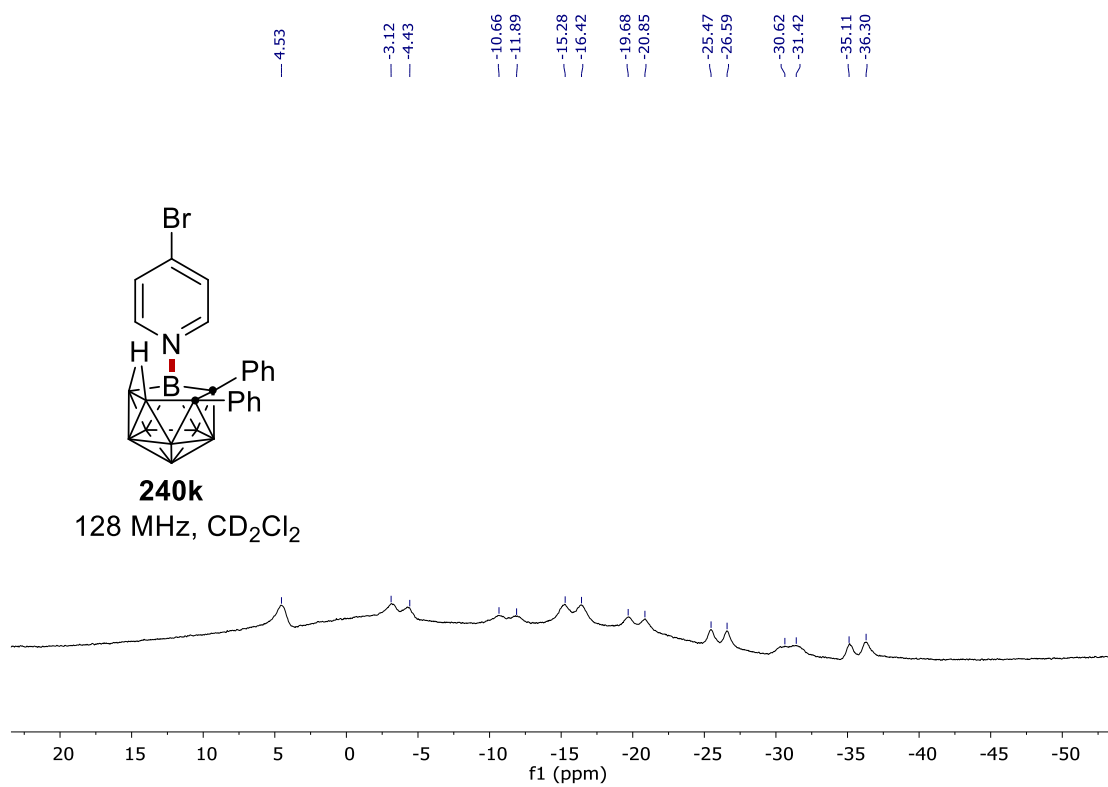
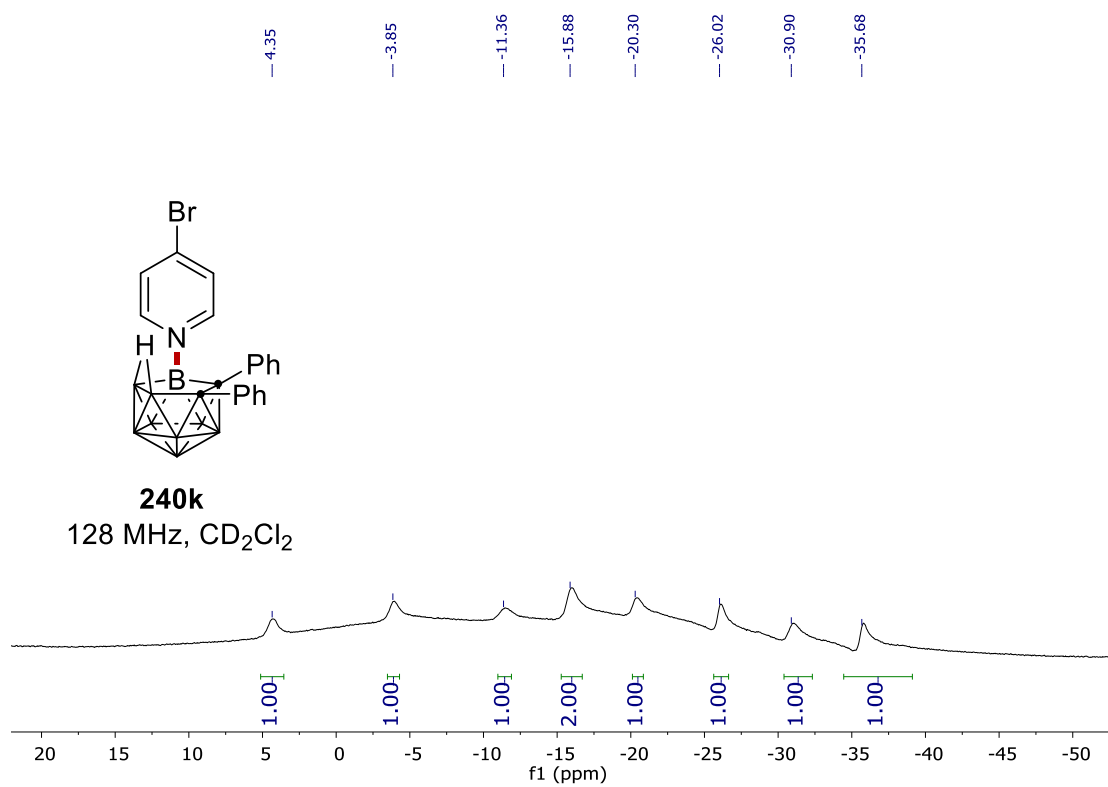
7. NMR Spectra



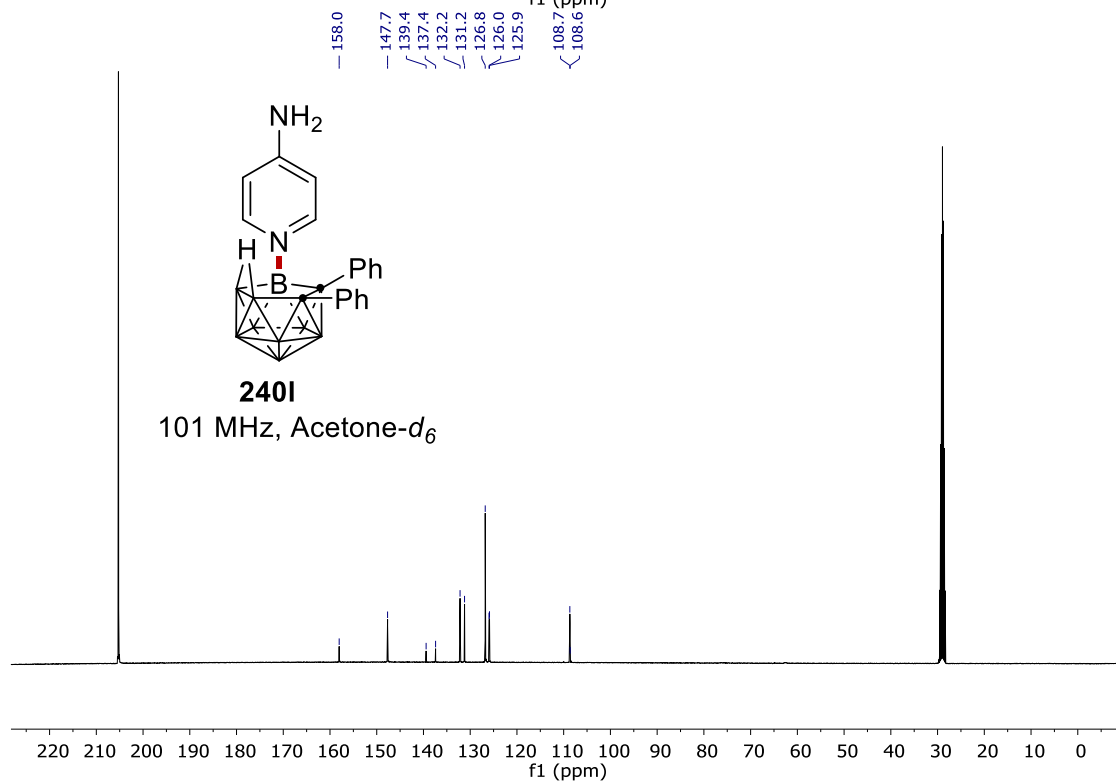
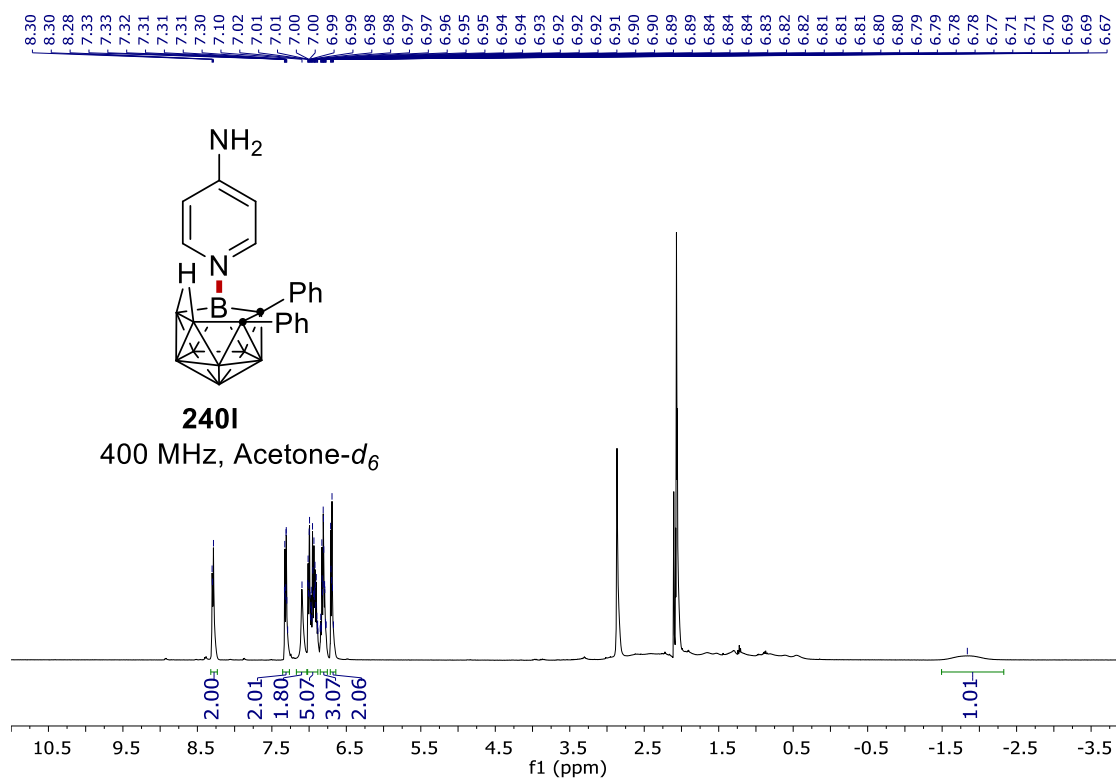
7. NMR Spectra



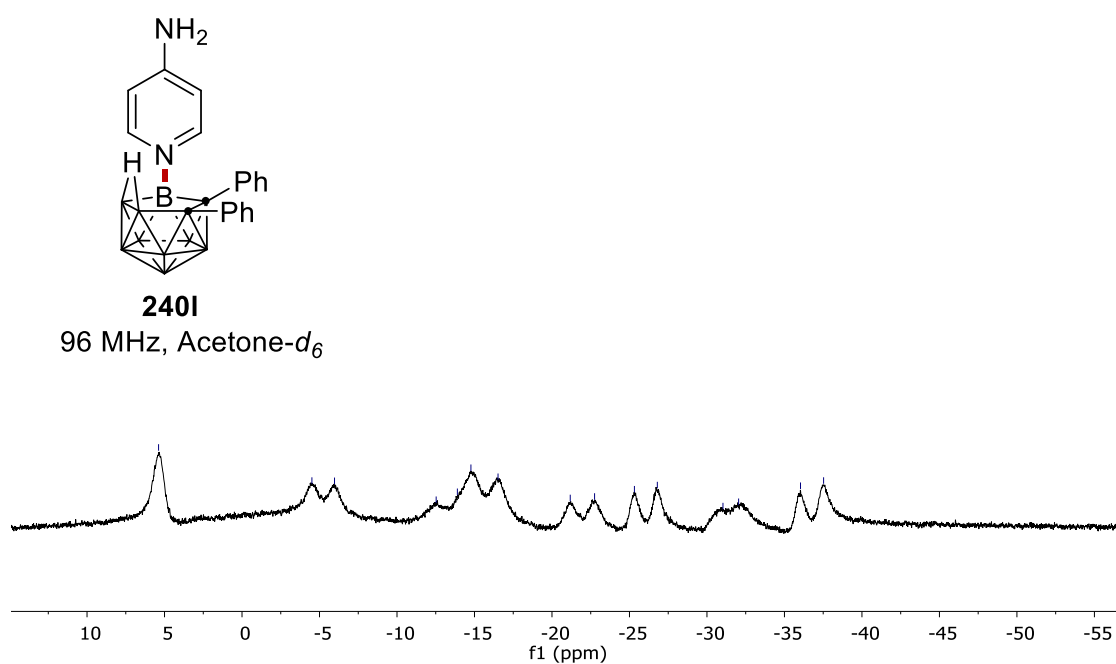
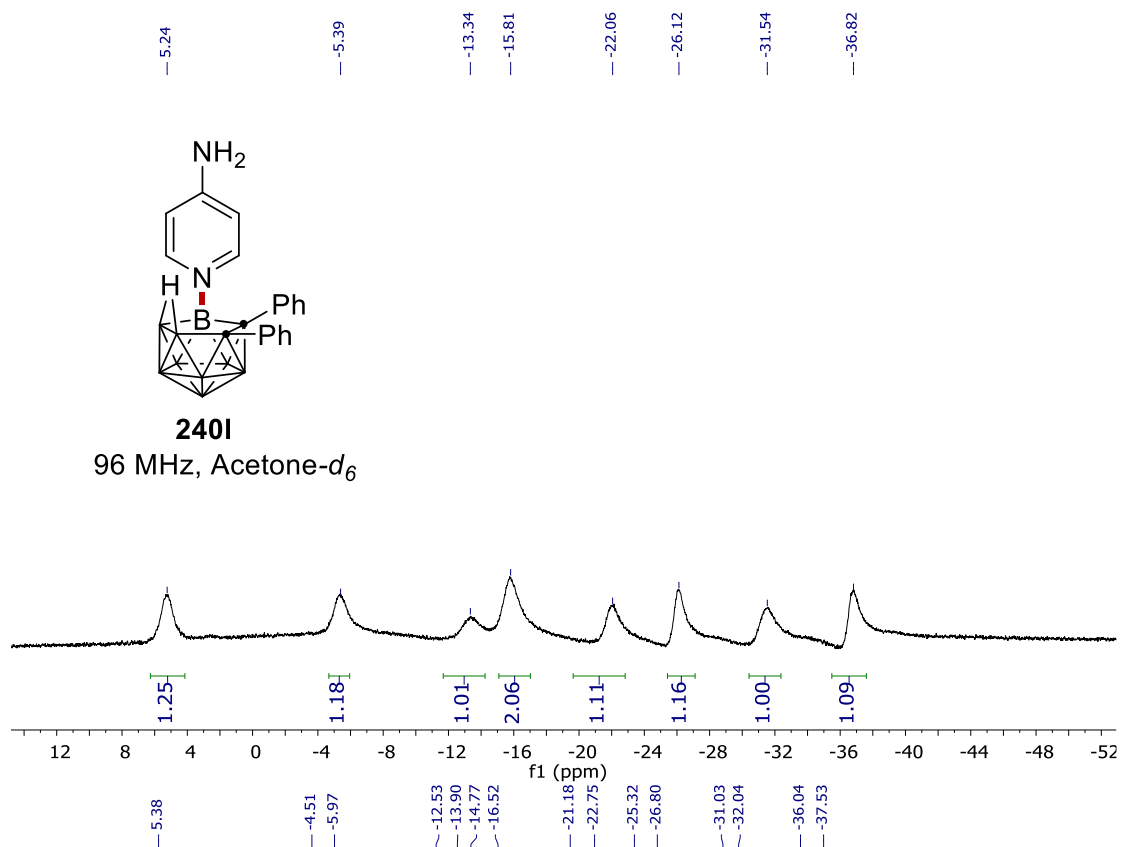
7. NMR Spectra



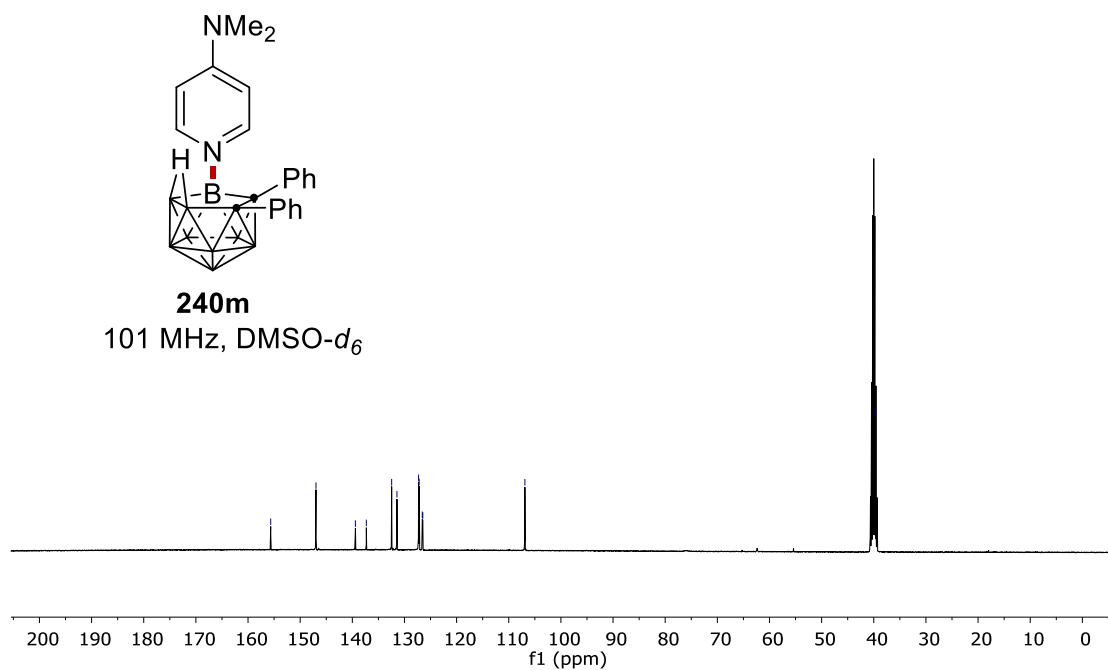
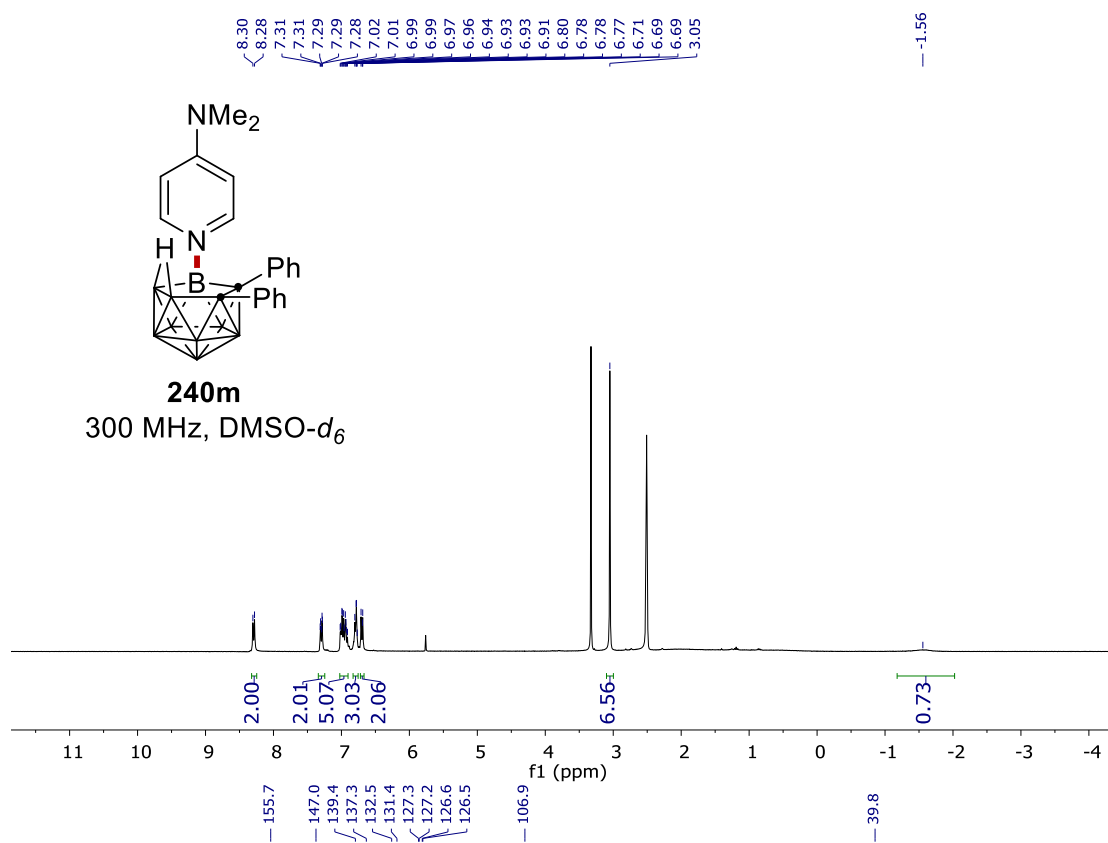
7. NMR Spectra



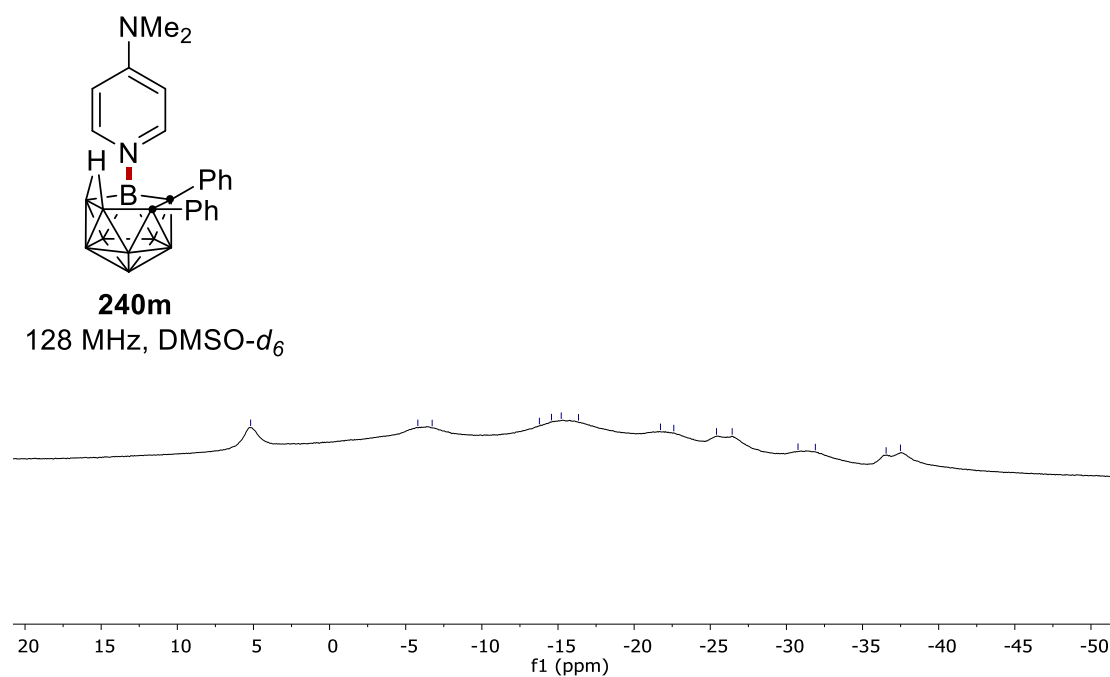
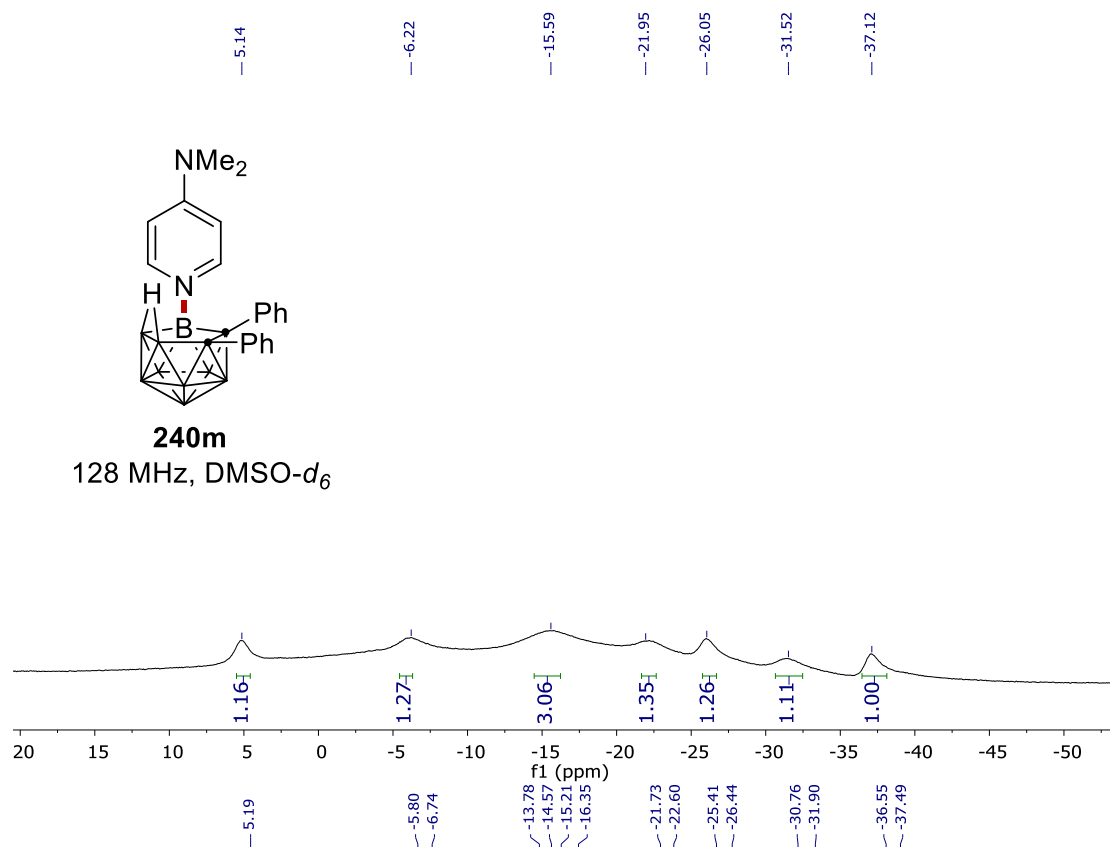
7. NMR Spectra



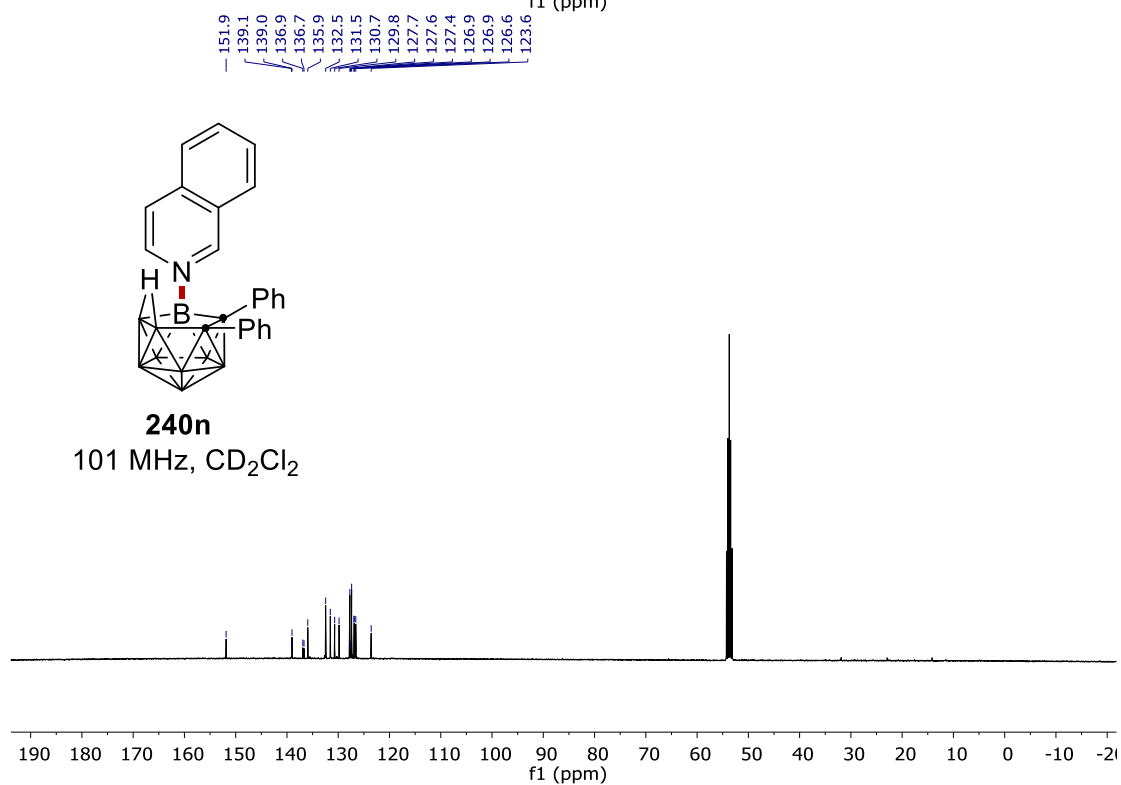
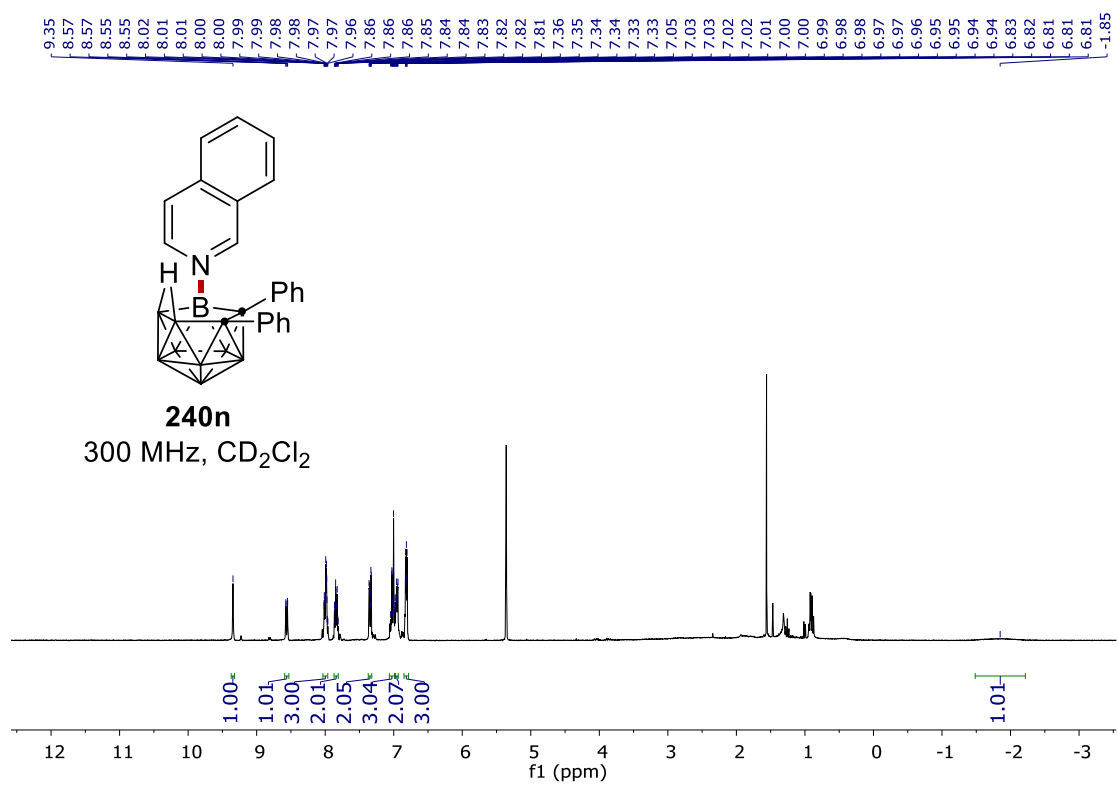
7. NMR Spectra



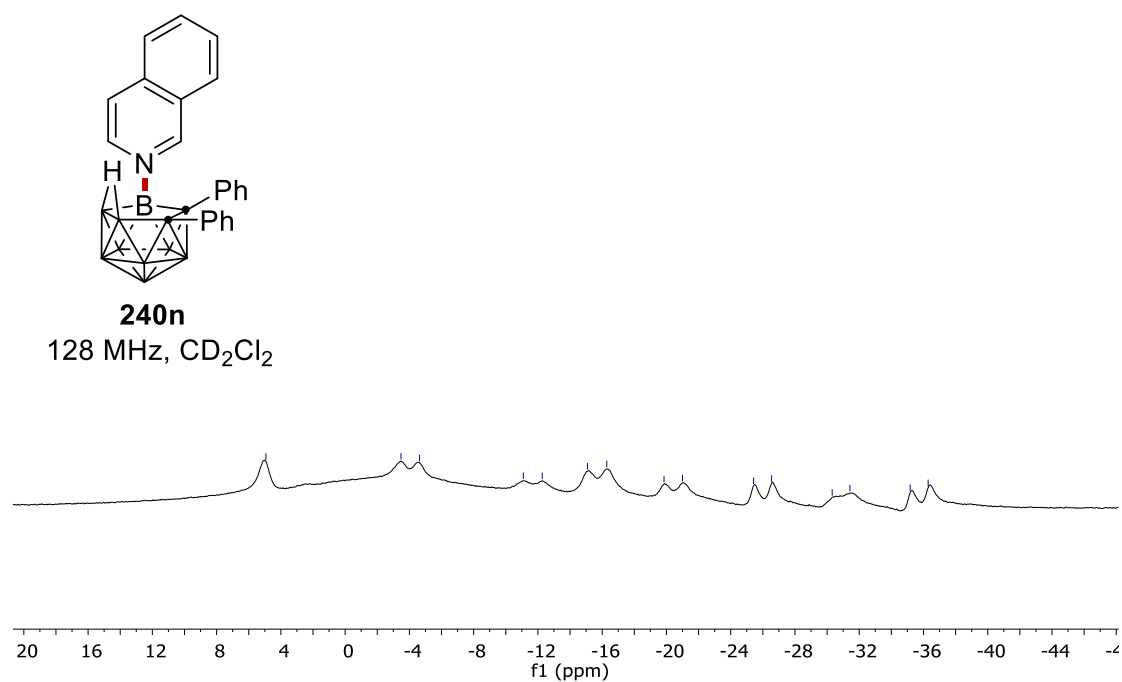
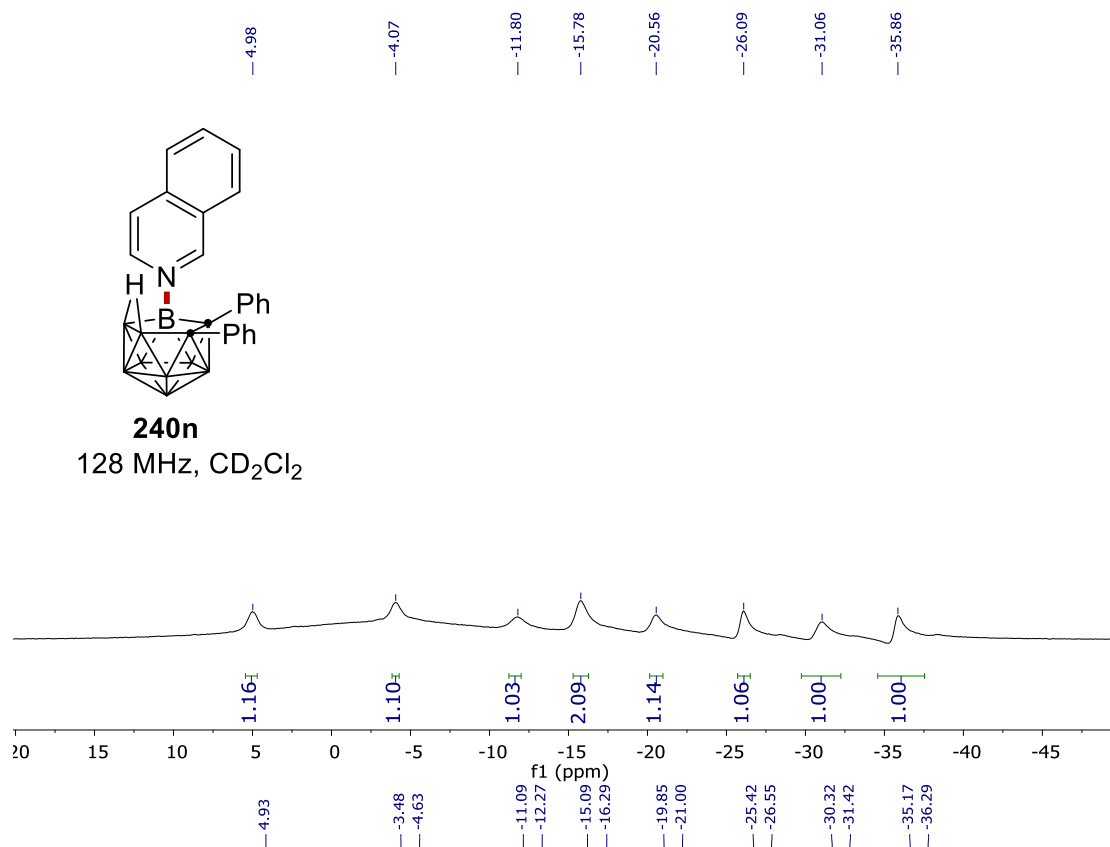
7. NMR Spectra



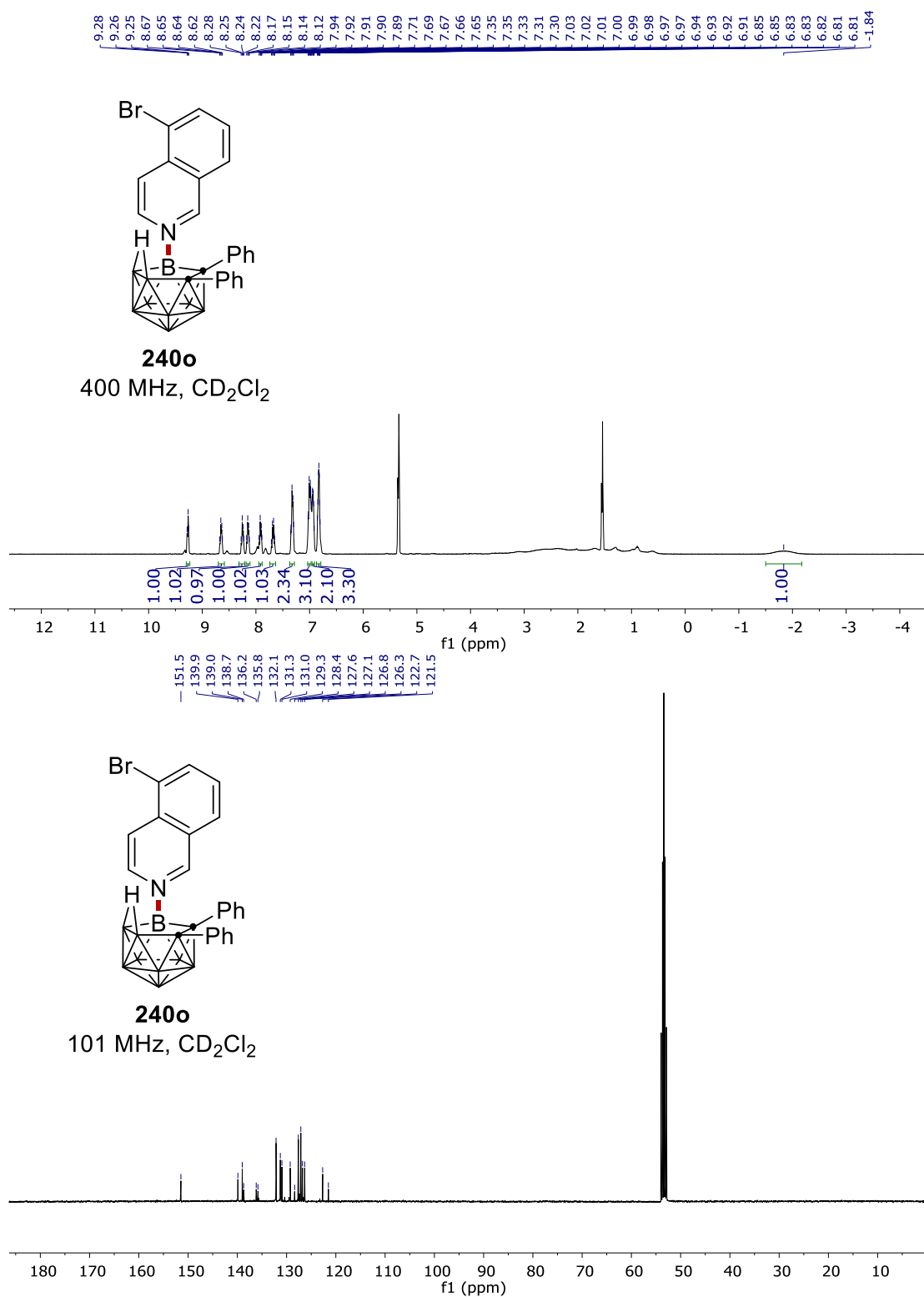
7. NMR Spectra



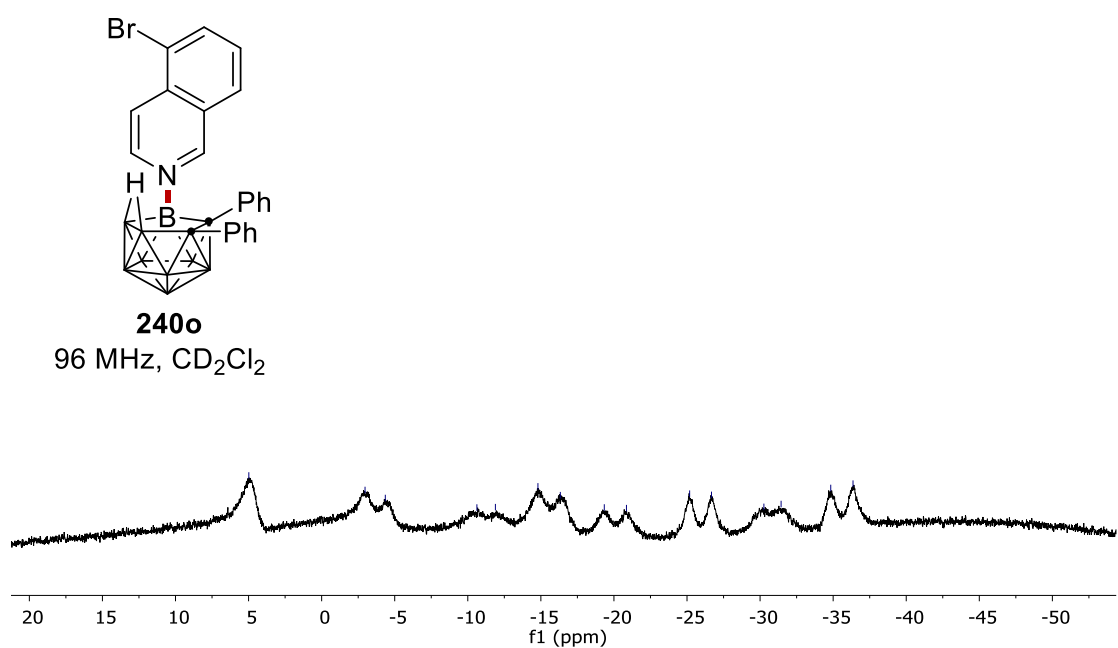
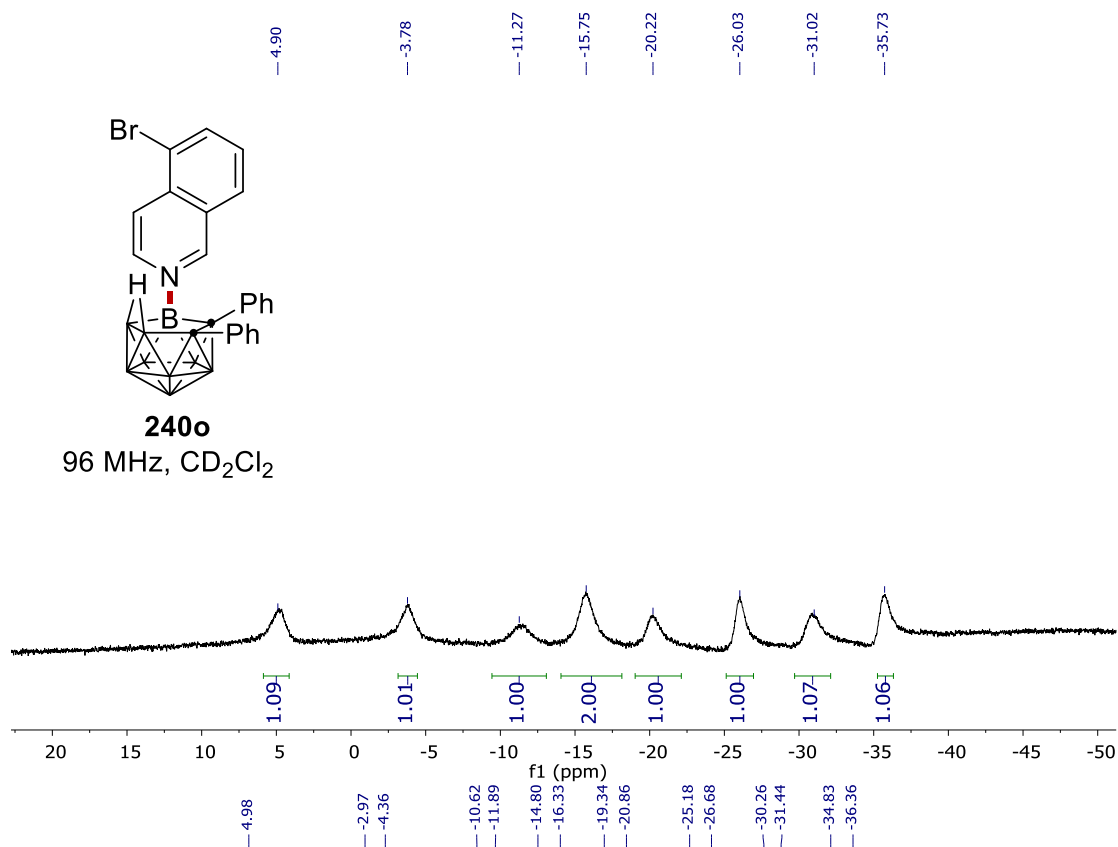
7. NMR Spectra



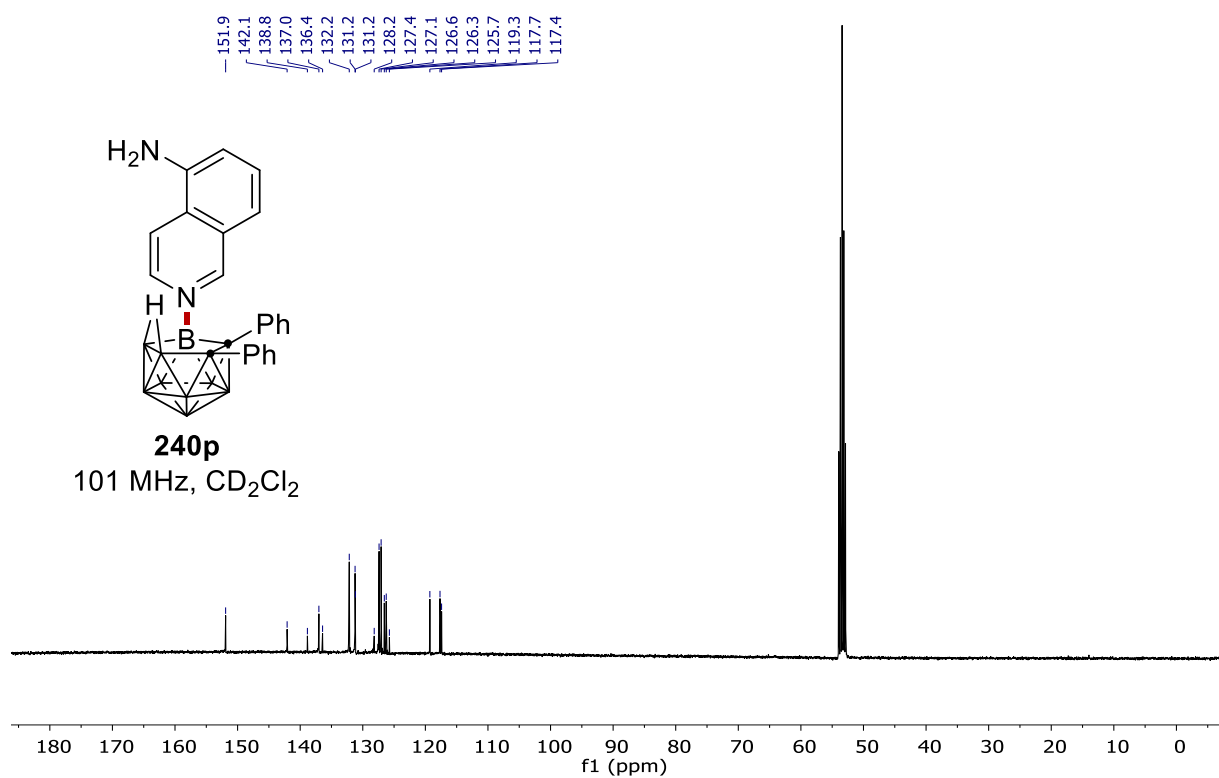
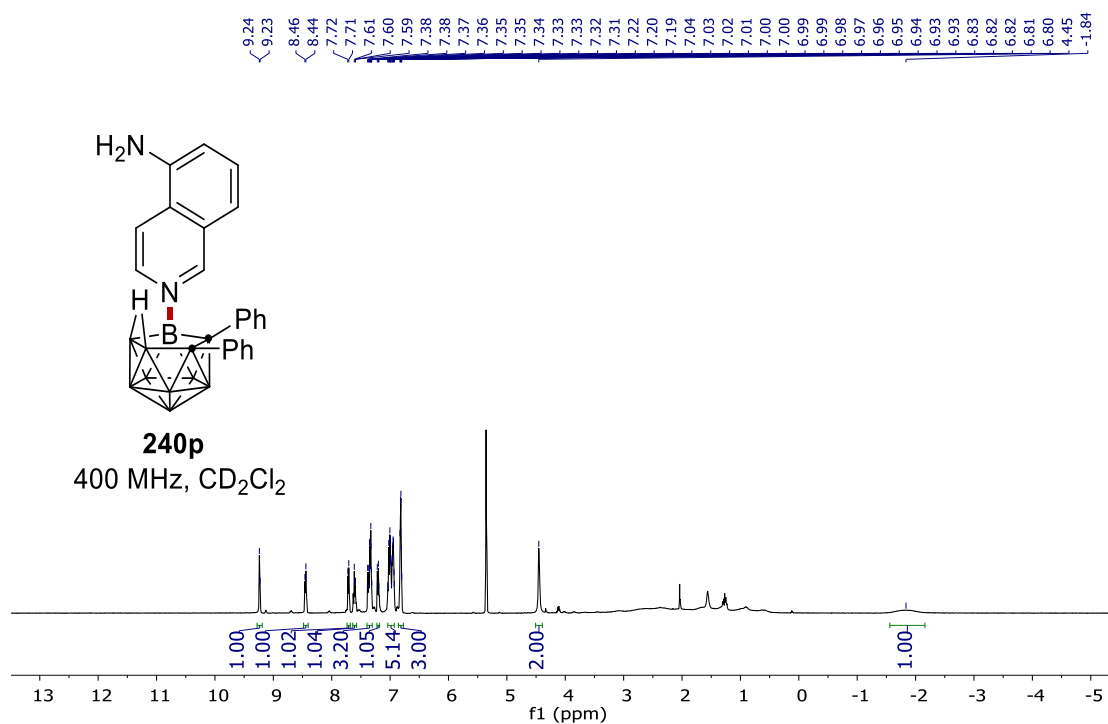
7. NMR Spectra



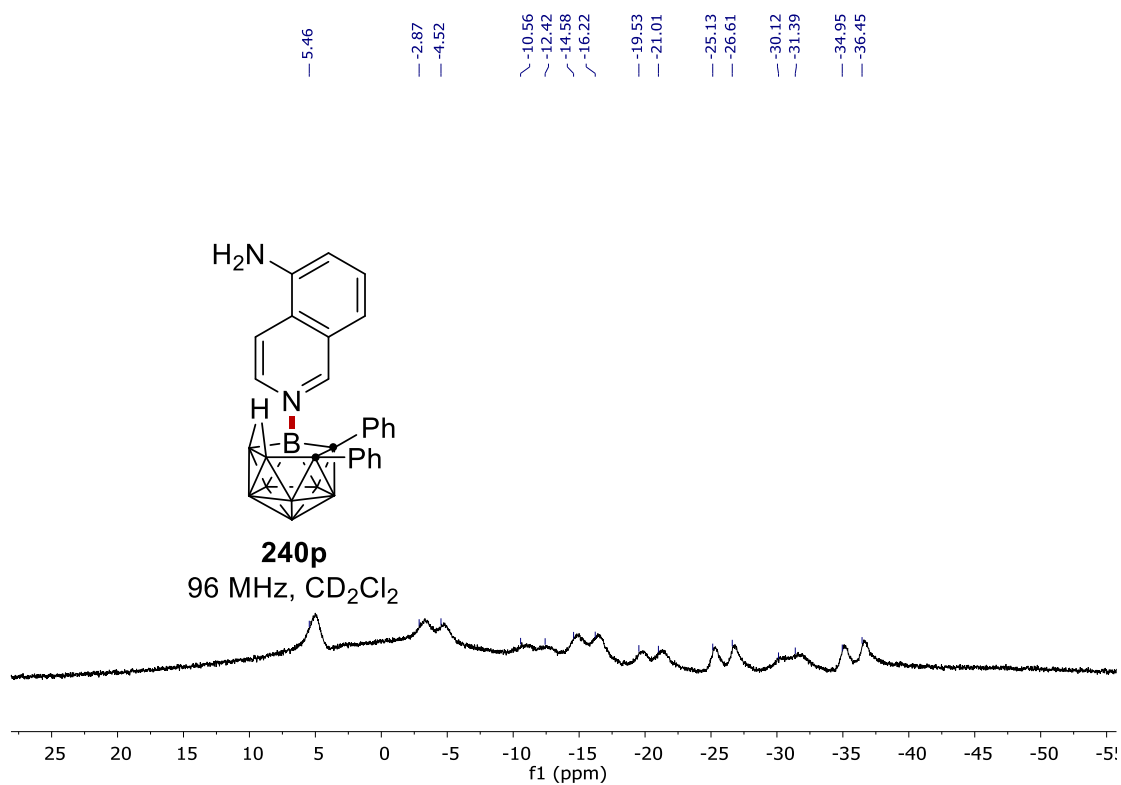
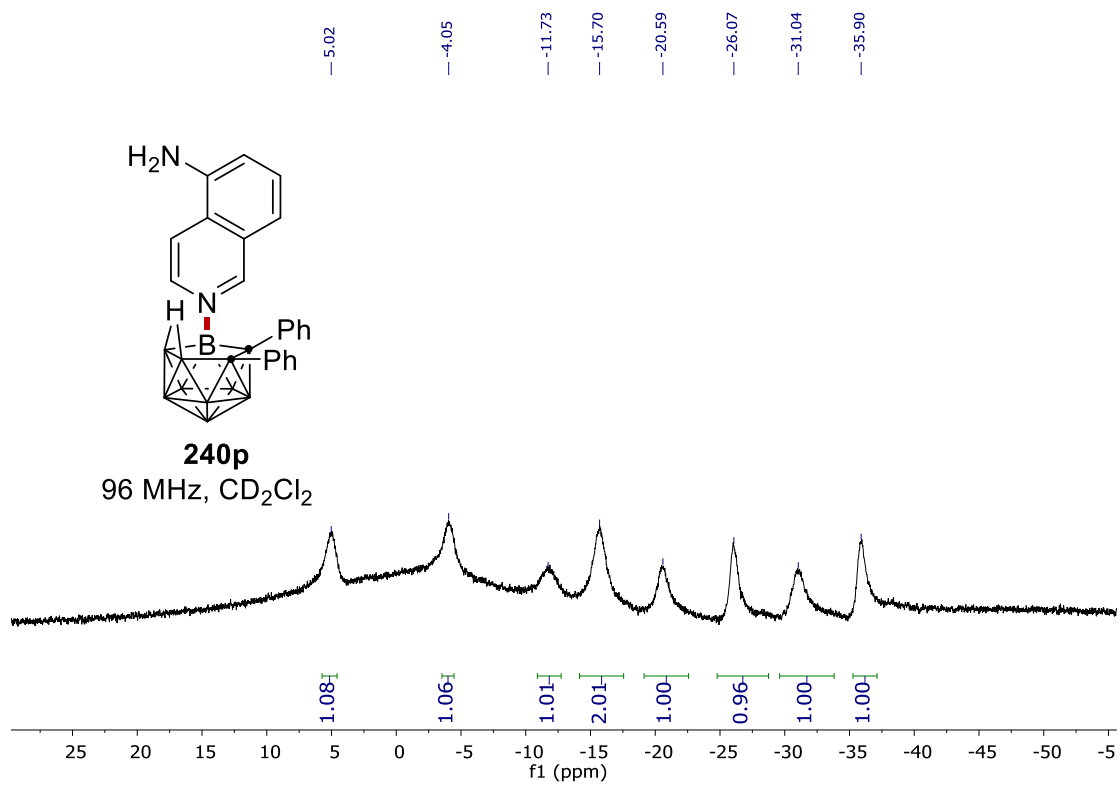
7. NMR Spectra



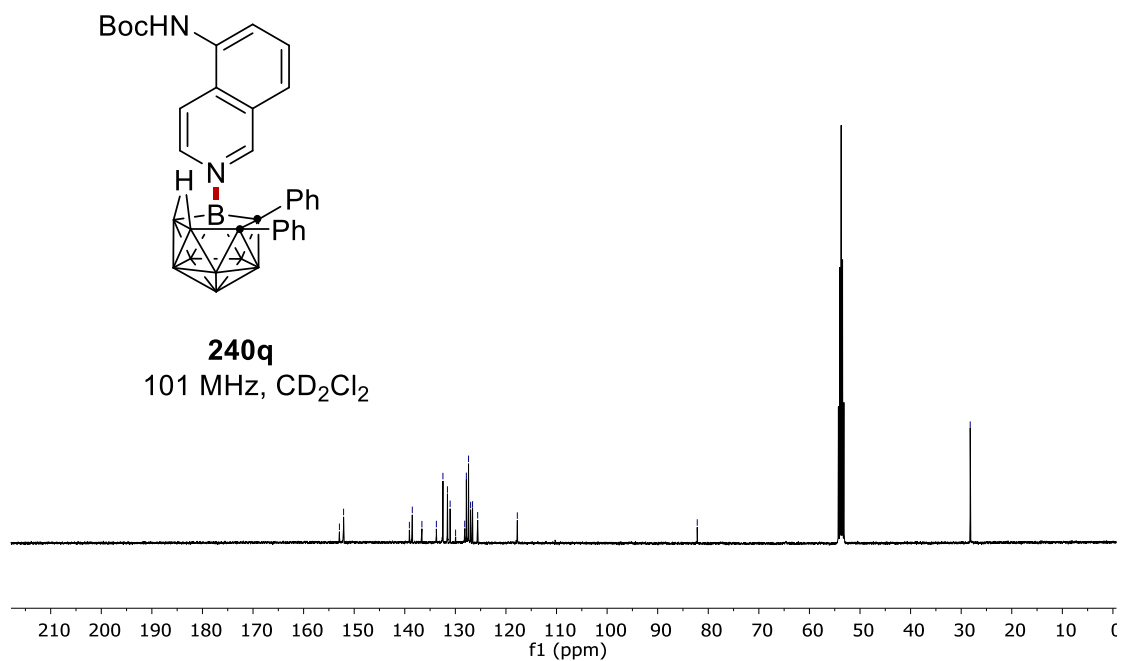
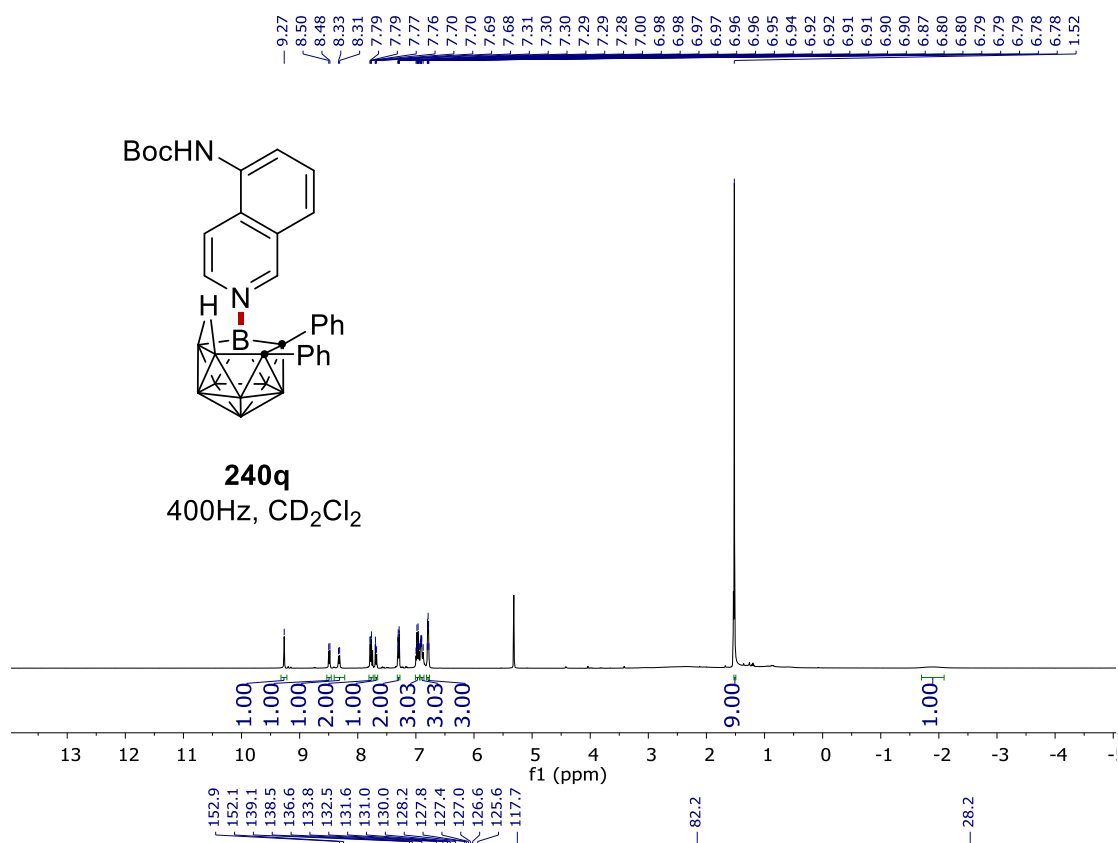
7. NMR Spectra



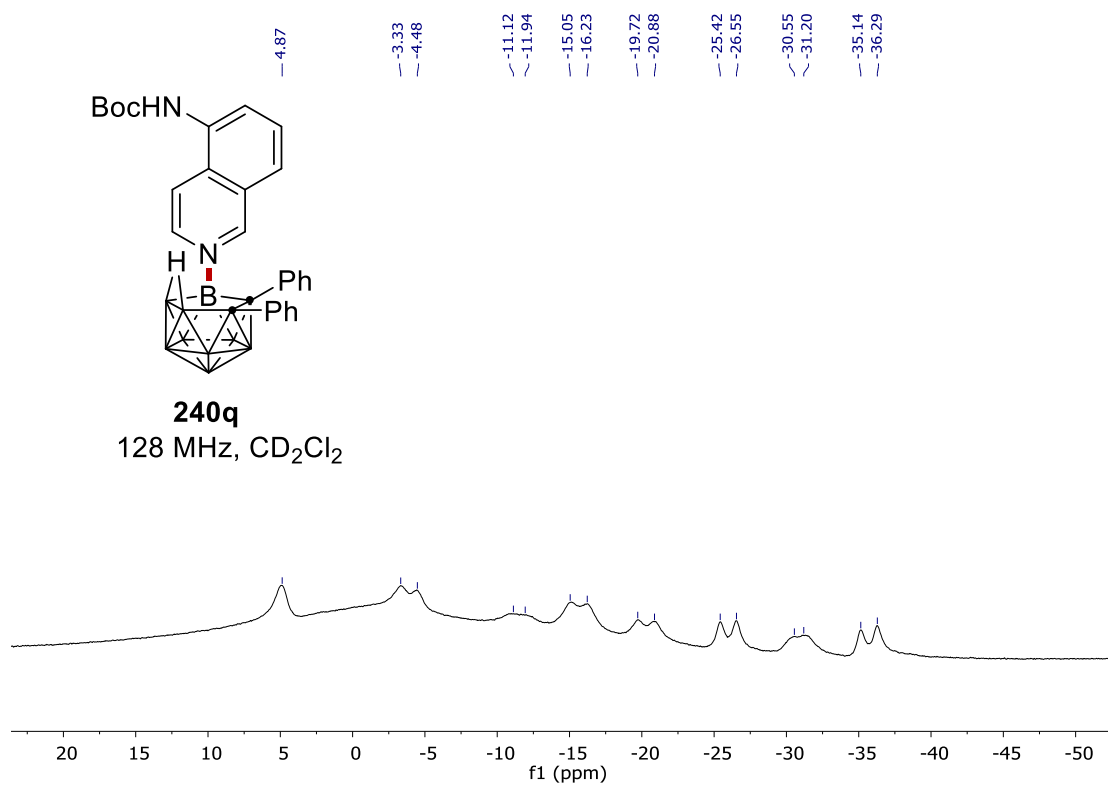
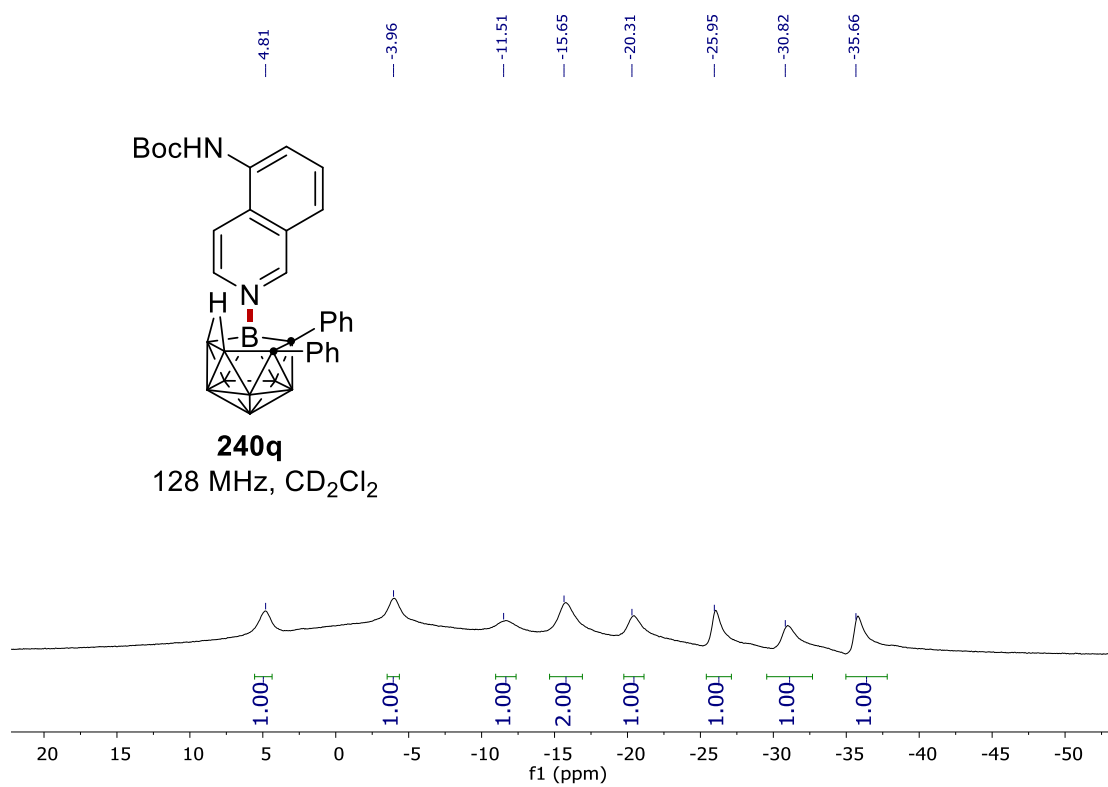
7. NMR Spectra

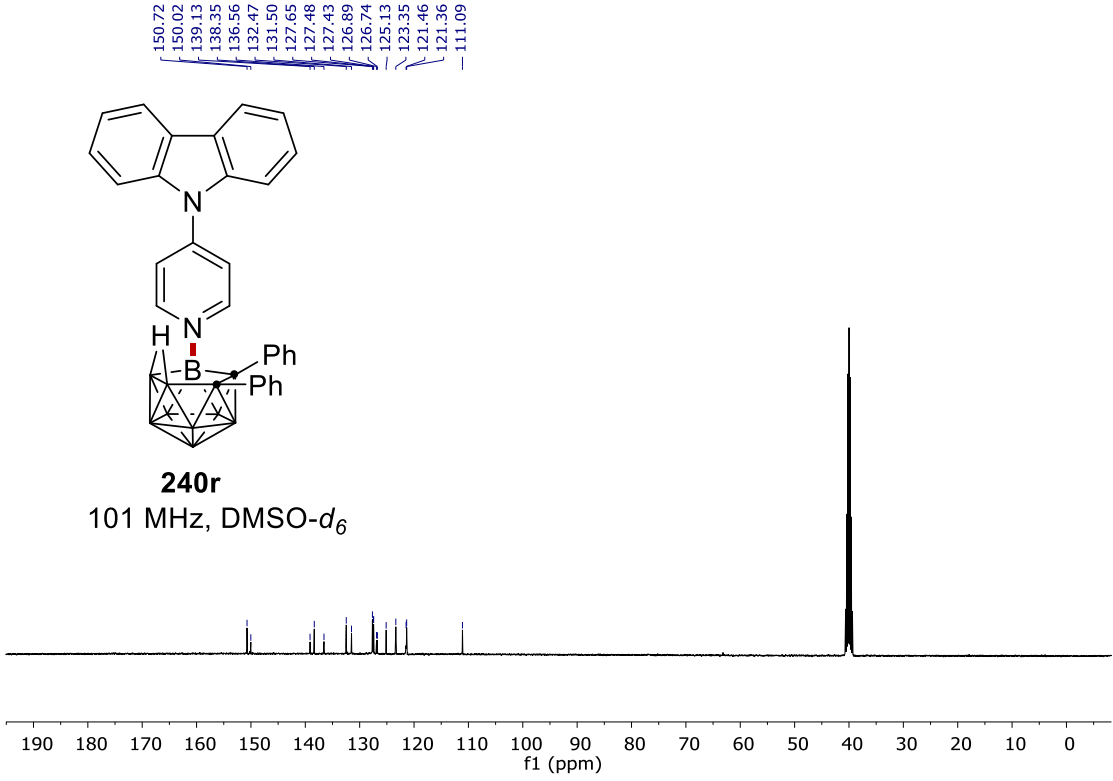
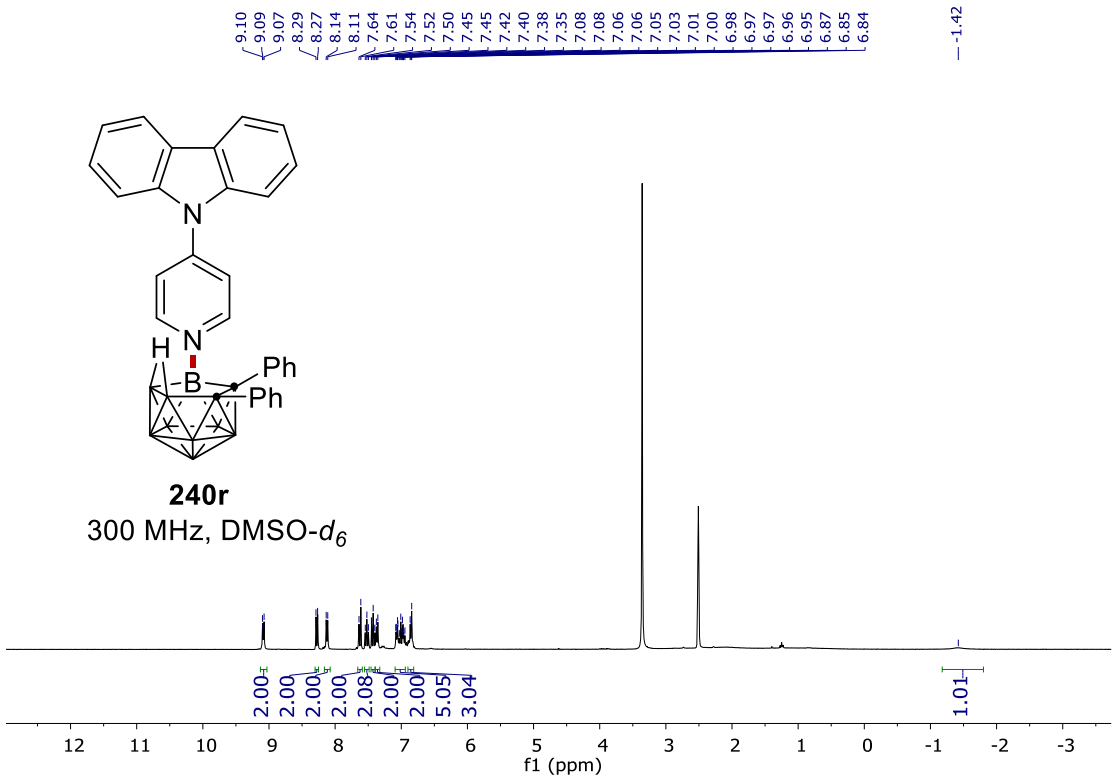


7. NMR Spectra

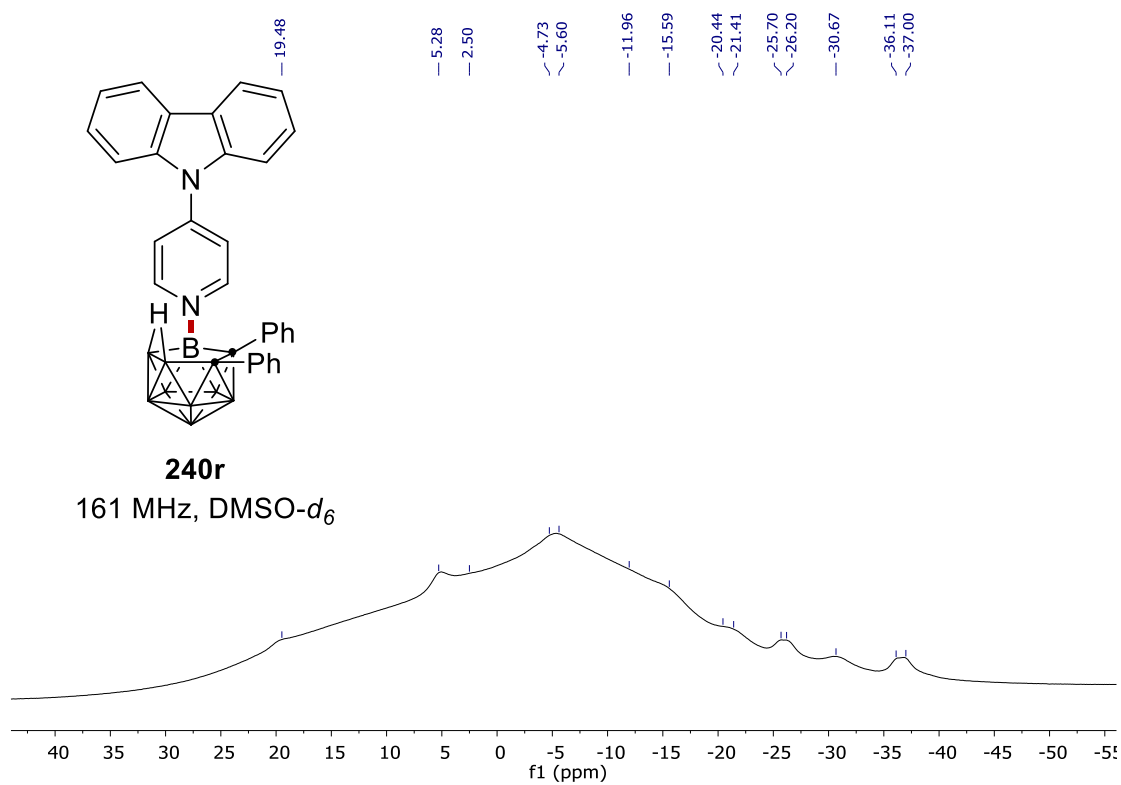
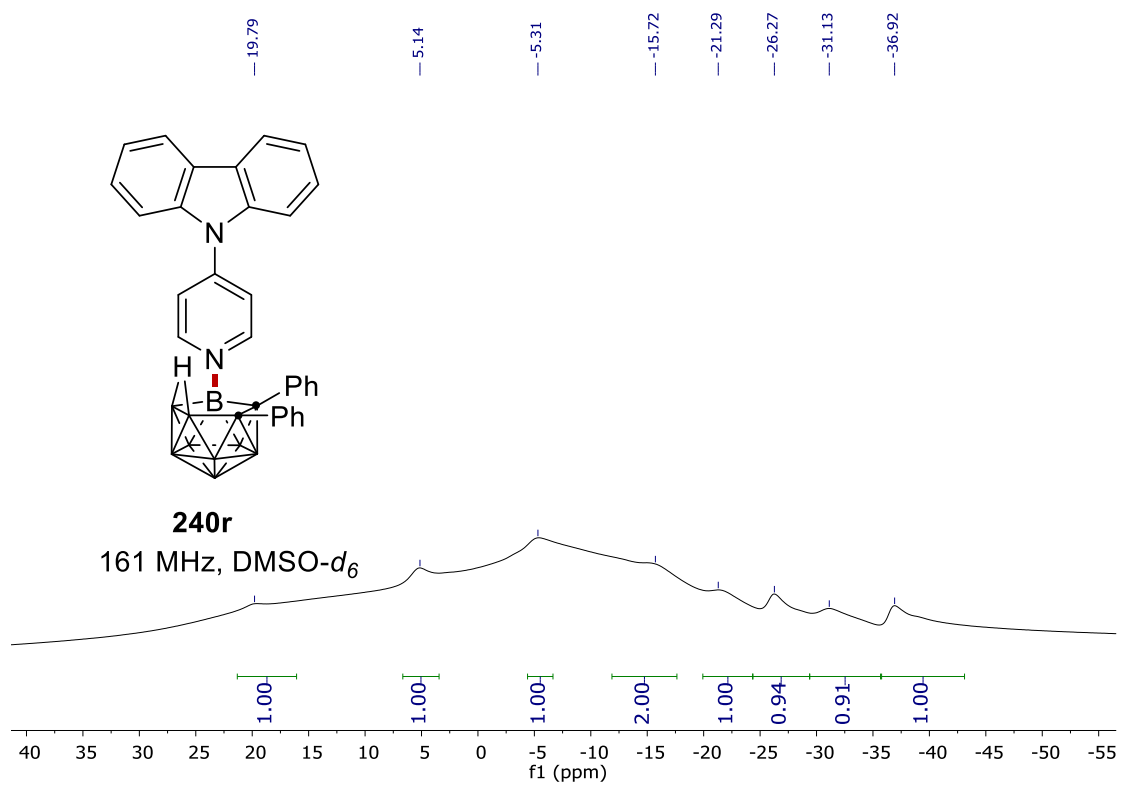


7. NMR Spectra

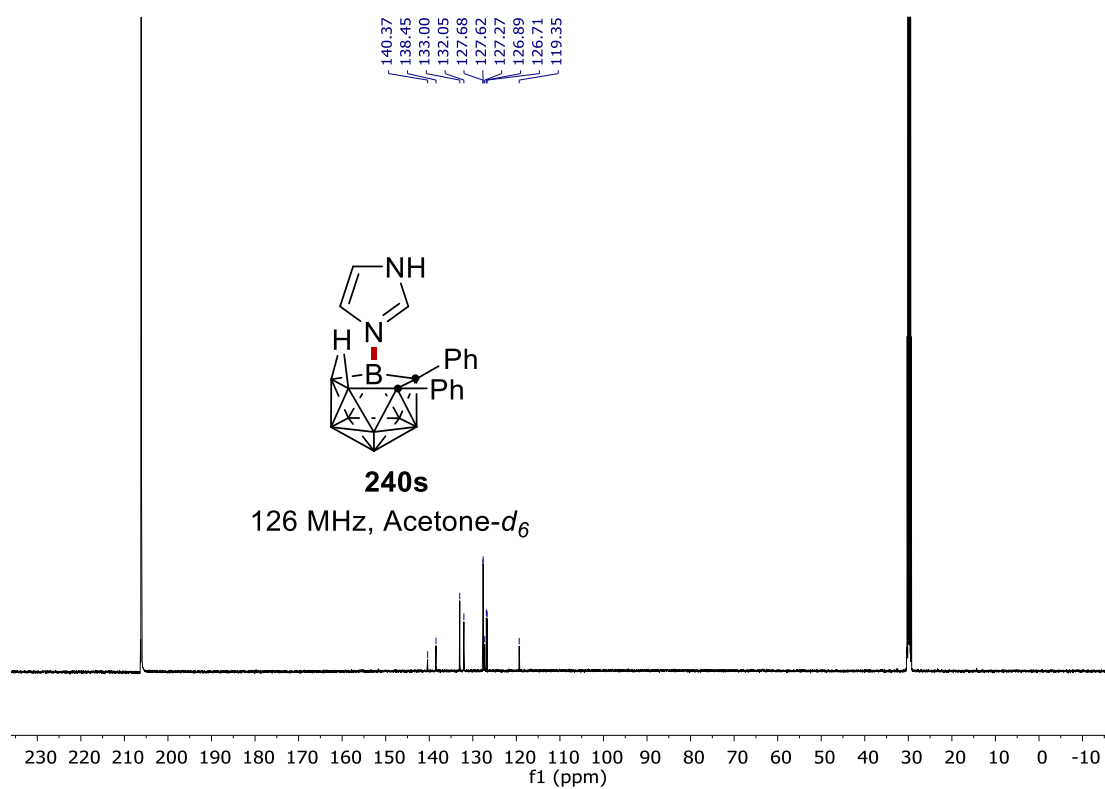
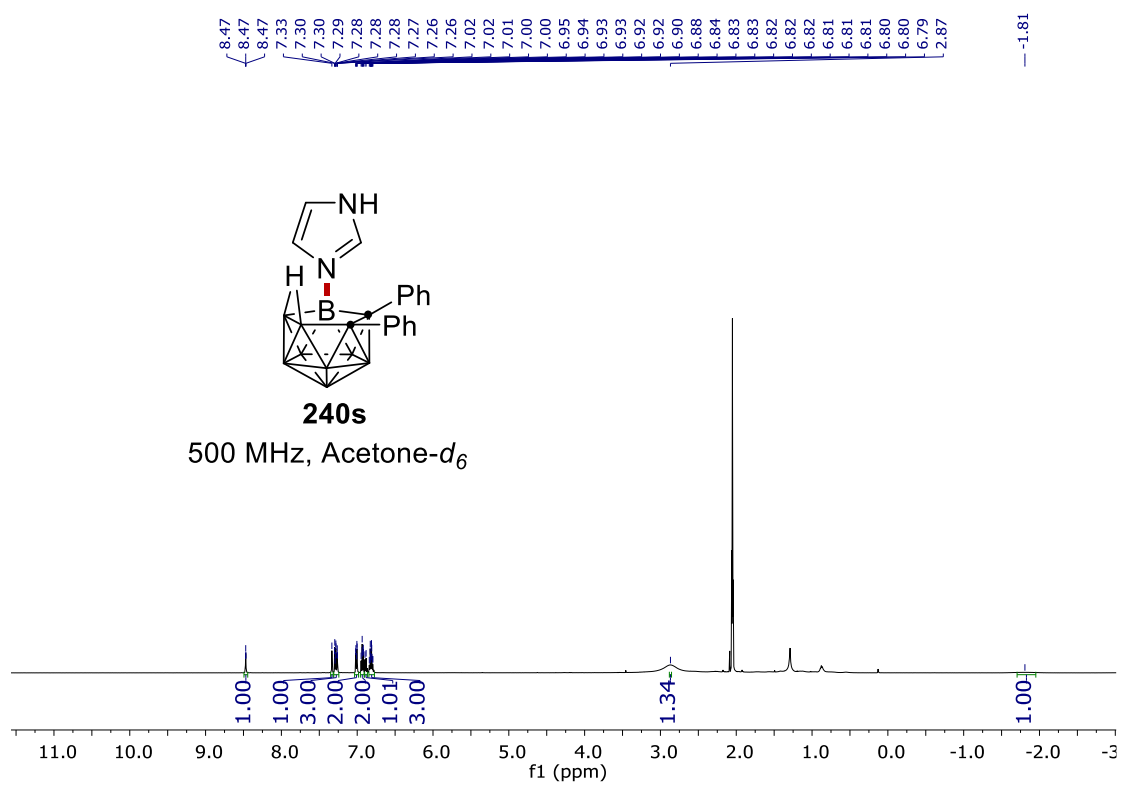




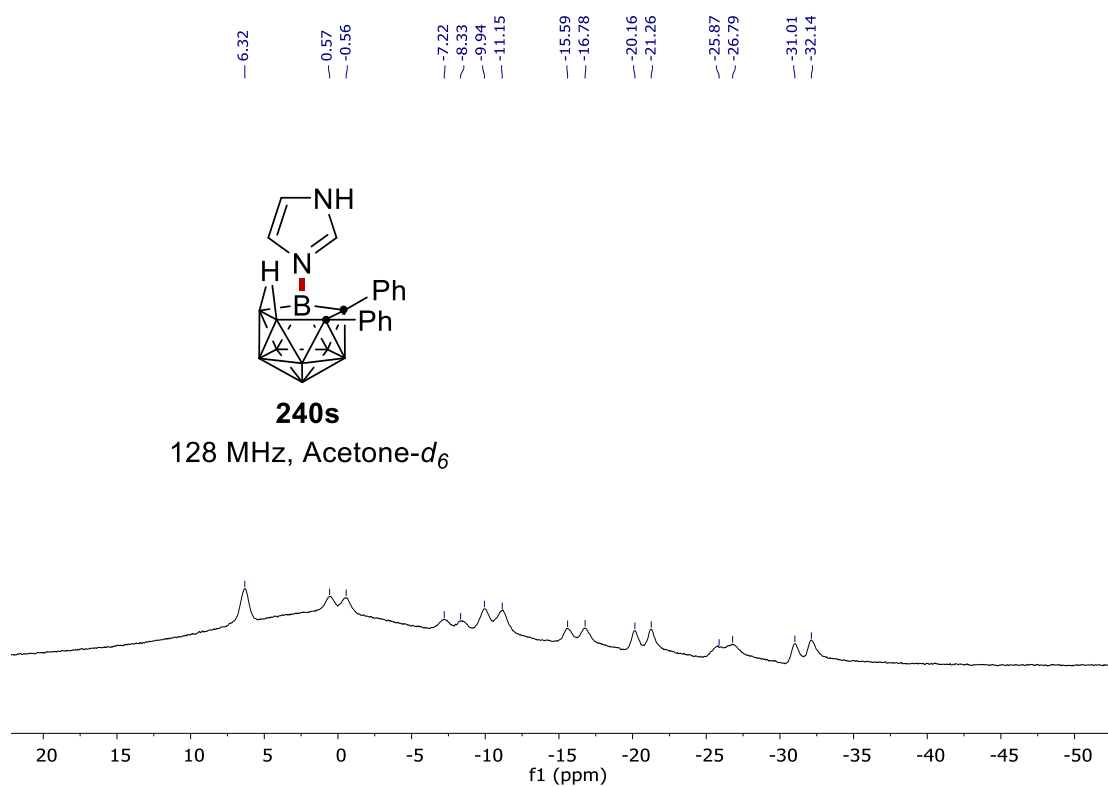
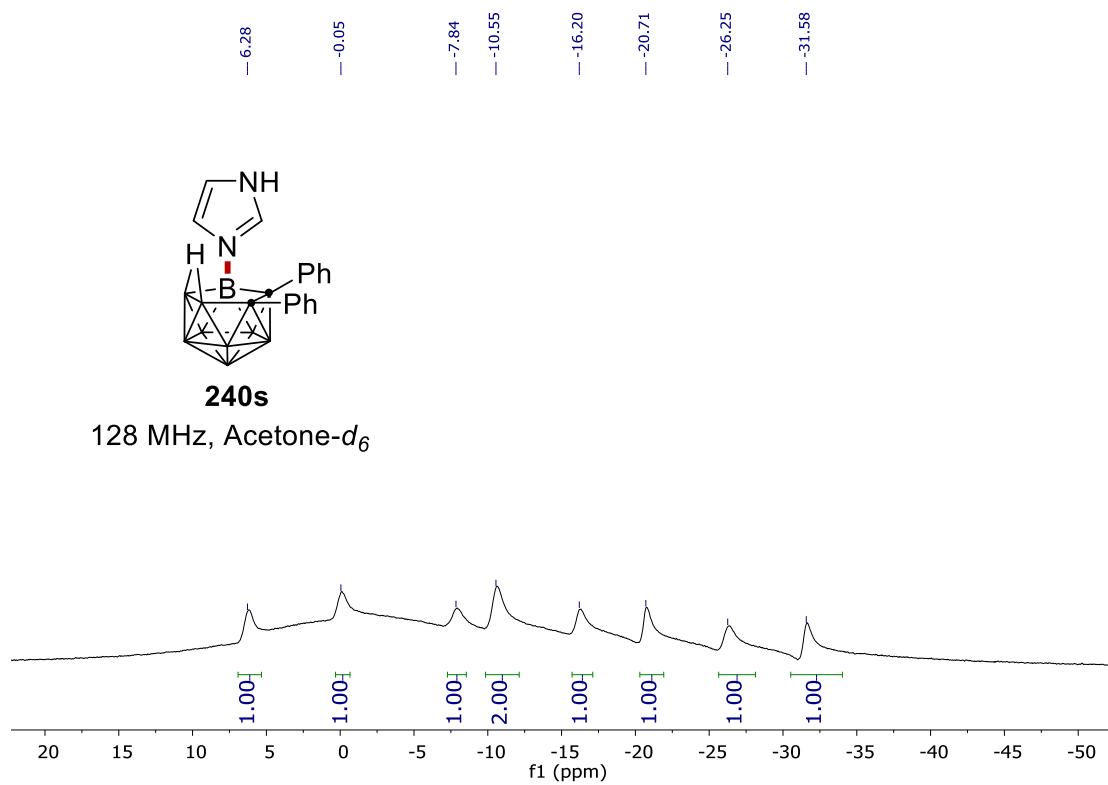
7. NMR Spectra



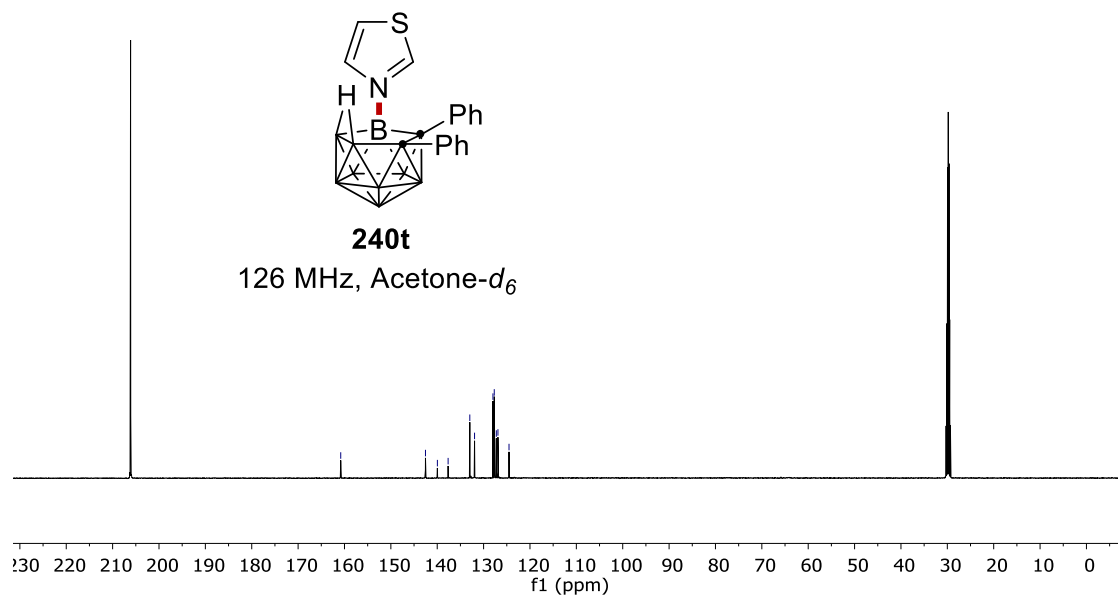
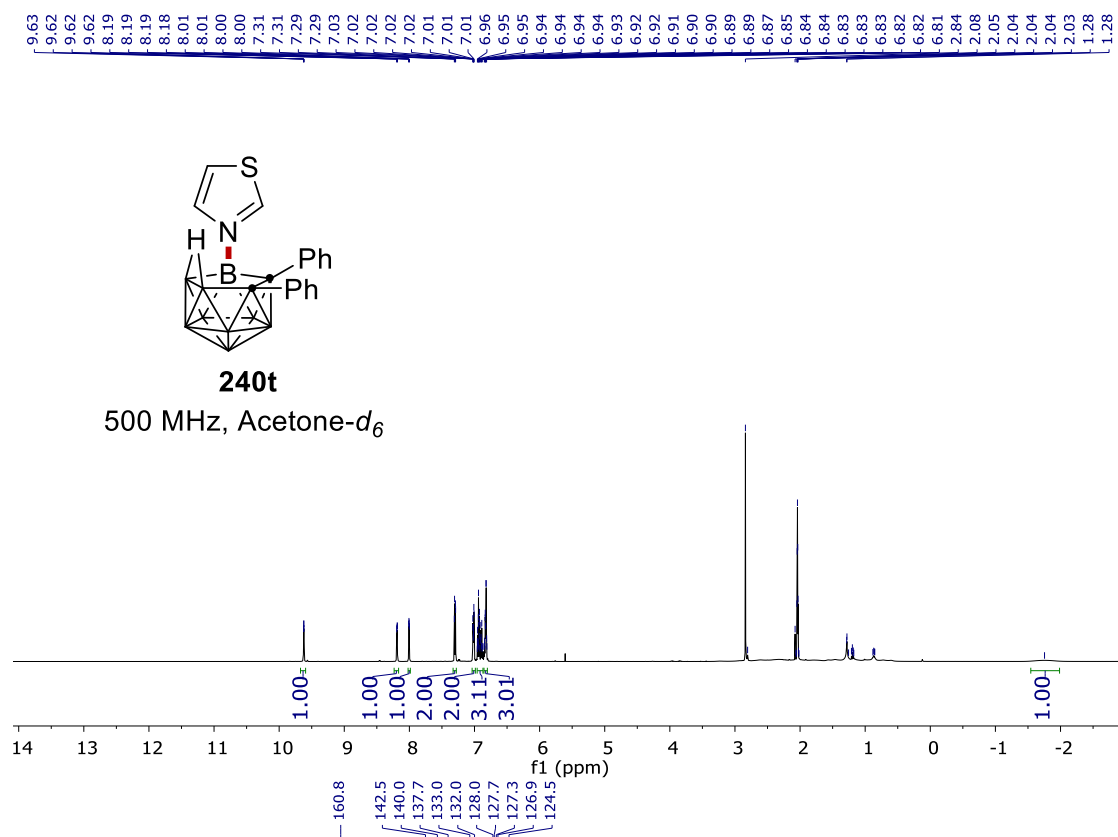
7. NMR Spectra



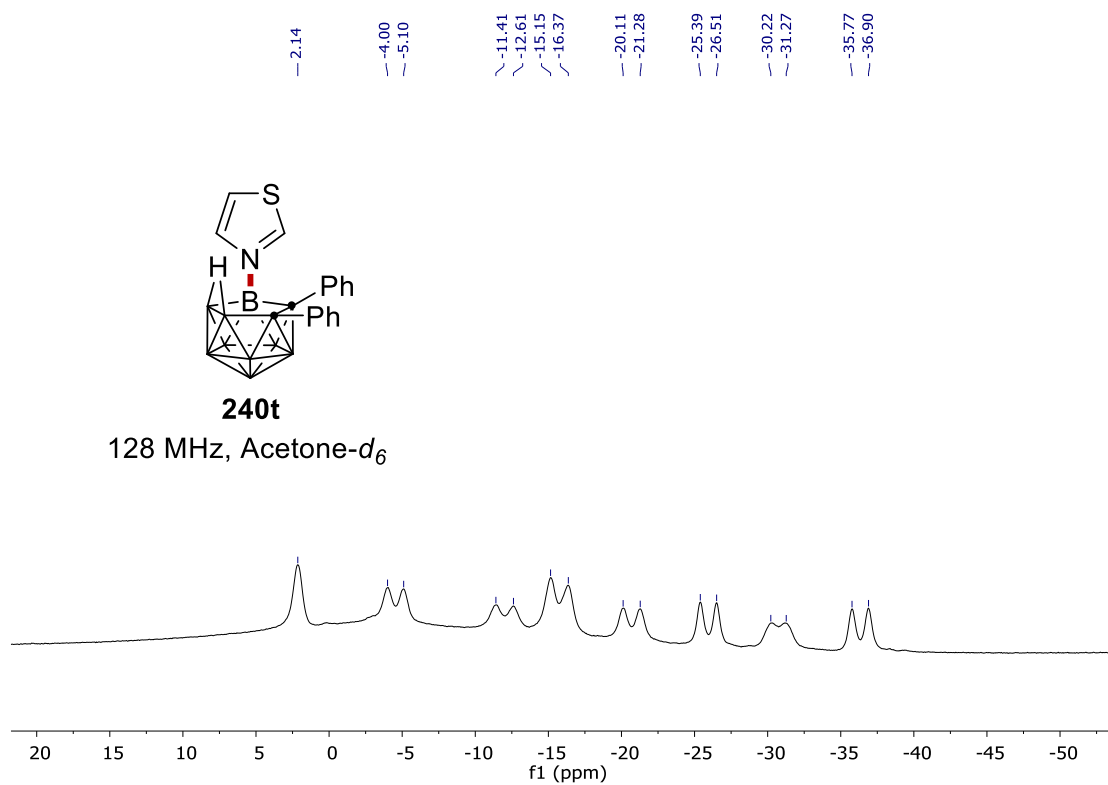
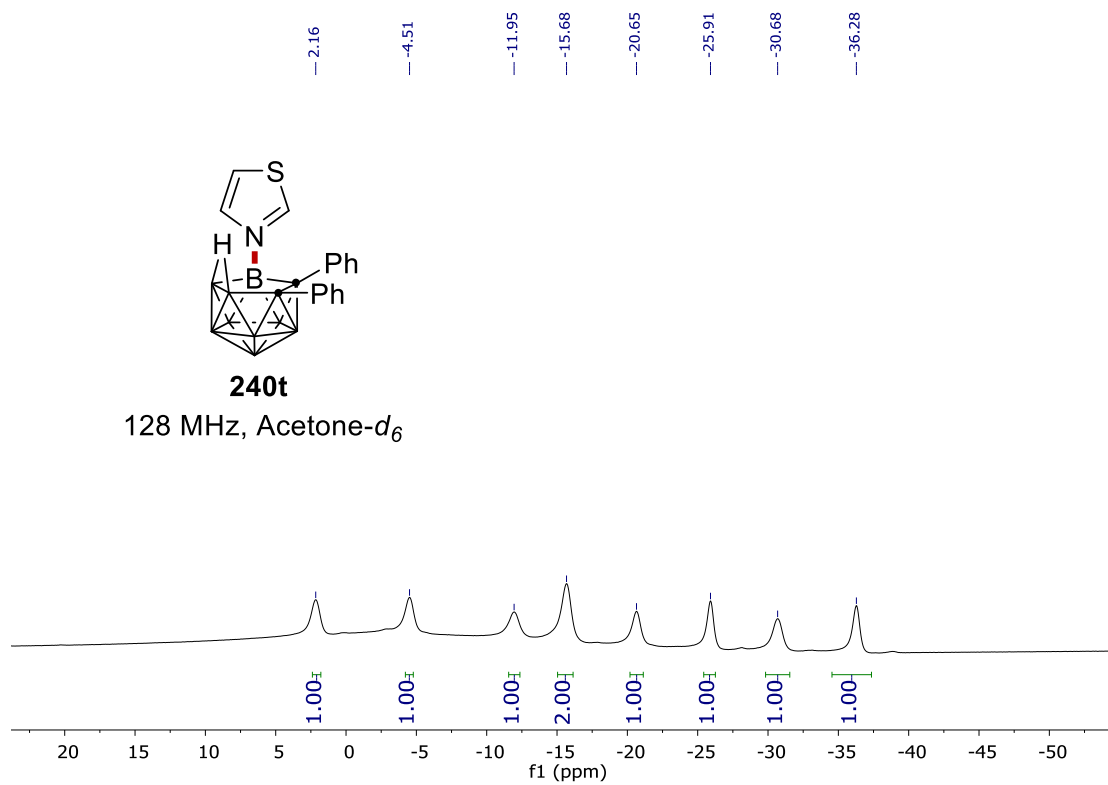
7. NMR Spectra



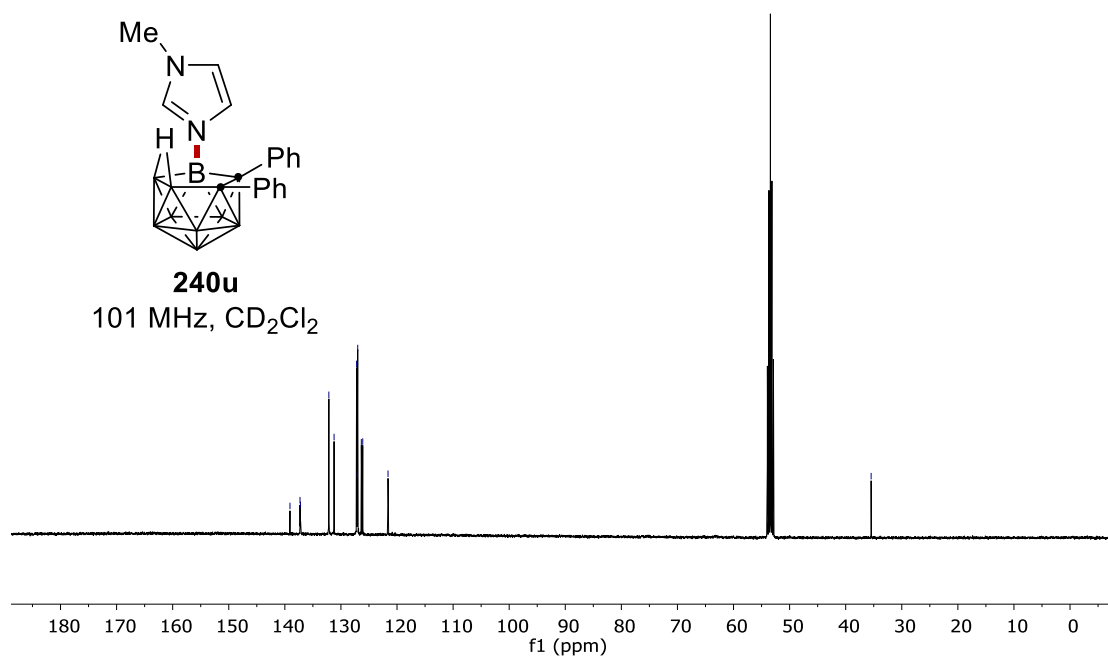
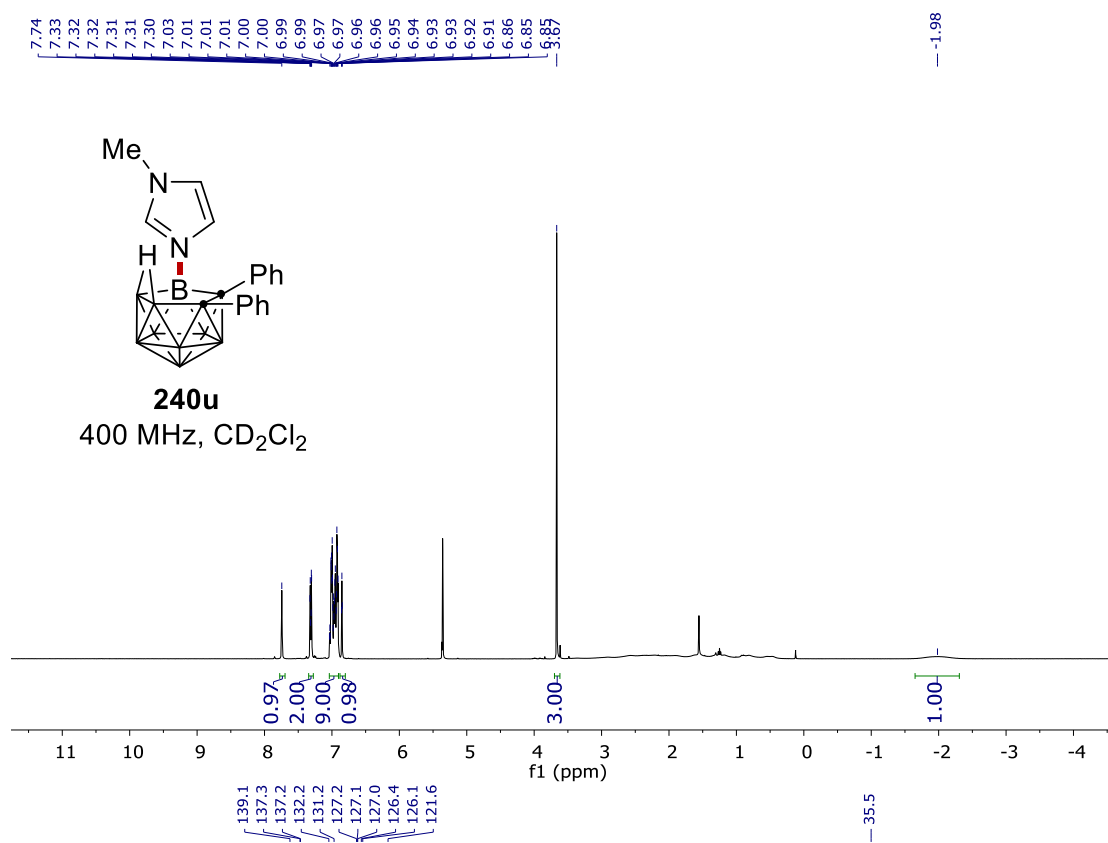
7. NMR Spectra



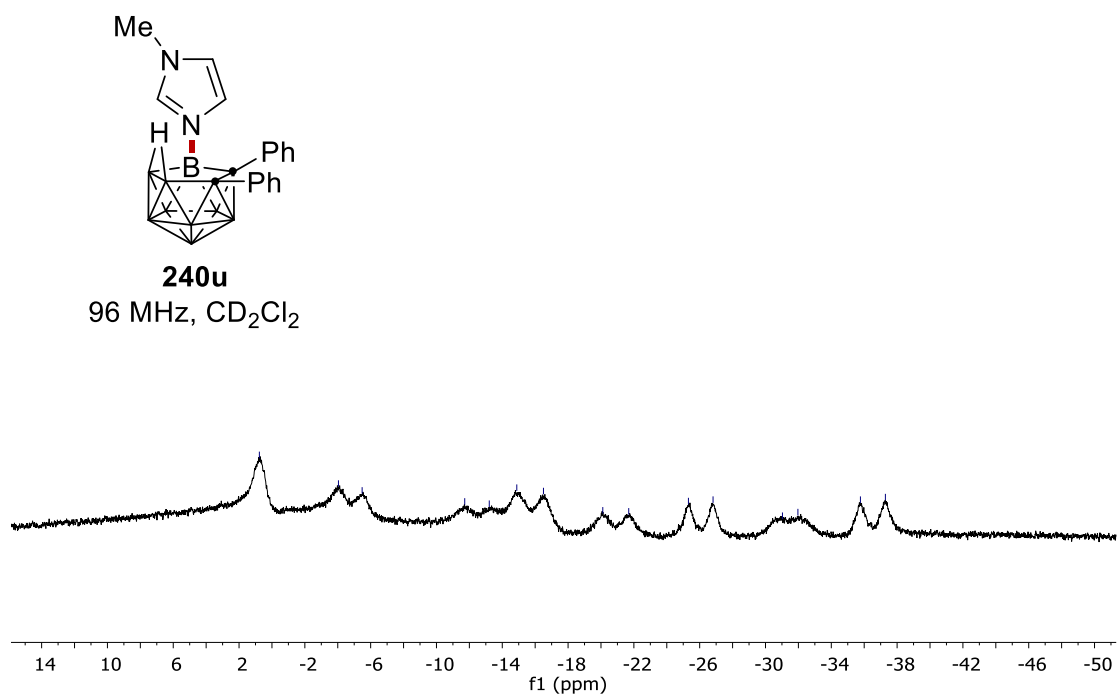
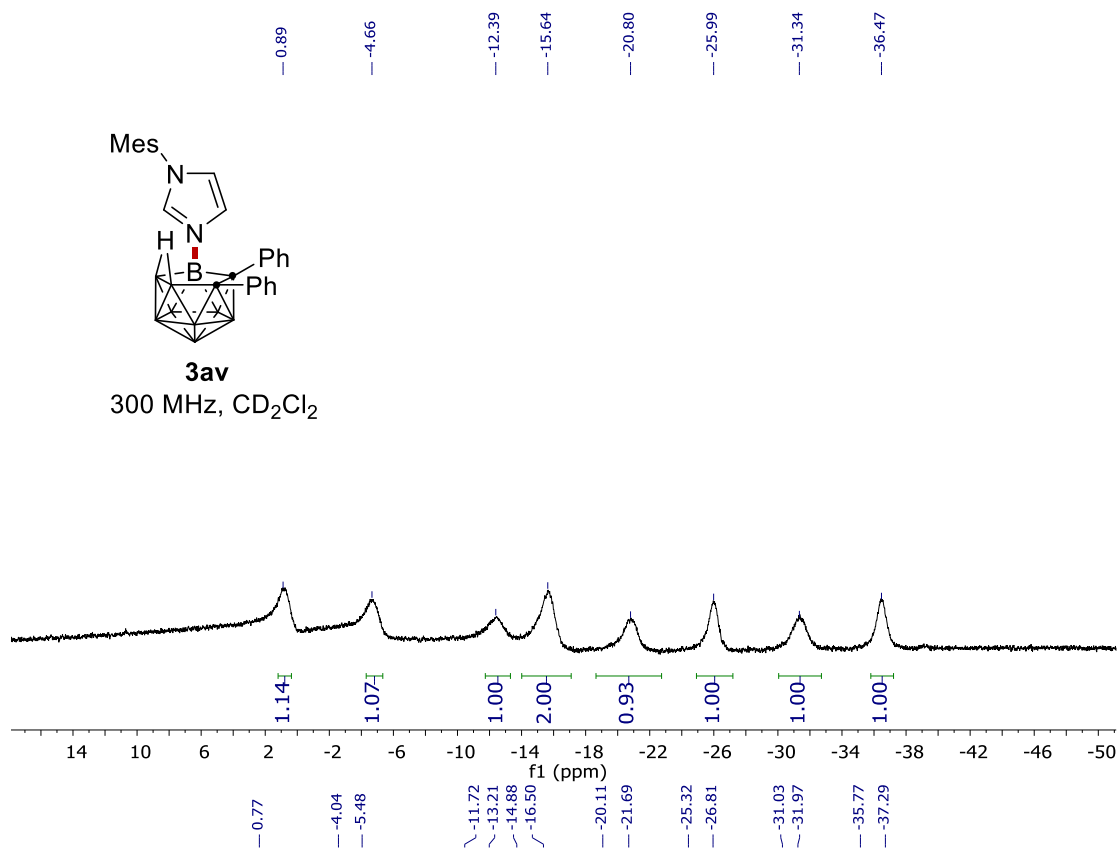
7. NMR Spectra



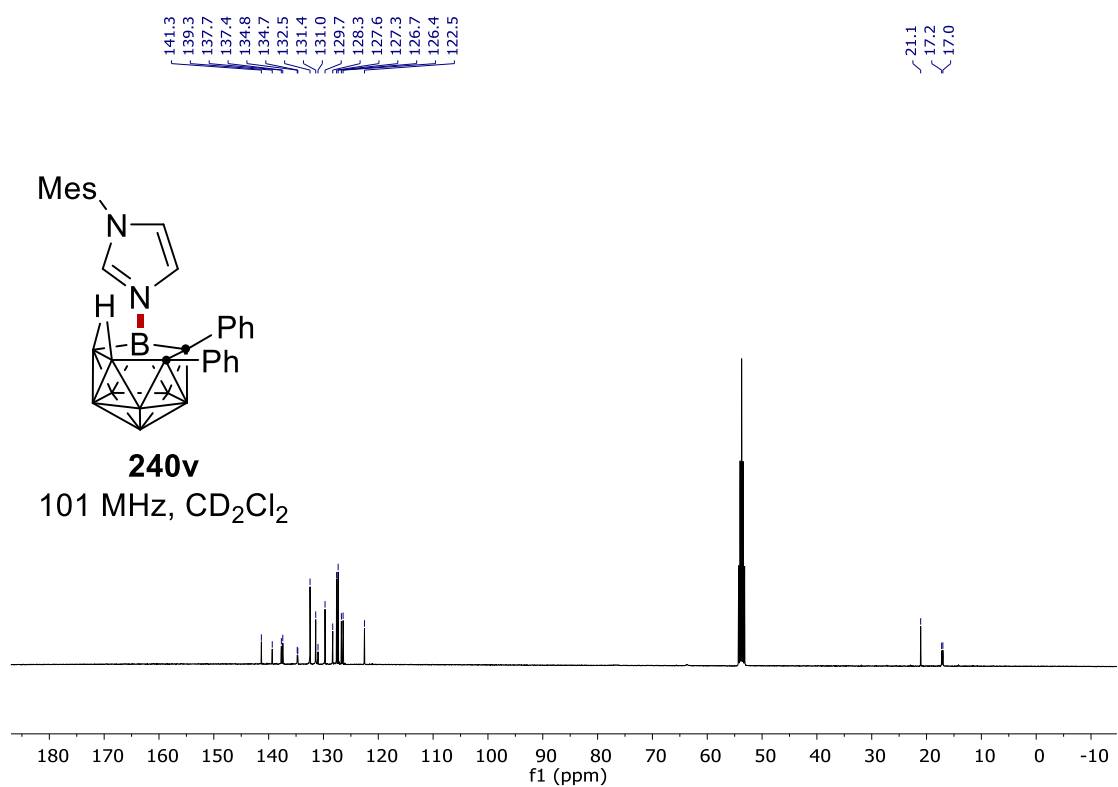
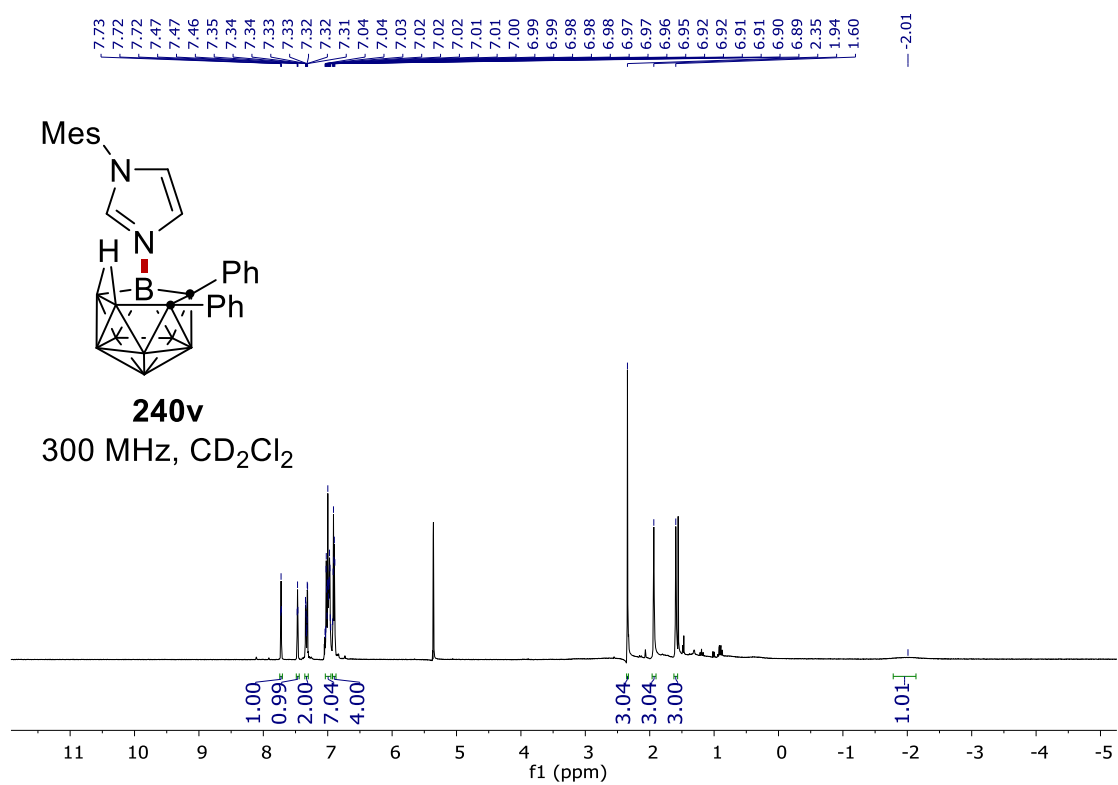
7. NMR Spectra



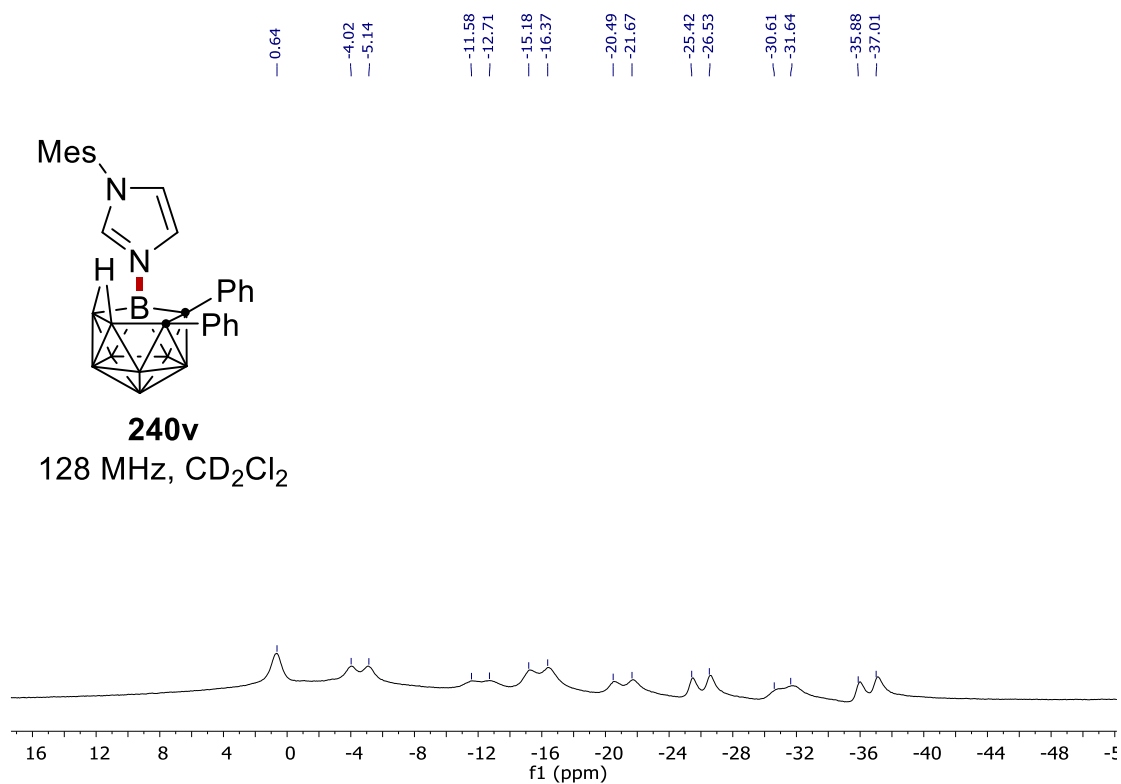
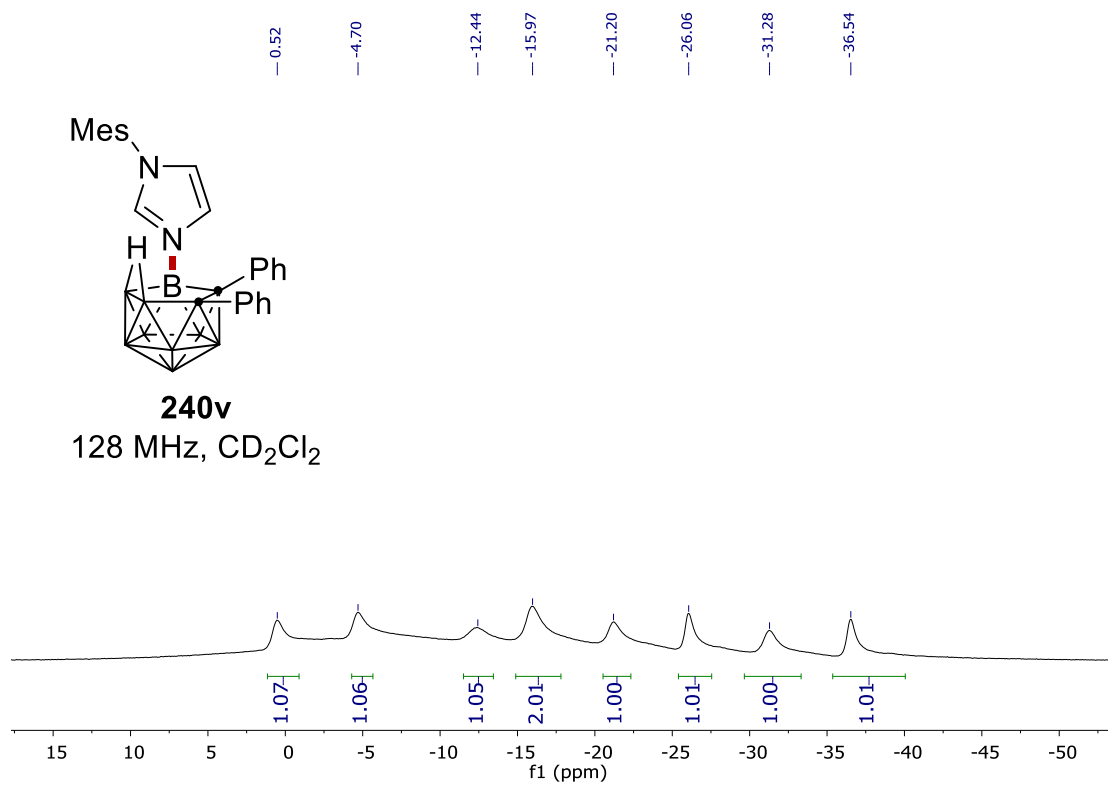
7. NMR Spectra



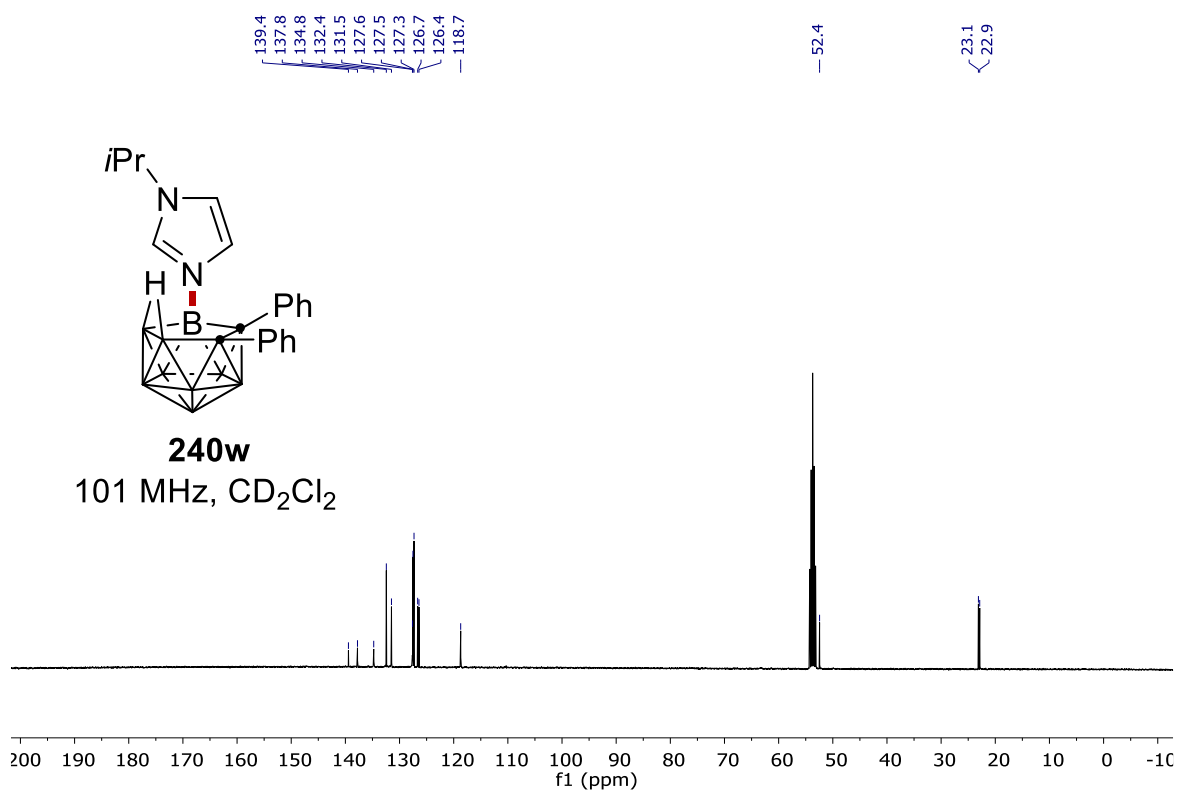
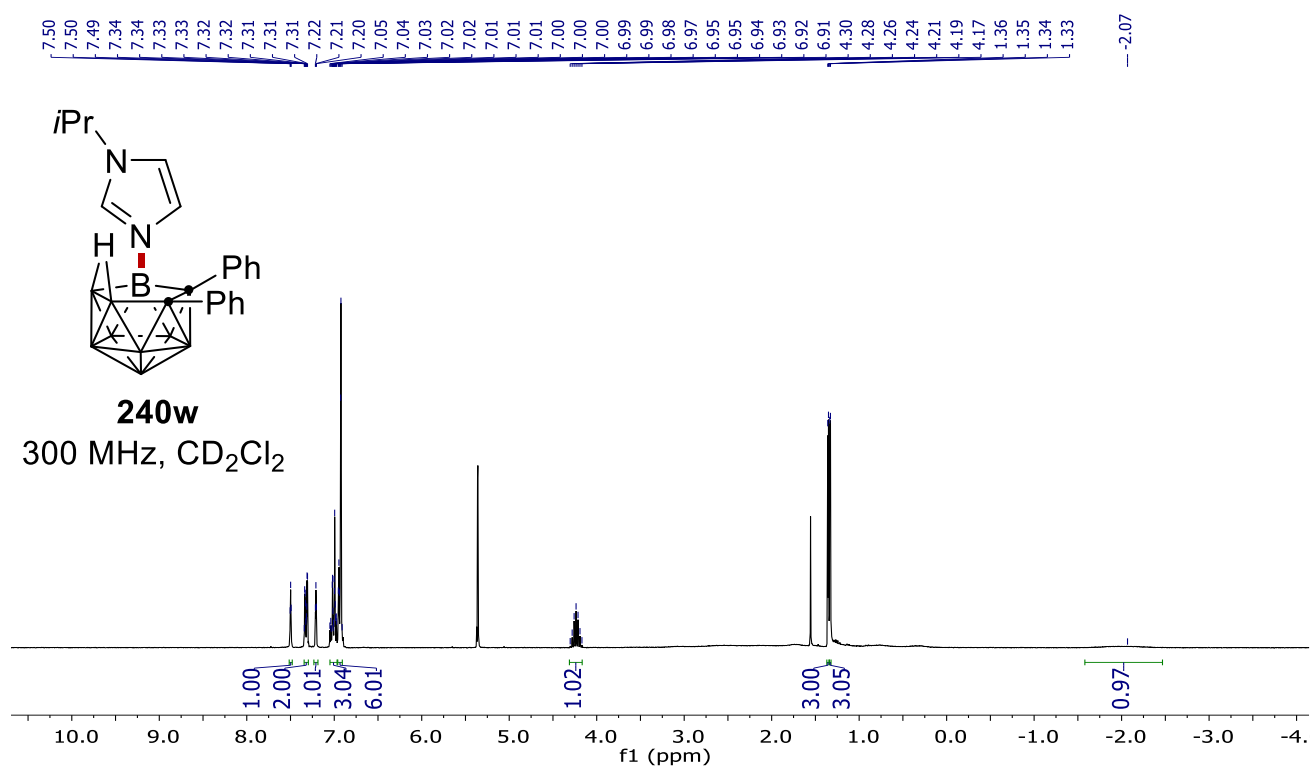
7. NMR Spectra



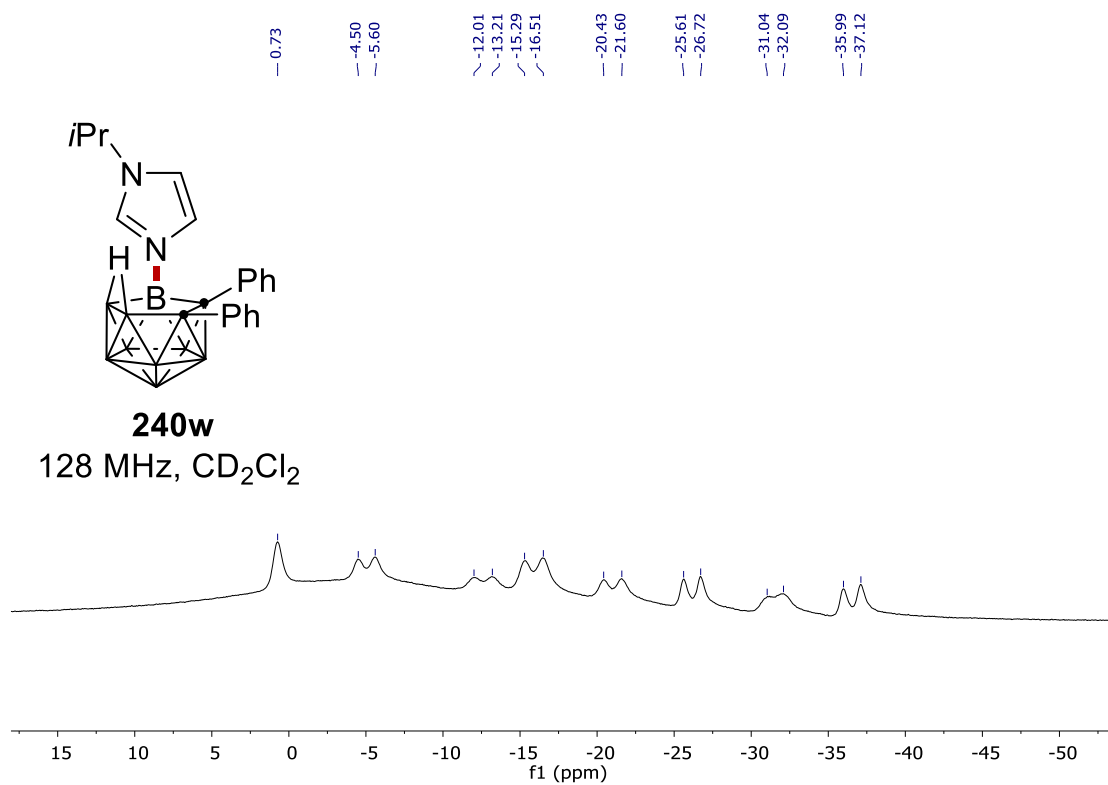
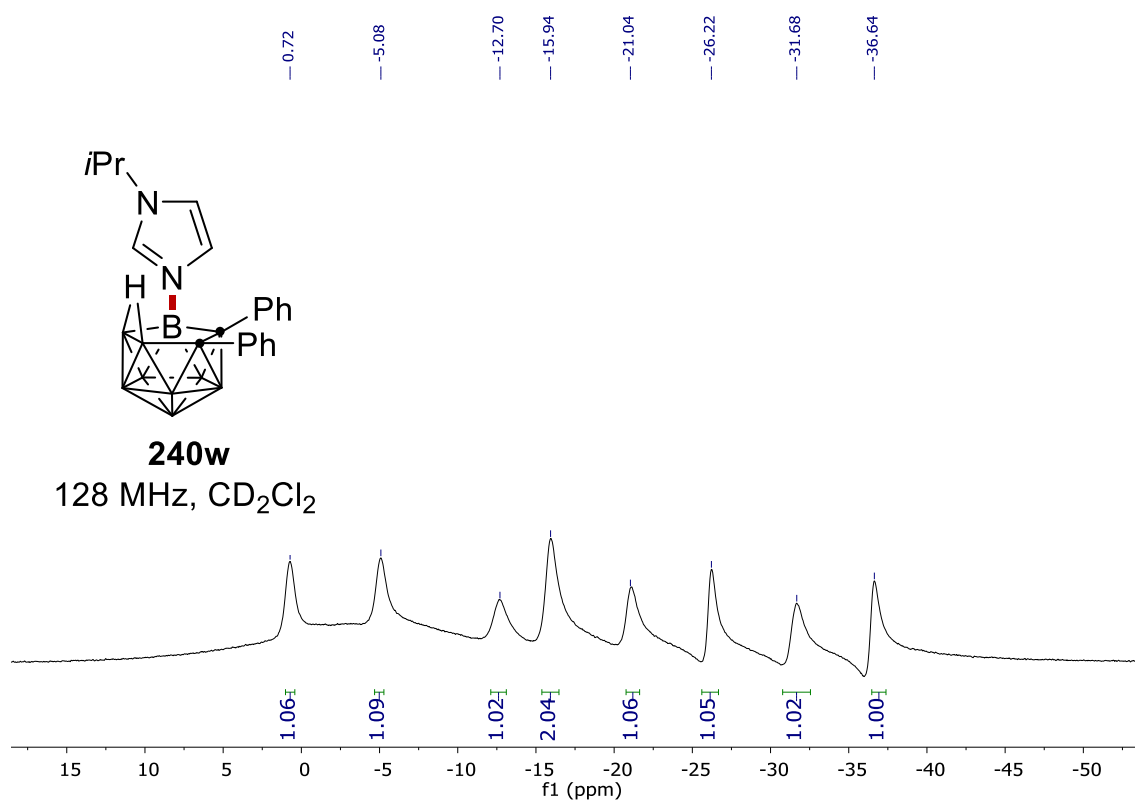
7. NMR Spectra



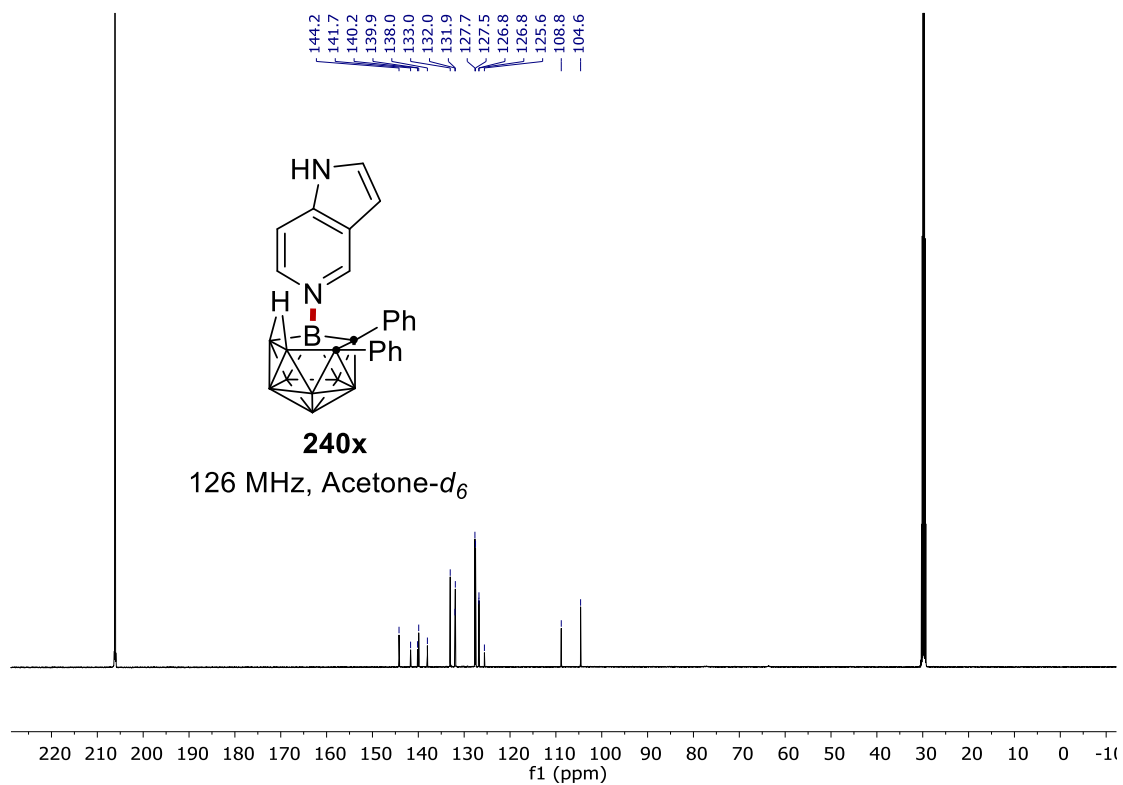
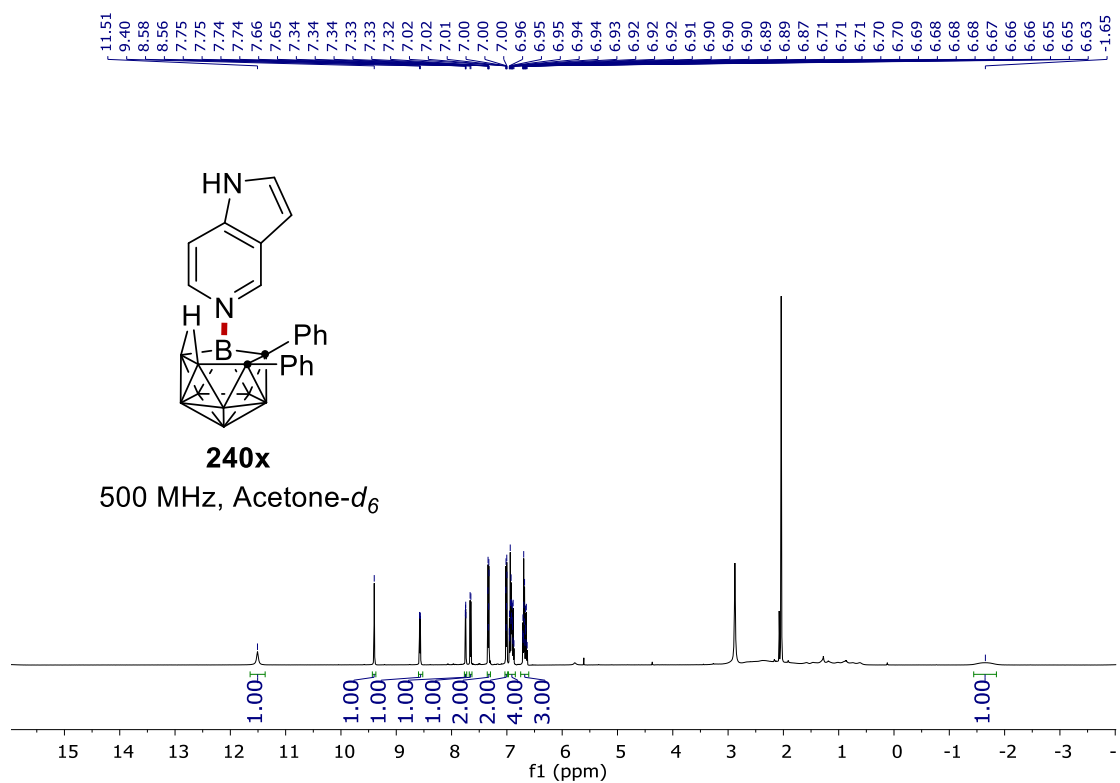
7. NMR Spectra



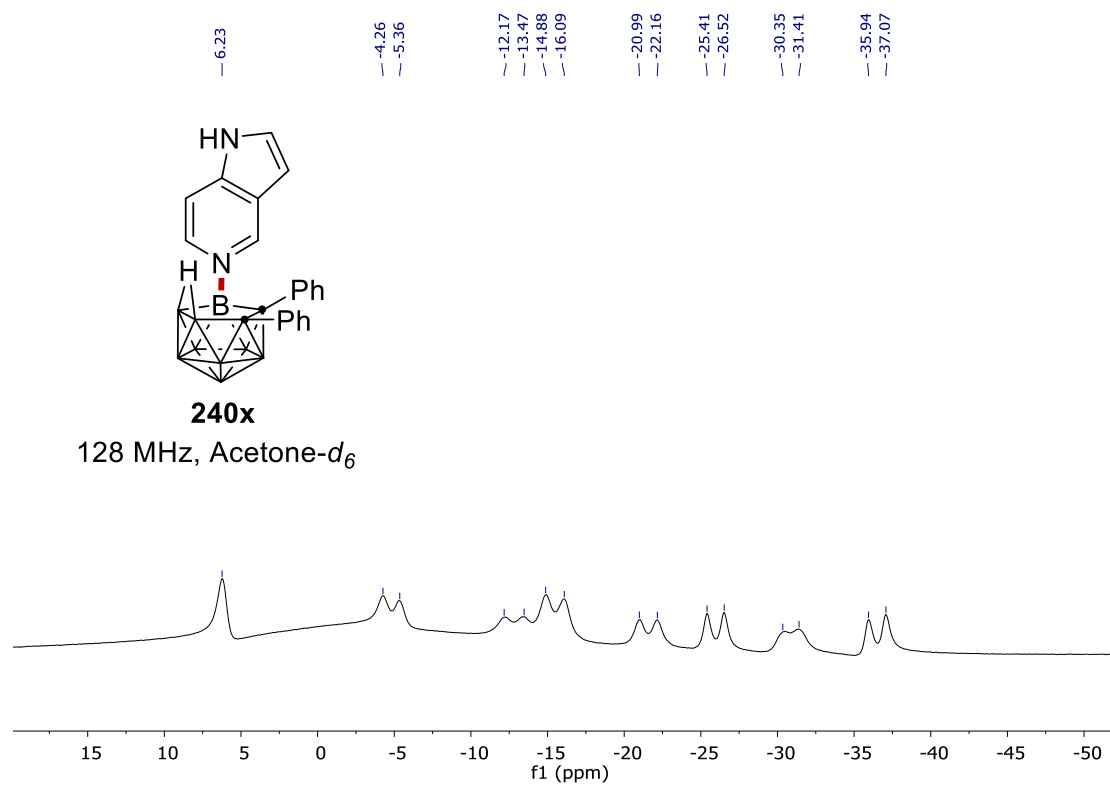
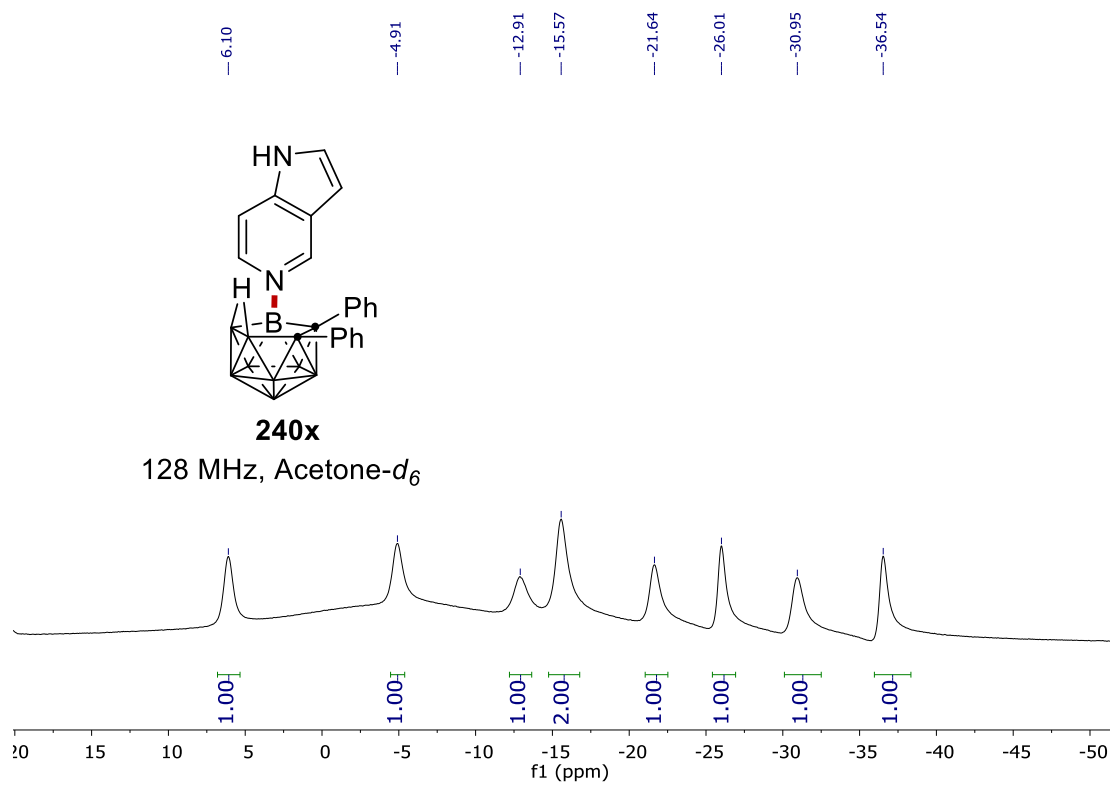
7. NMR Spectra



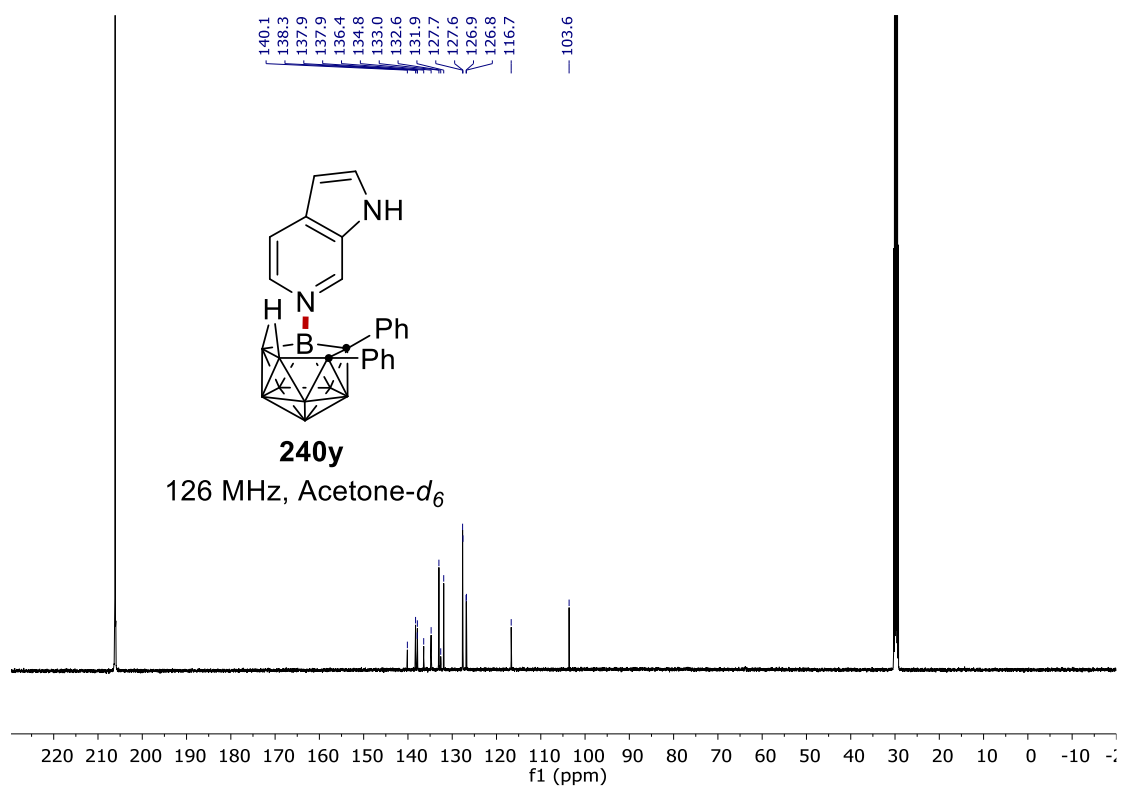
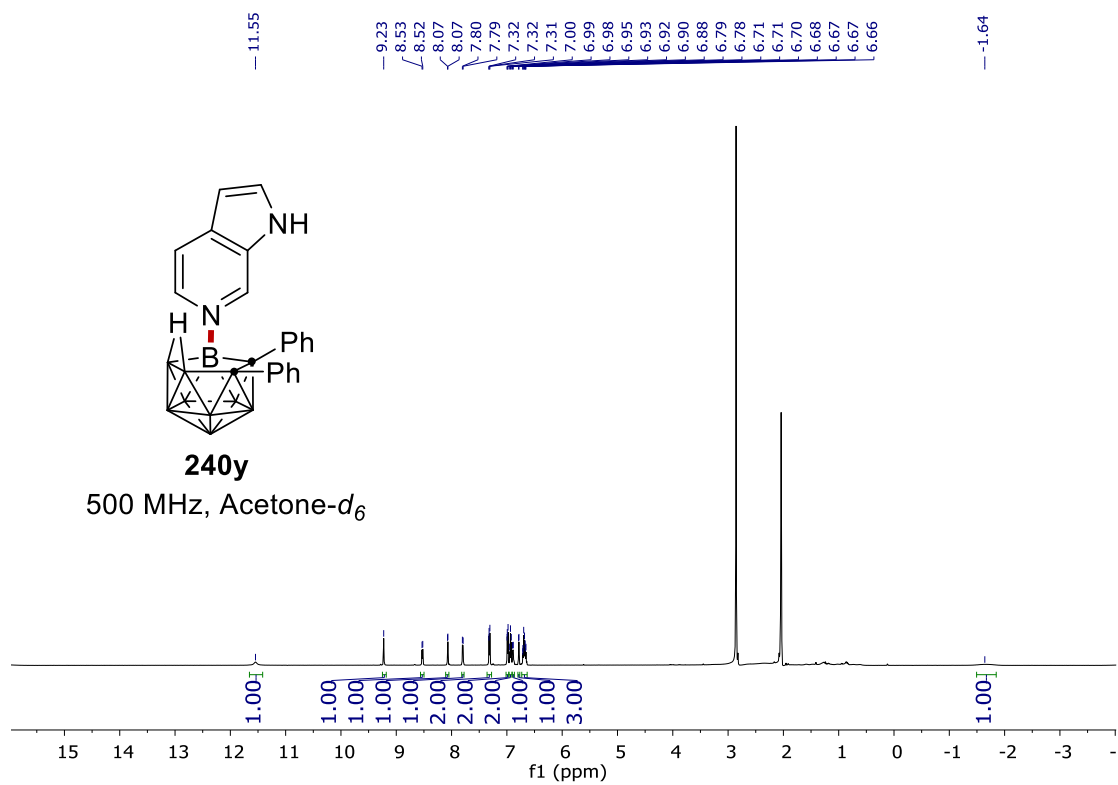
7. NMR Spectra



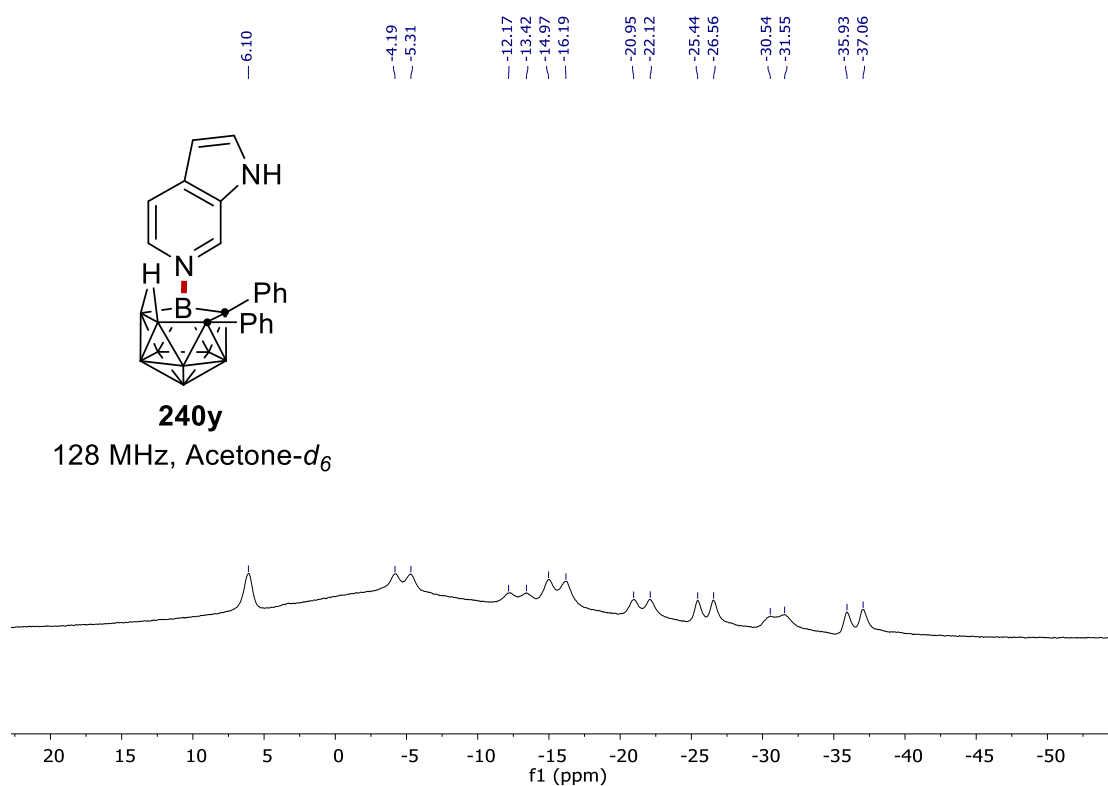
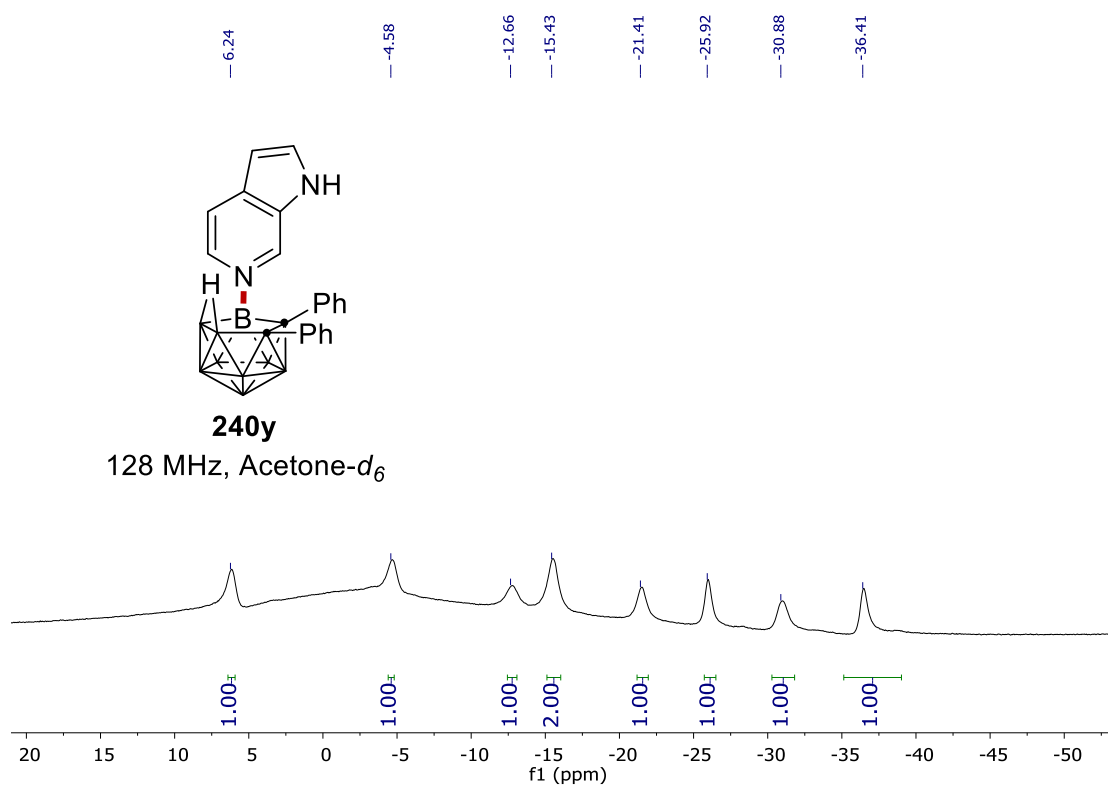
7. NMR Spectra



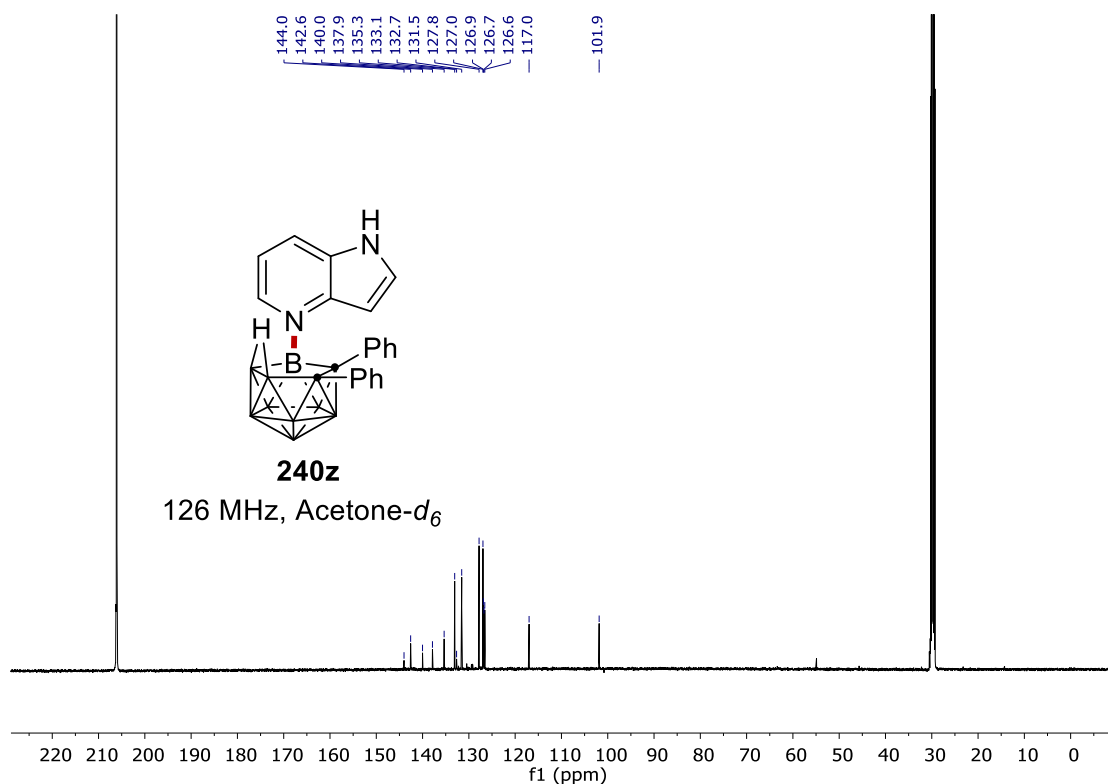
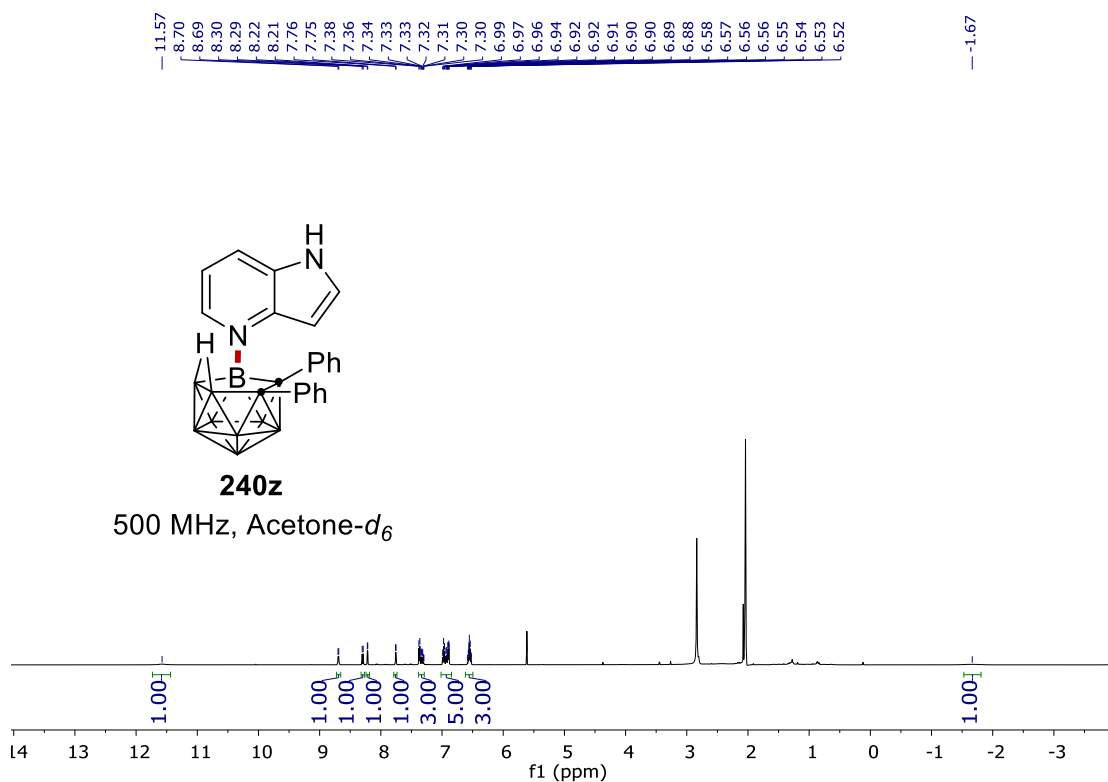
7. NMR Spectra

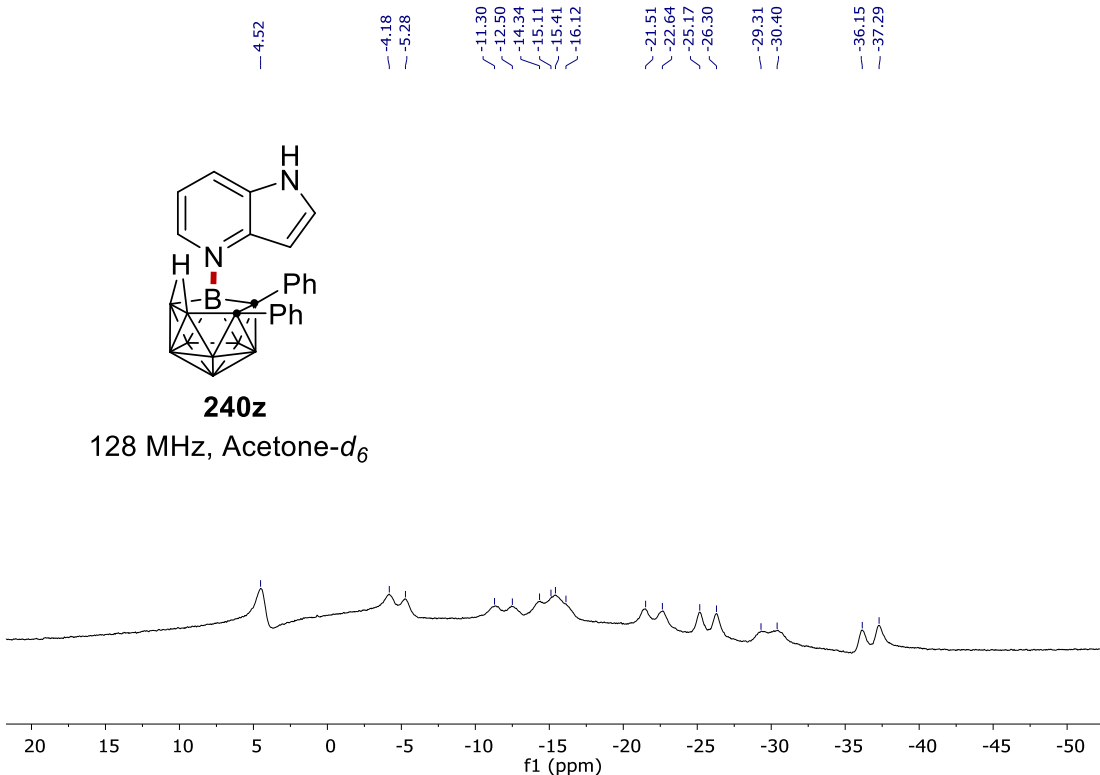


7. NMR Spectra

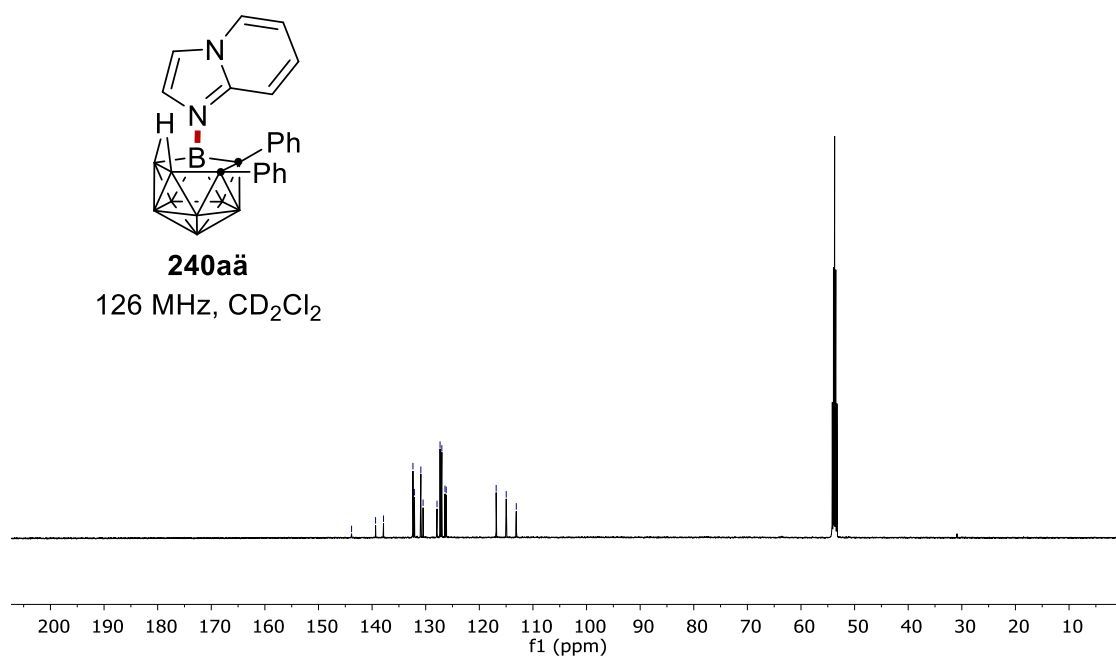
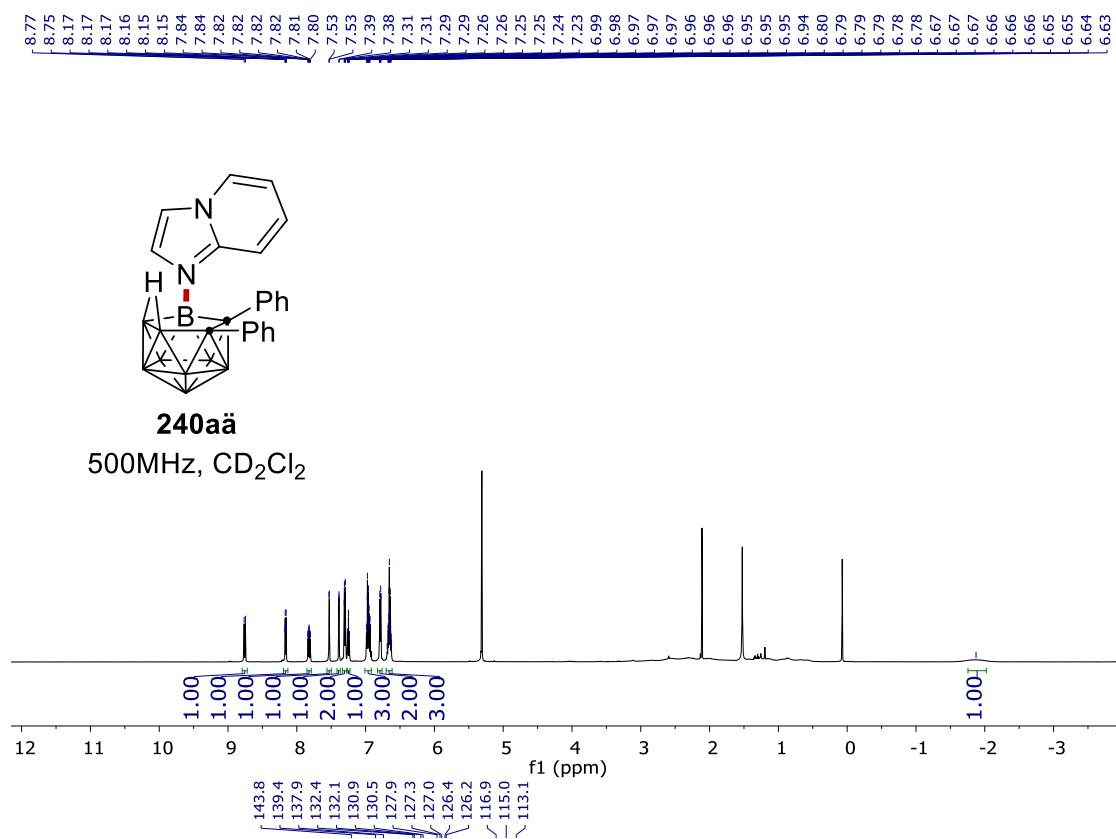


7. NMR Spectra

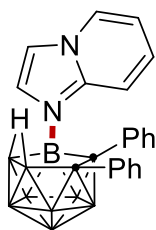




7. NMR Spectra

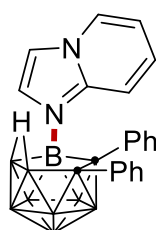
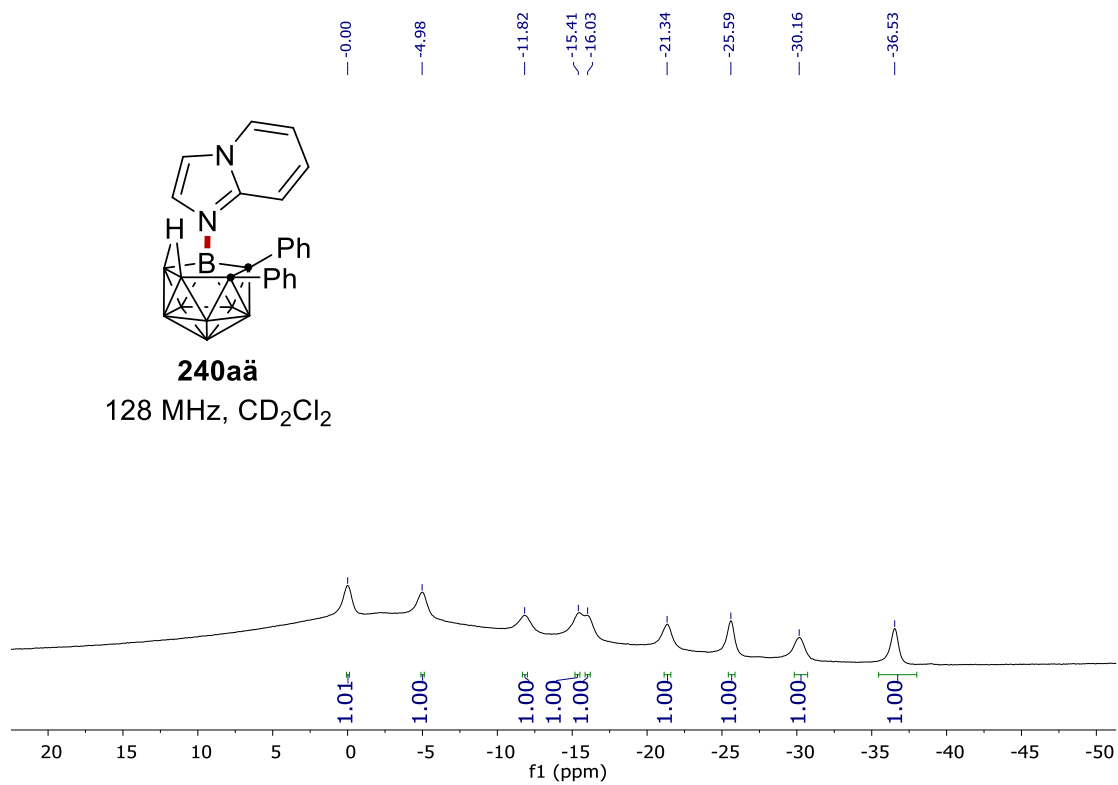


7. NMR Spectra



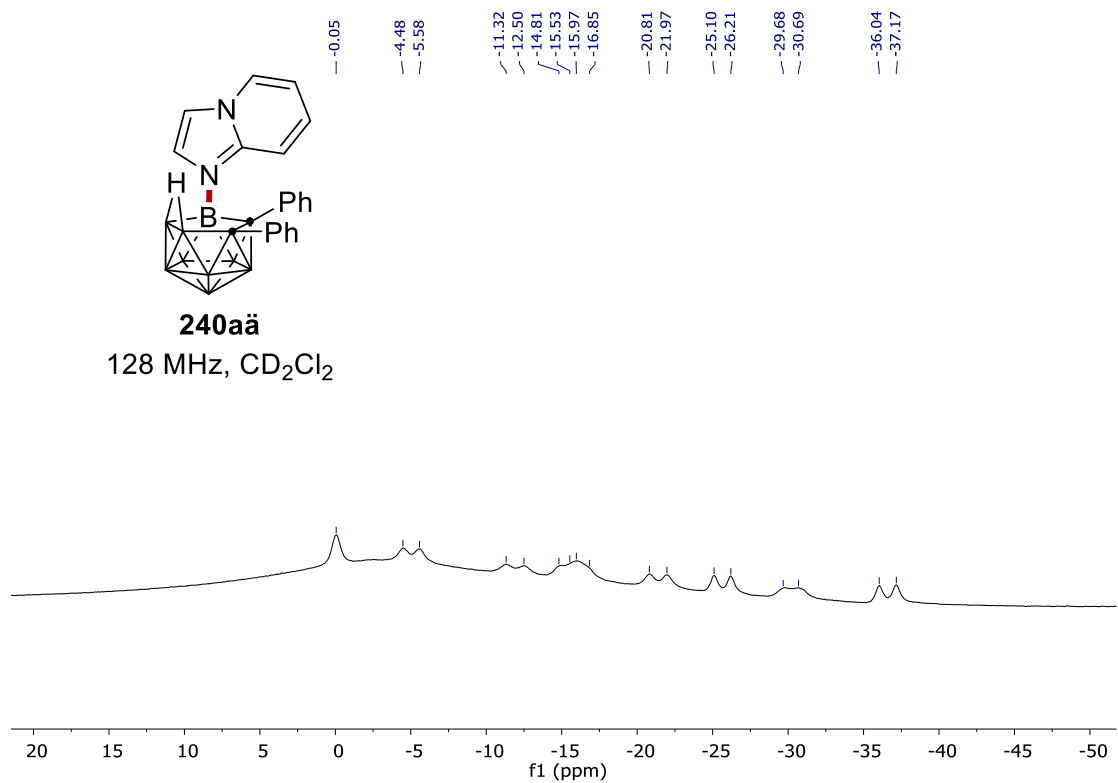
240aa

128 MHz, CD₂Cl₂

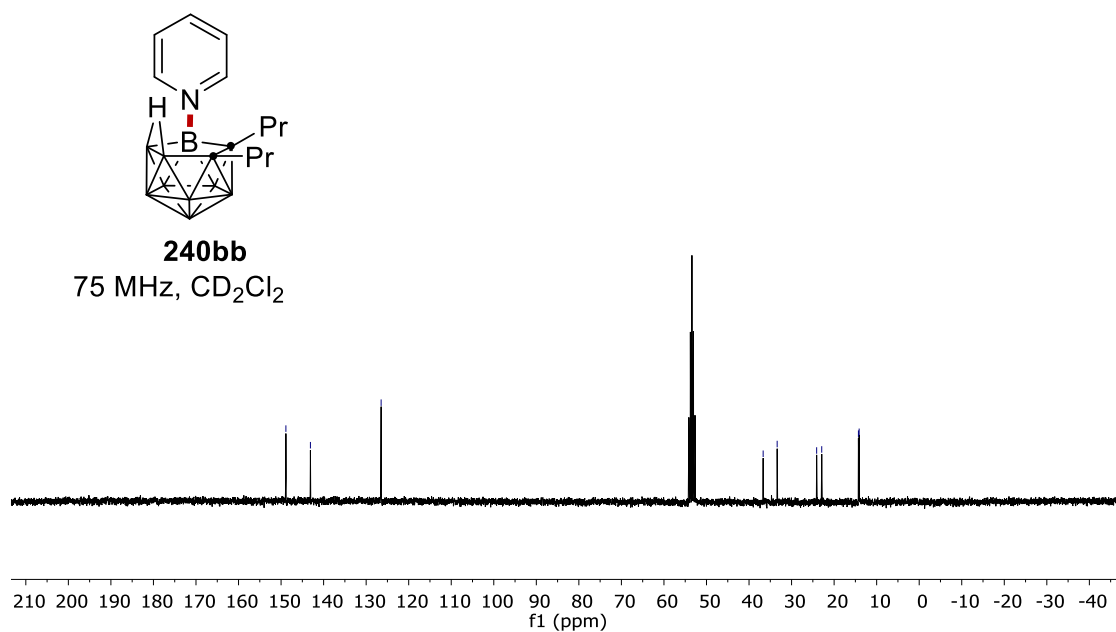
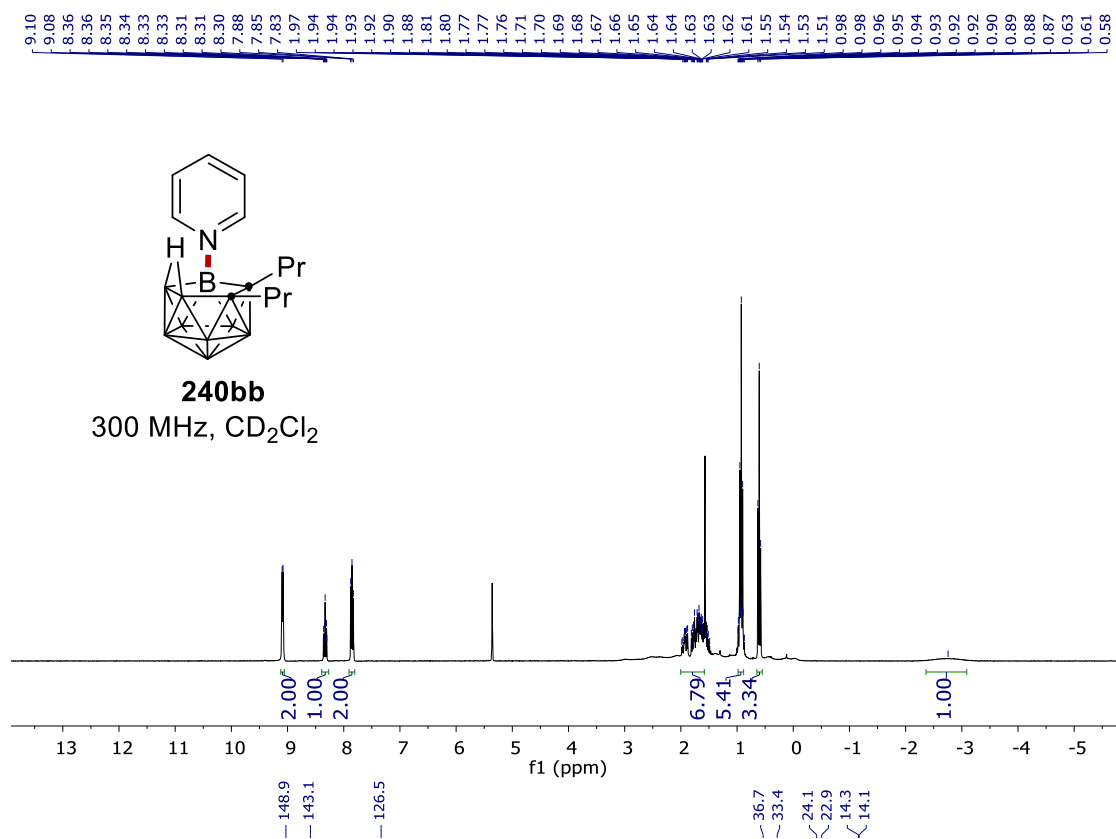


240aa

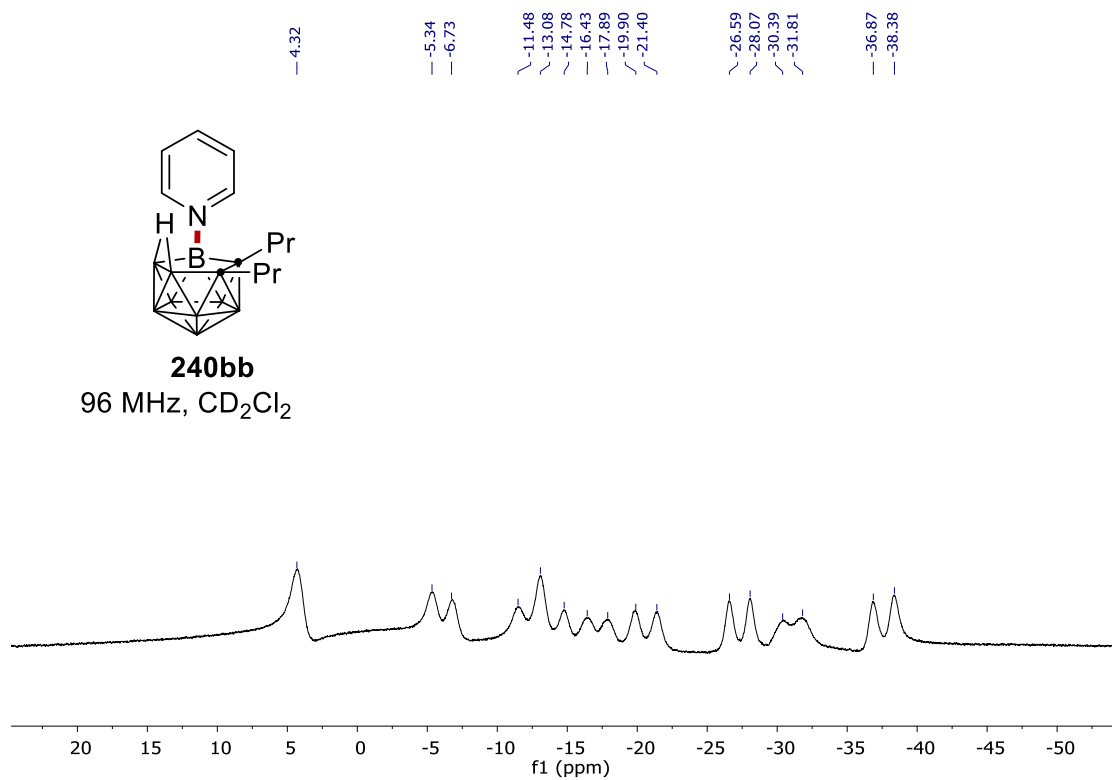
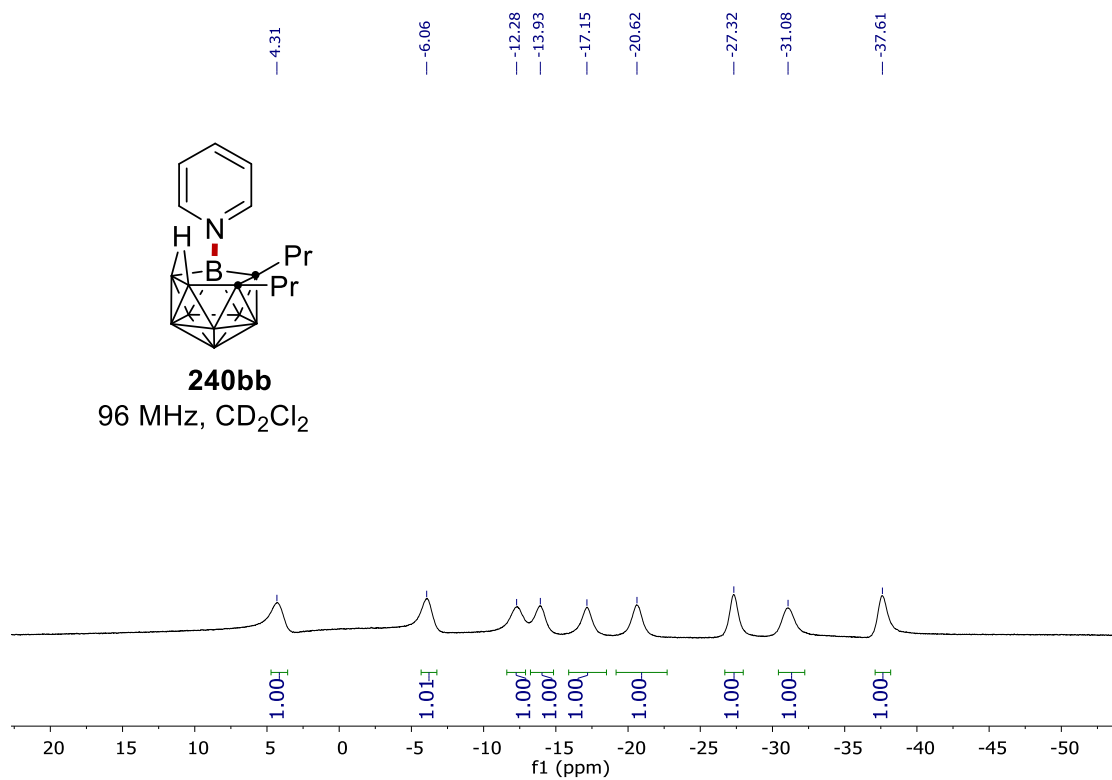
128 MHz, CD₂Cl₂



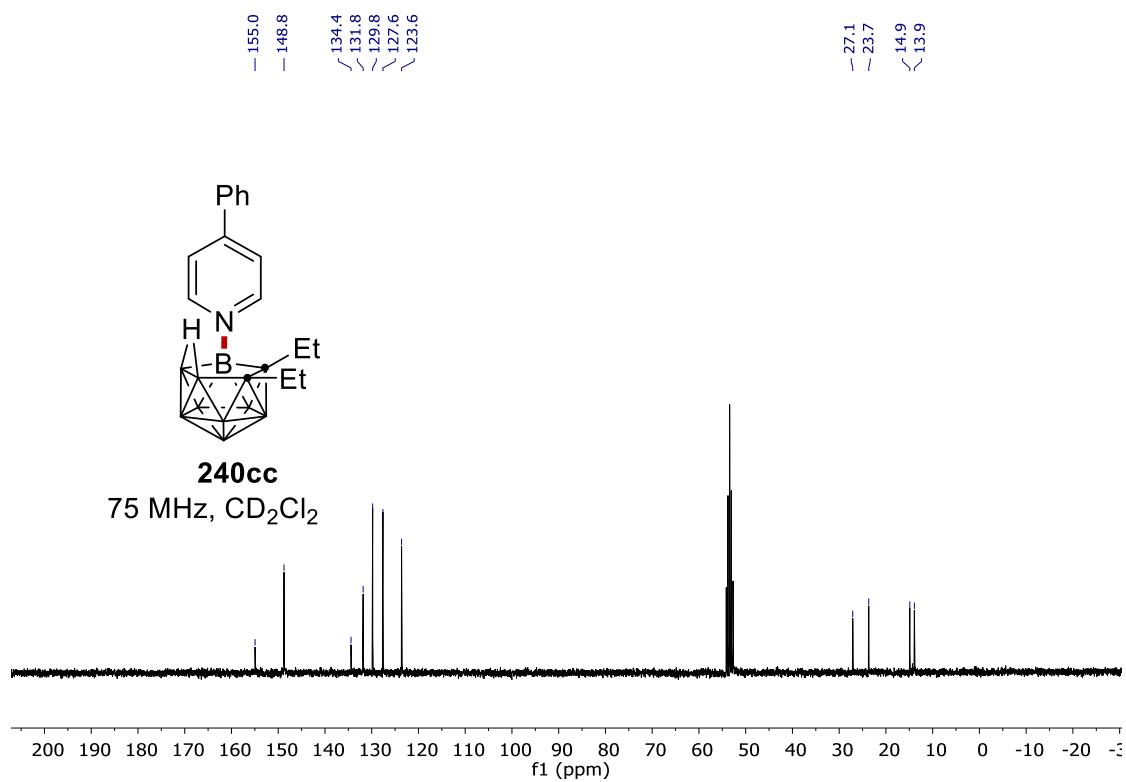
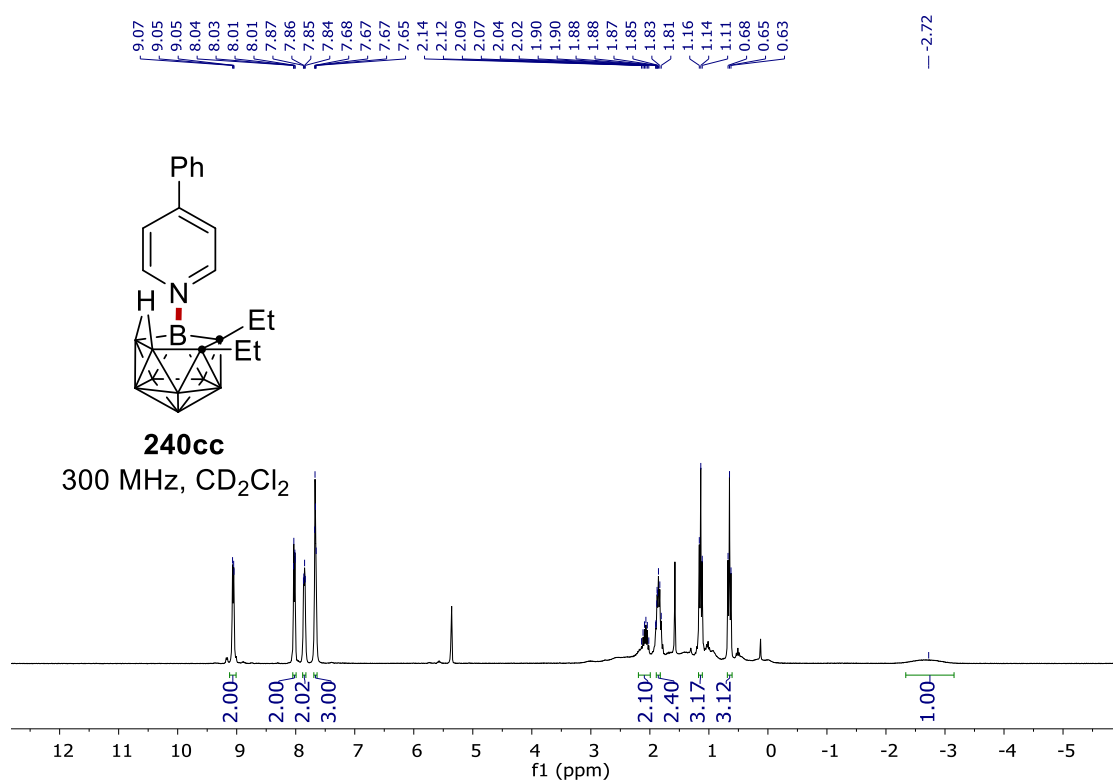
7. NMR Spectra



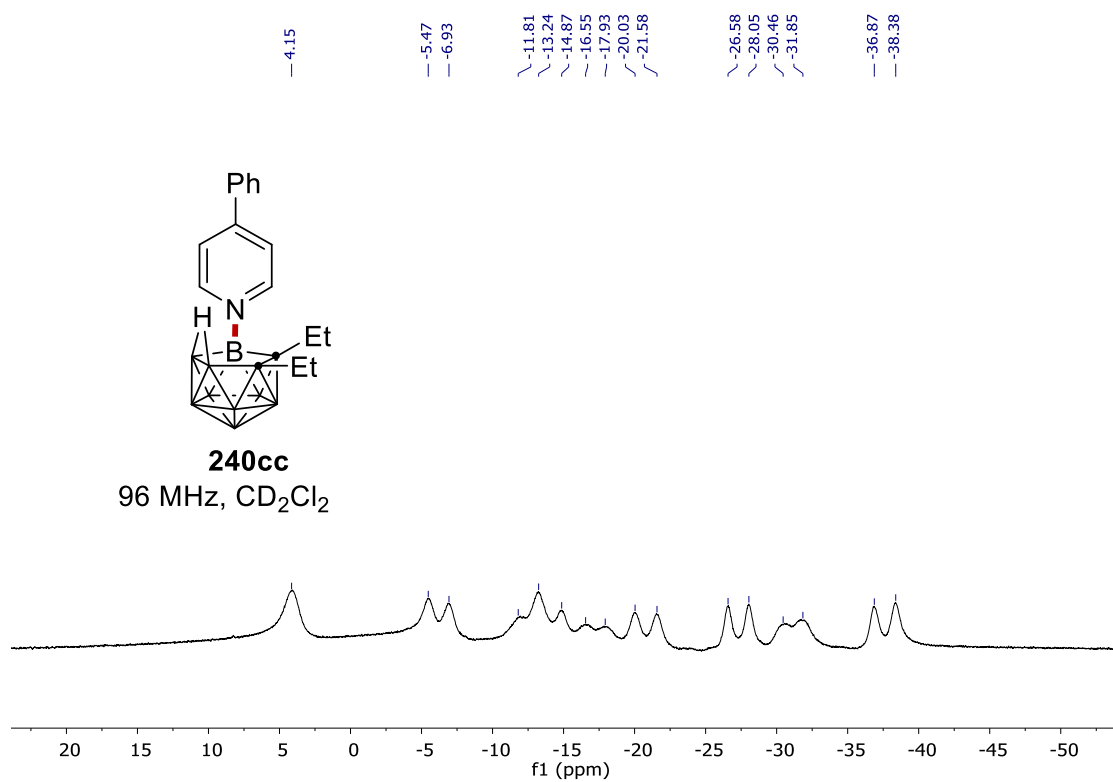
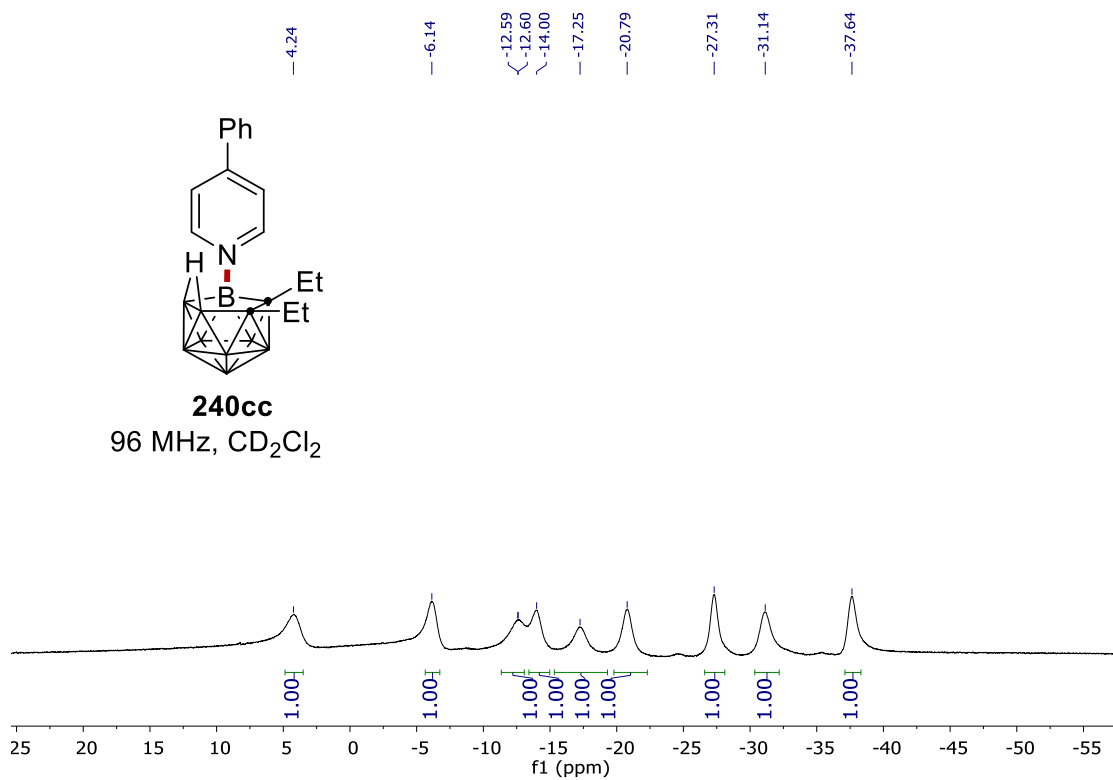
7. NMR Spectra



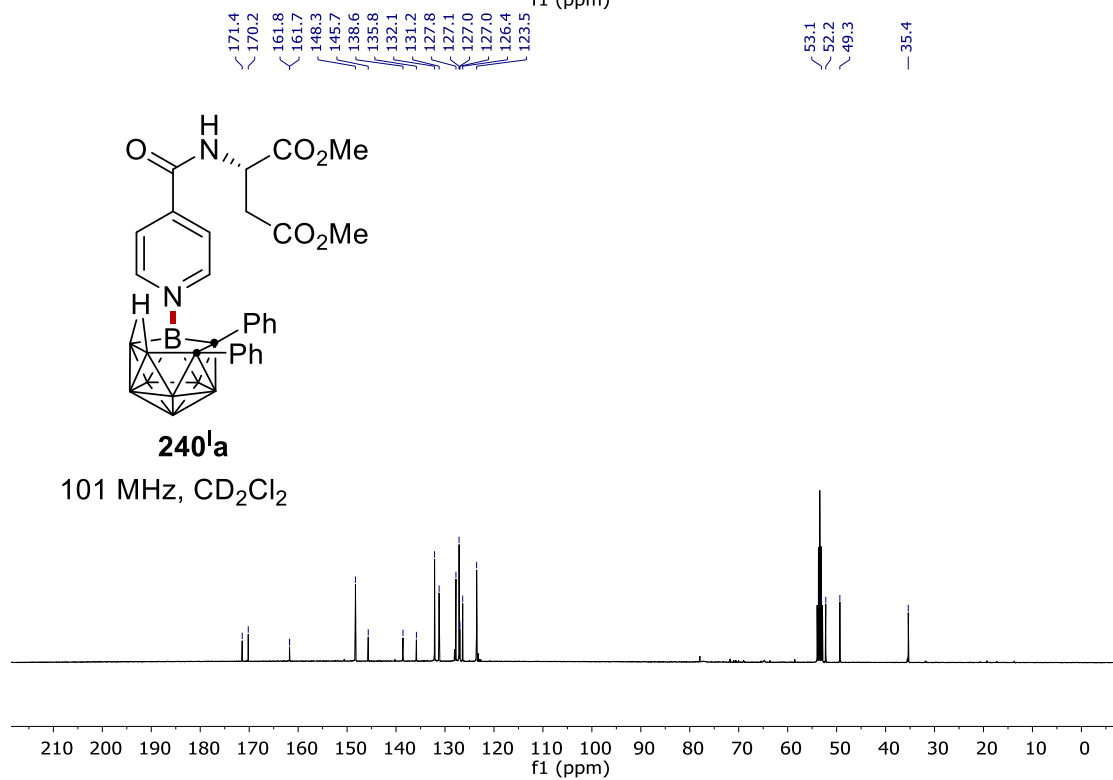
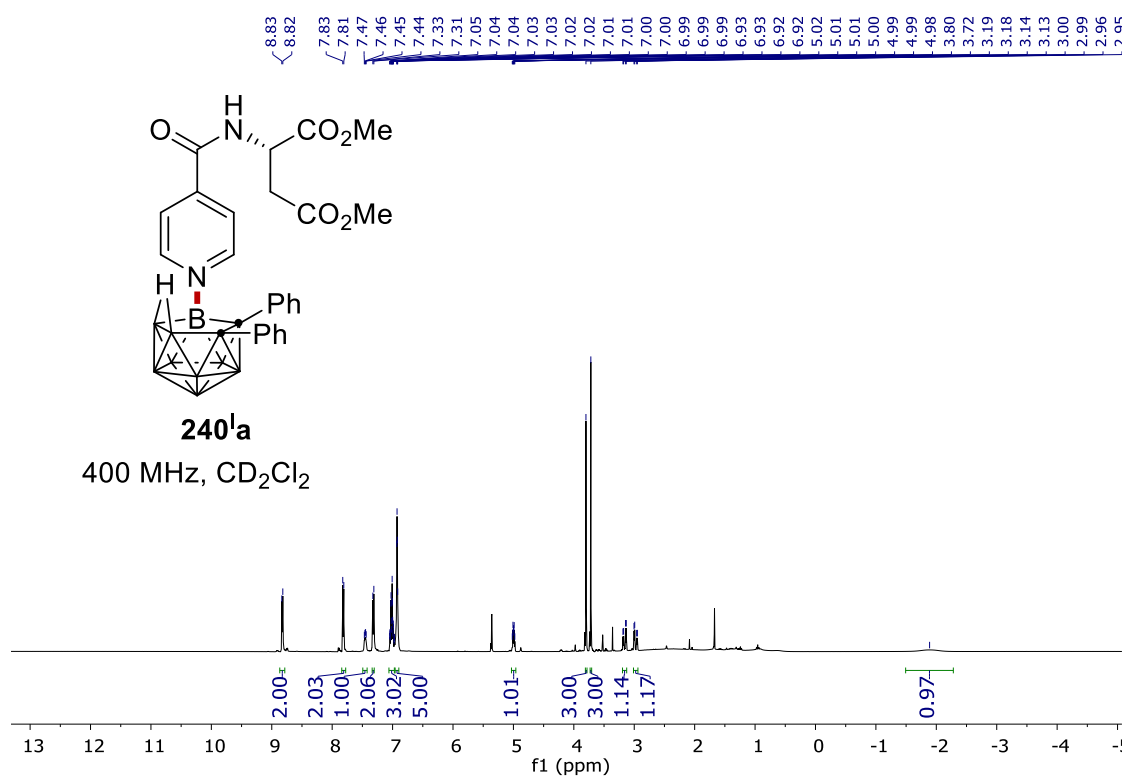
7. NMR Spectra



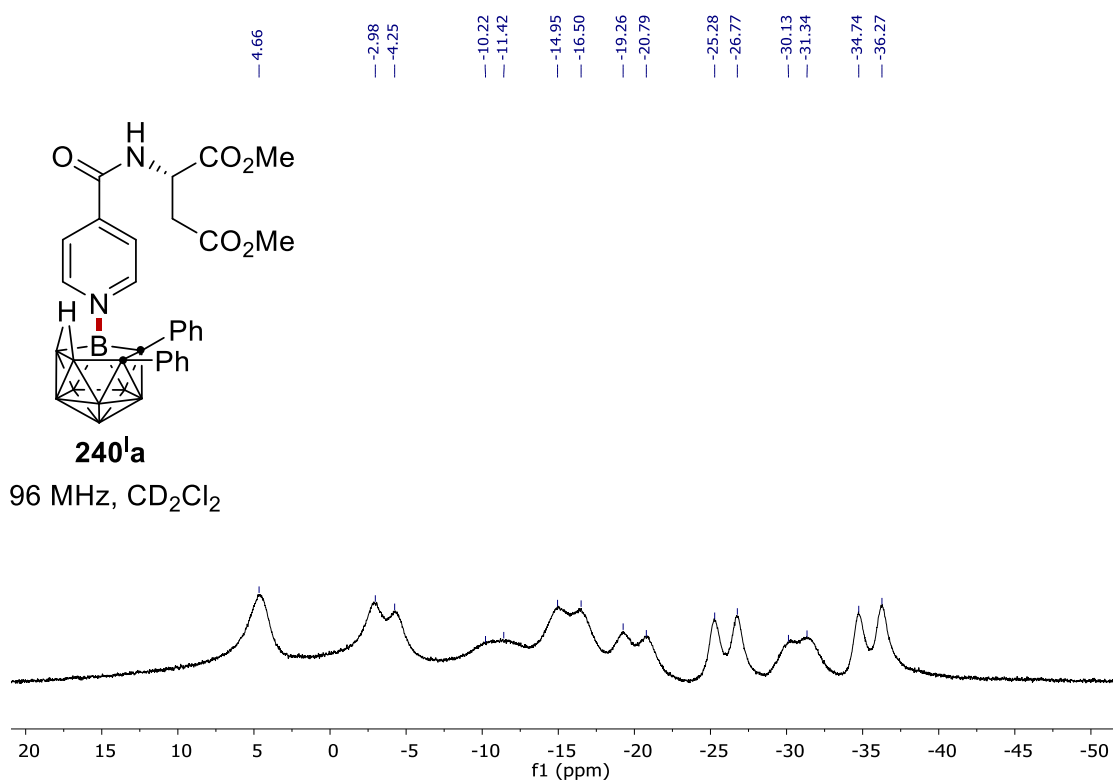
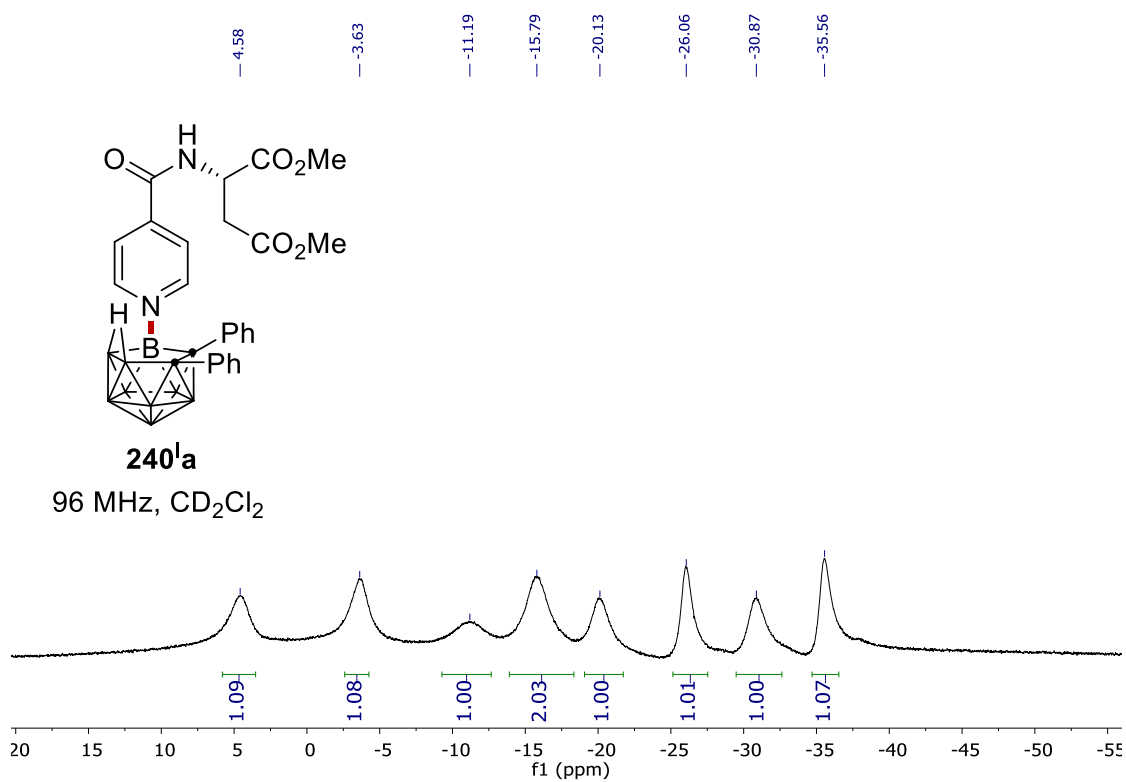
7. NMR Spectra



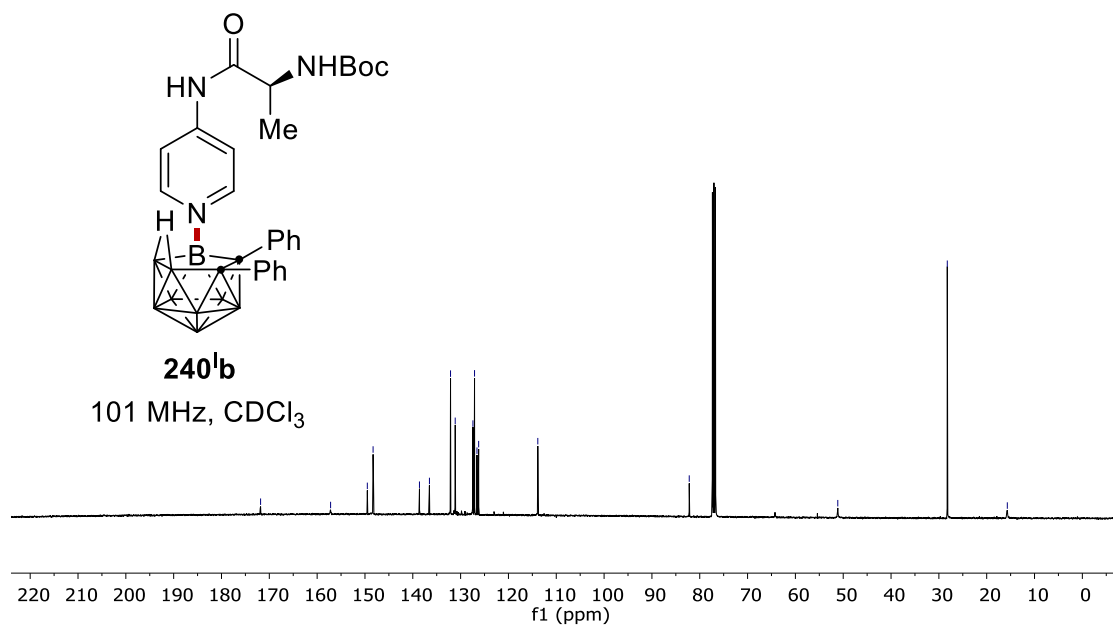
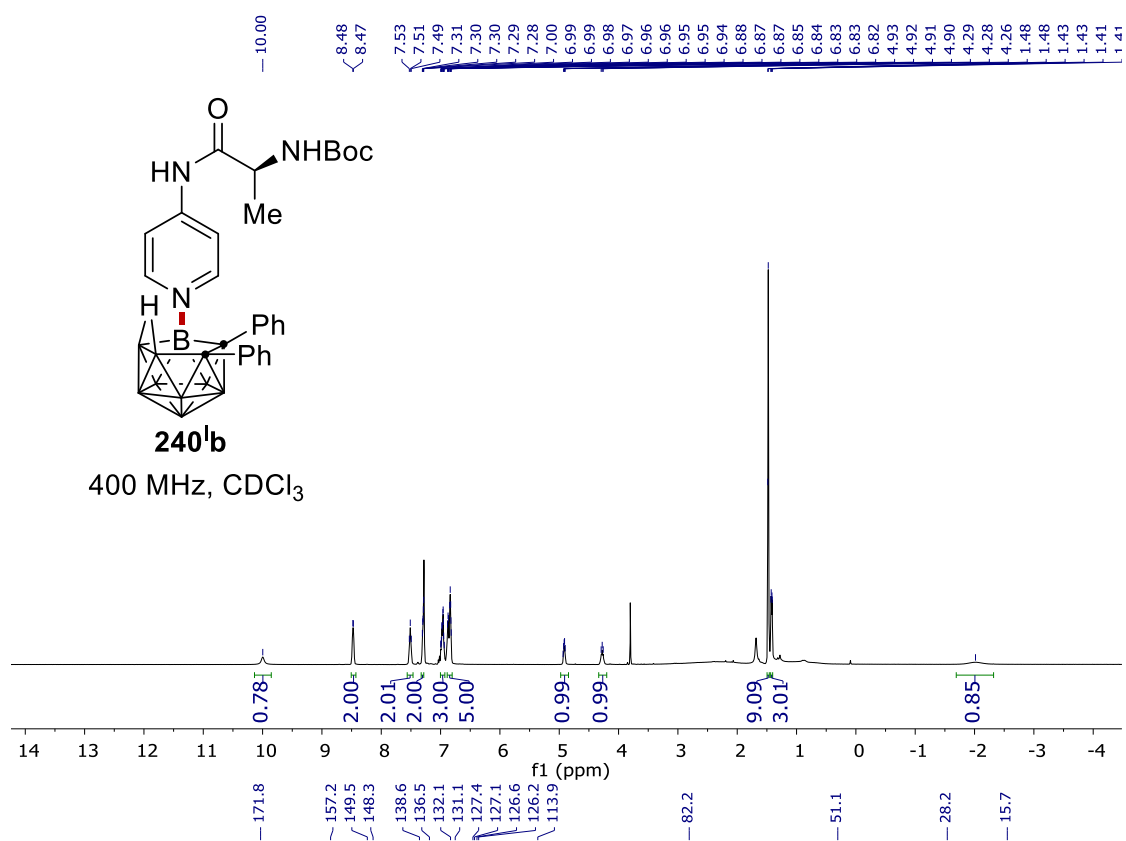
7. NMR Spectra



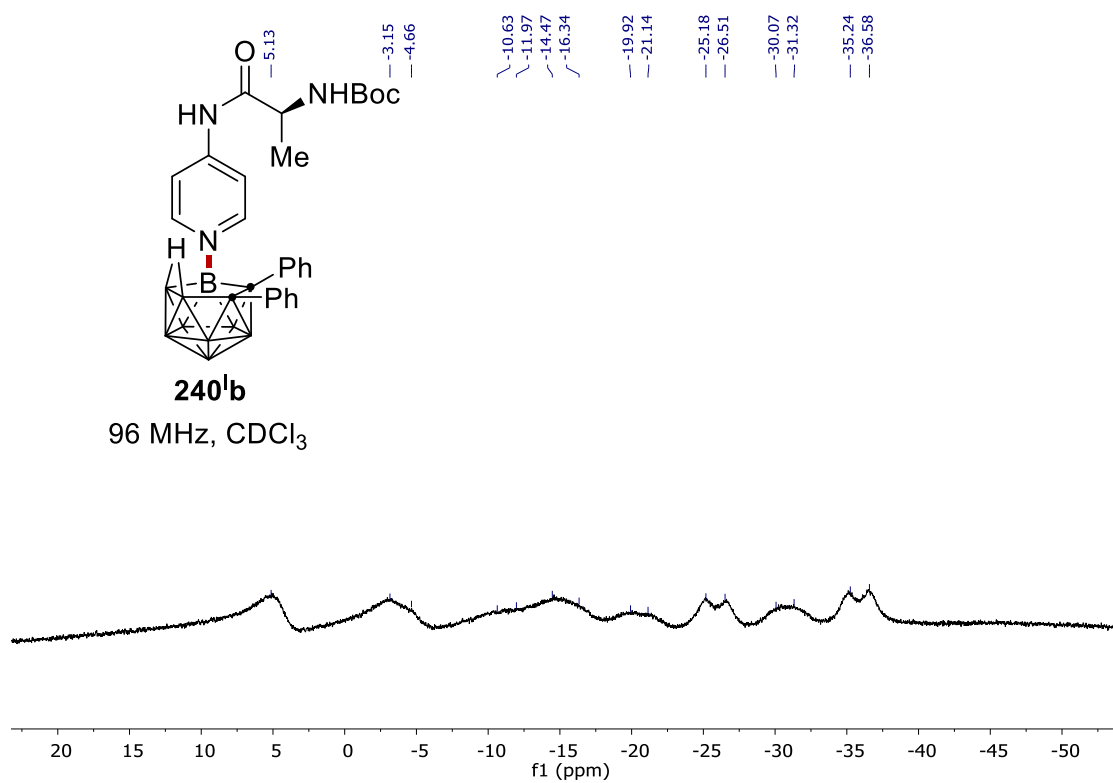
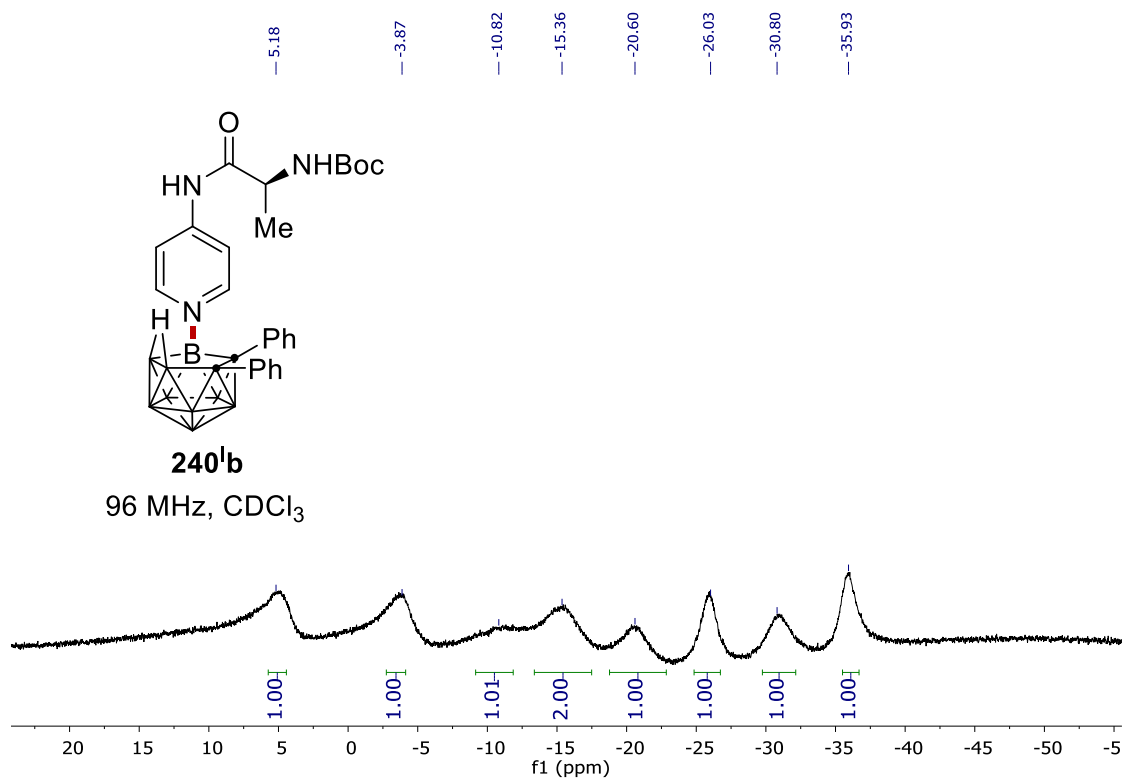
7. NMR Spectra

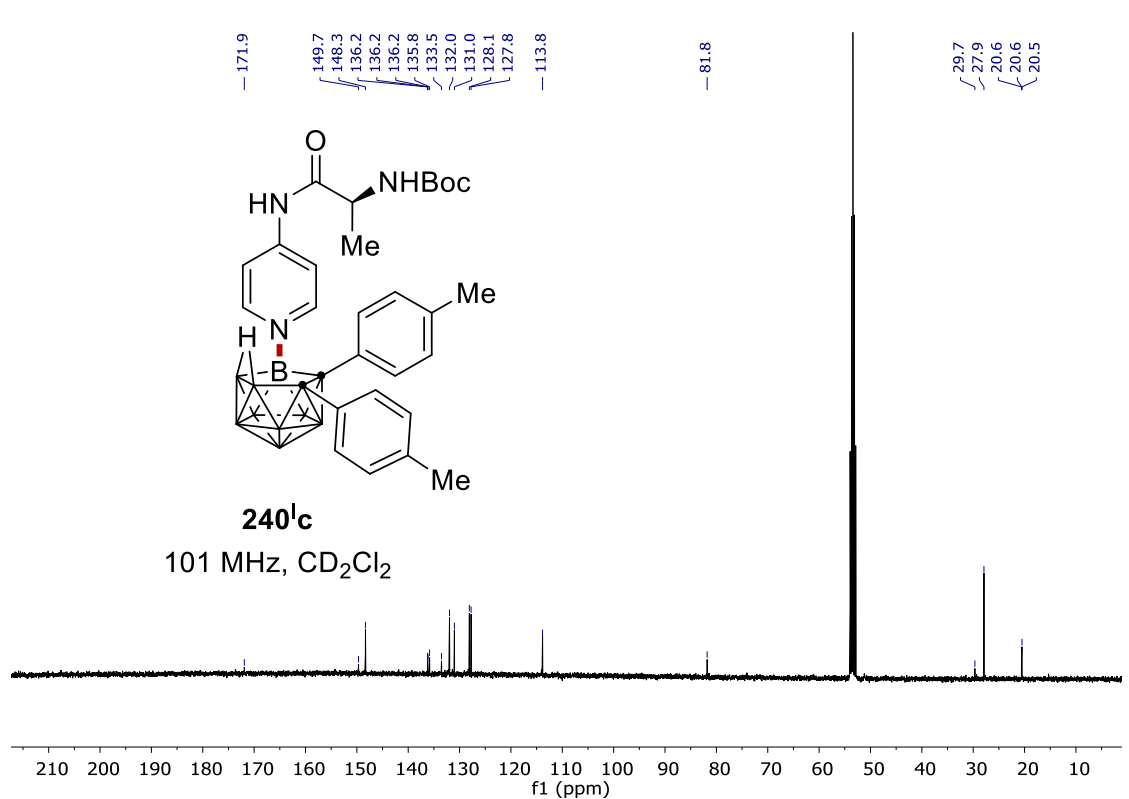


7. NMR Spectra

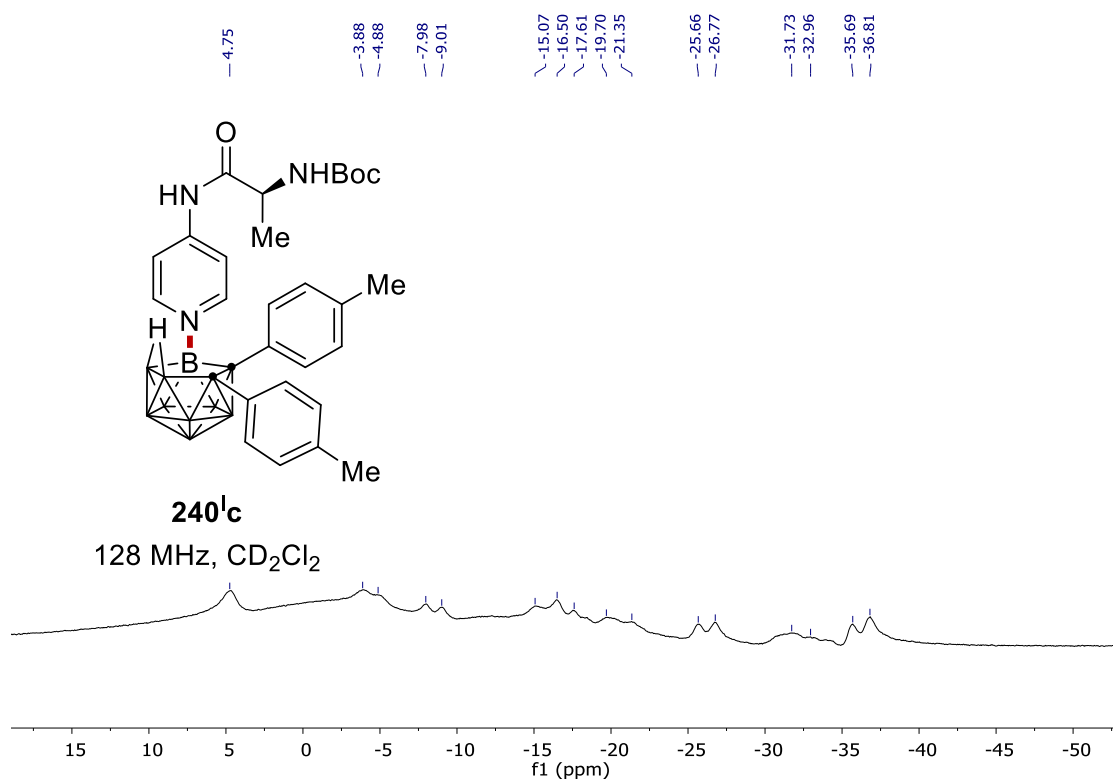
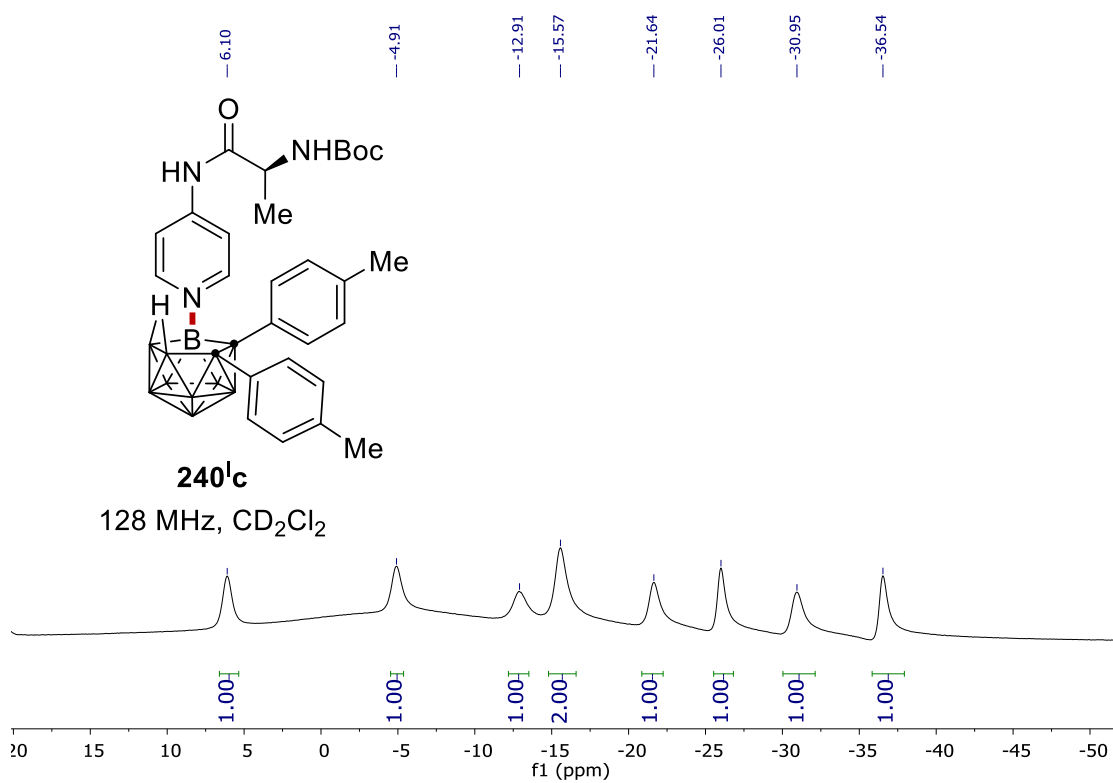


7. NMR Spectra

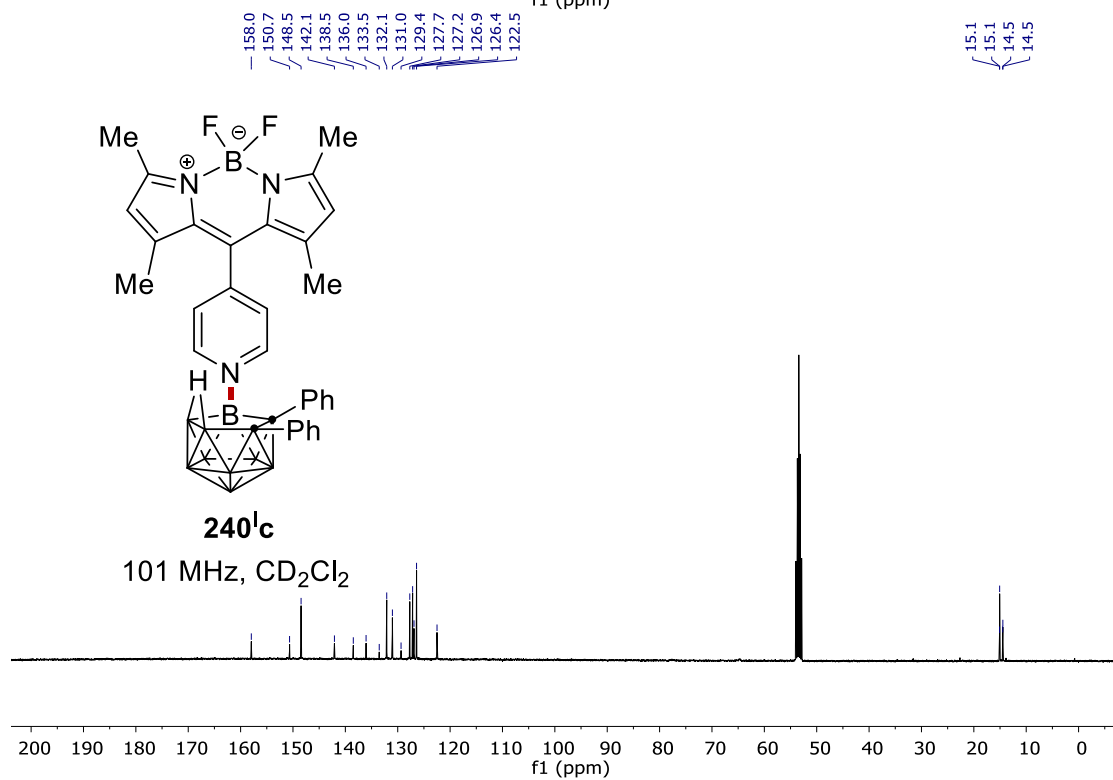
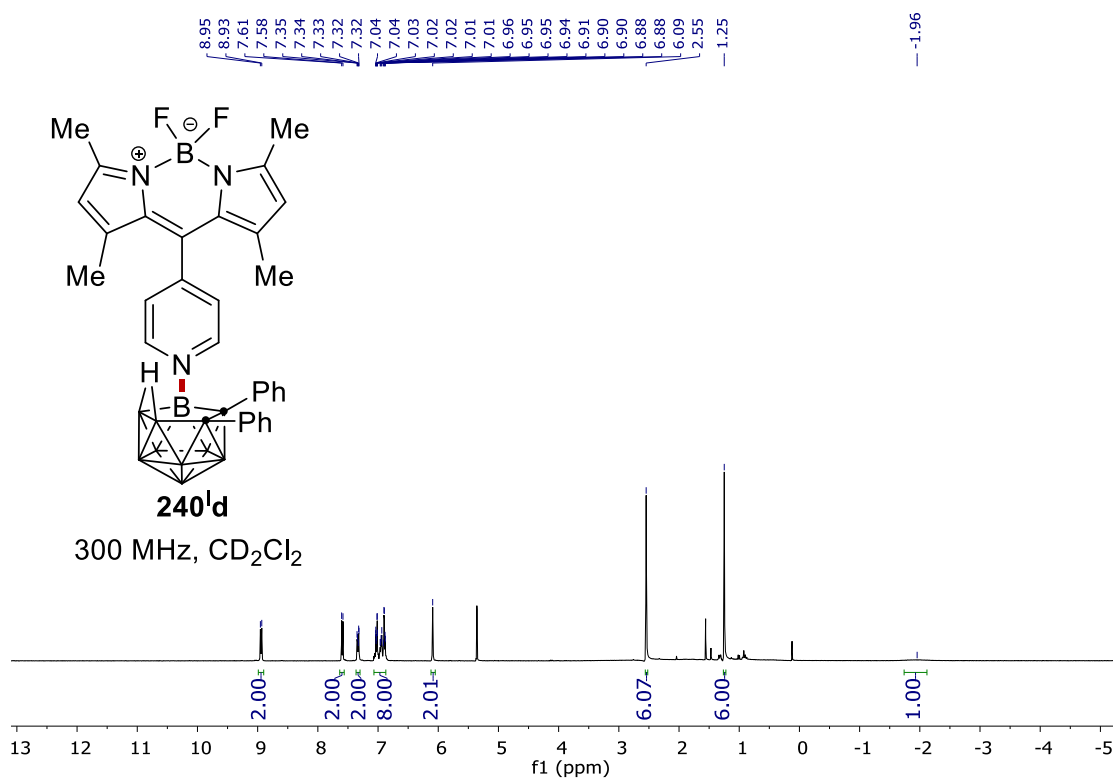




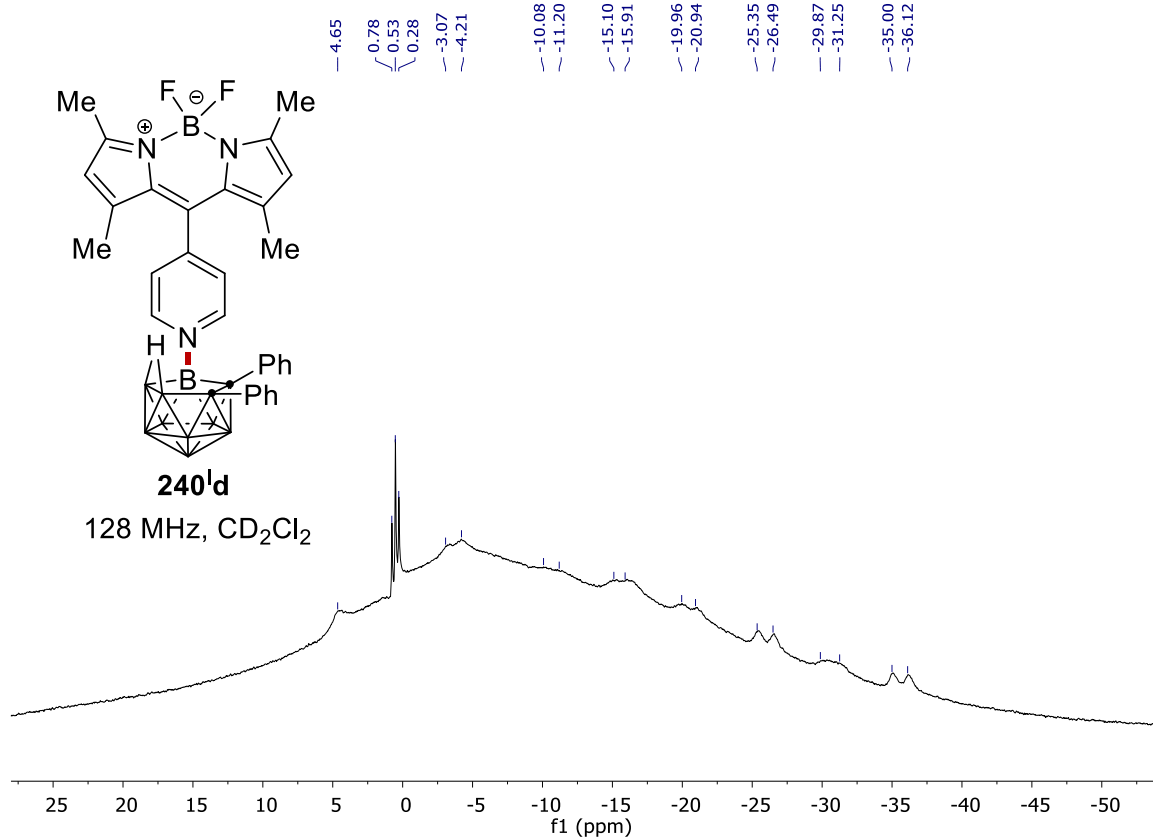
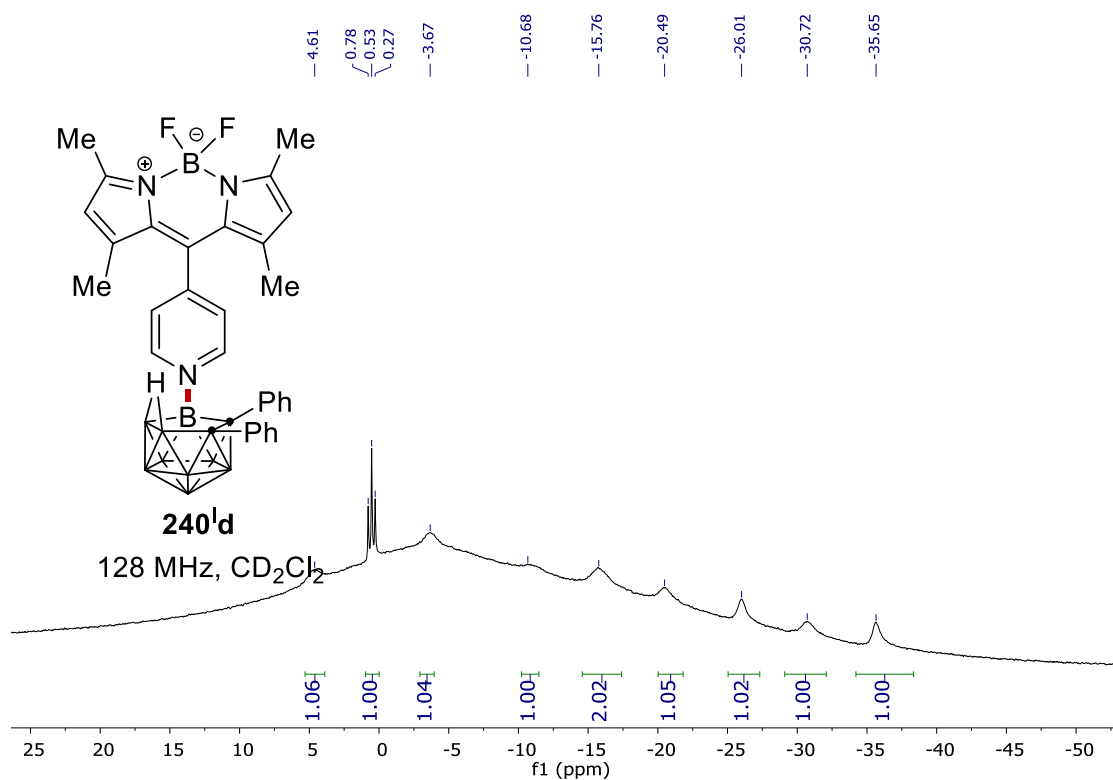
7. NMR Spectra



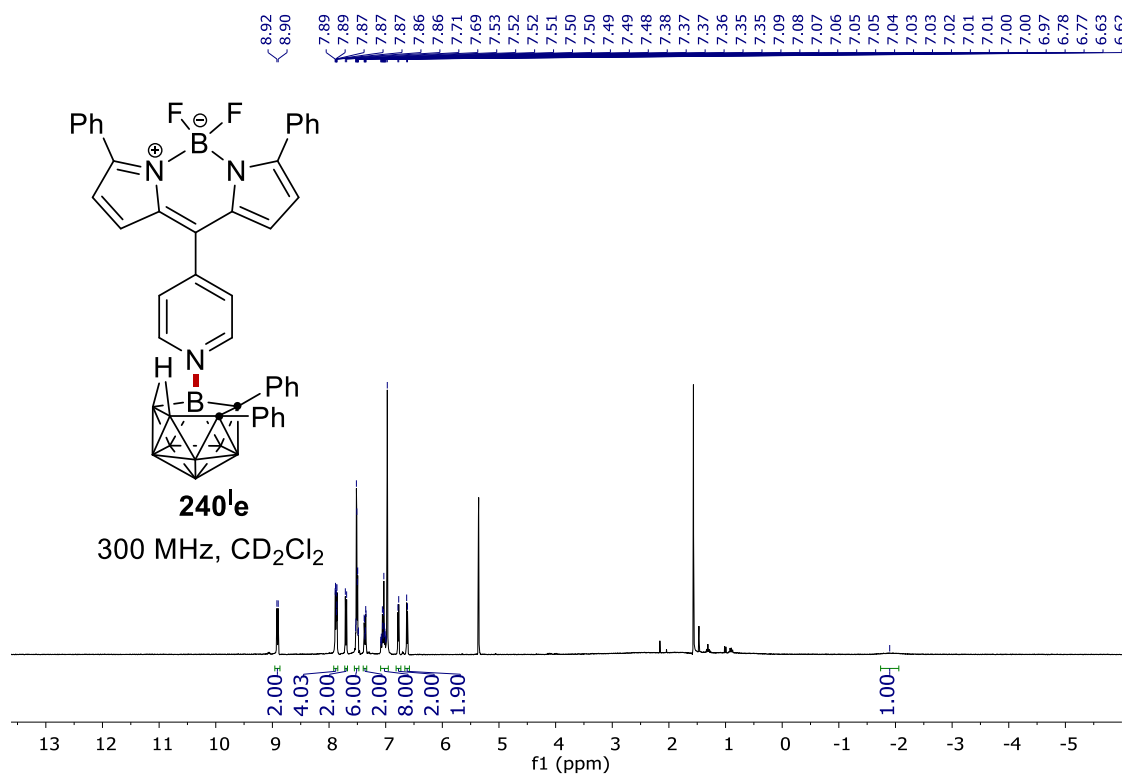
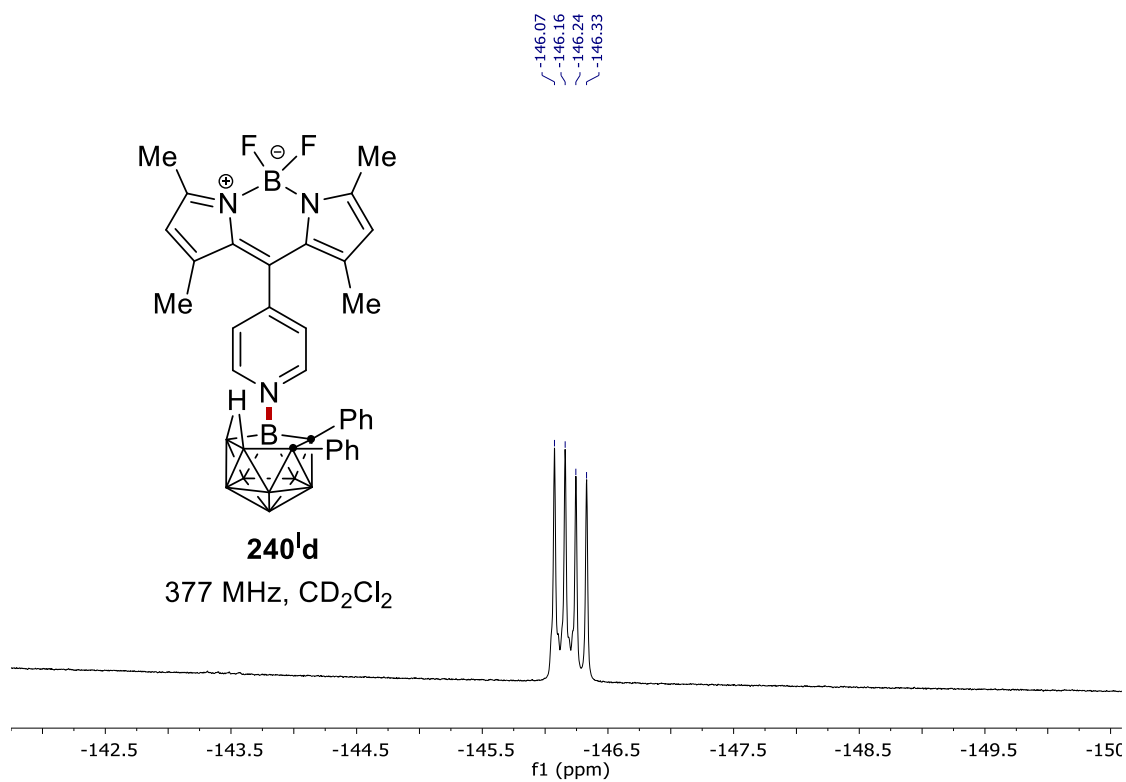
7. NMR Spectra



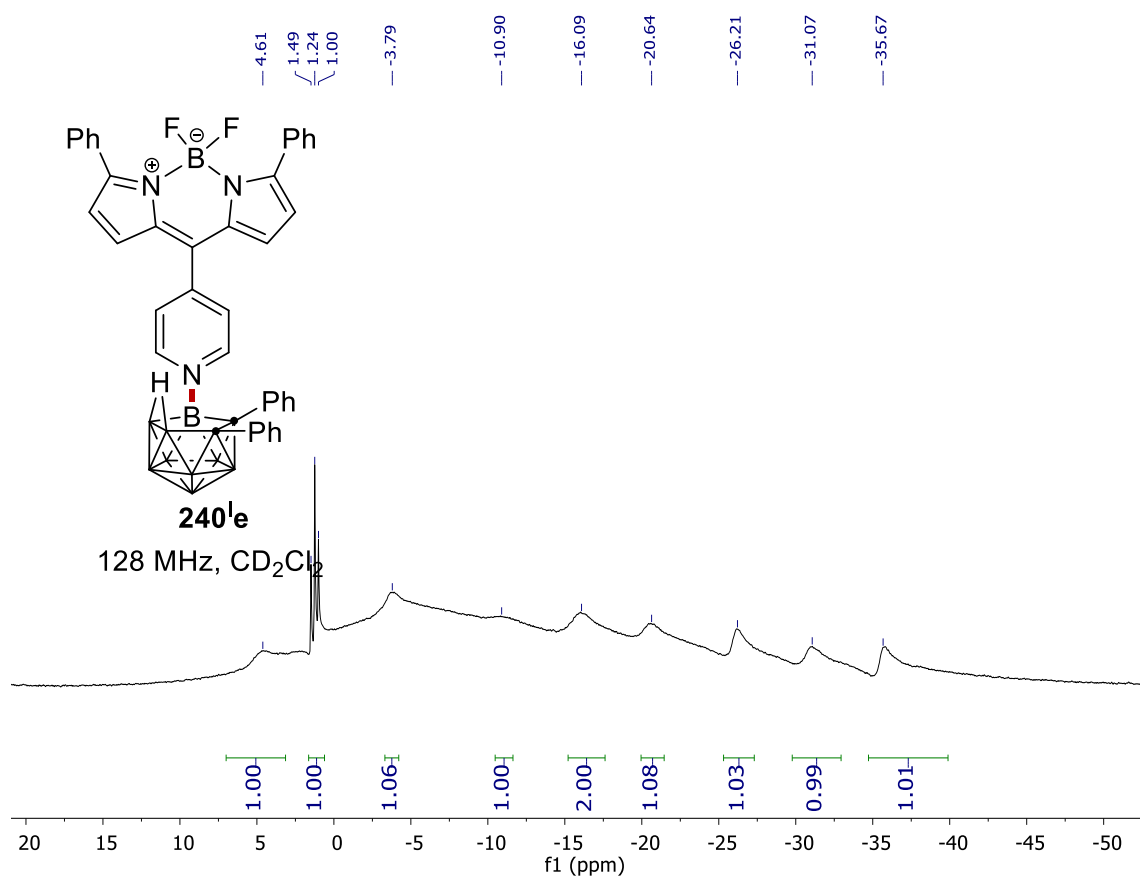
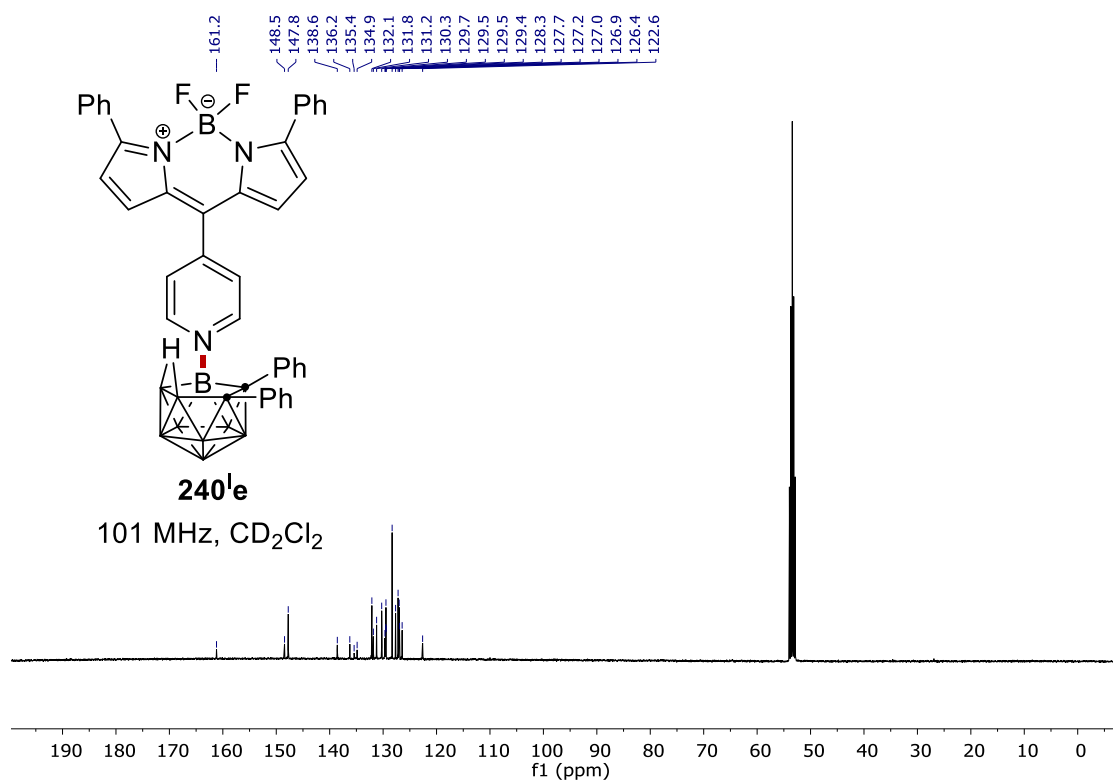
7. NMR Spectra



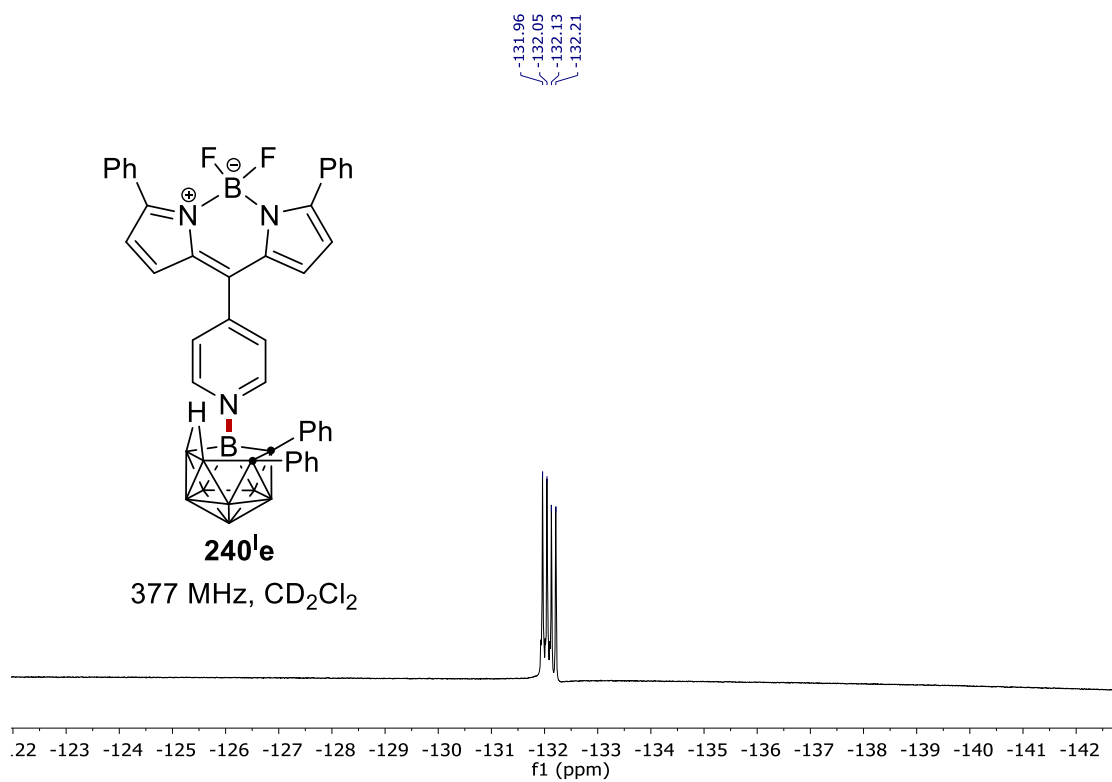
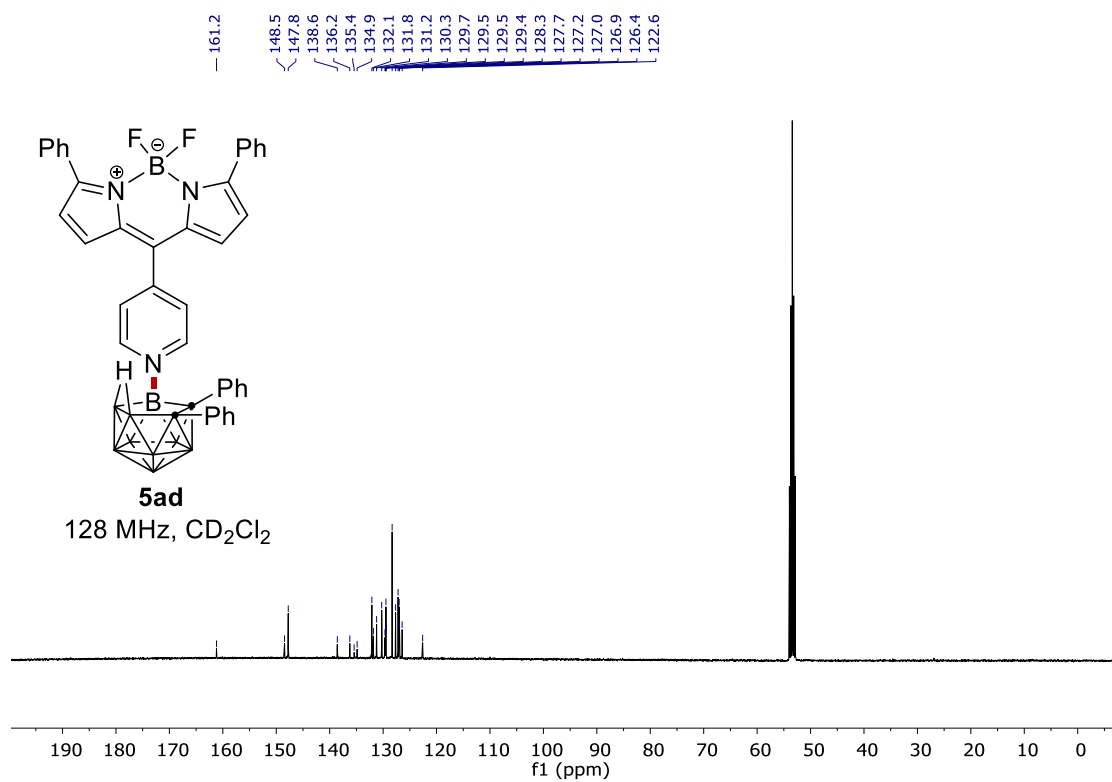
7. NMR Spectra

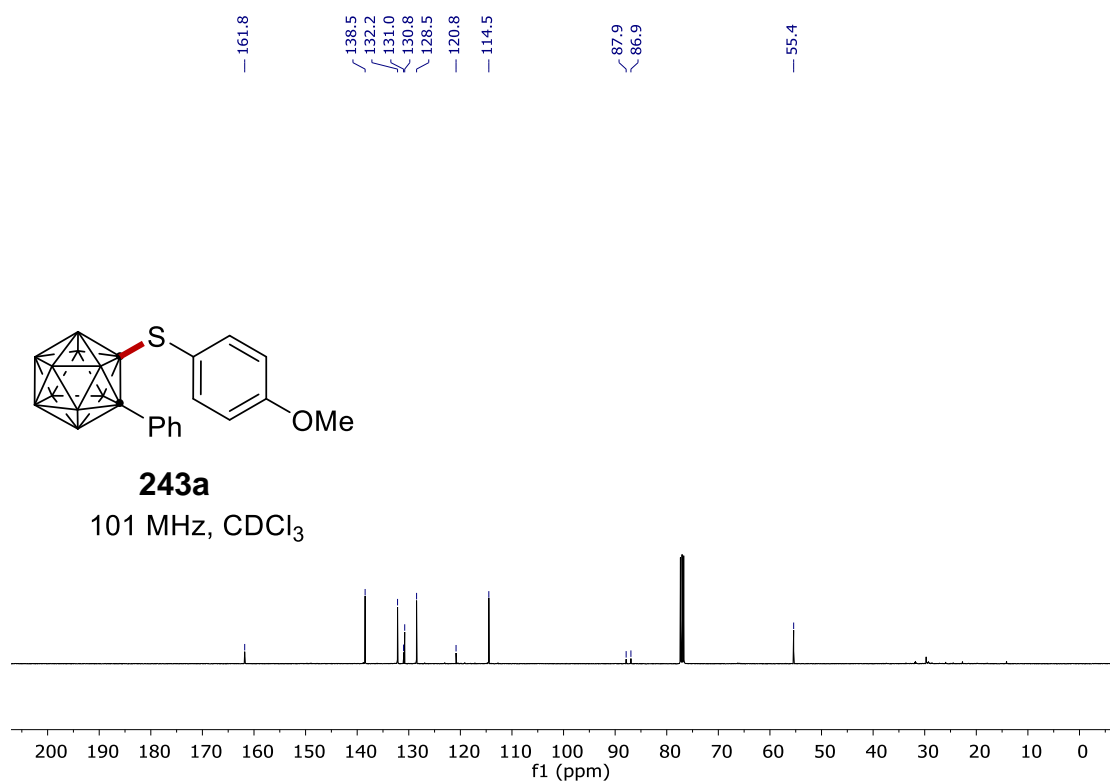
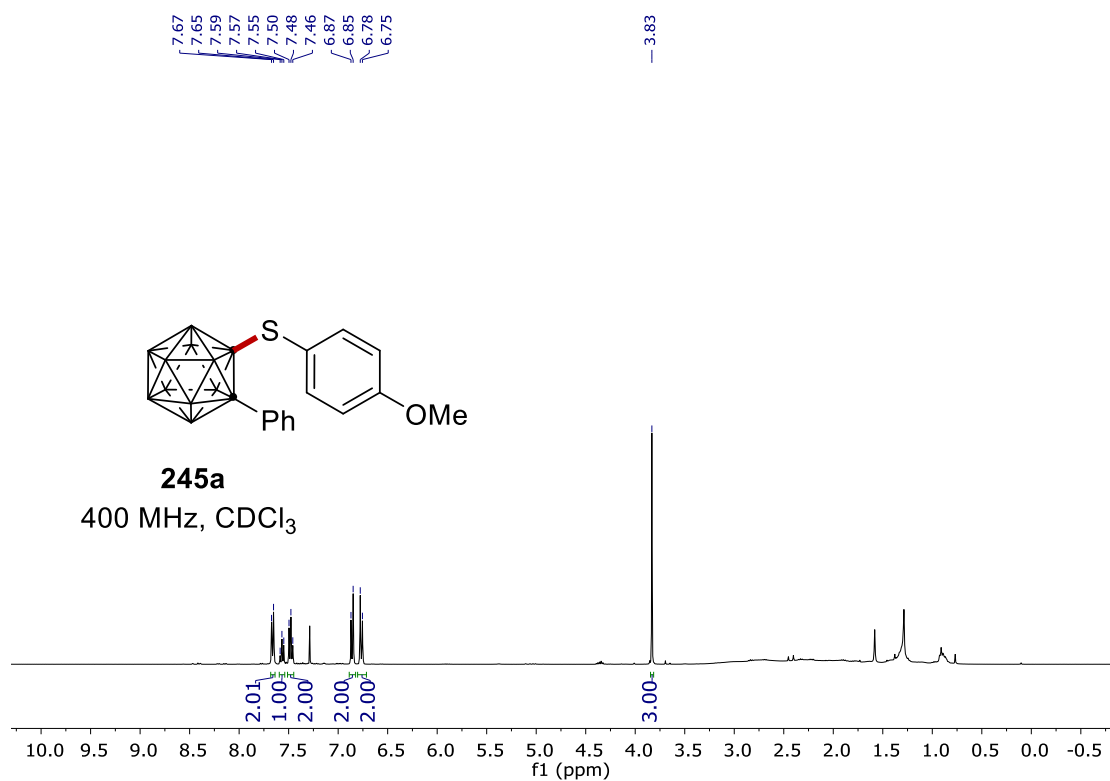


7. NMR Spectra

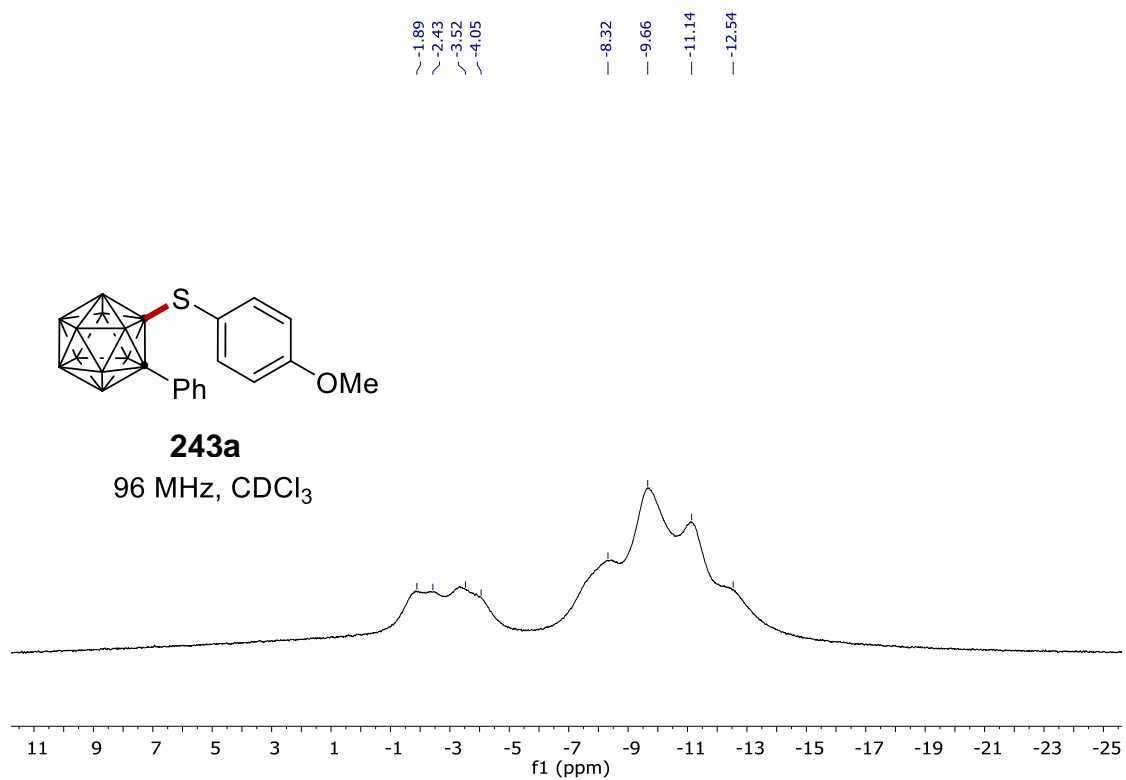
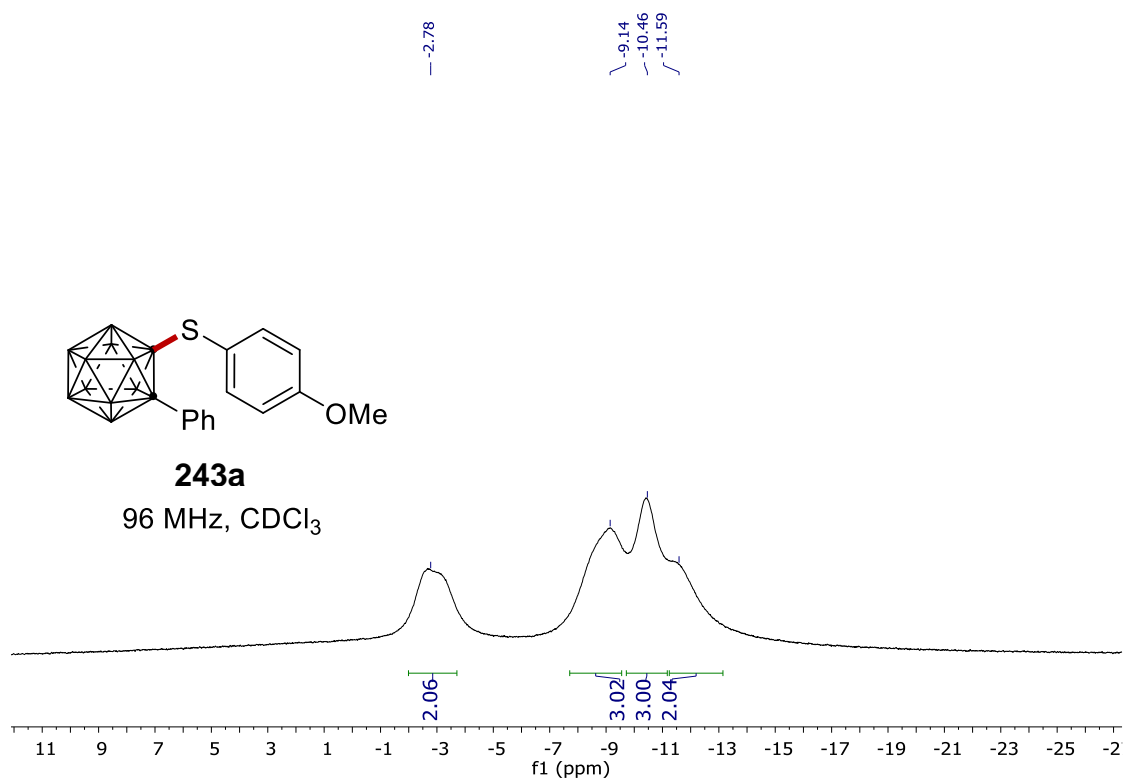


7. NMR Spectra

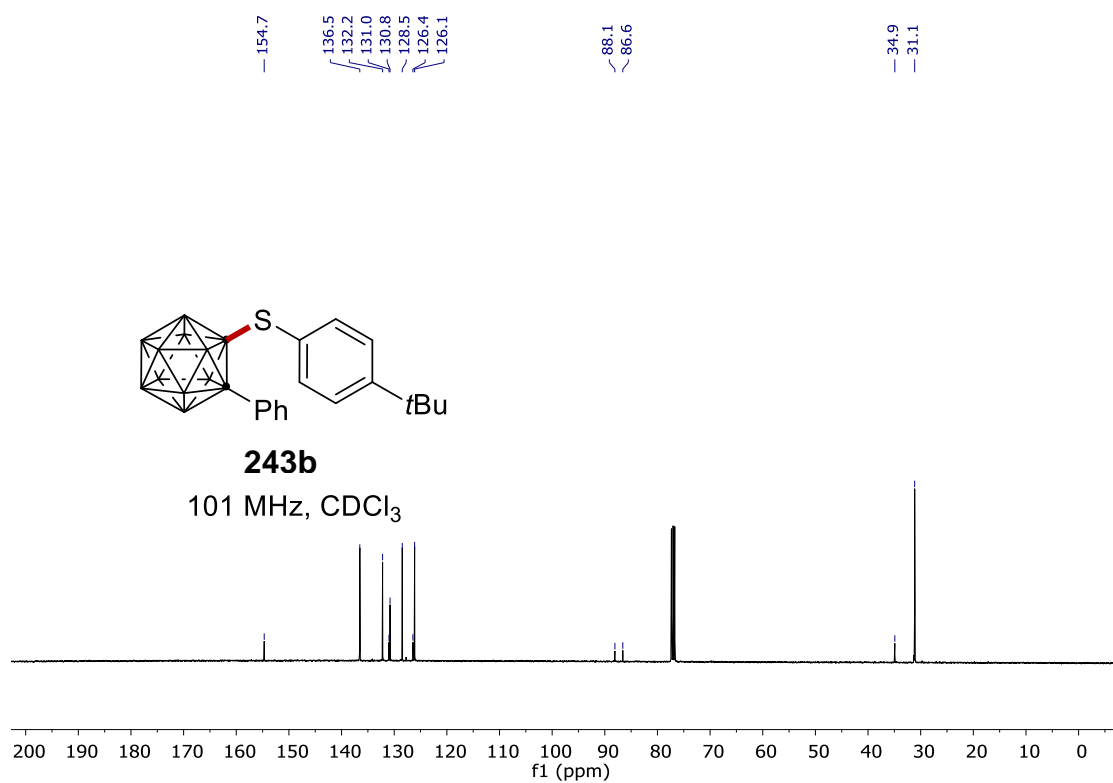
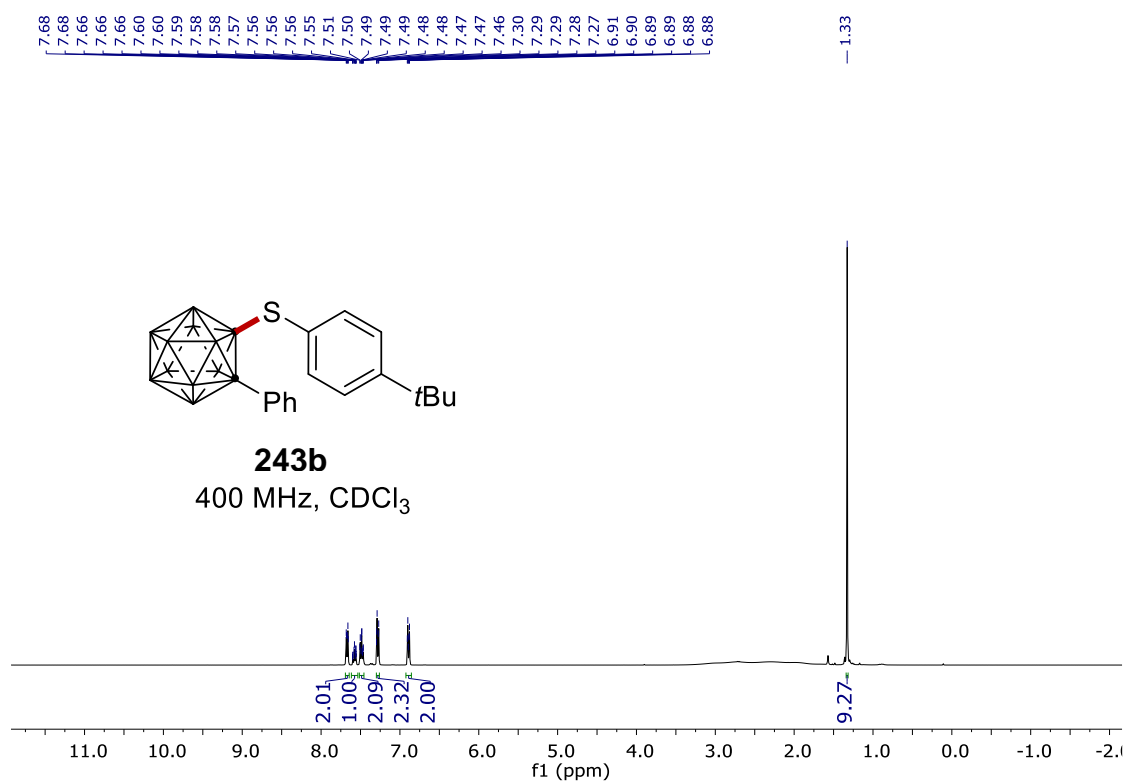


7.2 Cupra-electro-catalyzed cage chalcogenation of α -carboranes

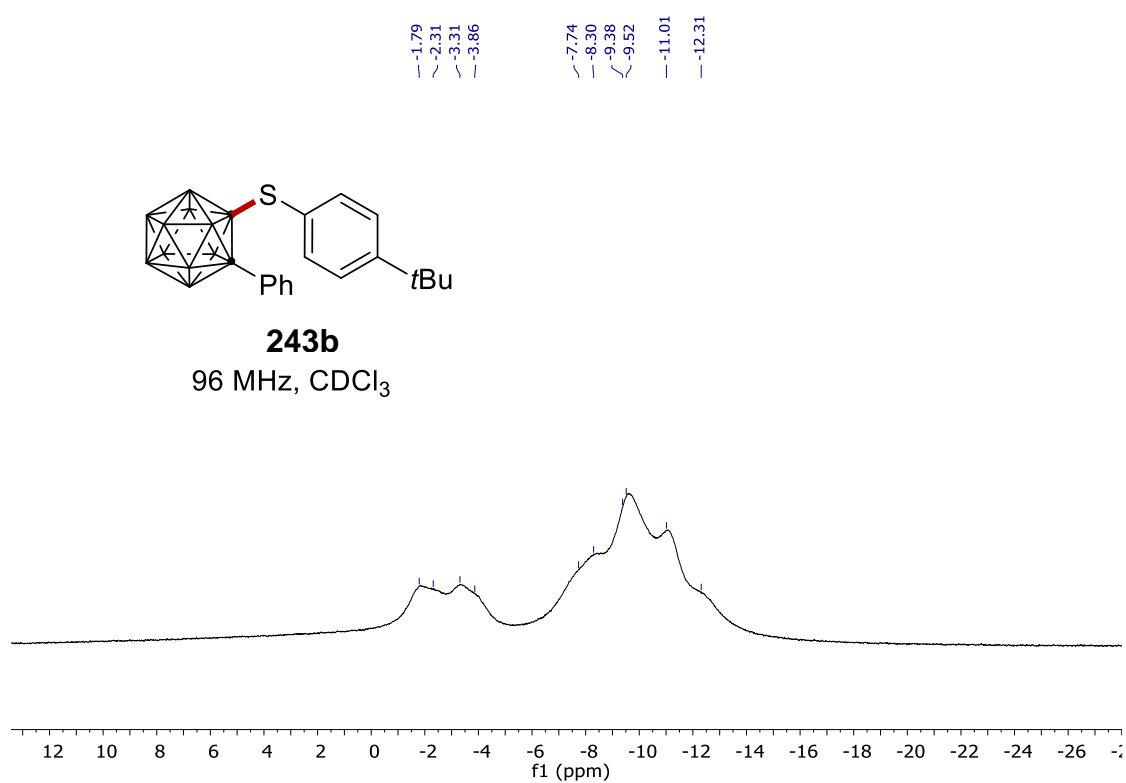
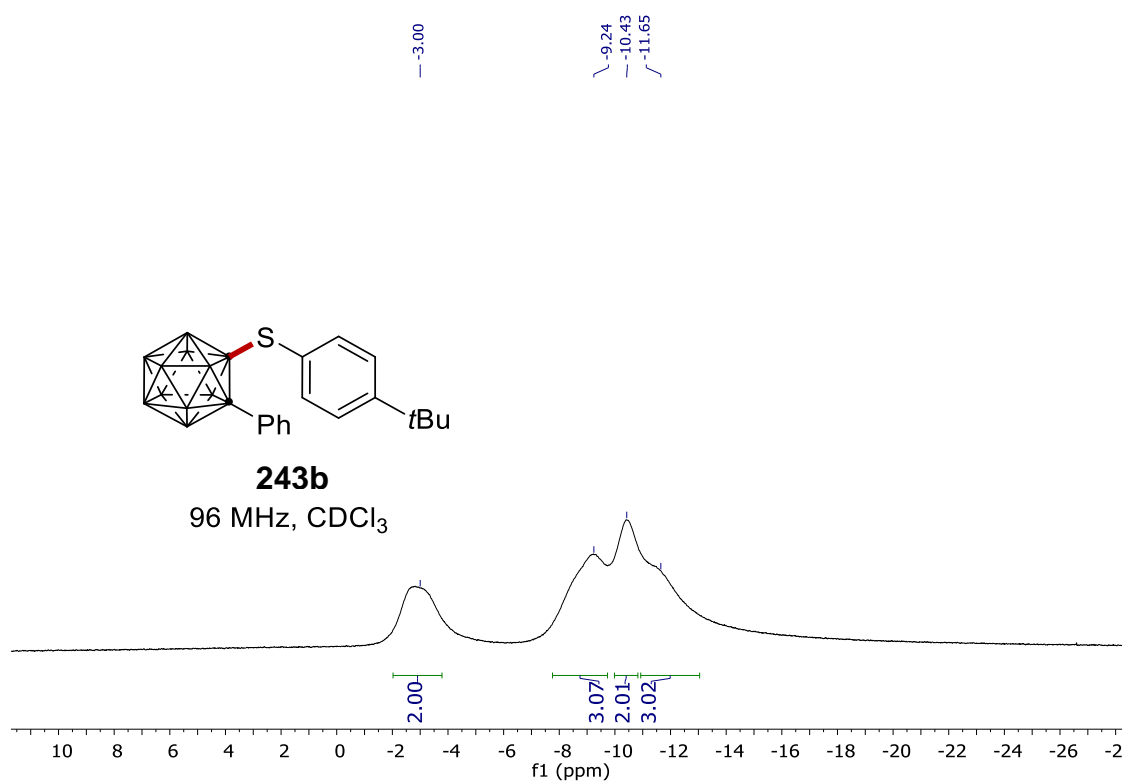
7. NMR Spectra



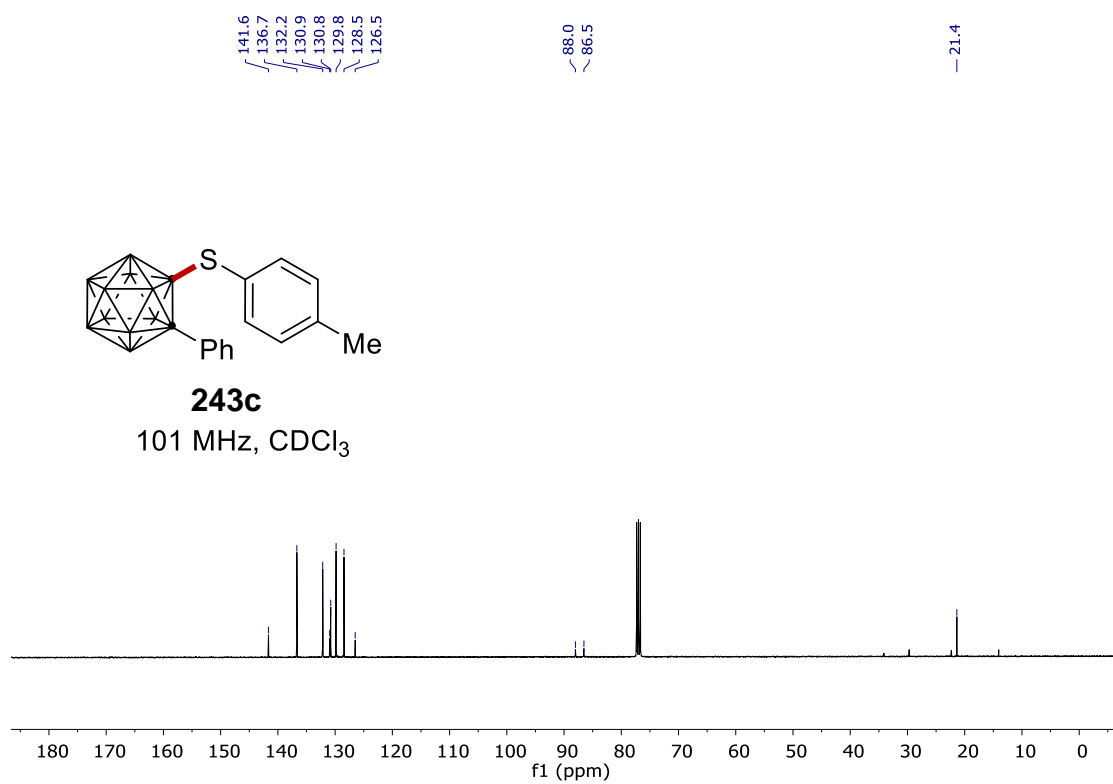
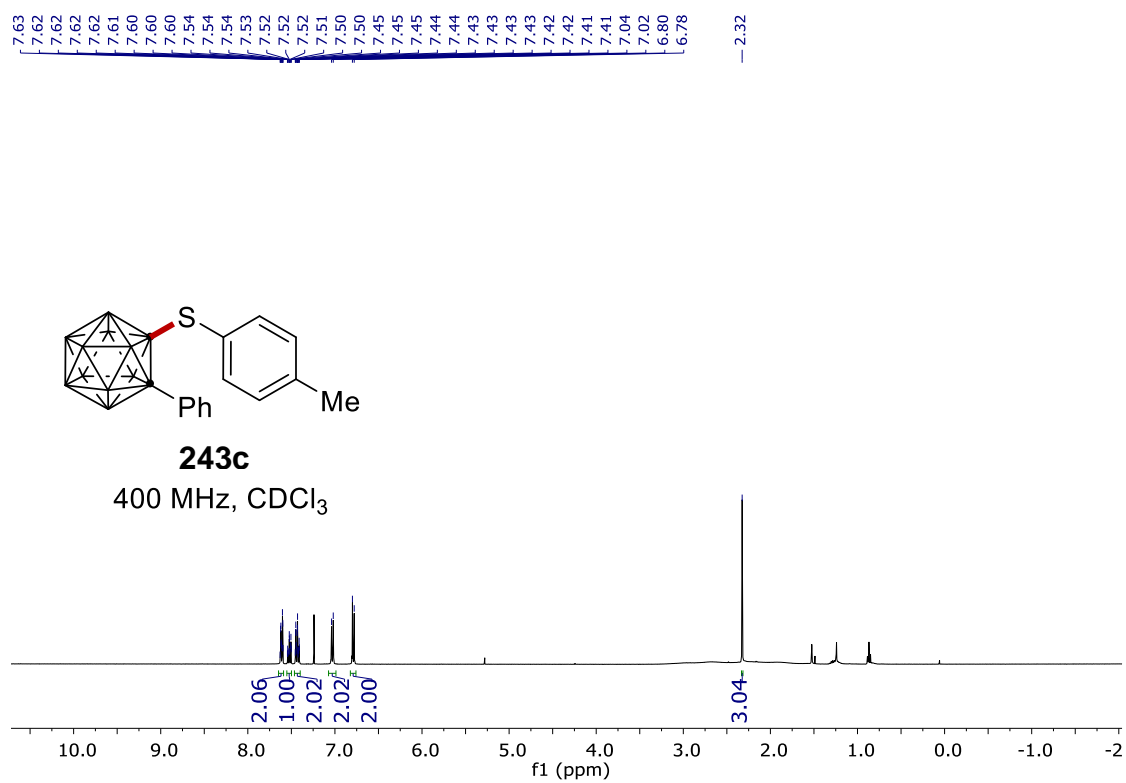
7. NMR Spectra



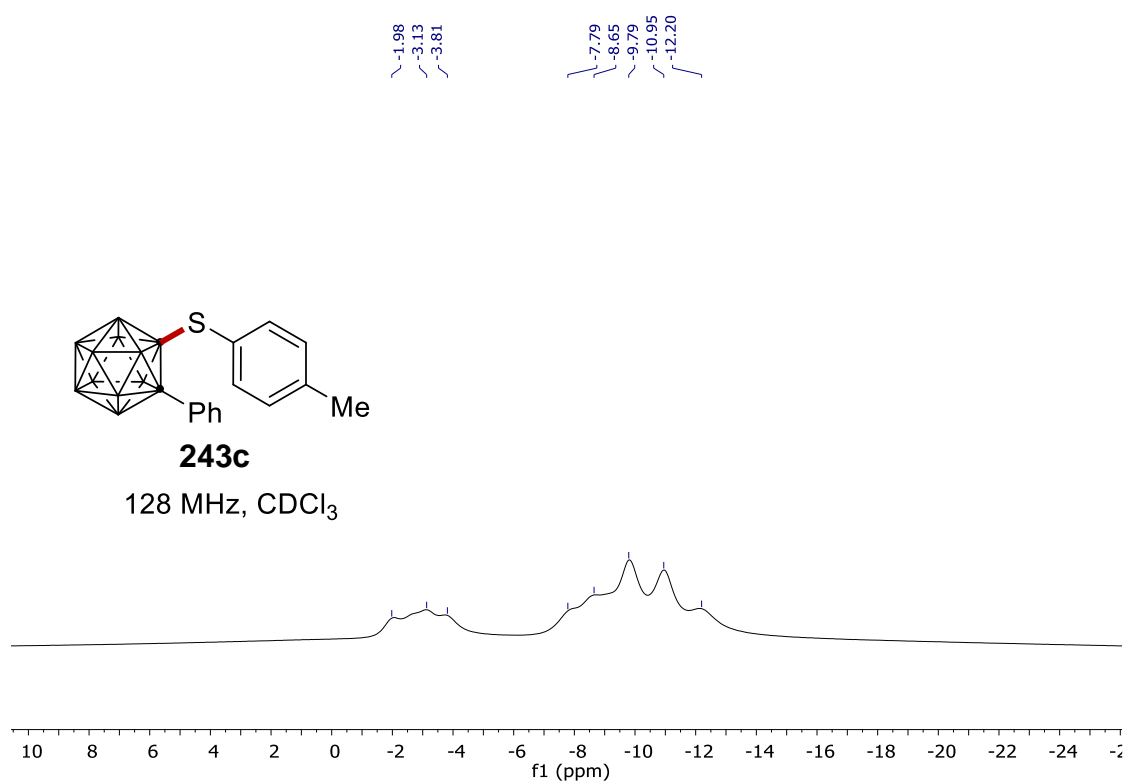
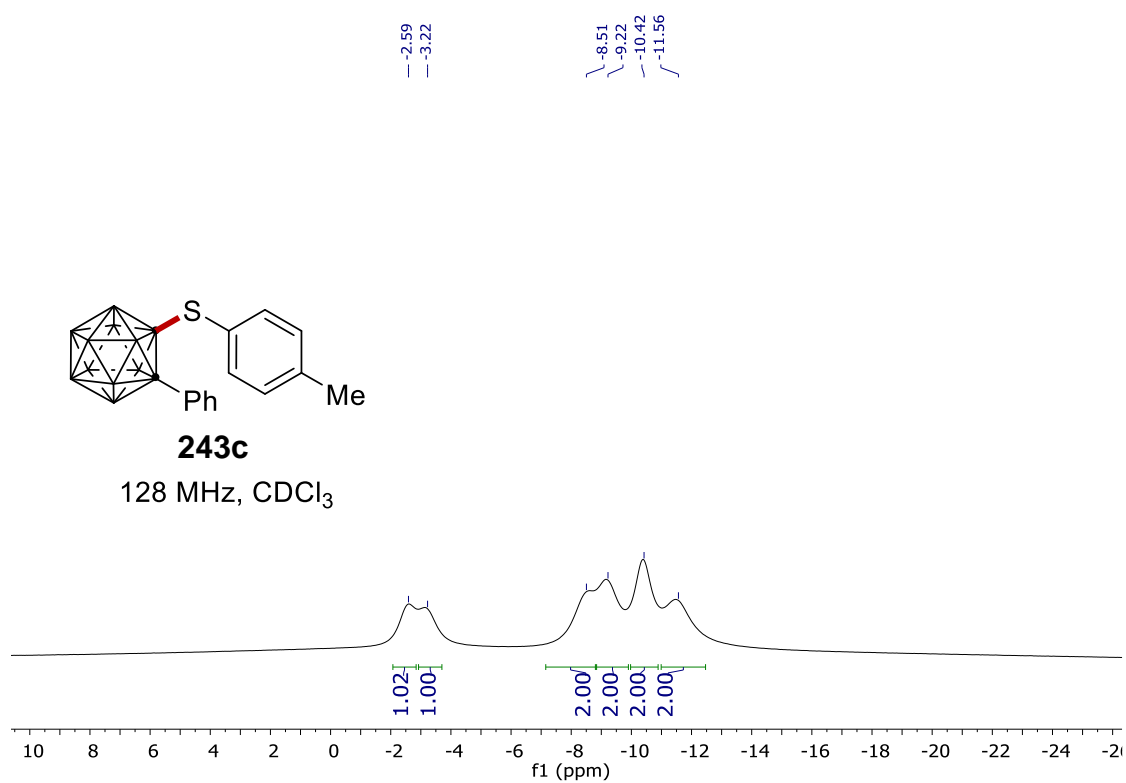
7. NMR Spectra



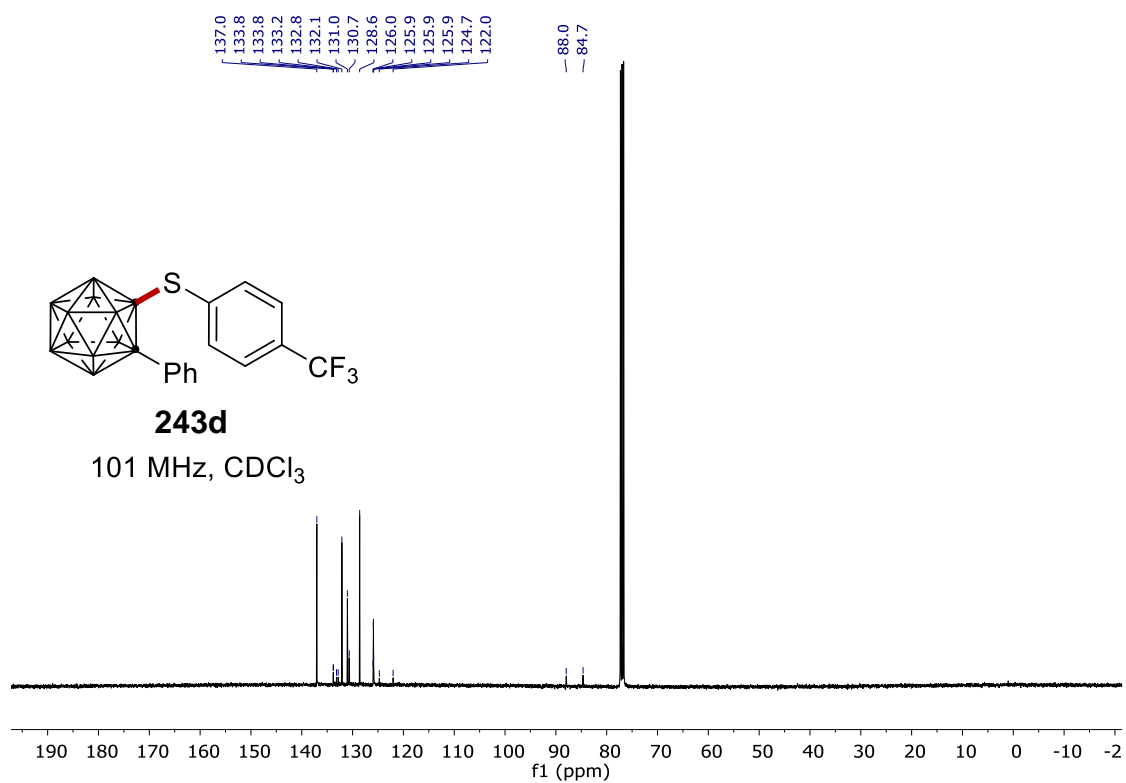
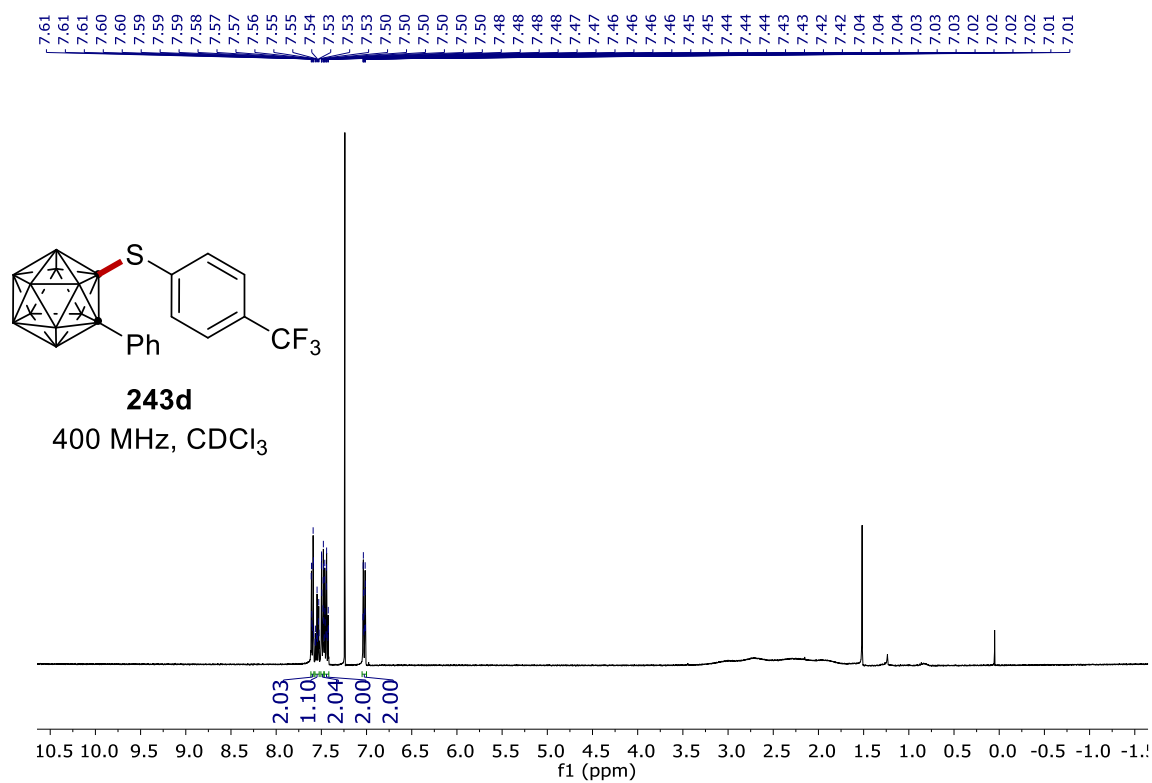
7. NMR Spectra



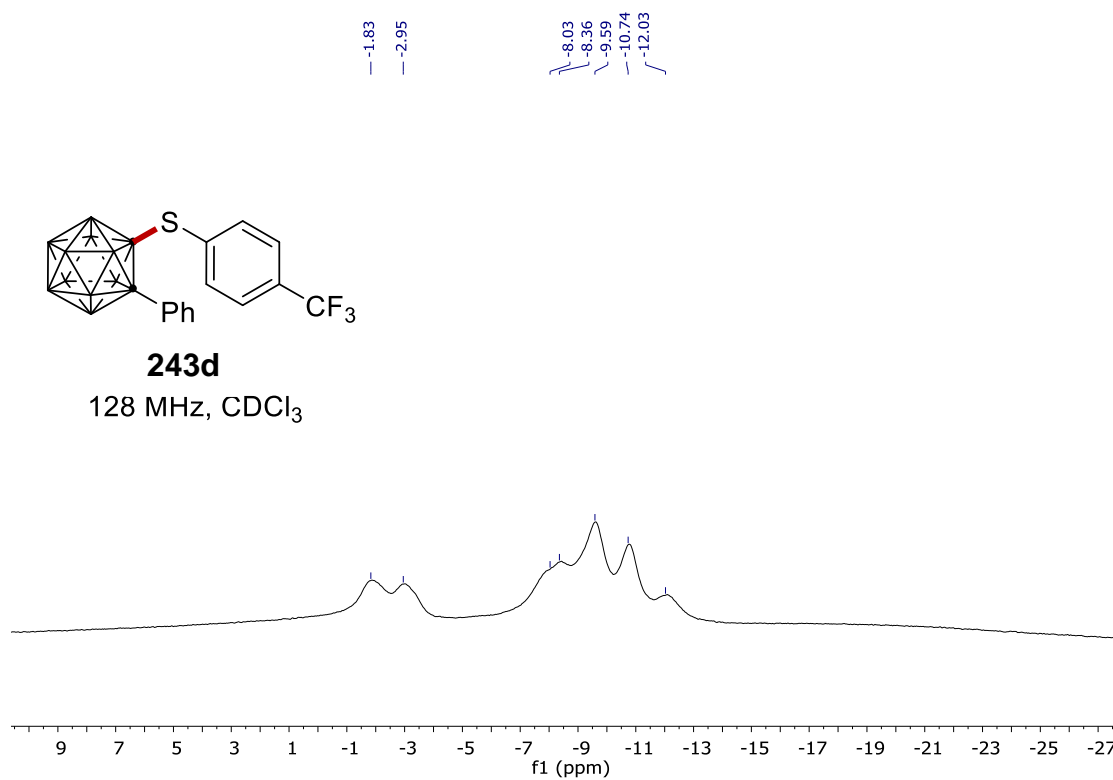
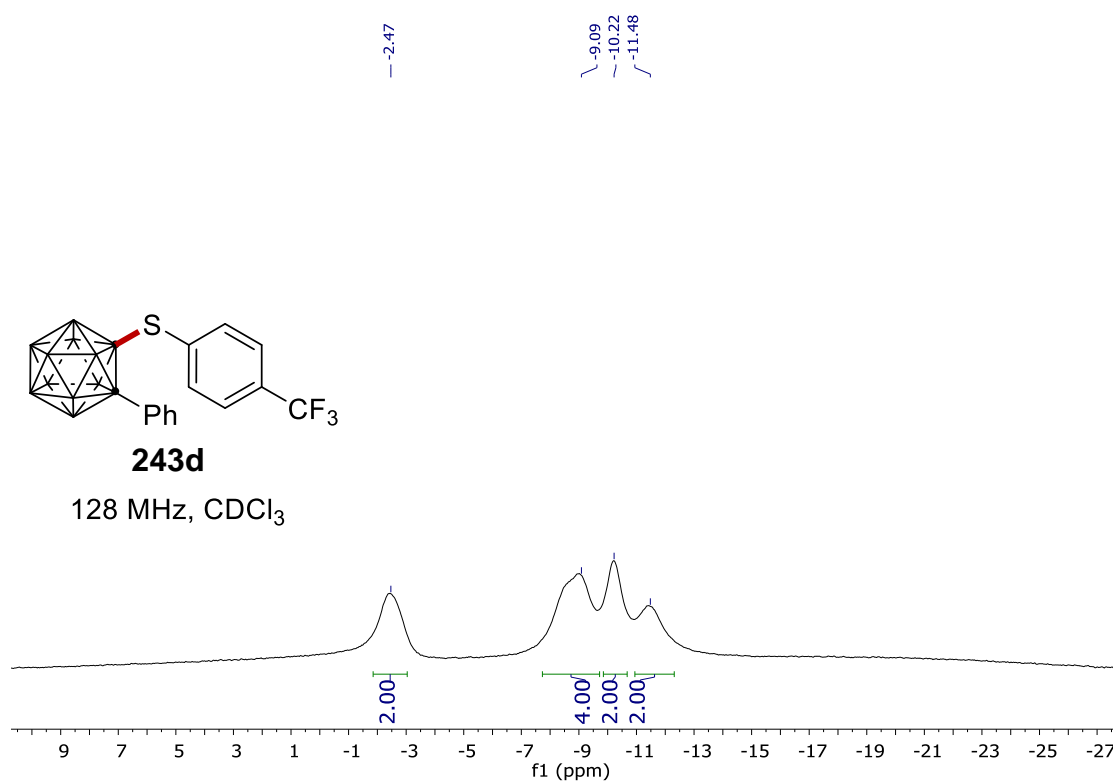
7. NMR Spectra



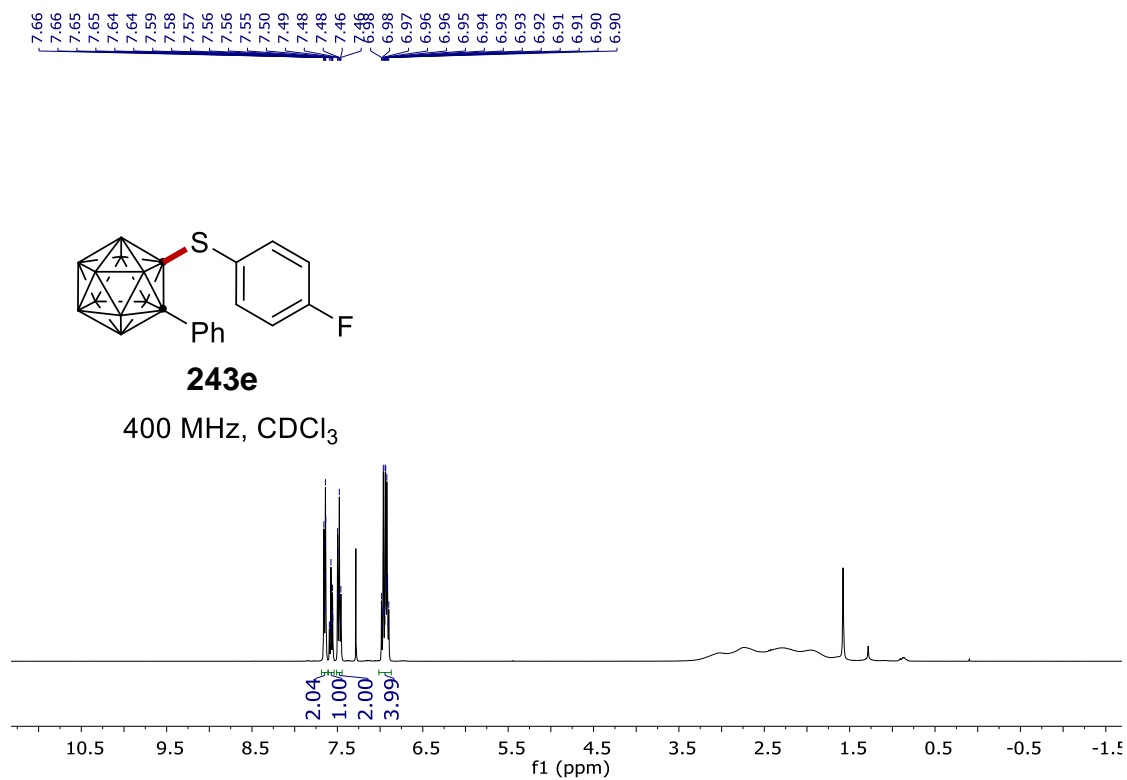
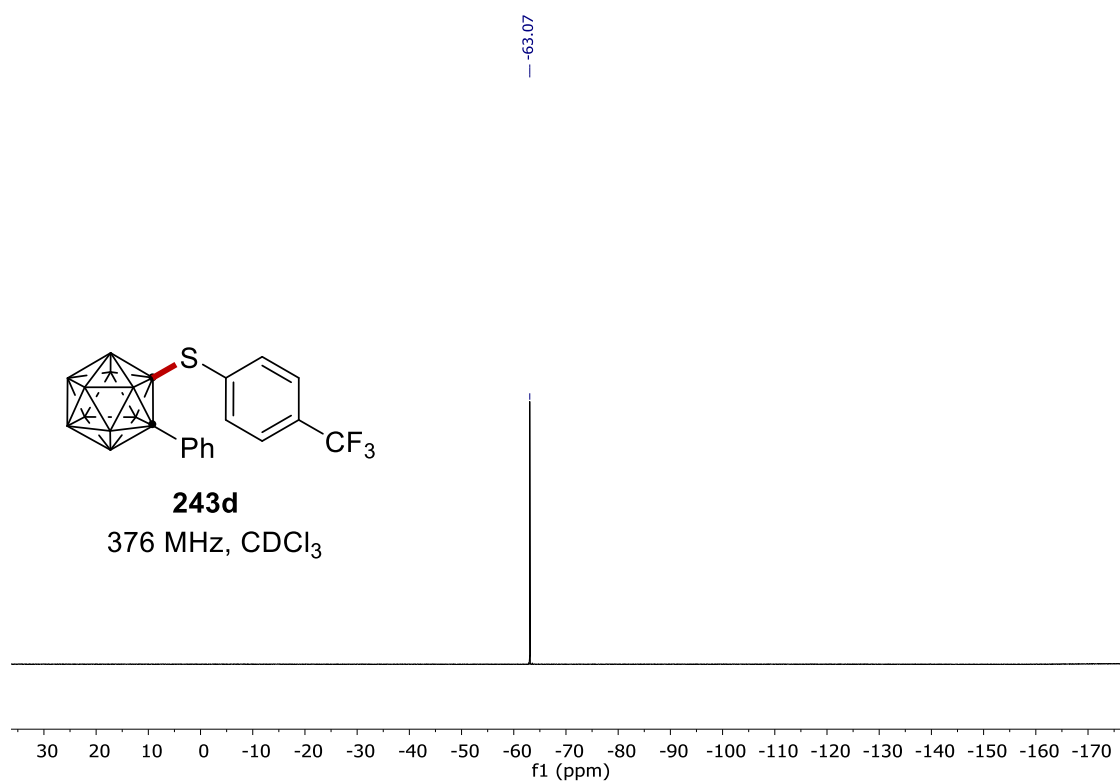
7. NMR Spectra



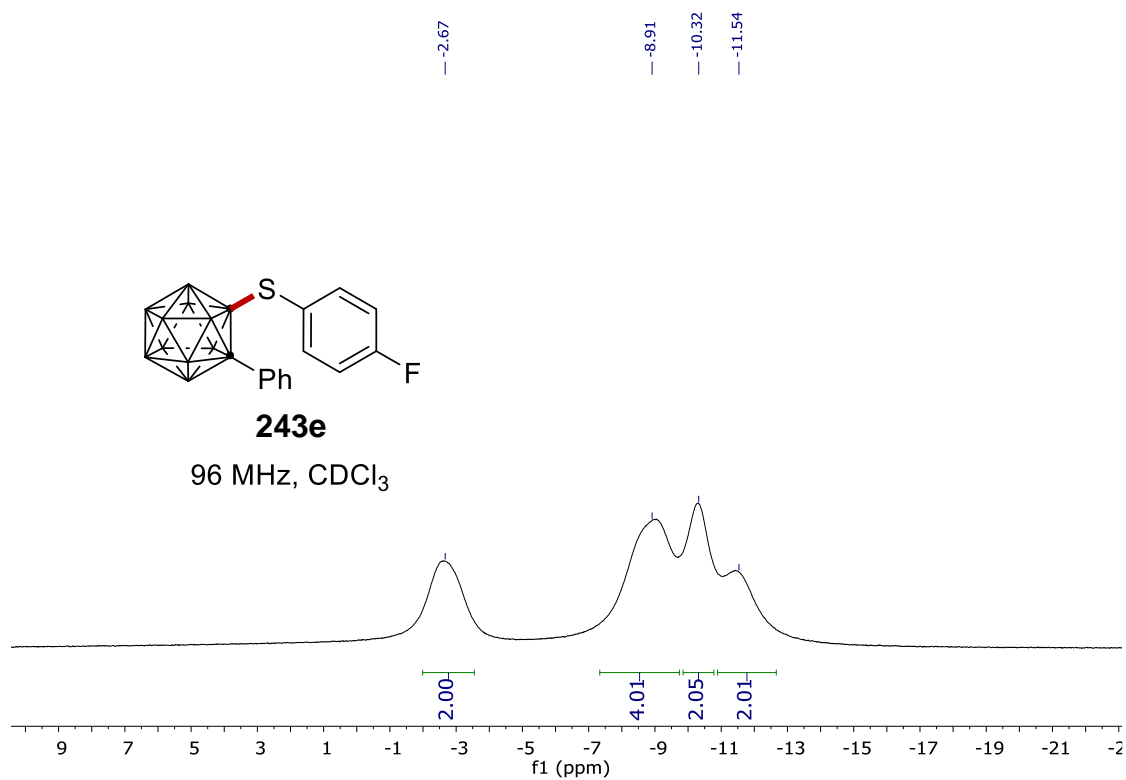
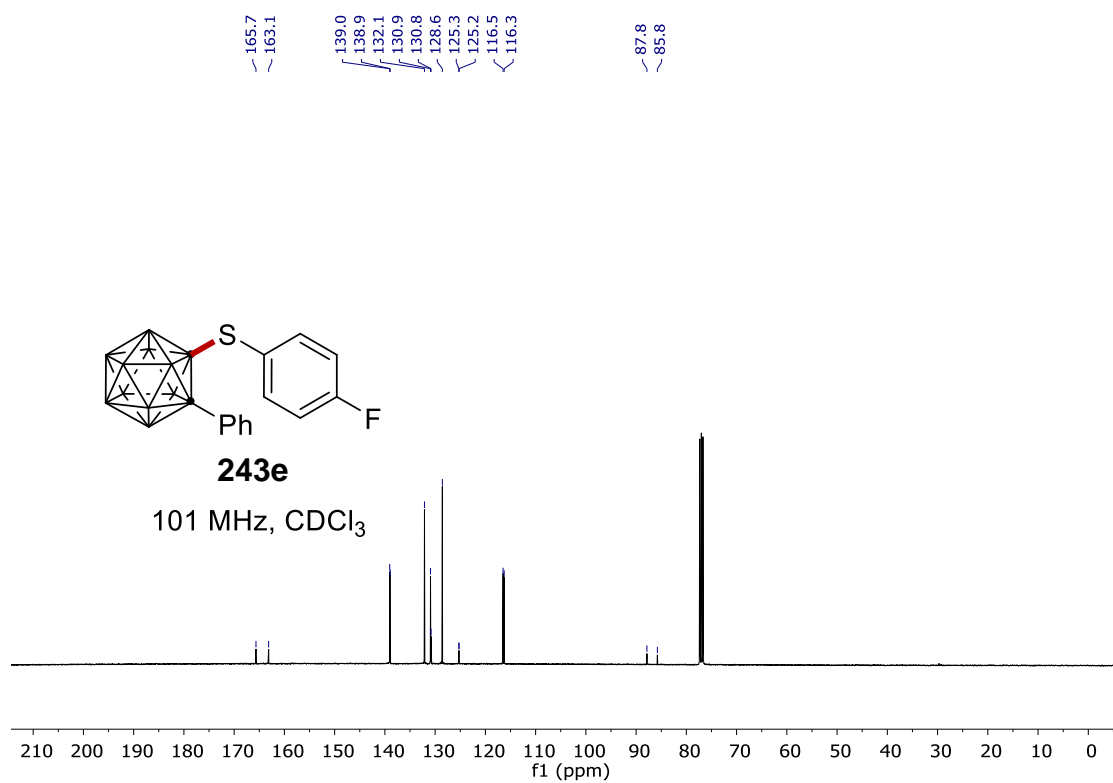
7. NMR Spectra



7. NMR Spectra

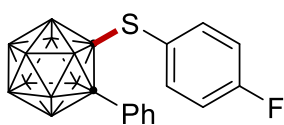


7. NMR Spectra



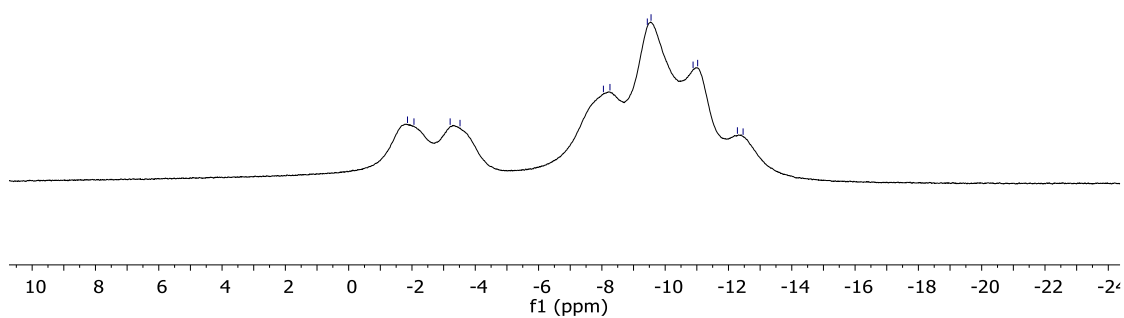
7. NMR Spectra

¹H NMR peaks (ppm):
 -1.86, -2.06, -3.21, -3.52, -8.05, -8.26, -9.44, -9.55, -10.88, -11.03, -12.28, -12.46

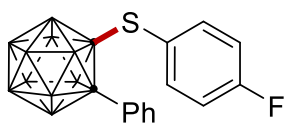


243e

96 MHz, CDCl₃

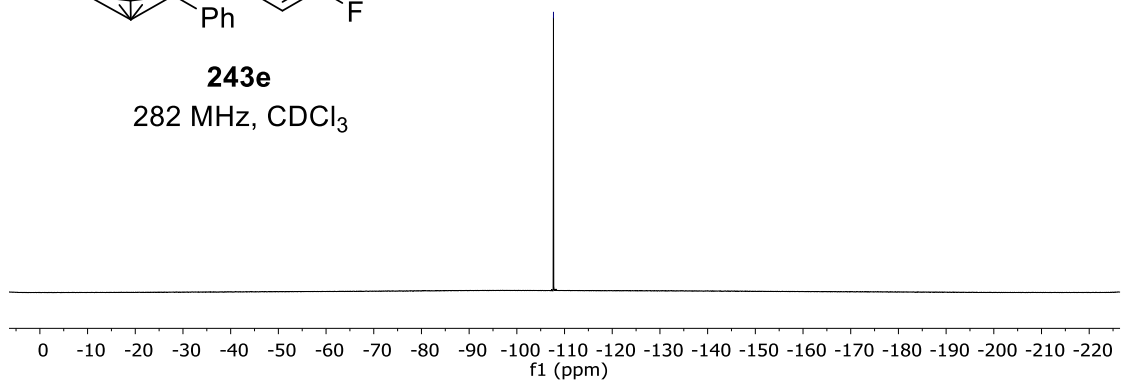


¹³C NMR peak (ppm):
 -107.68



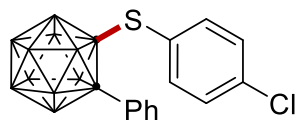
243e

282 MHz, CDCl₃



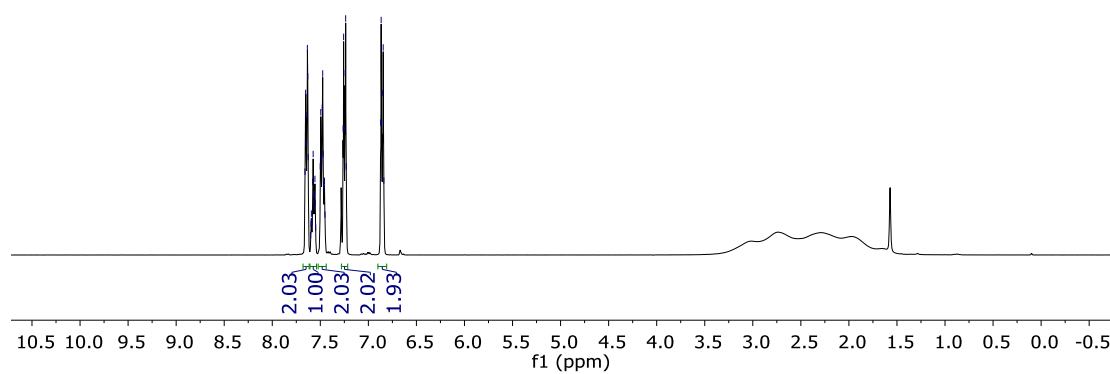
7. NMR Spectra

7.66
7.65
7.65
7.64
7.63
7.63
7.60
7.60
7.59
7.59
7.58
7.58
7.57
7.57
7.56
7.56
7.56
7.55
7.55
7.50
7.50
7.49
7.48
7.48
7.47
7.47
7.46
7.46
7.45
7.45
7.26
7.26
7.25
7.25
7.24
7.24
7.23
7.23
6.87
6.87
6.86
6.86
6.85
6.85
6.84



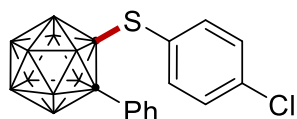
243f

400 MHz, CDCl₃



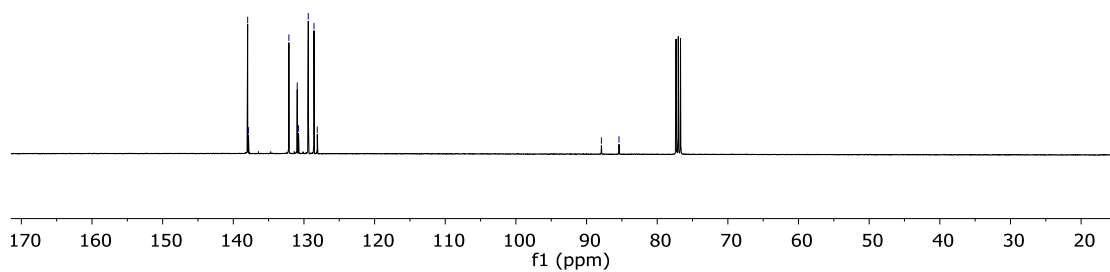
138.0
137.9
132.1
131.0
130.8
129.4
128.6
128.1

87.9
85.4

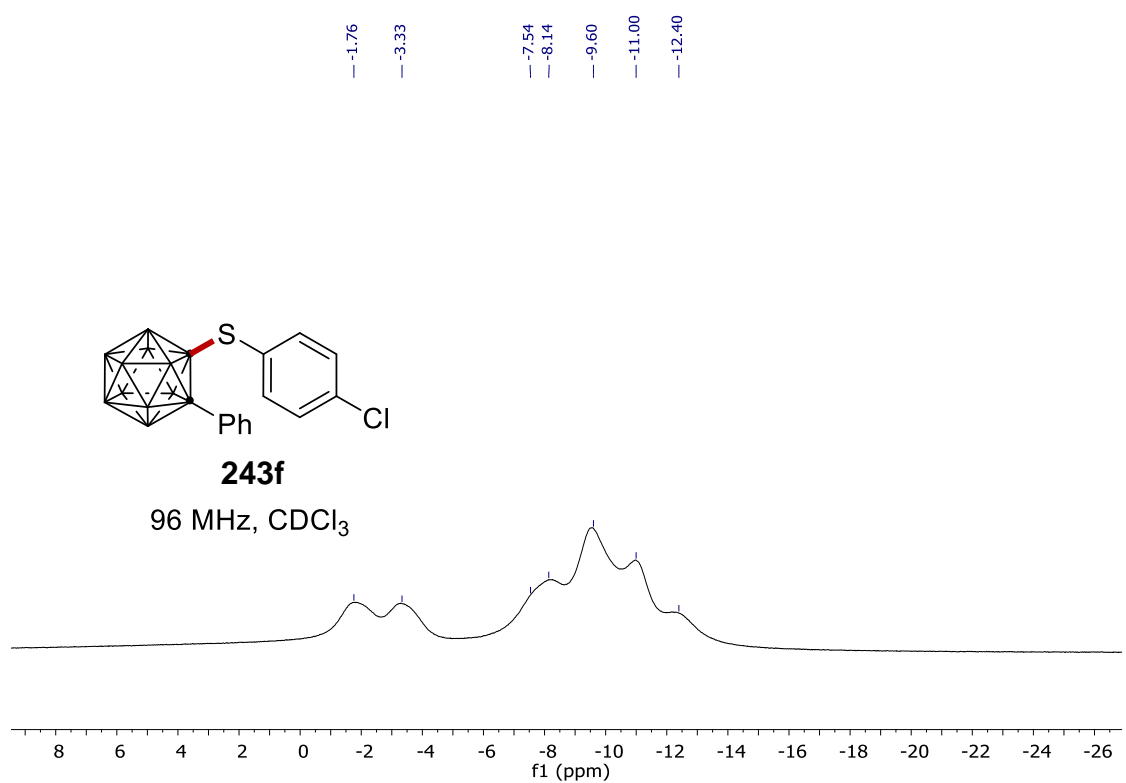
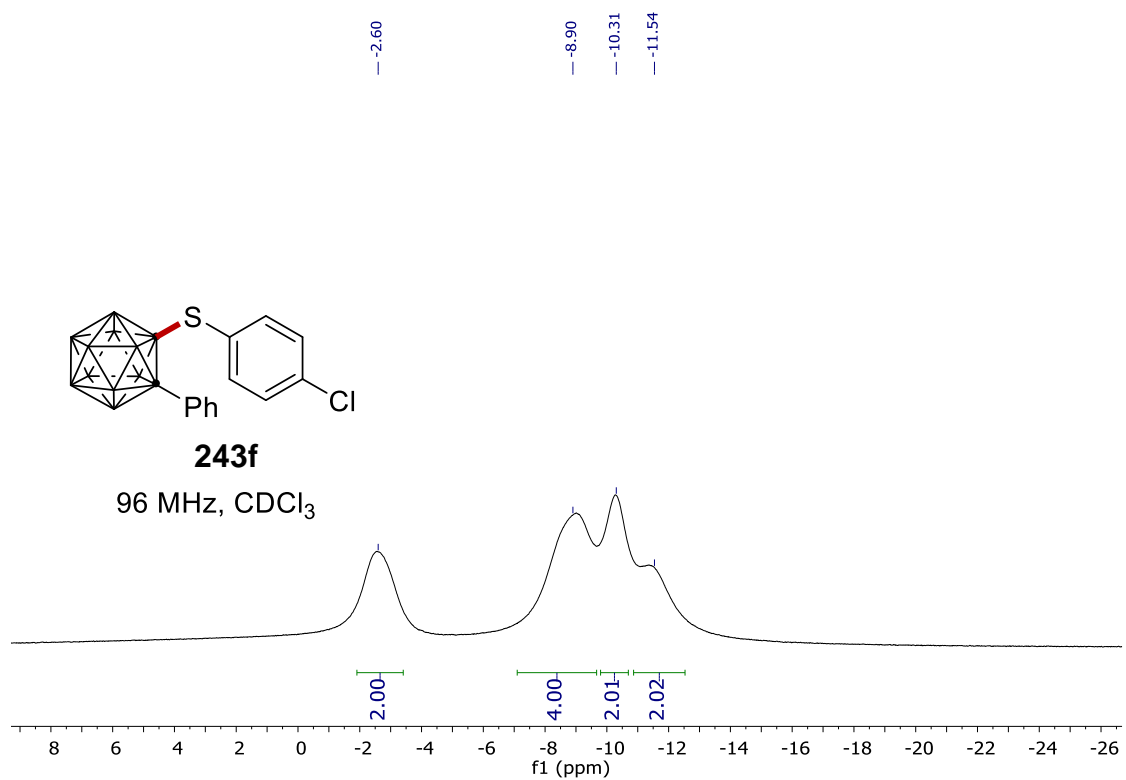


243f

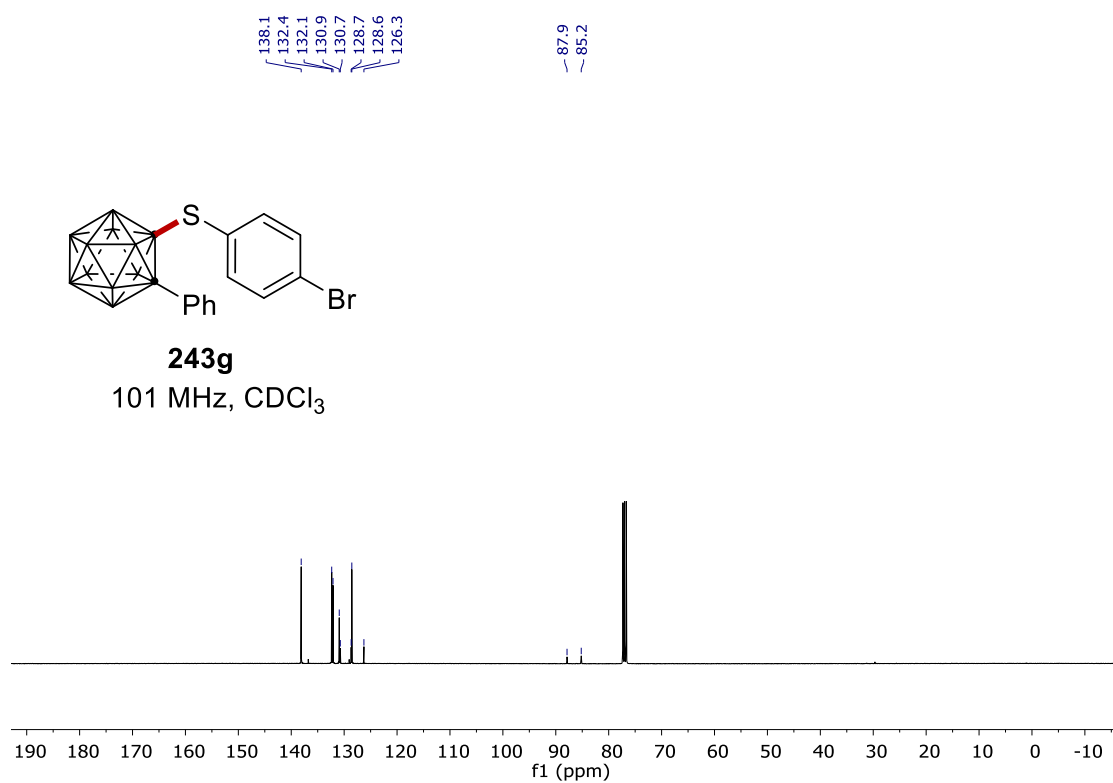
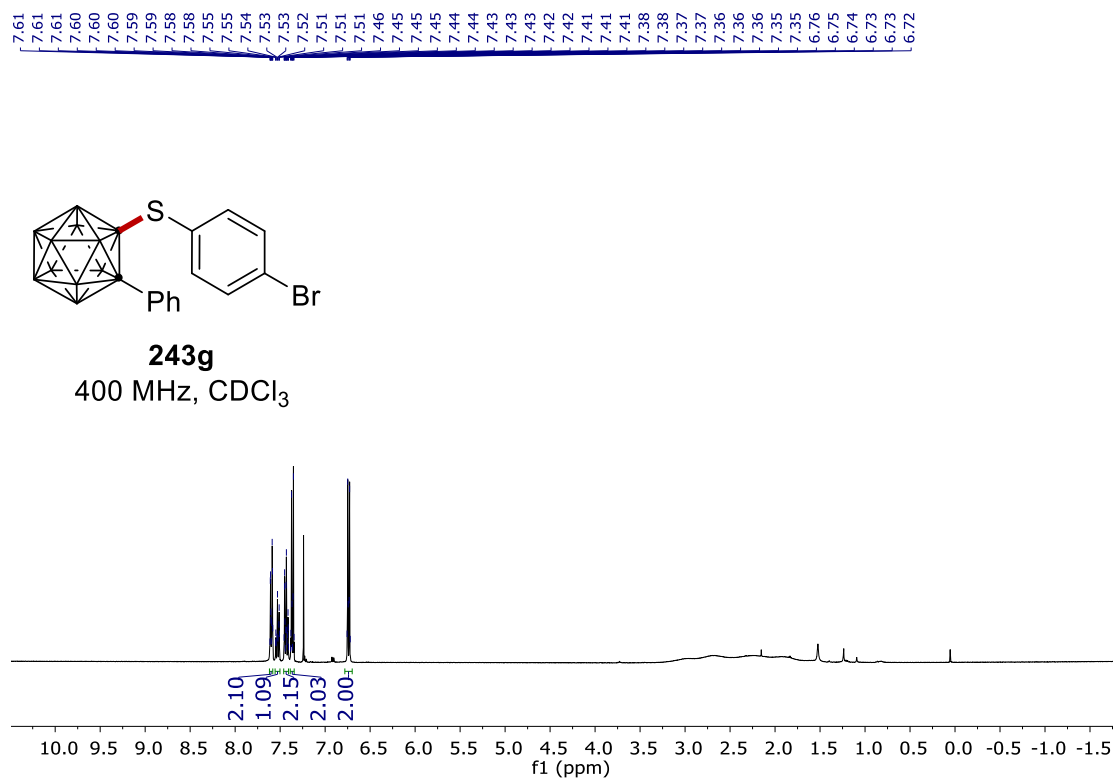
101 MHz, CDCl₃



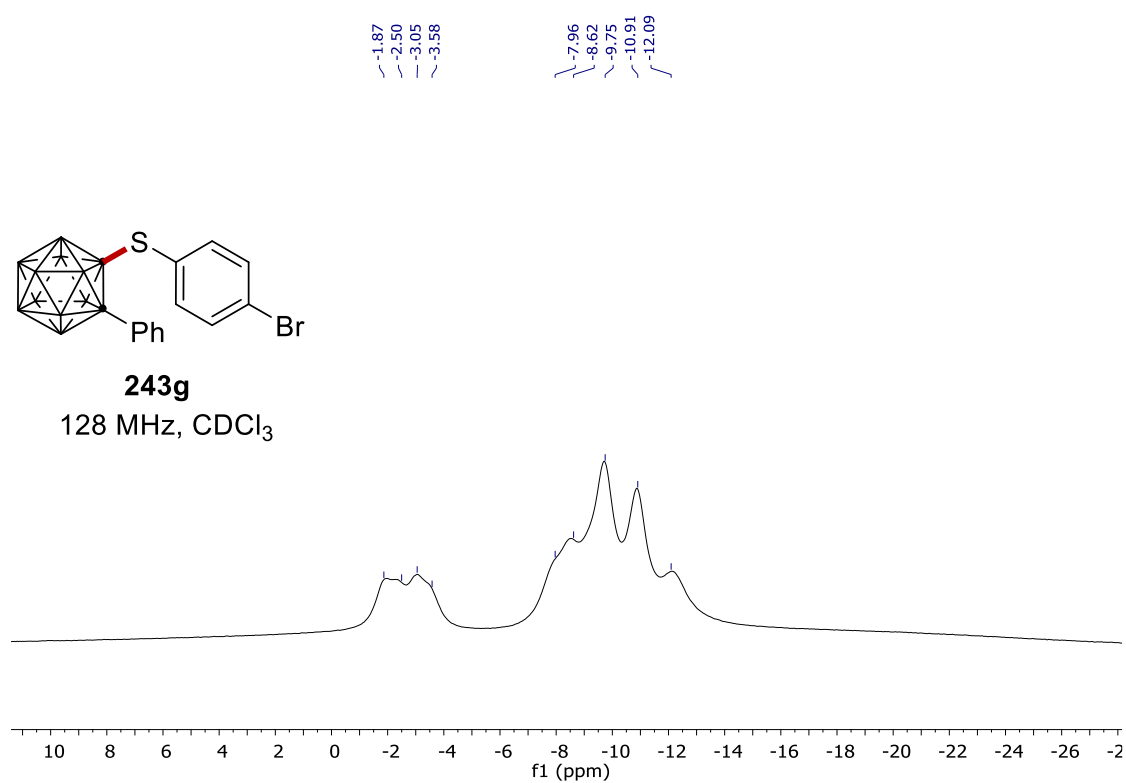
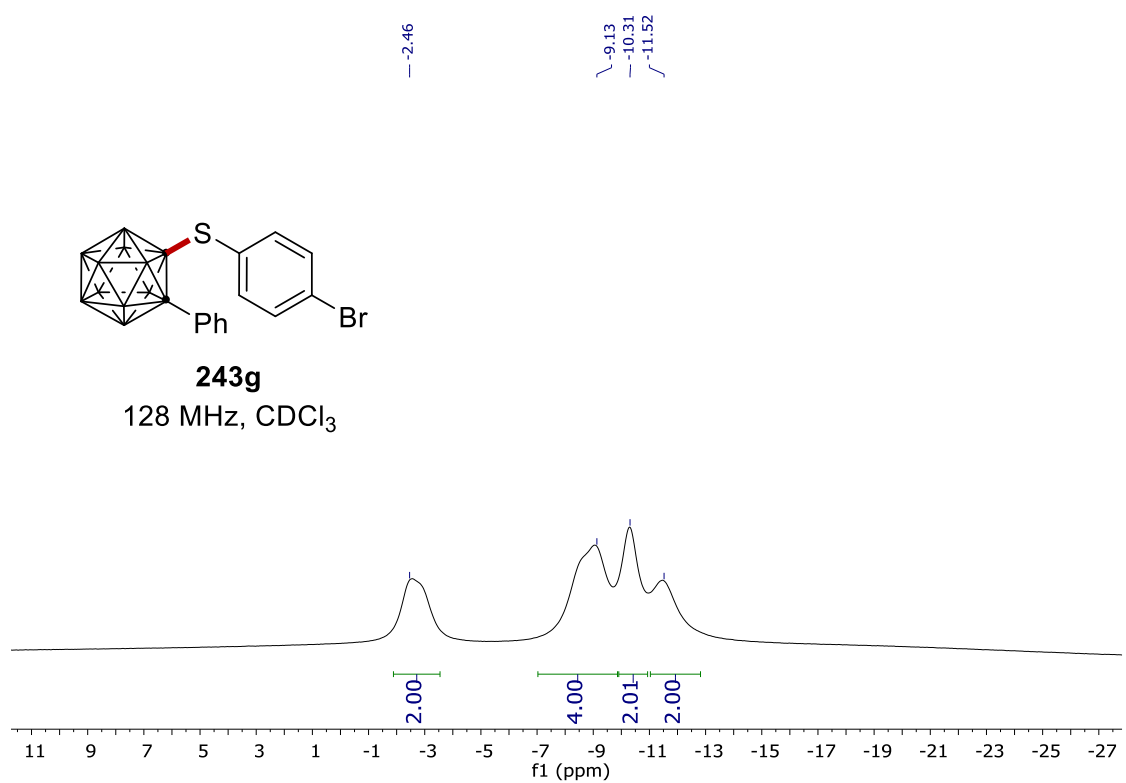
7. NMR Spectra



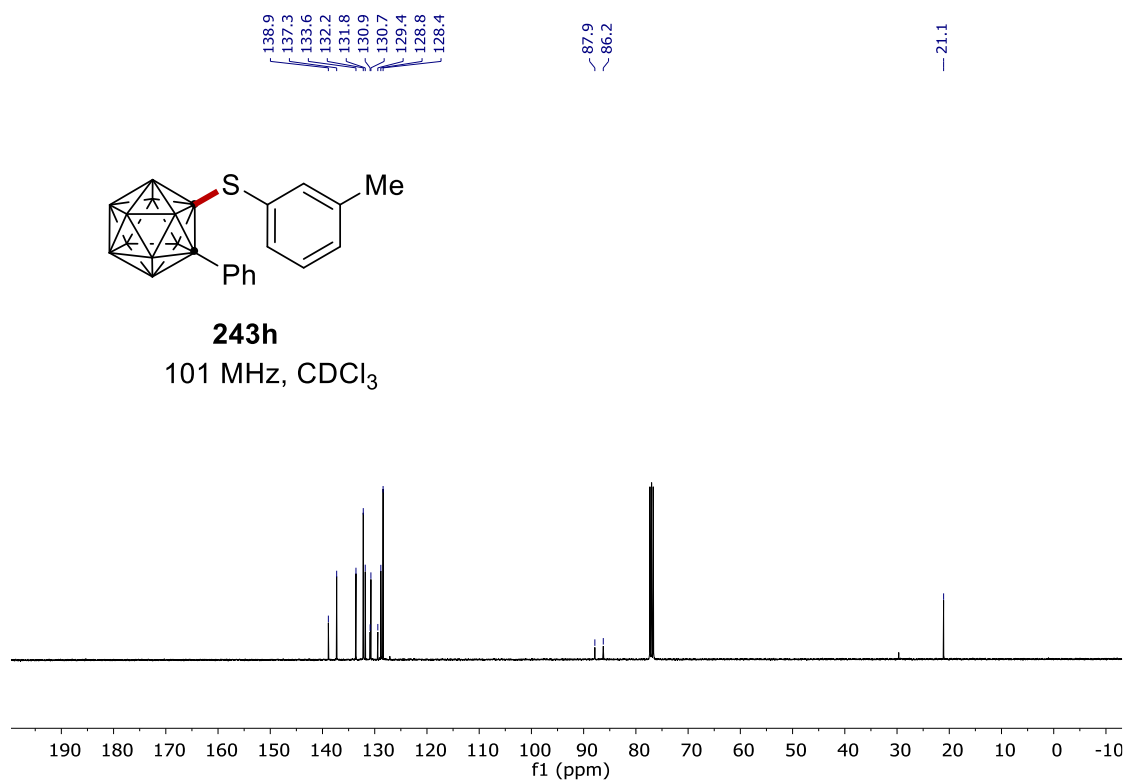
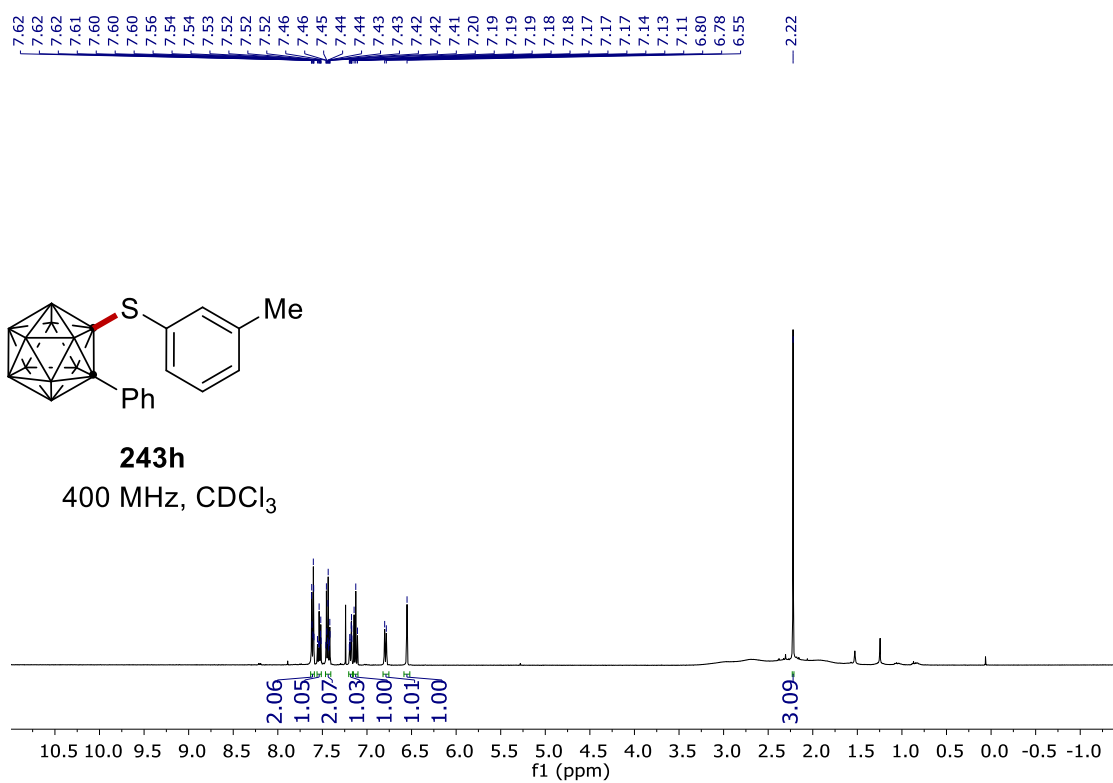
7. NMR Spectra



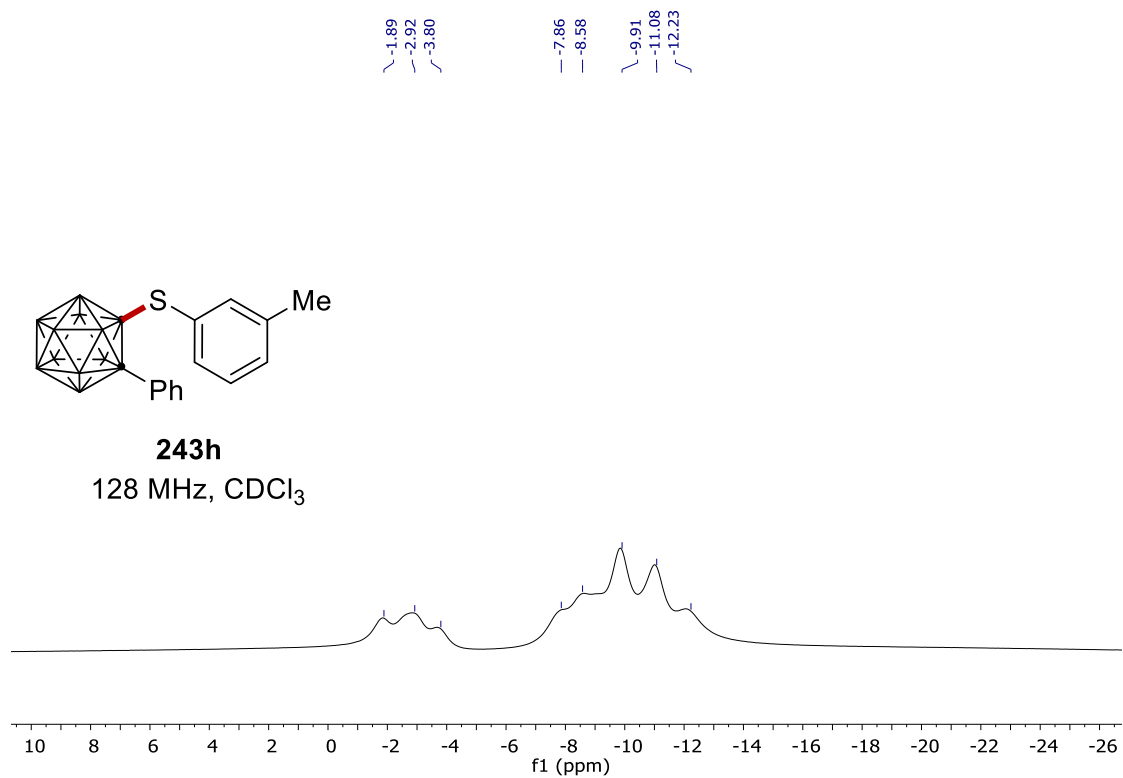
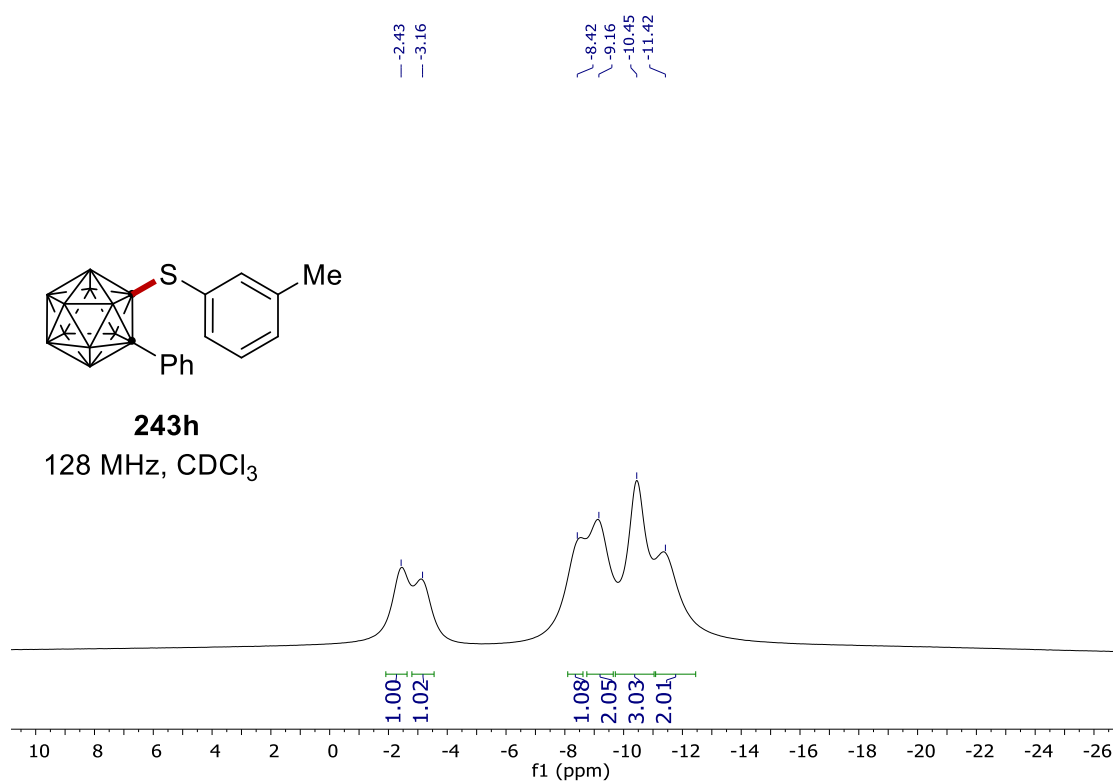
7. NMR Spectra



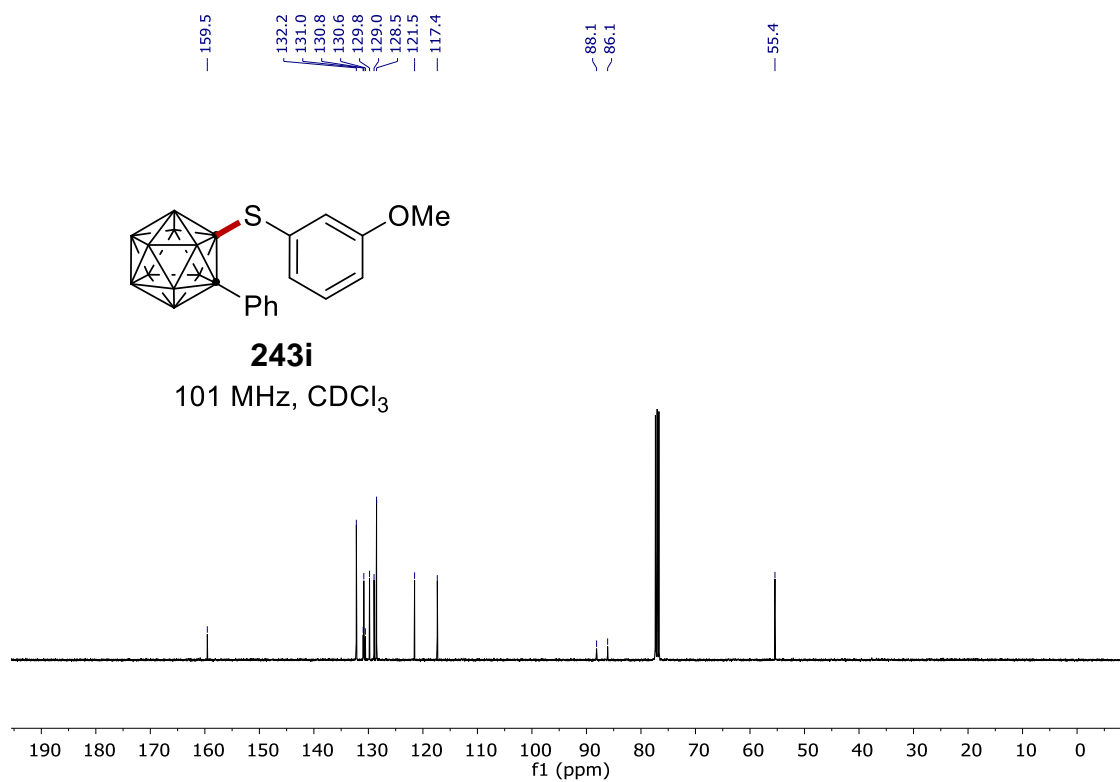
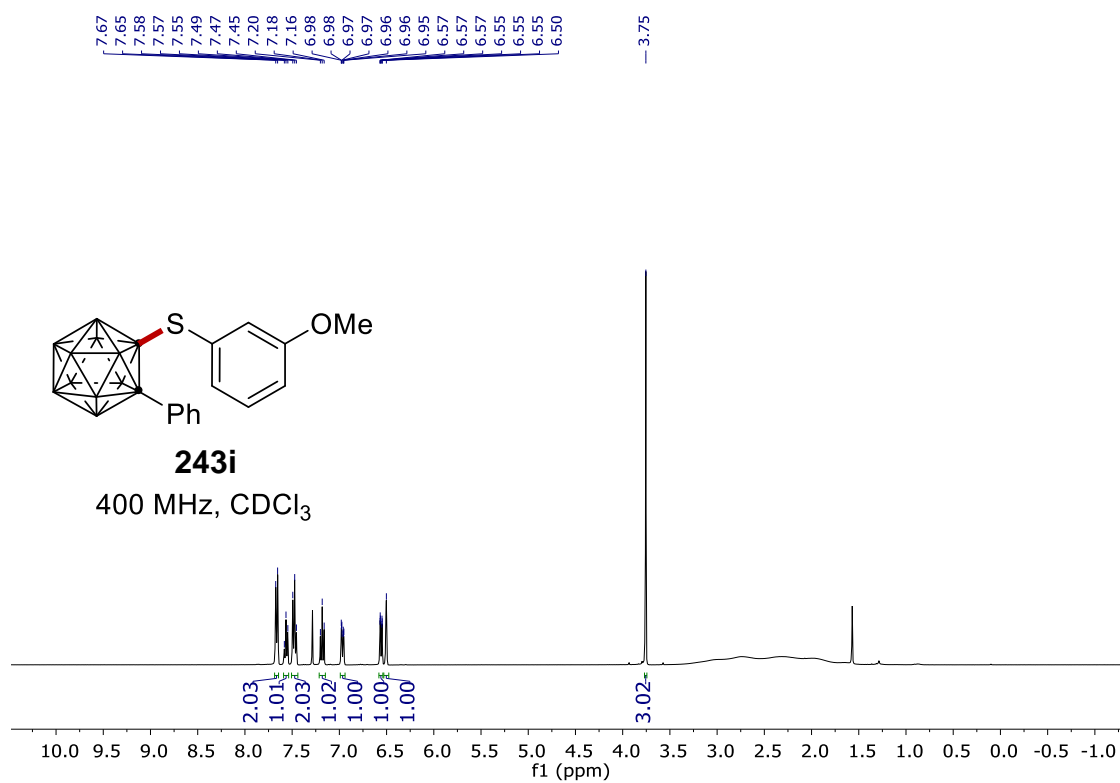
7. NMR Spectra



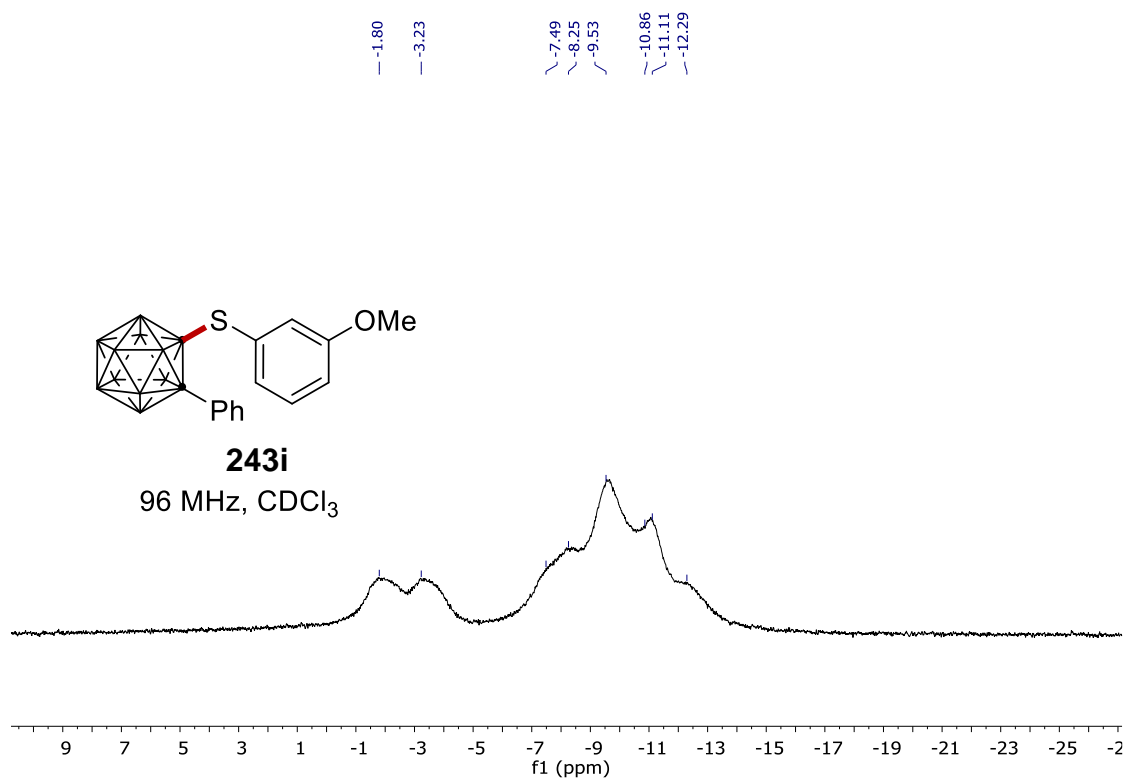
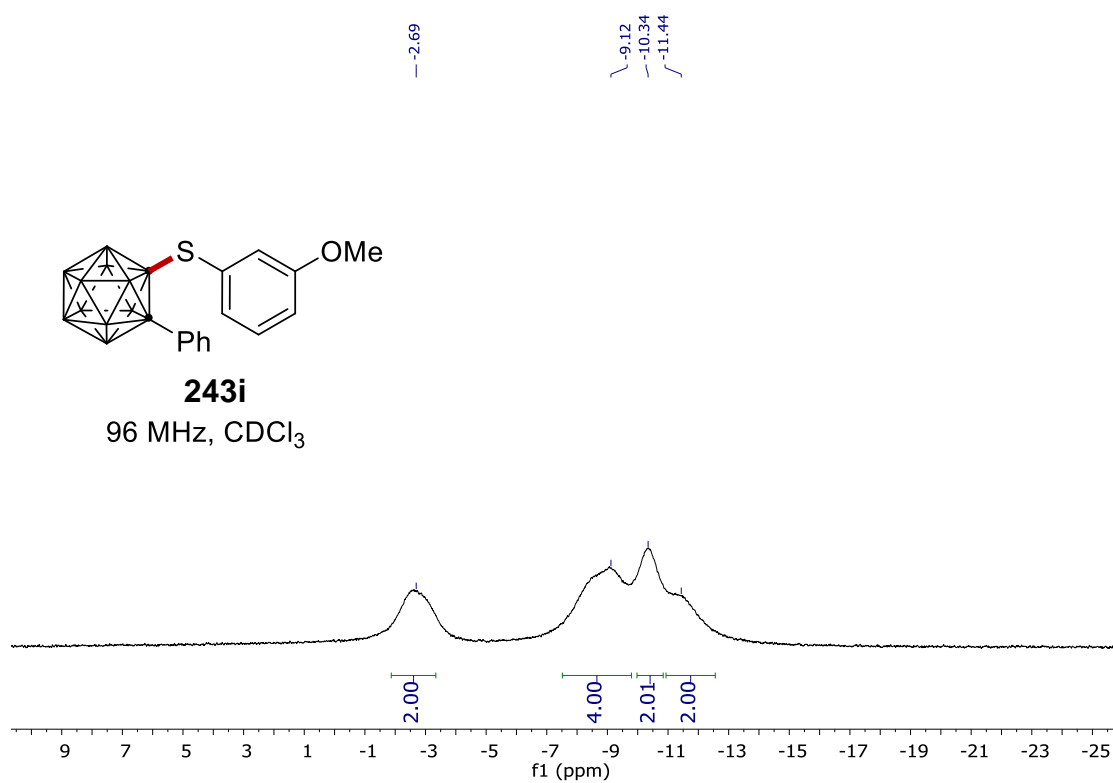
7. NMR Spectra



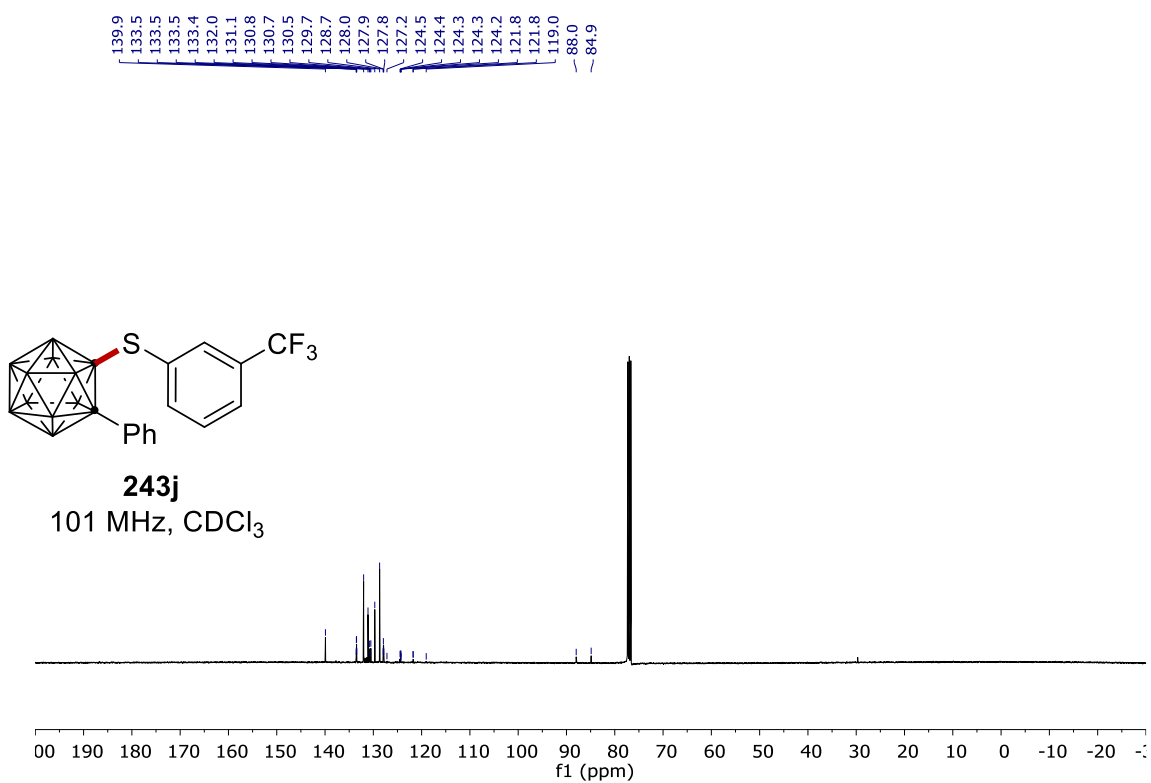
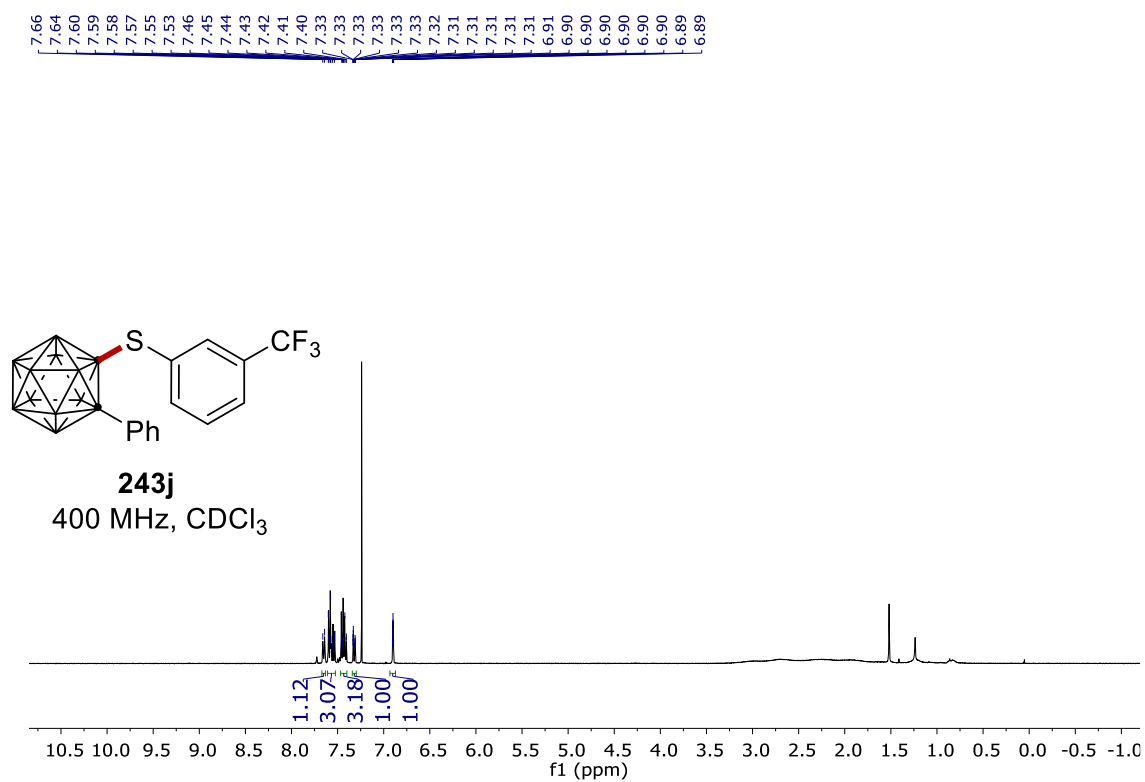
7. NMR Spectra



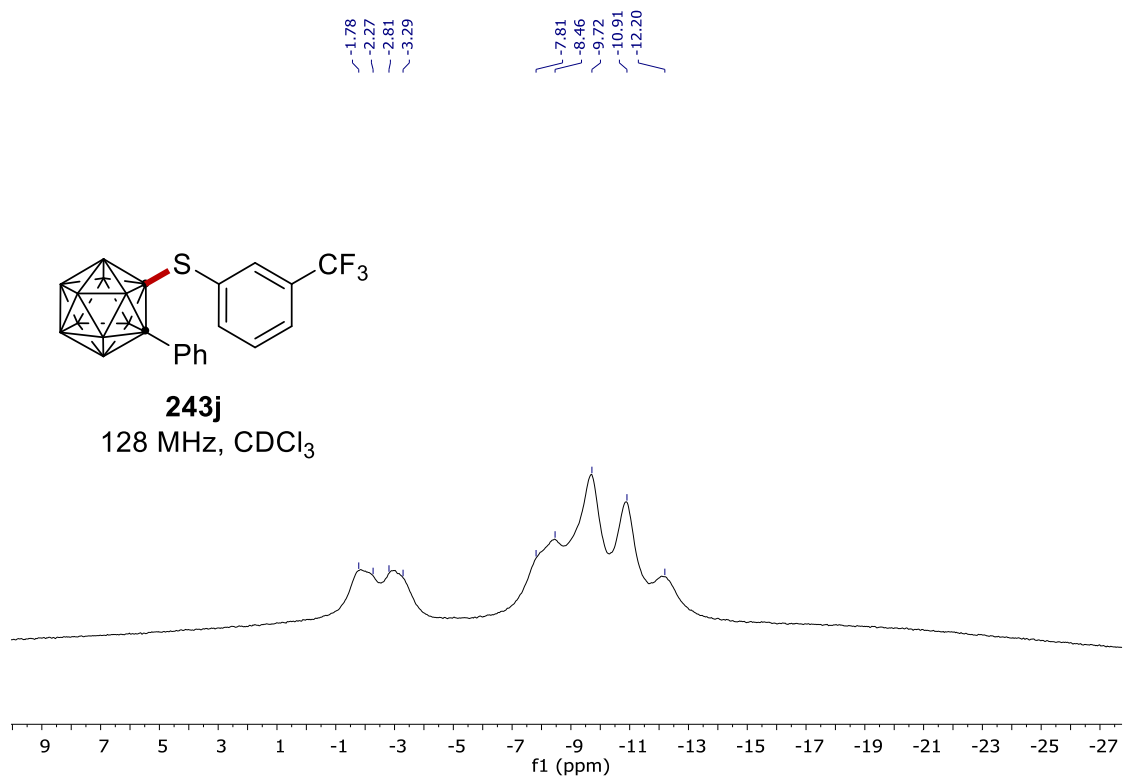
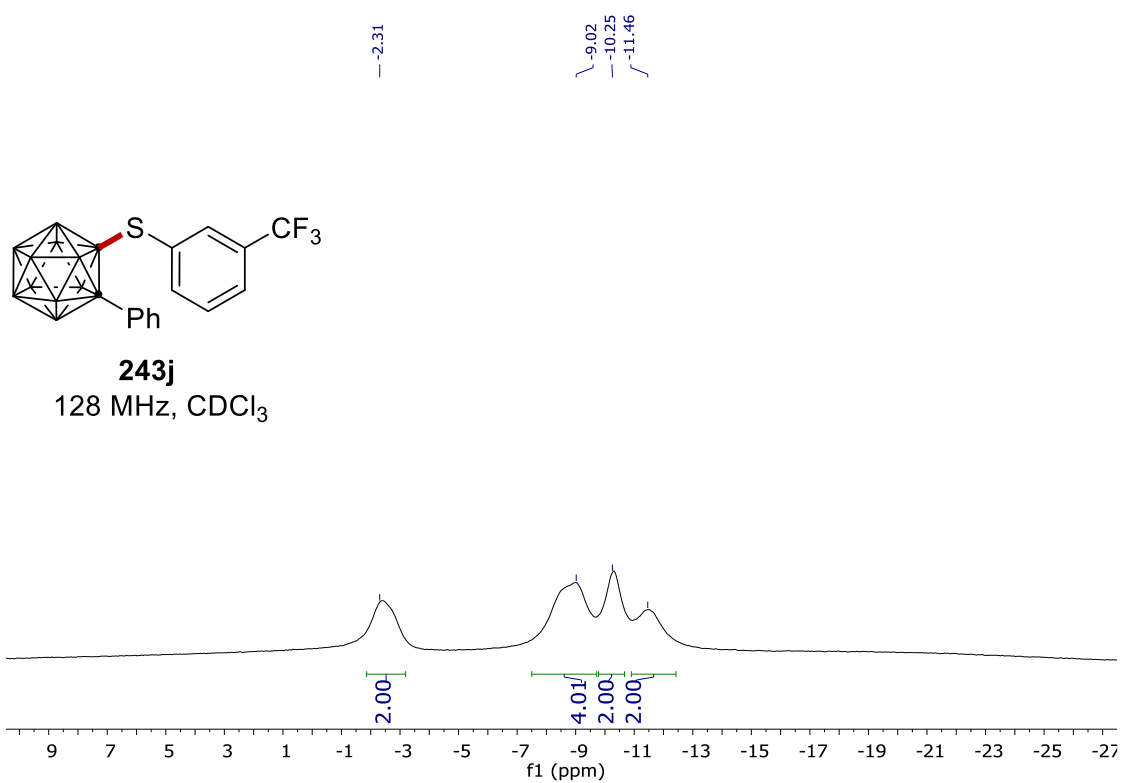
7. NMR Spectra



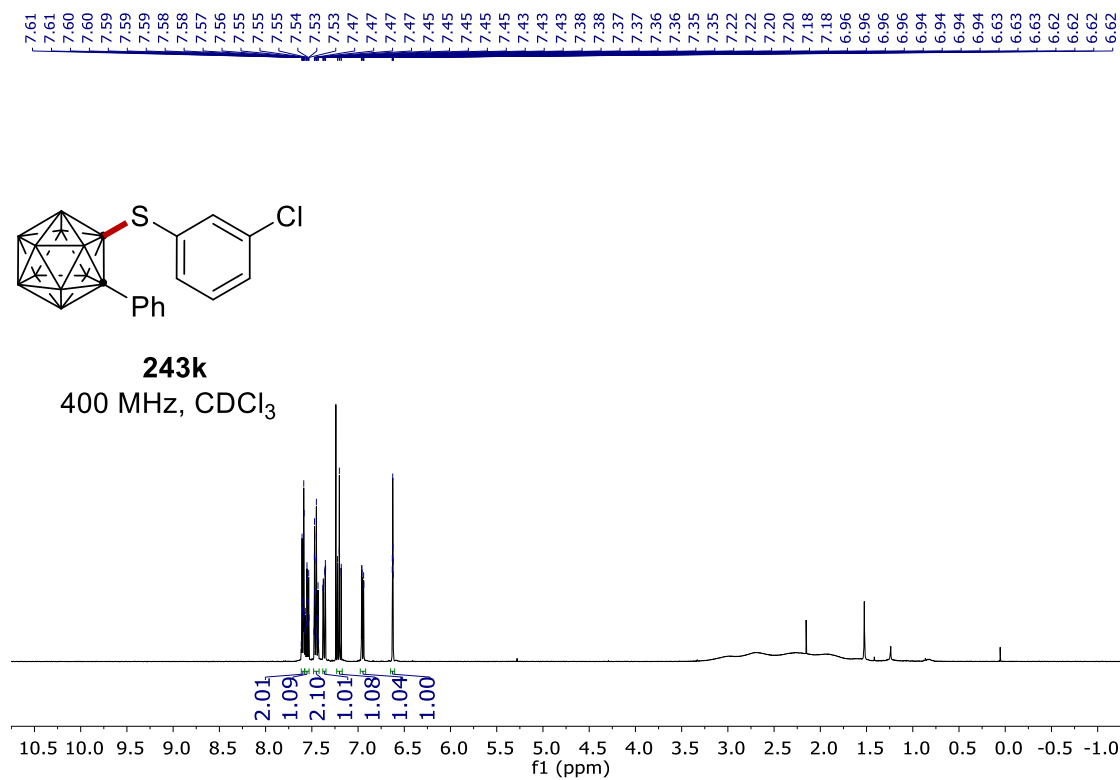
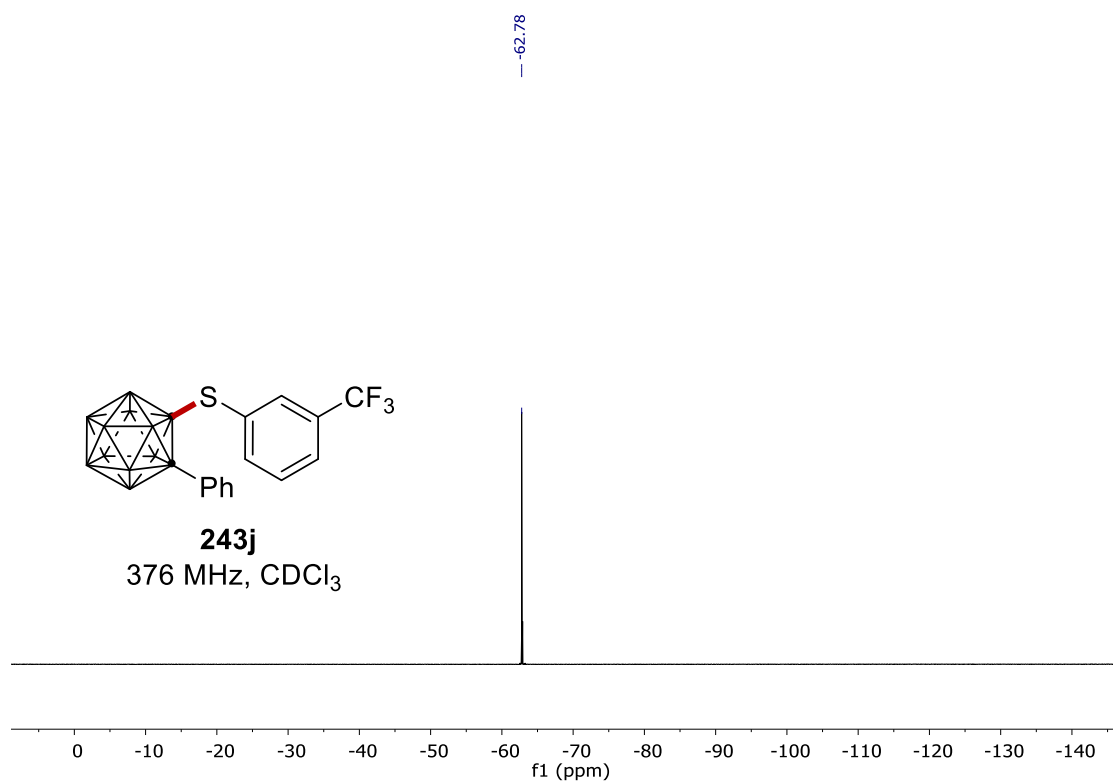
7. NMR Spectra



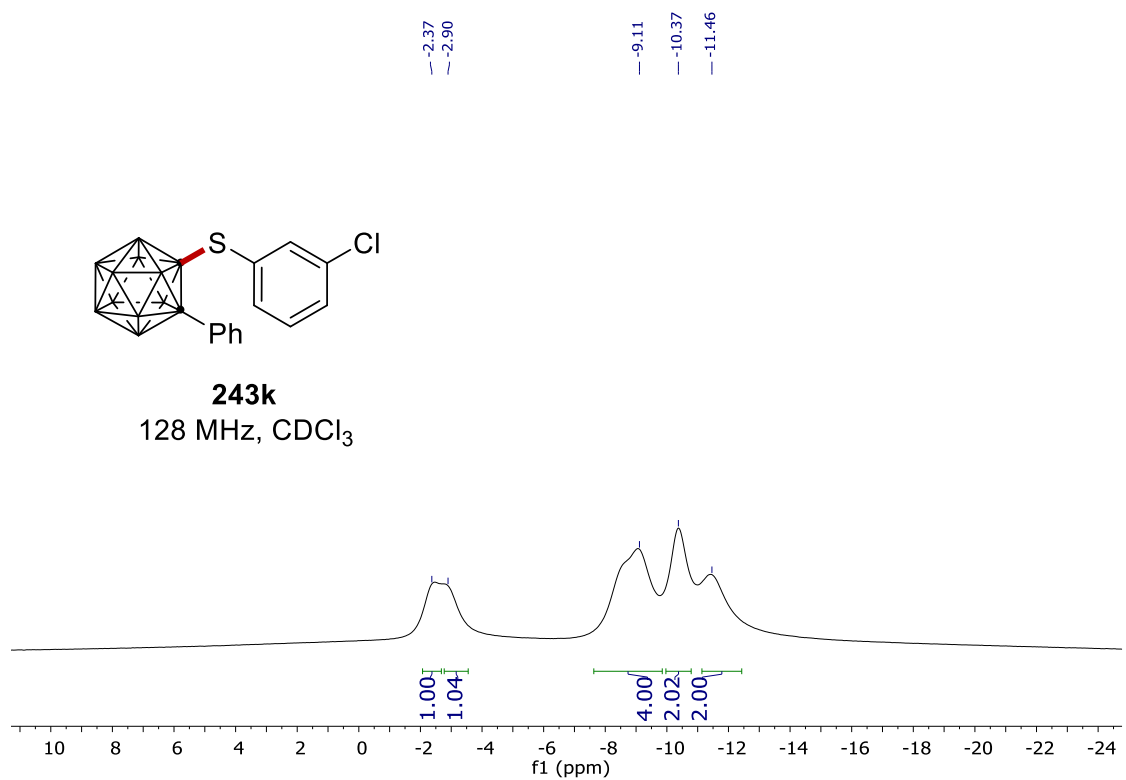
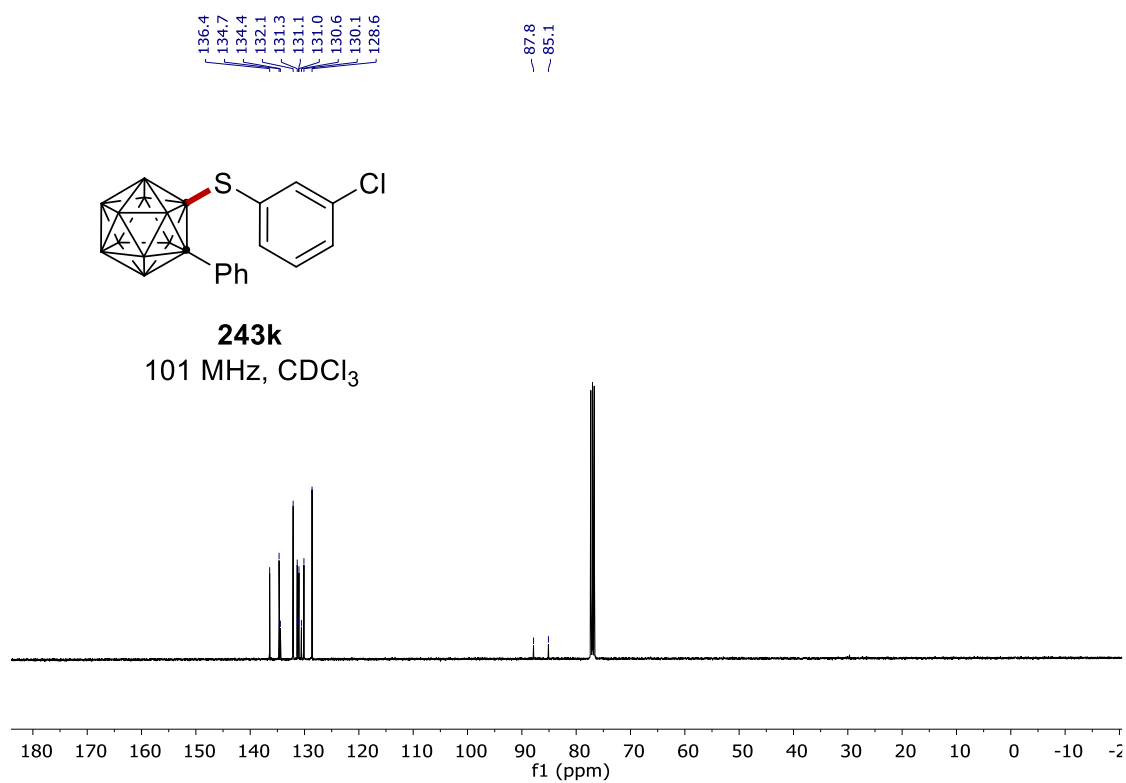
7. NMR Spectra



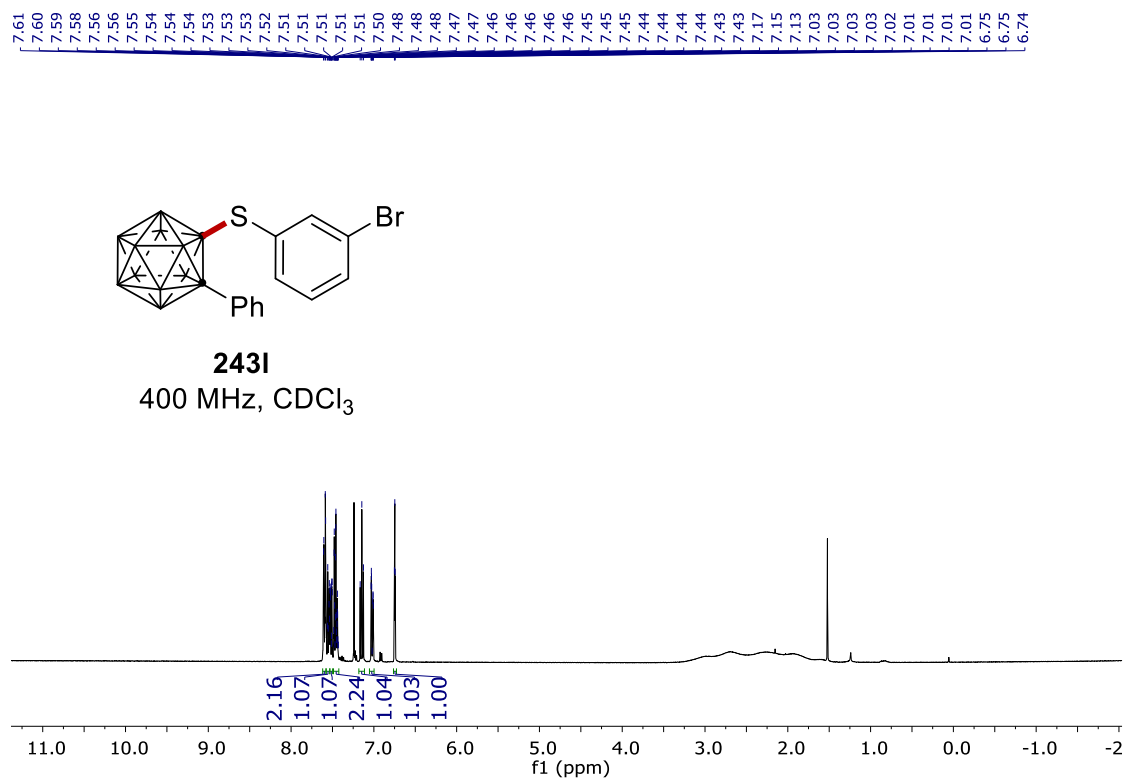
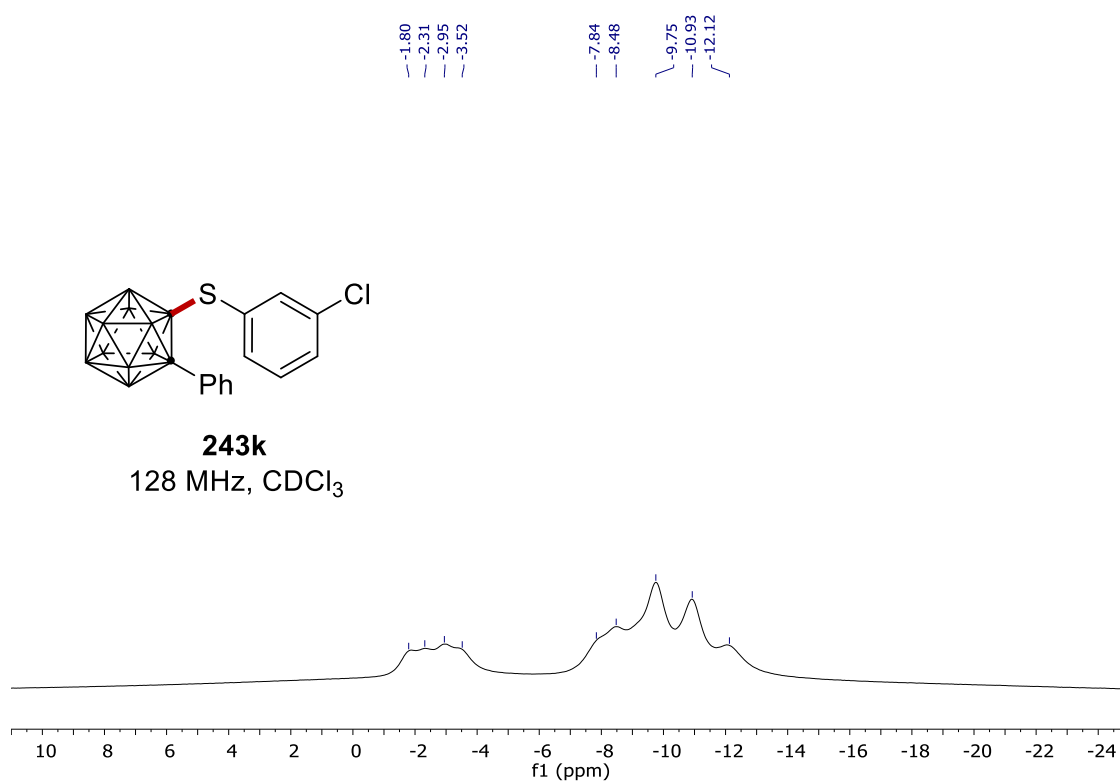
7. NMR Spectra



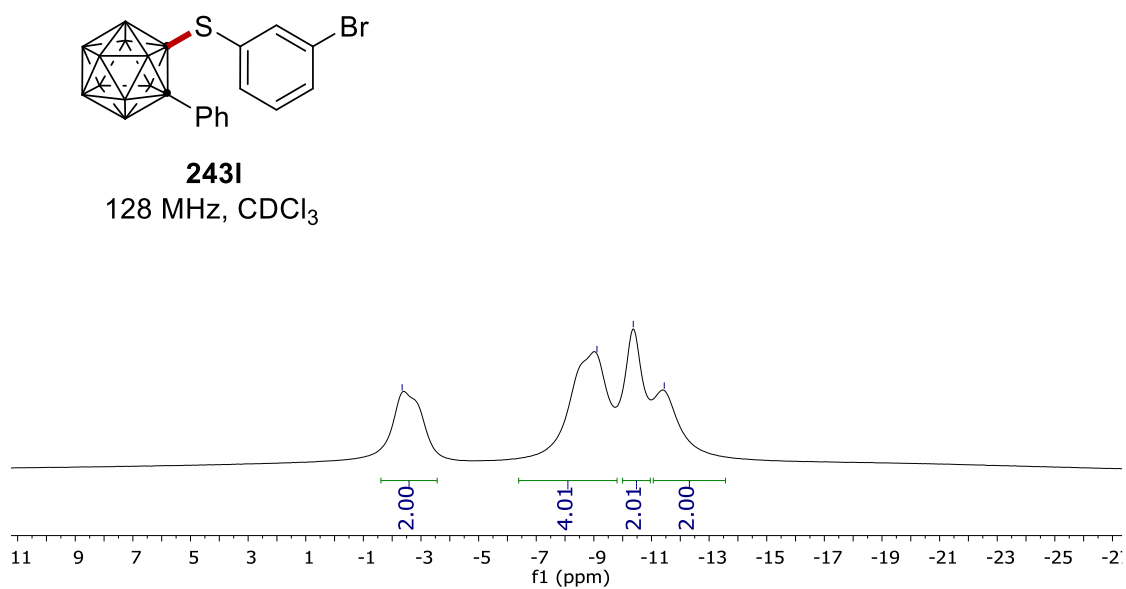
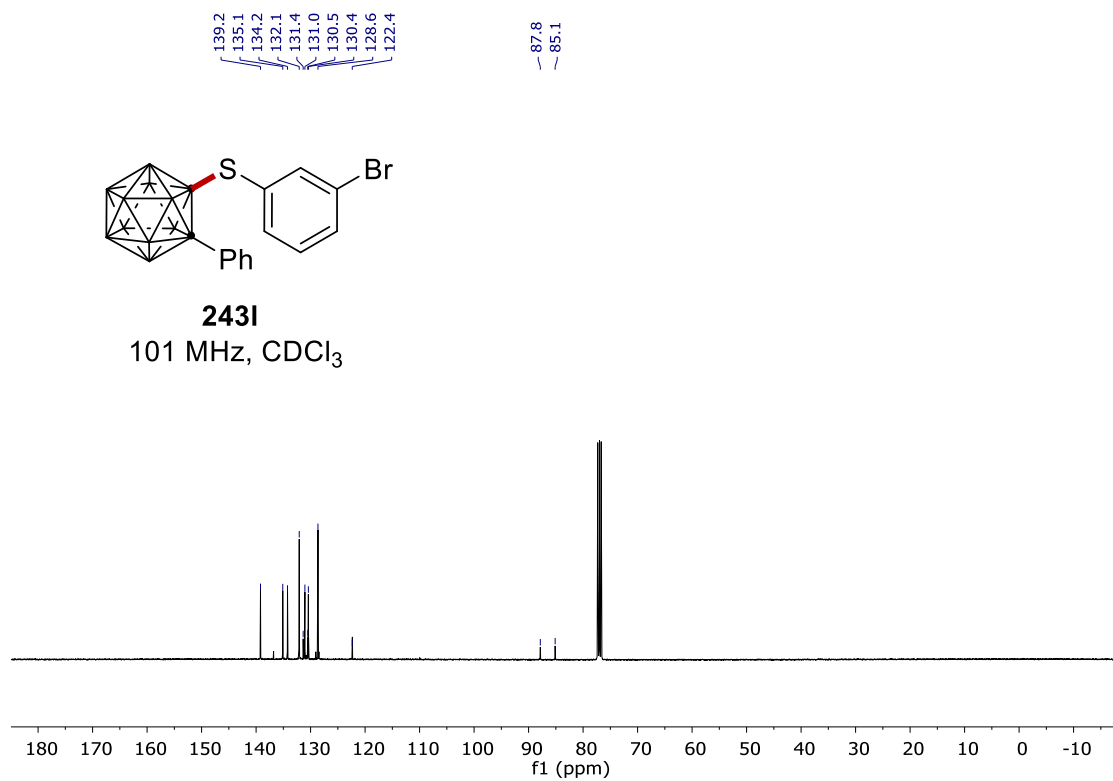
7. NMR Spectra



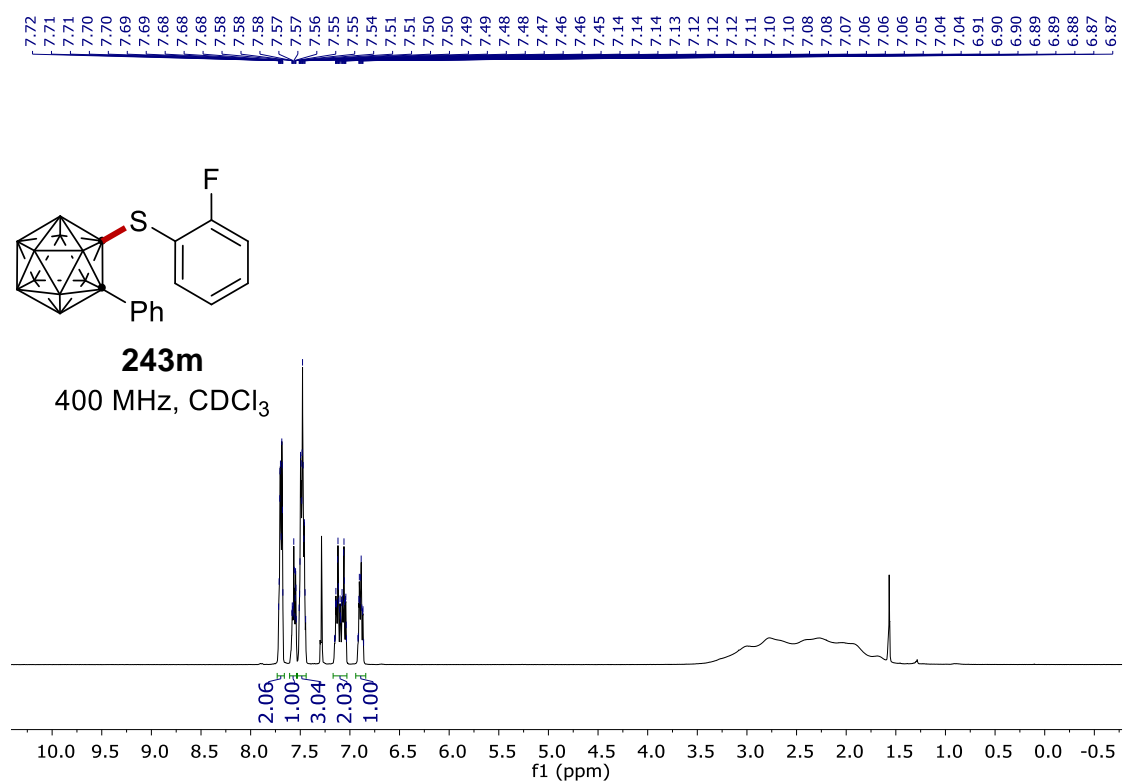
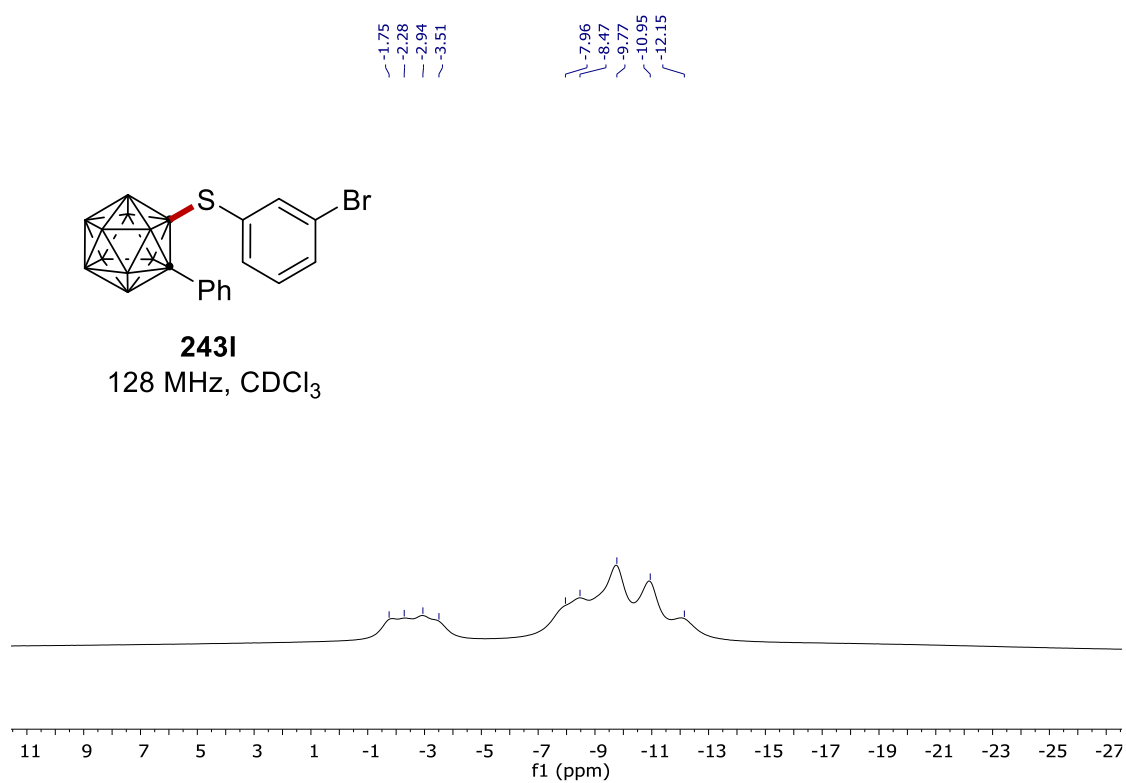
7. NMR Spectra



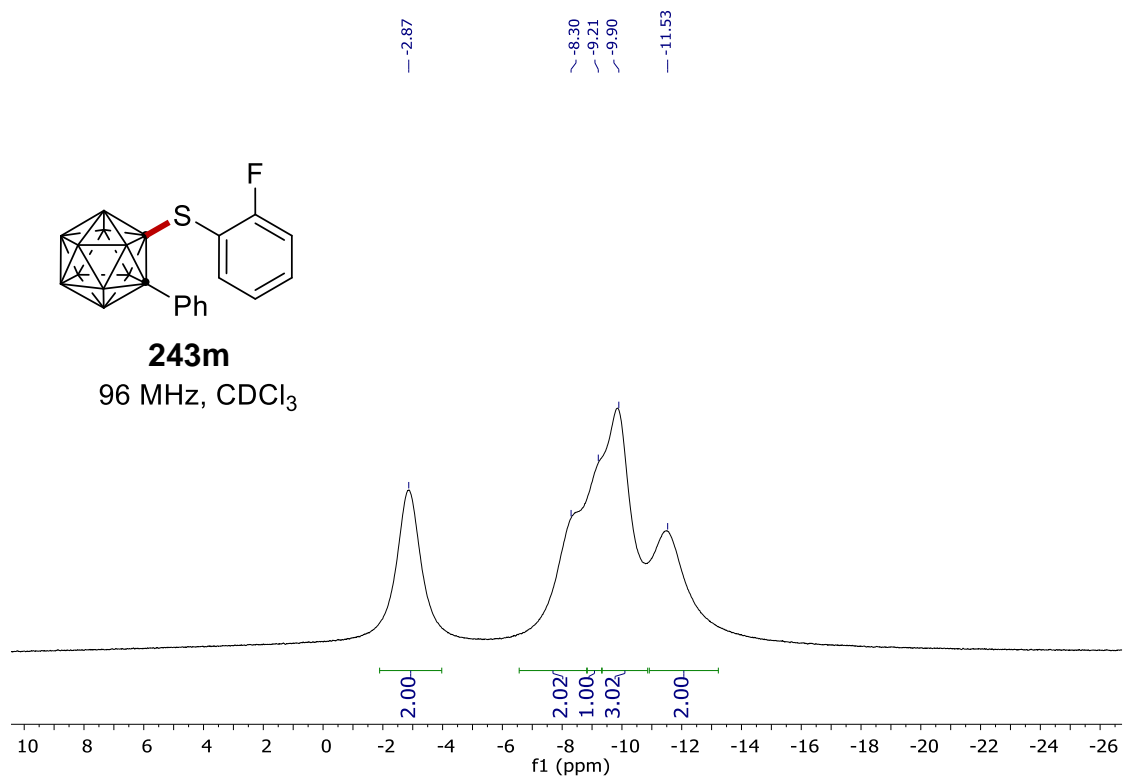
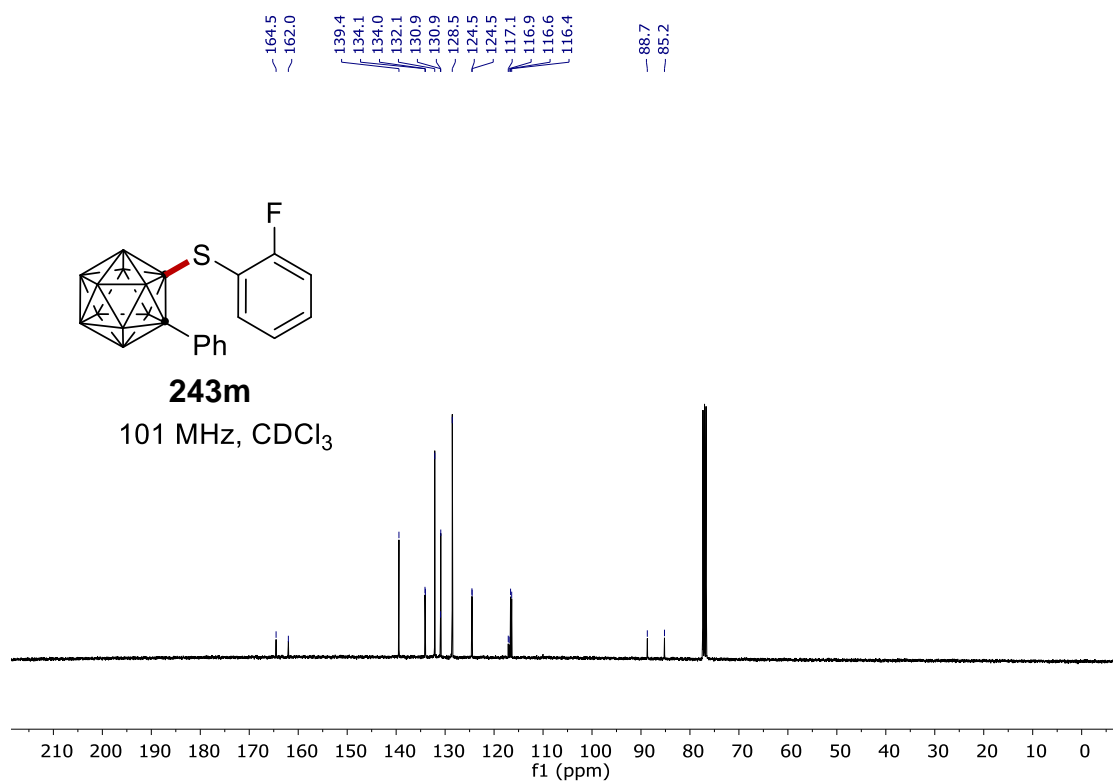
7. NMR Spectra



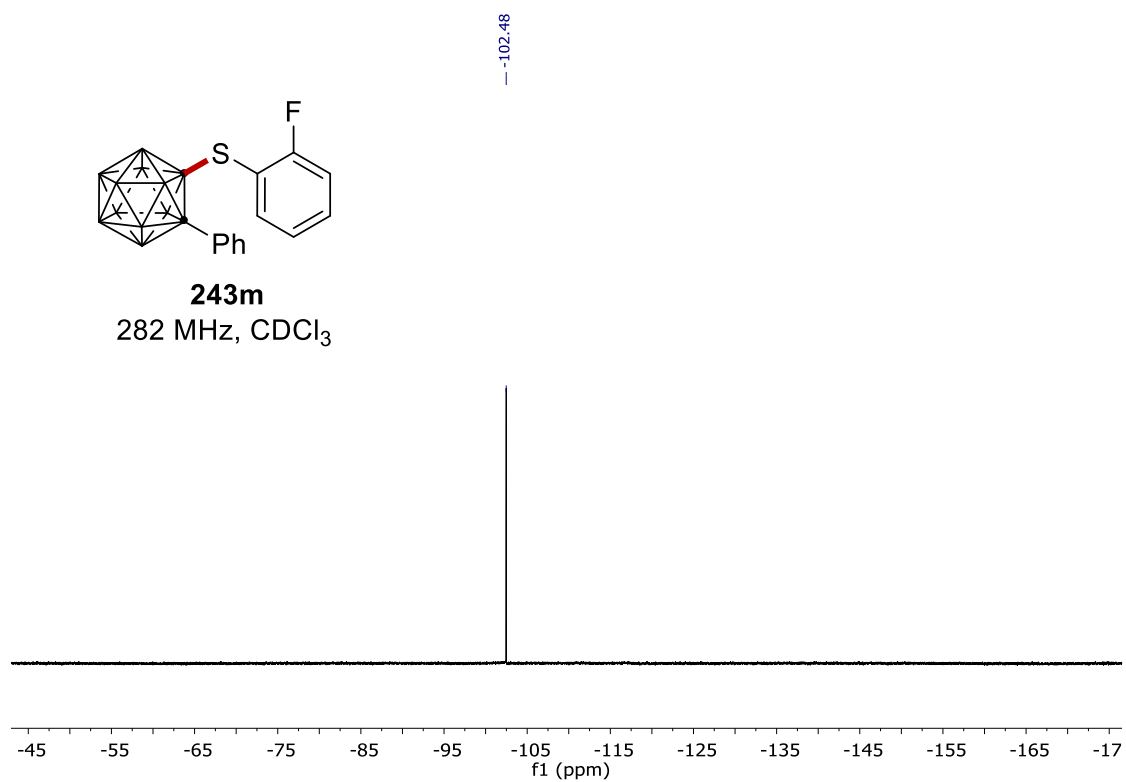
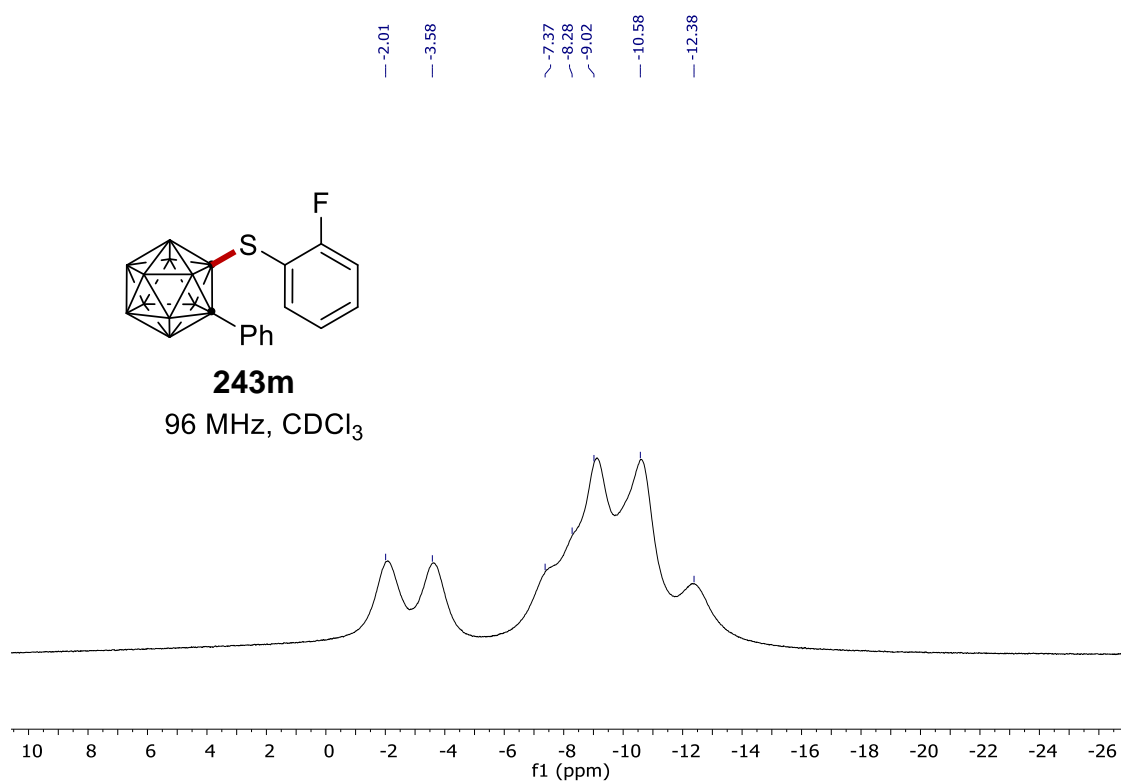
7. NMR Spectra



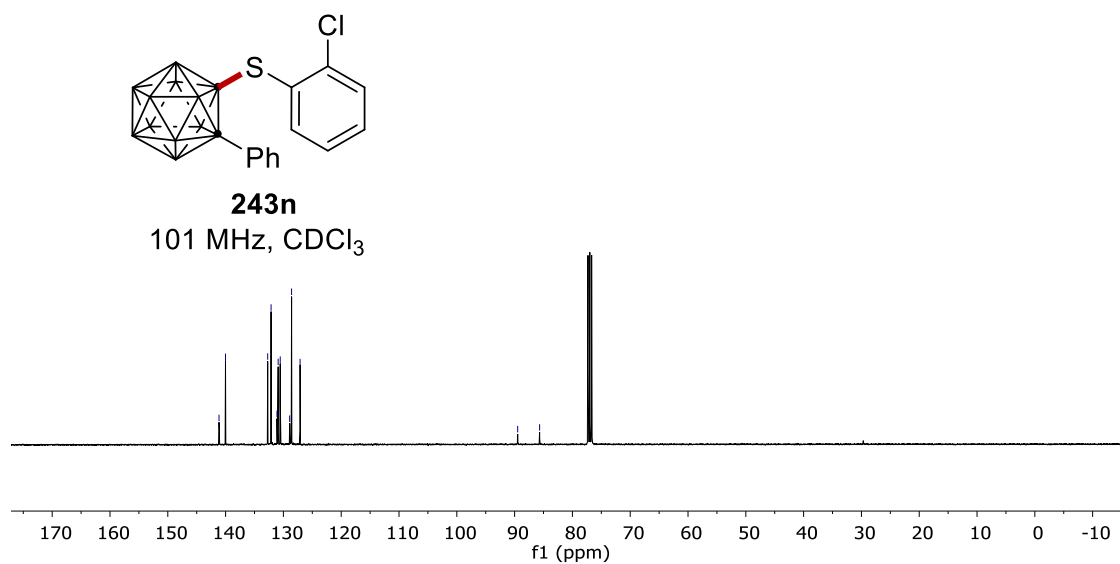
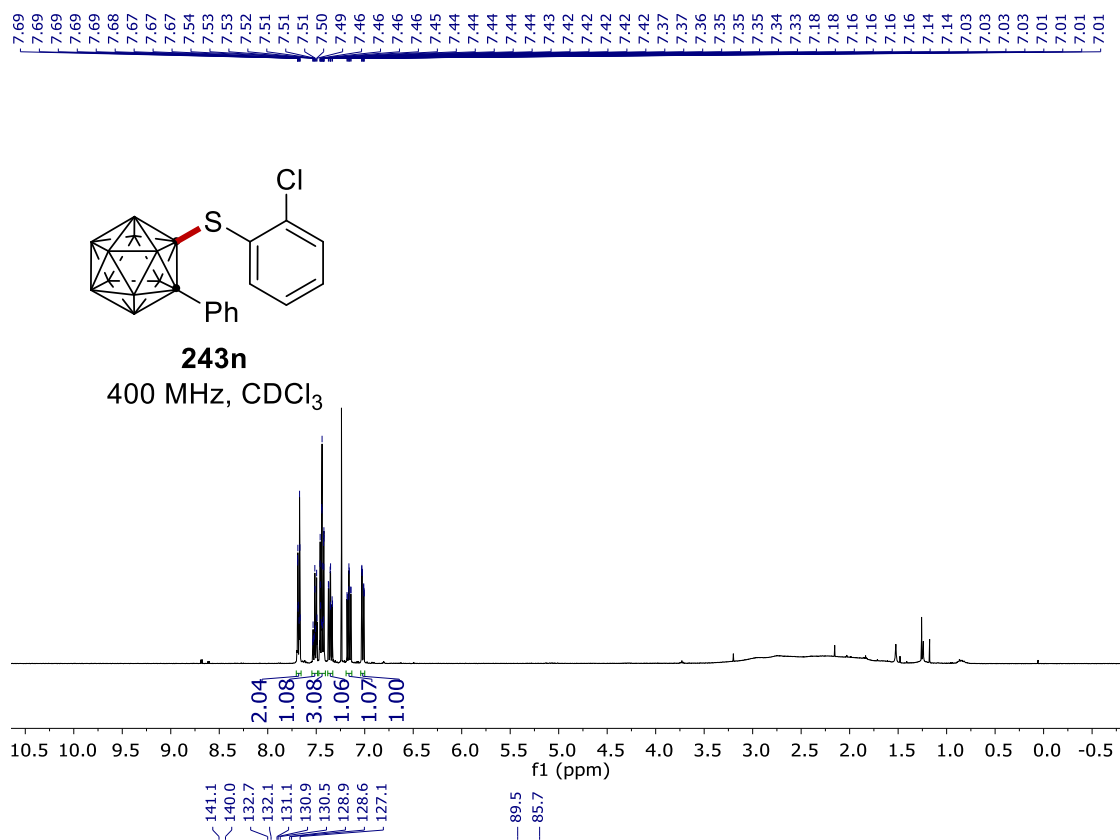
7. NMR Spectra



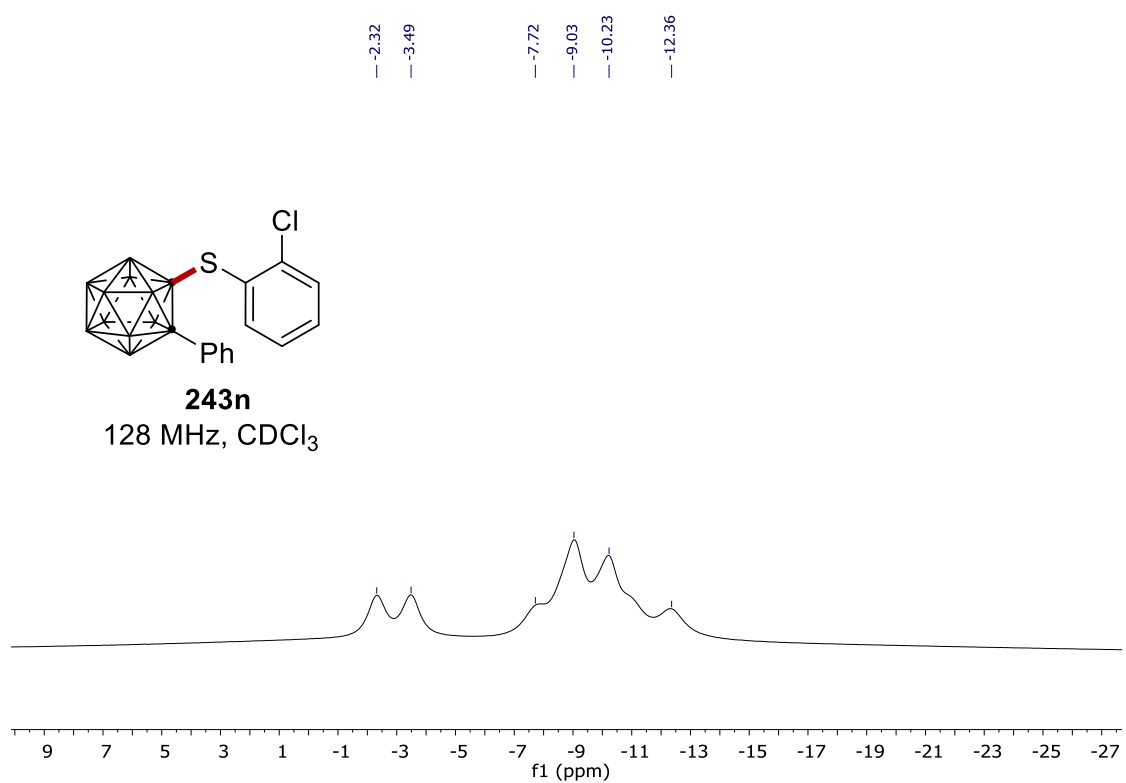
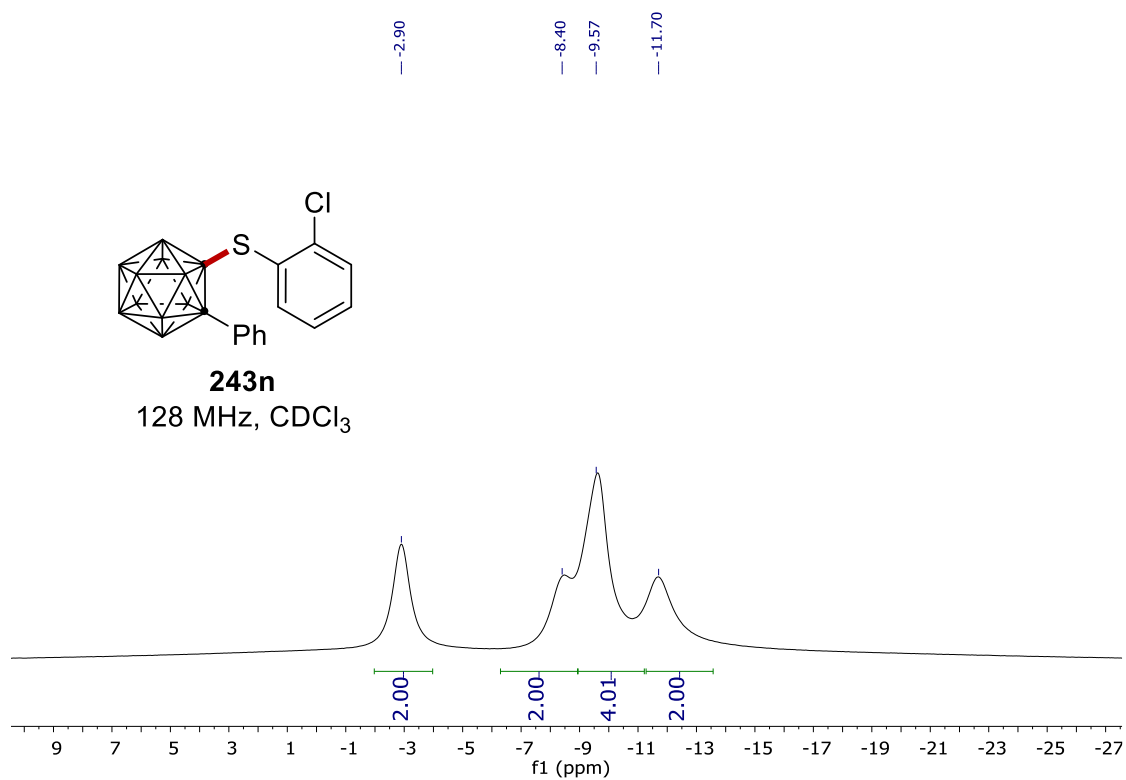
7. NMR Spectra



7. NMR Spectra

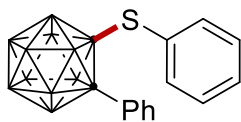


7. NMR Spectra



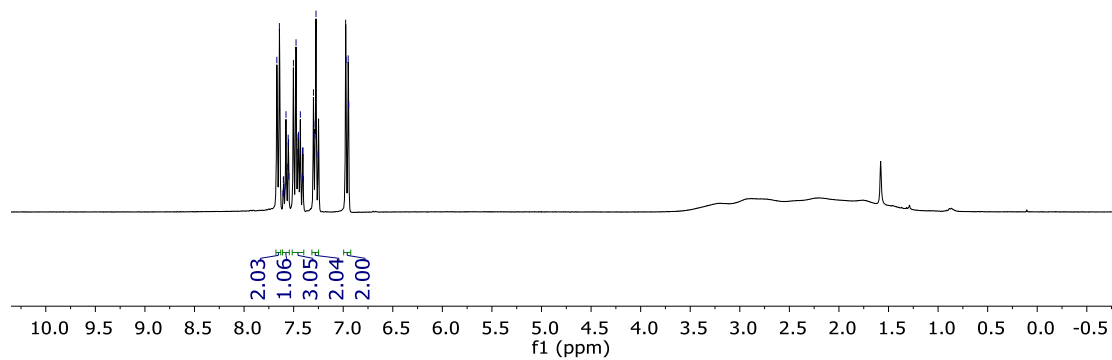
7. NMR Spectra

7.67
7.64
7.61
7.60
7.60
7.59
7.58
7.56
7.55
7.55
7.50
7.48
7.46
7.46
7.45
7.43
7.41
7.41
7.40
7.30
7.29
7.28
7.27
7.25
6.98
6.97
6.95
6.94

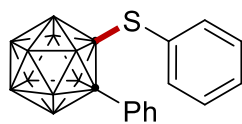


243o

300 MHz, CDCl₃

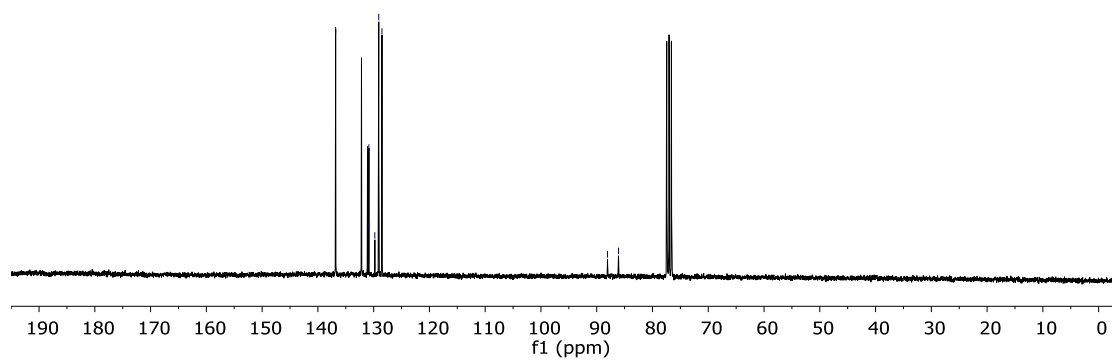


136.8
132.2
131.1
130.9
129.8
129.1
128.5
88.1
86.1

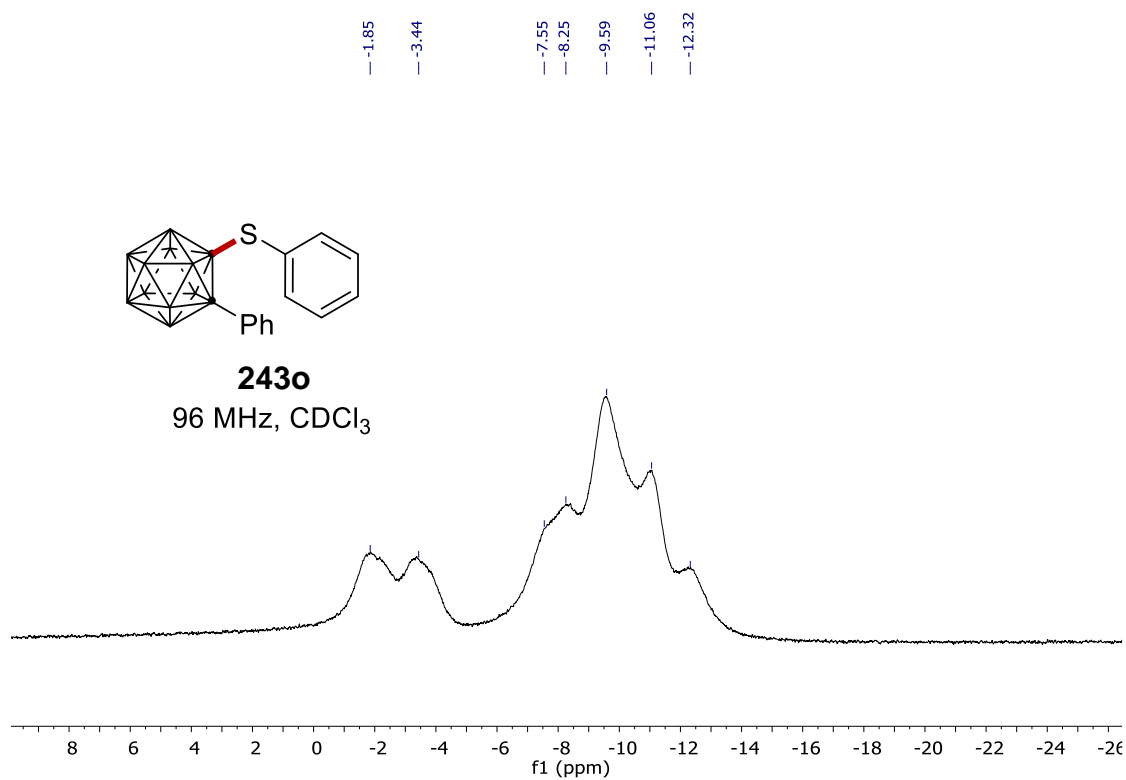
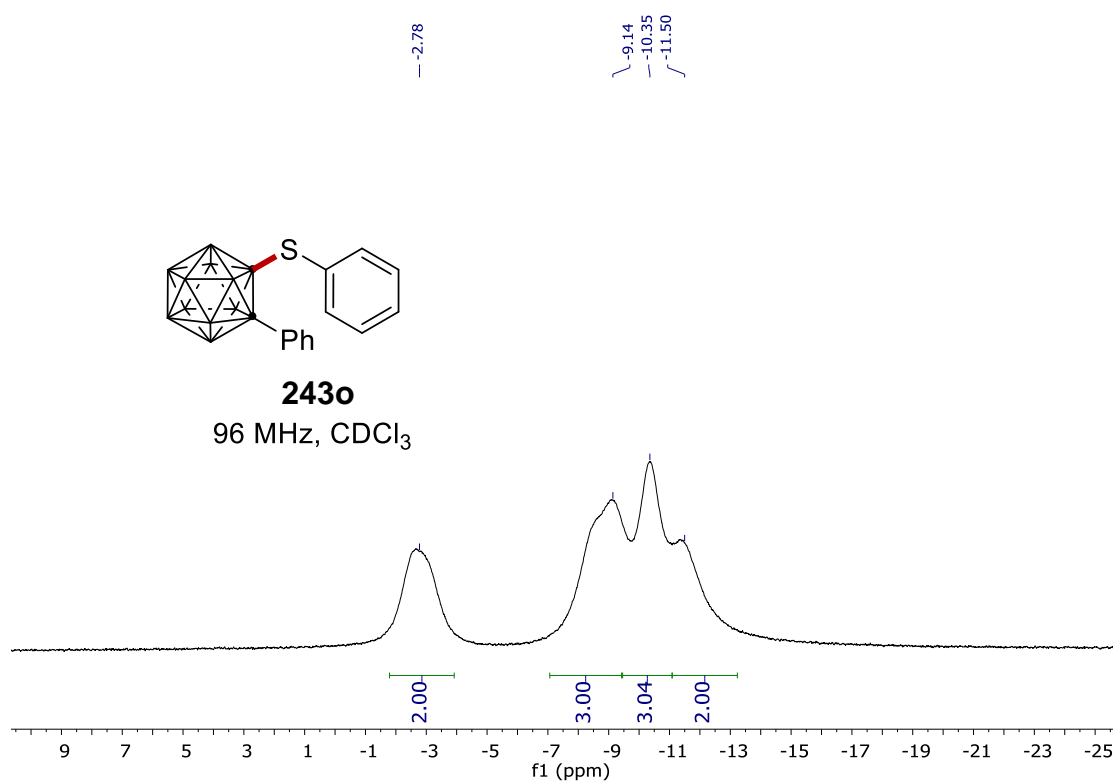


243o

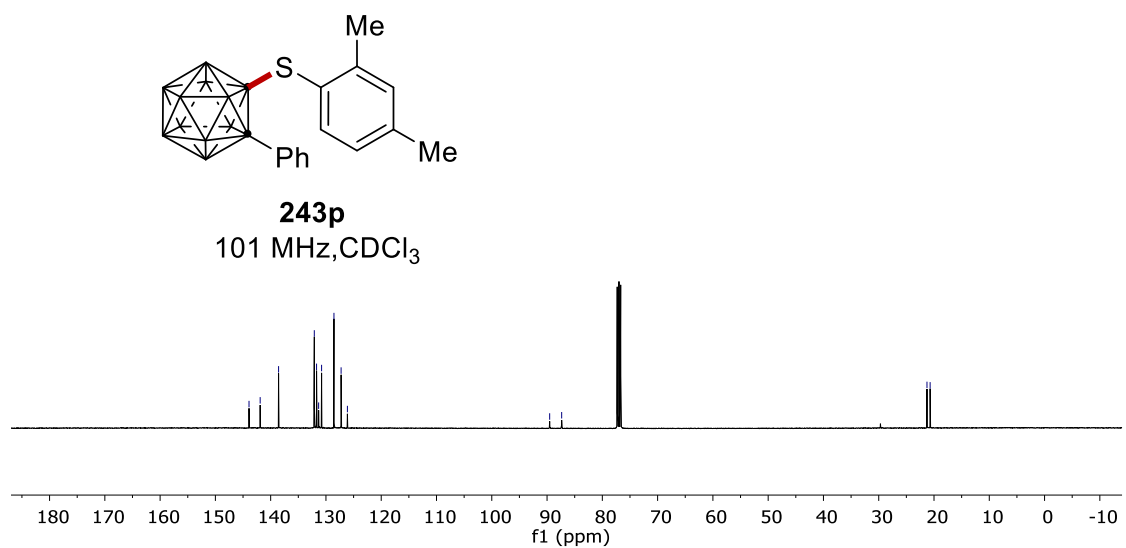
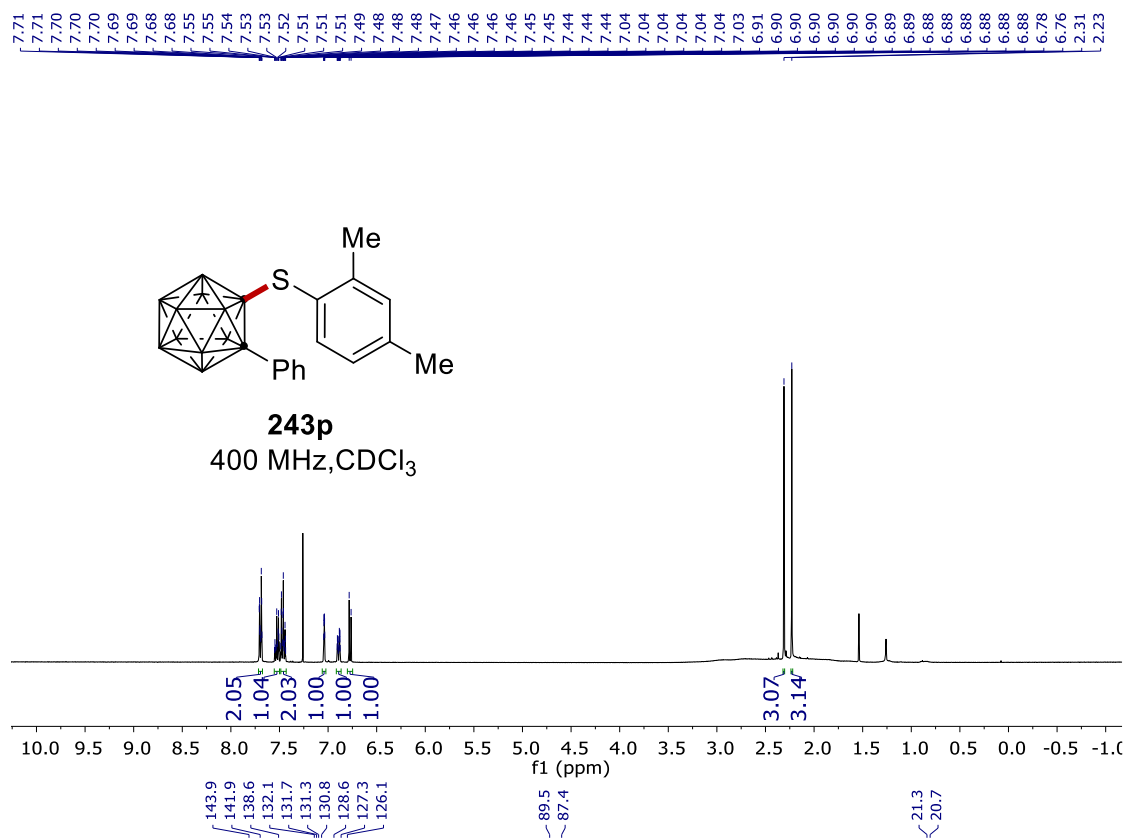
75 MHz, CDCl₃



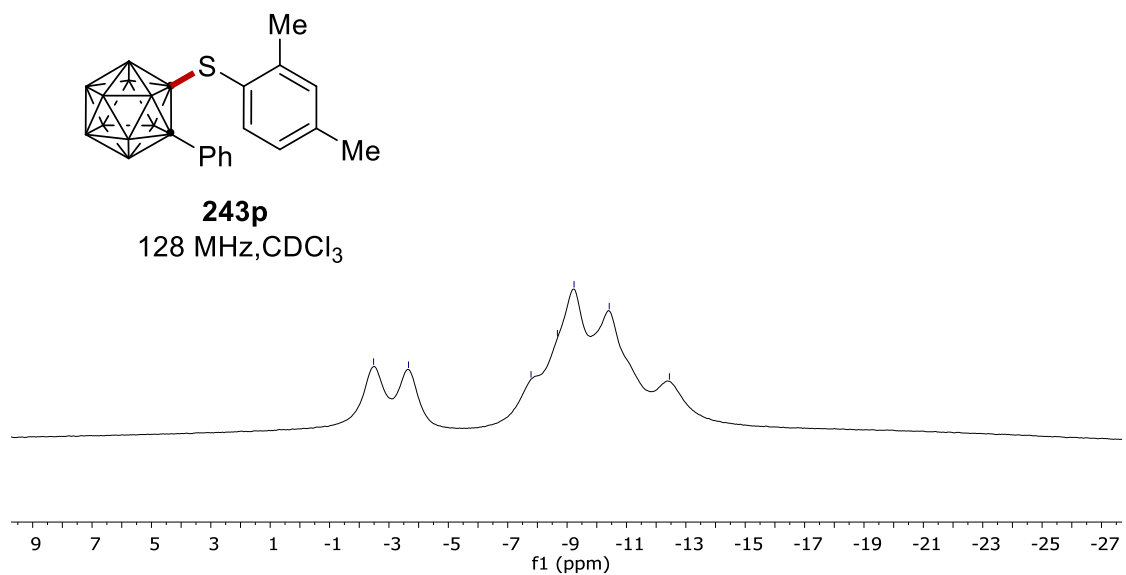
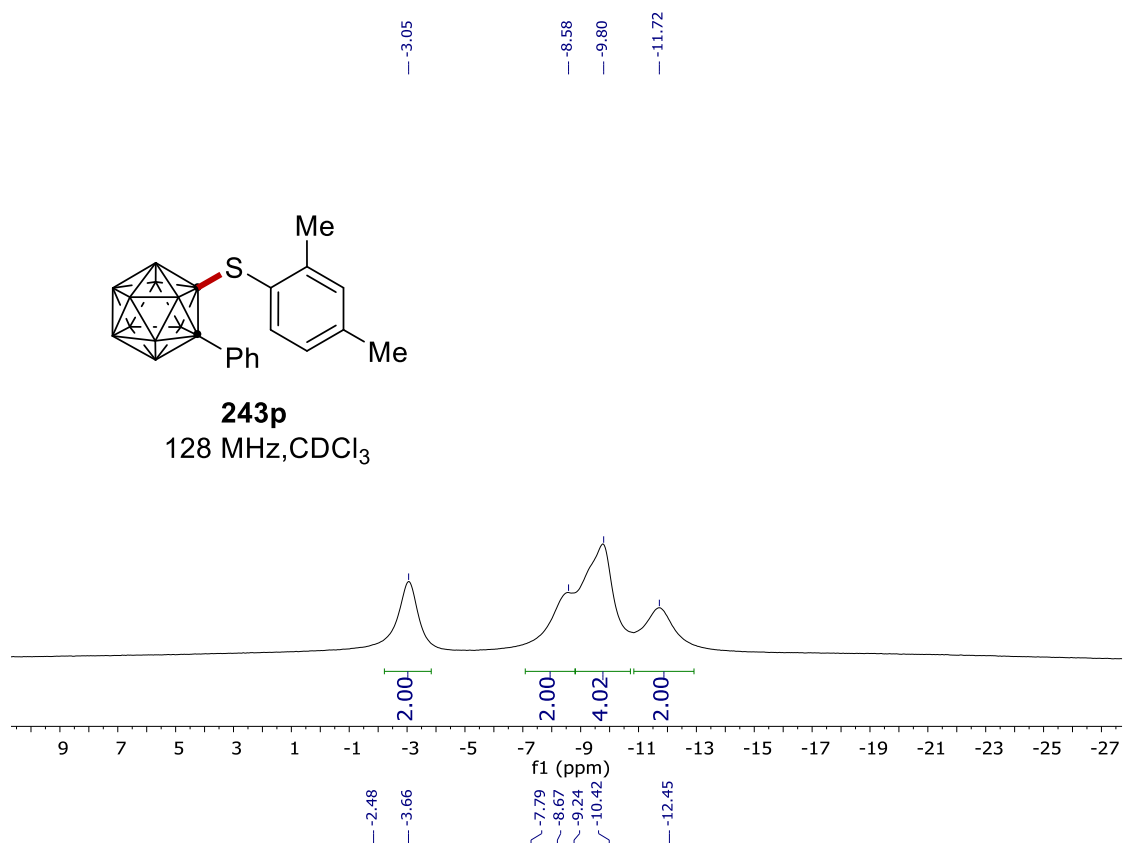
7. NMR Spectra



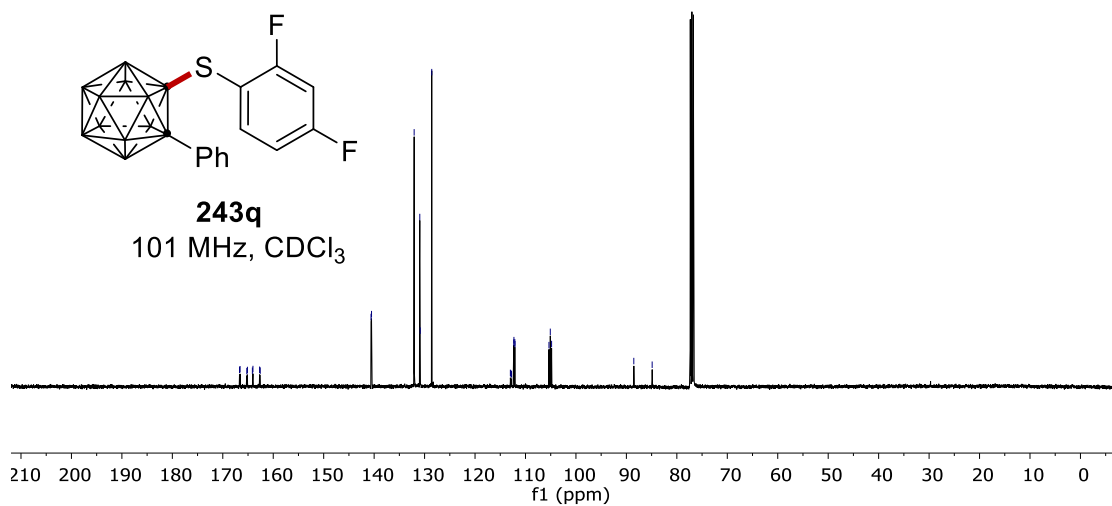
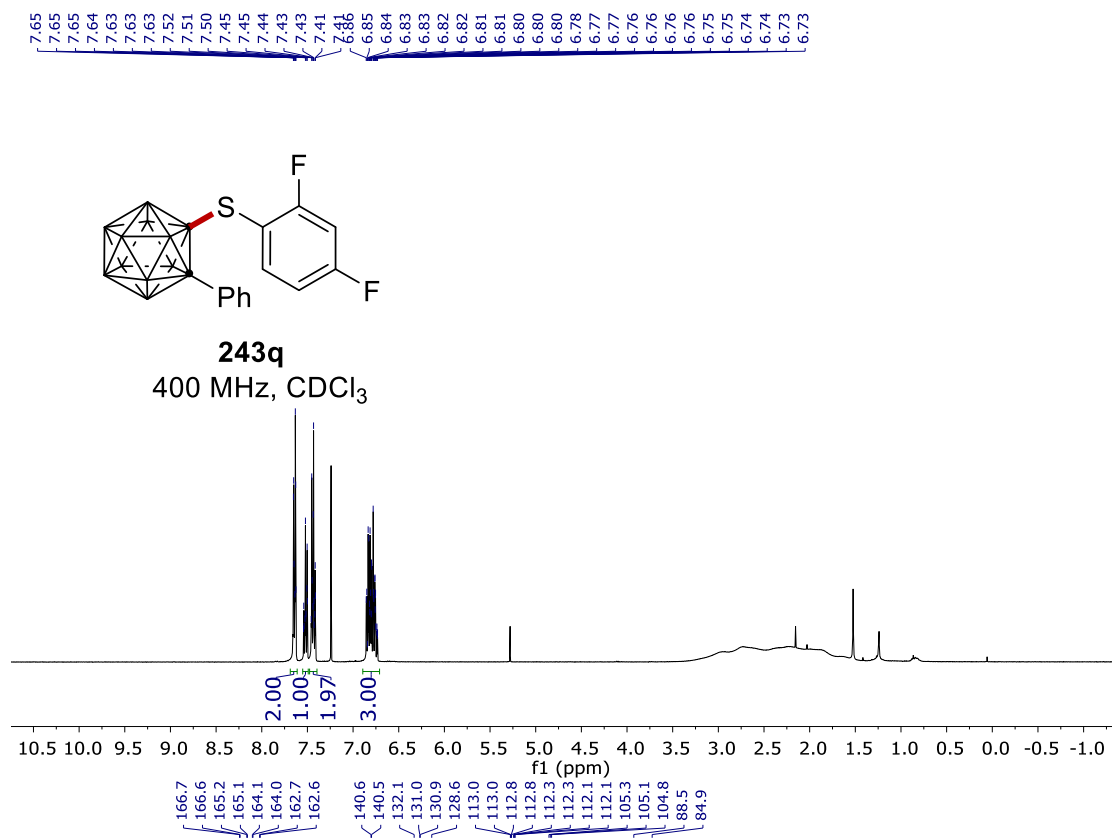
7. NMR Spectra



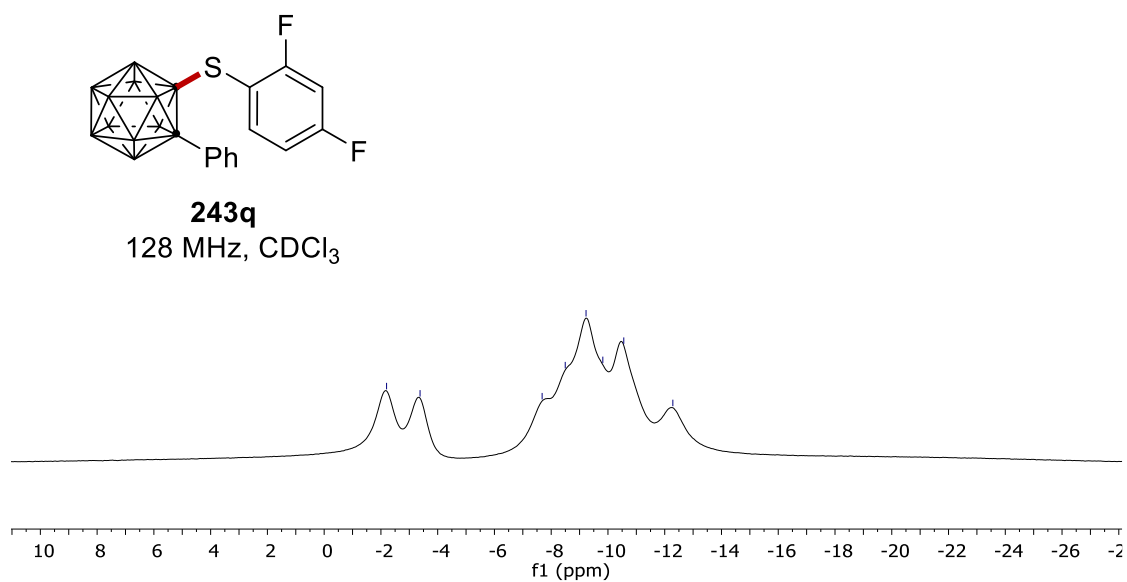
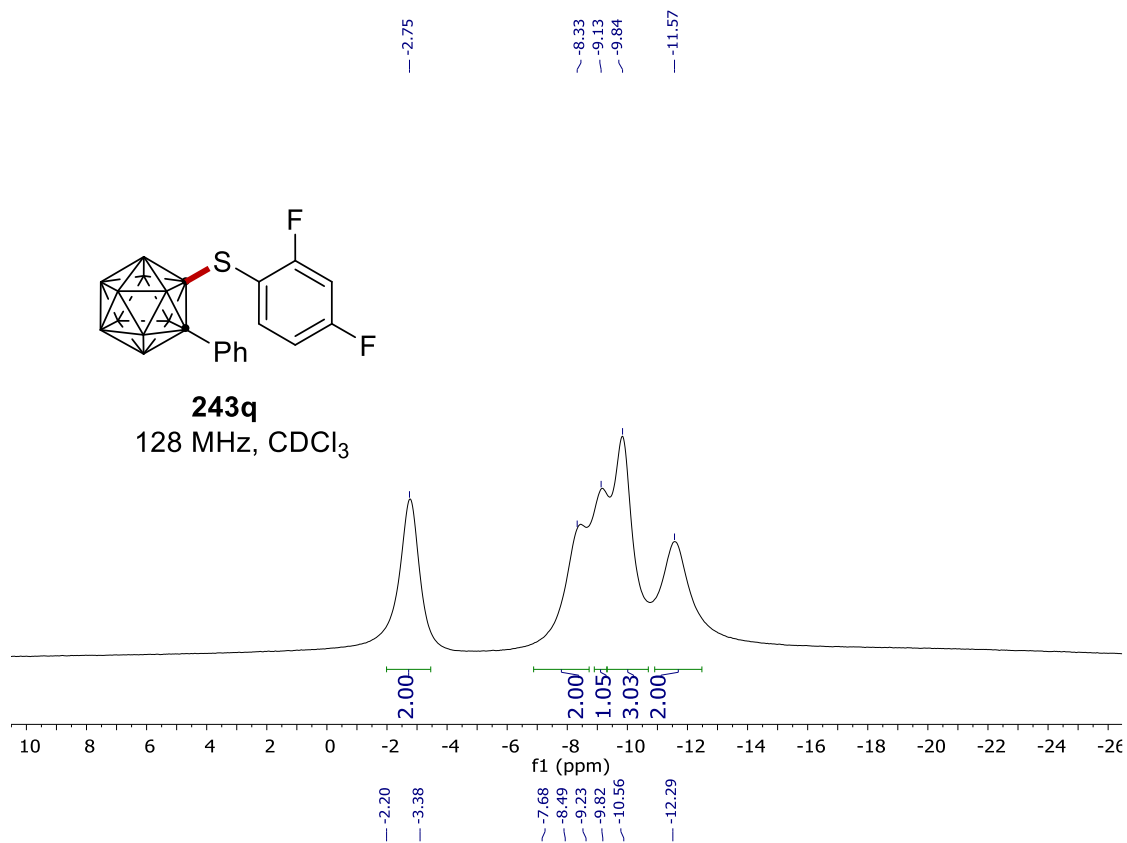
7. NMR Spectra



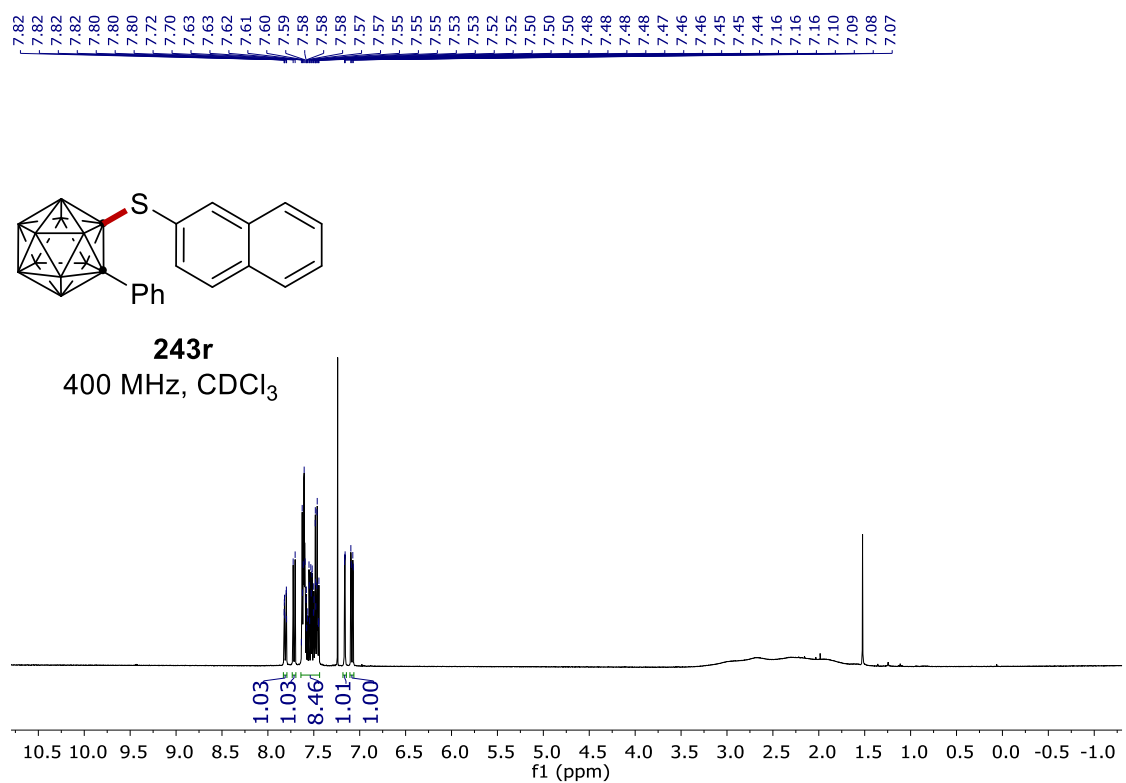
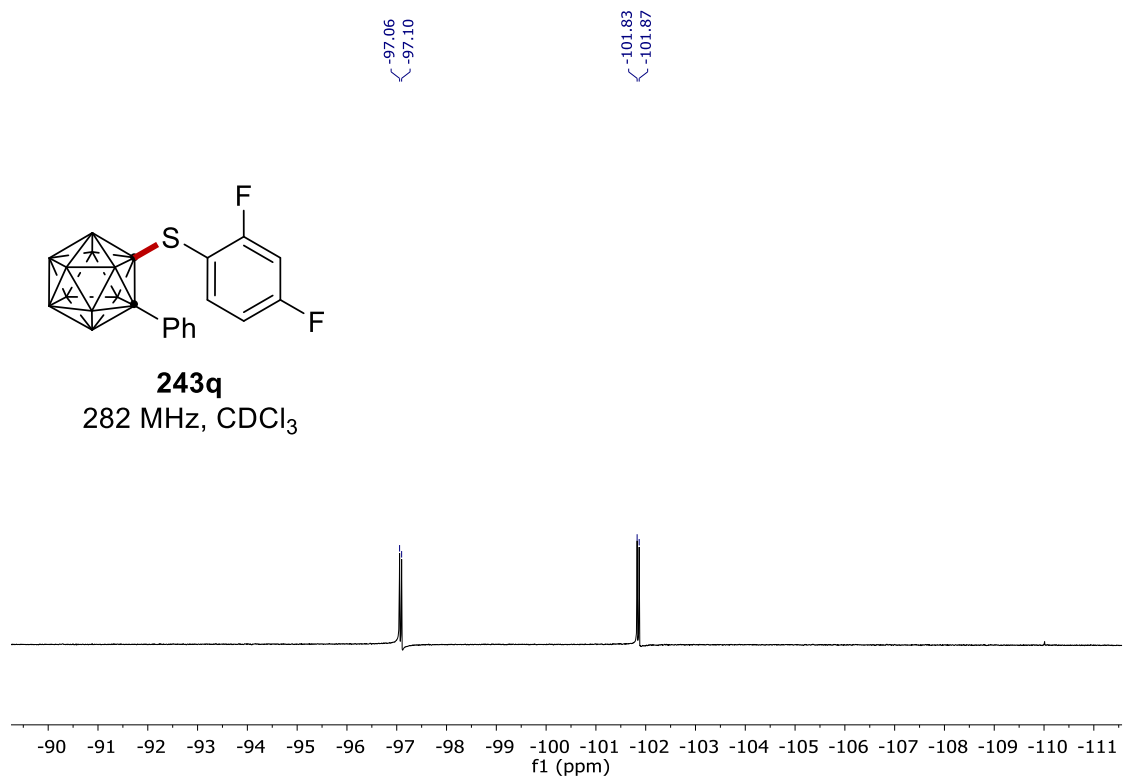
7. NMR Spectra



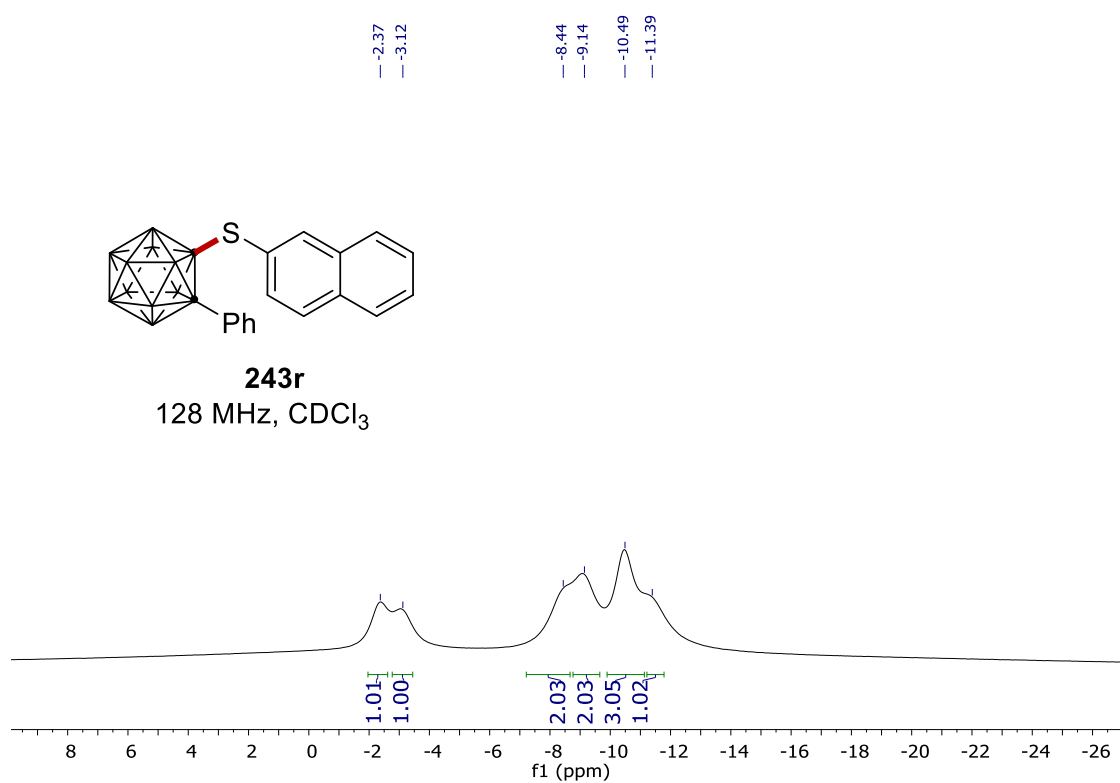
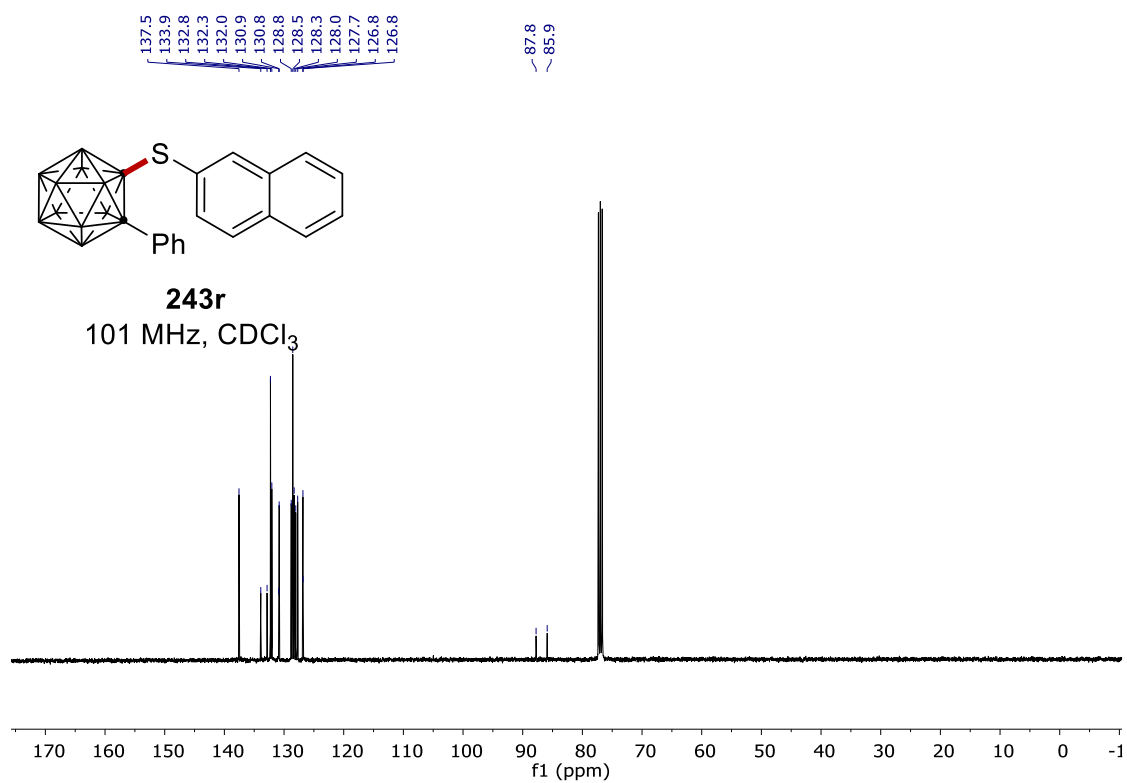
7. NMR Spectra



7. NMR Spectra

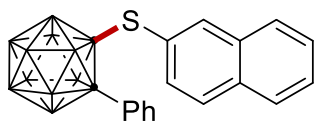


7. NMR Spectra

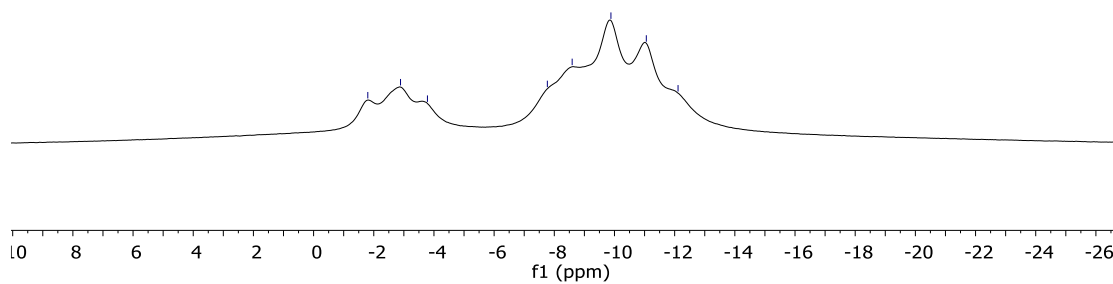


7. NMR Spectra

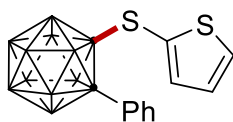
~ -1.80
 ~ -2.89
 ~ -3.78
 -7.77
 -8.59
 ~ -9.88
 ~ -11.06
 ~ -12.11



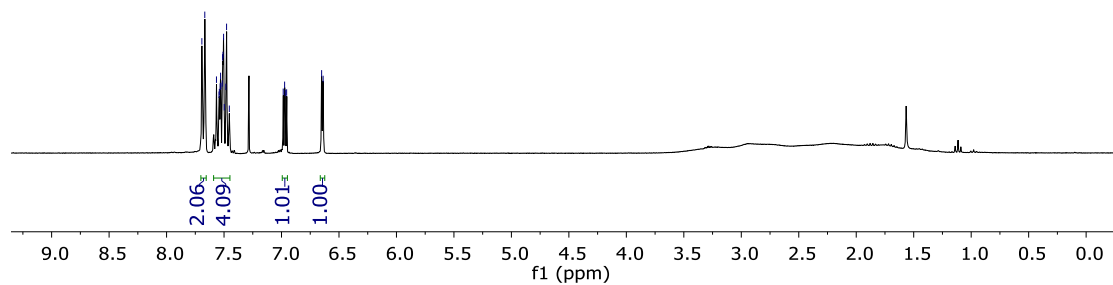
243r
128 MHz, CDCl_3



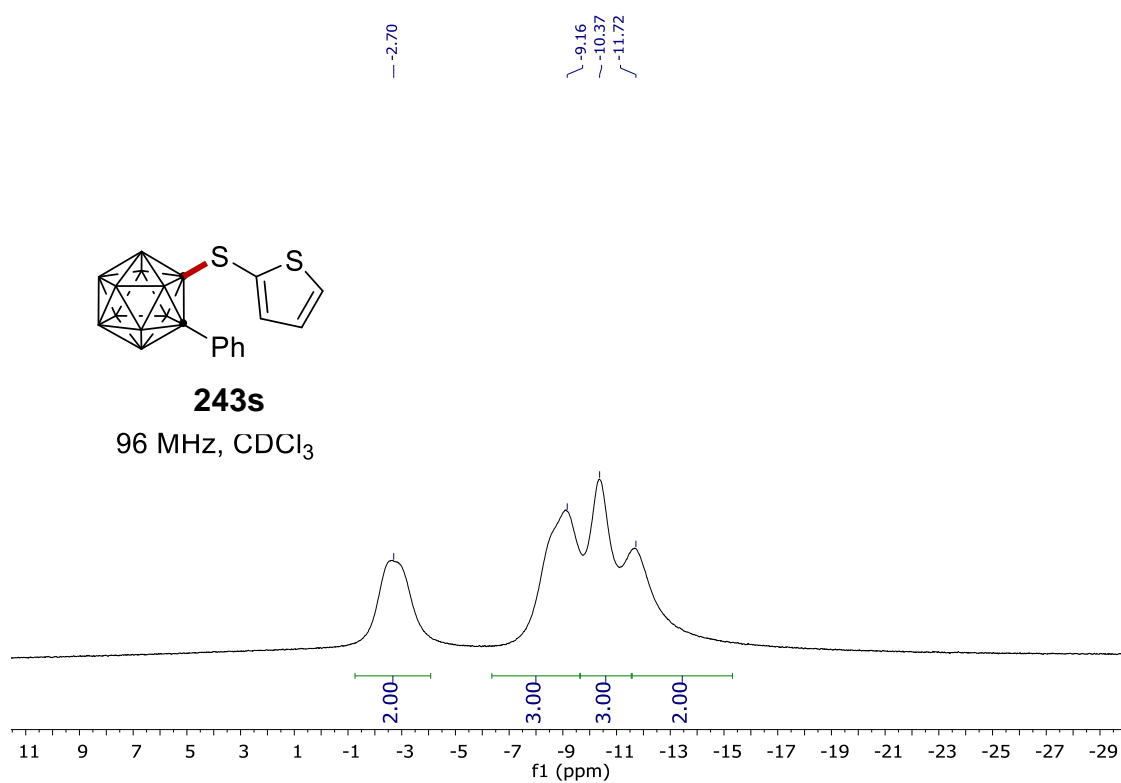
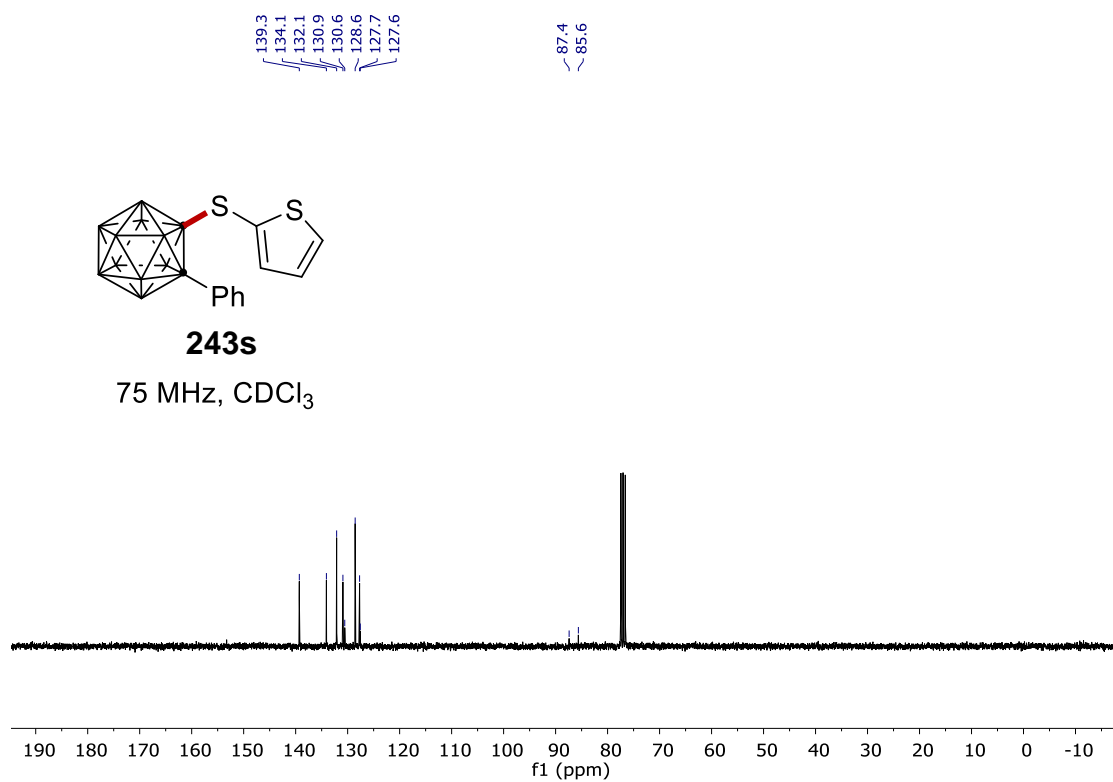
7.69
 7.67
 7.57
 7.53
 7.53
 7.53
 7.52
 7.51
 7.51
 7.50
 7.48
 7.48
 6.97
 6.96
 6.65
 6.64



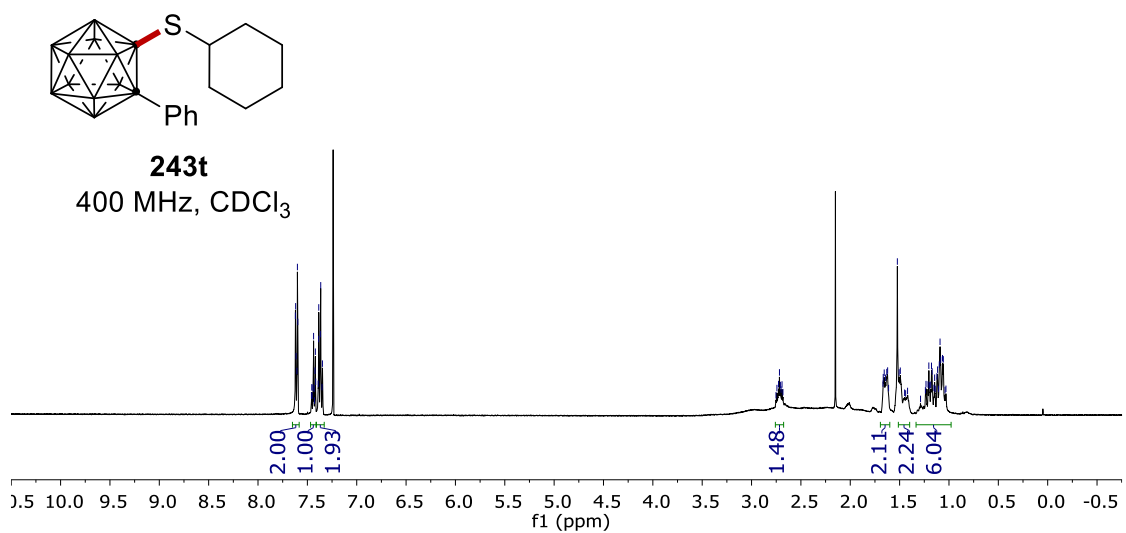
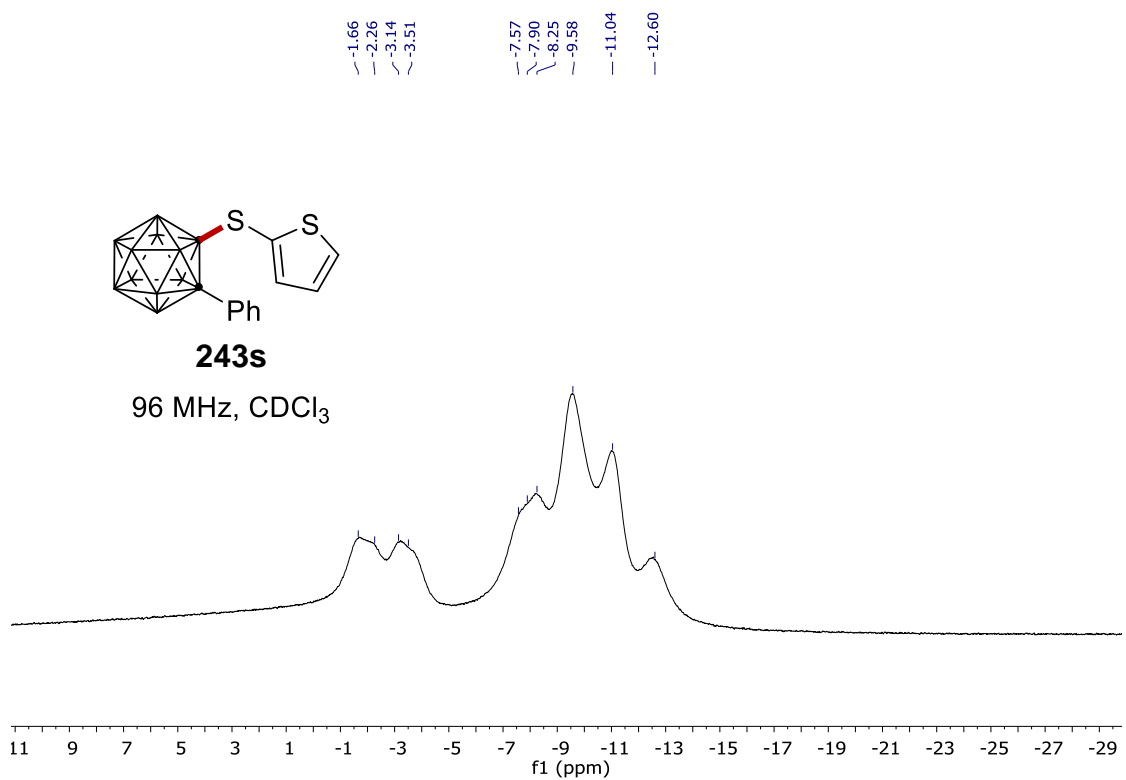
243s
300 MHz, CDCl_3



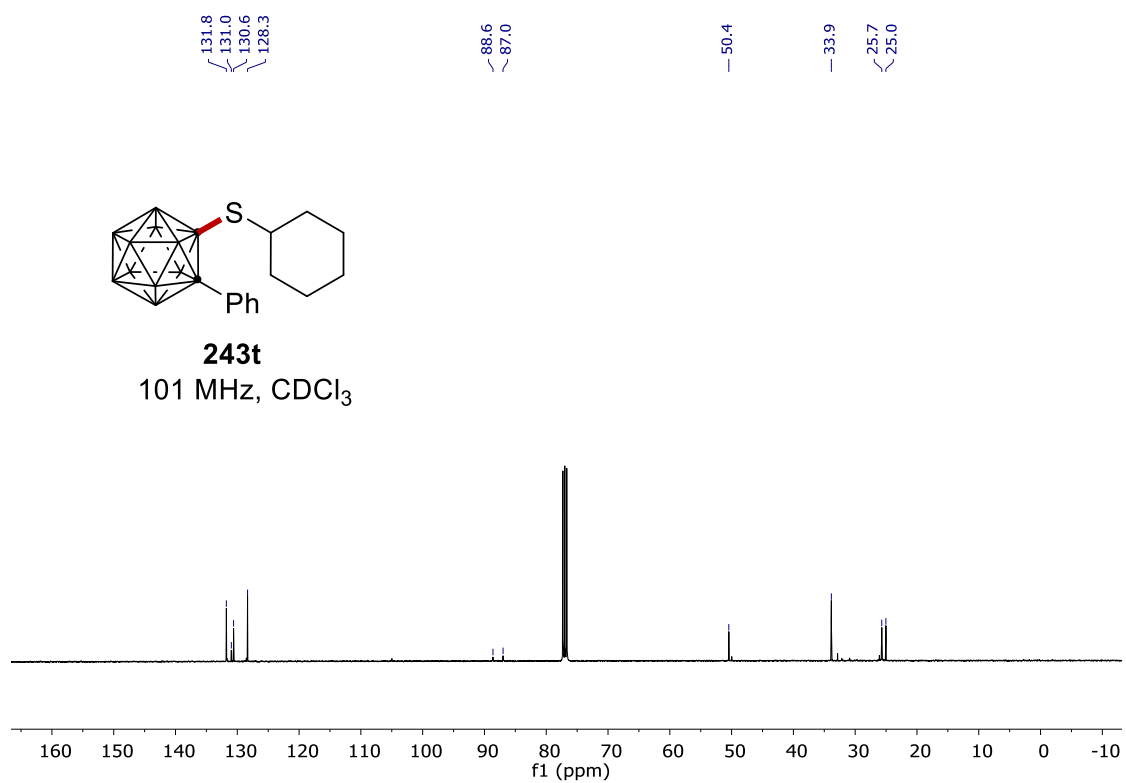
7. NMR Spectra



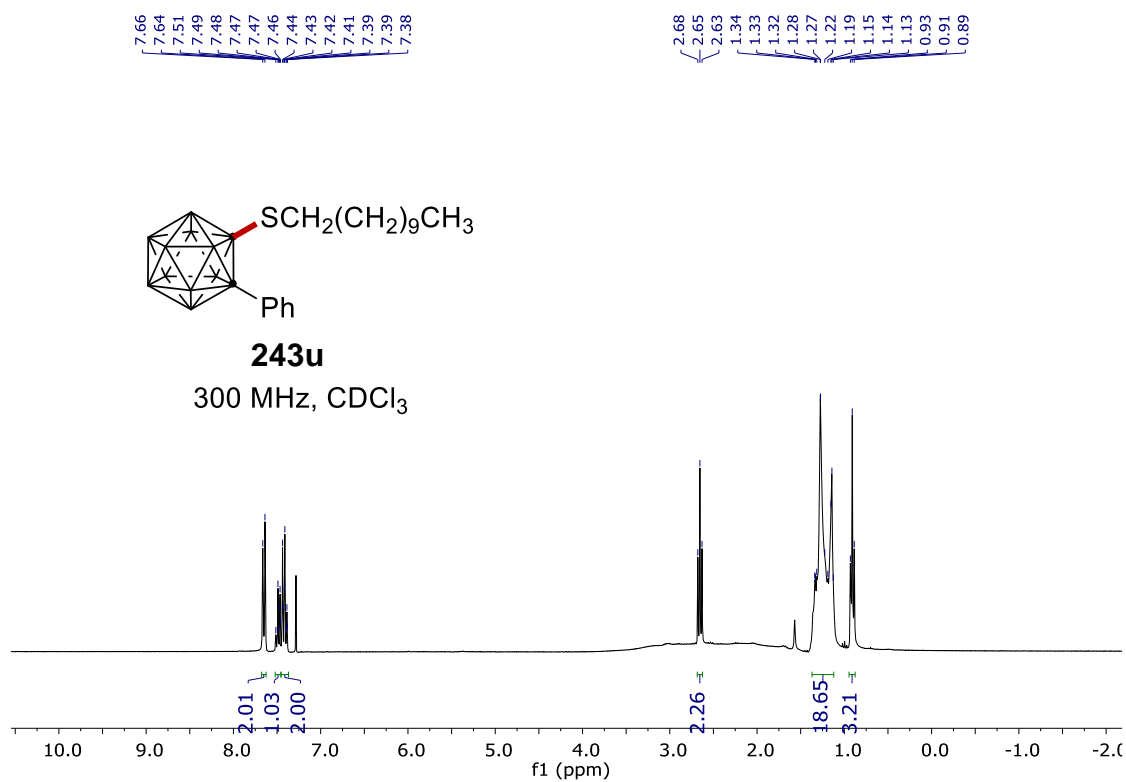
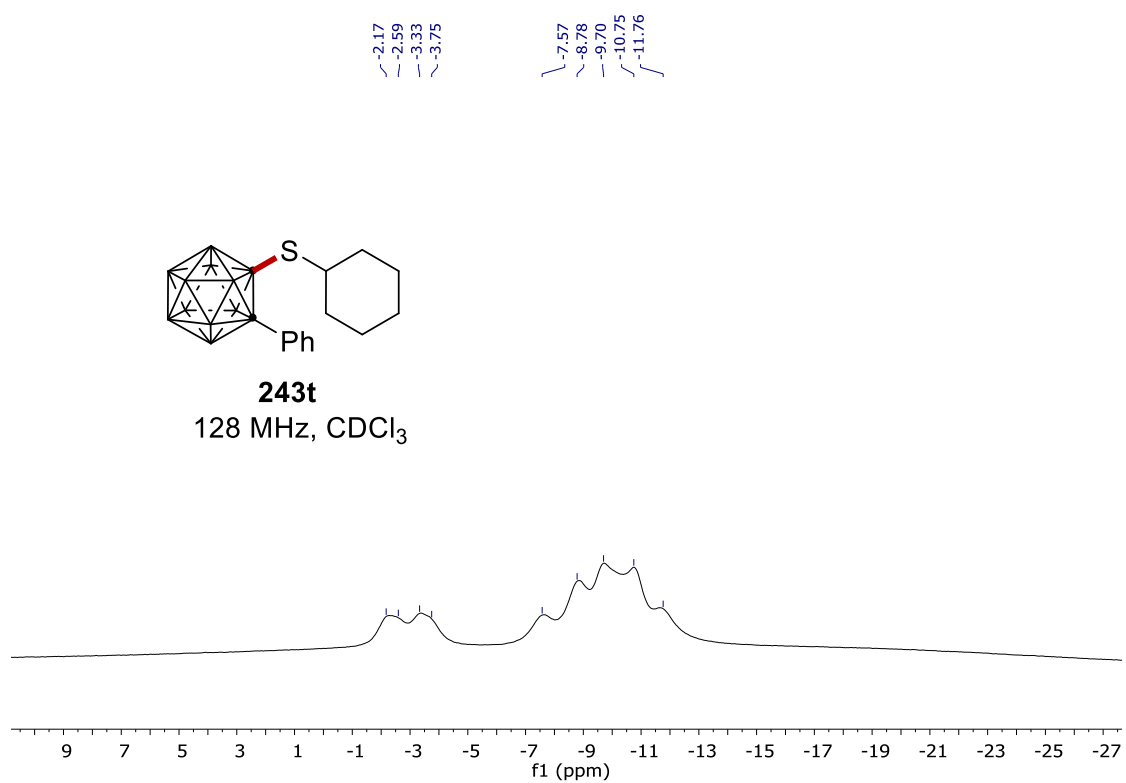
7. NMR Spectra



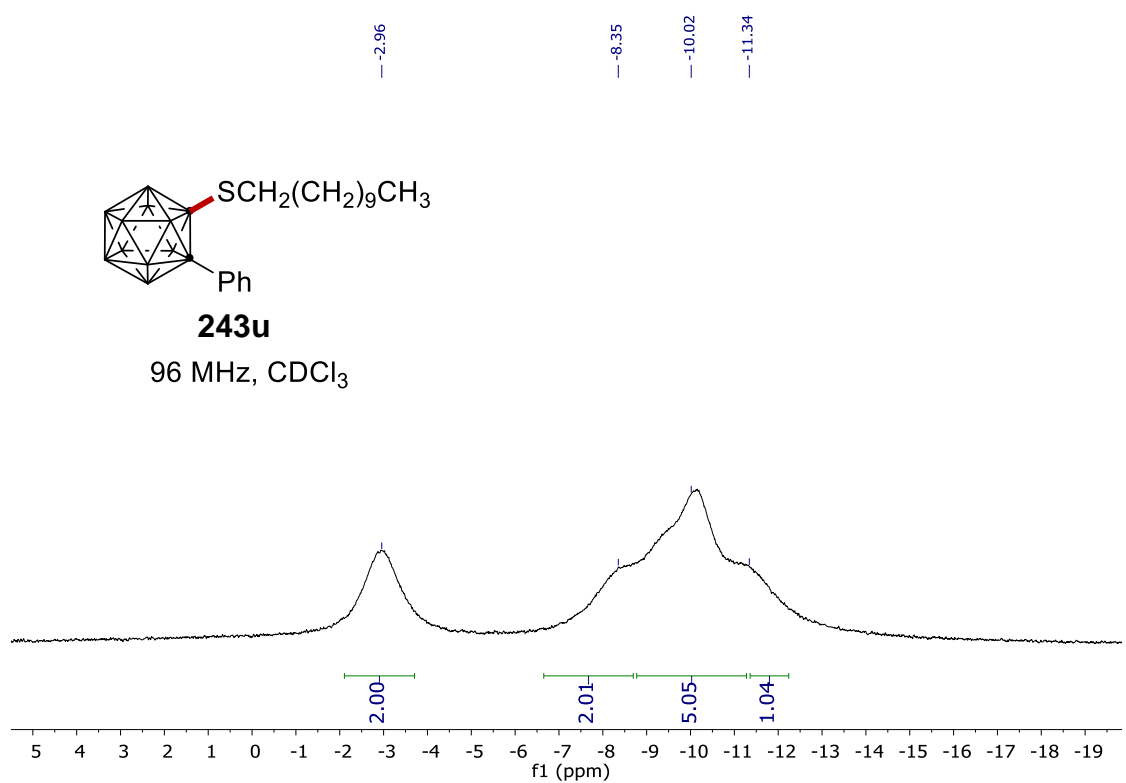
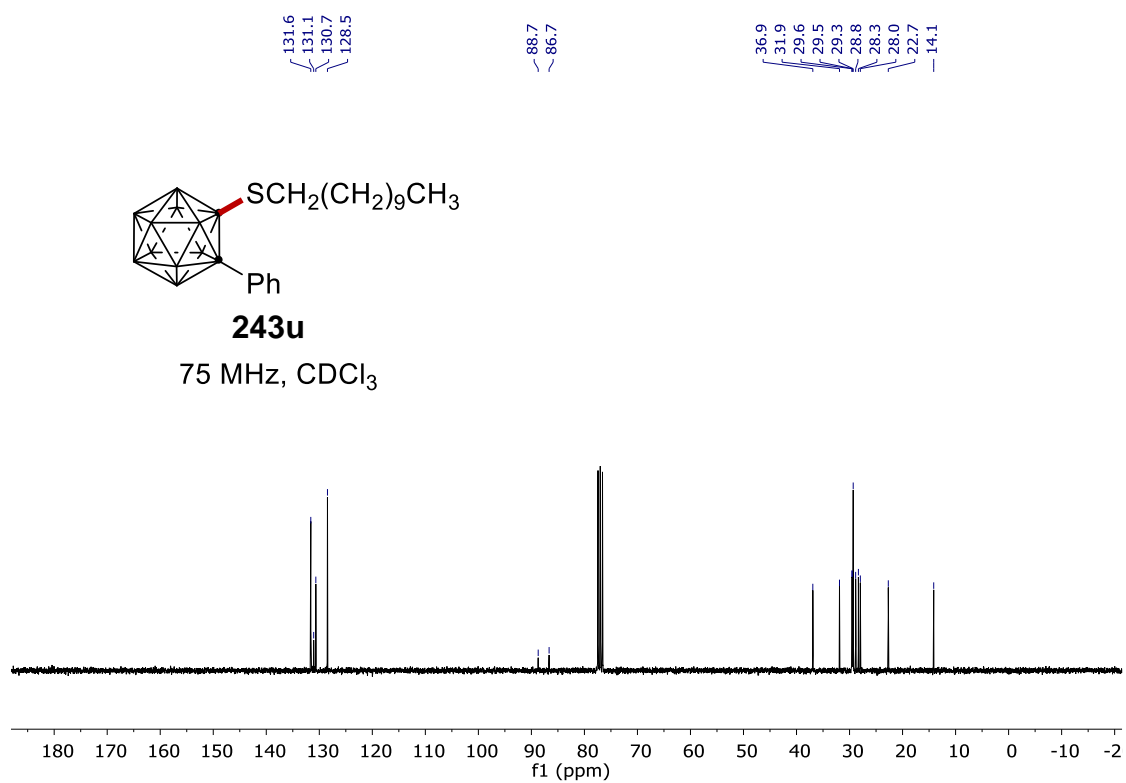
7. NMR Spectra



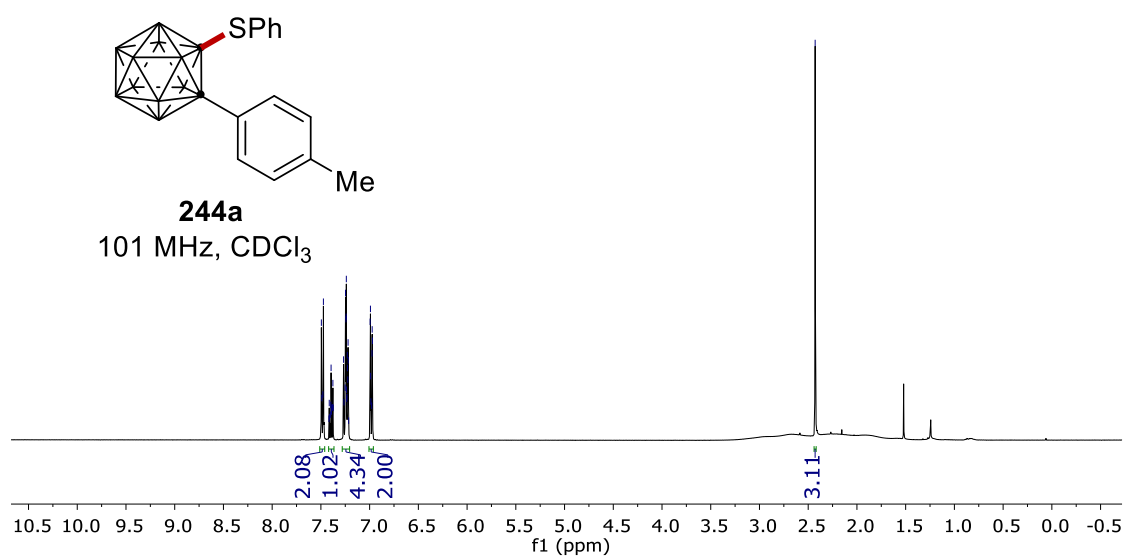
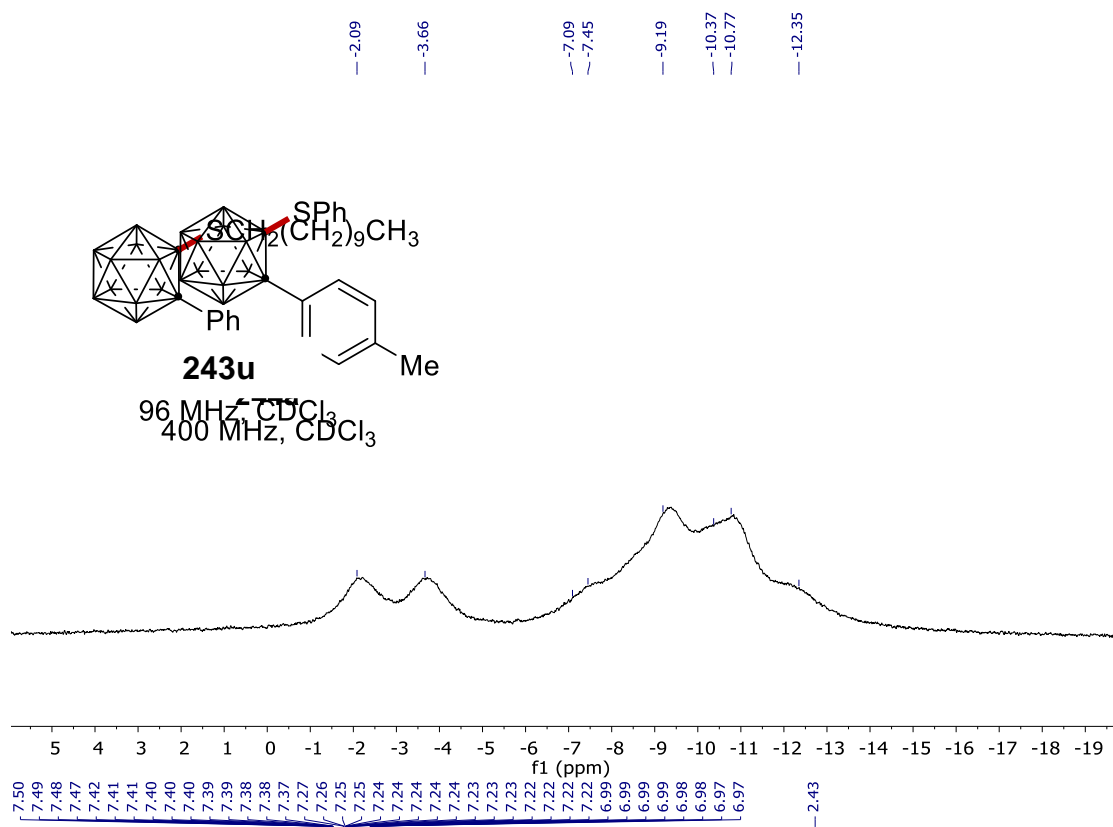
7. NMR Spectra



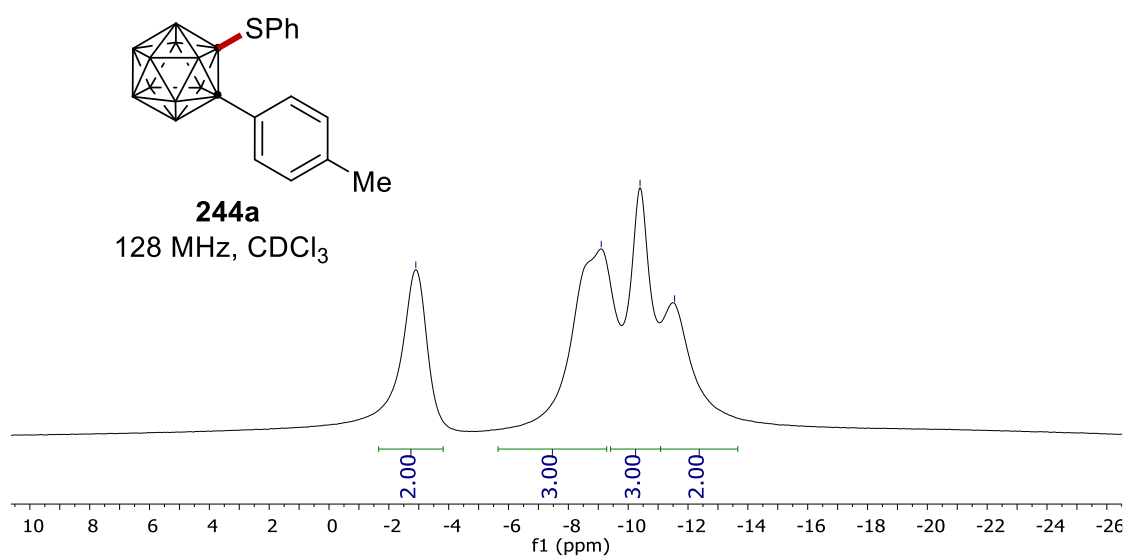
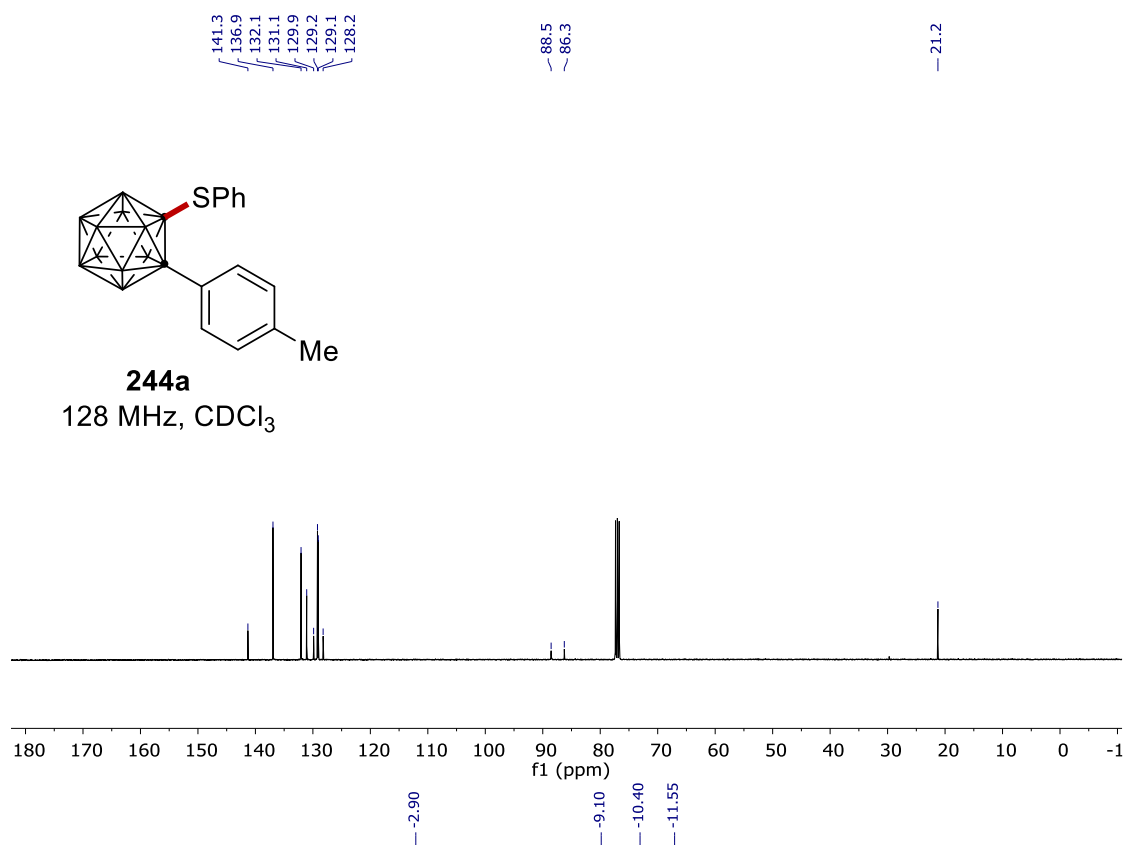
7. NMR Spectra



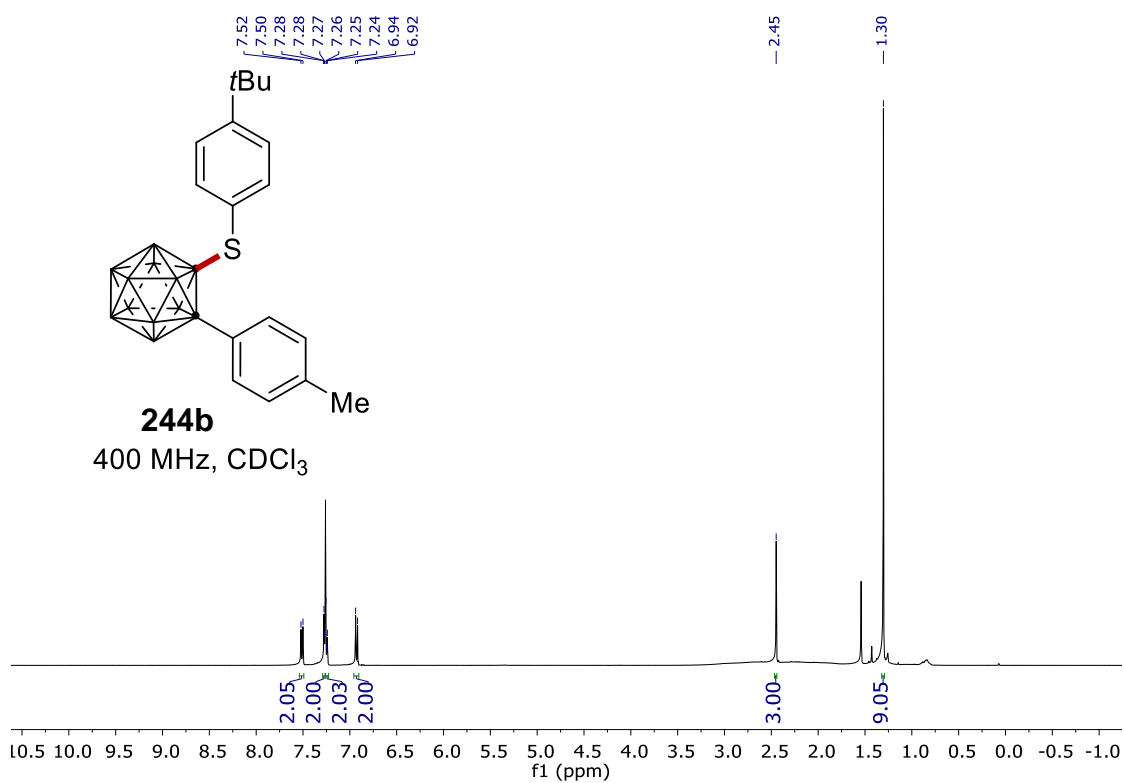
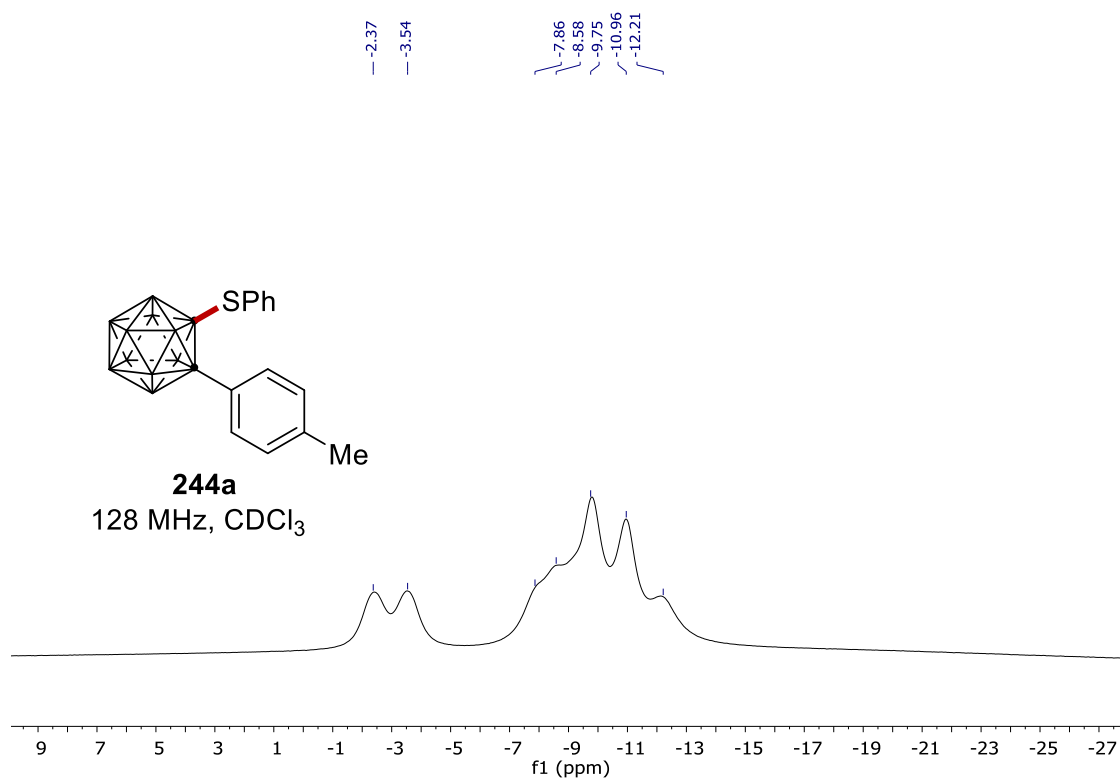
7. NMR Spectra



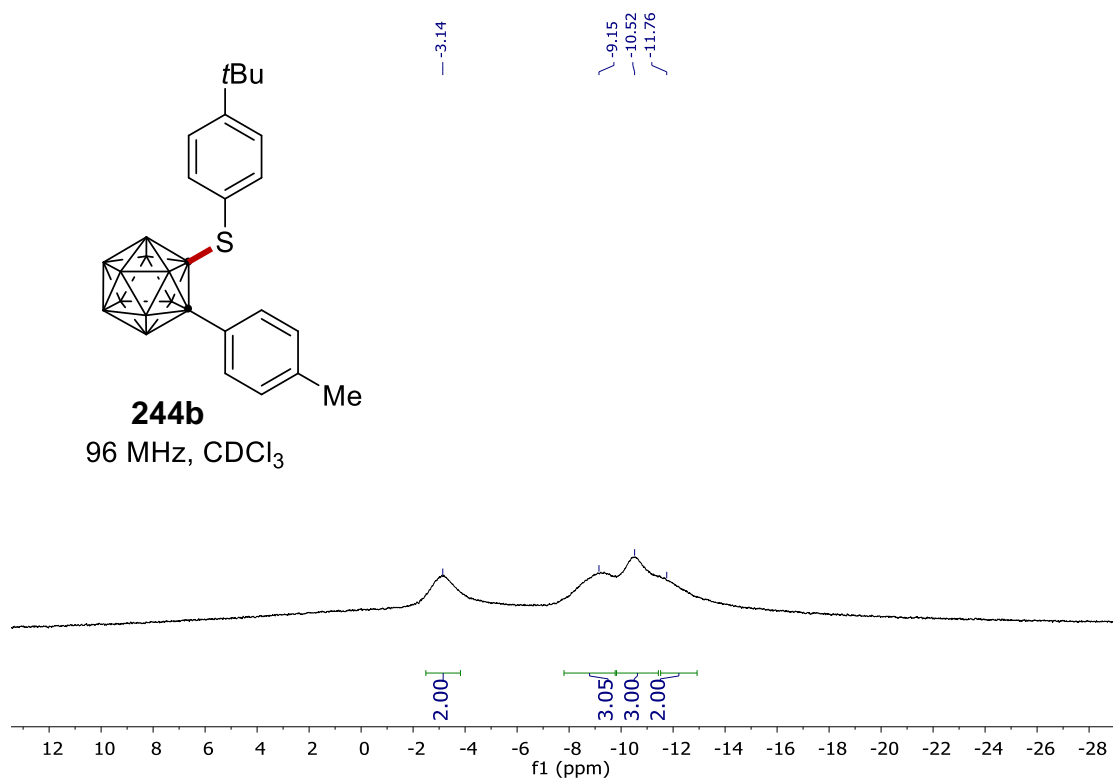
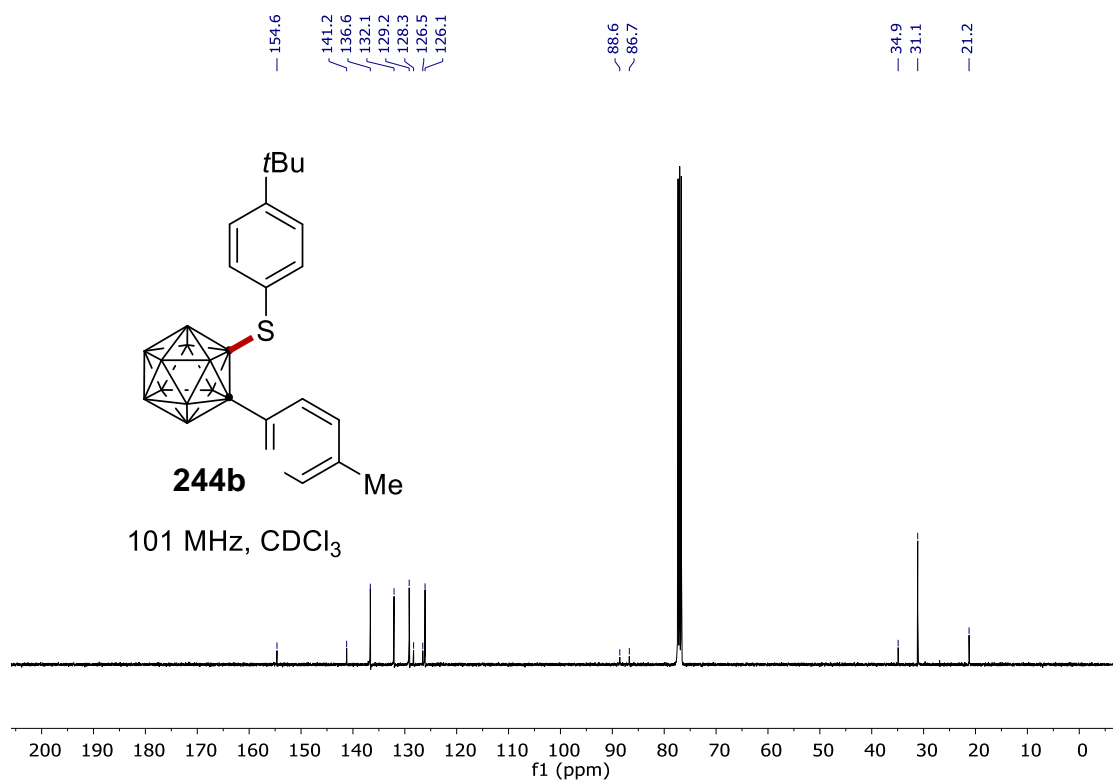
7. NMR Spectra



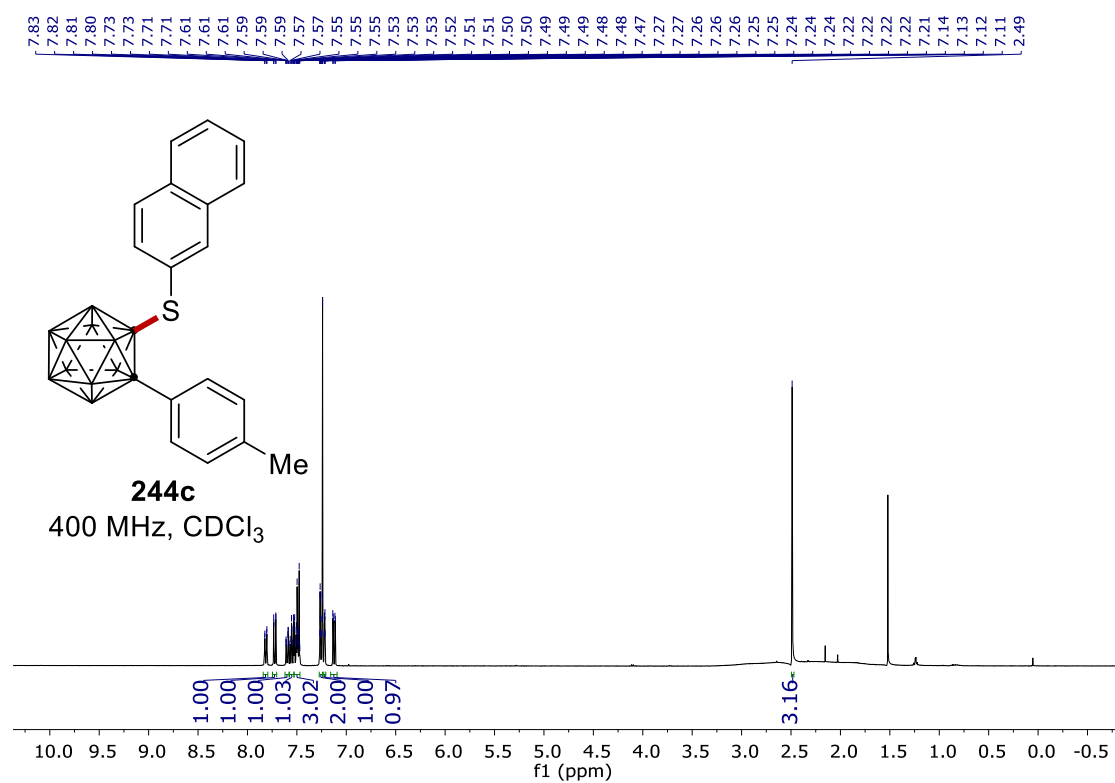
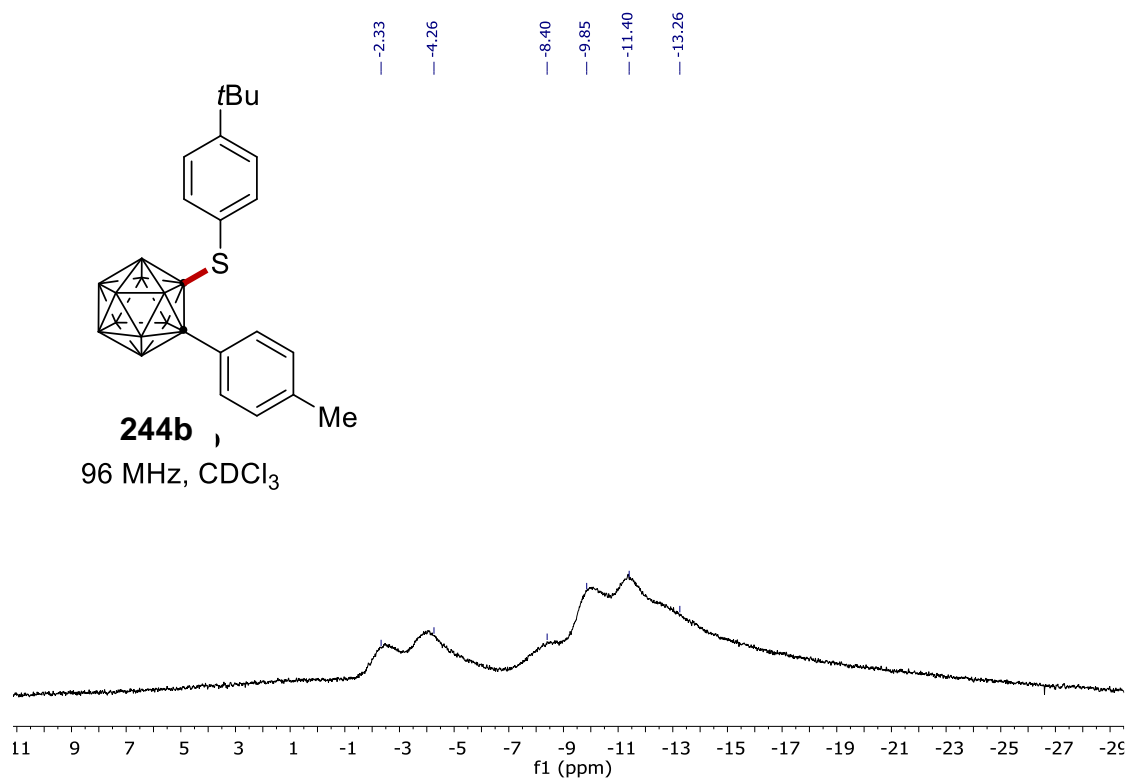
7. NMR Spectra



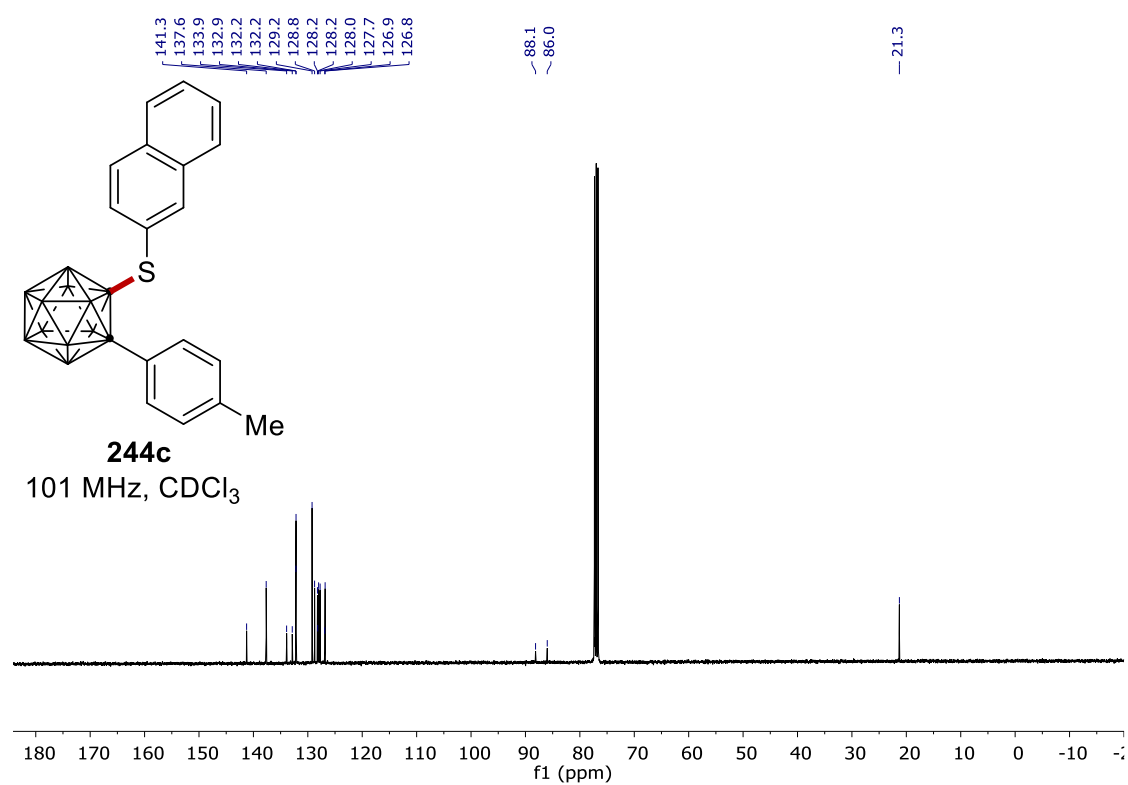
7. NMR Spectra



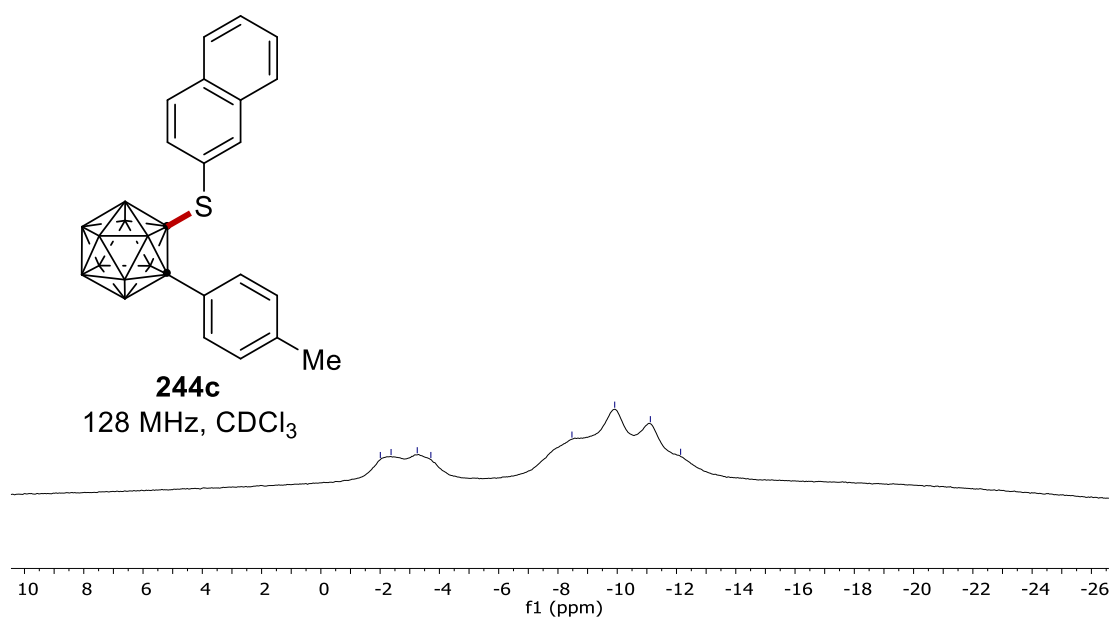
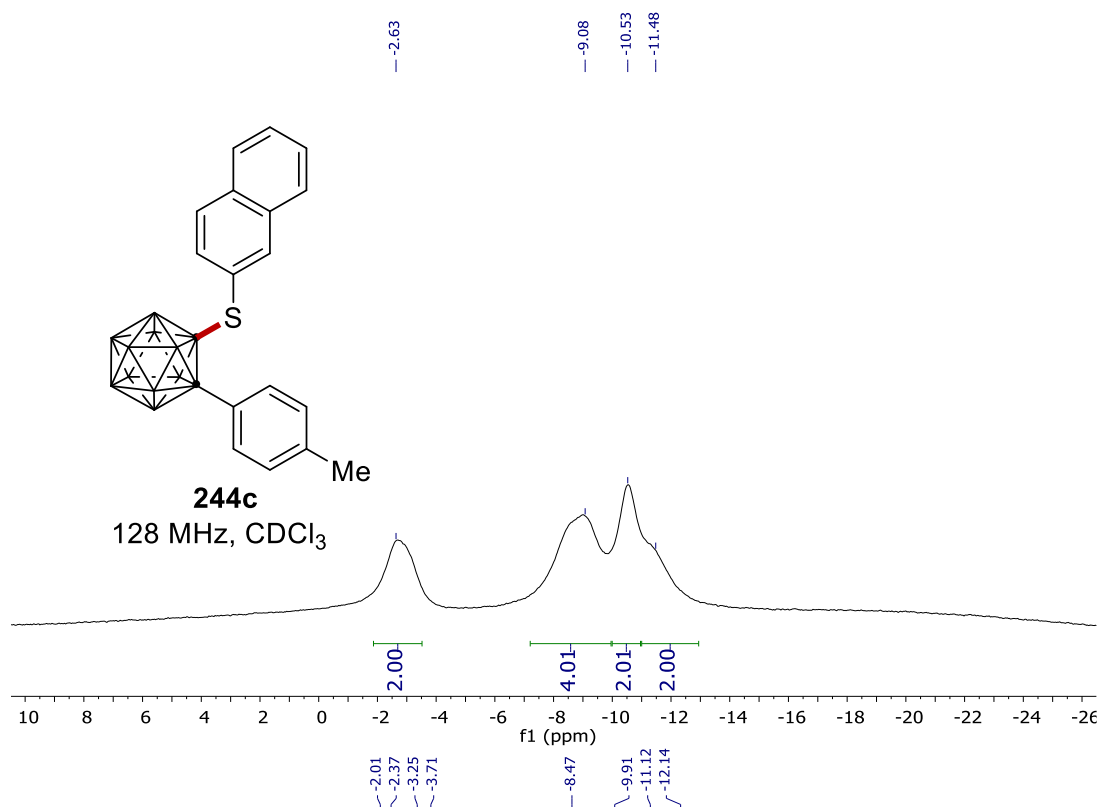
7. NMR Spectra



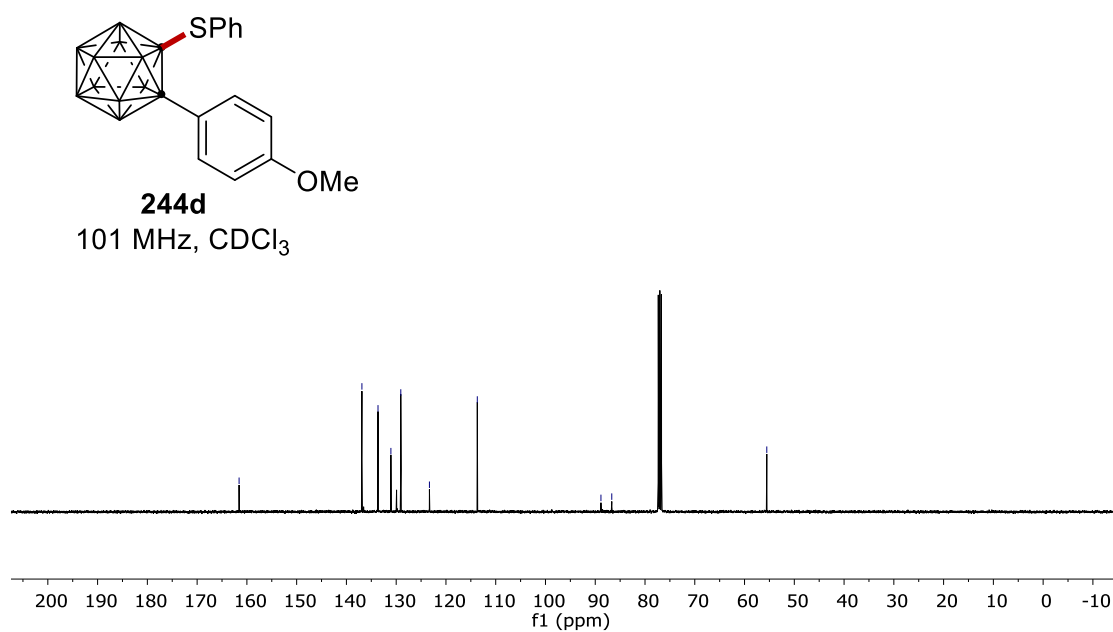
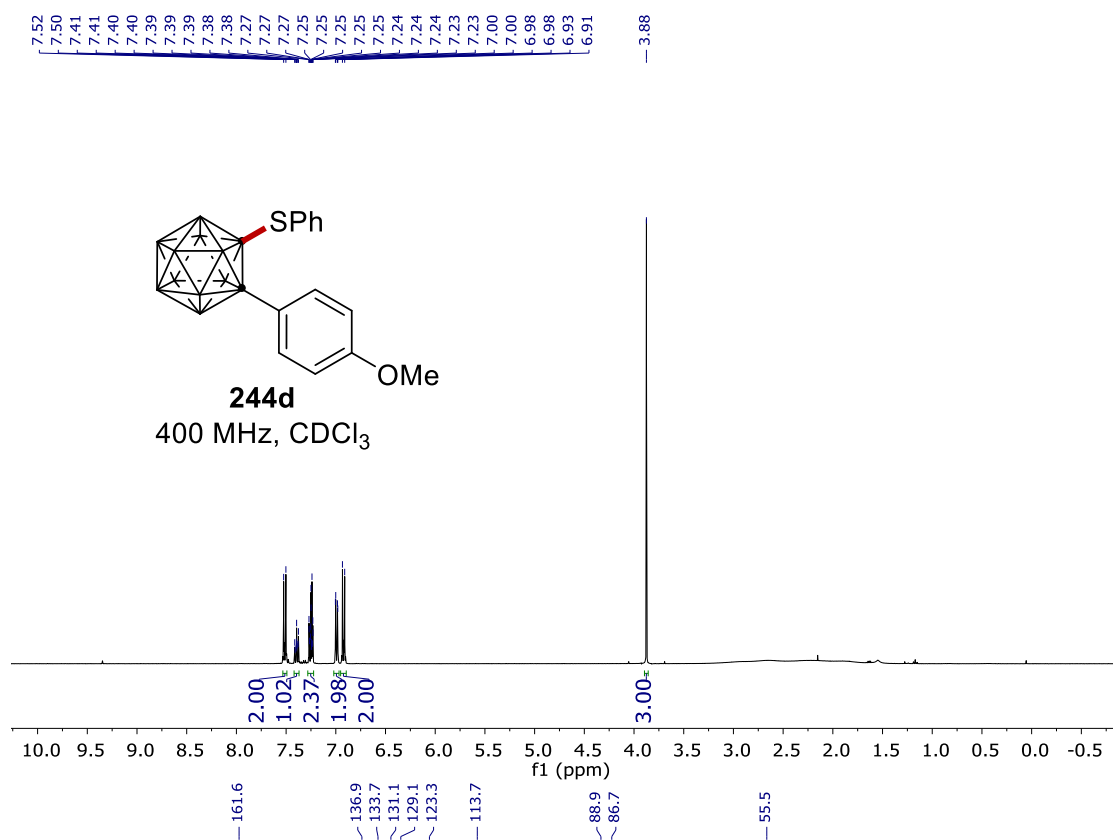
7. NMR Spectra



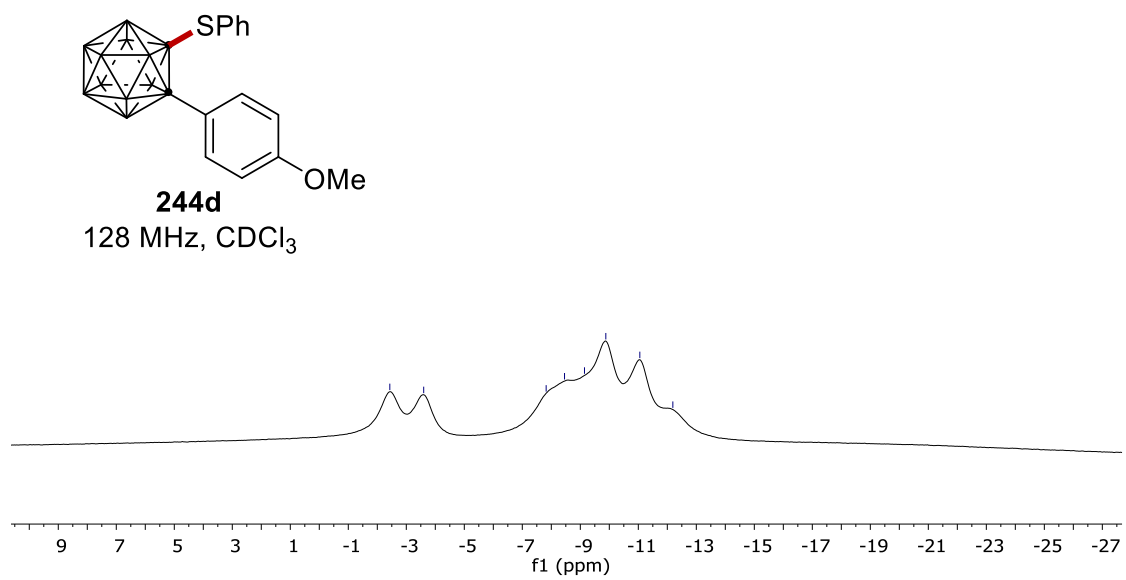
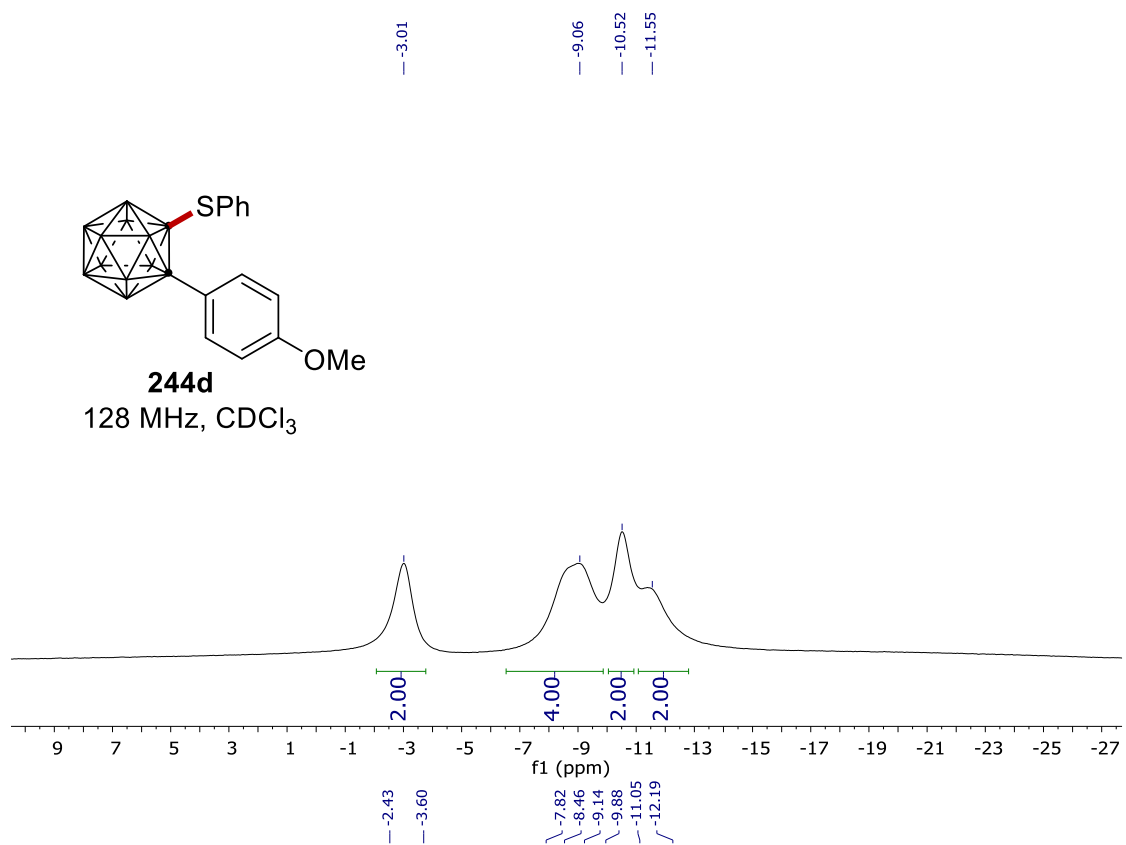
7. NMR Spectra



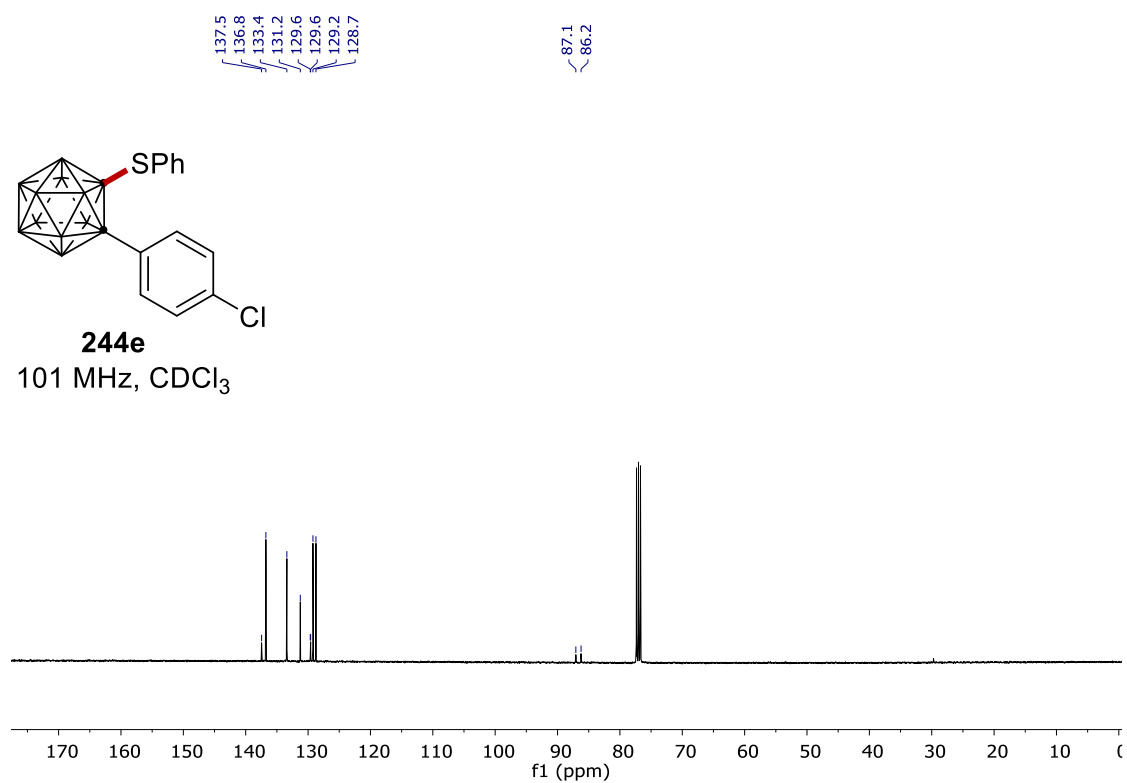
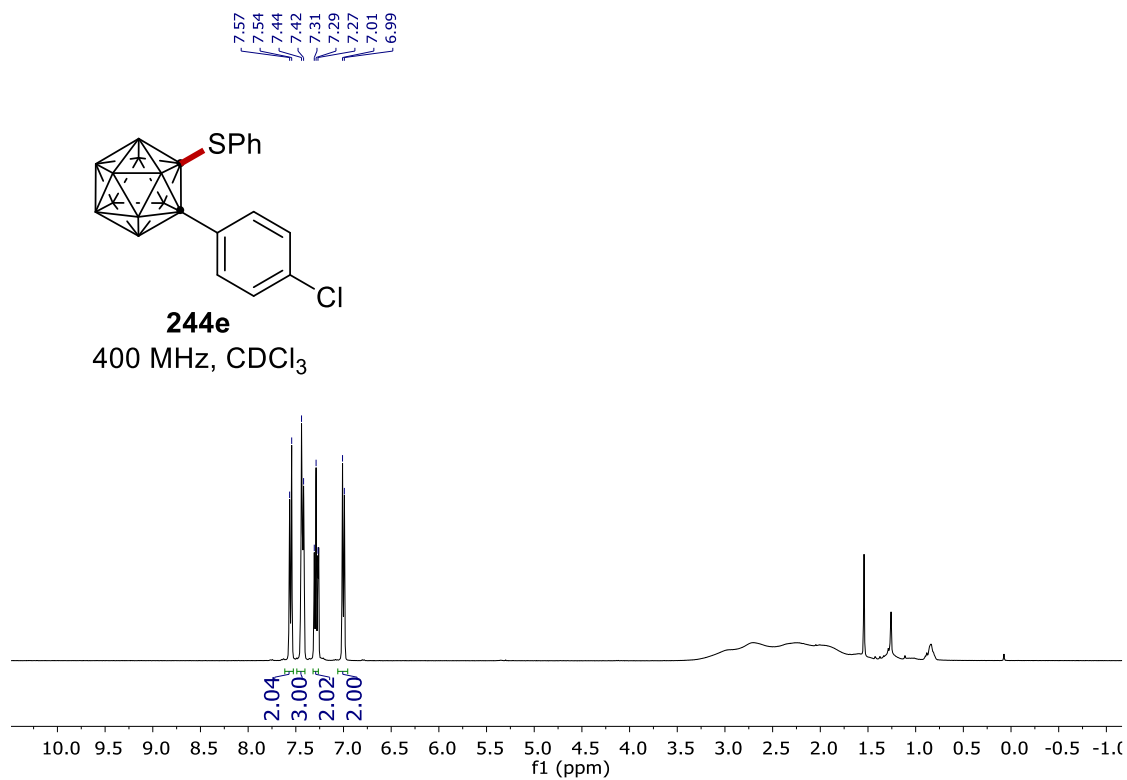
7. NMR Spectra

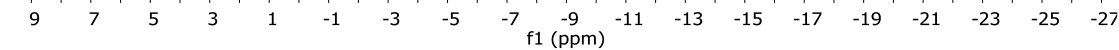
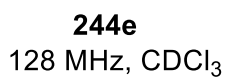
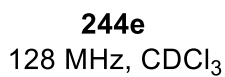


7. NMR Spectra

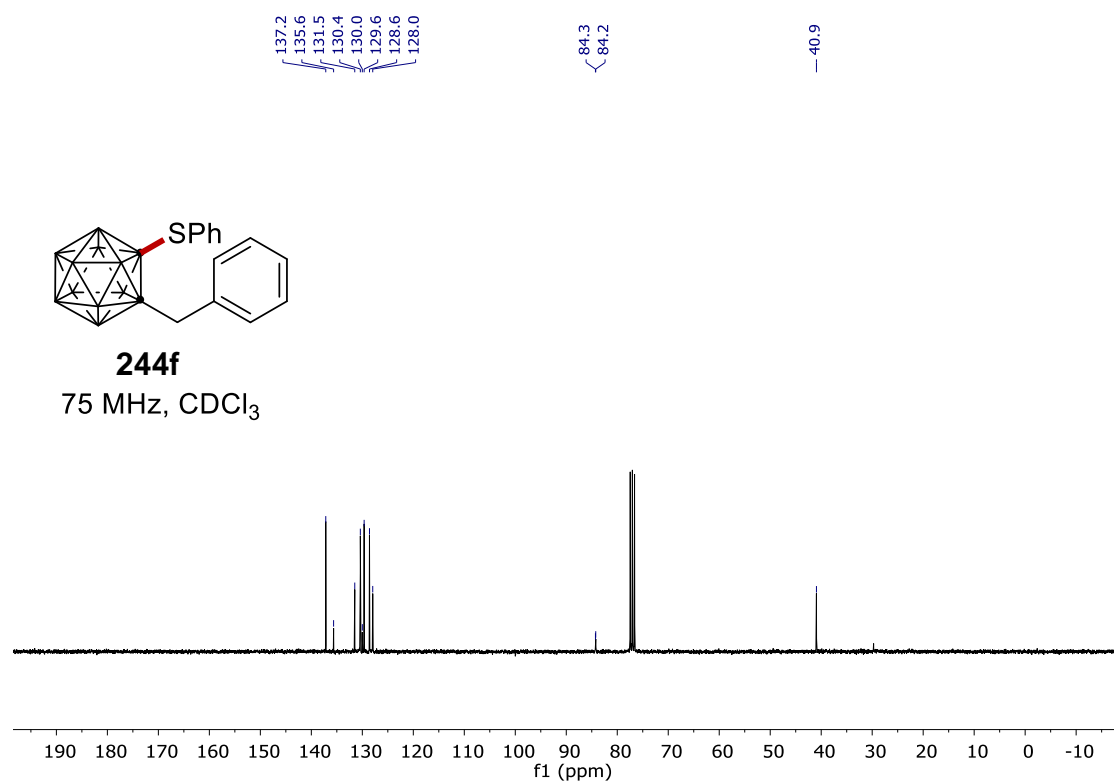
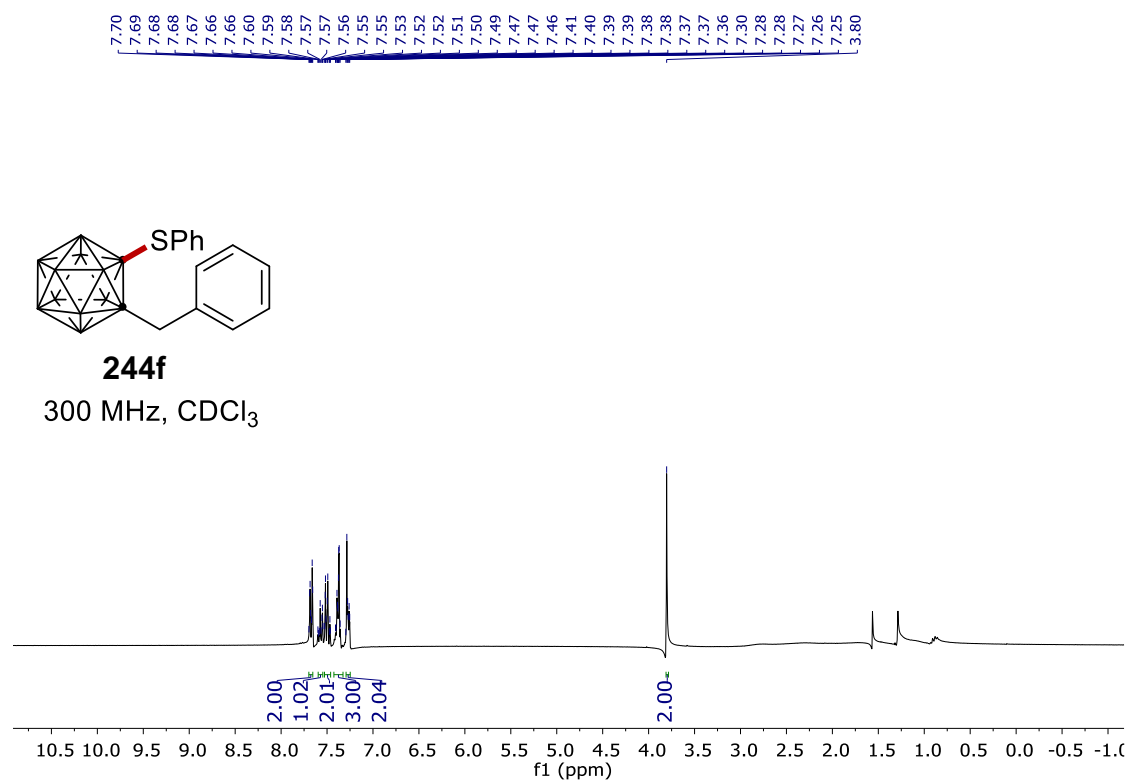


7. NMR Spectra

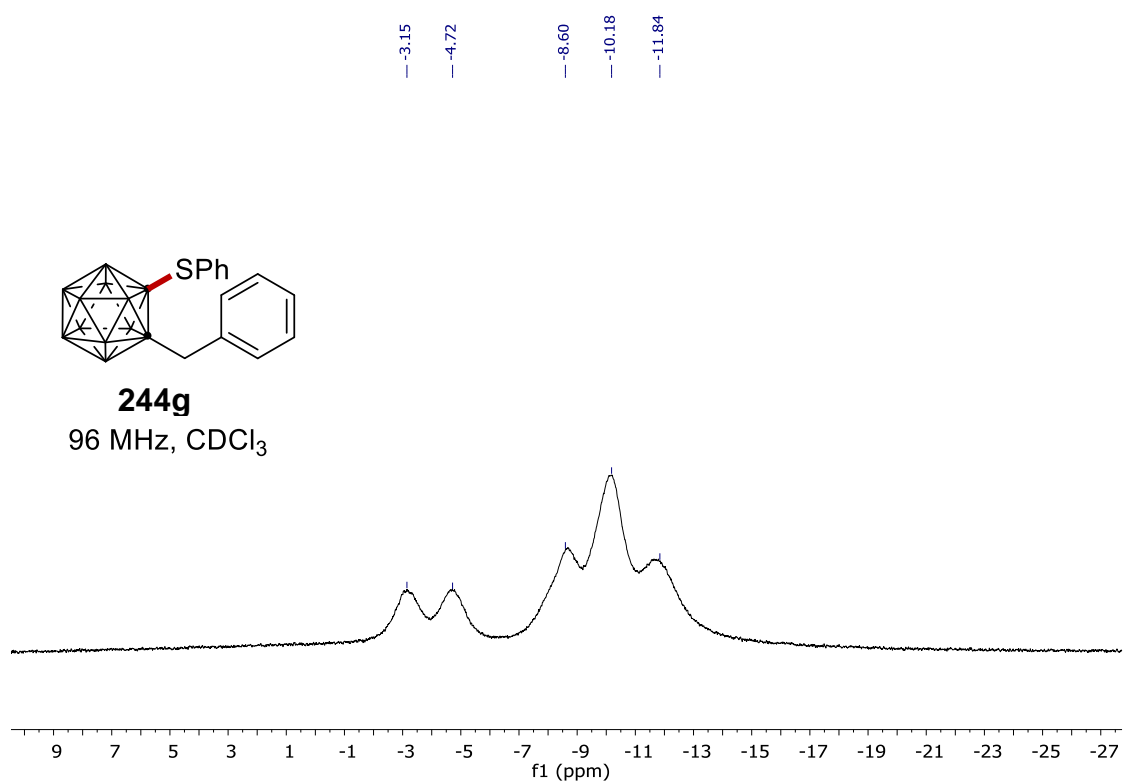
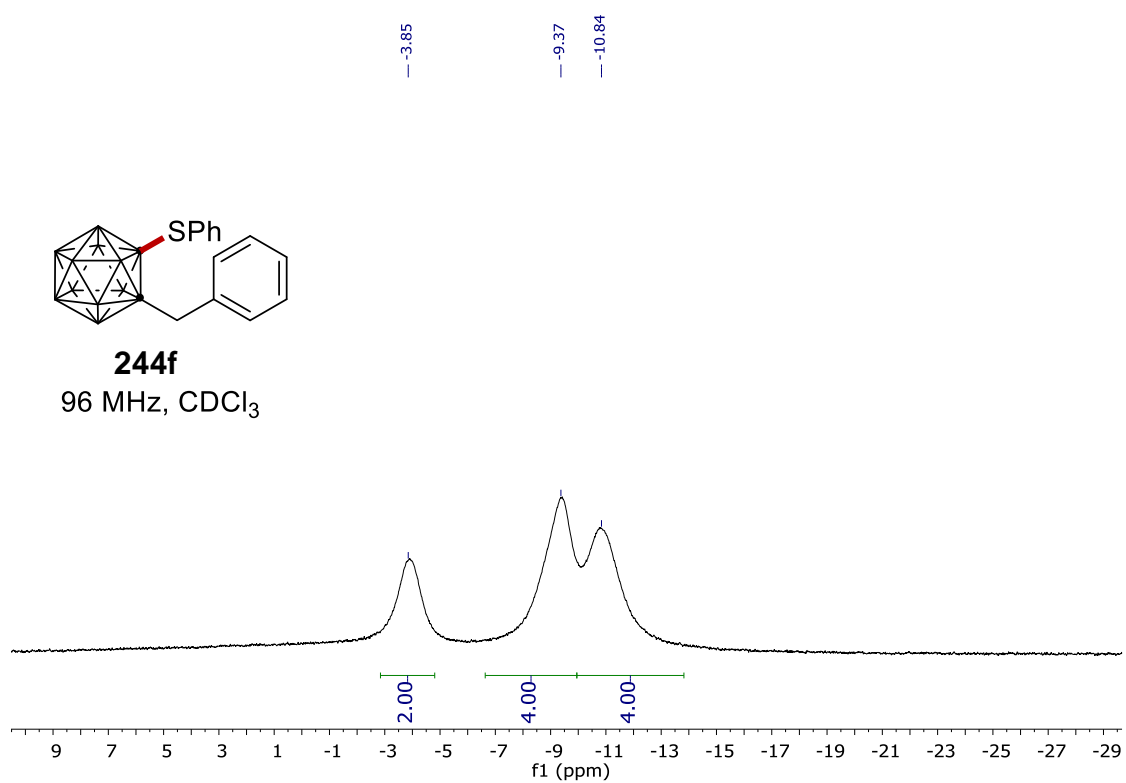




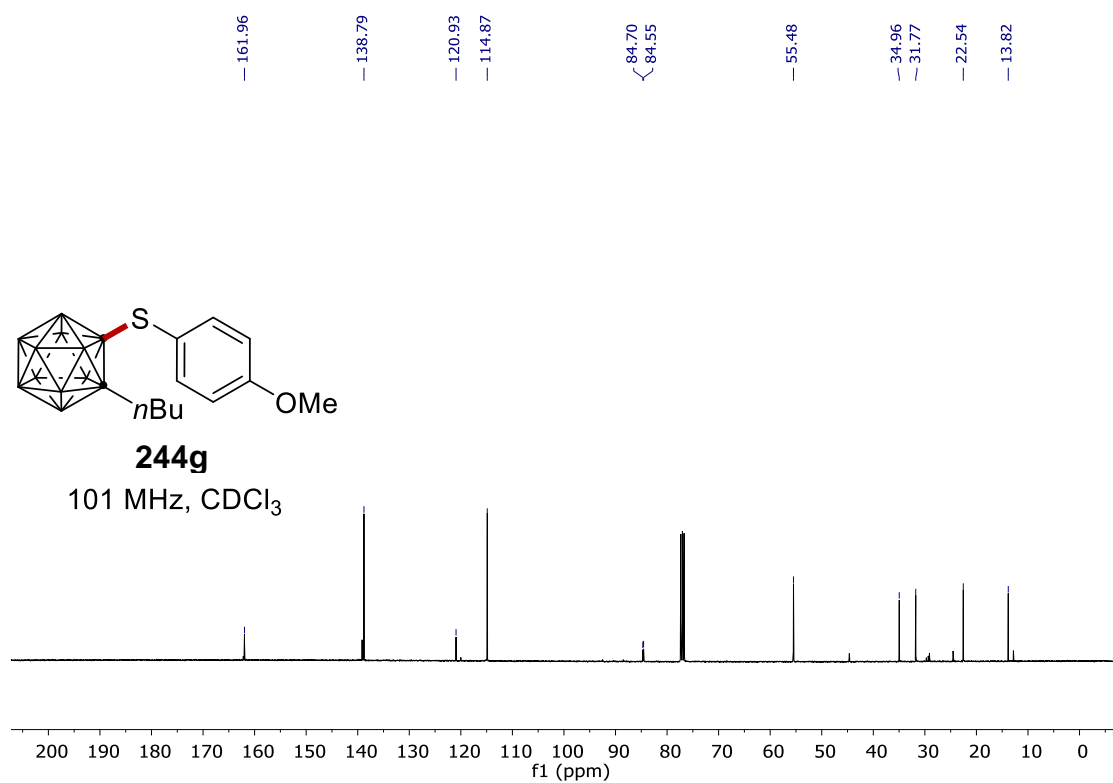
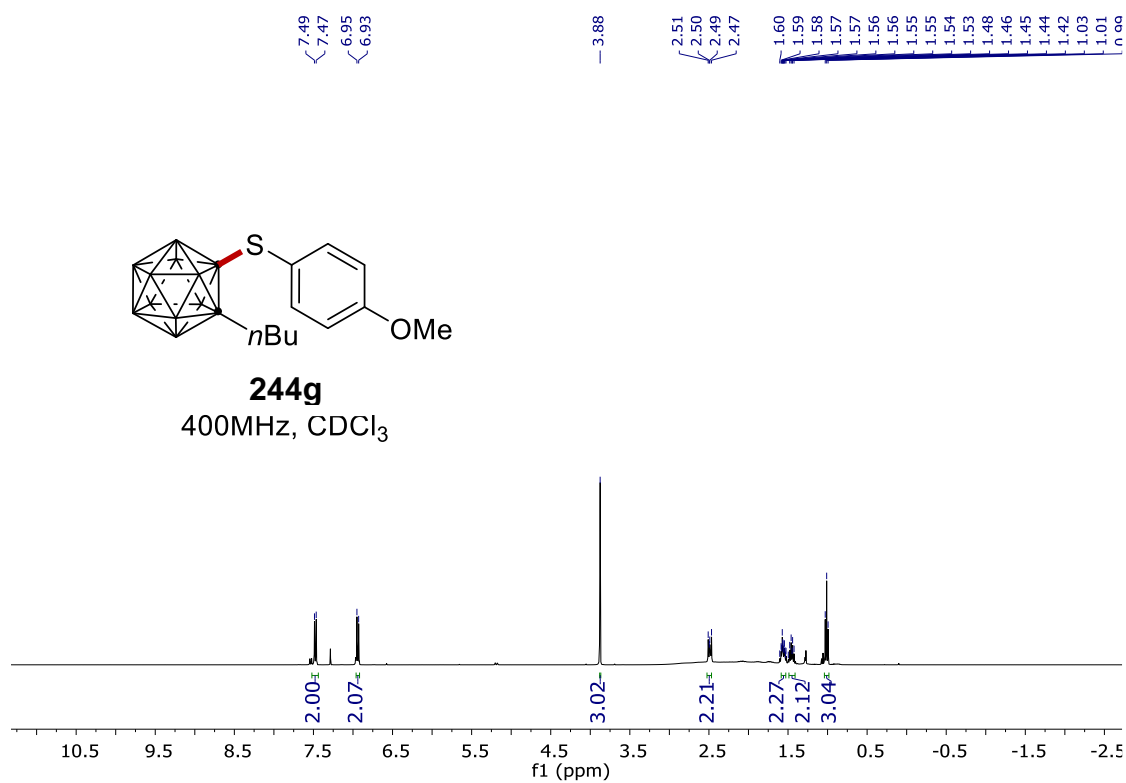
7. NMR Spectra



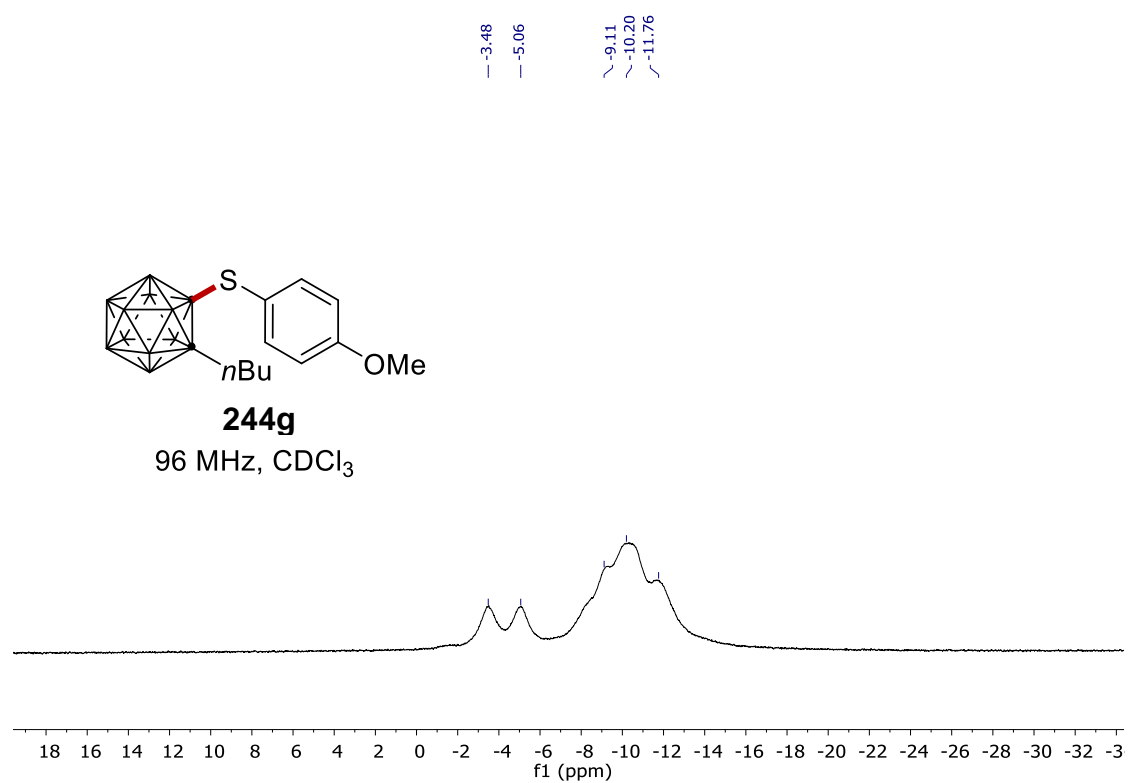
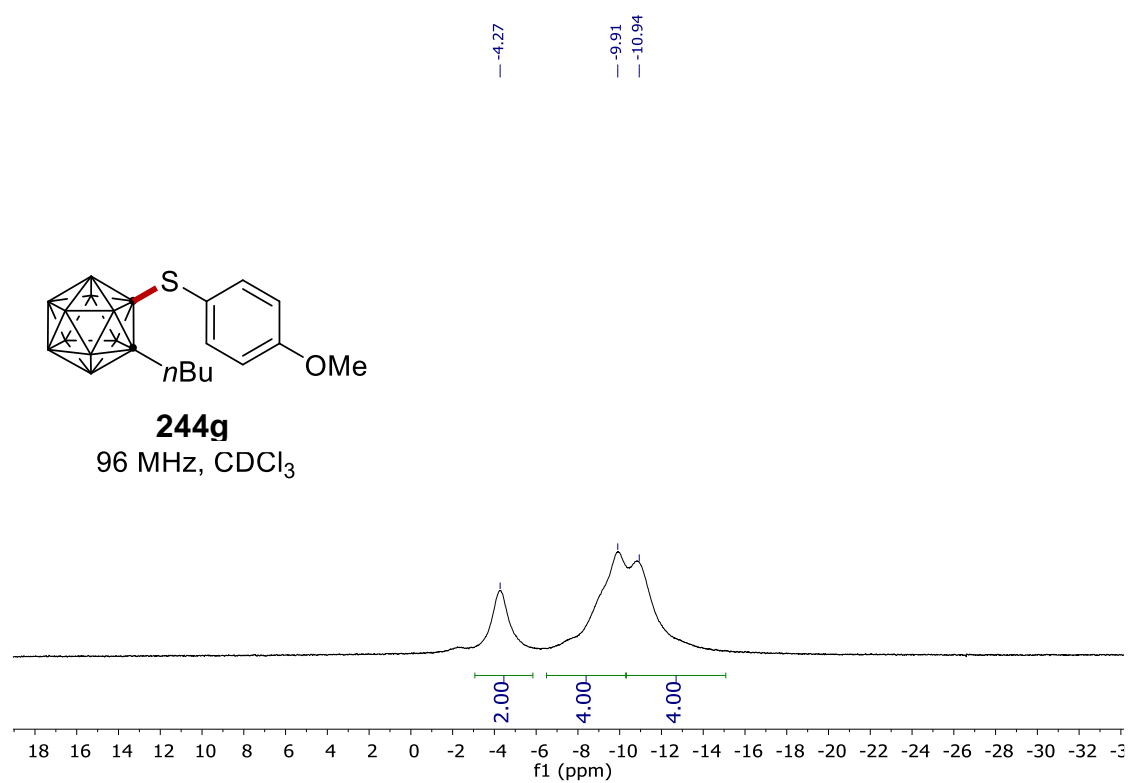
7. NMR Spectra

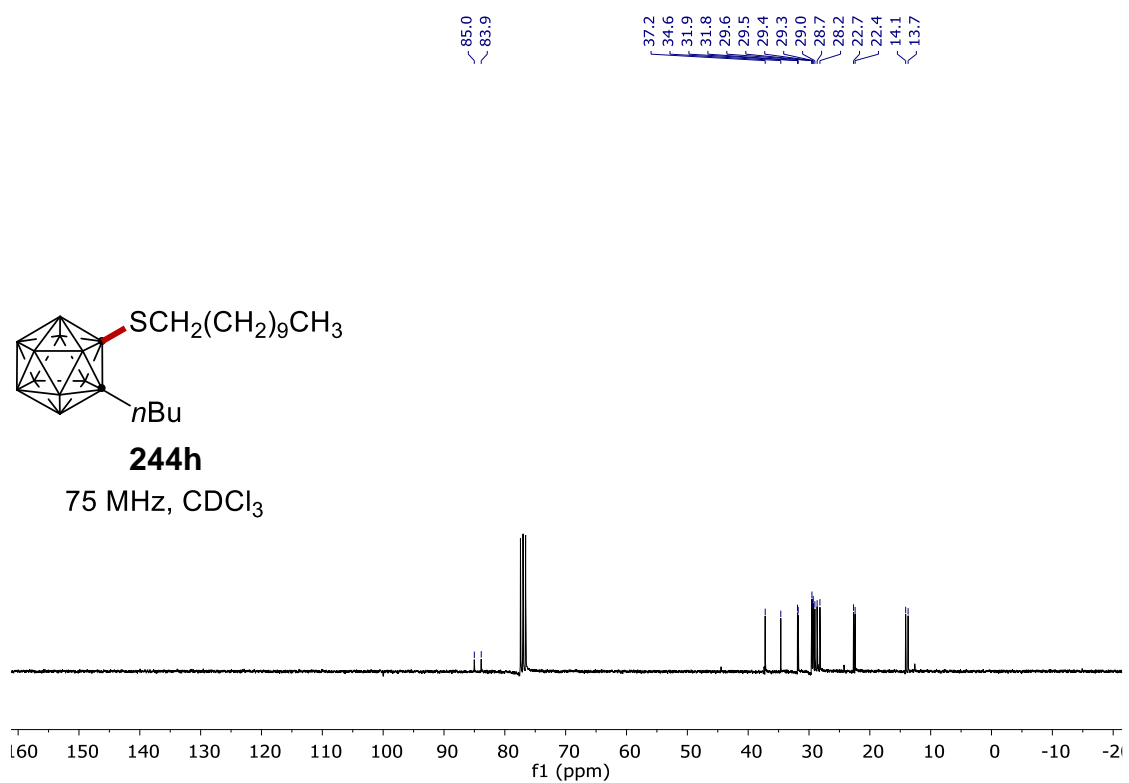


7. NMR Spectra

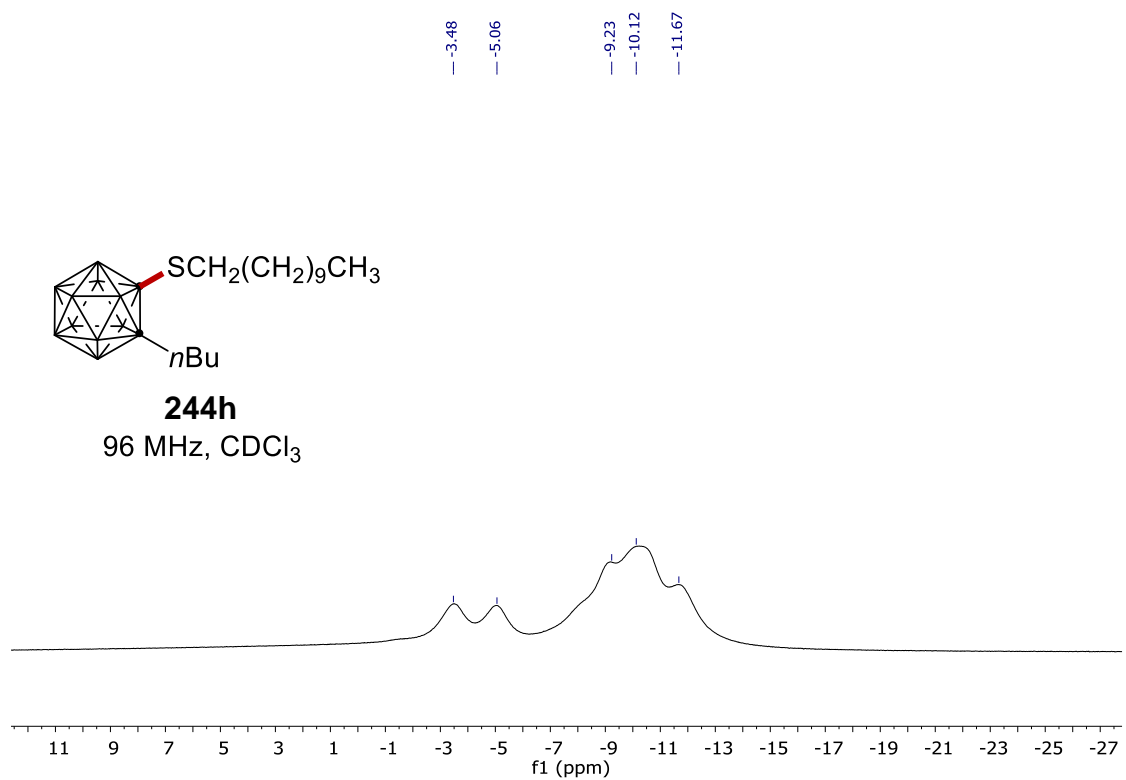
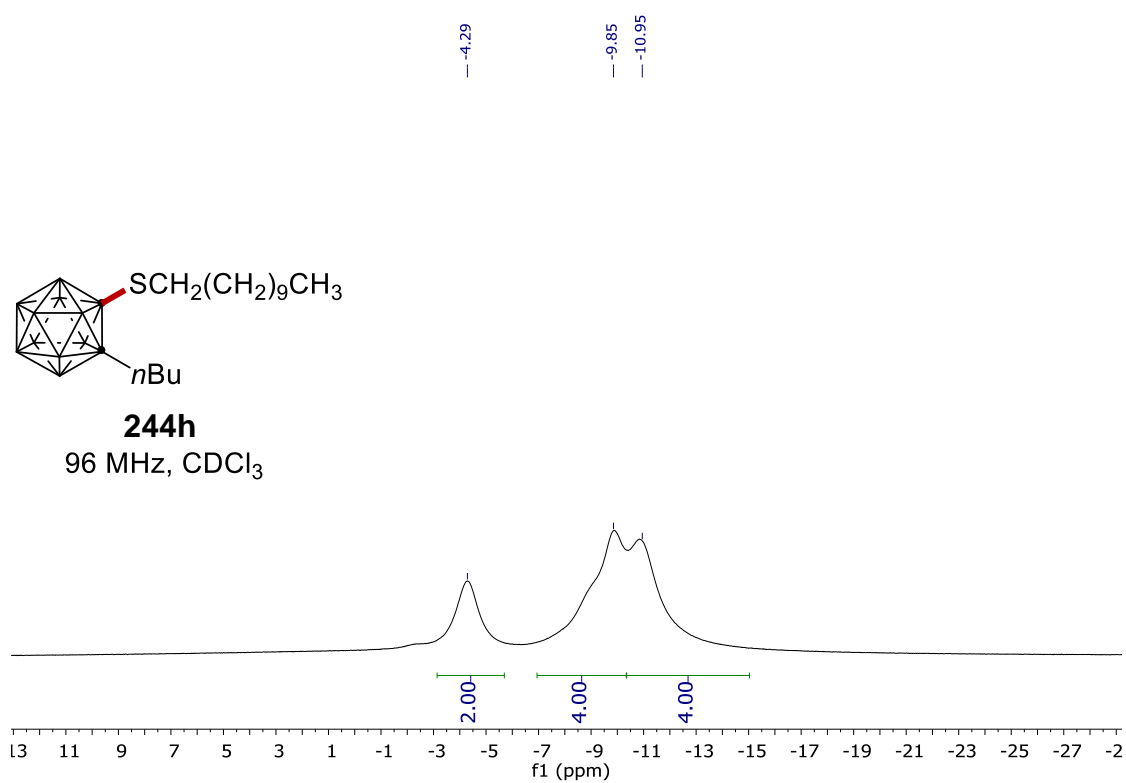


7. NMR Spectra

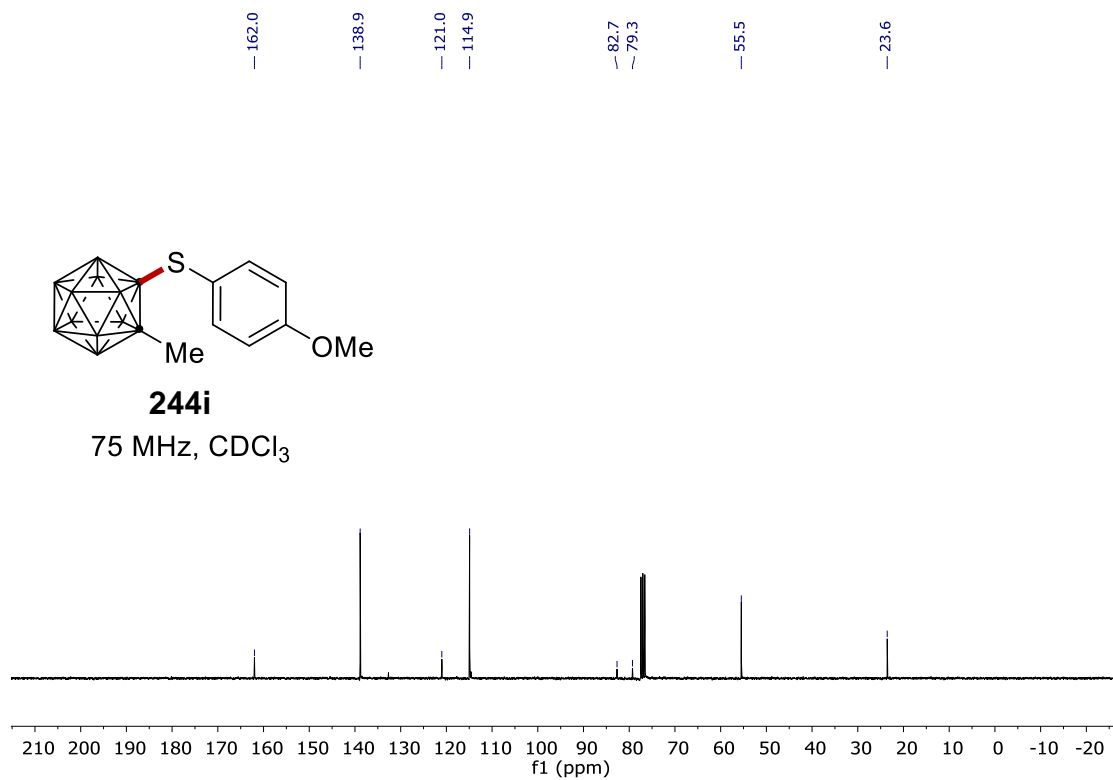
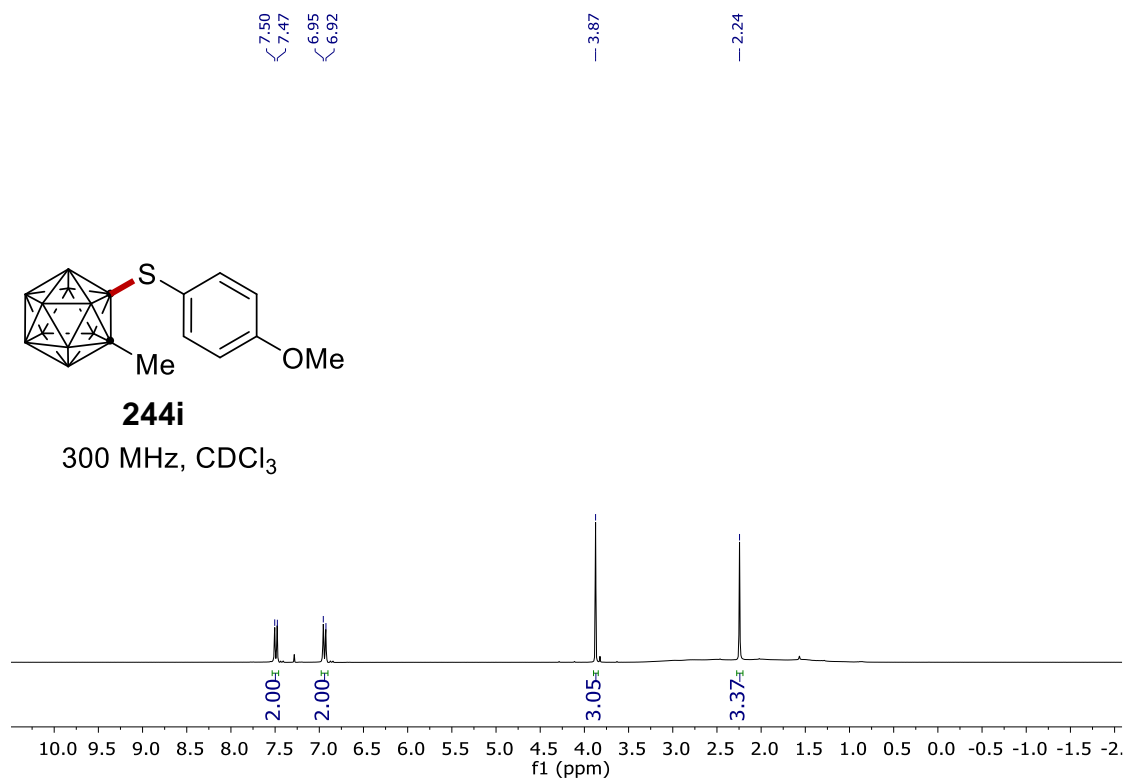




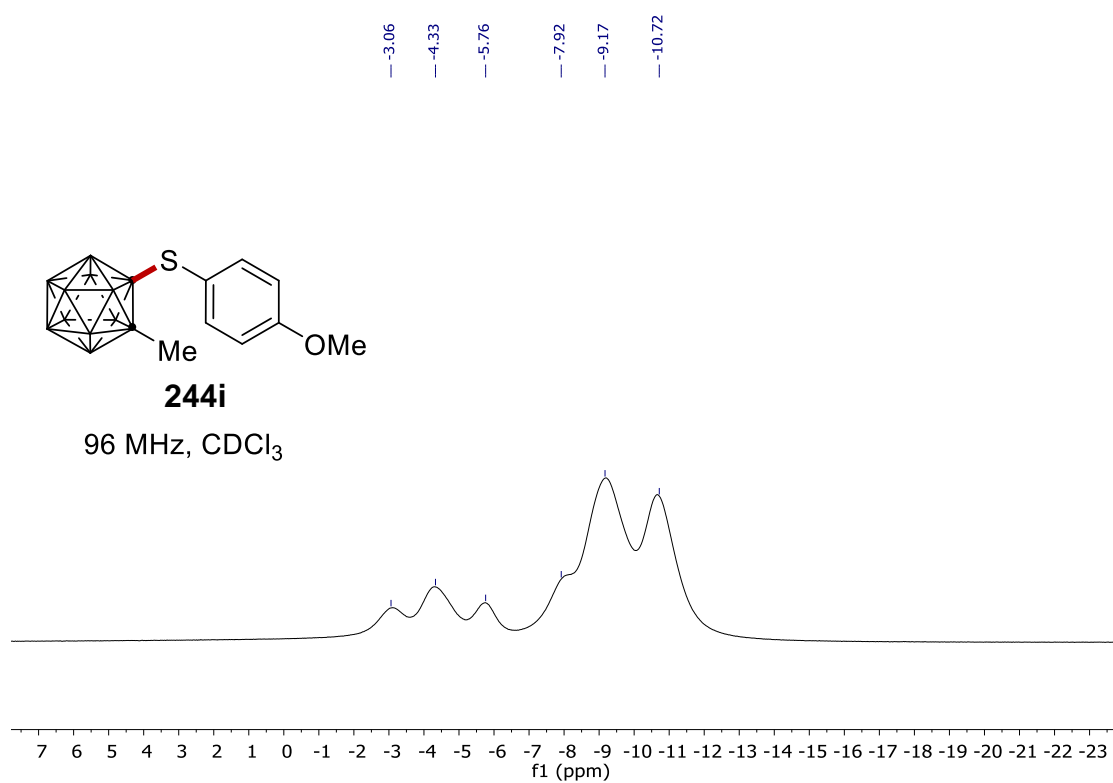
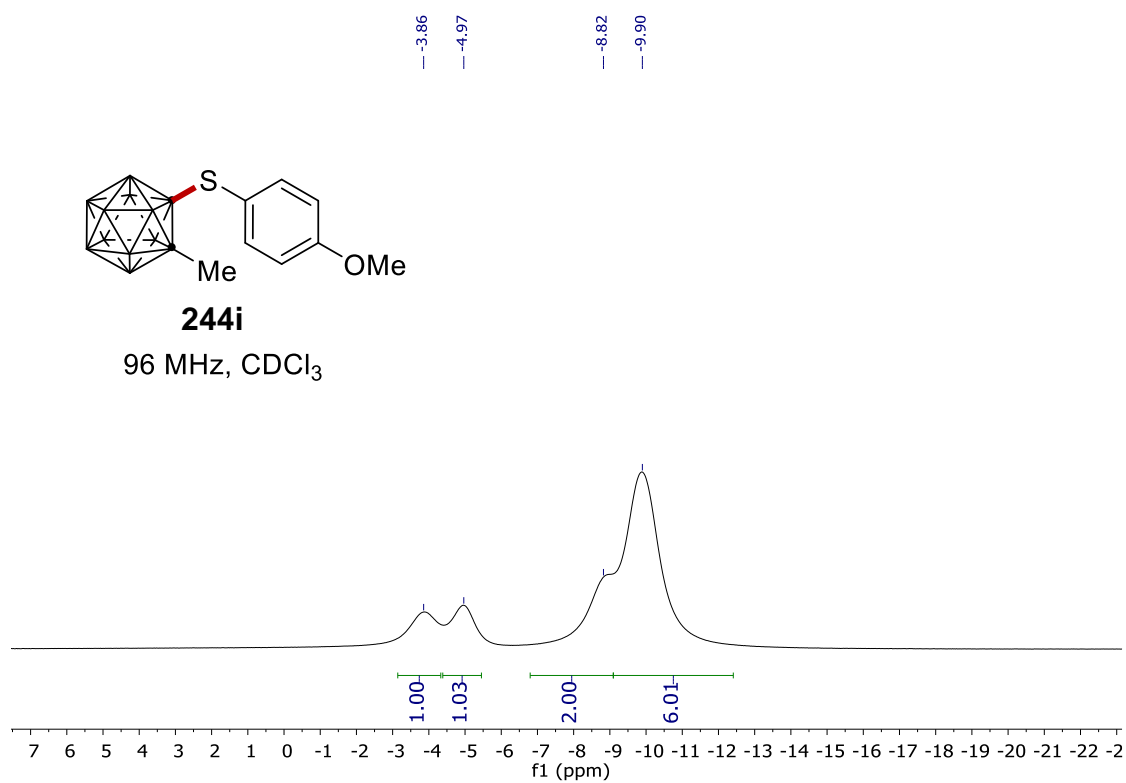
7. NMR Spectra



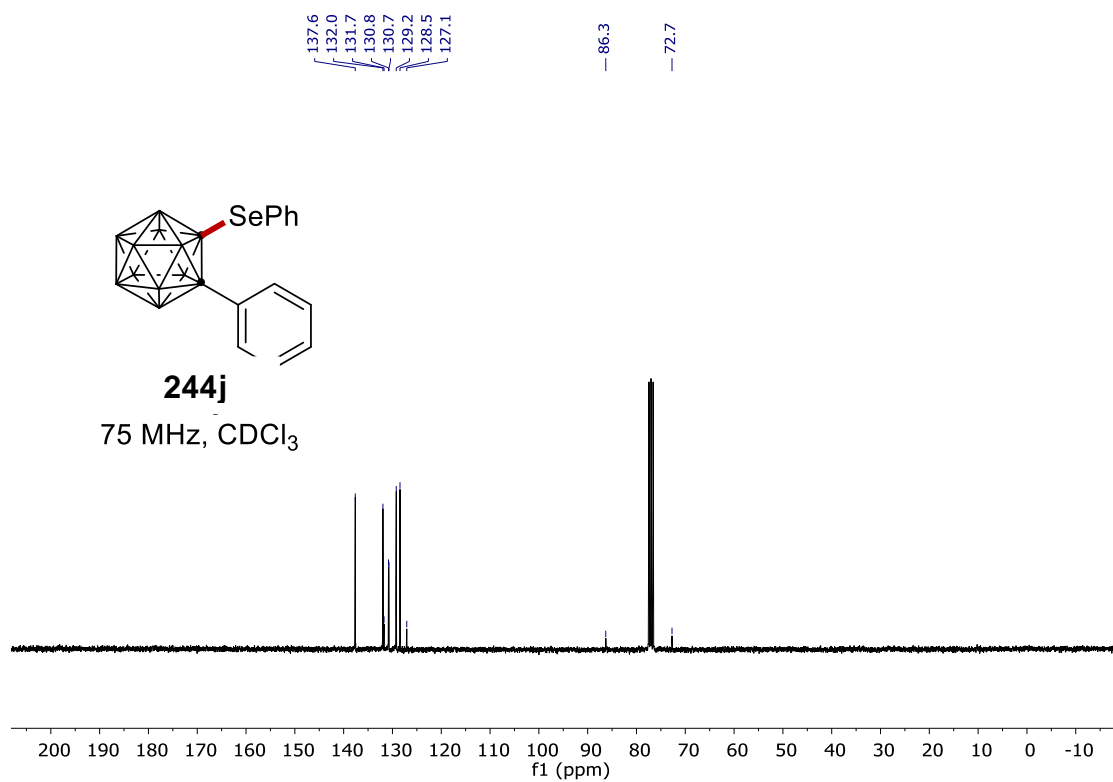
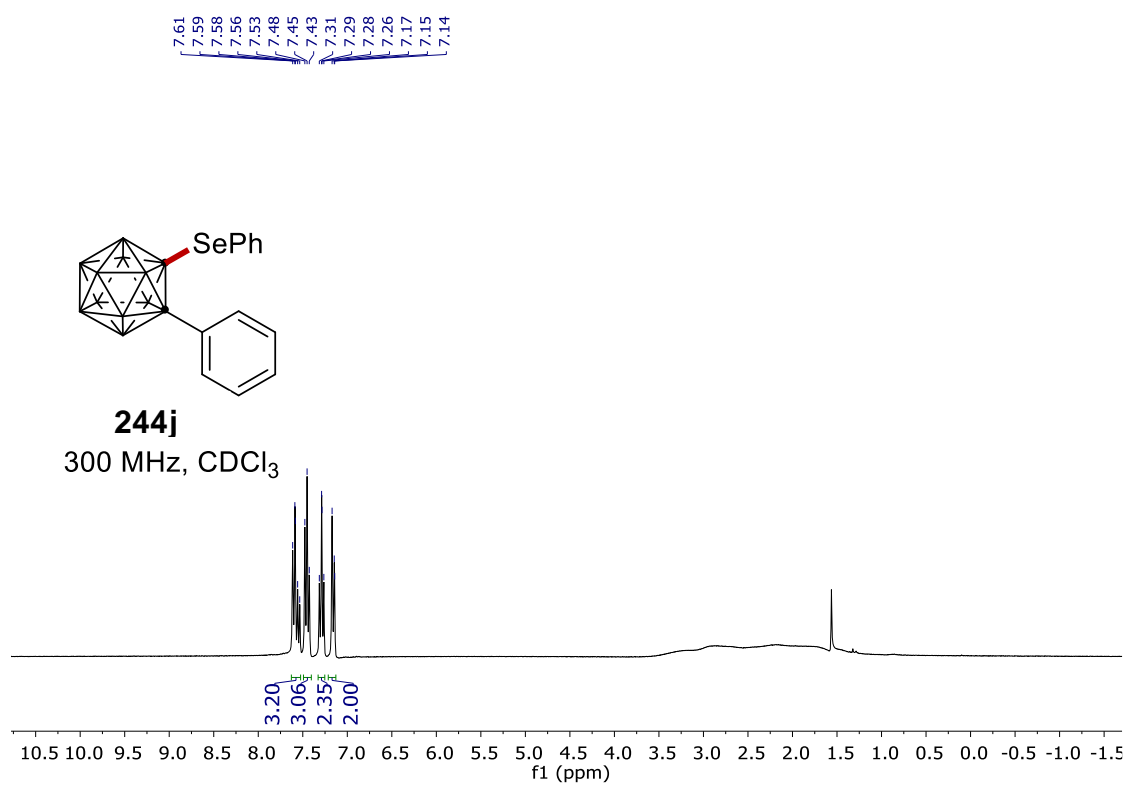
7. NMR Spectra



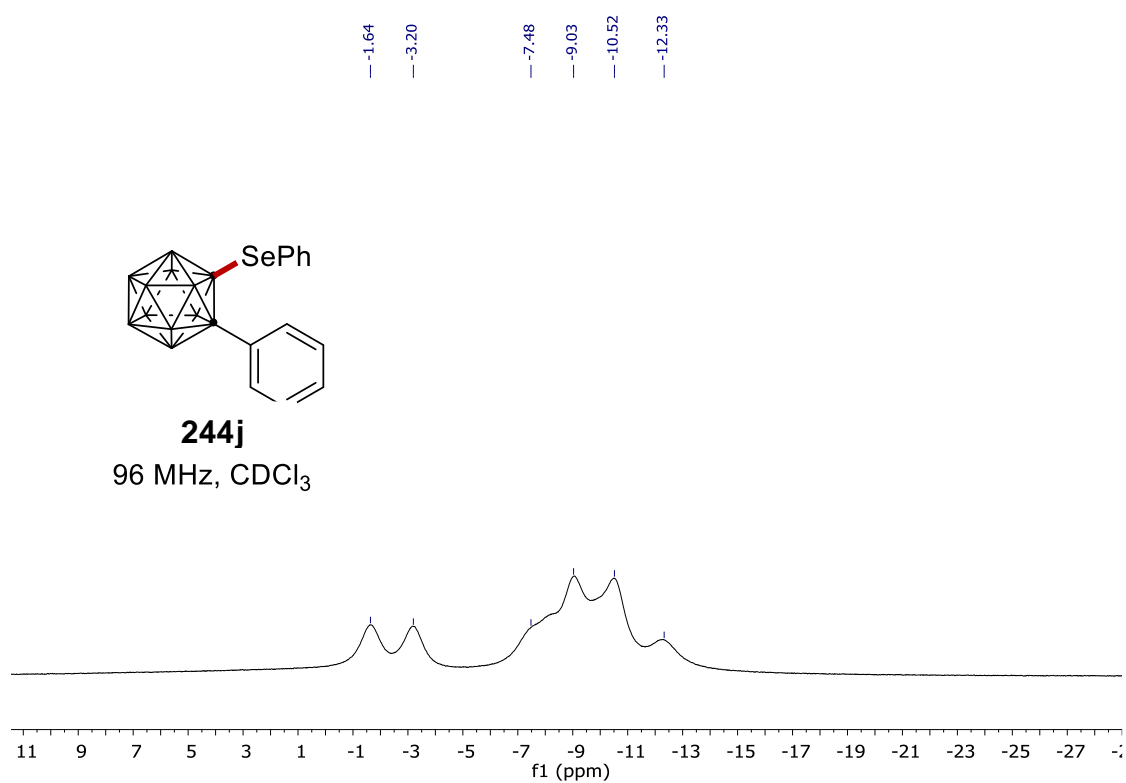
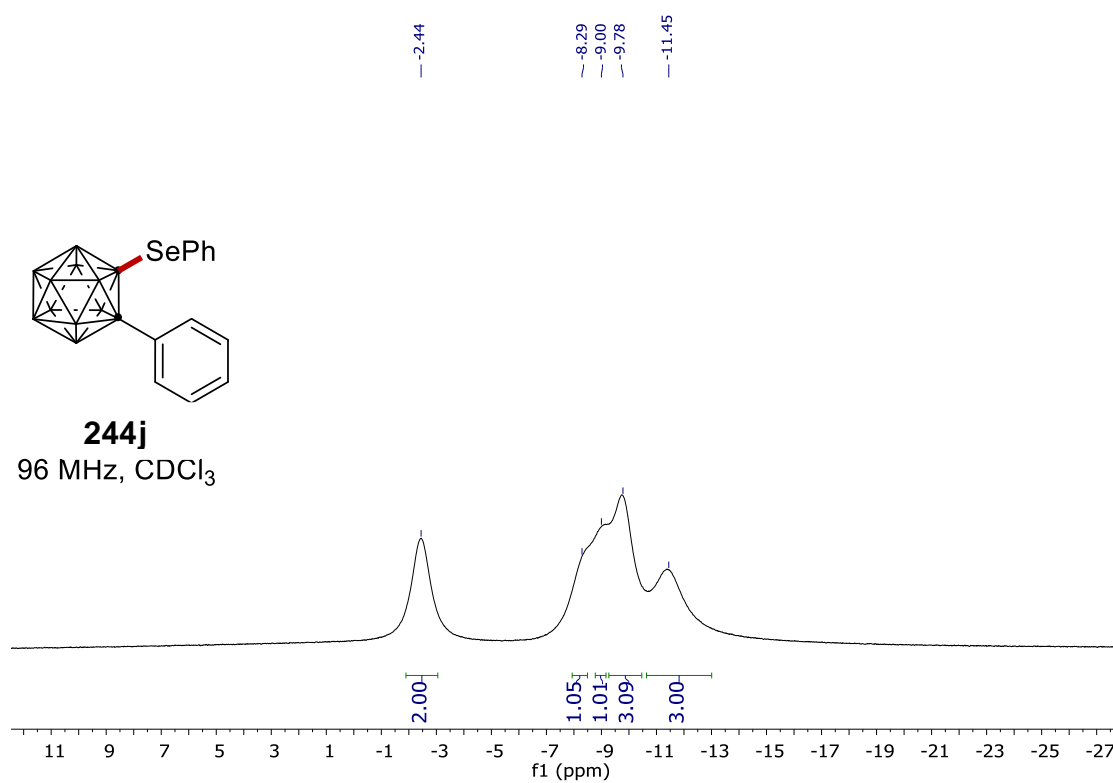
7. NMR Spectra



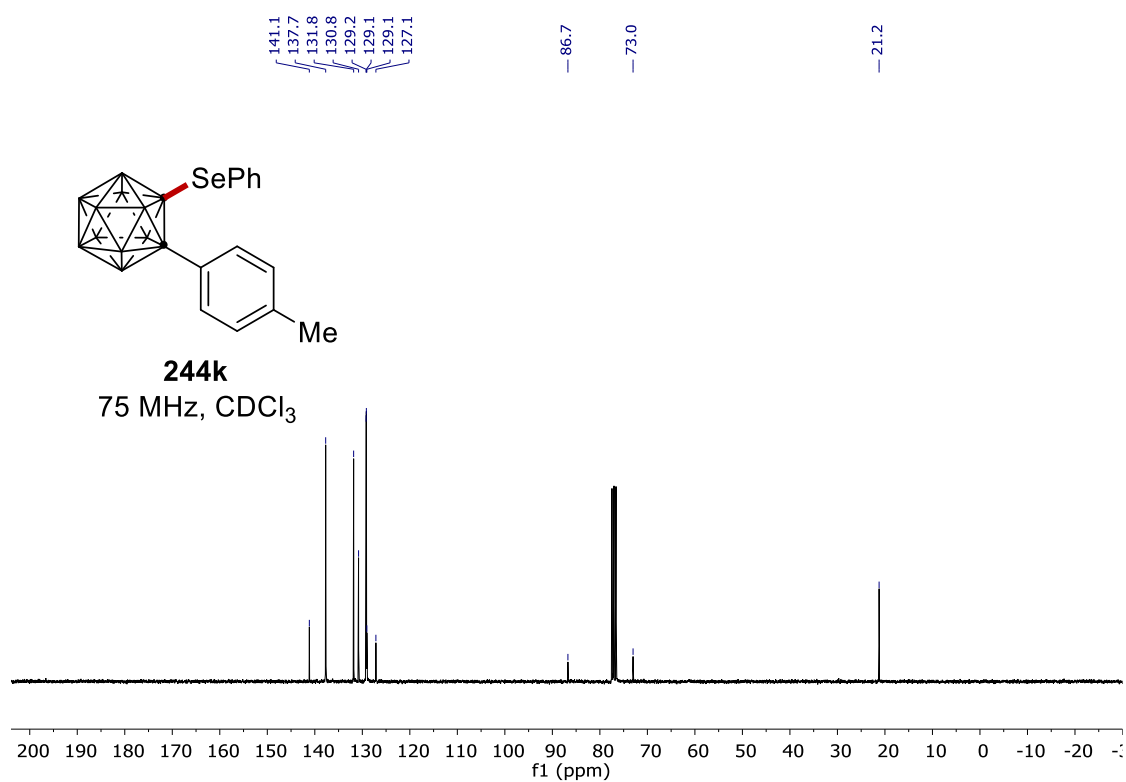
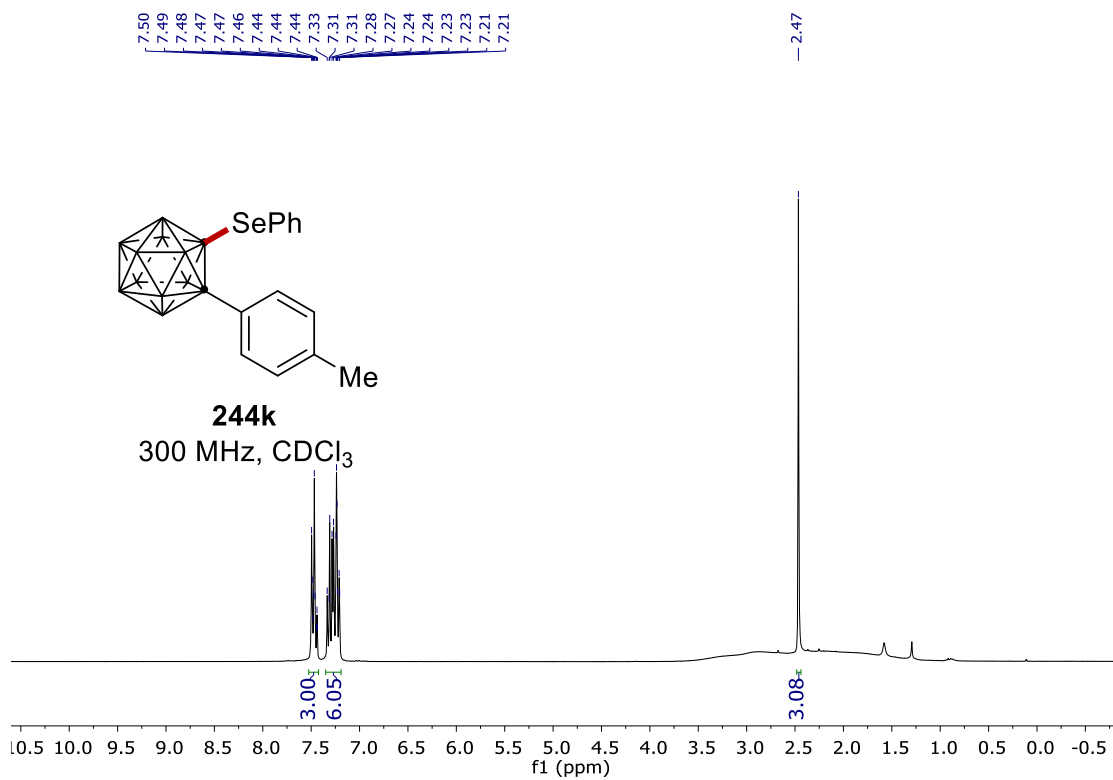
7. NMR Spectra



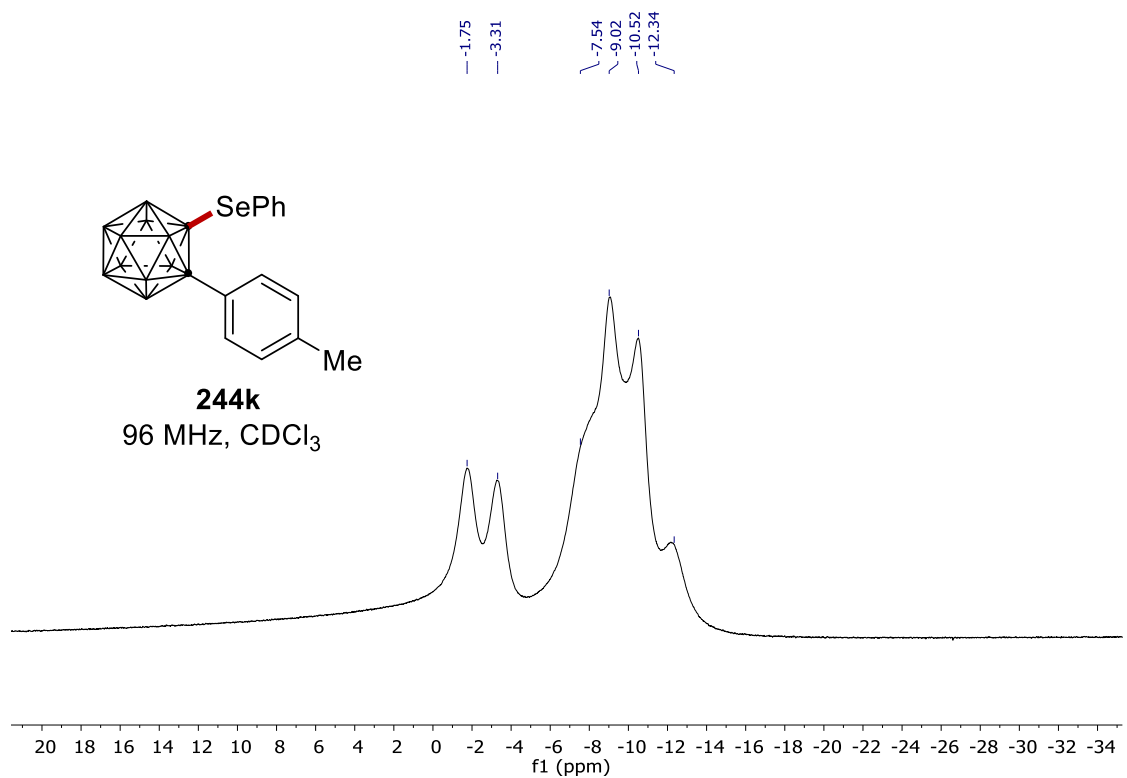
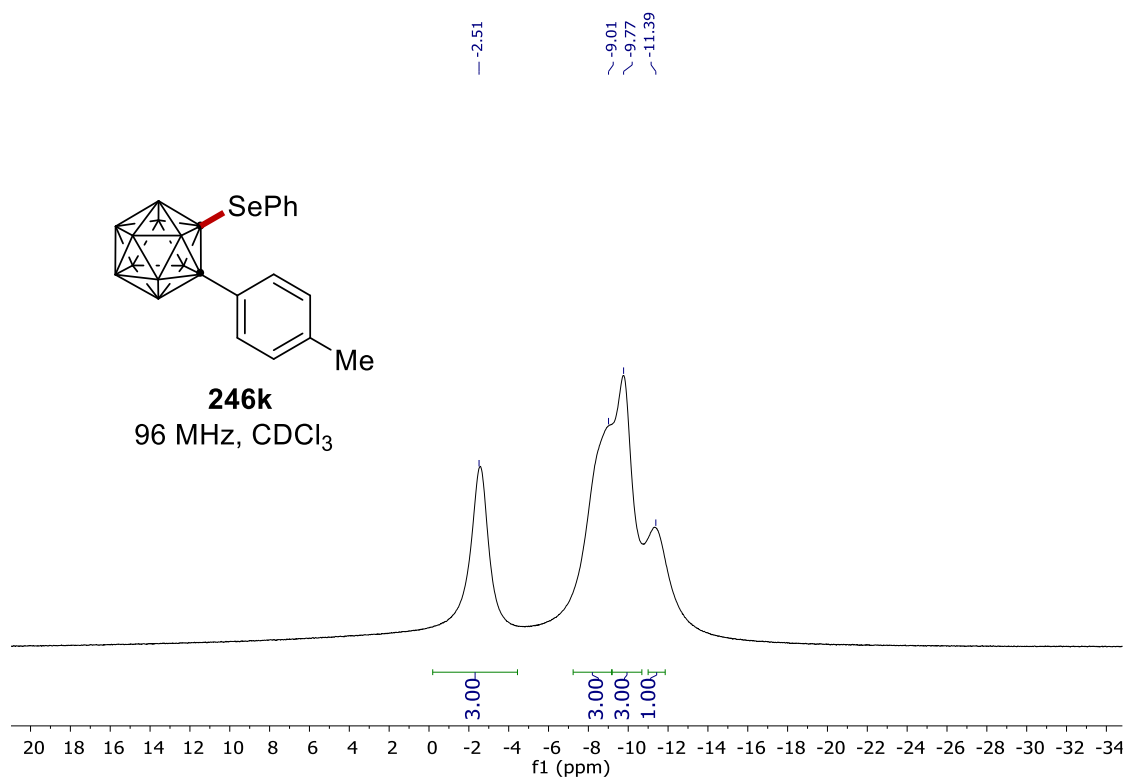
7. NMR Spectra



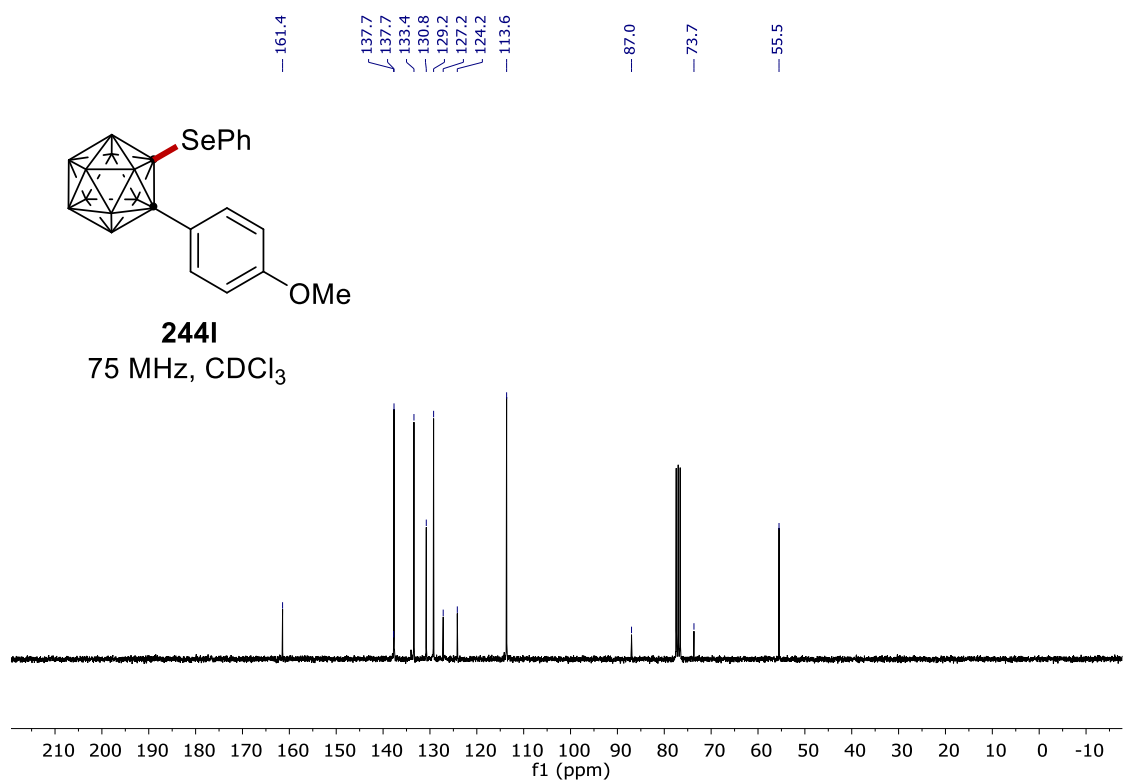
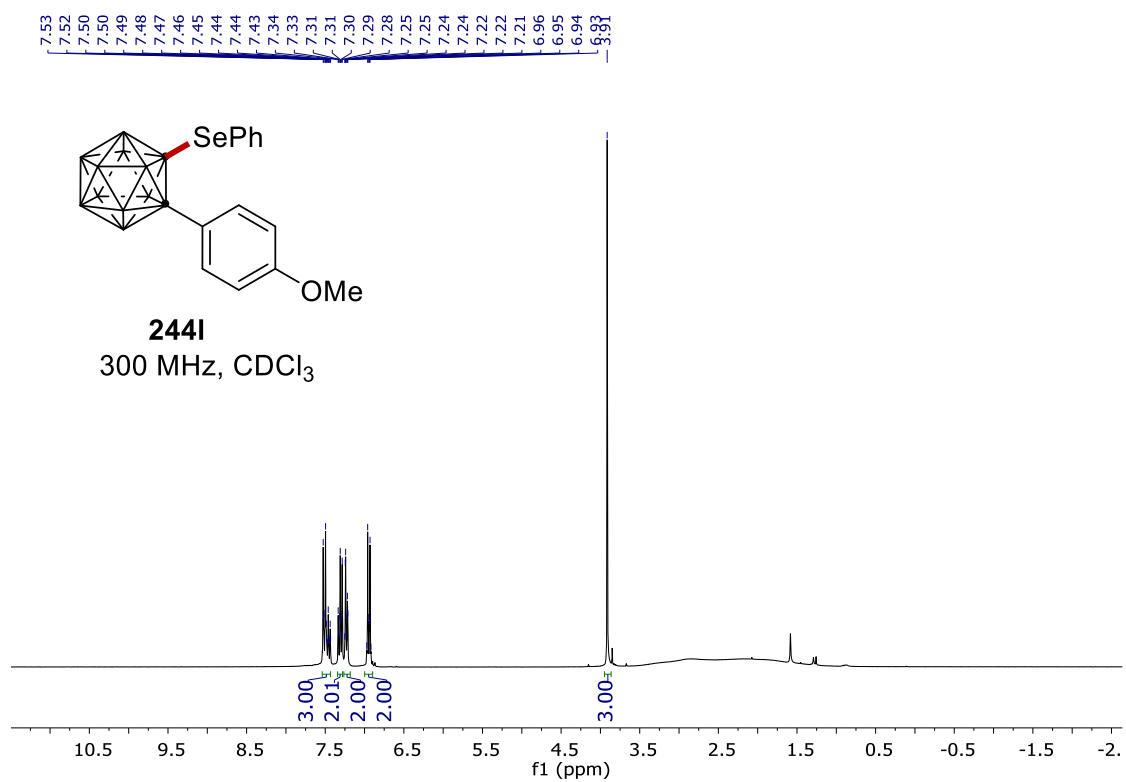
7. NMR Spectra



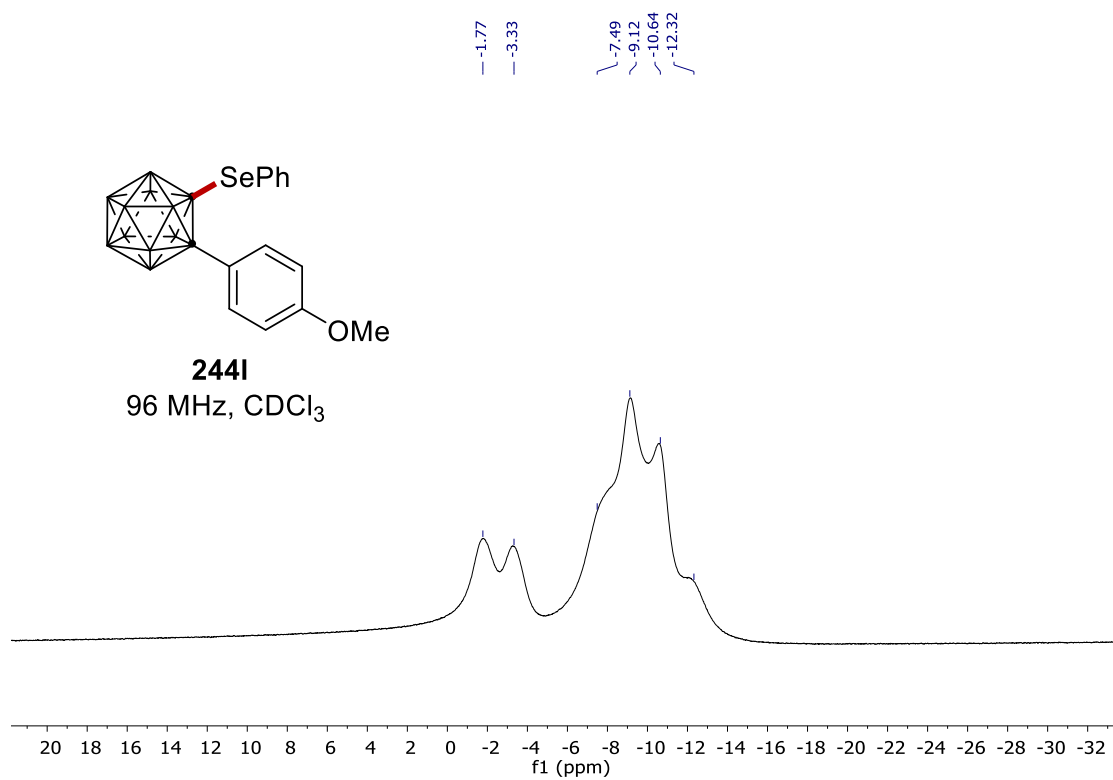
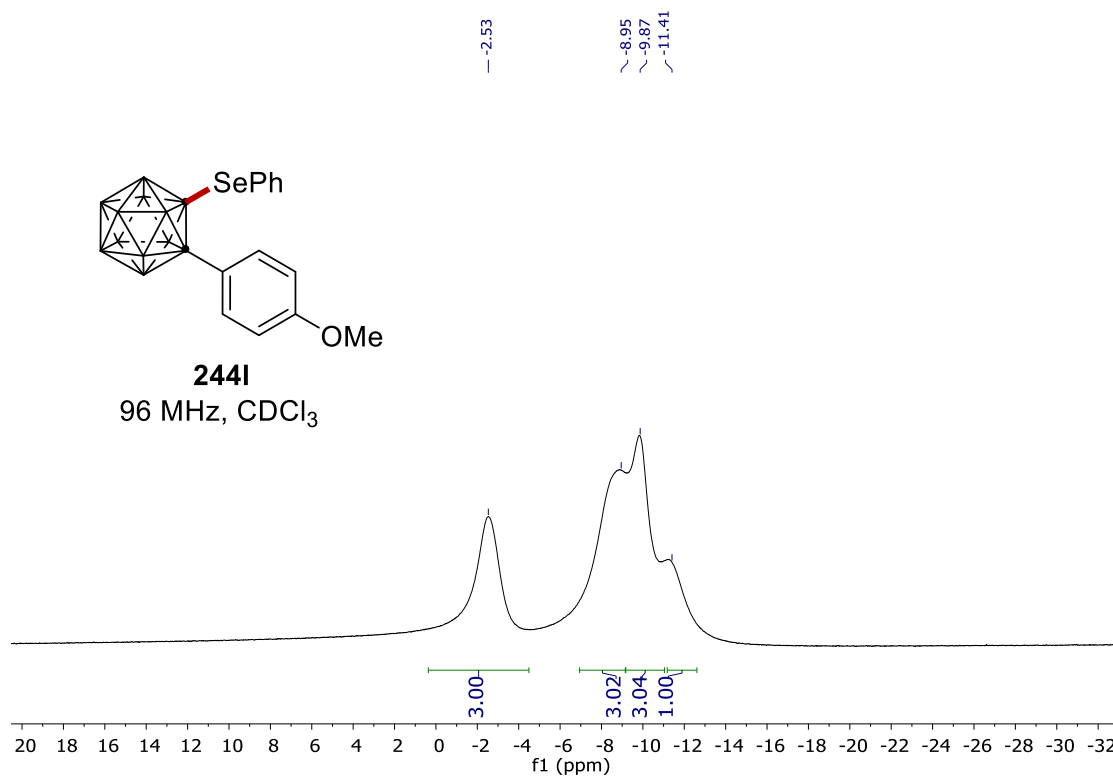
7. NMR Spectra



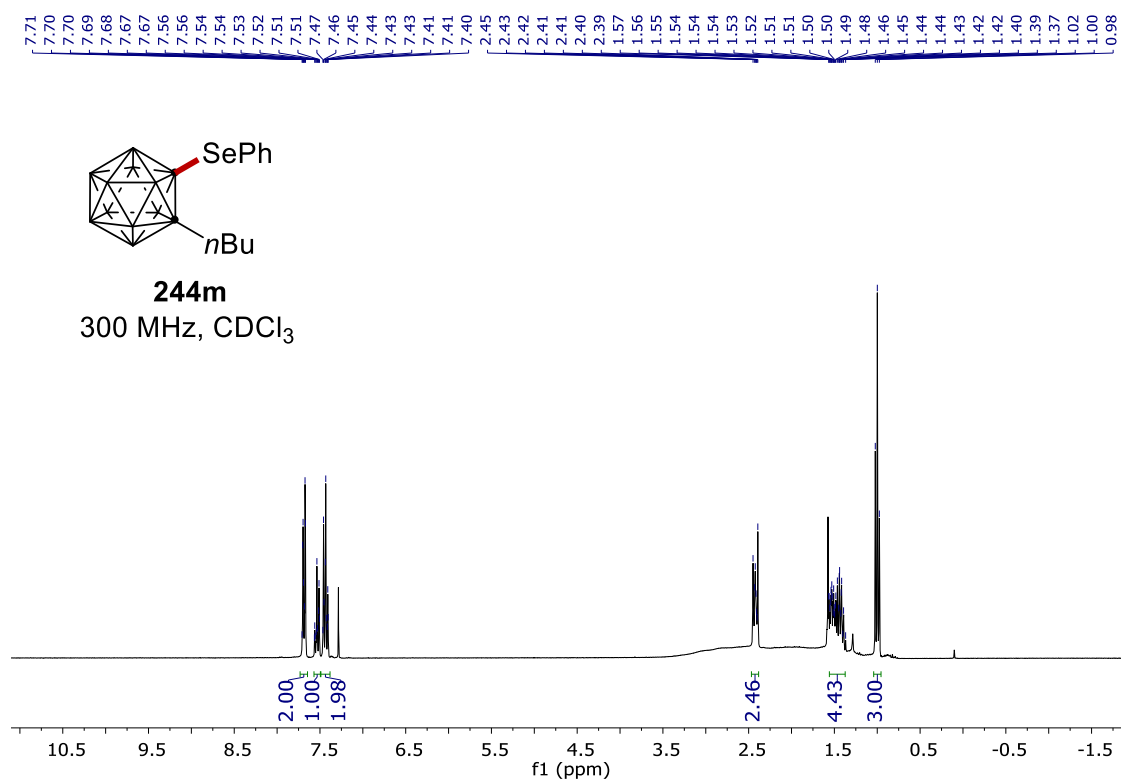
7. NMR Spectra



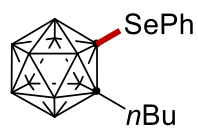
7. NMR Spectra



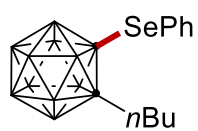
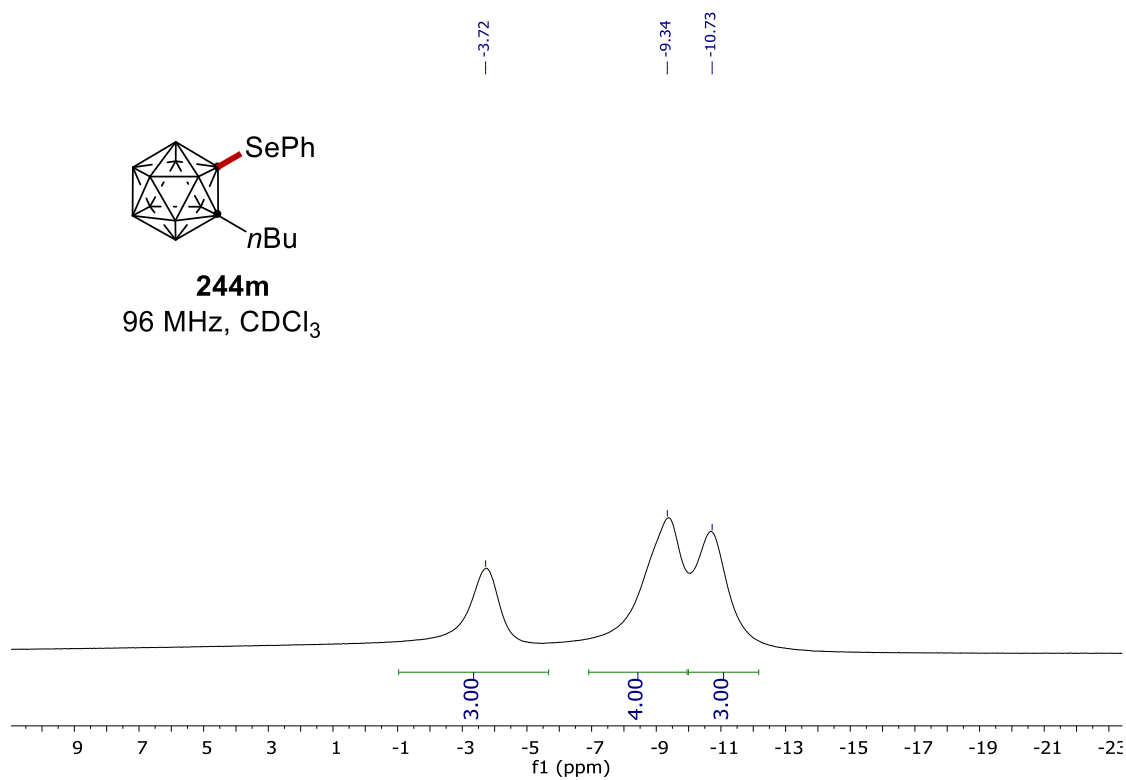
7. NMR Spectra



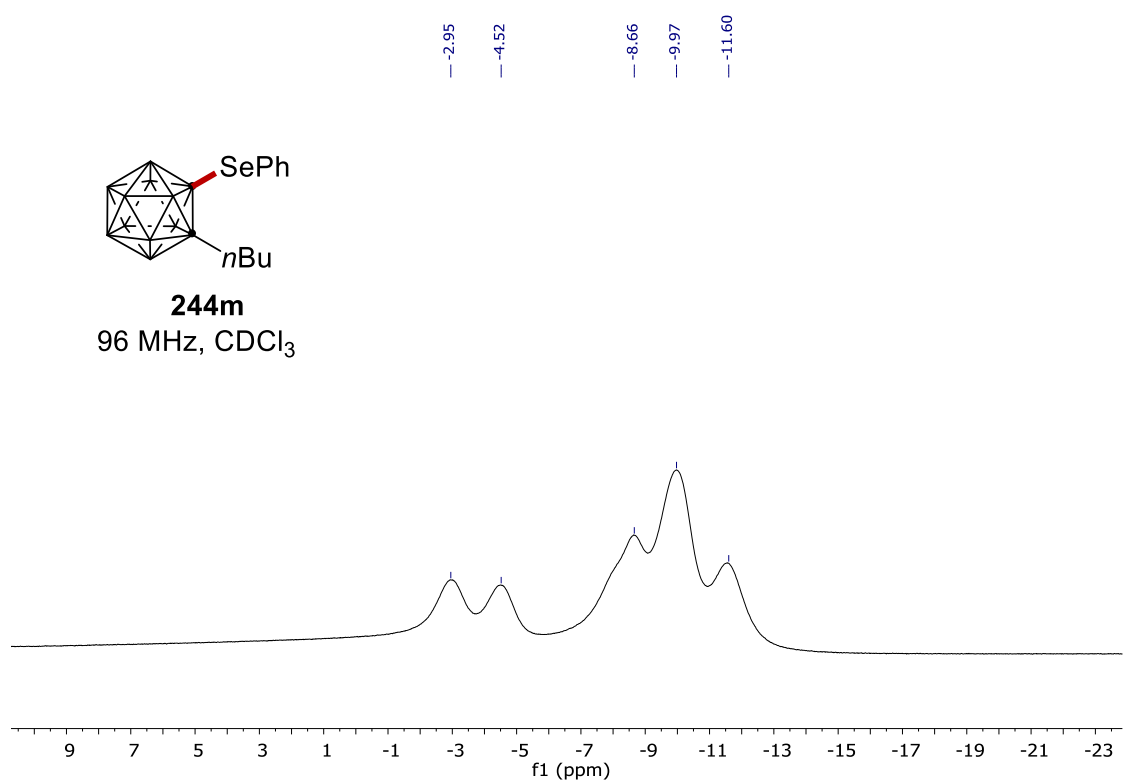
7. NMR Spectra



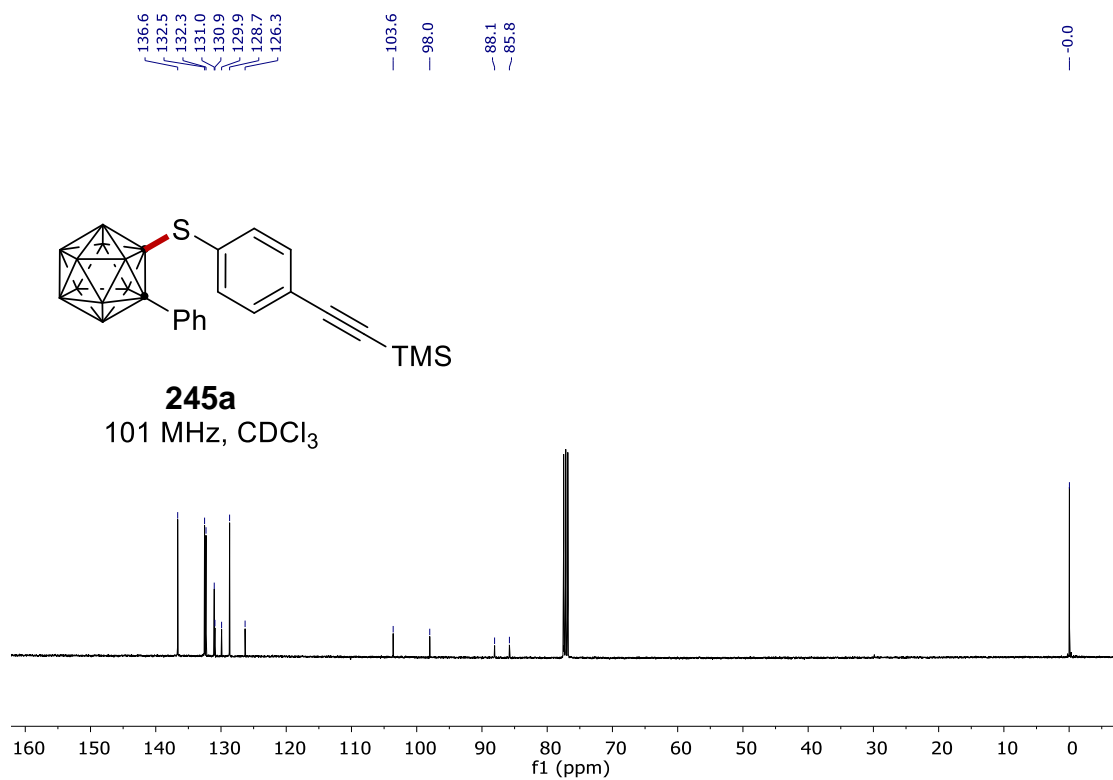
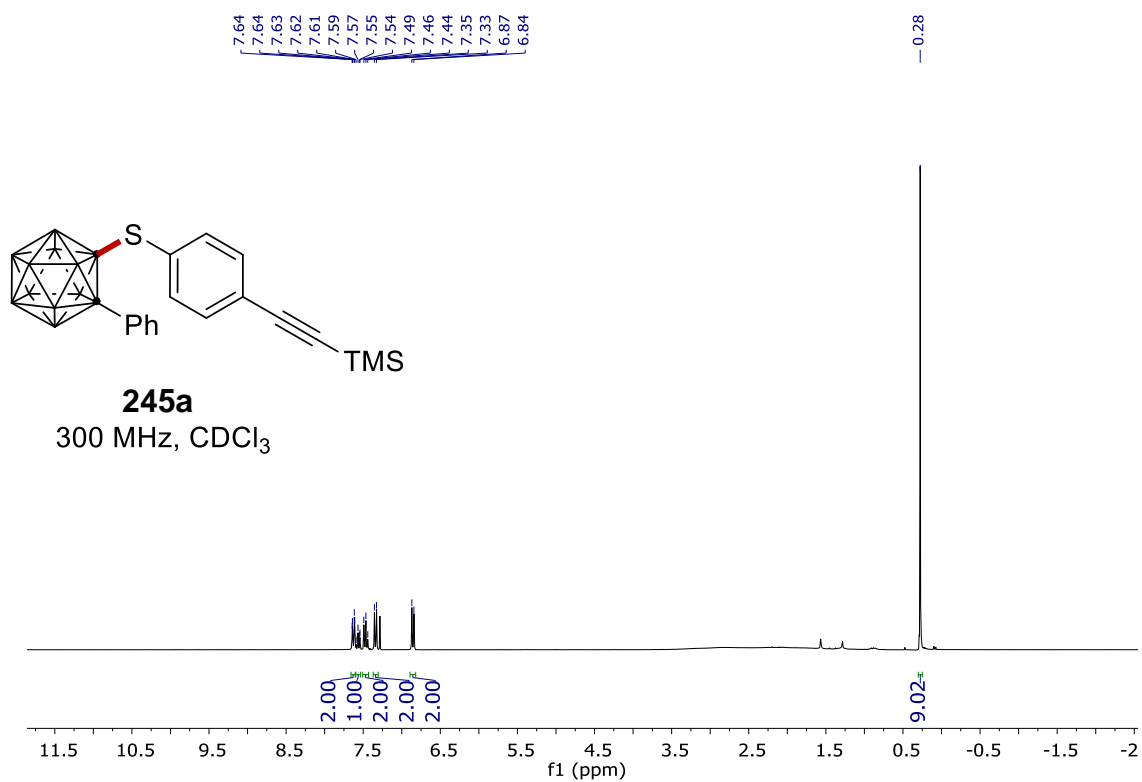
244m
96 MHz, CDCl₃



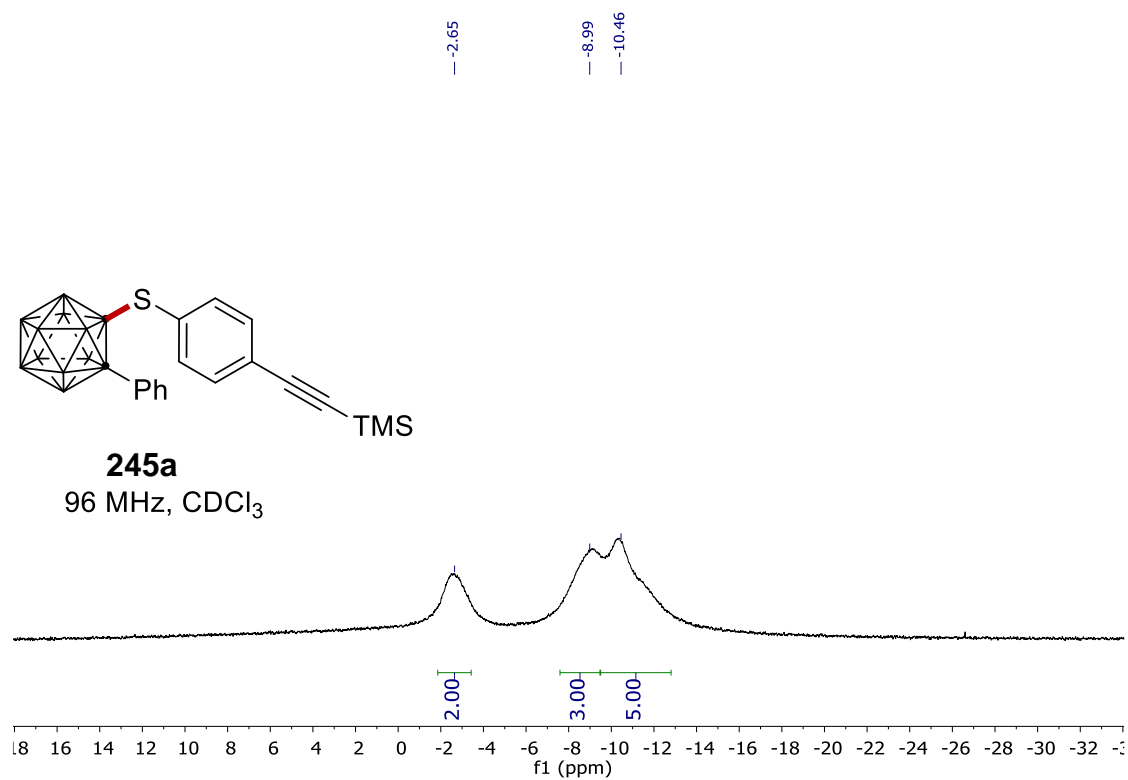
244m
96 MHz, CDCl₃



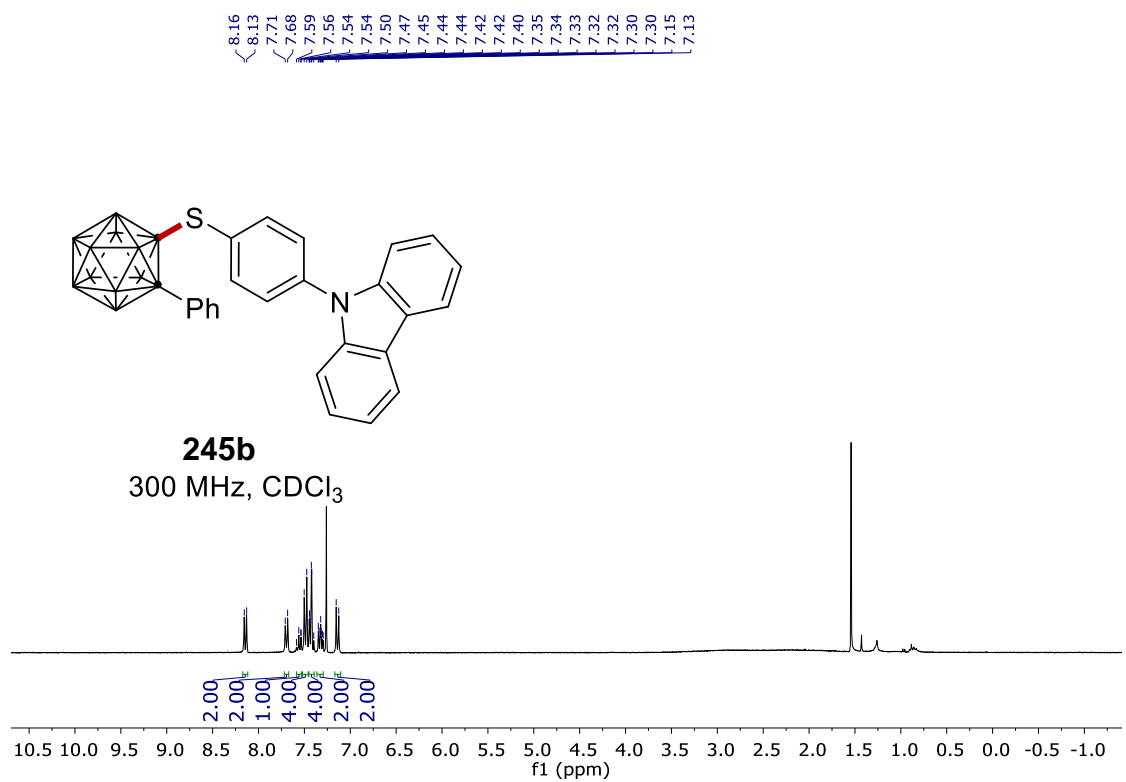
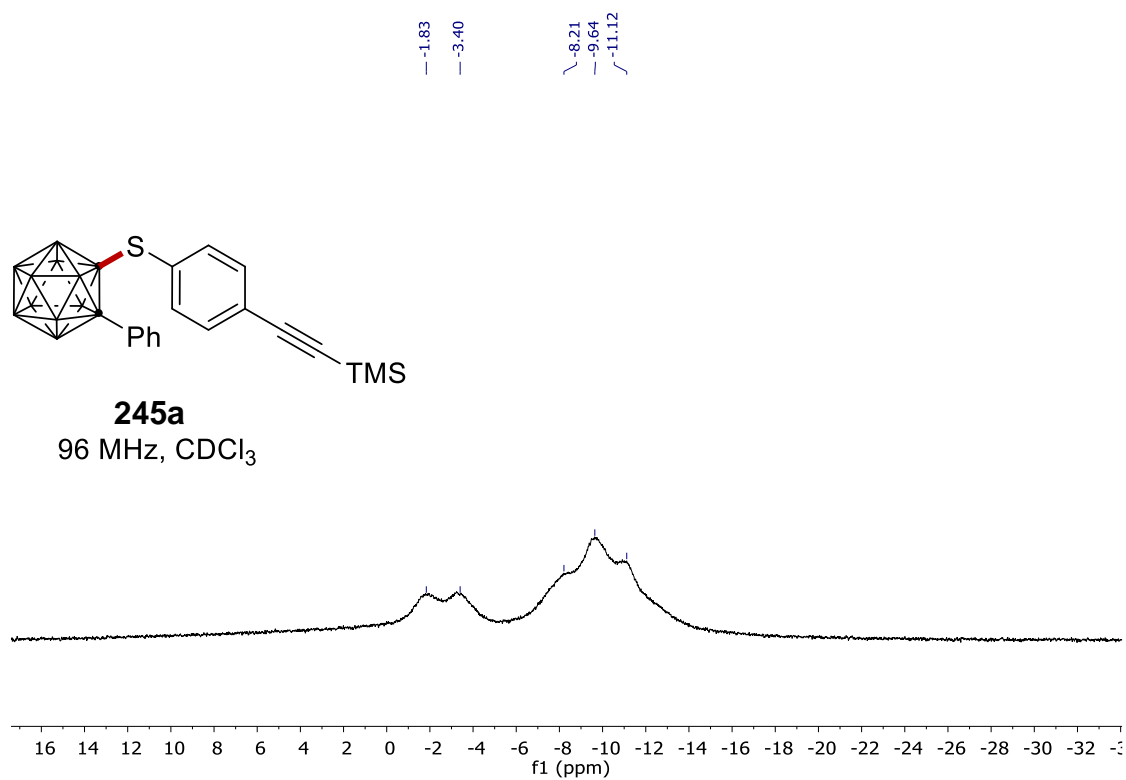
7. NMR Spectra



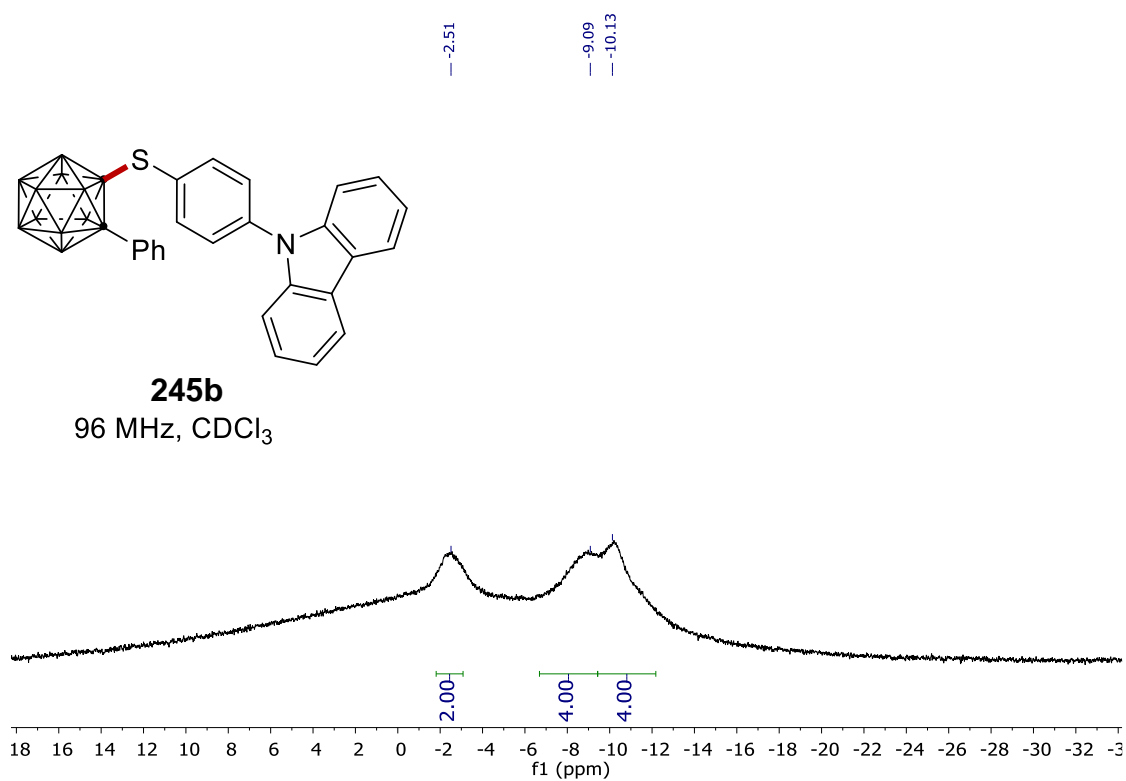
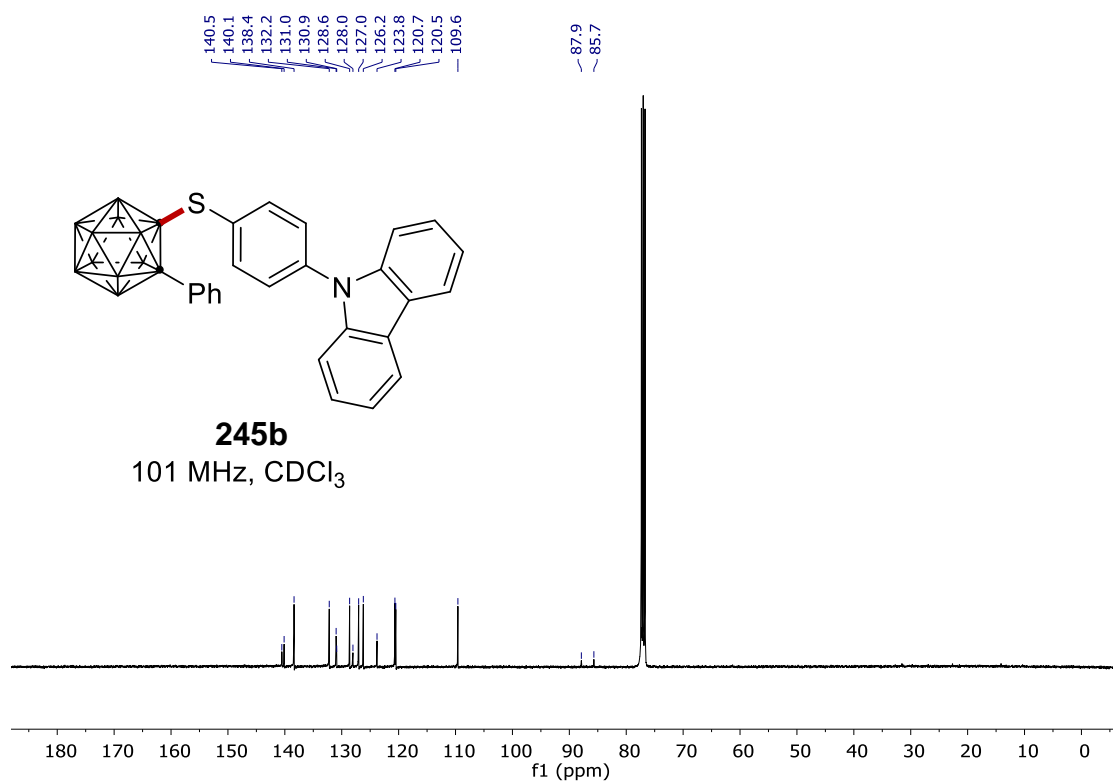
7. NMR Spectra



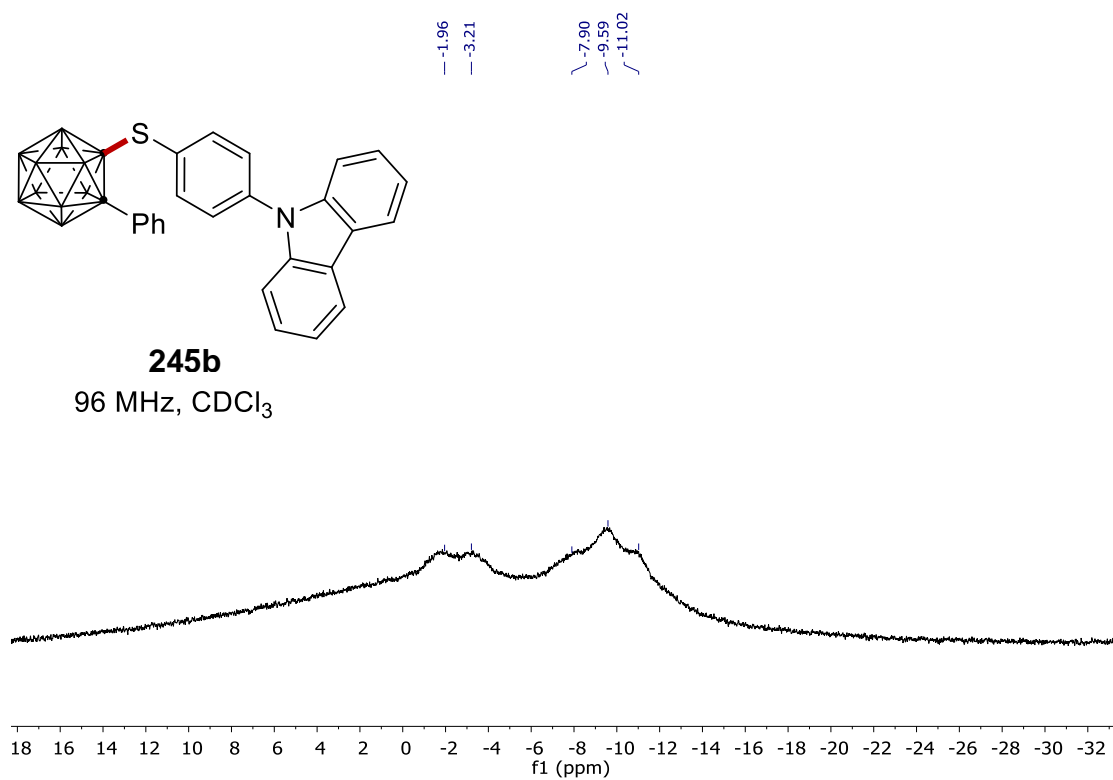
7. NMR Spectra



7. NMR Spectra

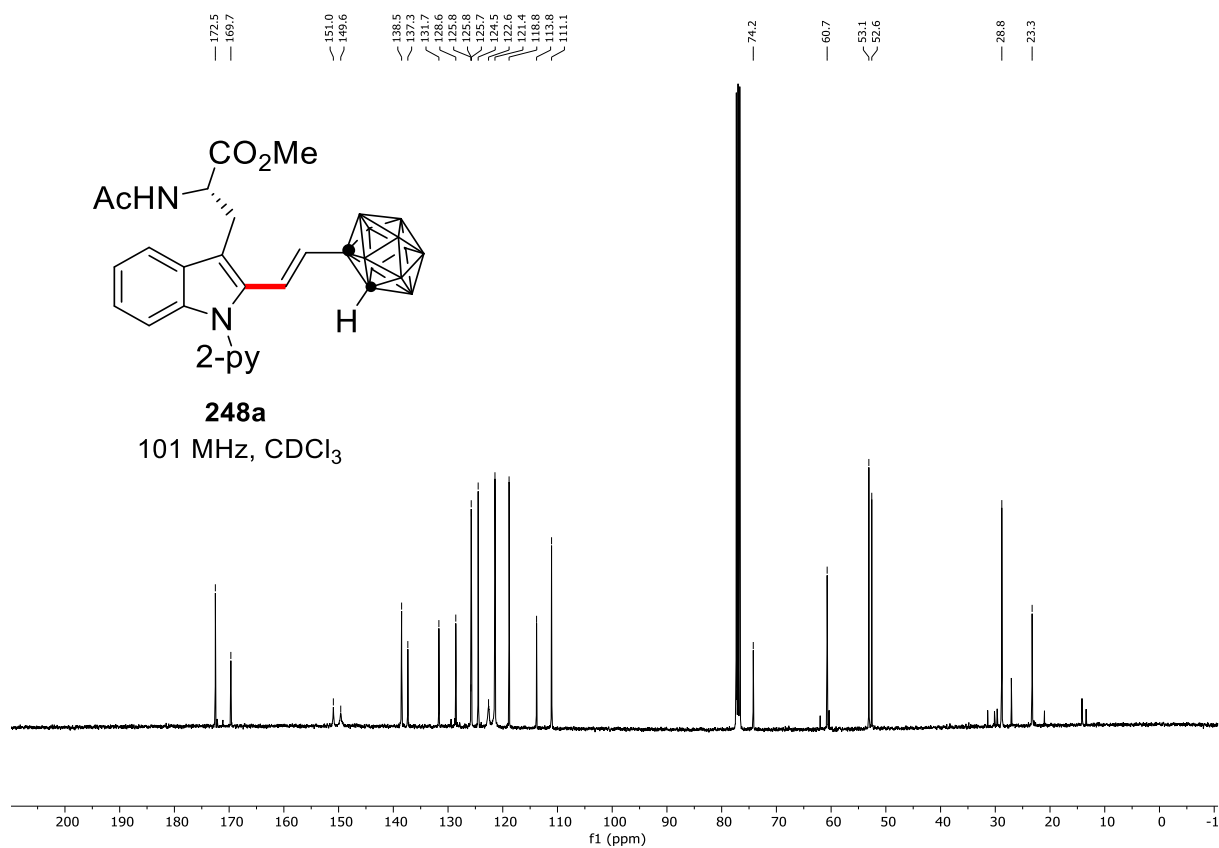
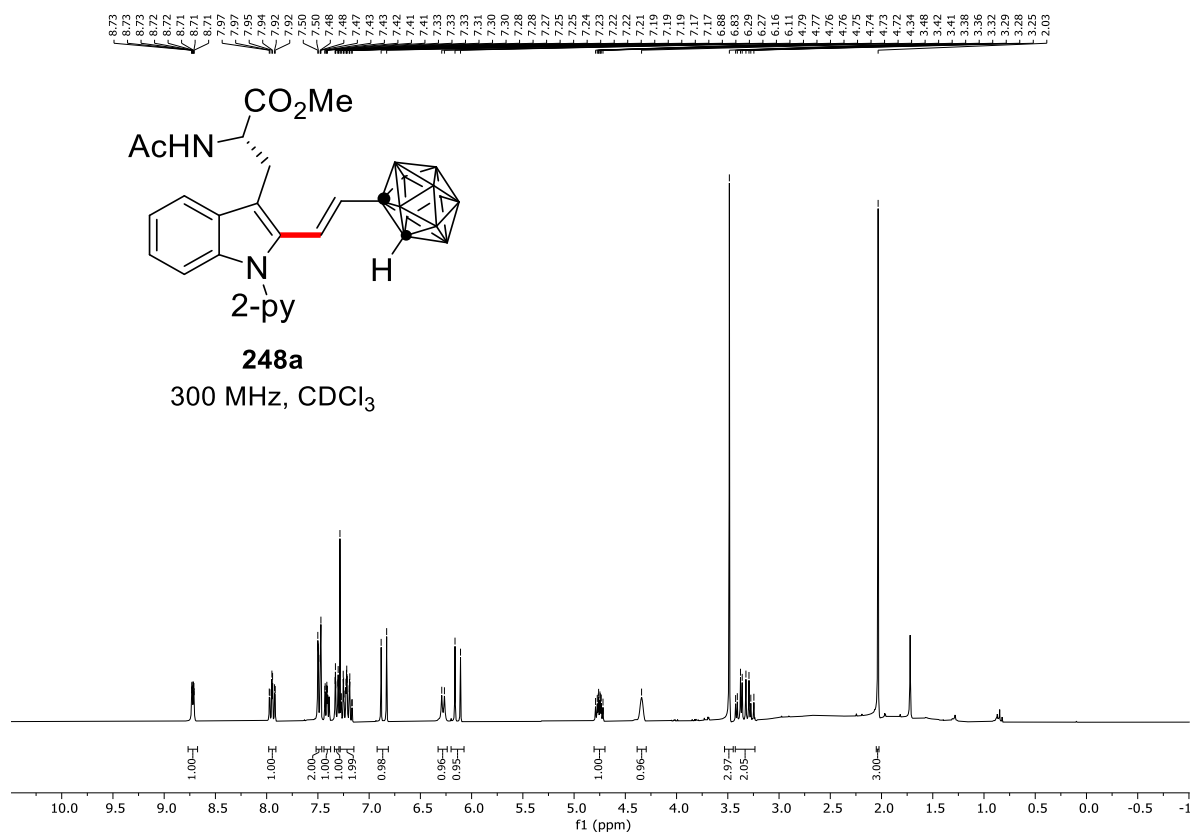


7. NMR Spectra

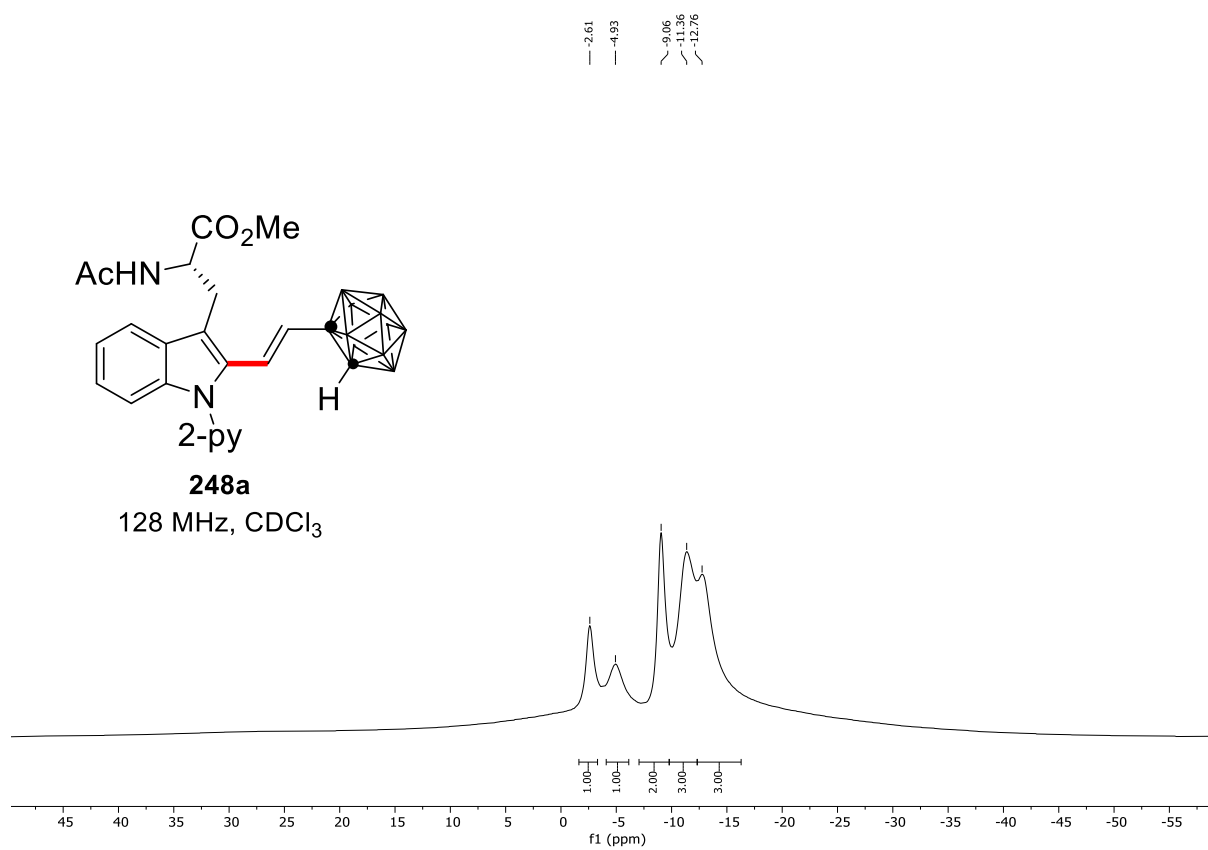


7. NMR Spectra

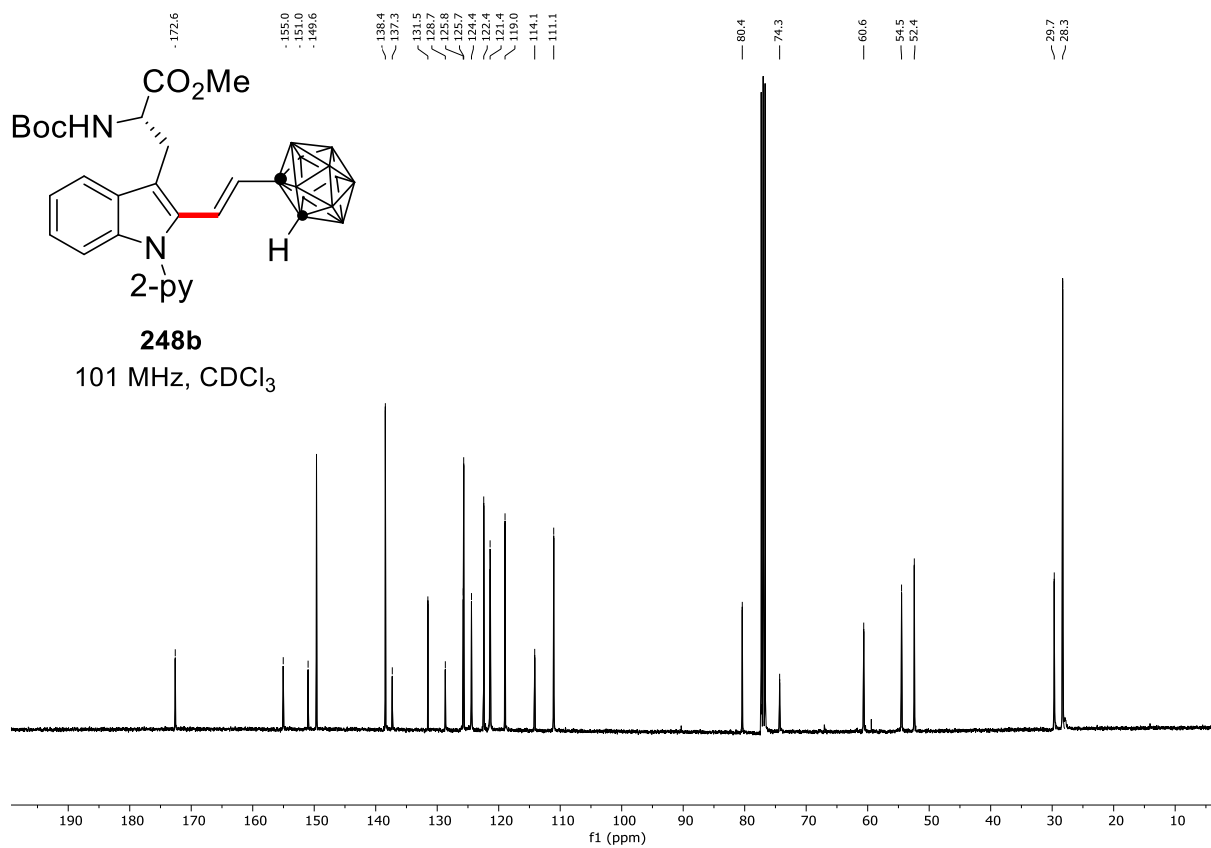
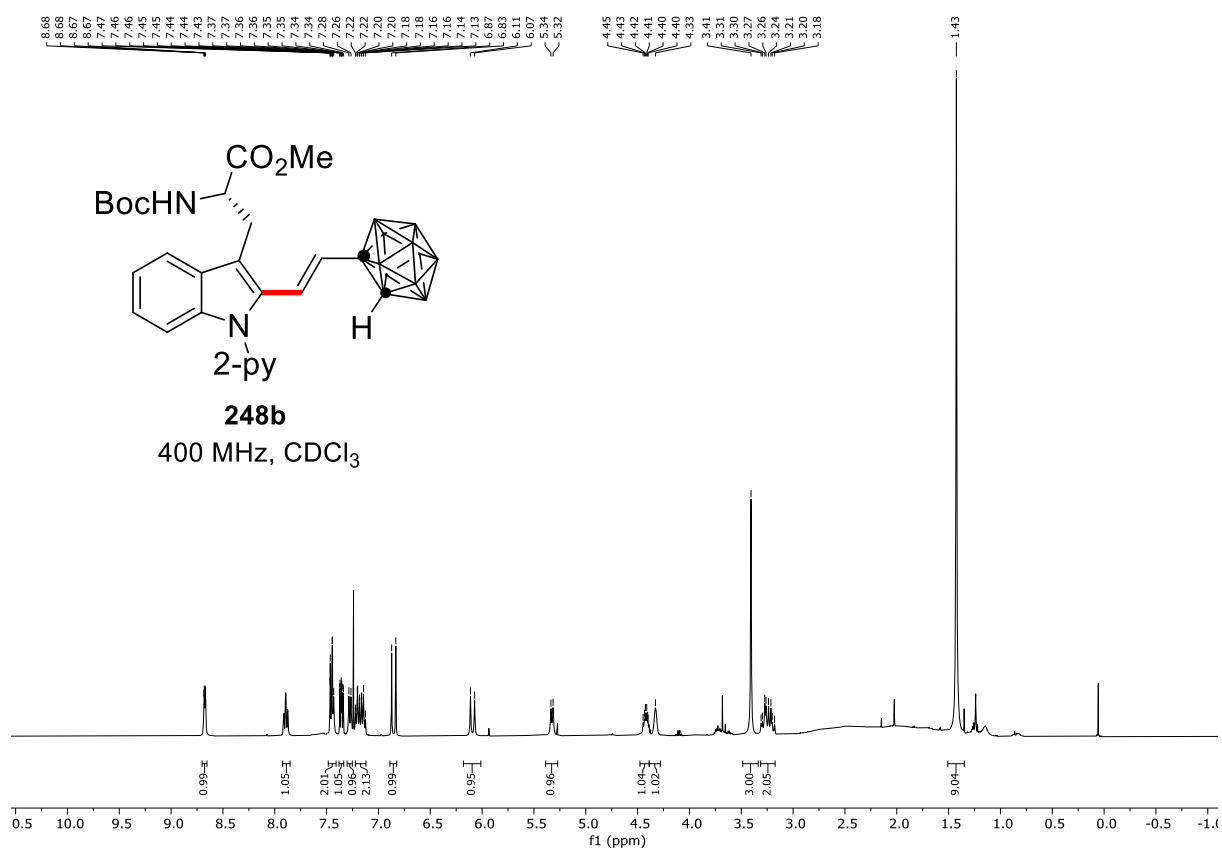
7.3 Manganese(I)-catalyzed selective labeling of peptides with α -carboranes via C–H activation.



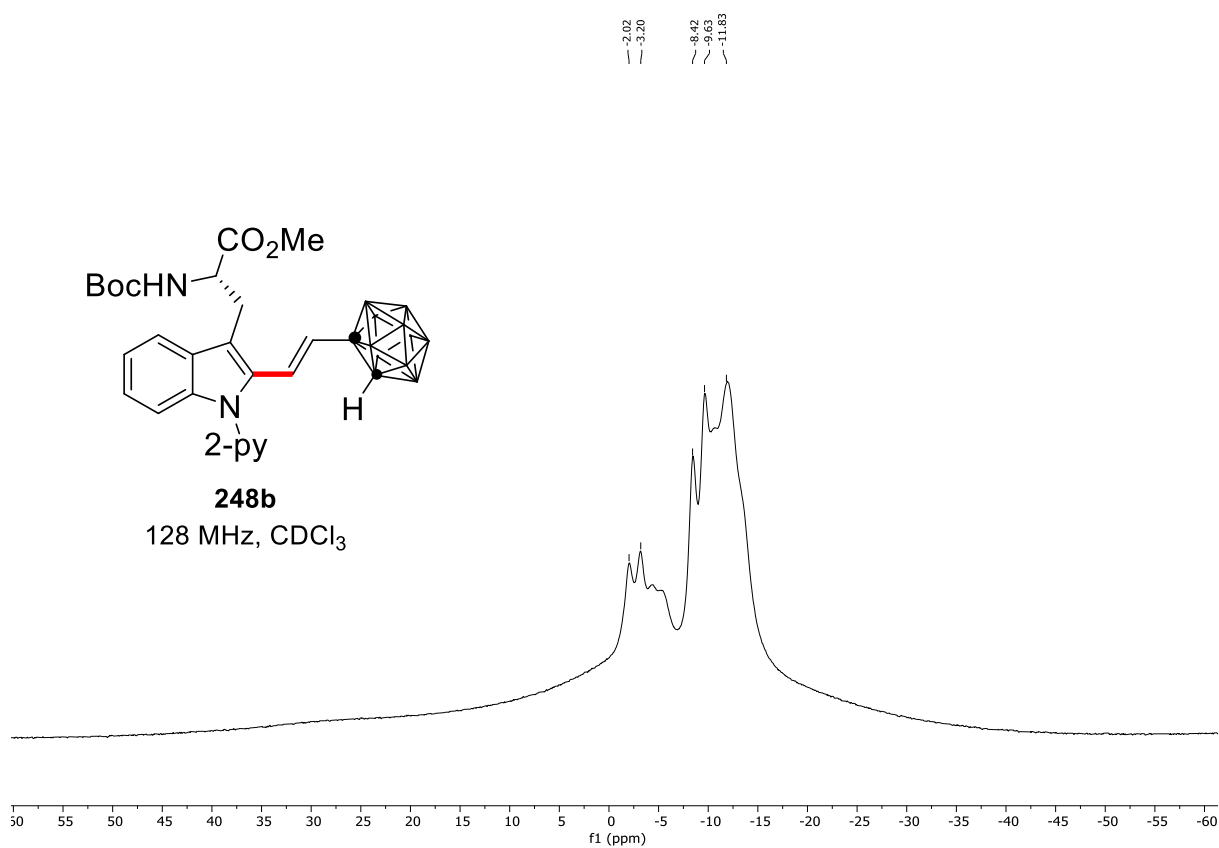
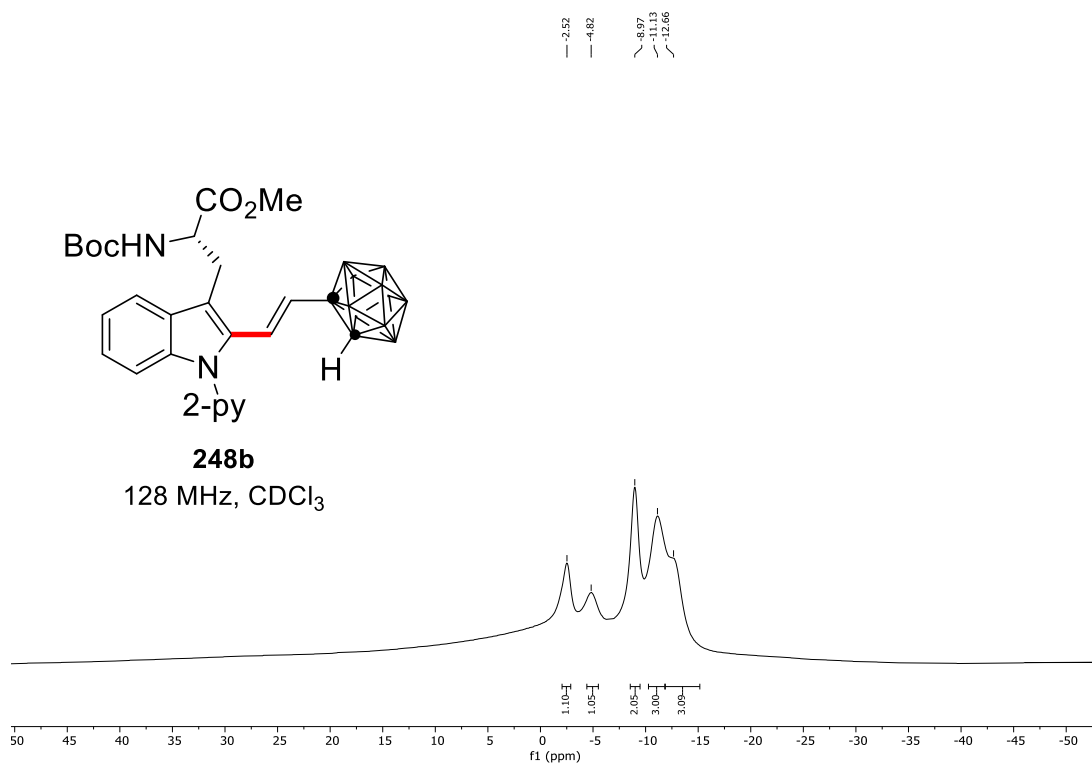
7. NMR Spectra



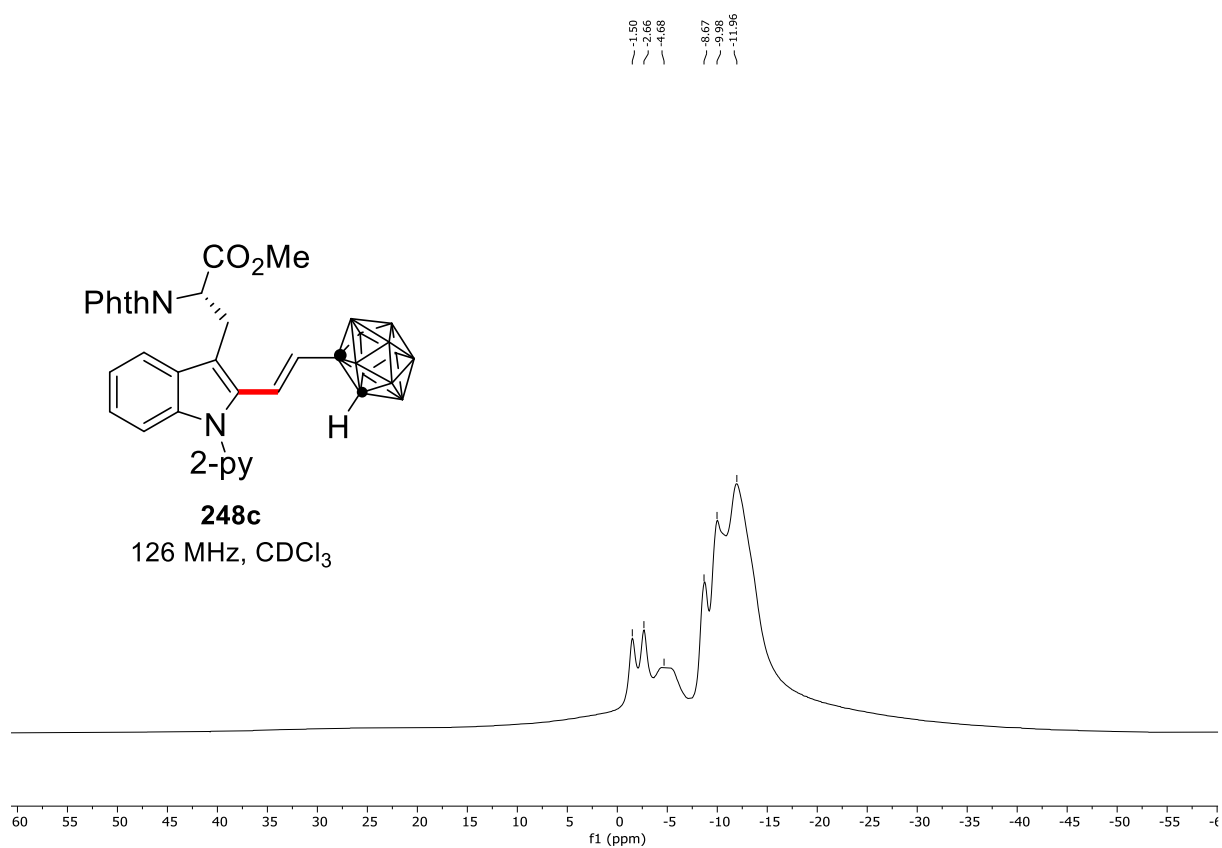
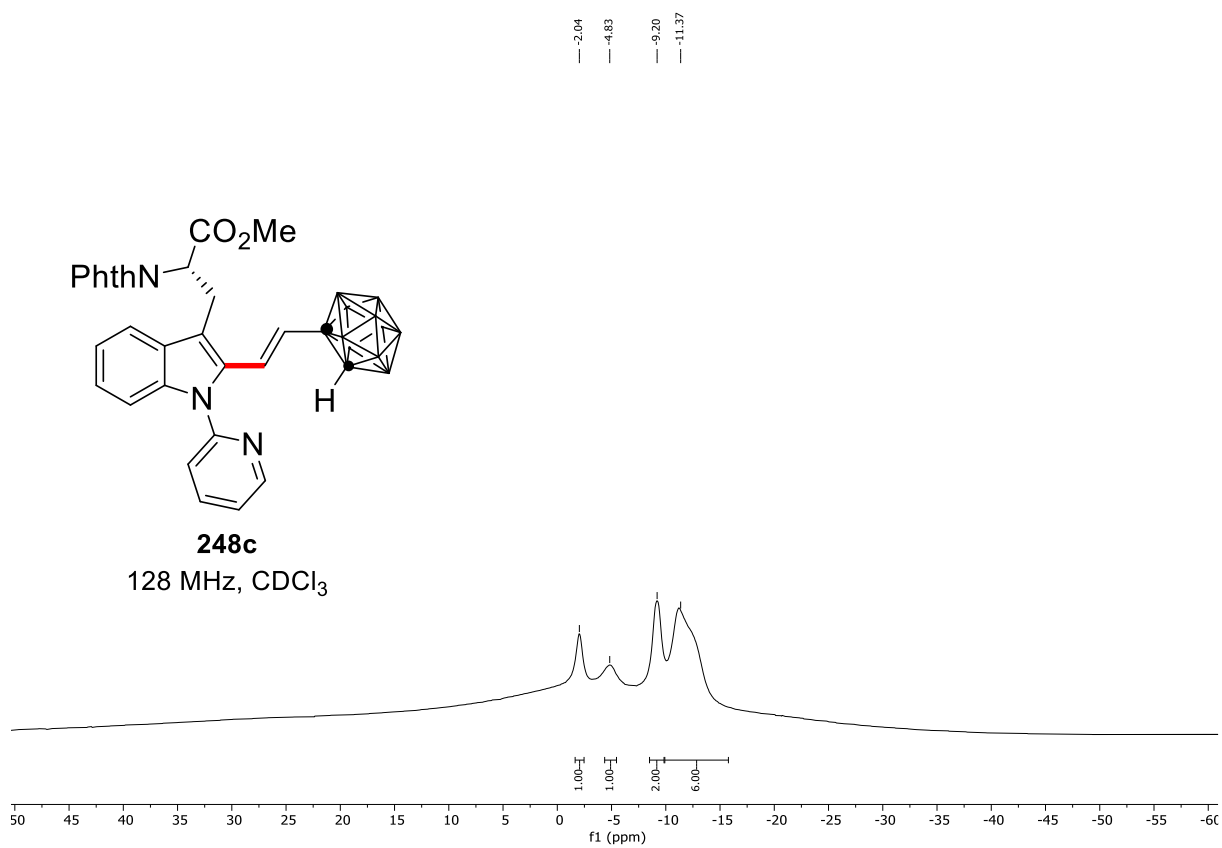
7. NMR Spectra

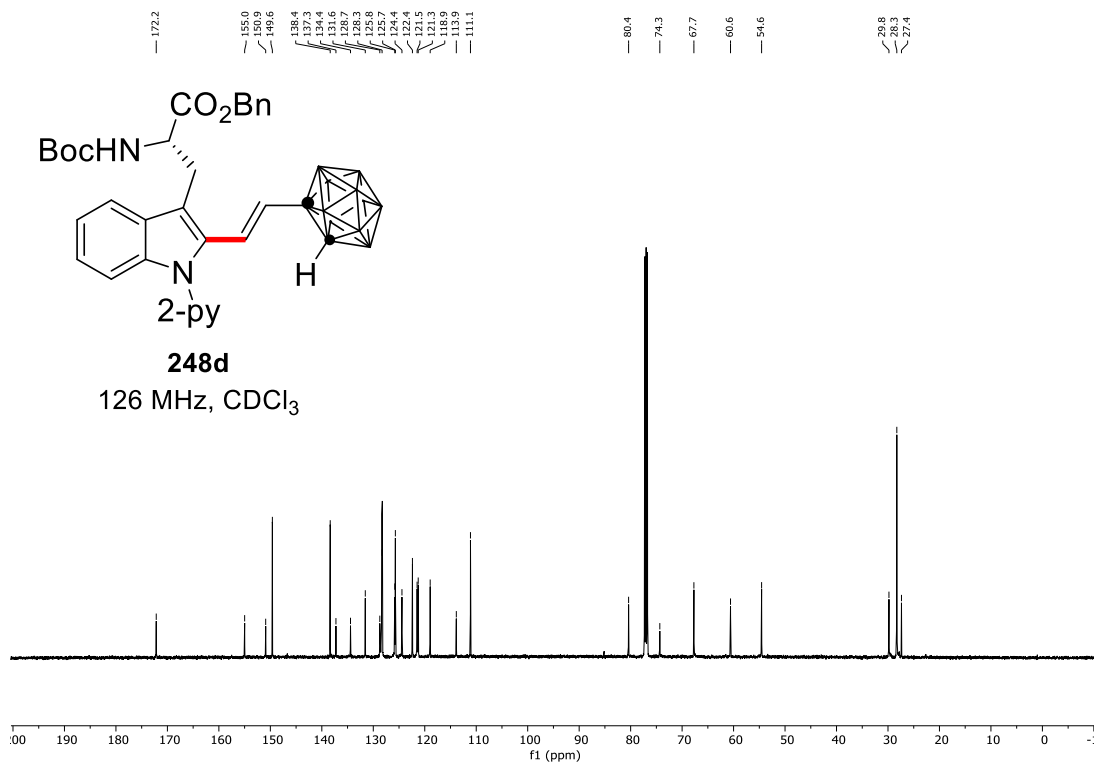


7. NMR Spectra

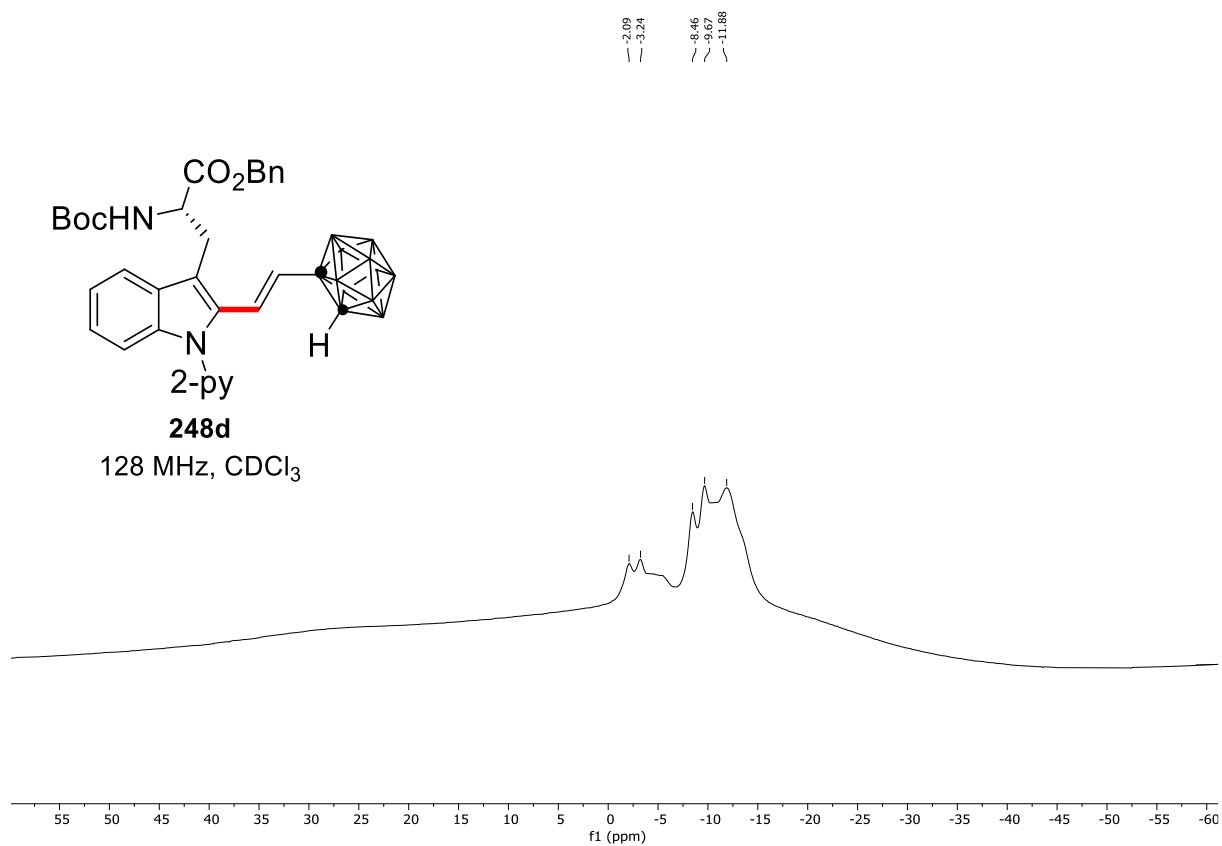
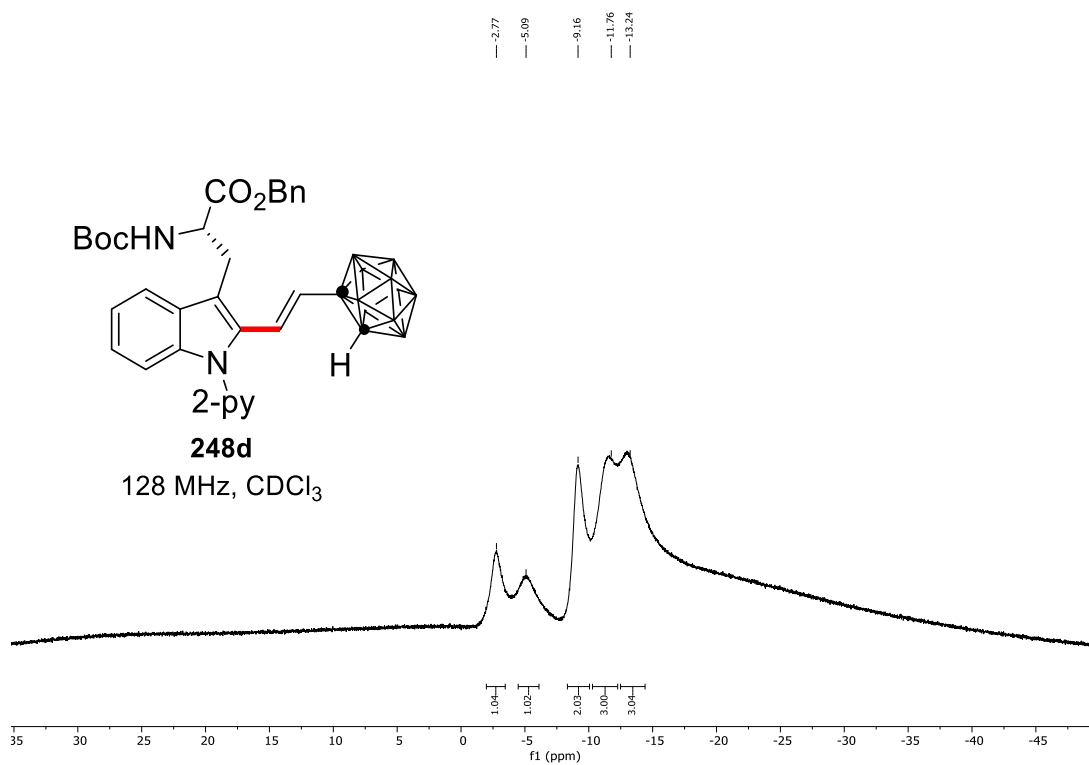


7. NMR Spectra

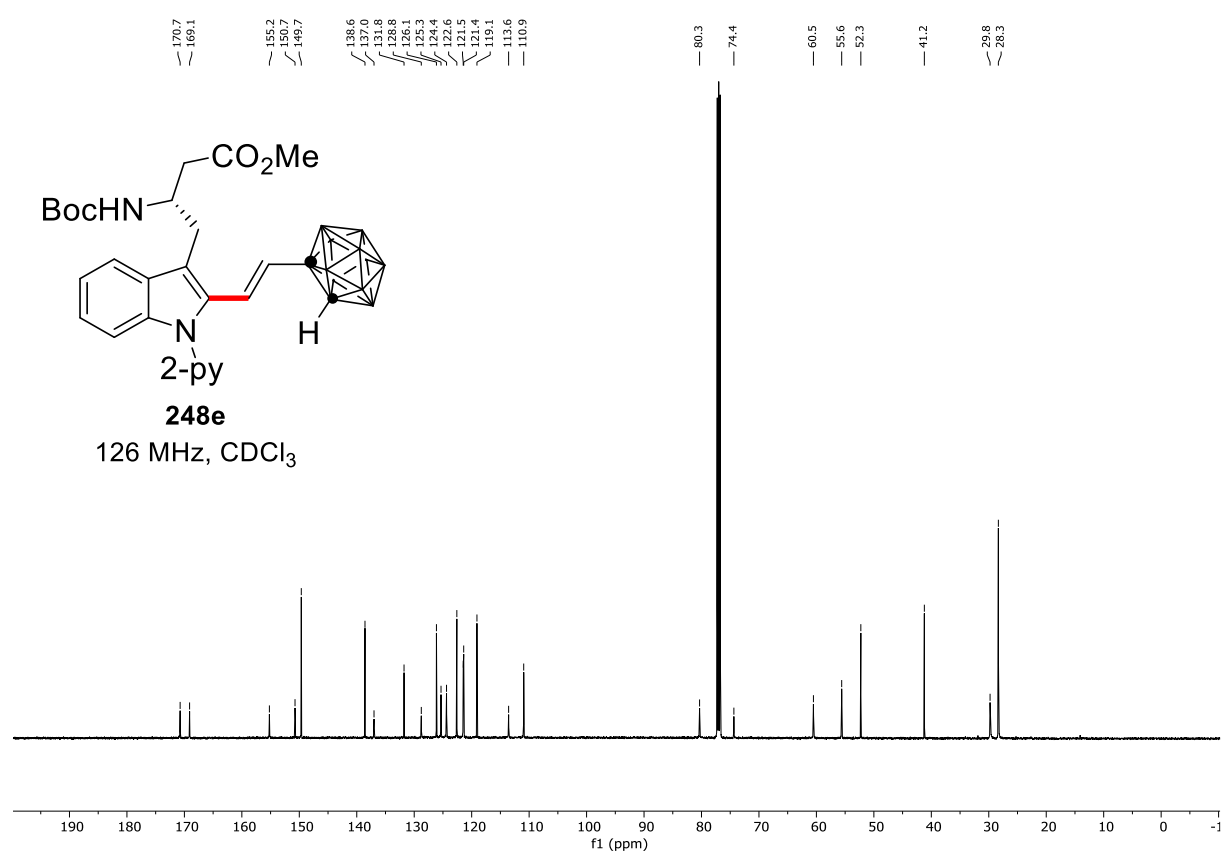
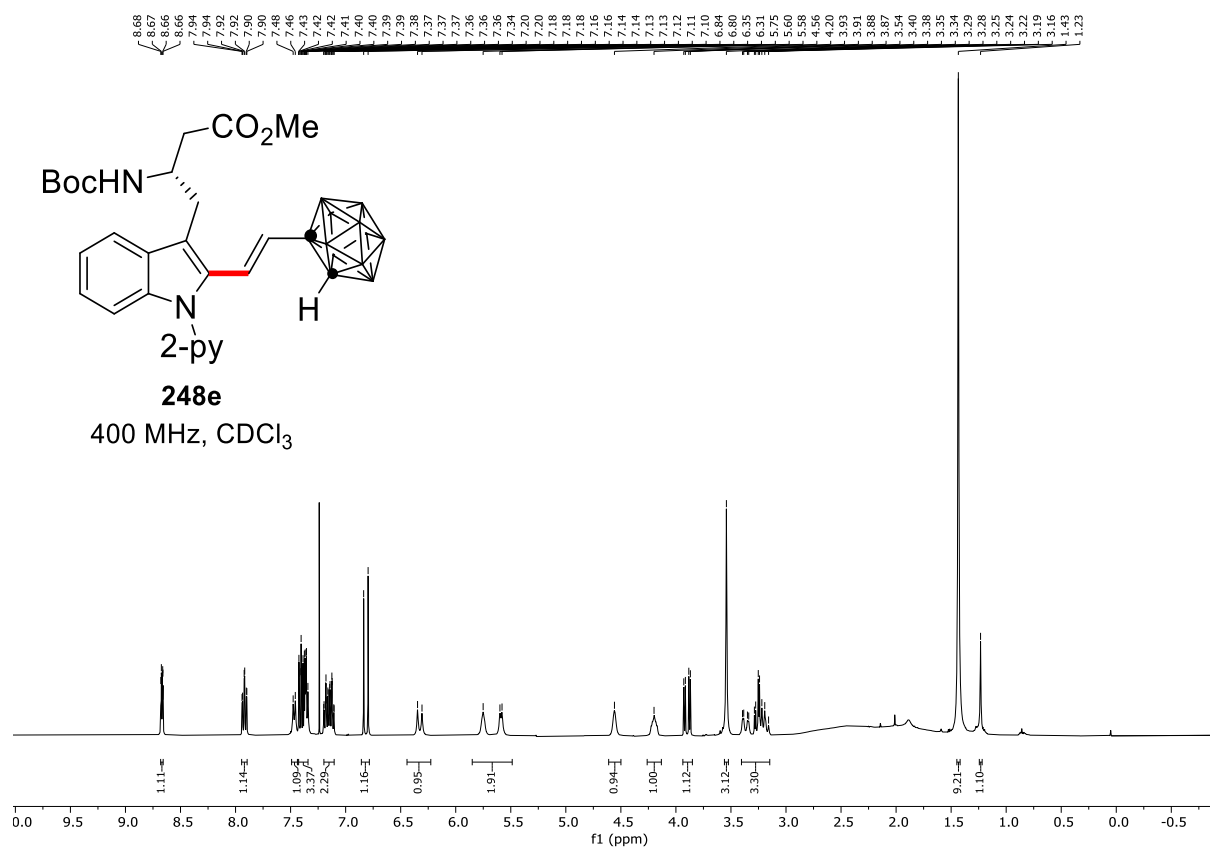




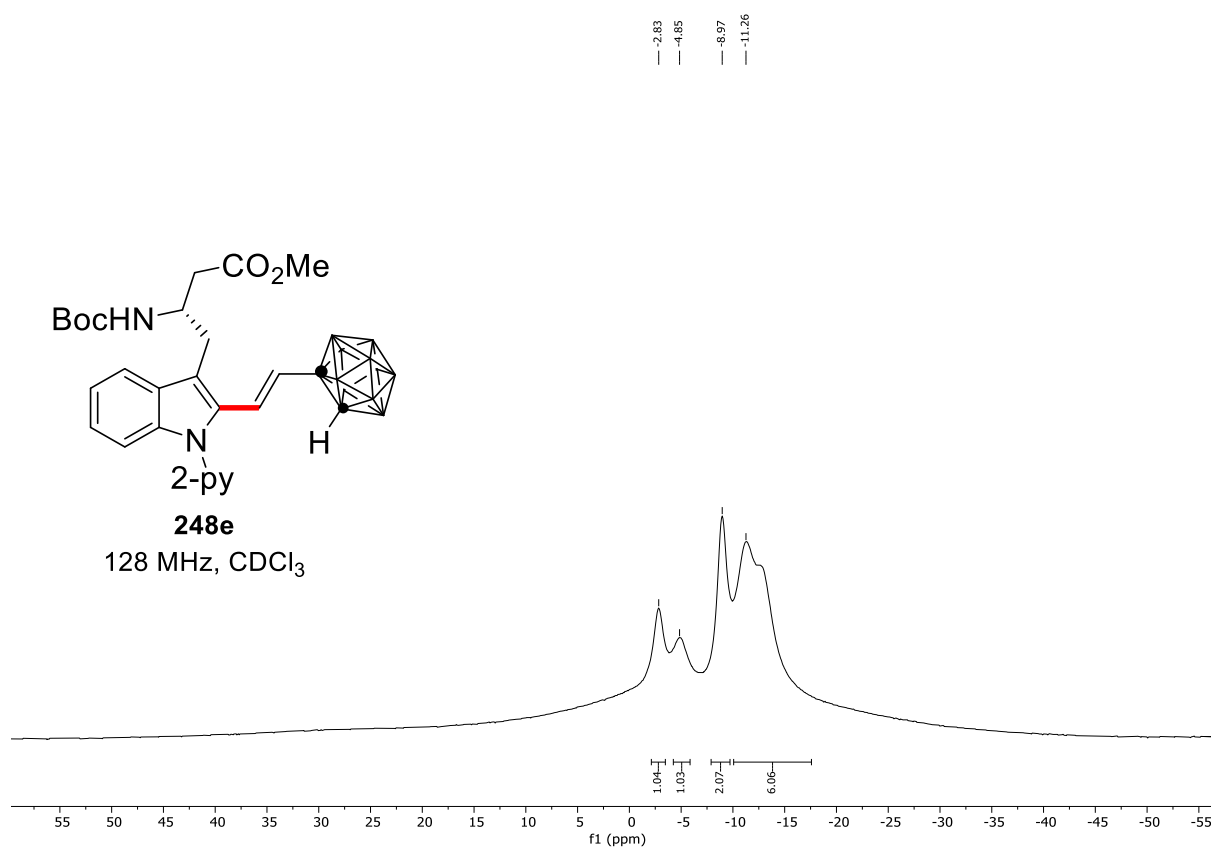
7. NMR Spectra



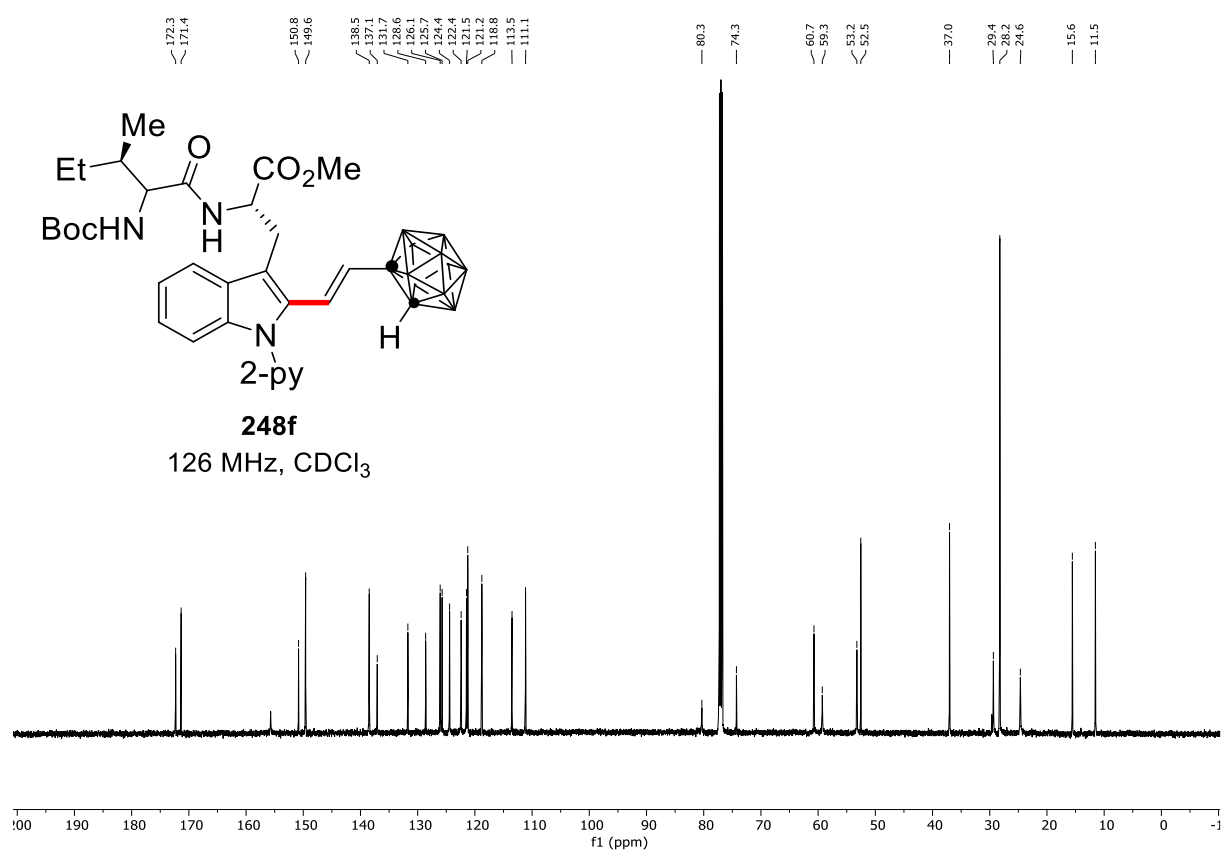
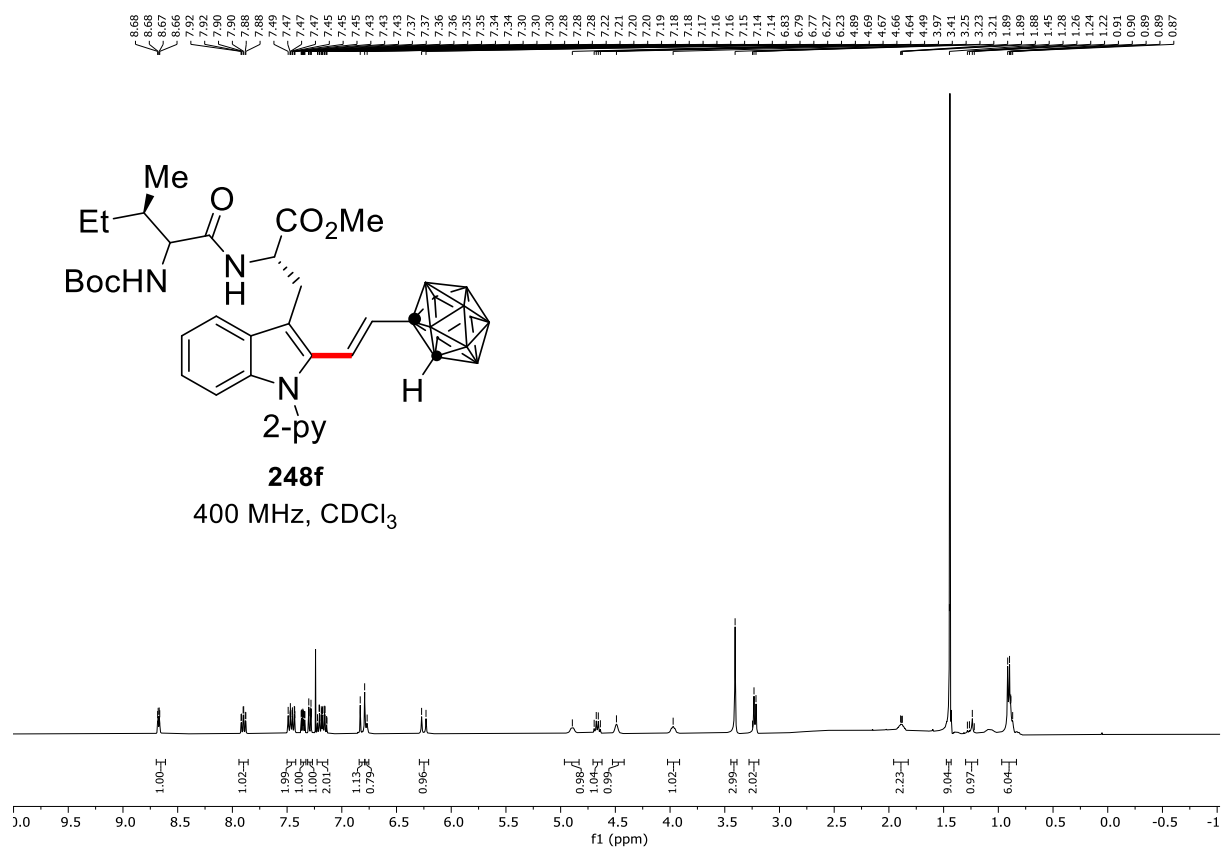
7. NMR Spectra



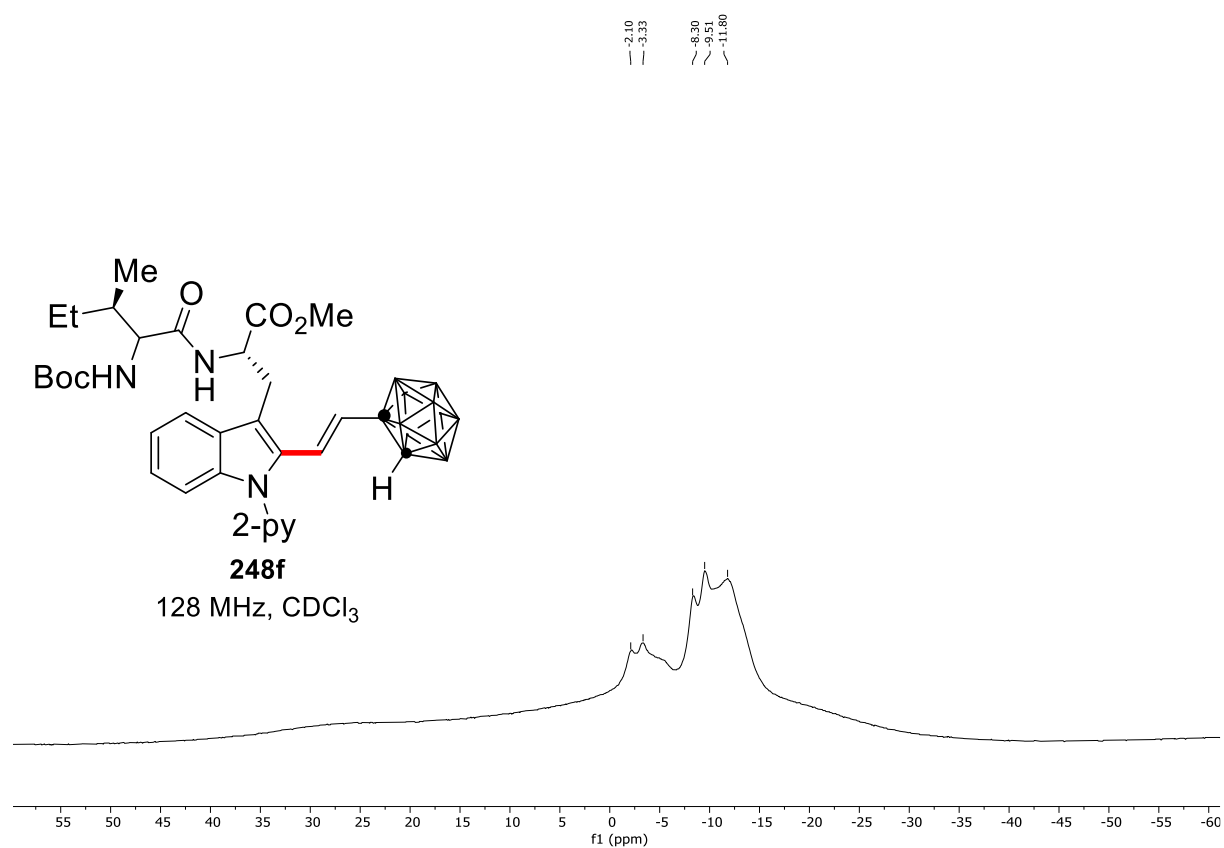
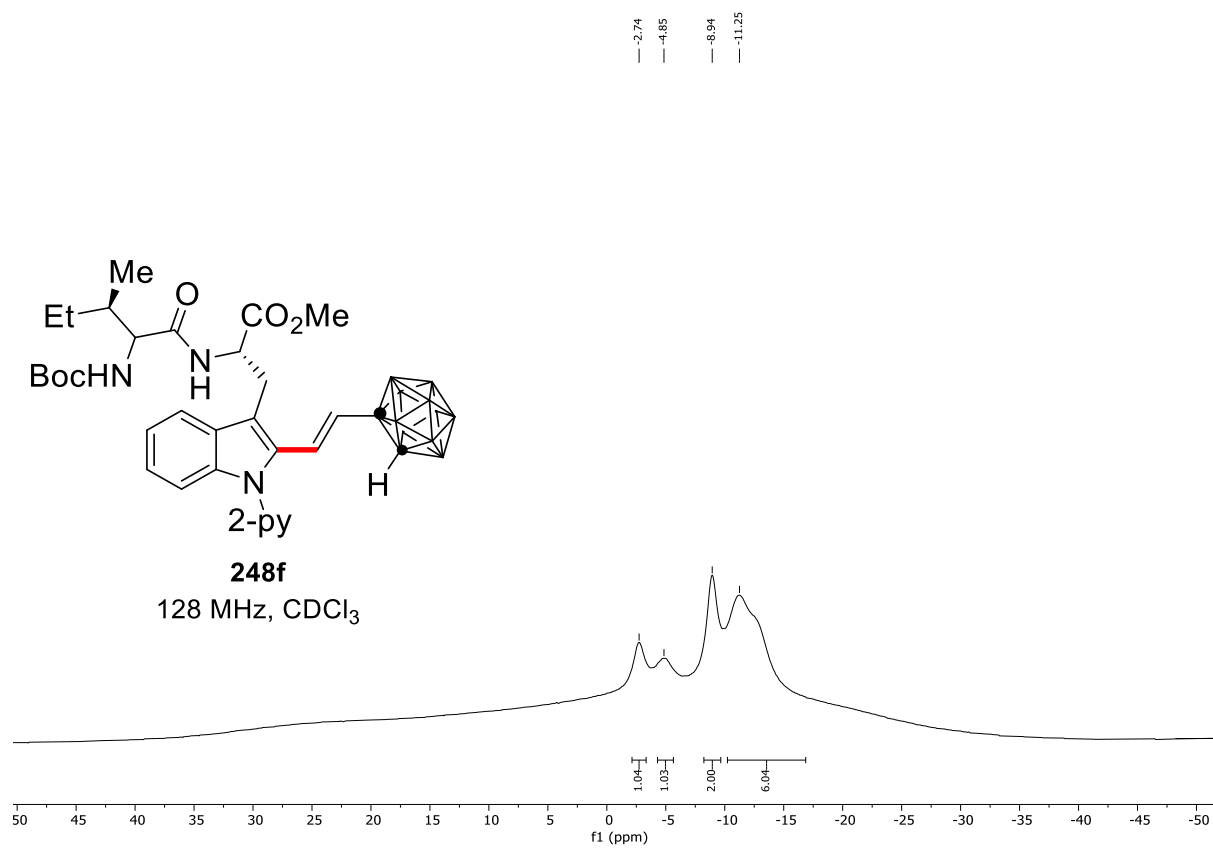
7. NMR Spectra



7. NMR Spectra

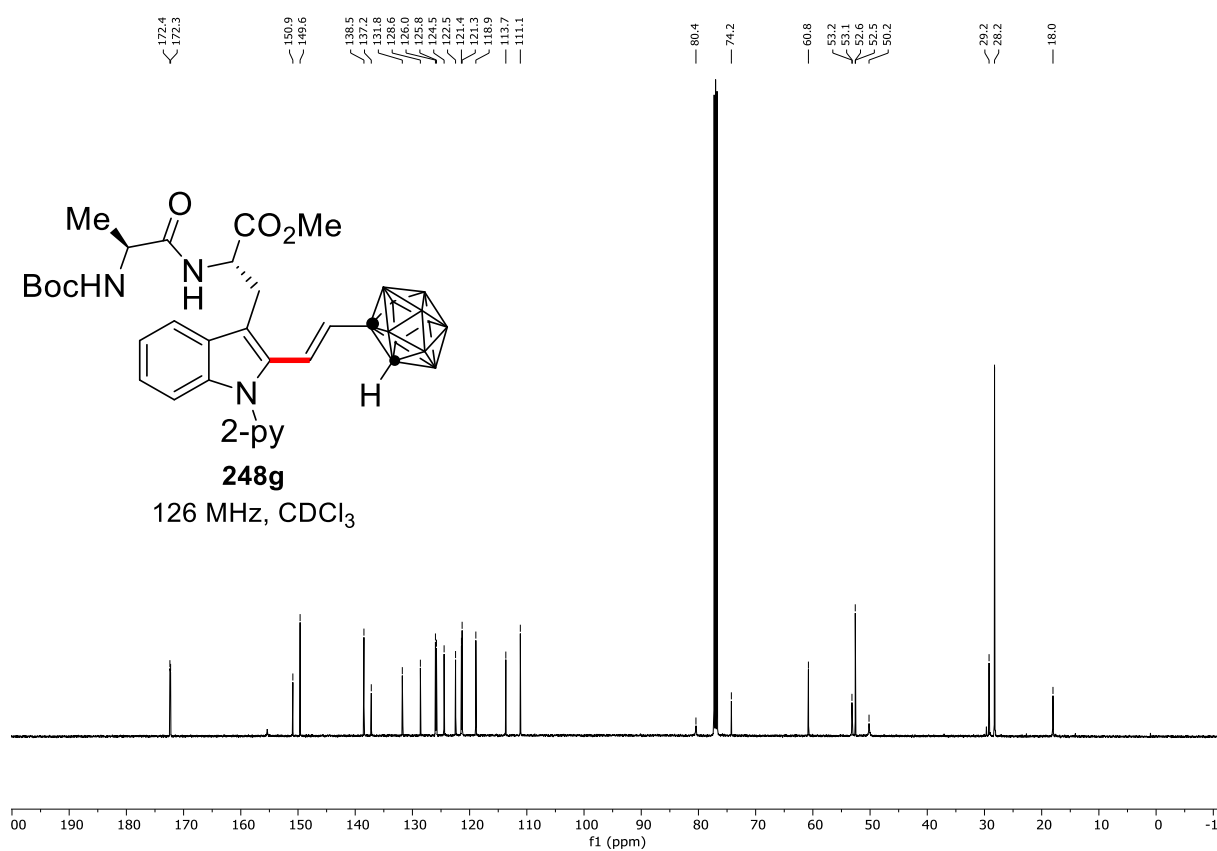


7. NMR Spectra

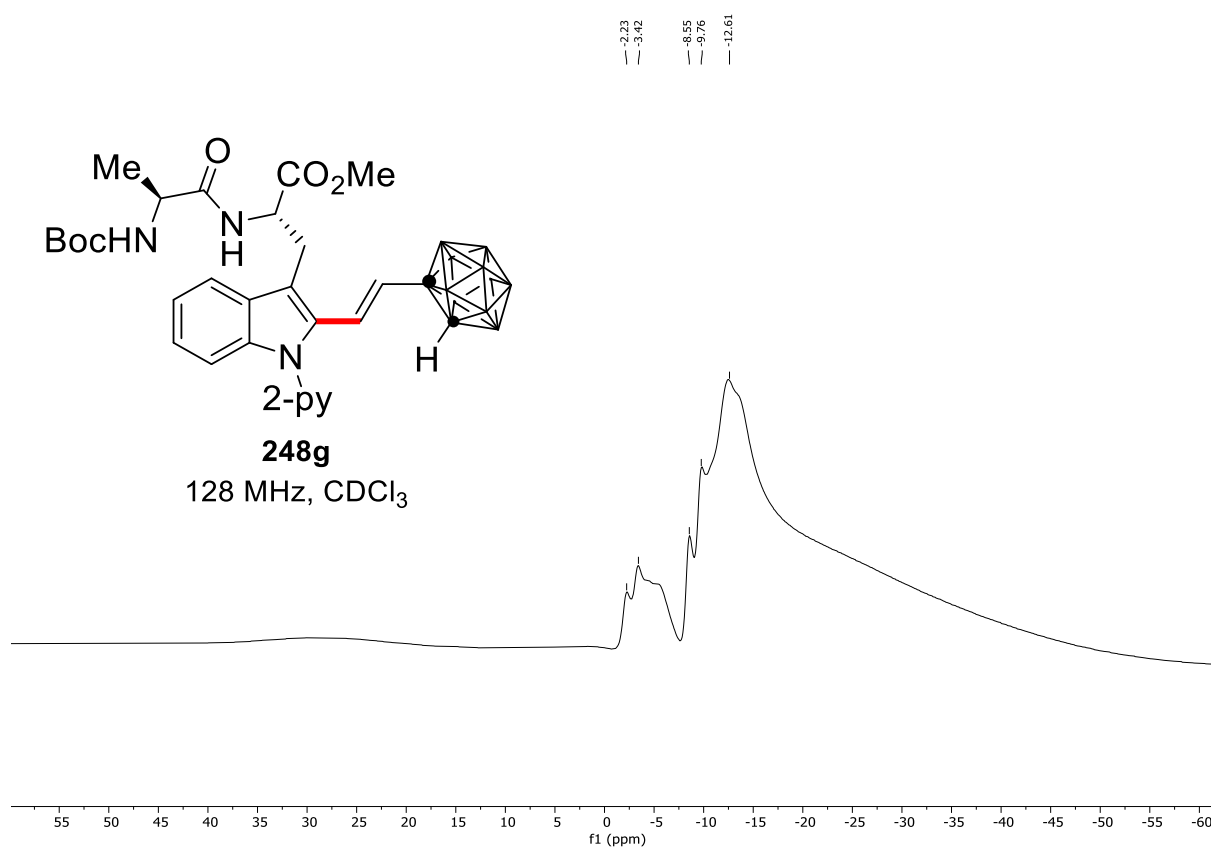
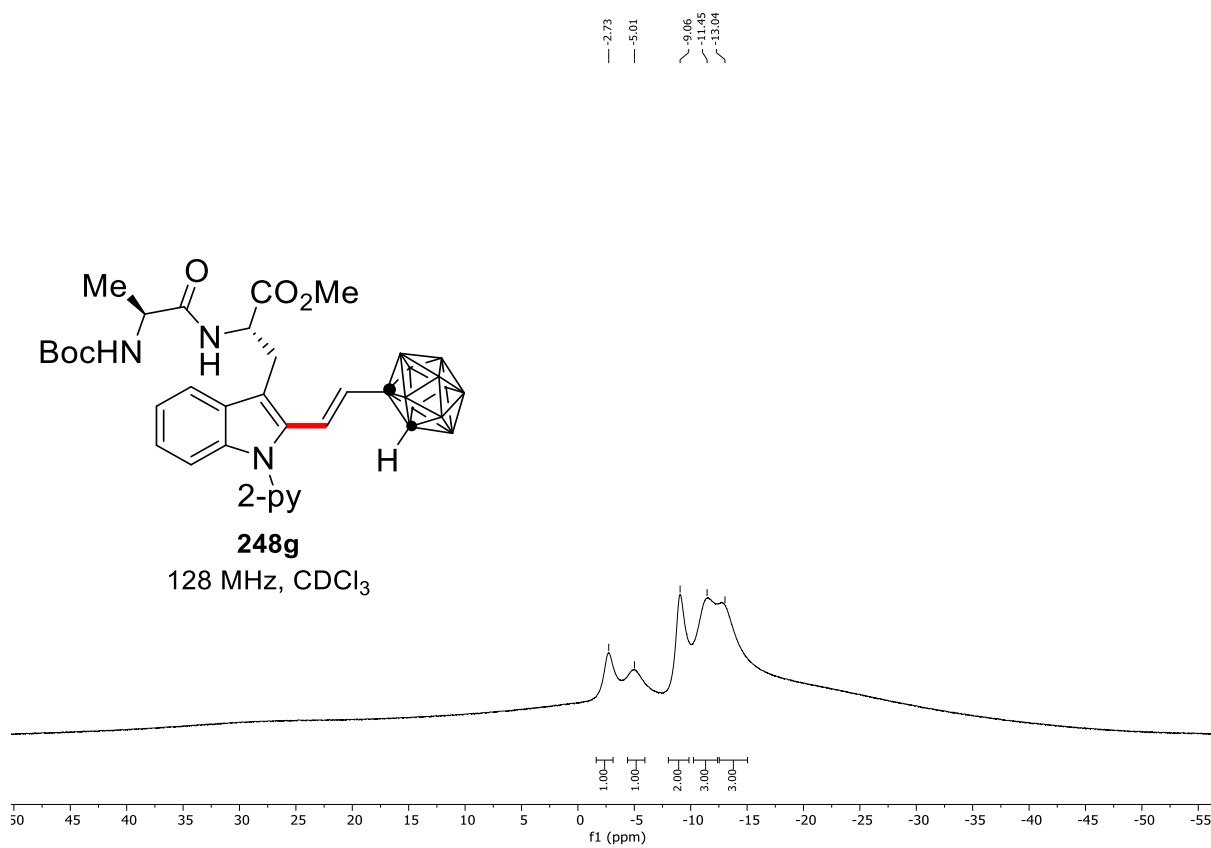


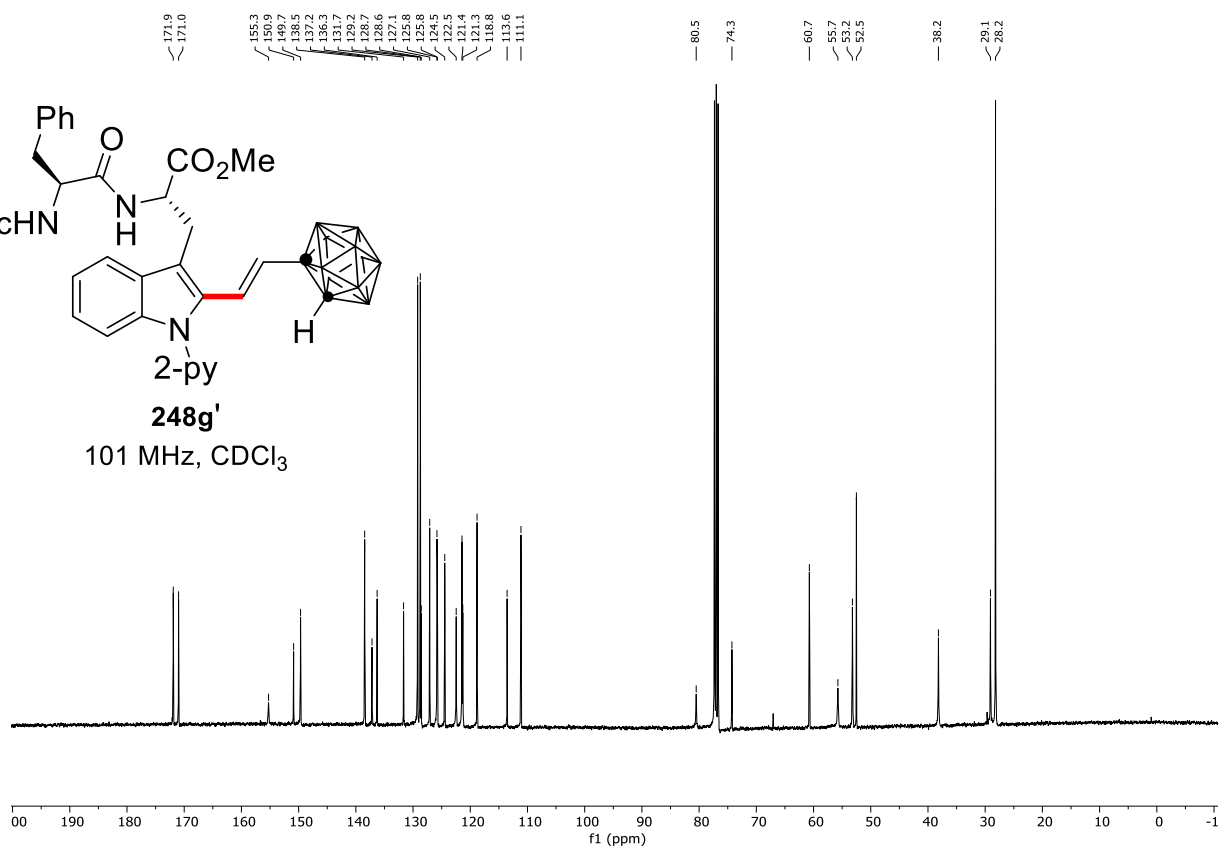
Chemical structure of **248g** is shown, a 2-pyridyl derivative. The structure features a pyridine ring substituted with a BocHN group, a CO₂Me group, and a 2-pyridyl group. The structure is labeled **248g** and the solvent is CDCl₃.

The ¹H NMR spectrum (400 MHz, CDCl₃) is displayed below the structure. The x-axis represents the chemical shift in ppm (f1), ranging from 0.0 to 10.0. The spectrum shows several peaks, including aromatic signals between 6.5 and 8.7 ppm, a broad peak around 7.2 ppm, and a sharp peak at 1.43 ppm. Integration values are provided for several peaks: 1.00, 1.00, 2.00, 1.00, 1.01, 2.00, 0.87, 0.92, 0.86, 1.00, 0.90, 0.87, 3.00, 2.00, 9.00, and 3.00.

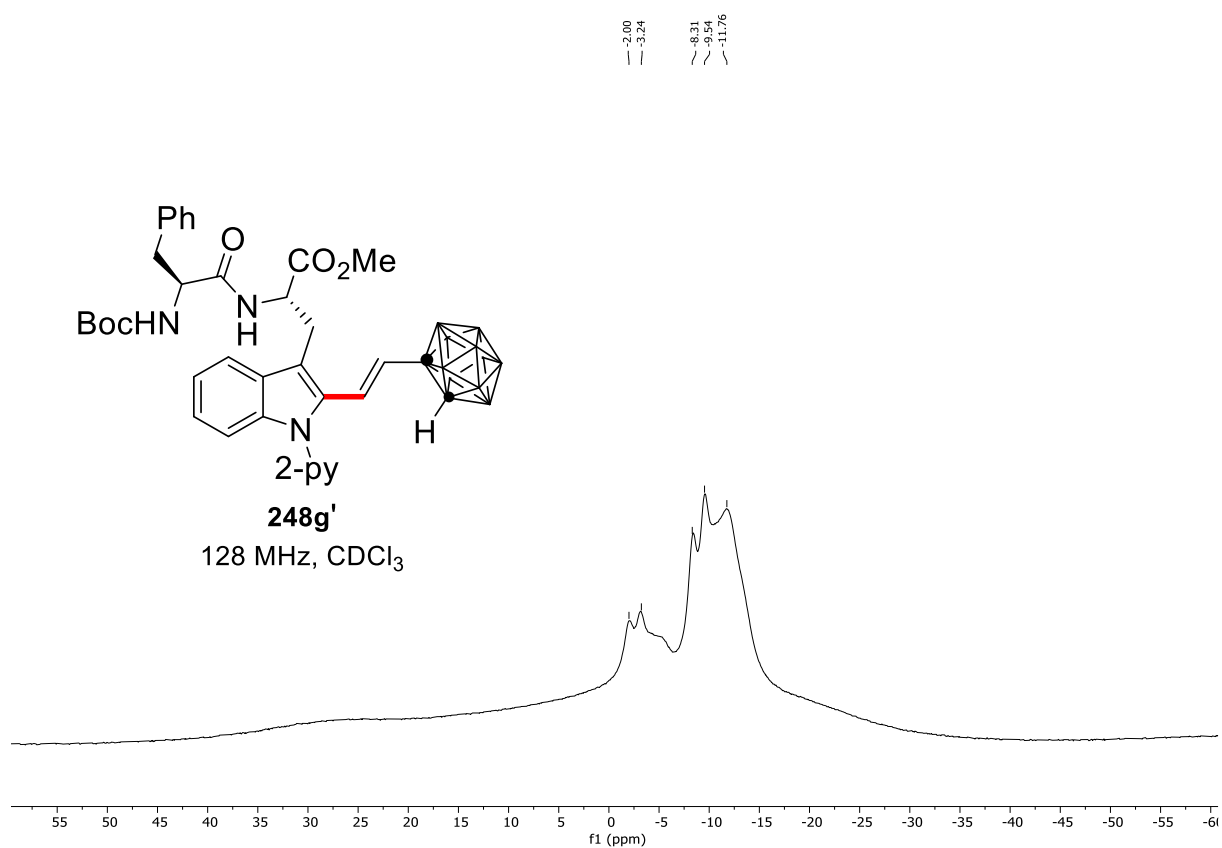
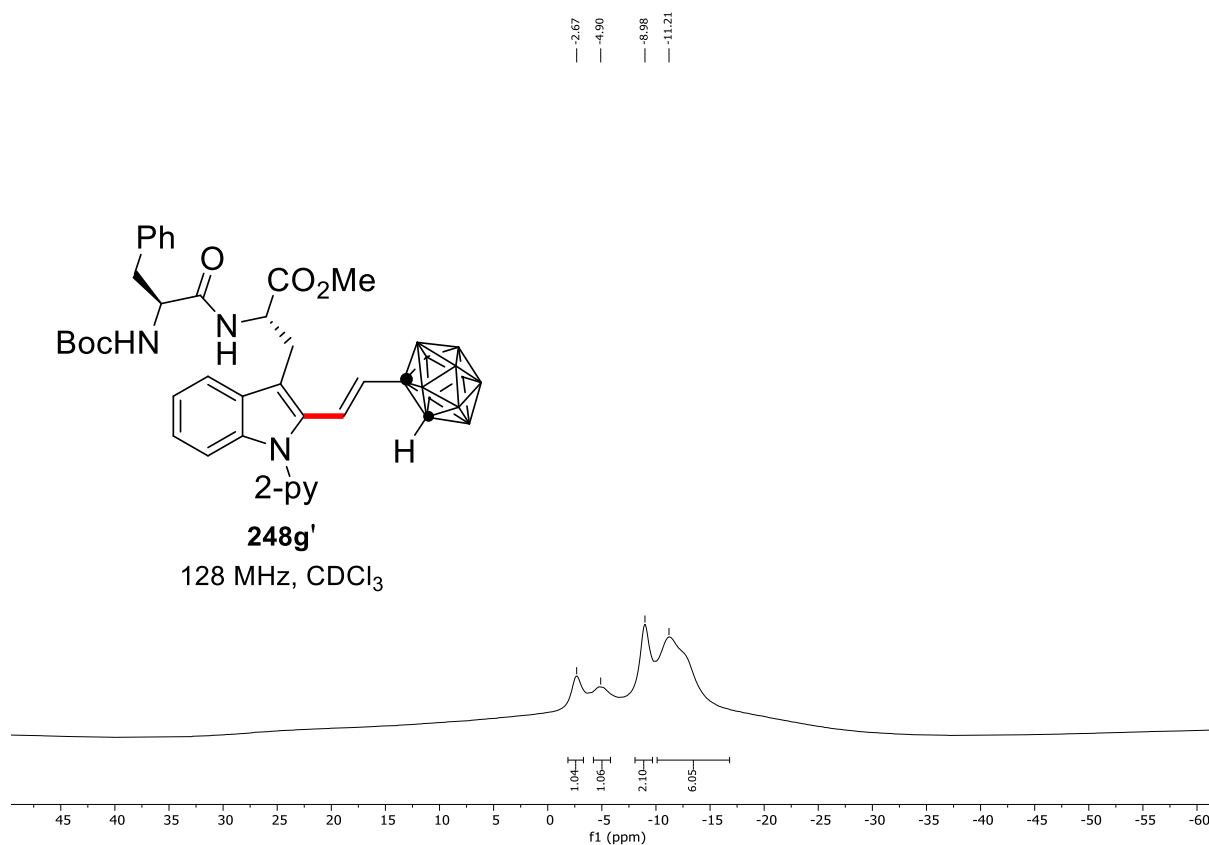


7. NMR Spectra

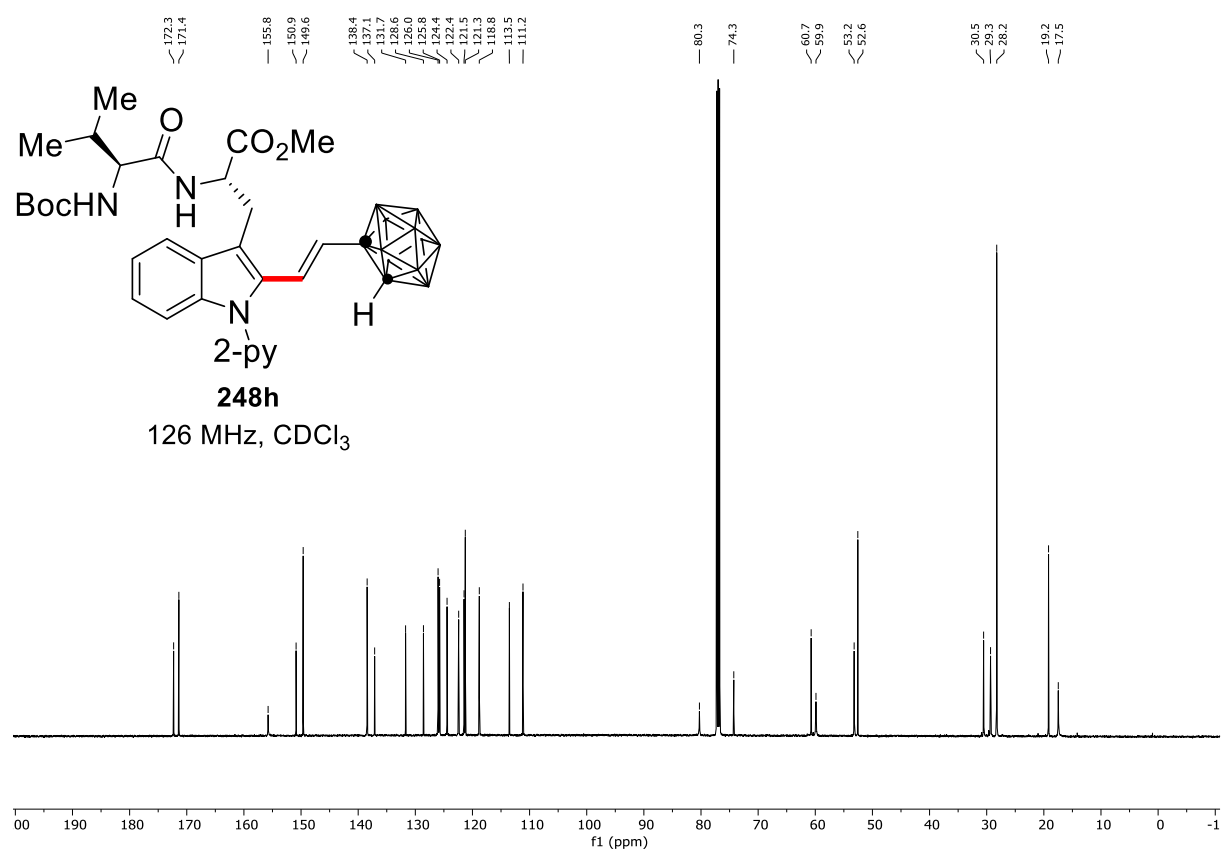
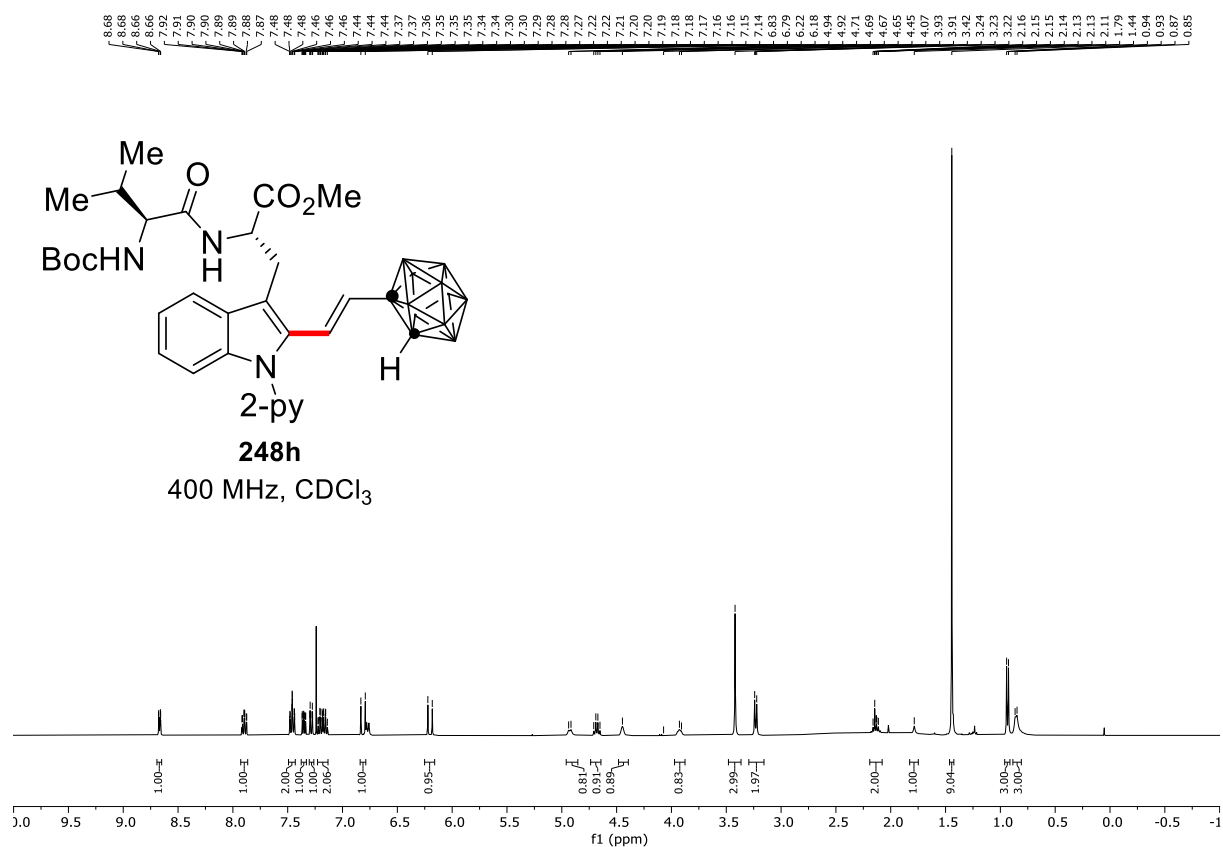




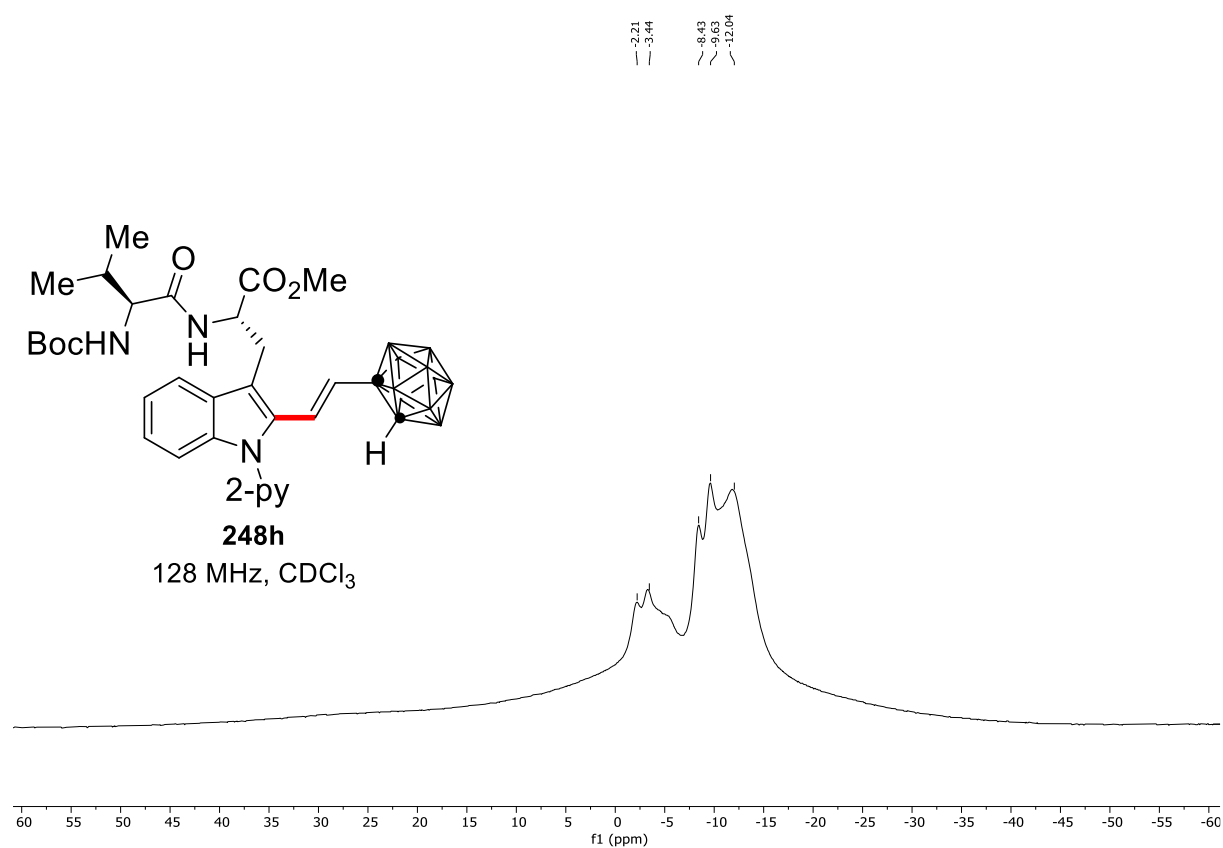
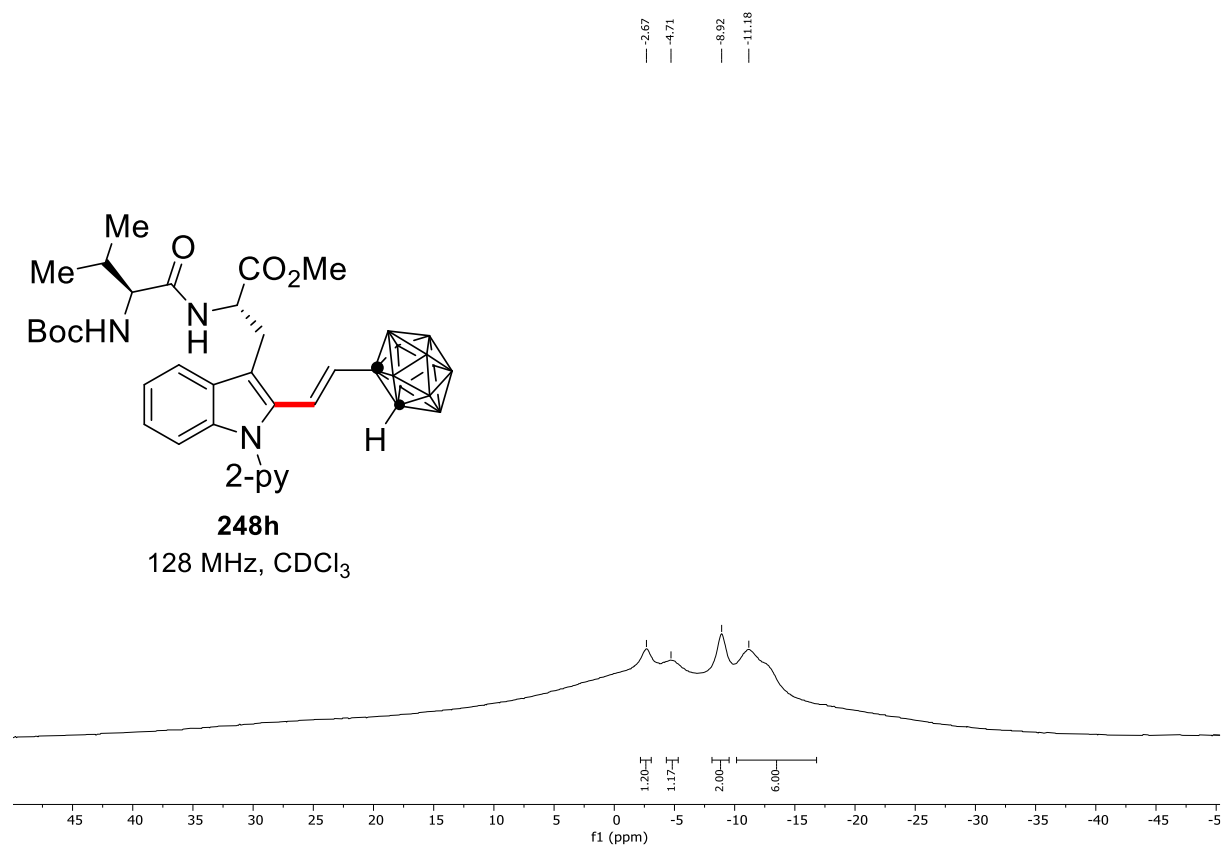
7. NMR Spectra



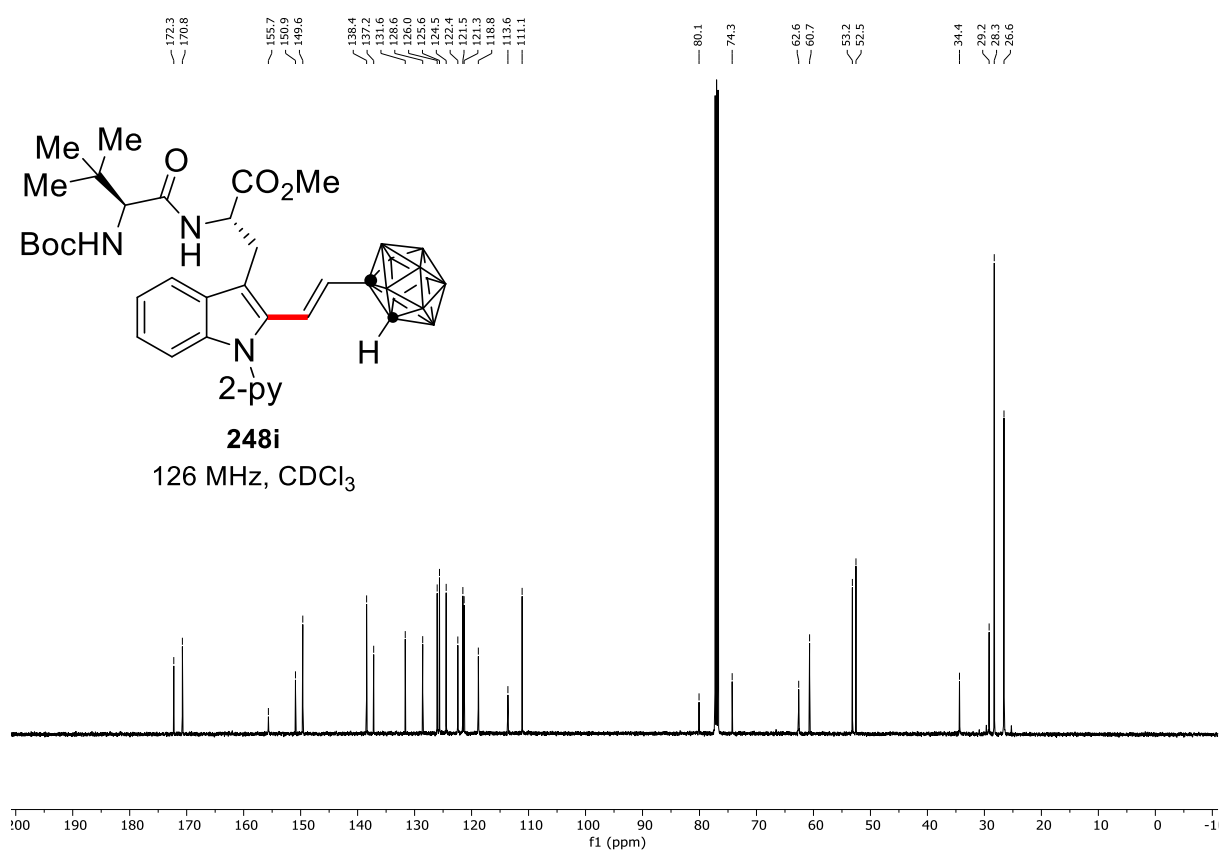
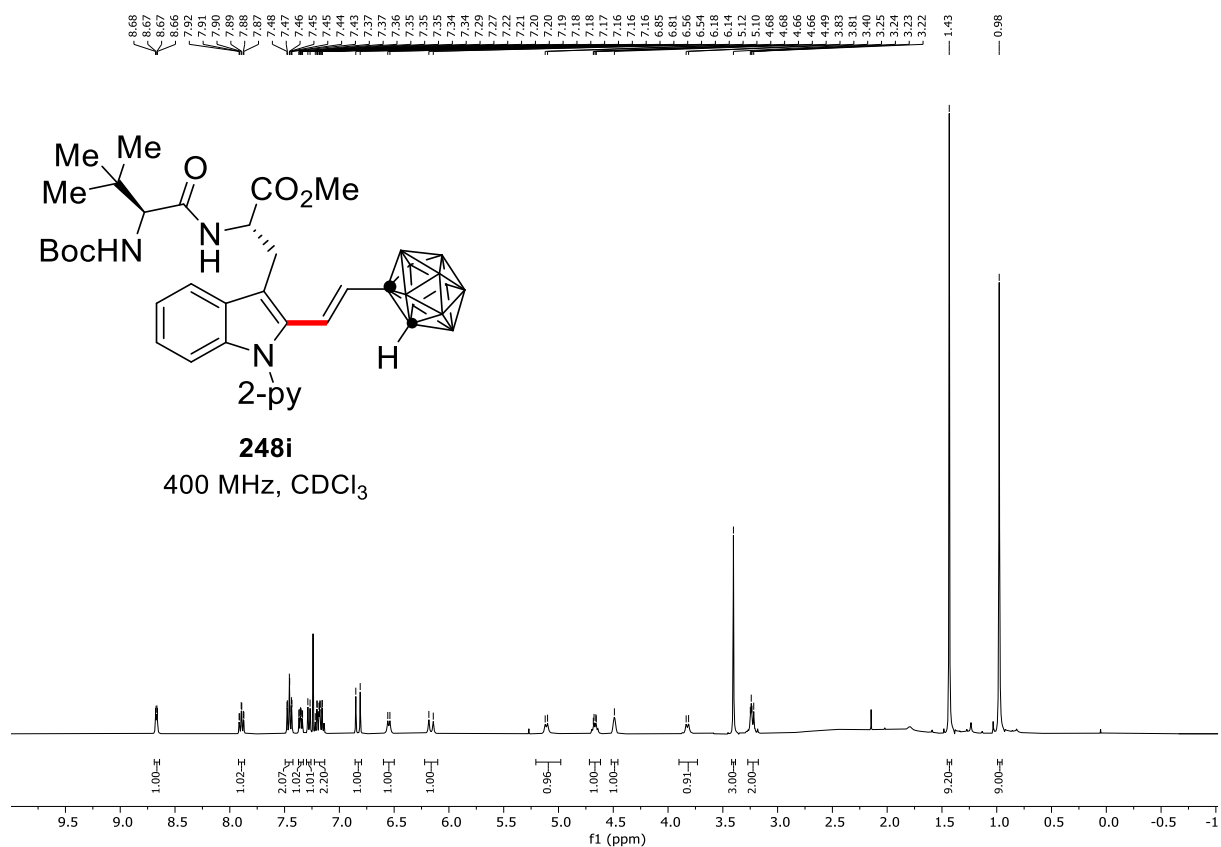
7. NMR Spectra



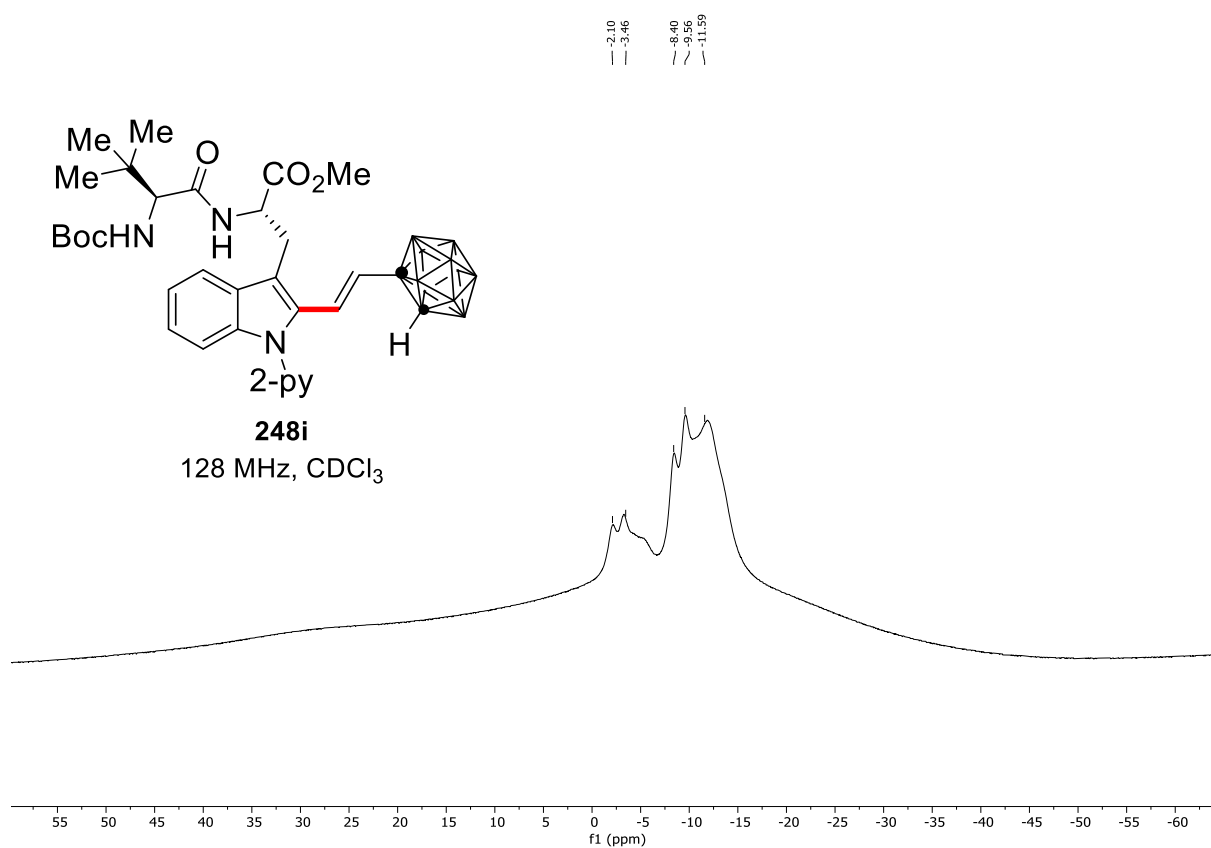
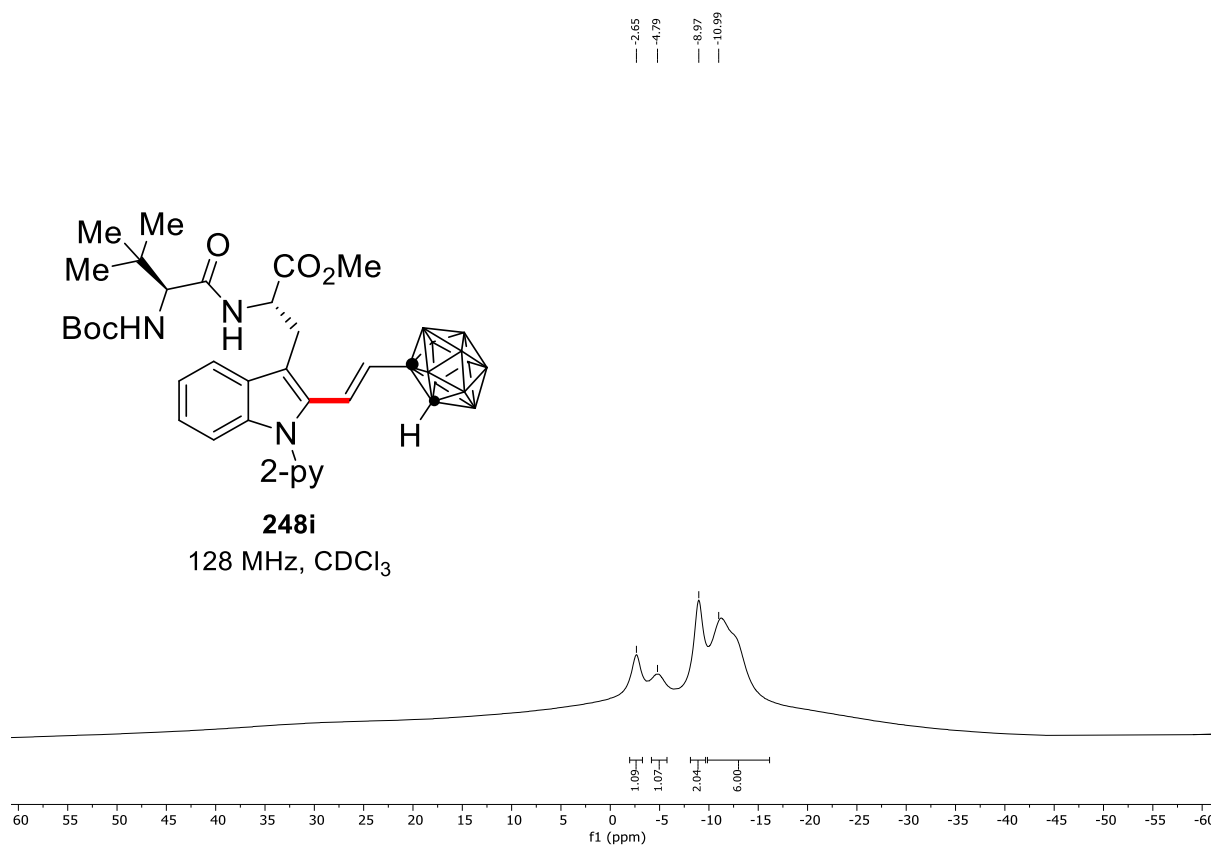
7. NMR Spectra



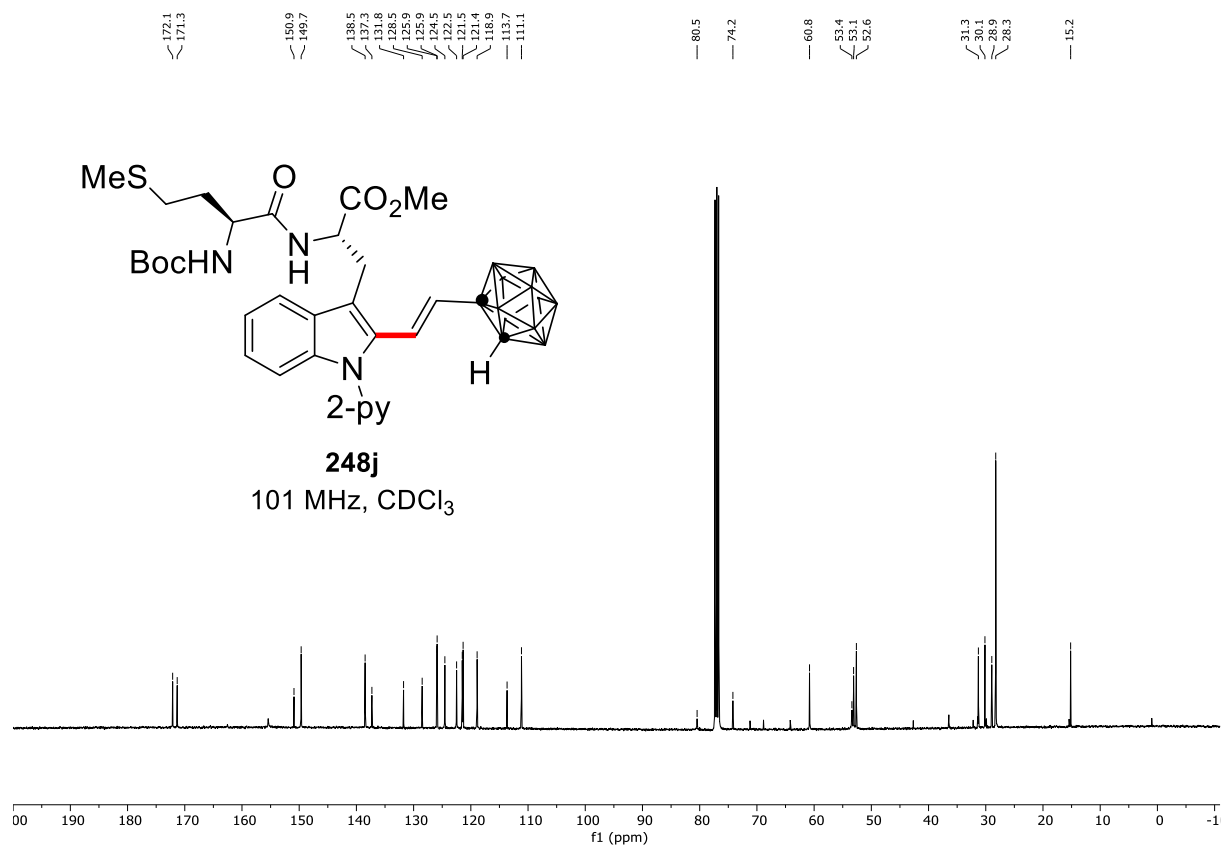
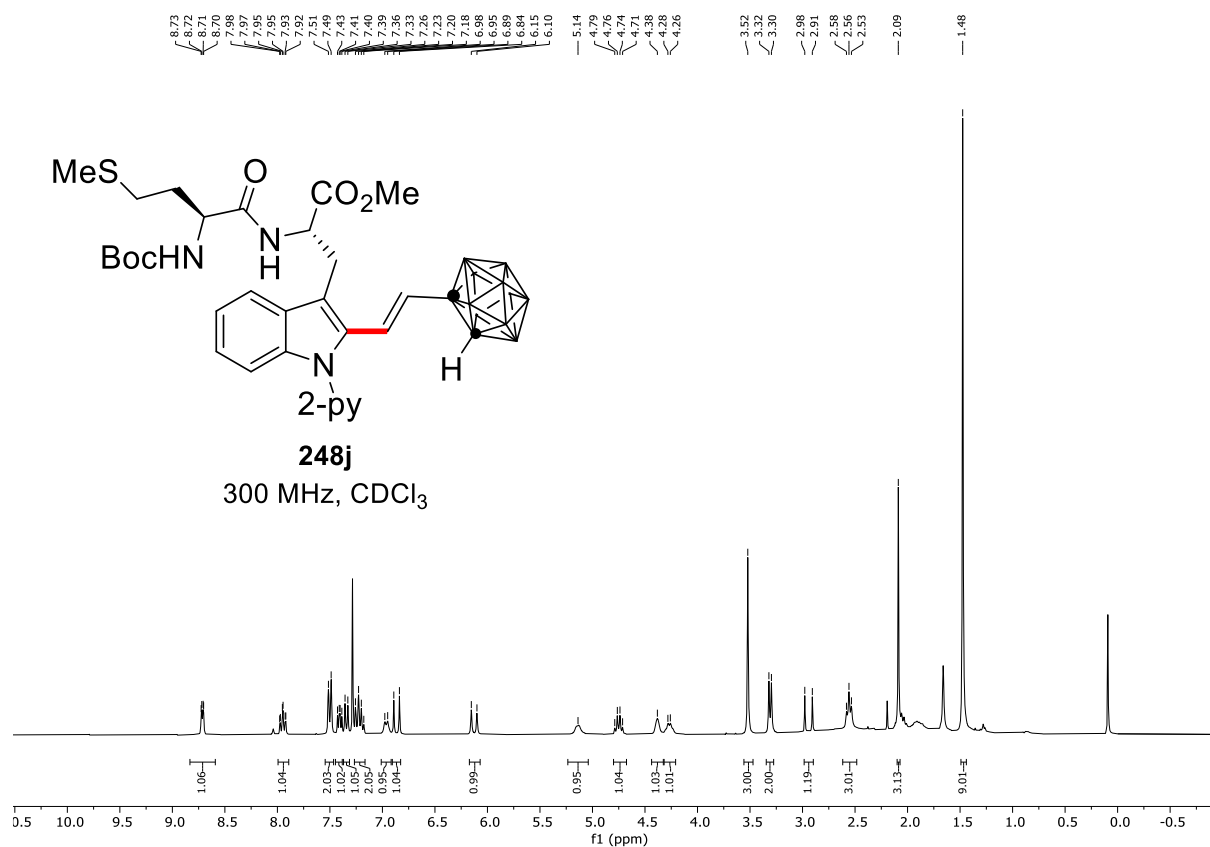
7. NMR Spectra



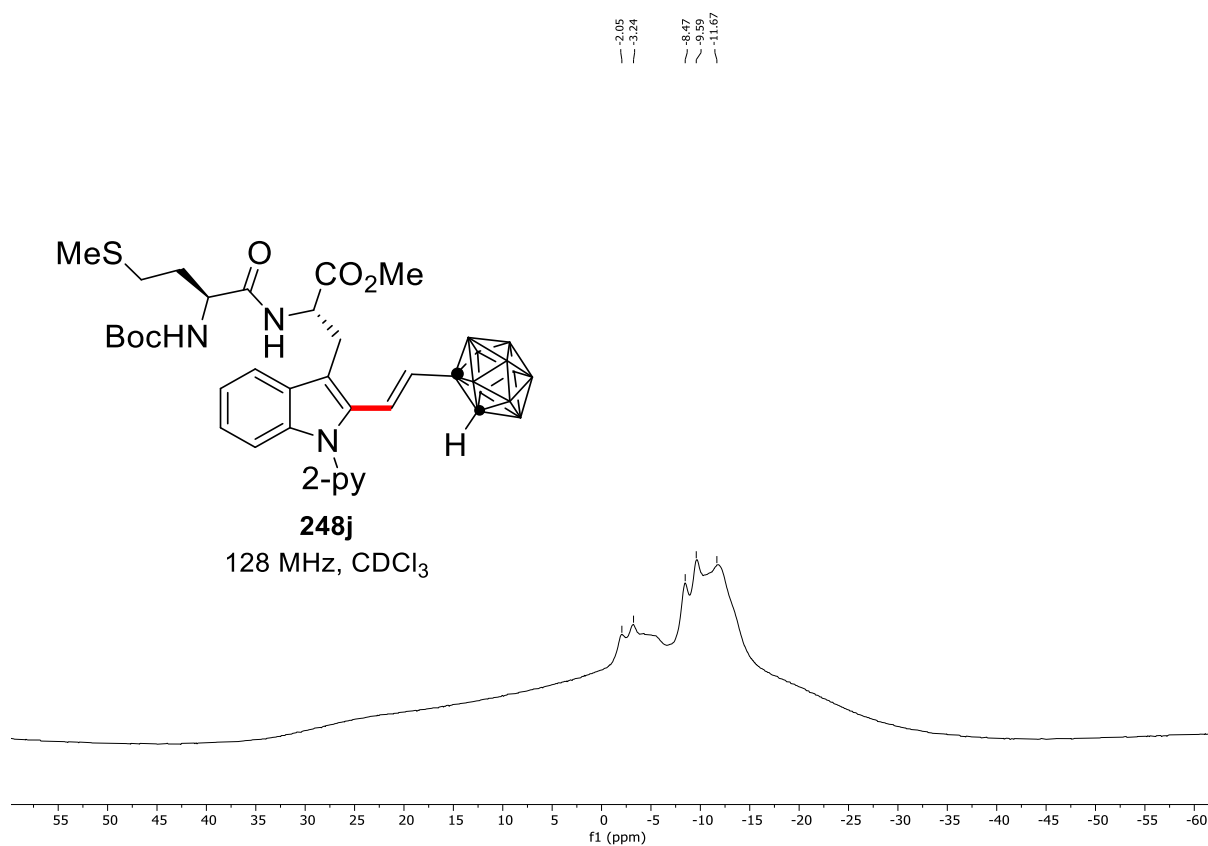
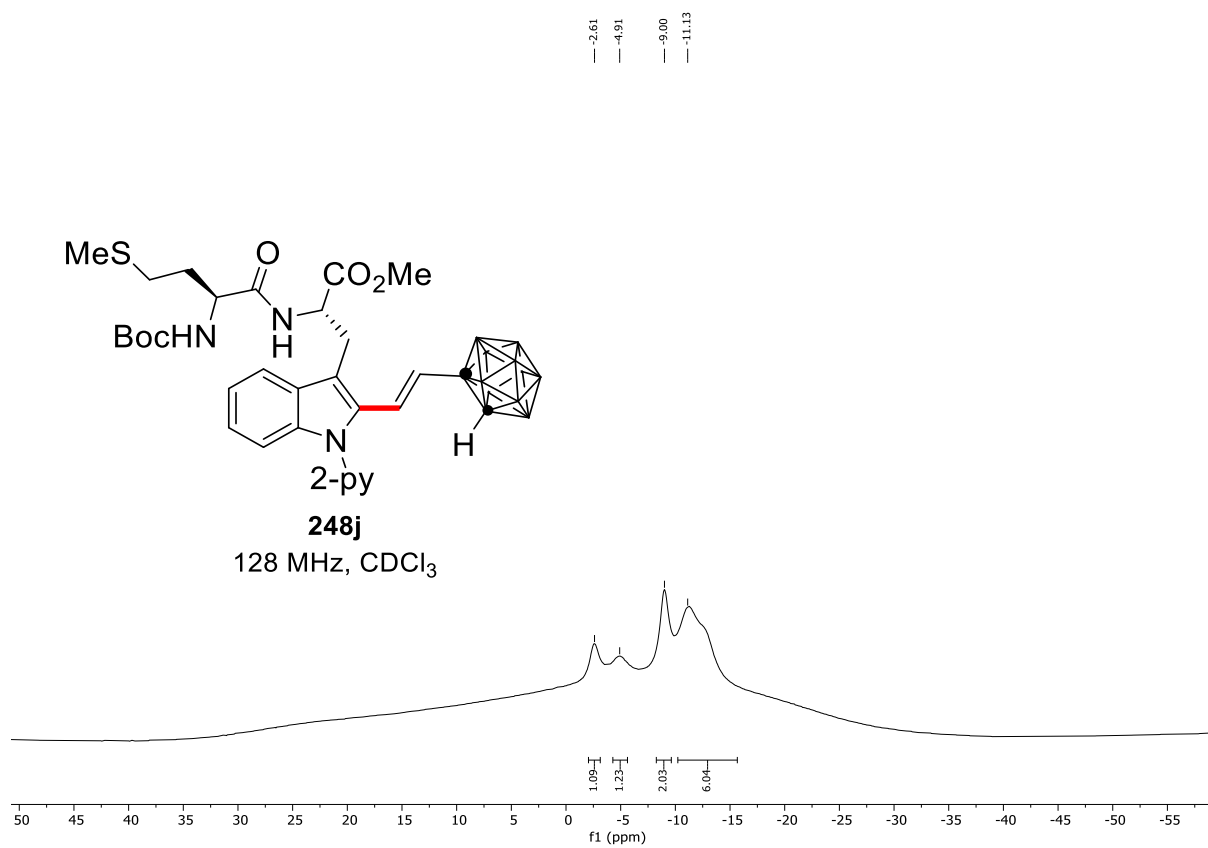
7. NMR Spectra



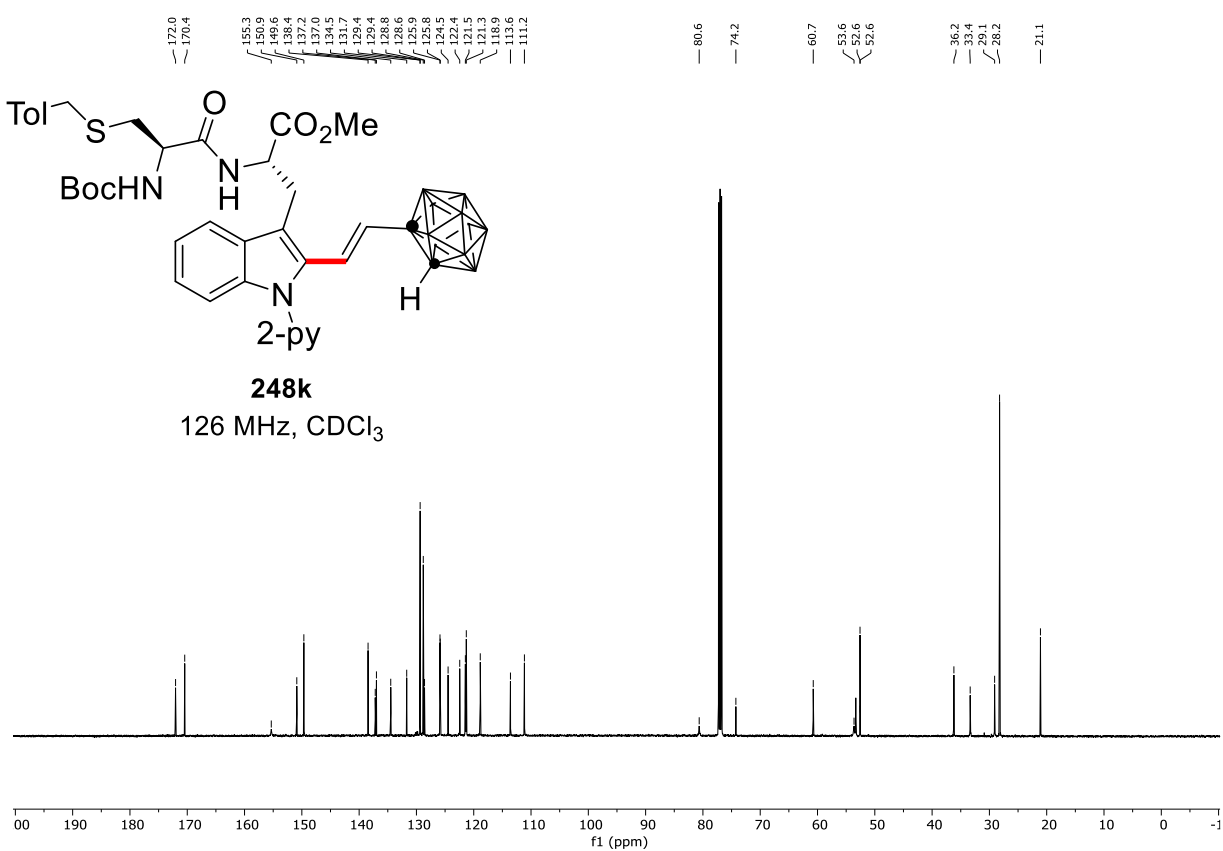
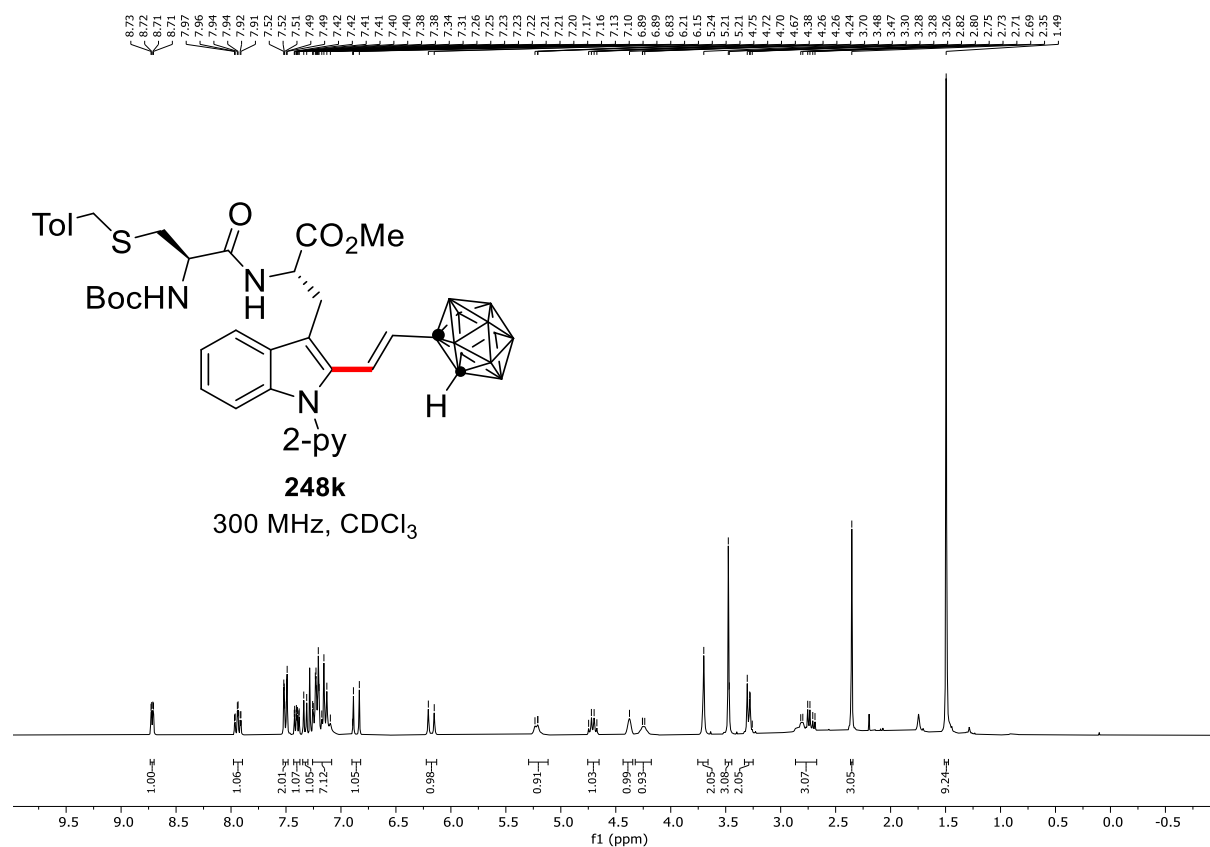
7. NMR Spectra



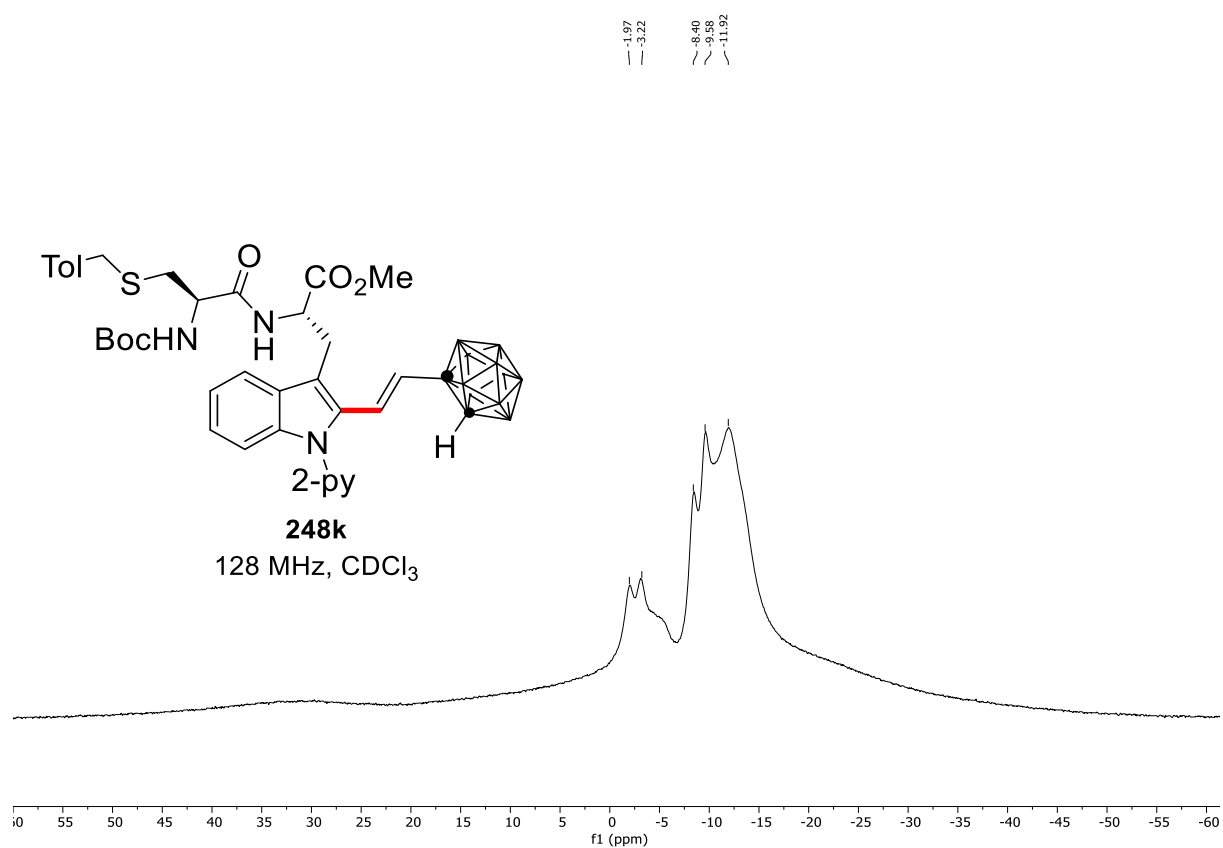
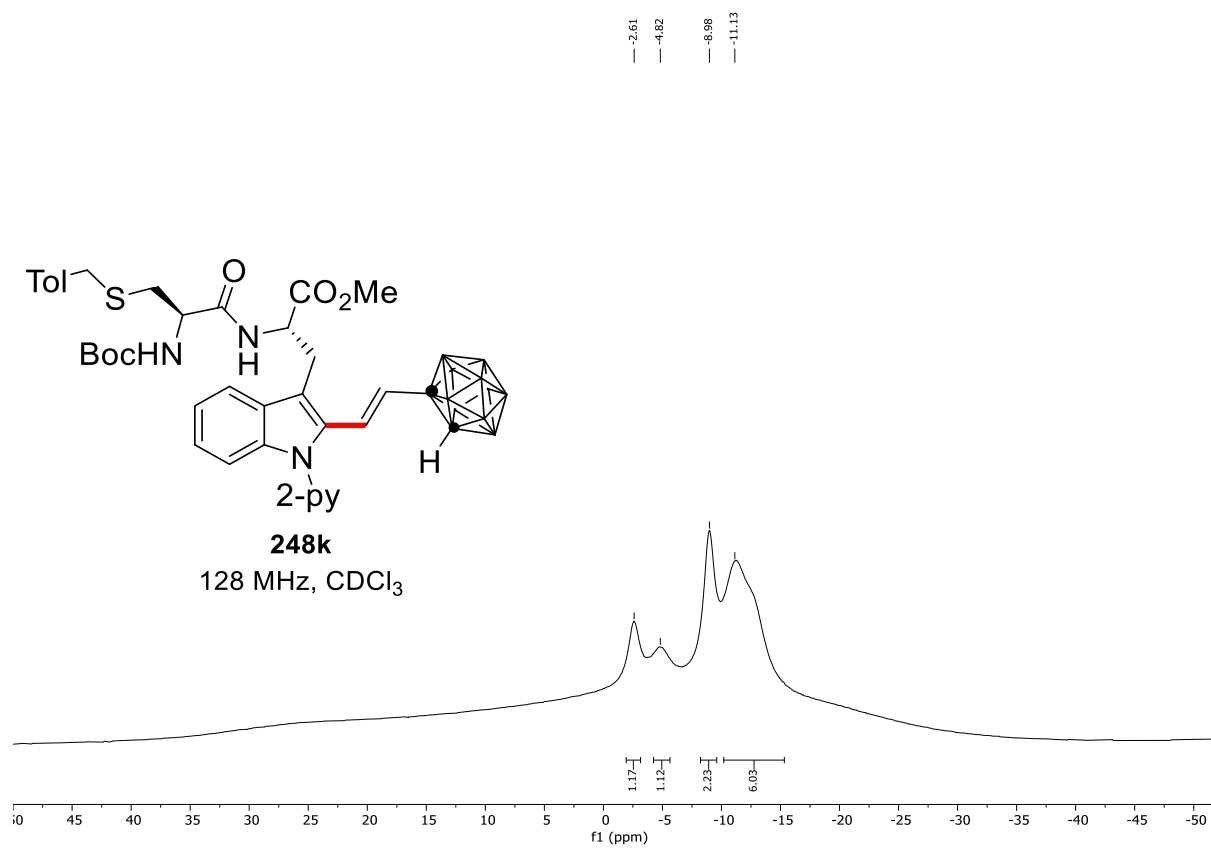
7. NMR Spectra



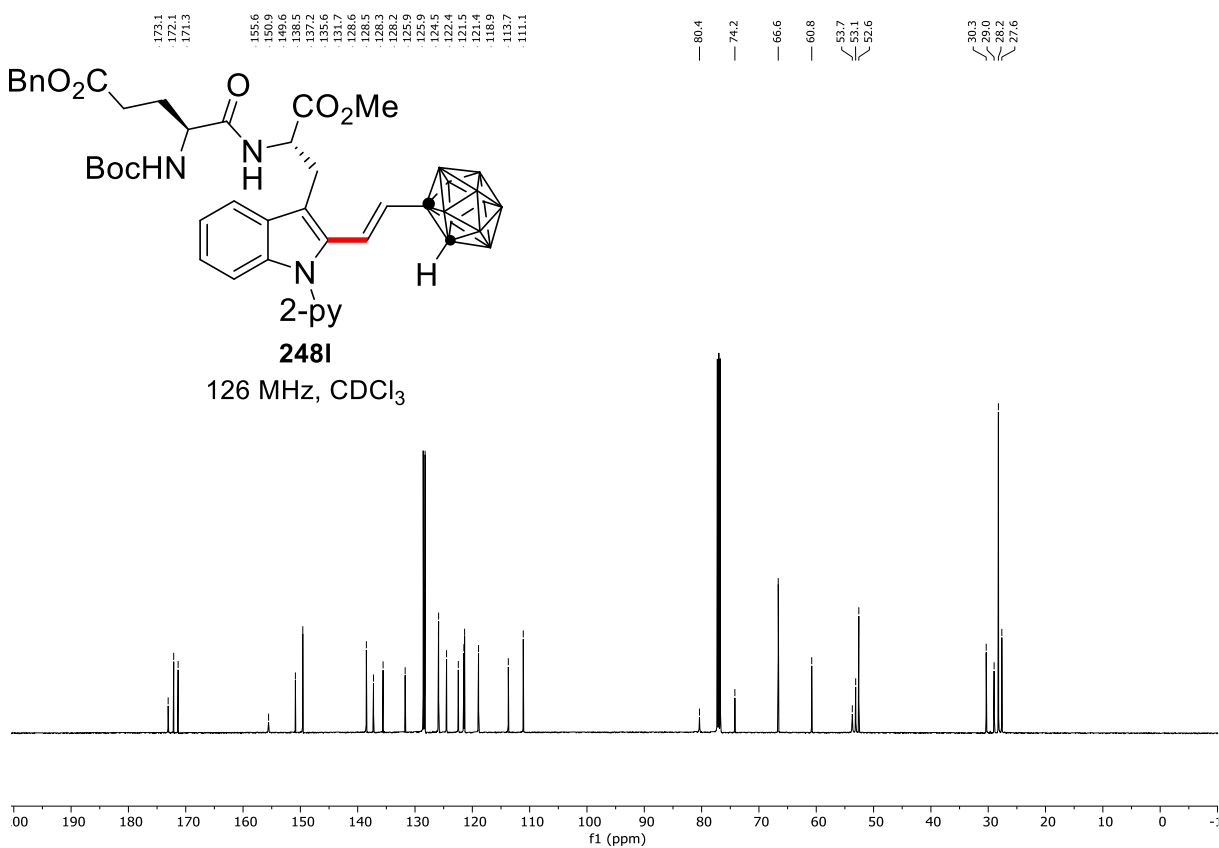
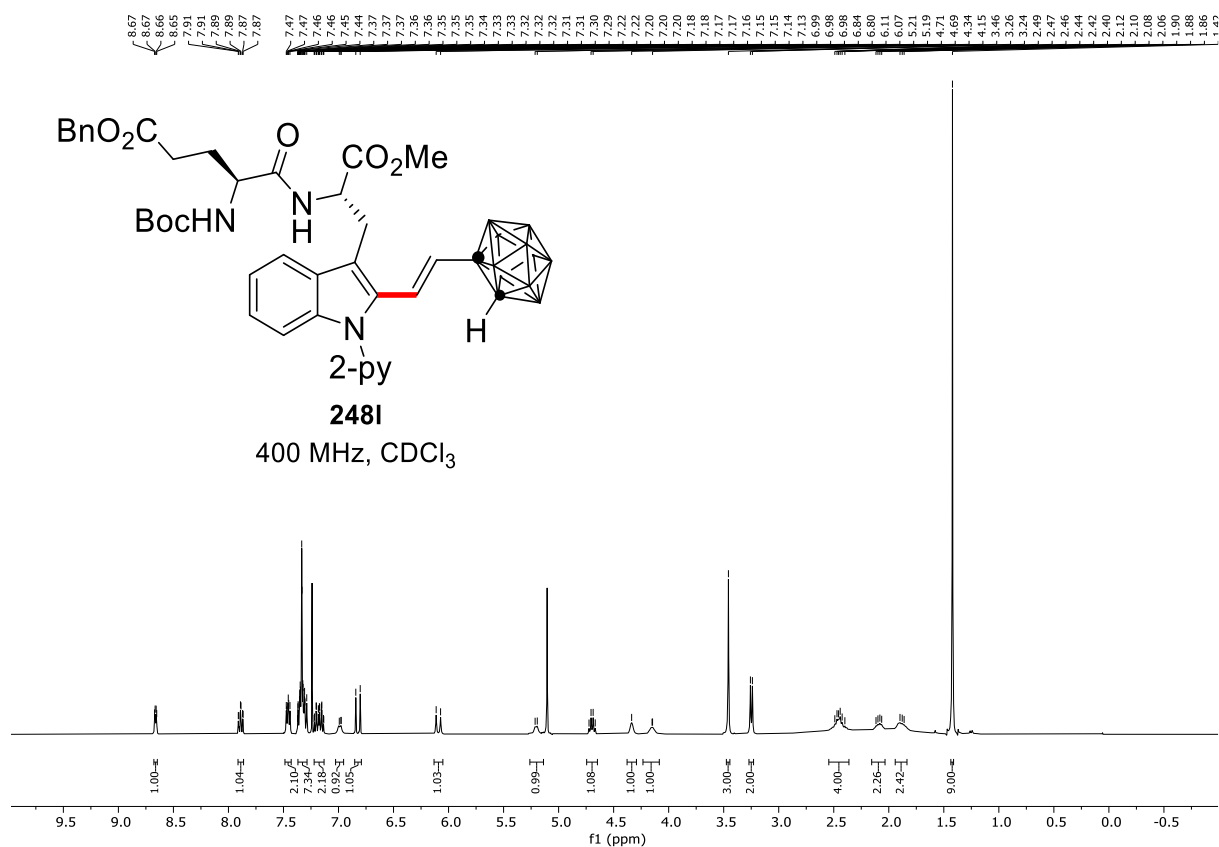
7. NMR Spectra



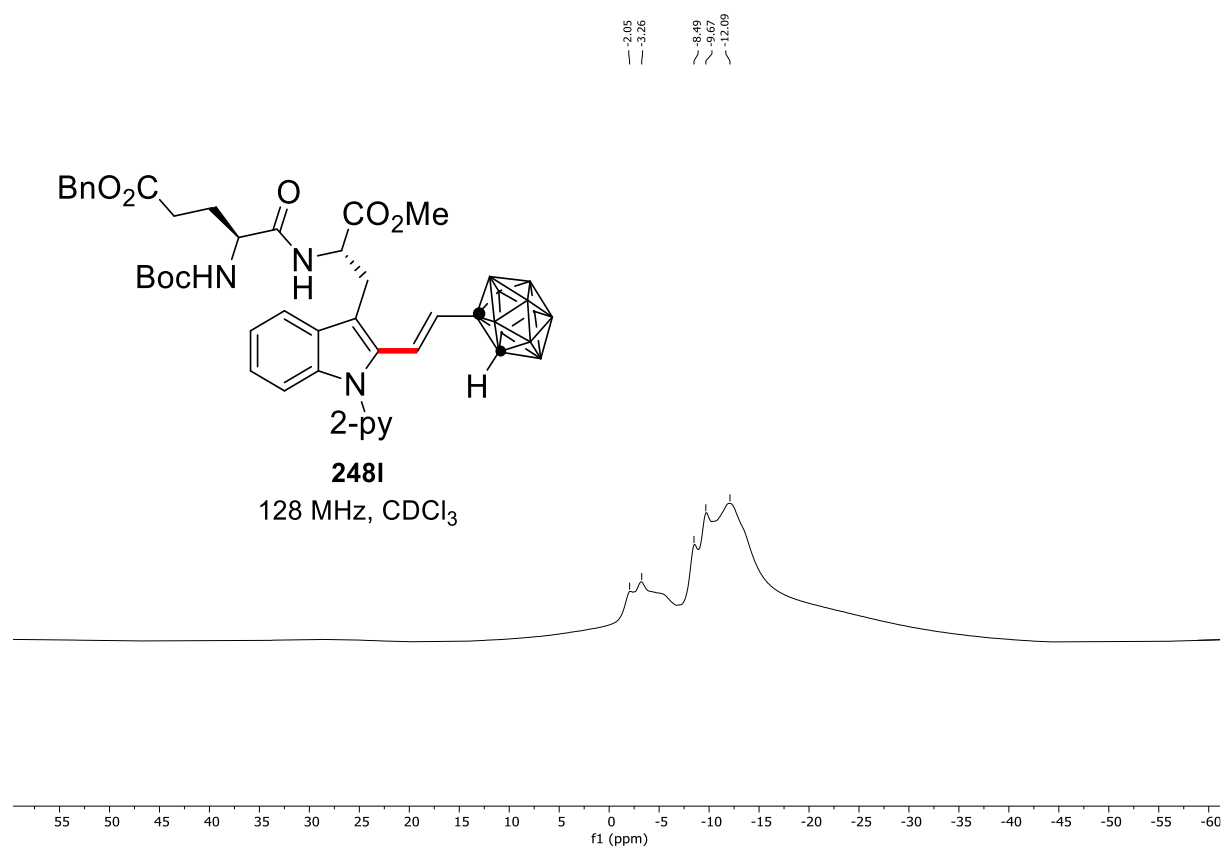
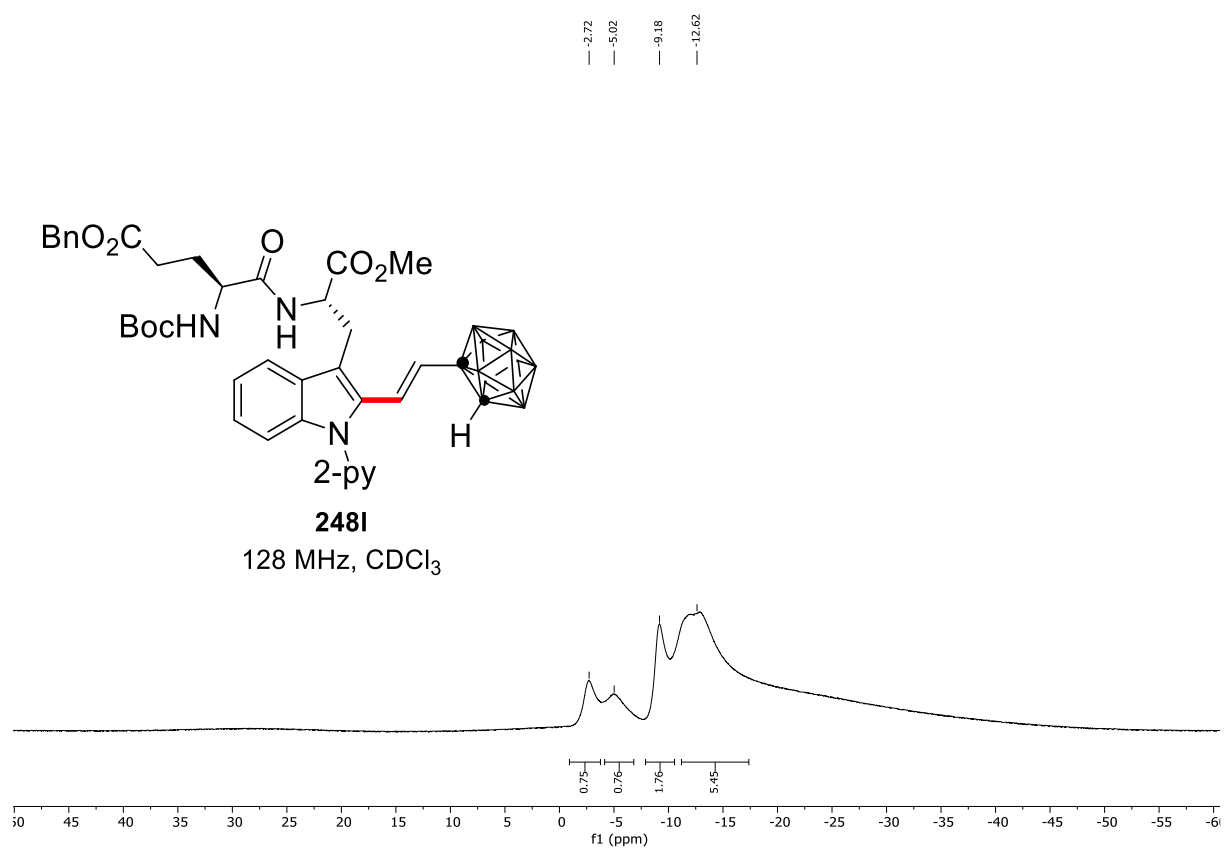
7. NMR Spectra

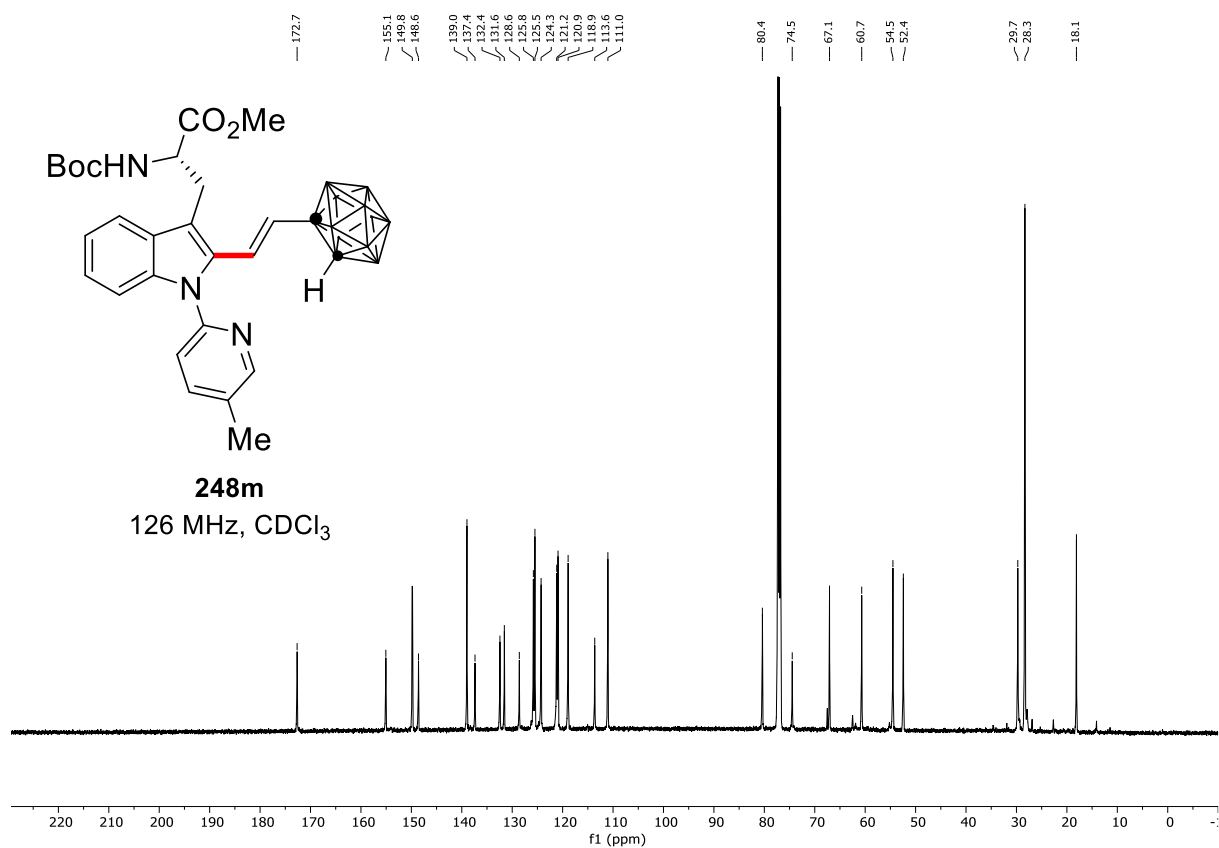


7. NMR Spectra

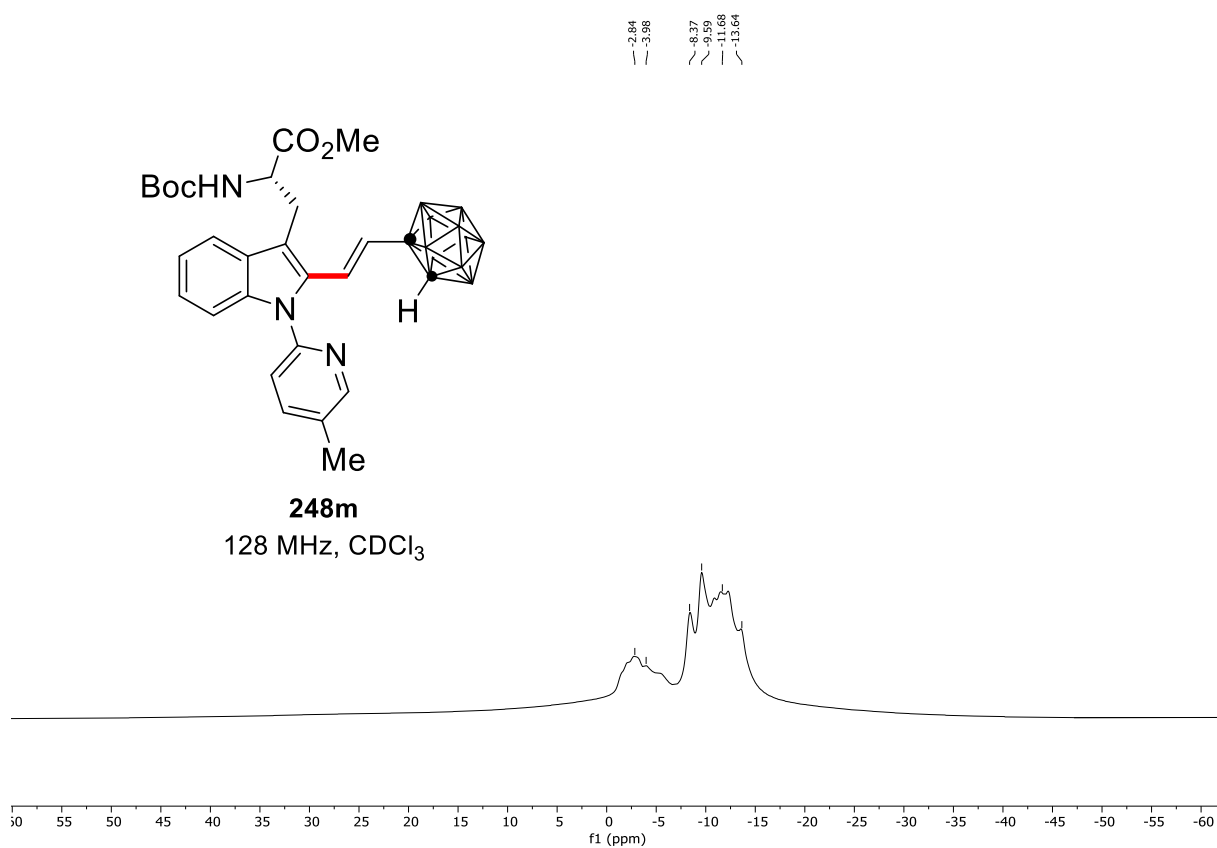
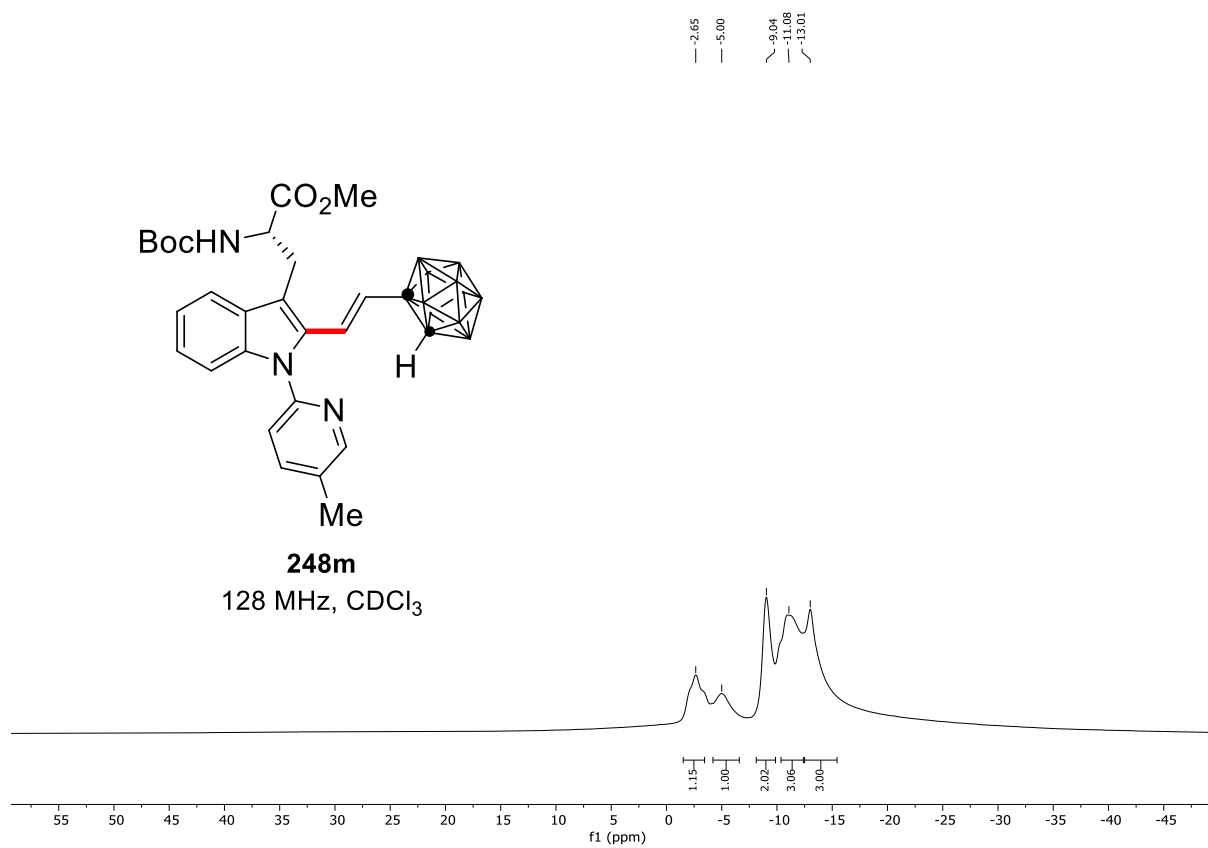


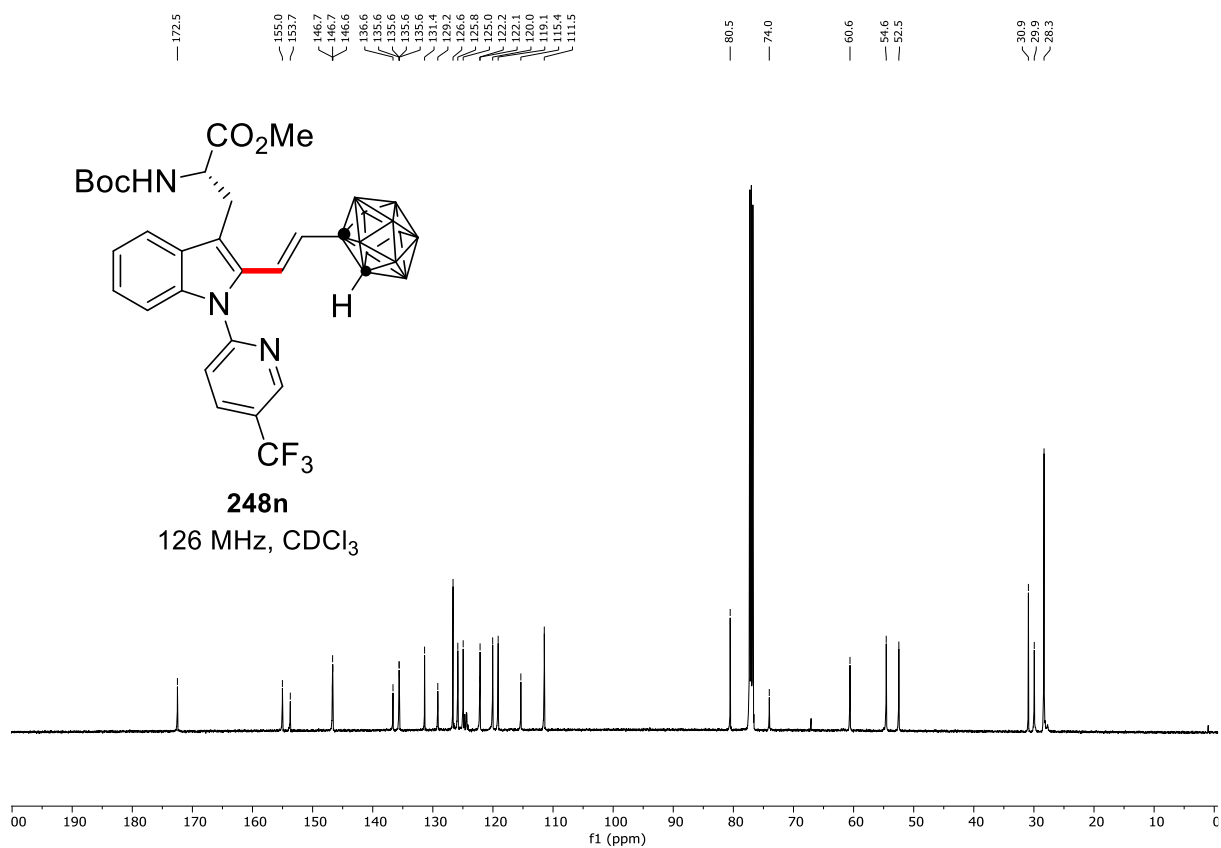
7. NMR Spectra



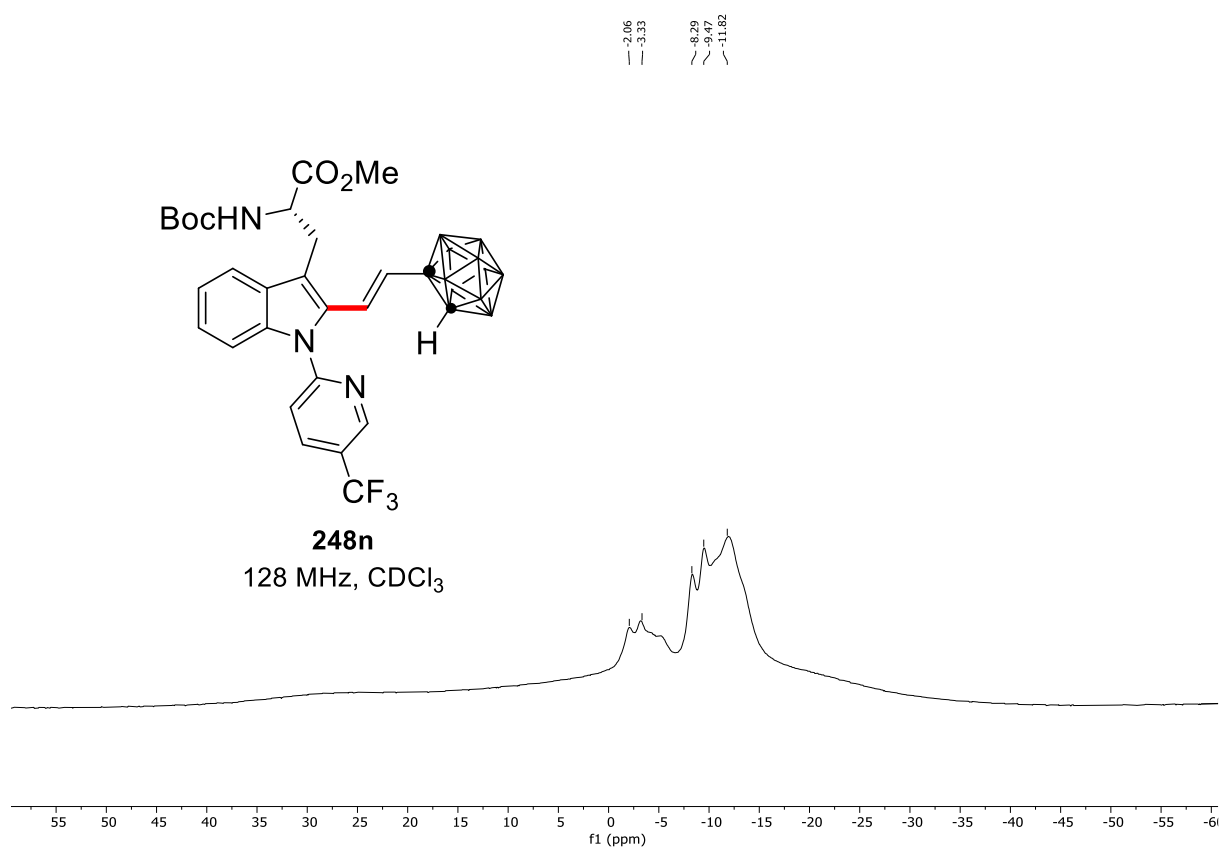
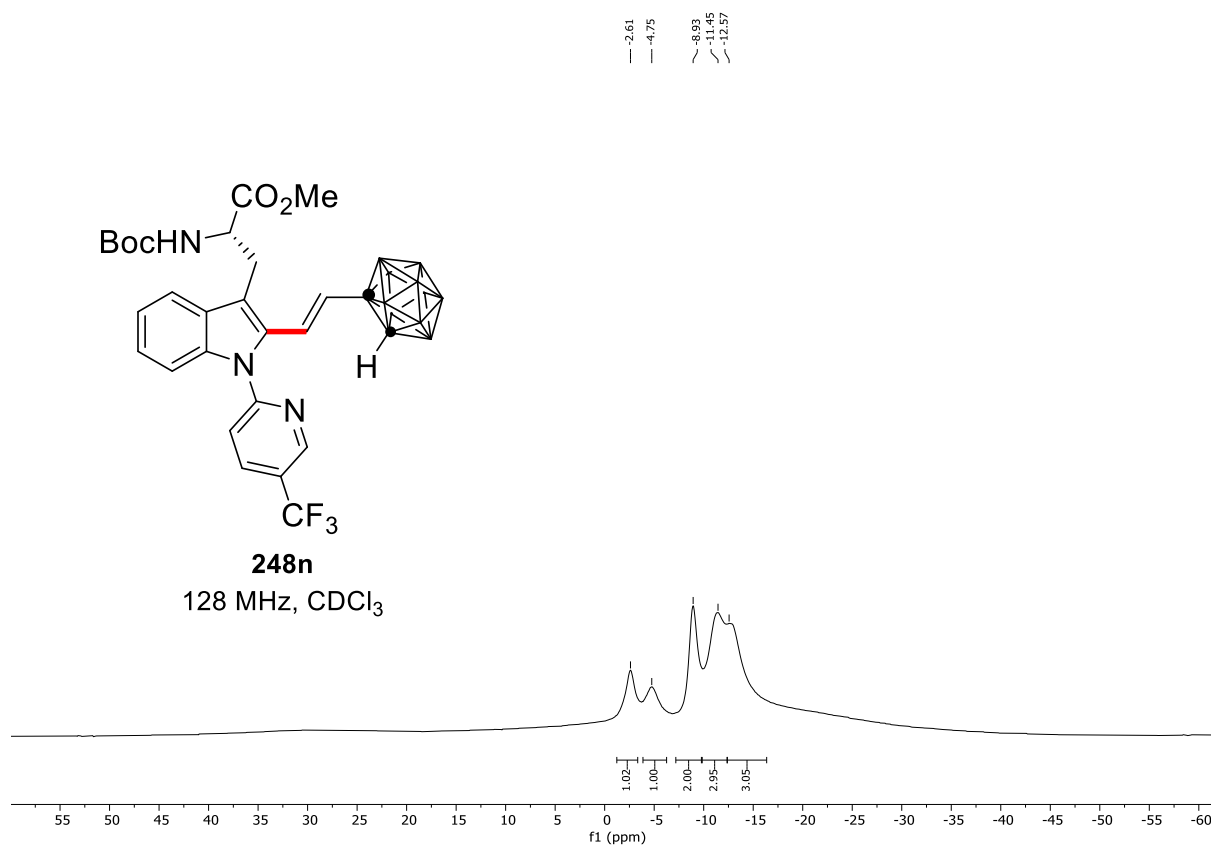


7. NMR Spectra

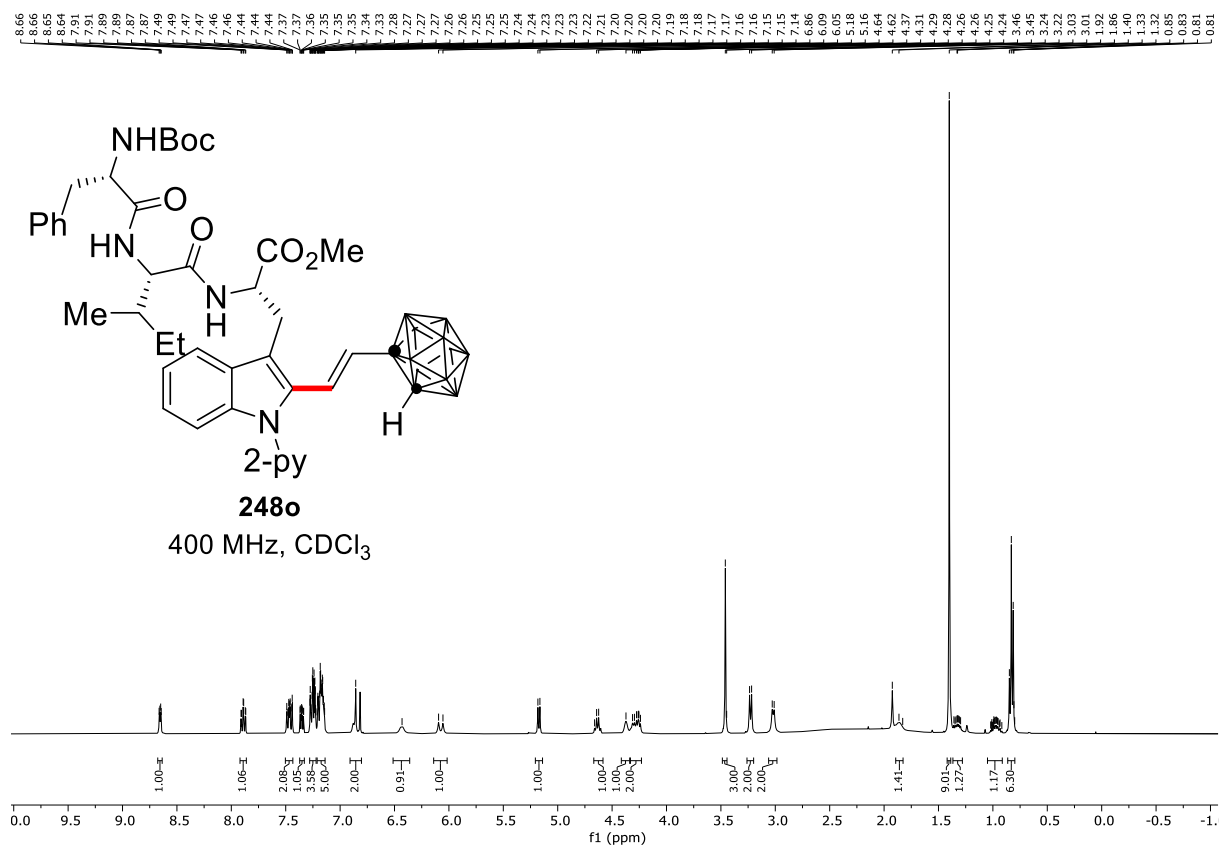
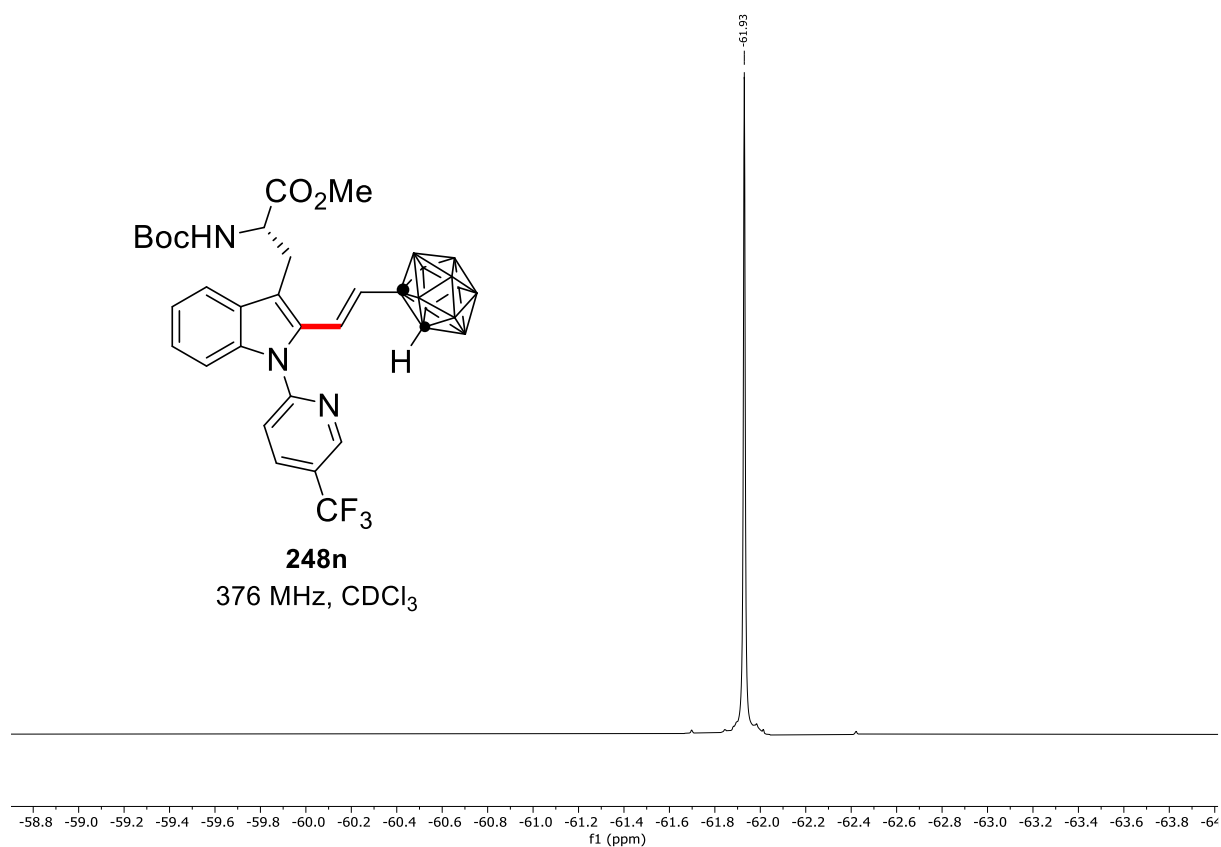


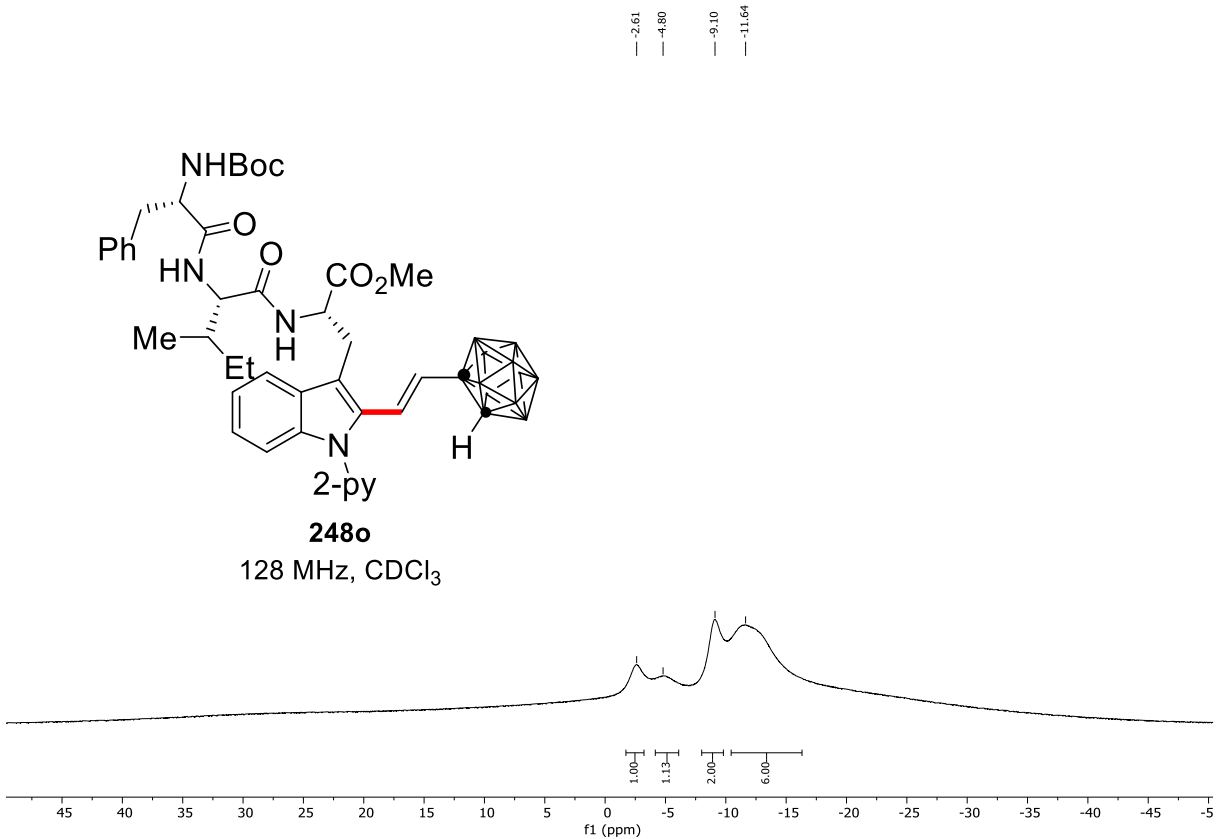


7. NMR Spectra

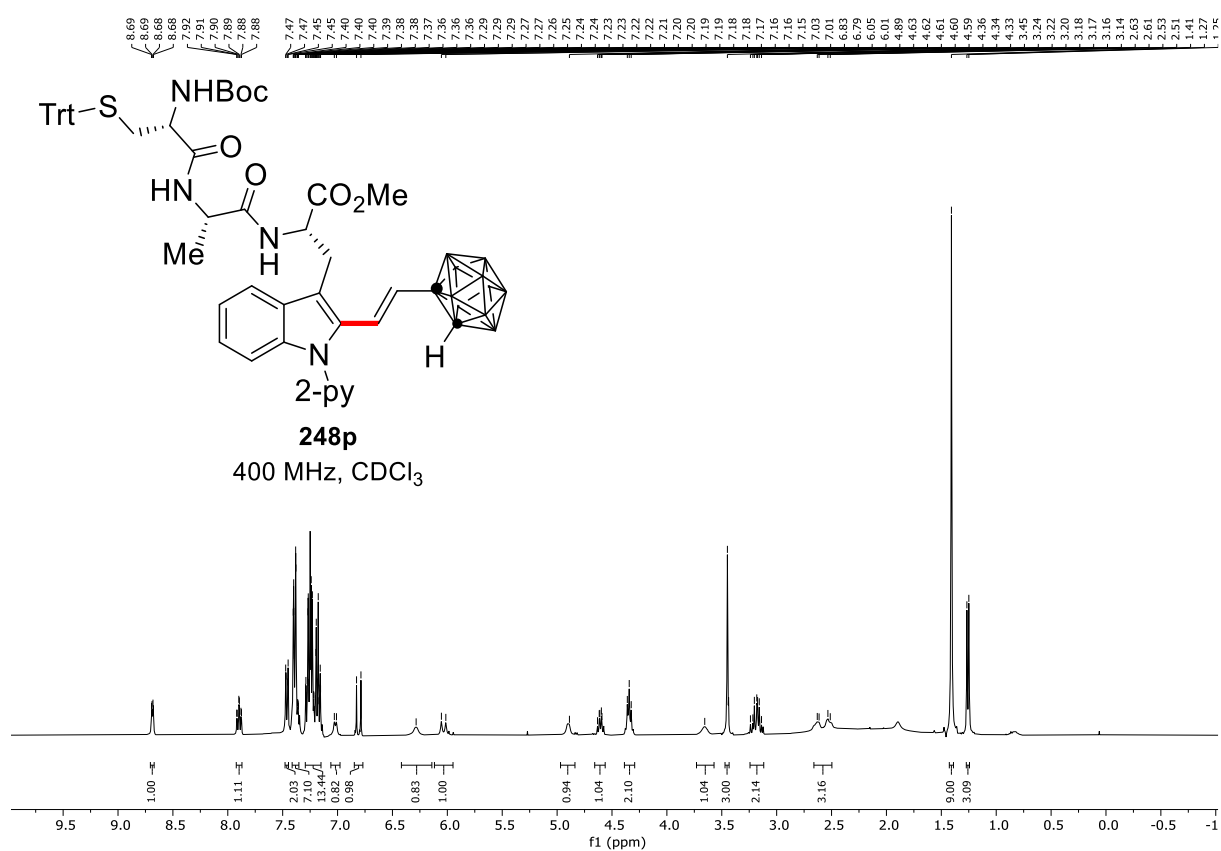
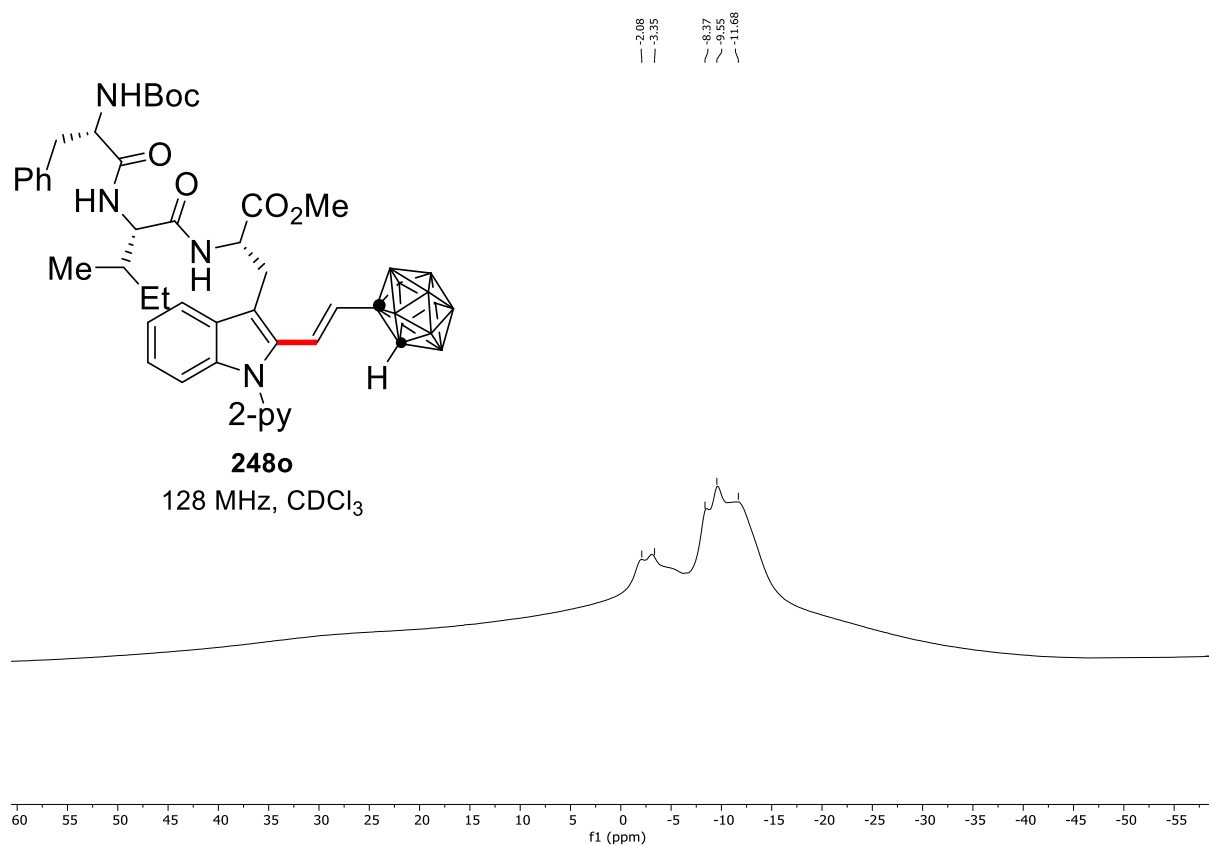


7. NMR Spectra

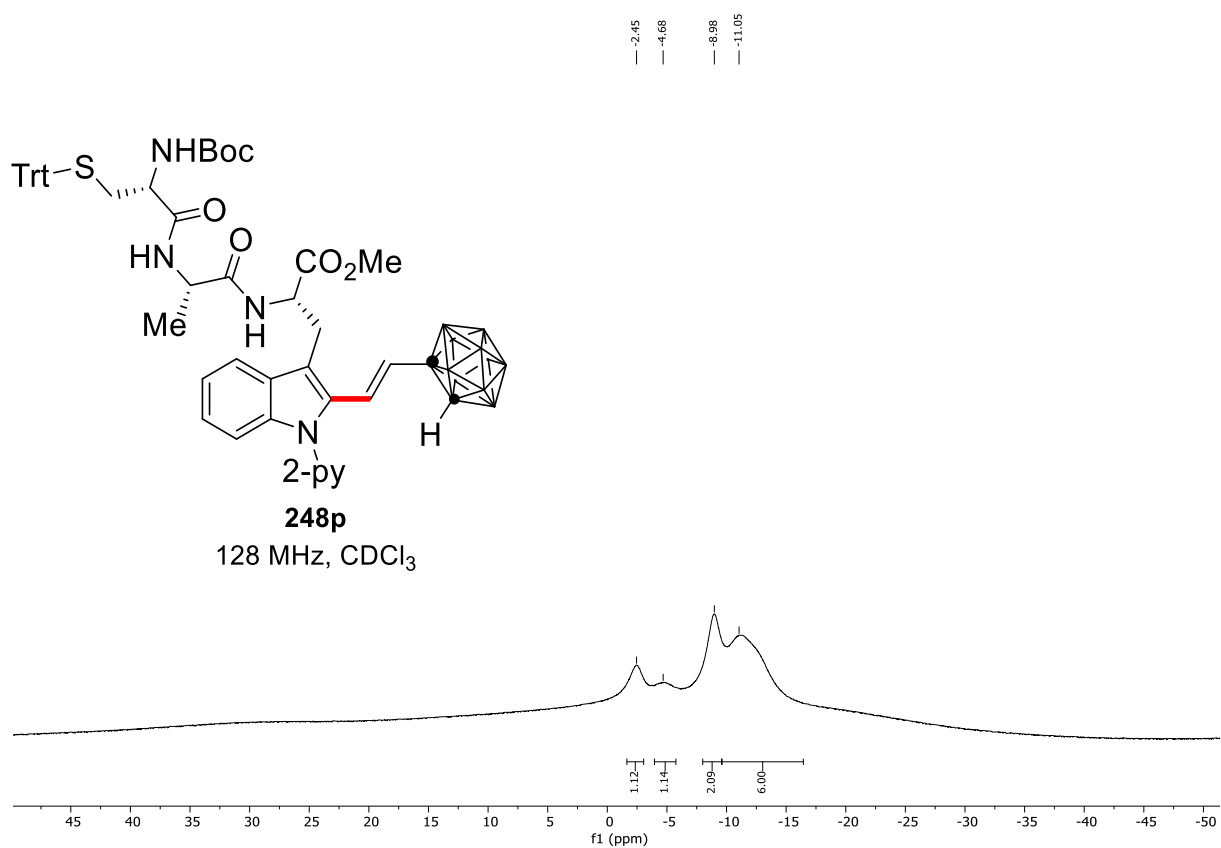
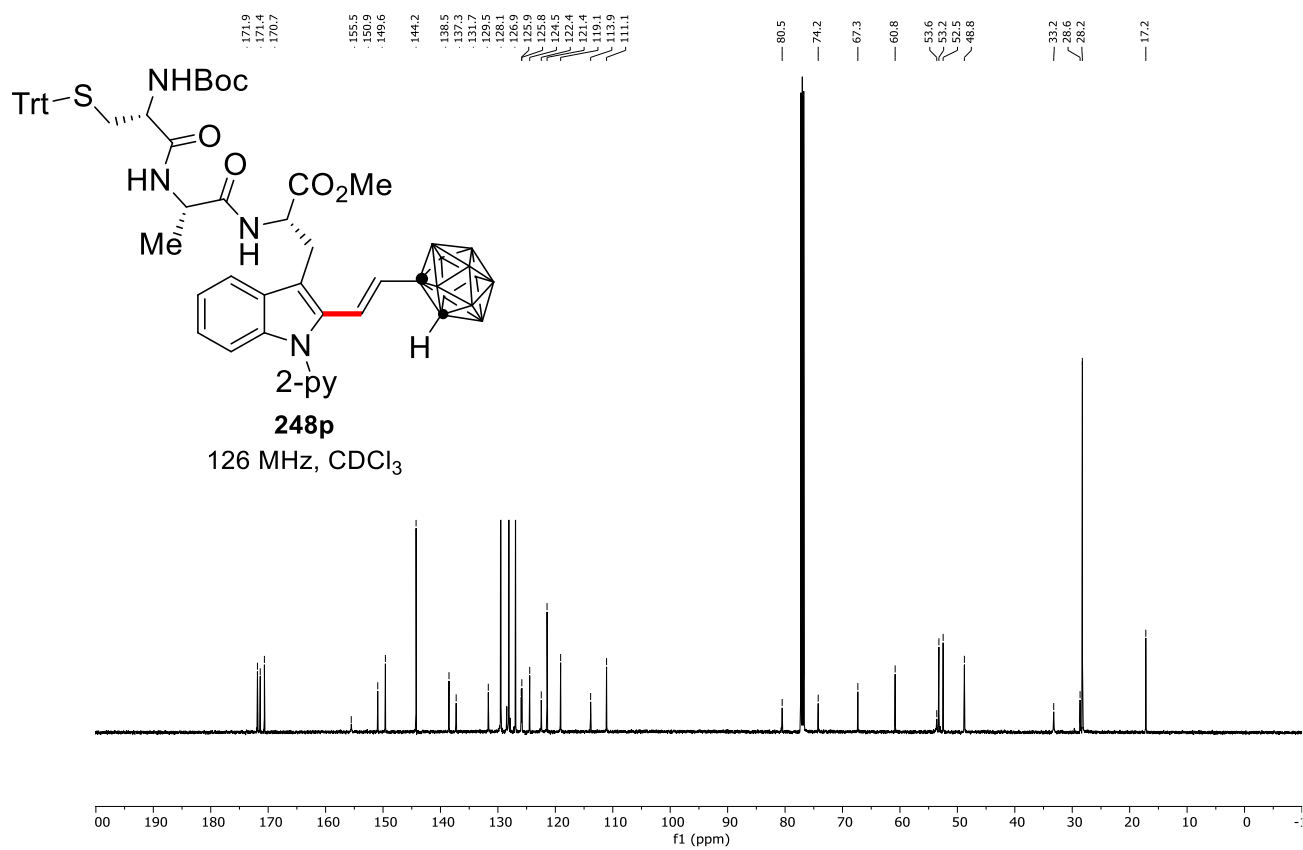




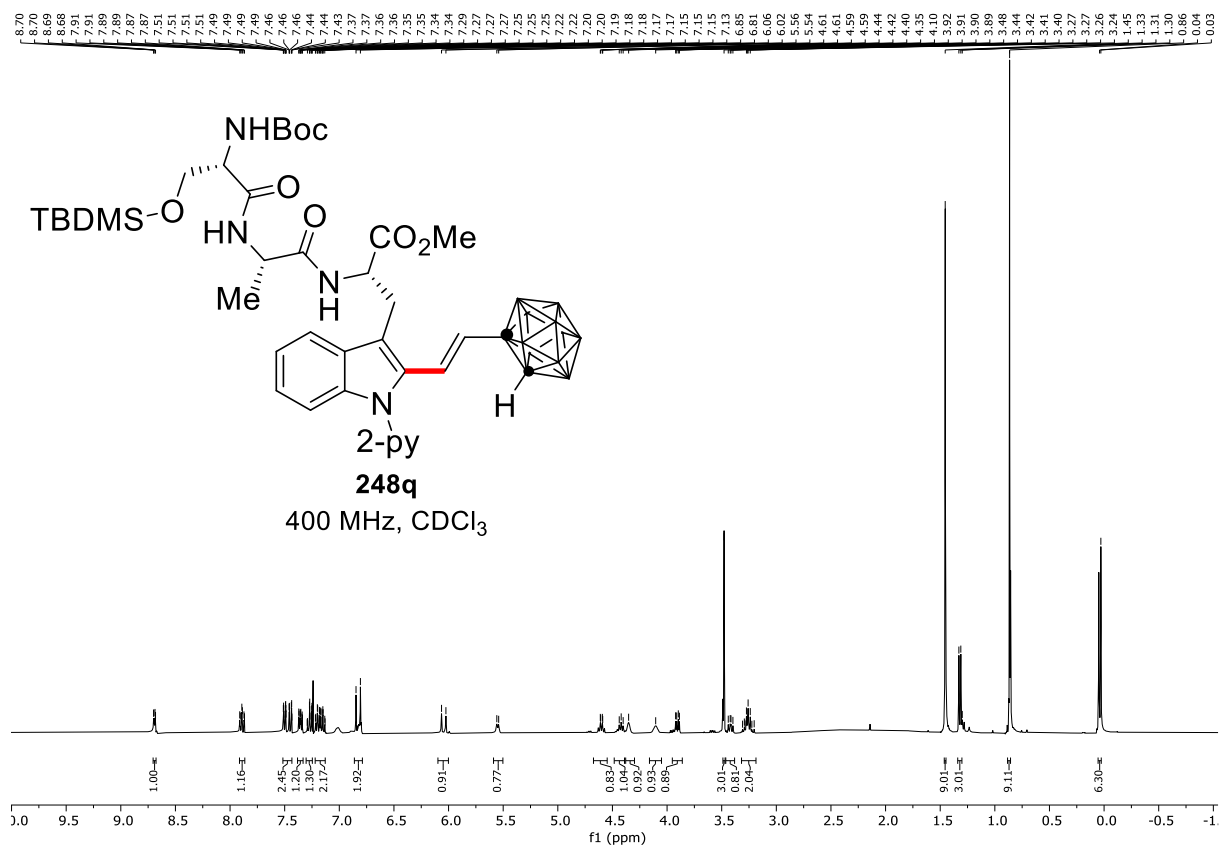
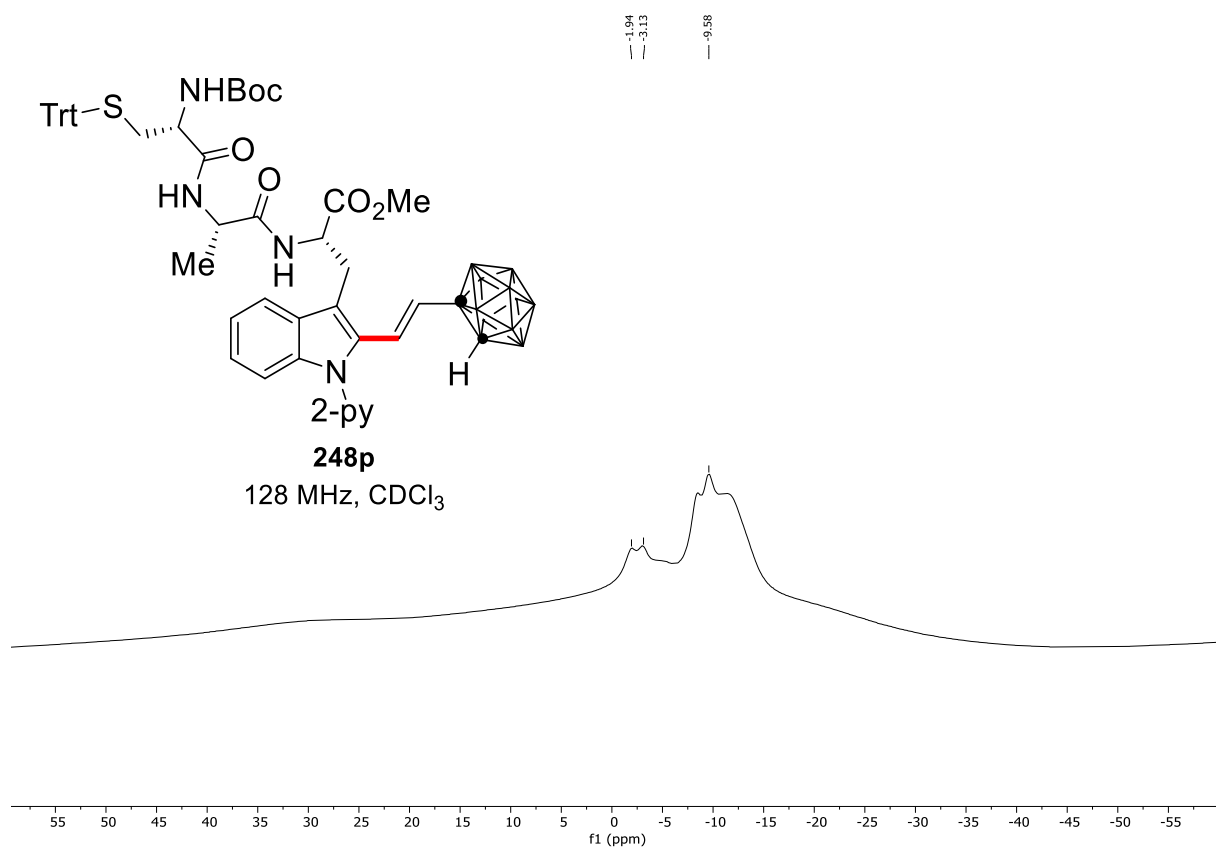
7. NMR Spectra

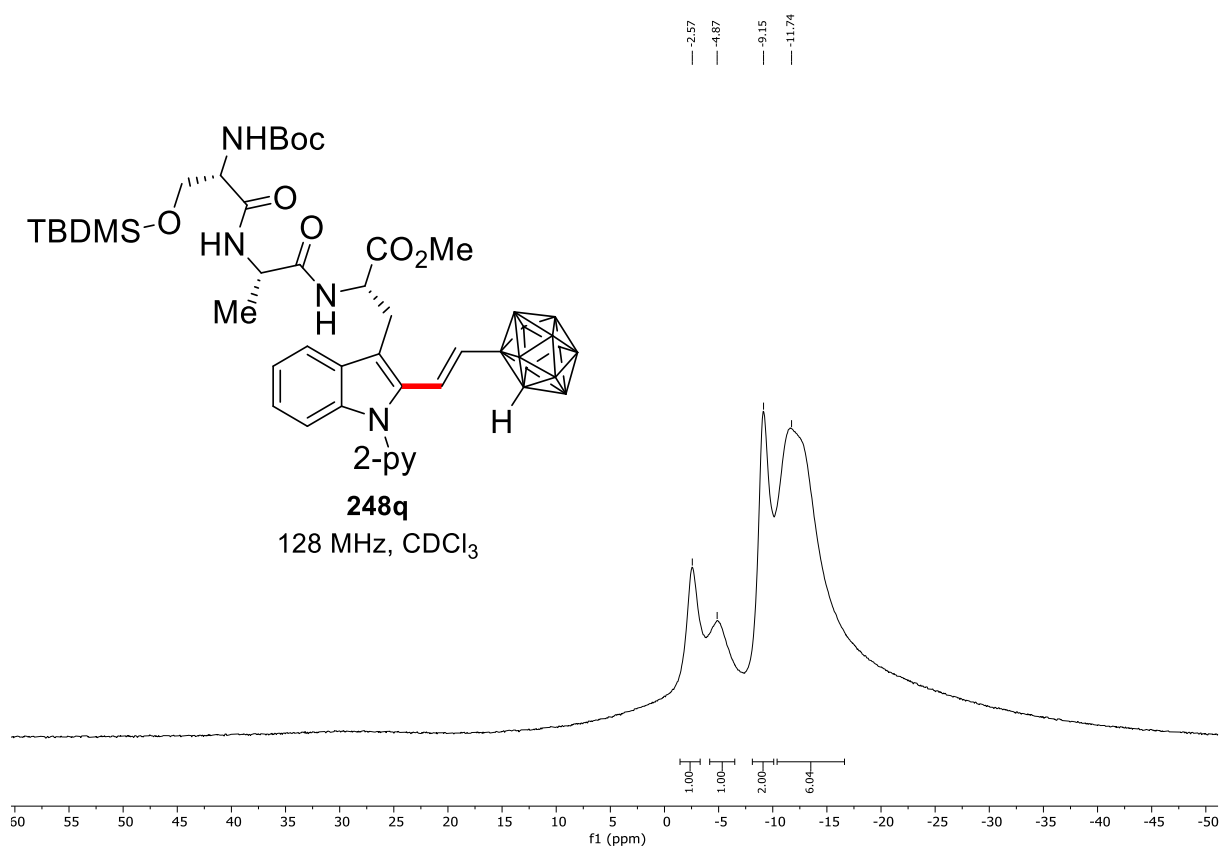


7. NMR Spectra

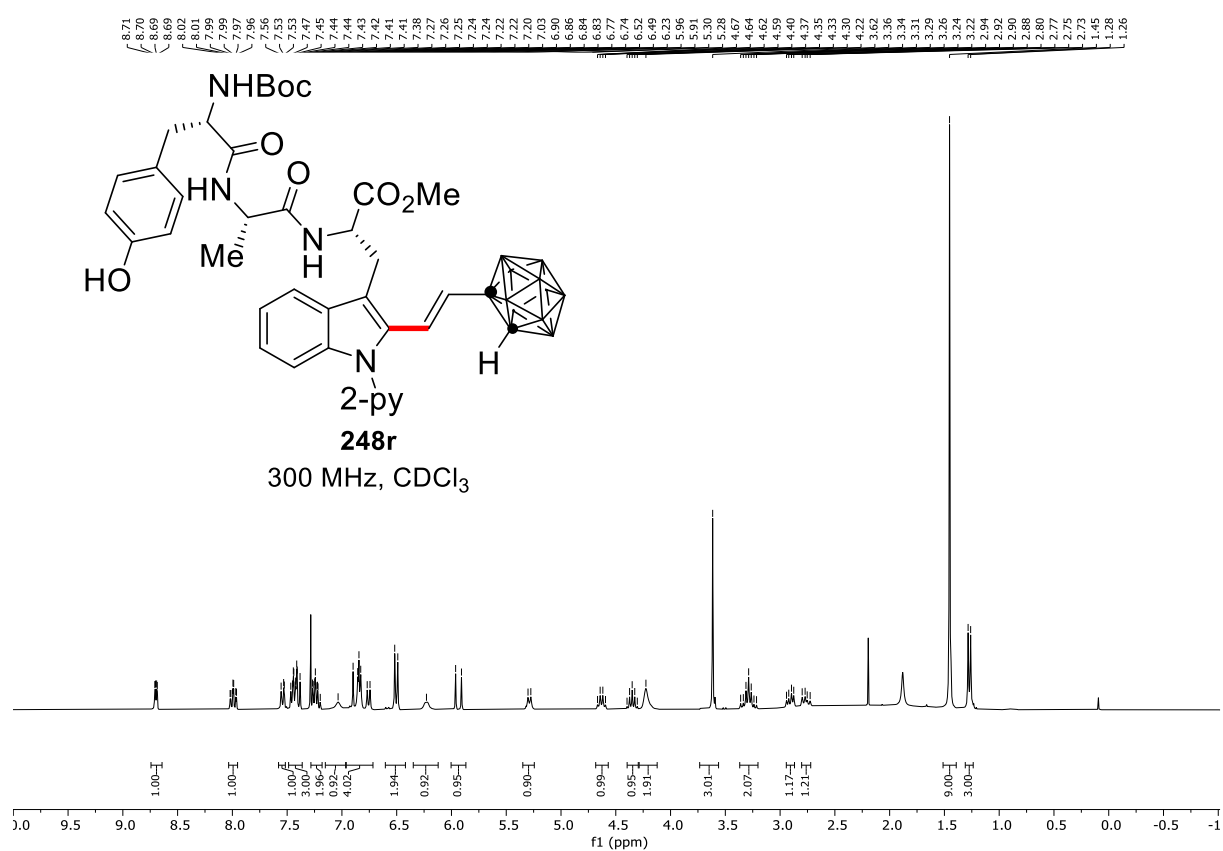
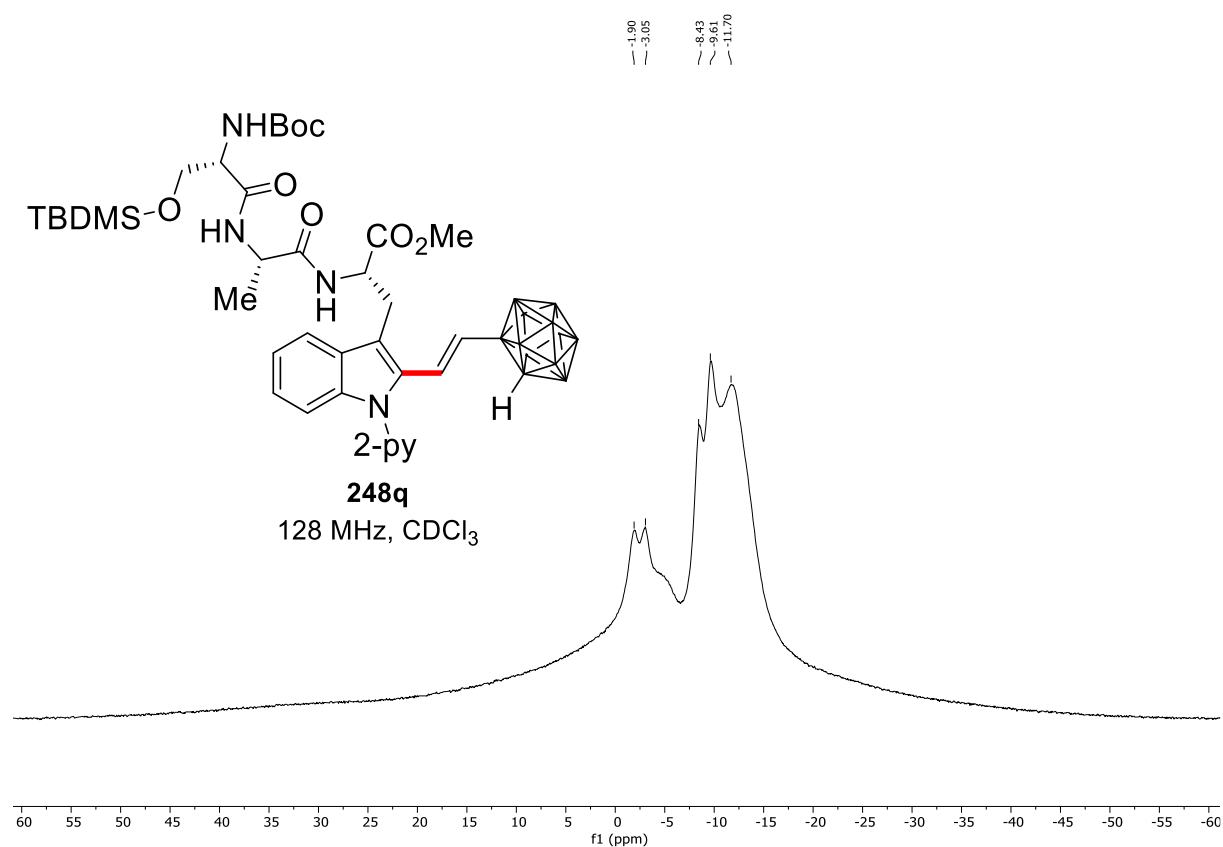


7. NMR Spectra

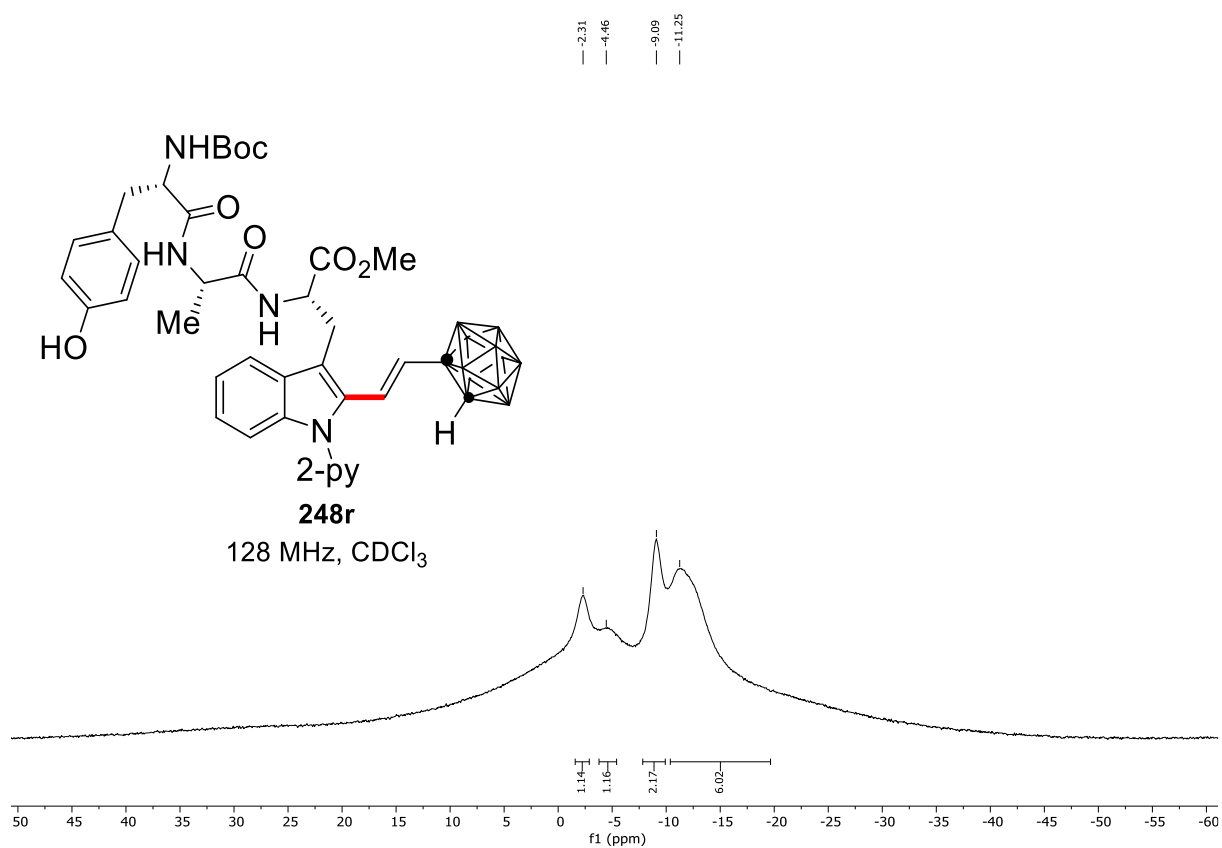
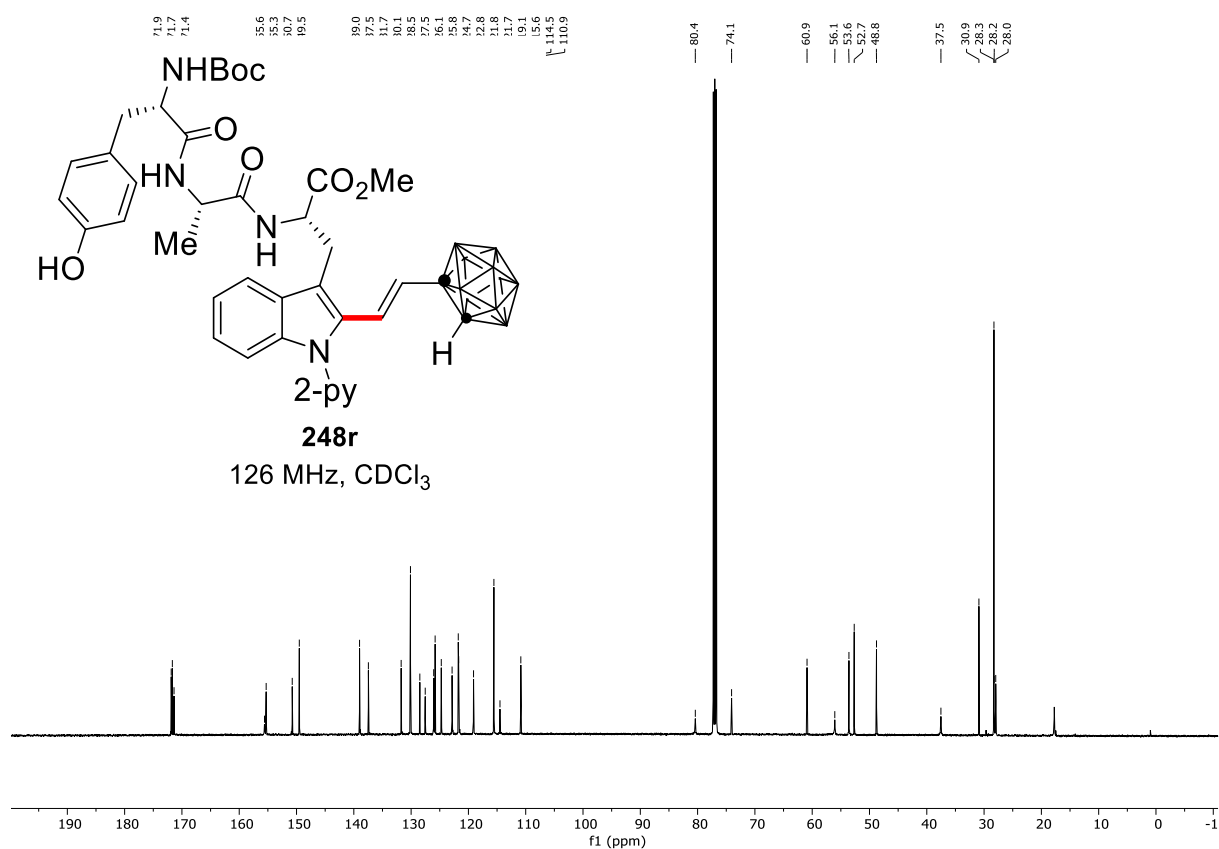




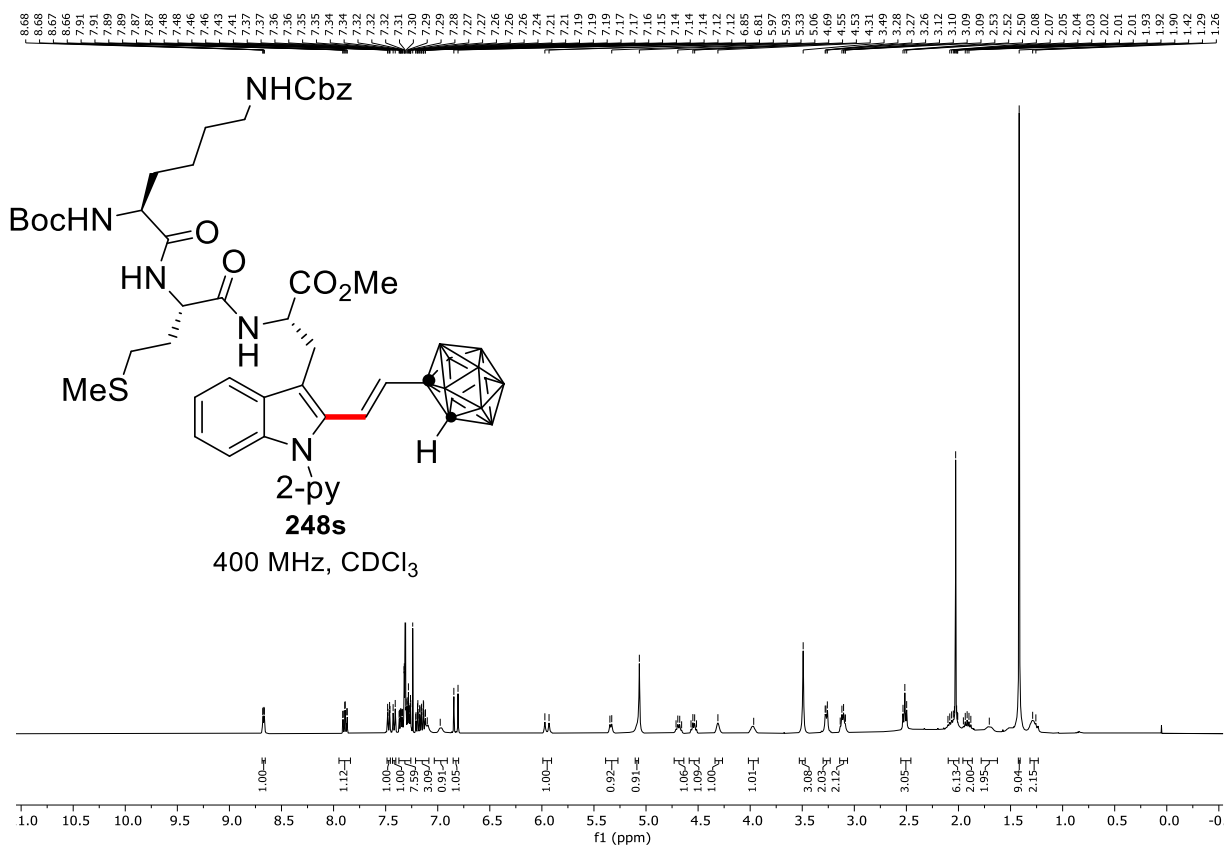
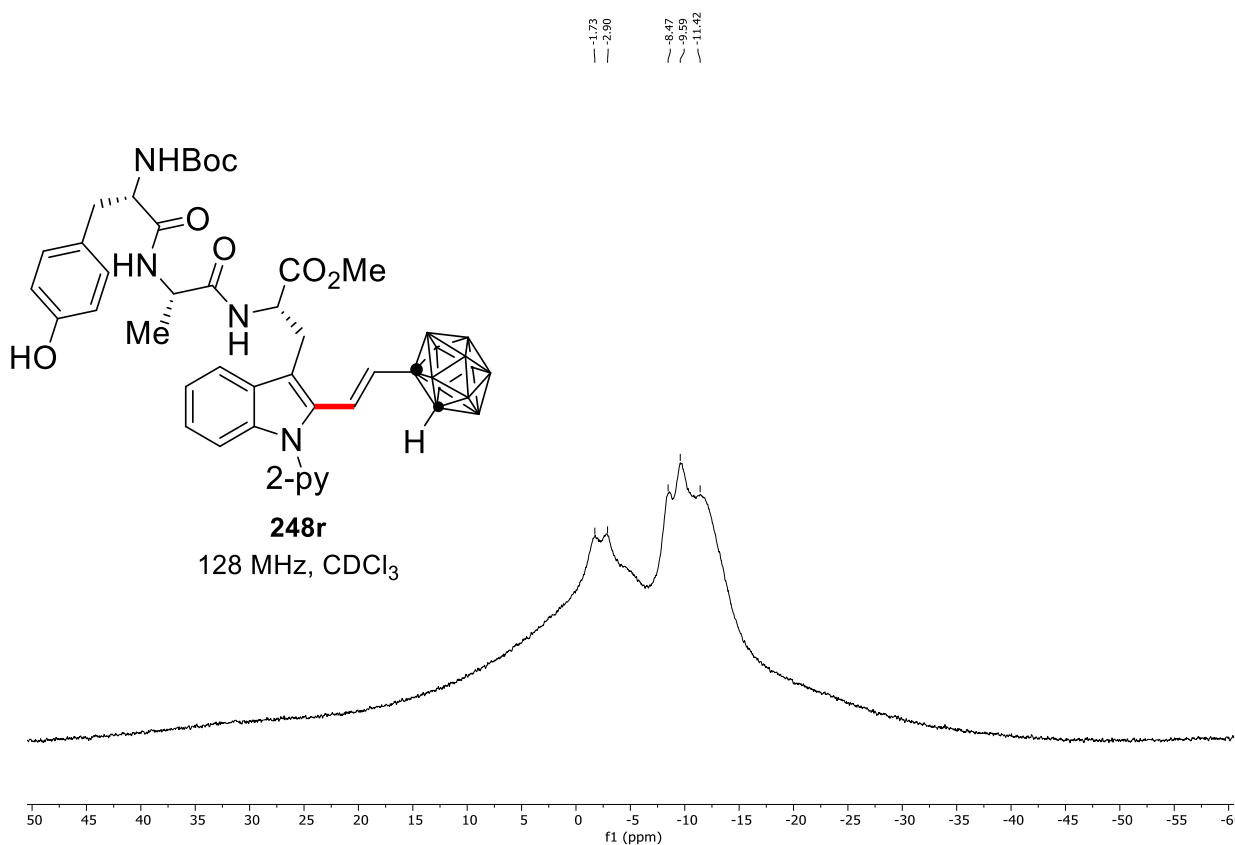
7. NMR Spectra



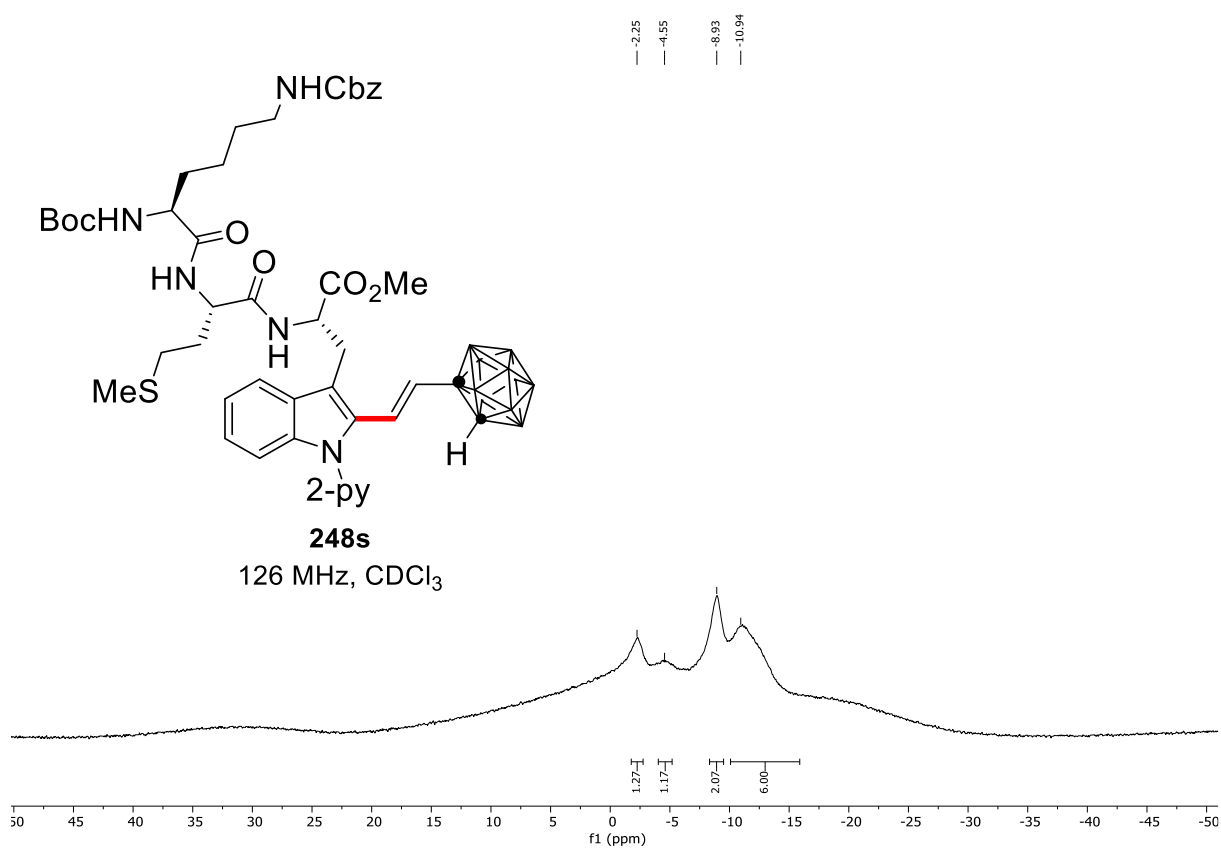
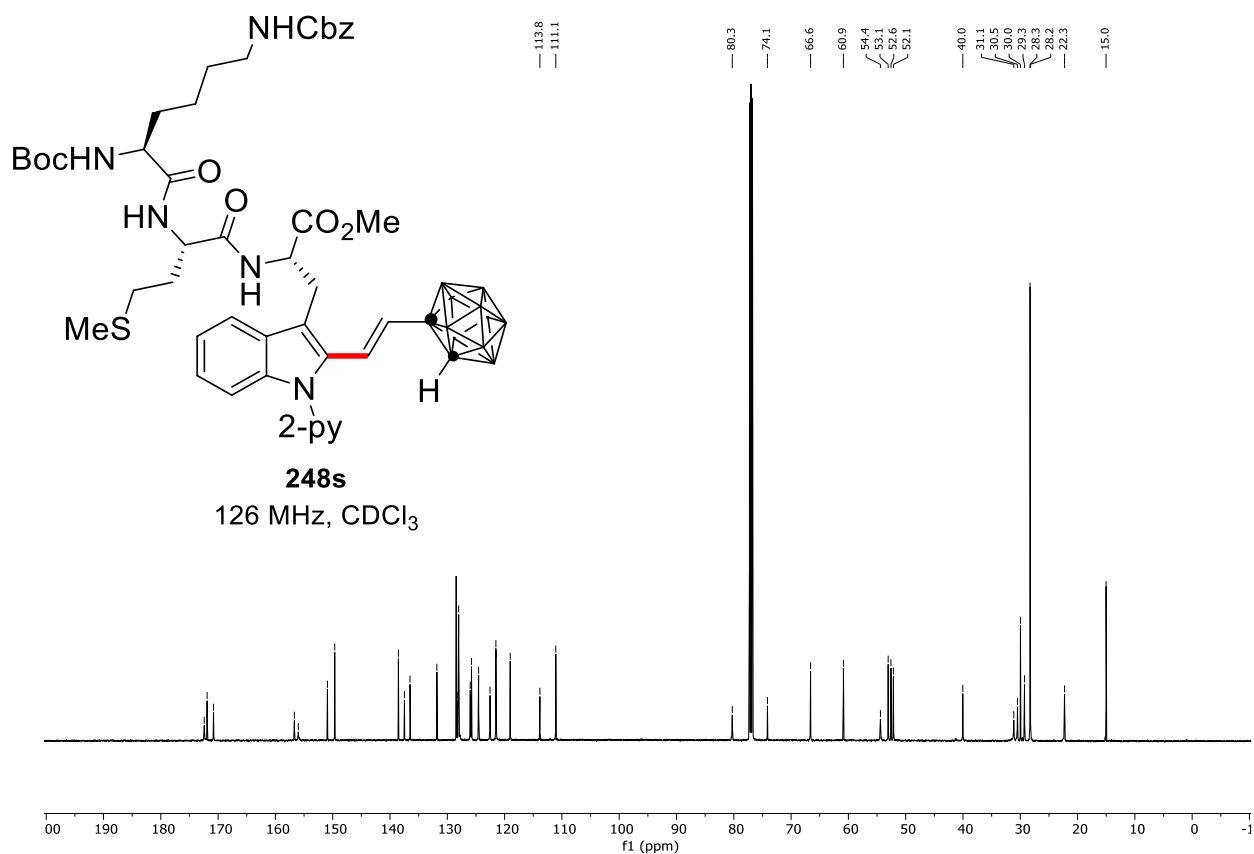
7. NMR Spectra

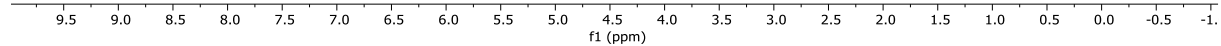
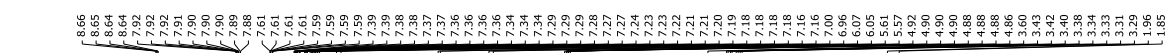


7. NMR Spectra

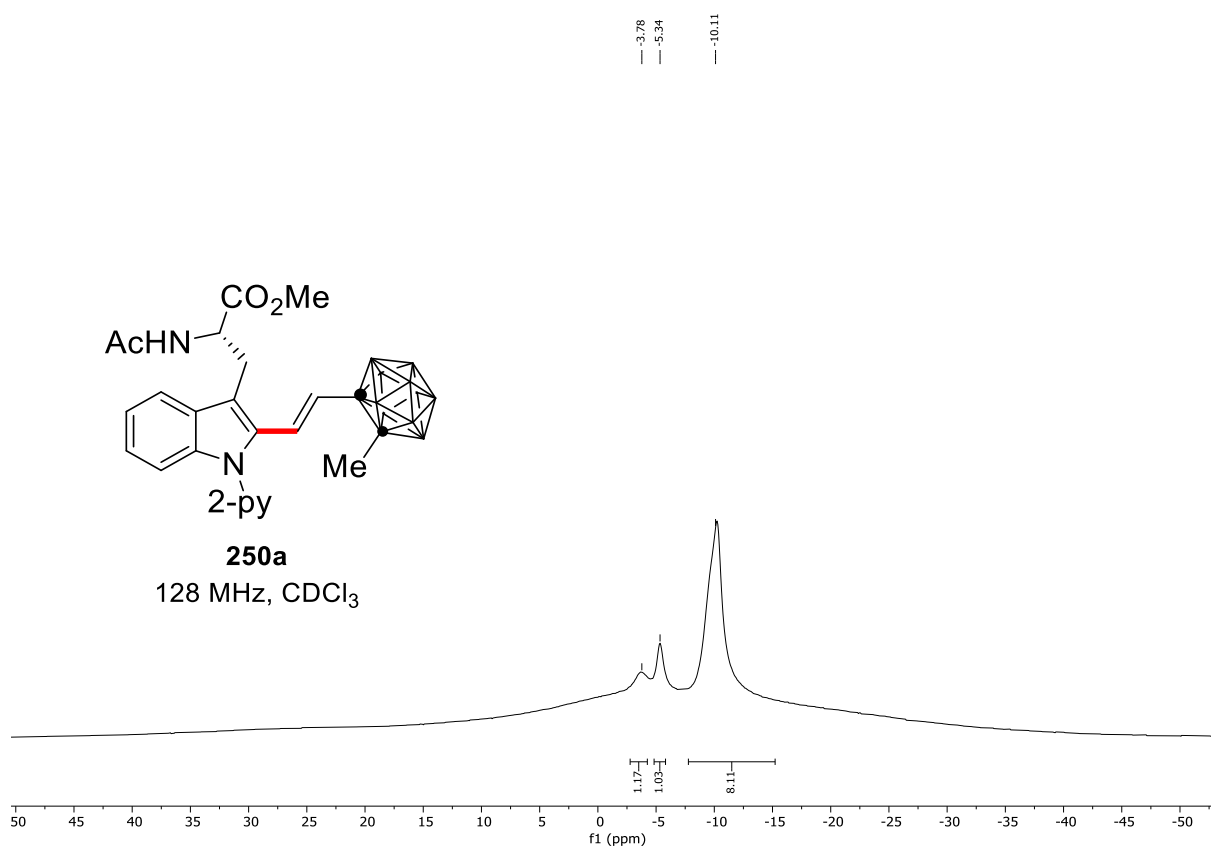
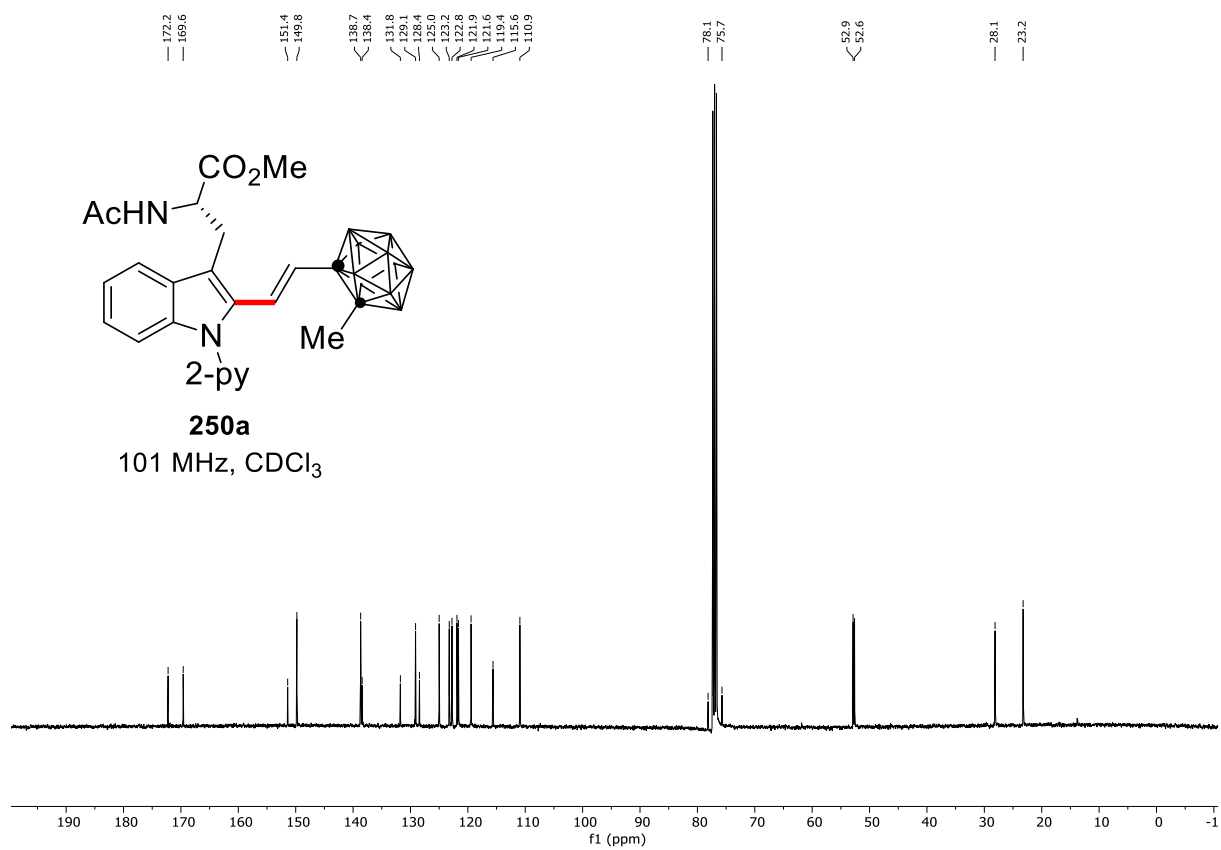


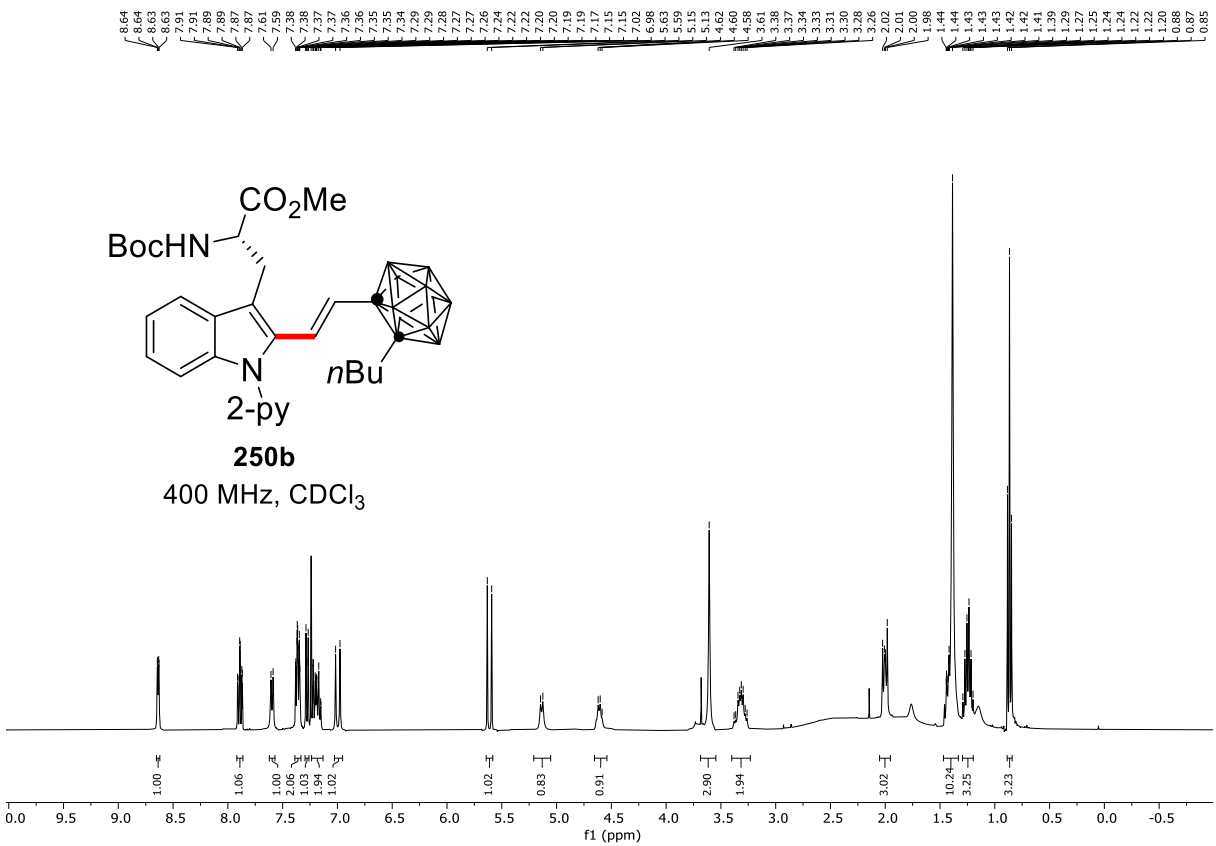
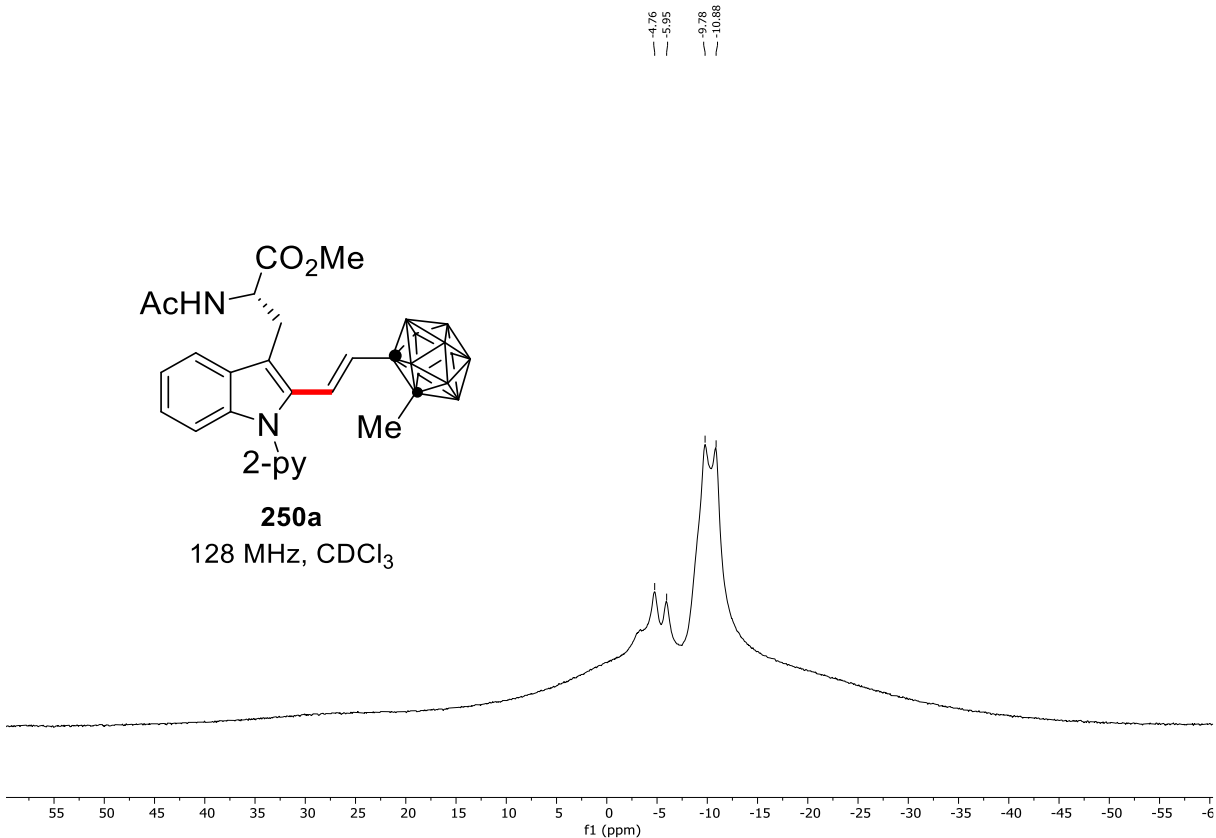
7. NMR Spectra



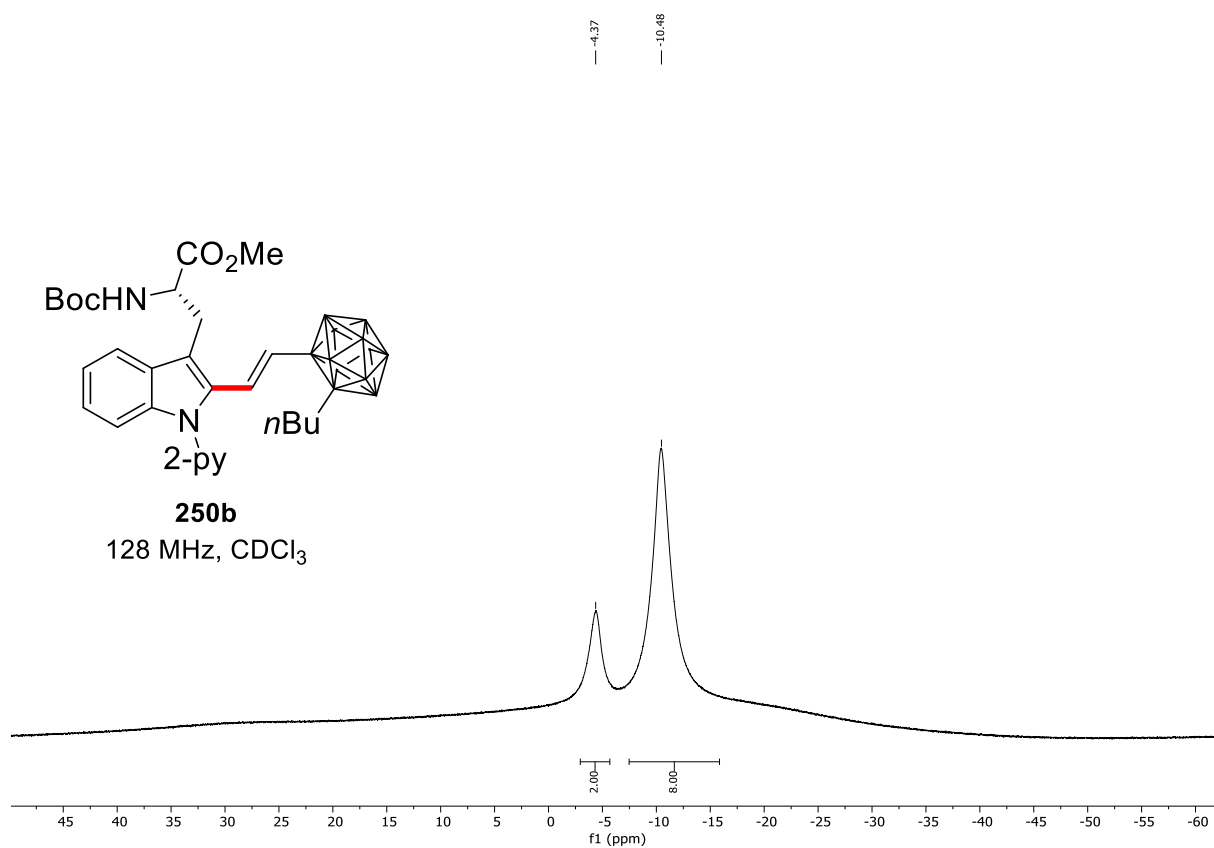
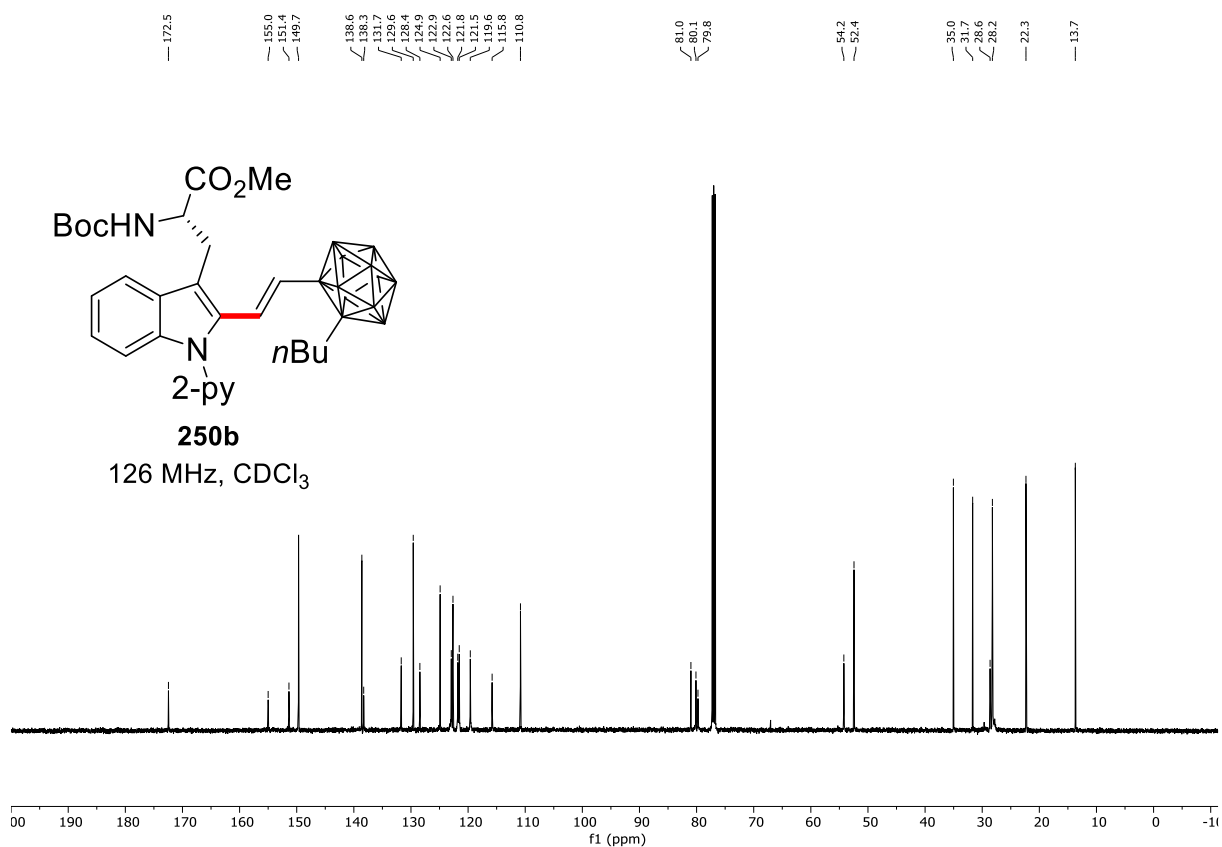


7. NMR Spectra

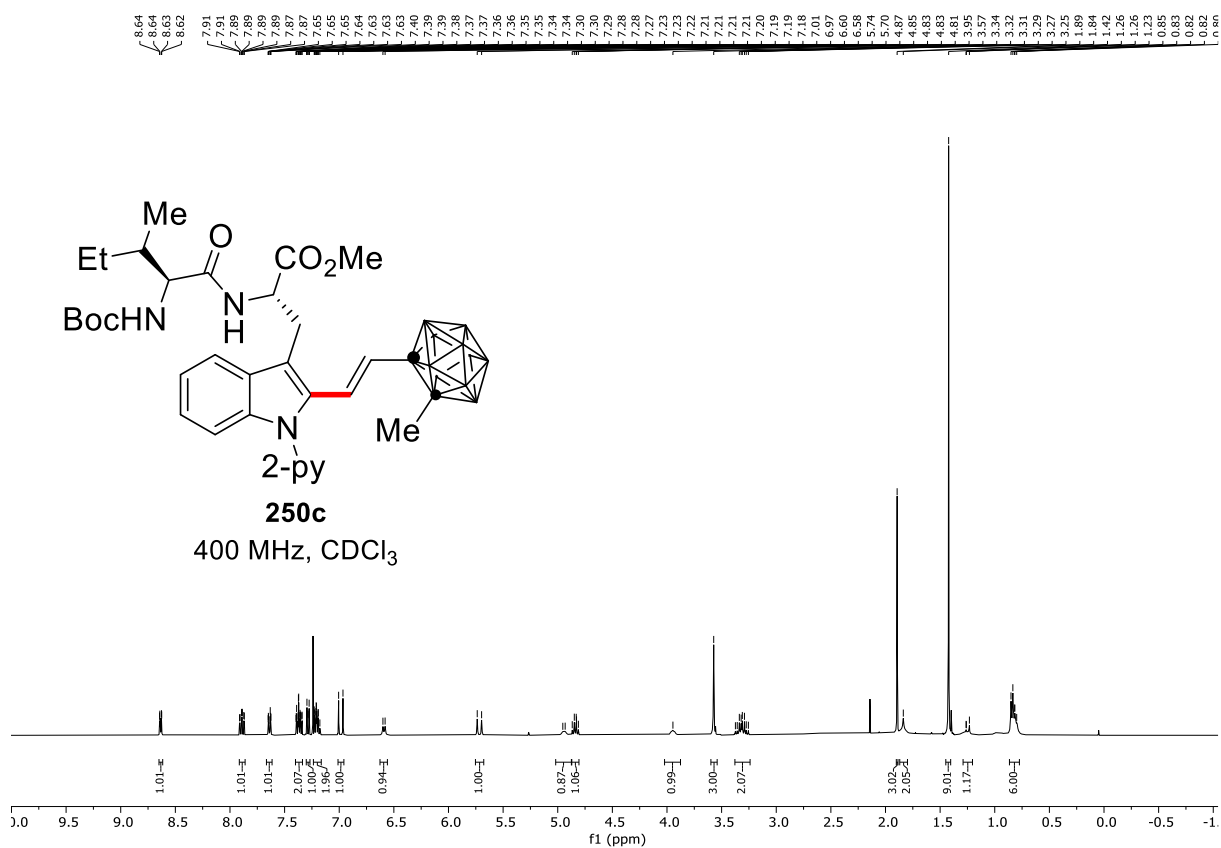
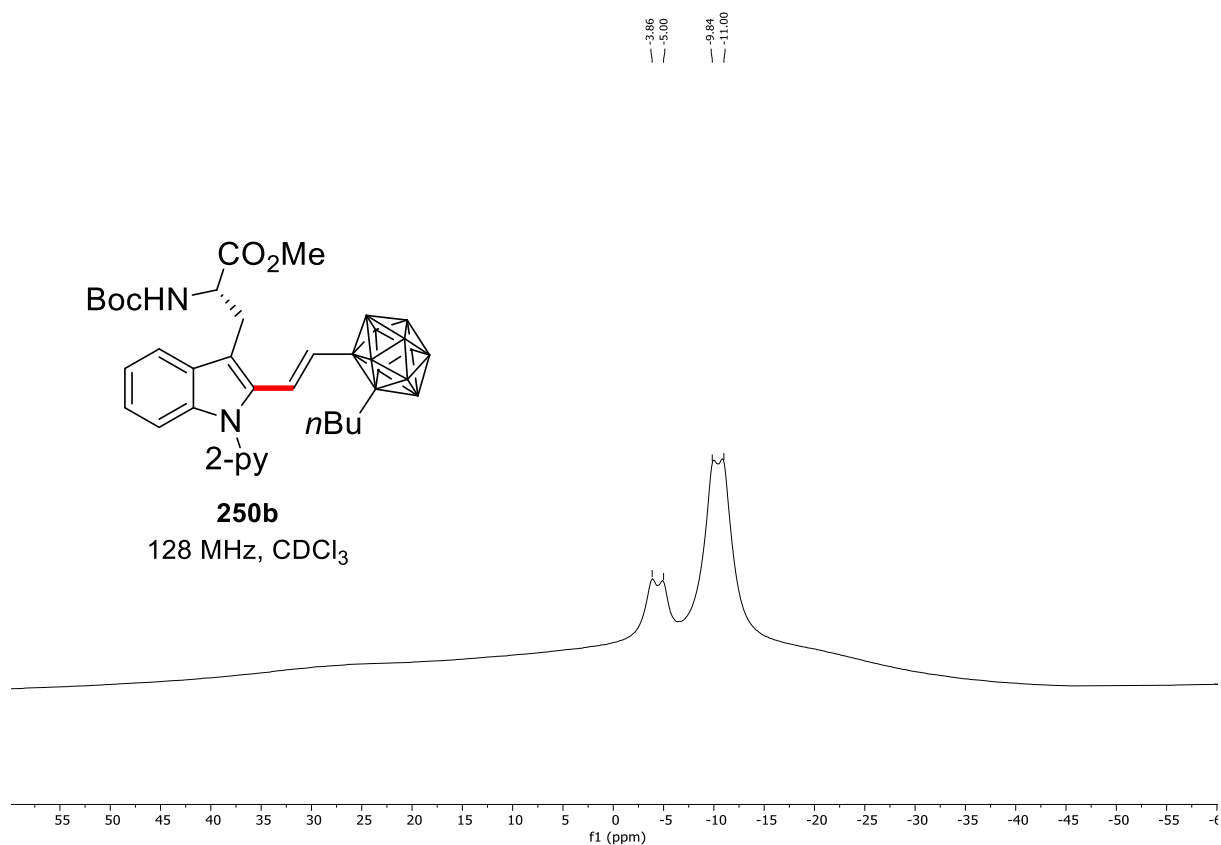




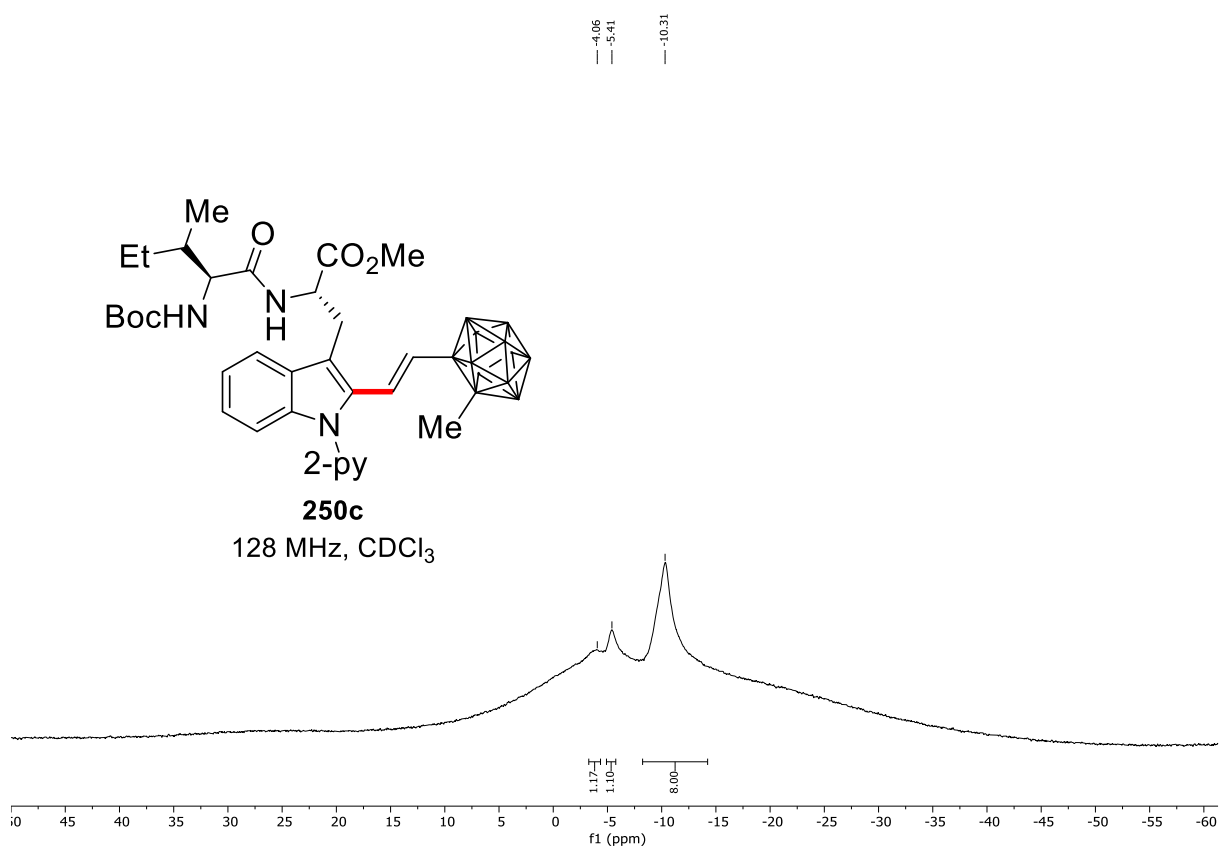
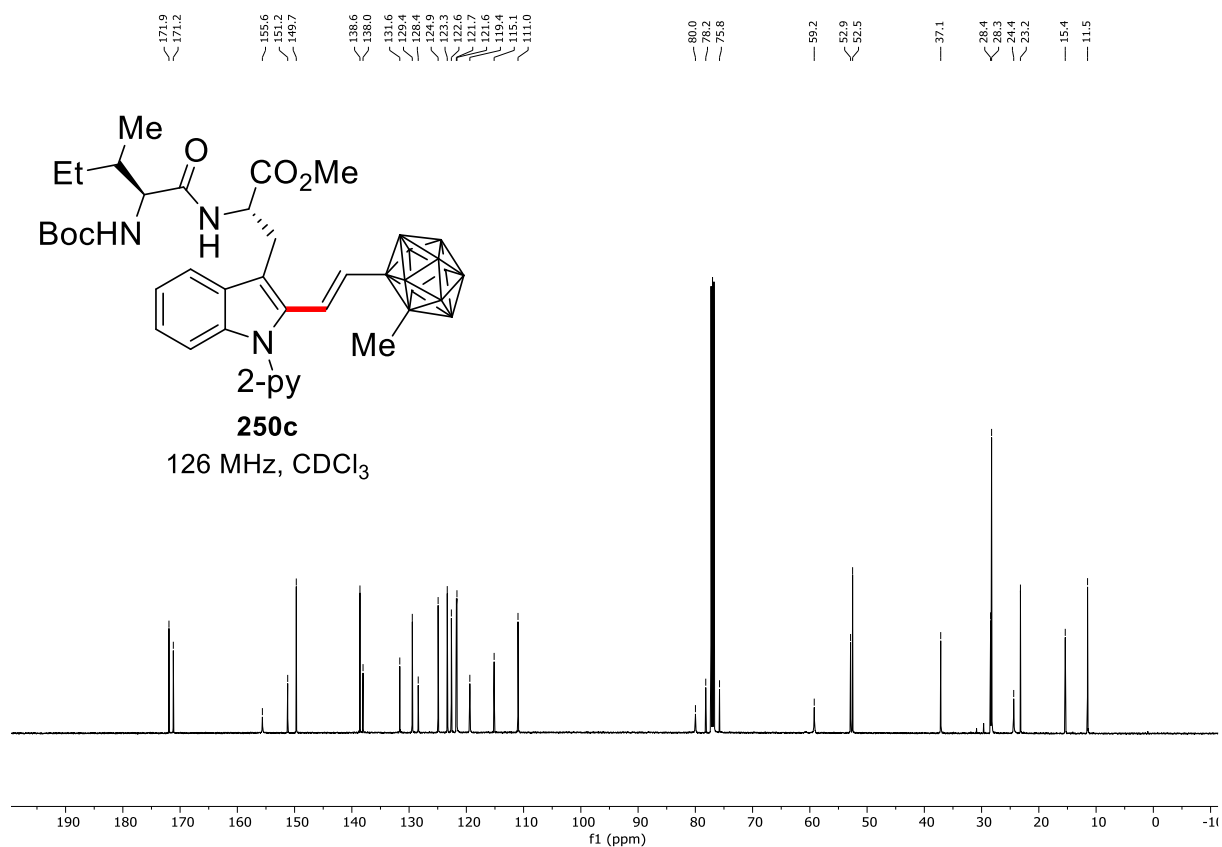
7. NMR Spectra



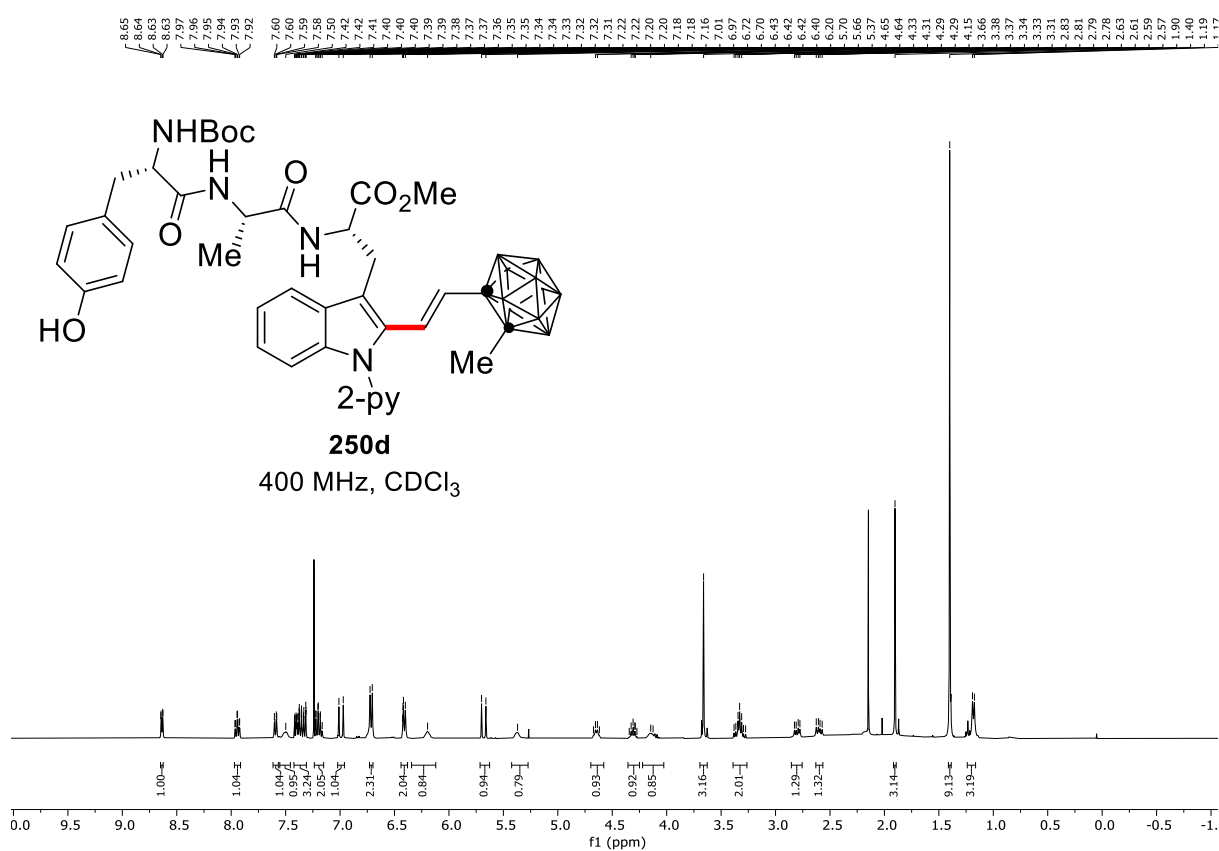
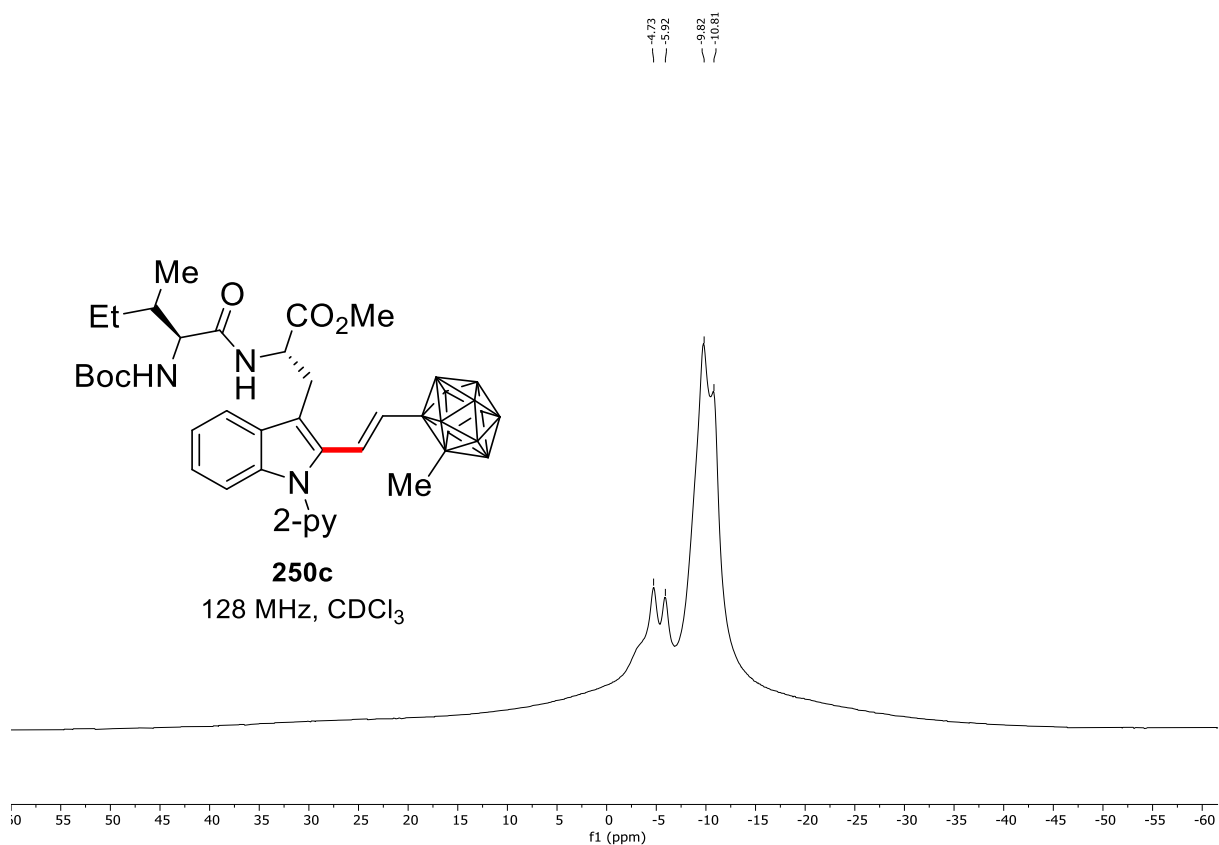
7. NMR Spectra



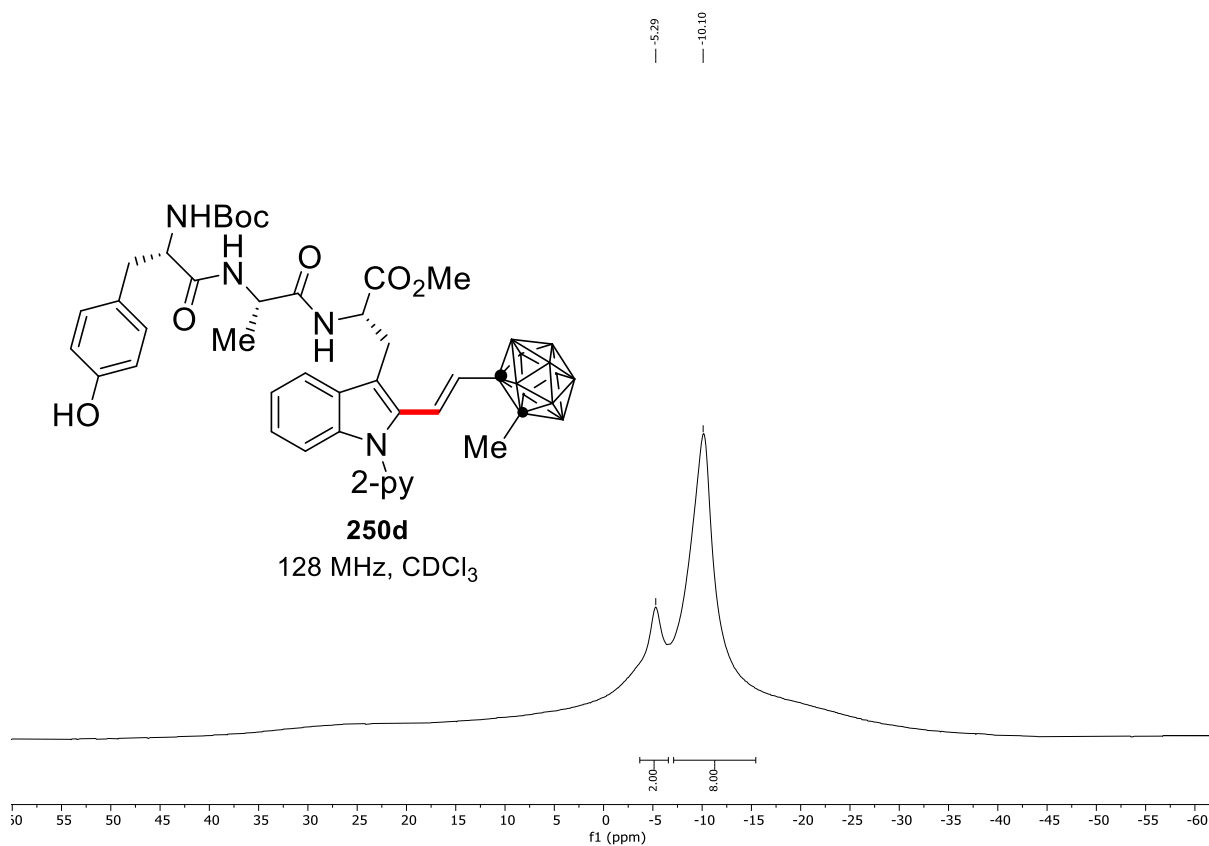
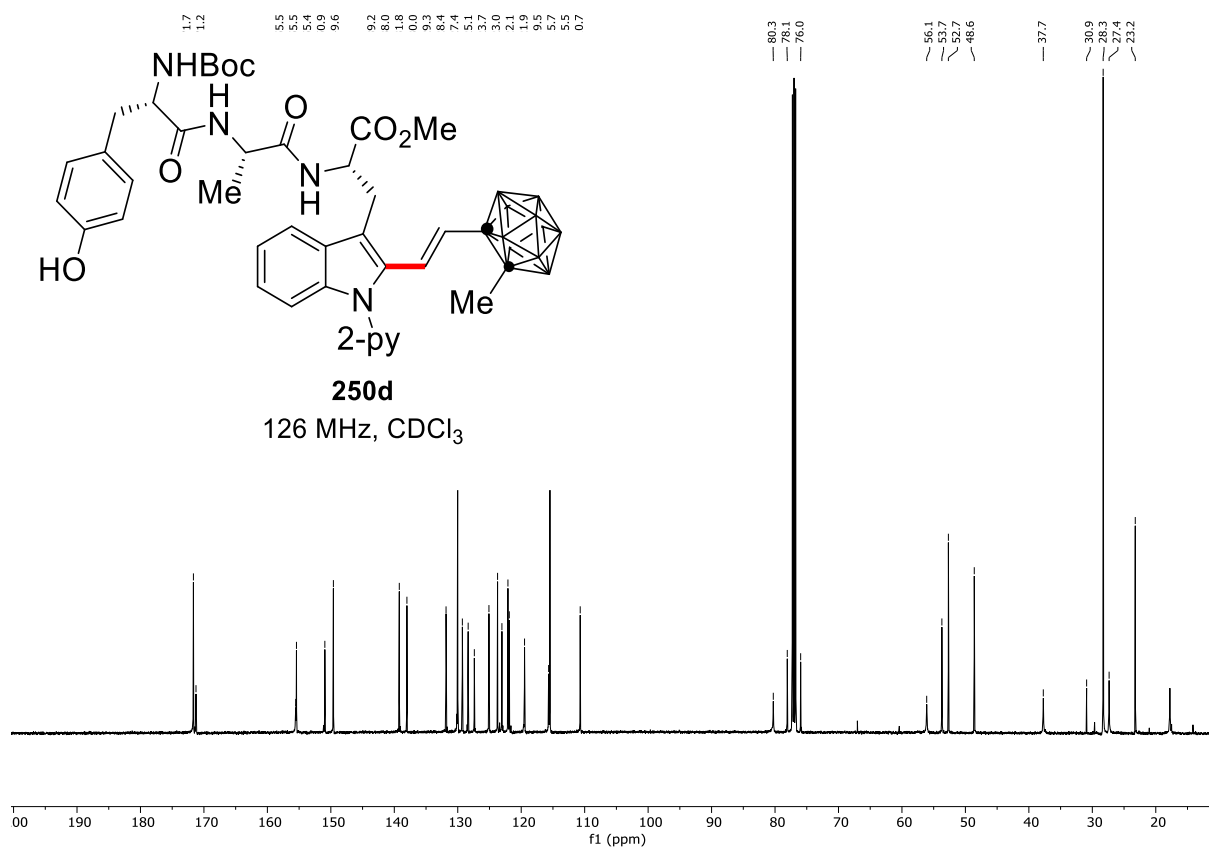
7. NMR Spectra



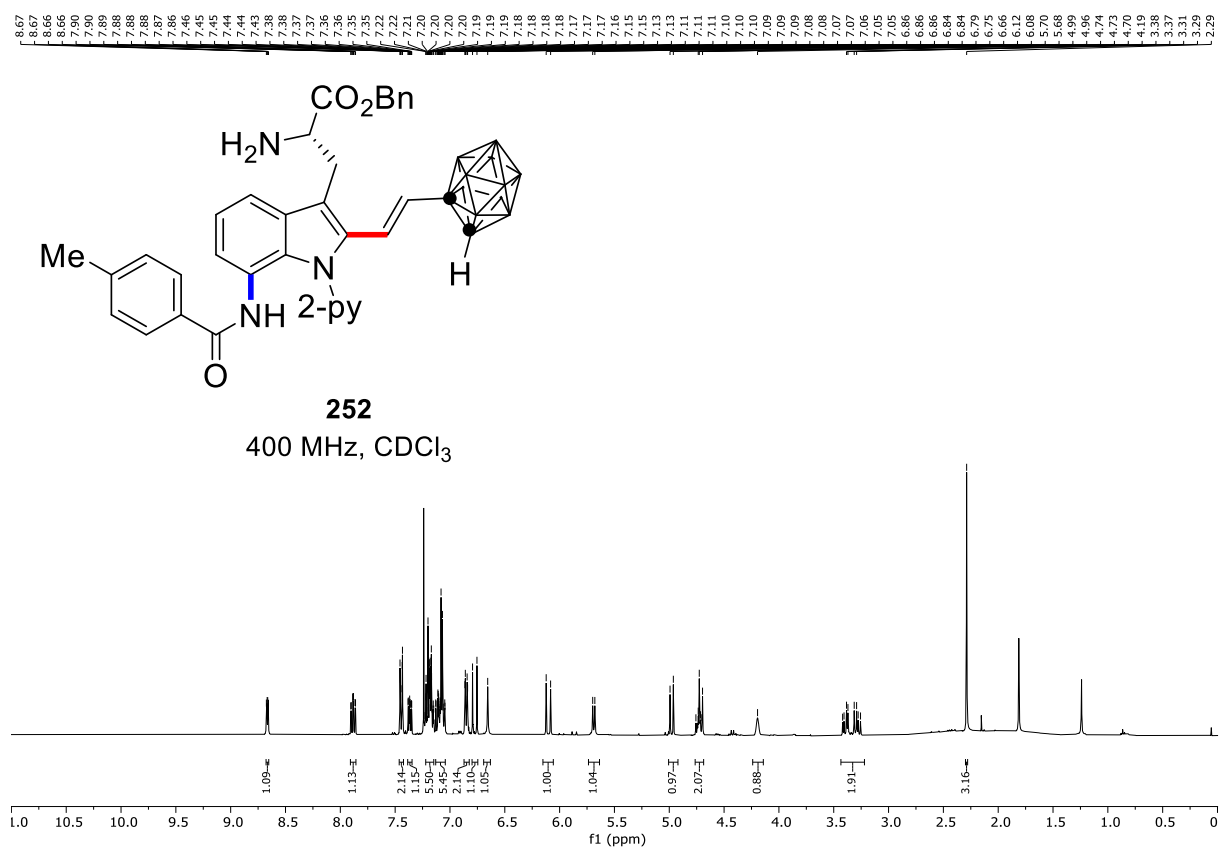
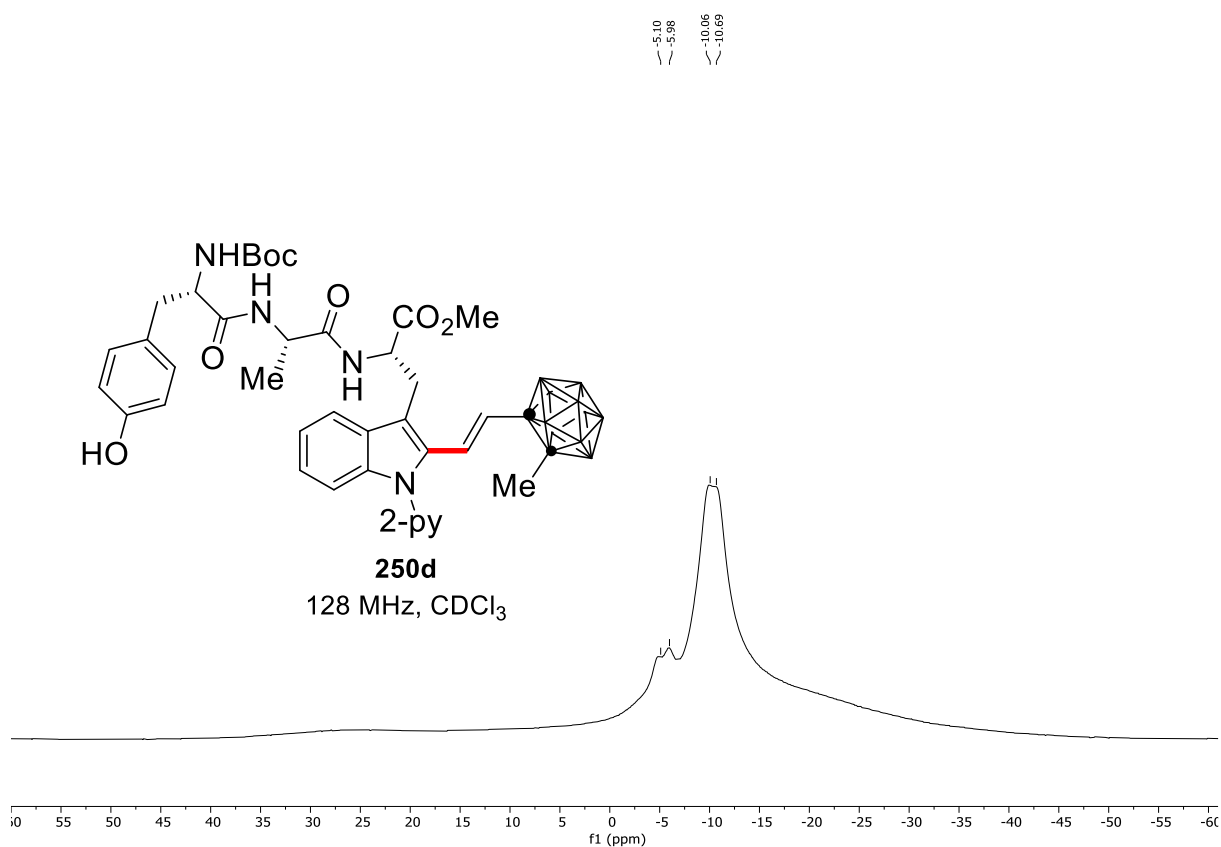
7. NMR Spectra



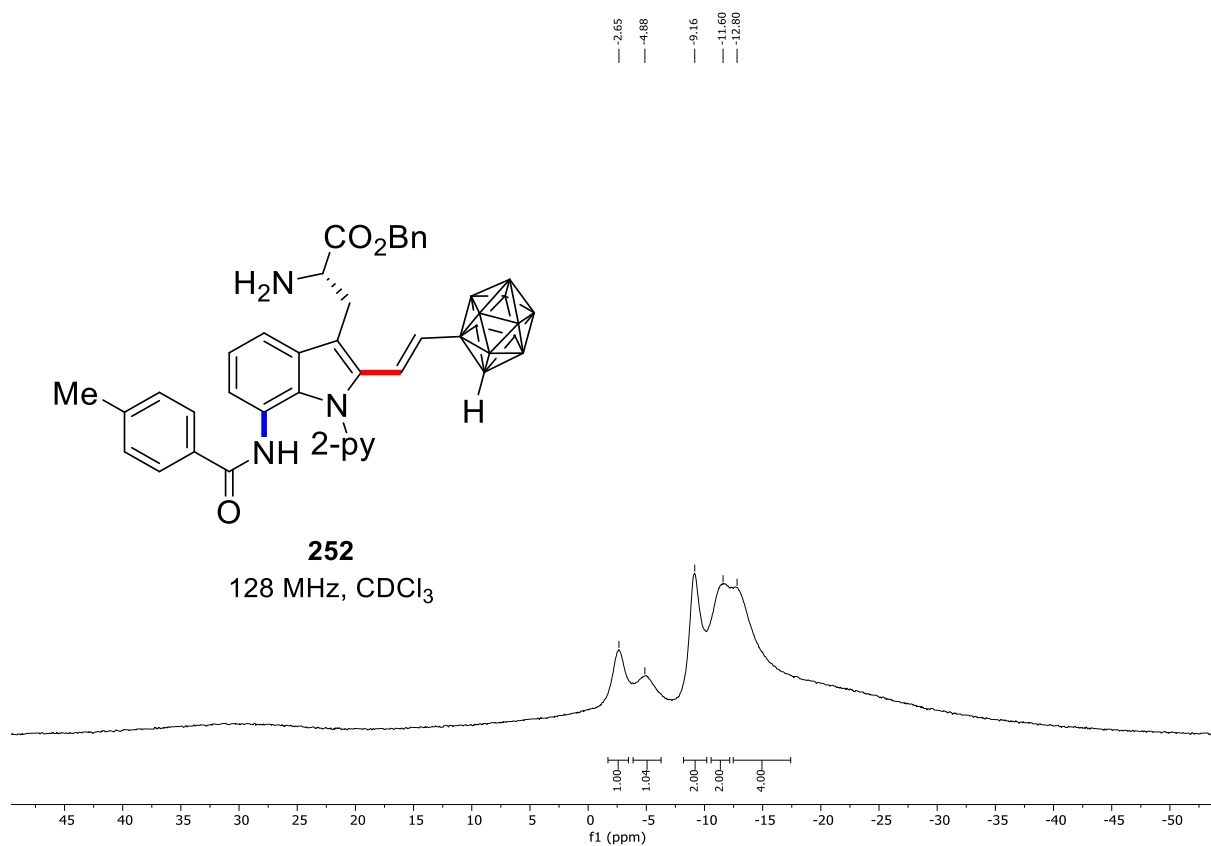
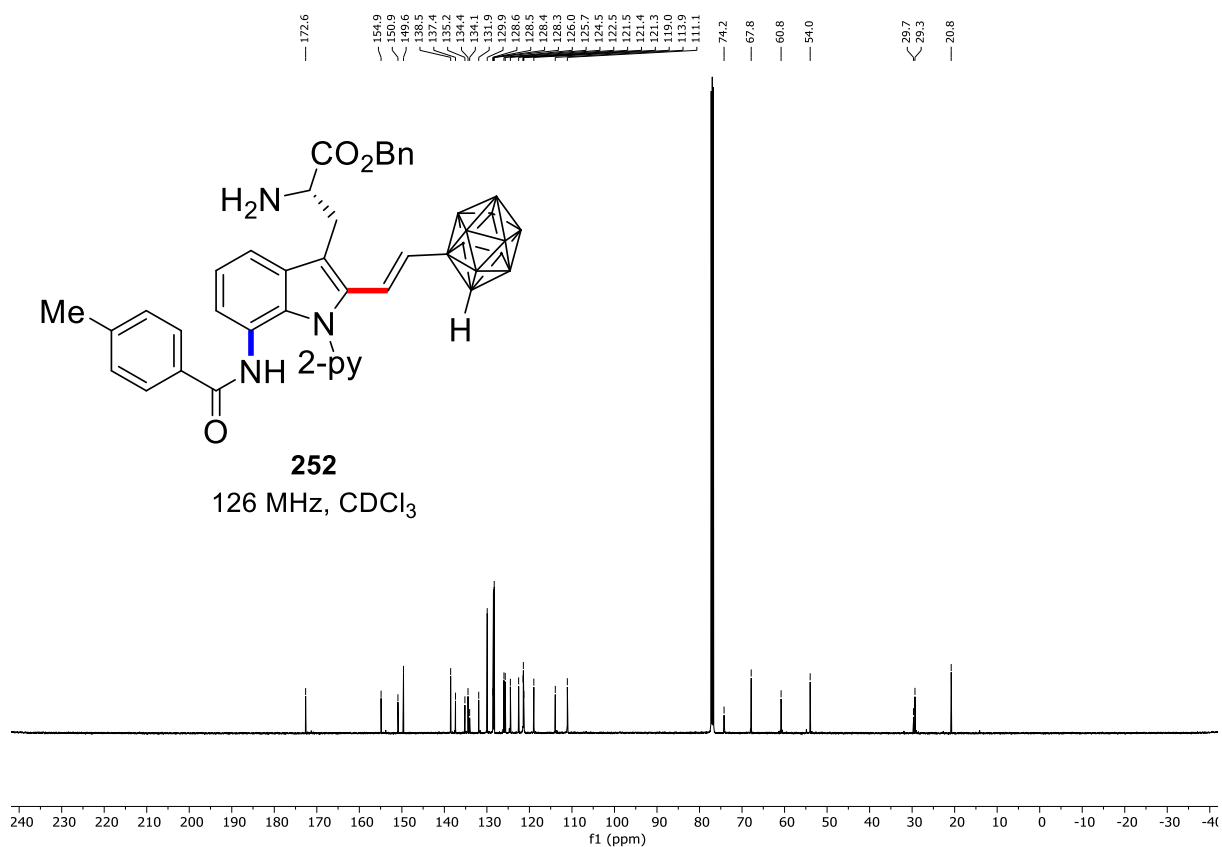
7. NMR Spectra



7. NMR Spectra



7. NMR Spectra



7. NMR Spectra

